The molecular and cellular basis of antigen recognition by CD1a-restricted T cells

Catriona Vi Nguyen-Robertson

B.Sci (Hons) Dip.Lang

ORCID 0000-0001-8751-4503

Department of Microbiology and Immunology

The University of Melbourne

The Peter Doherty Institute for Infection and Immunity

Submitted in total fulfilment of the requirements of the degree of

Doctor of Philosophy

April 2022

Abstract

In contrast to conventional T cells that recognise peptide antigens presented by MHC molecules, a group of "unconventional" T cells recognise lipid antigens presented by MHC-like CD1 family members, CD1a, CD1b, CD1c and CD1d. Studies suggest that CD1a-restricted T cells comprise a unique subset in human blood that recognise CD1a-lipid complexes and play a unique functional role in skin immunity. While they comprise a decent proportion of T cells compared to CD1d-restricted, natural killer T (NKT) cells, they remain relatively less well-understood.

This thesis describes the phenotypic characterisation of CD1a-restricted T cells in human tissues directly *ex vivo*. Phenotypic analyses and single cell RNA-sequencing of CD1a-restricted T cells revealed that they are distinct from other CD1-restricted T cells. They did not express typical innate-like markers such as CD161, IL-18R, and PLZF, which are expressed by NKT cells, distinguishing them as a unique population of unconventional T cells.

This thesis also elucidates how T cell receptors (TCRs) interact with CD1a-lipid complexes. Profiling the TCR repertoire of CD1a-restricted T cells, demonstrated that while diverse, there is a bias towards TCR variable genes that endow optimal TCR configurations to interact with CD1a and lipid antigens. Experiments with CD1a mutant cell lines revealed that individual TCRs bind at various sites across the entire binding cleft of CD1a, which likely increases the diversity of lipid antigens that can be recognised by CD1a-restricted T cells. Indeed, these T cells were observed to recognise numerous lipid antigens including self-lipids and dideoxymycobactin (DDM), a lipid antigen derived from *Mycobacterium tuberculosis*, with some CD1a-restricted TCRs even displaying cross-reactivity to lipids with distinct chemical structures.

Reagents were developed as tools to study lipid-reactive T cells in macaques, especially for non-human primate models of disease. A suite of CD1 tetramers were generated to isolate CD1-restricted T cells in pig-tailed macaques and for preliminary enumeration and phenotypic analysis of CD1-restricted T cell subsets in macaque tissues.

Lastly, tetramers were used to investigate CD1a-restricted T cells in human skin. Populations of lipid-reactive T cells and γδ-T cells were isolated for phenotypic analysis and TCR sequencing, thus demonstrating that they may play a role in healthy skin. C12-15 alkyl-benzoate, a common oil in dermatological products, was identified as a novel CD1a antigen, suggesting a role for CD1a-restricted T cells in allergic dermatitis.

These studies provide insight into the functional properties of CD1a-restricted T cells and their molecular interactions with CD1a-lipids. Collectively, they represent a step forward in characterising CD1a-restricted T cells and provide a greater understanding of their role in the immune system.

Declaration

This is to certify that:

1. This thesis comprises only my original work towards the PhD except where indicated in the preface
2. Due acknowledgment has been made in the text to all other material used
3. This thesis is less than 100,000 words in length, exclusive of tables, references and appendices

Catriona Vi Nguyen-Robertson, 8th April 2022

Preface

In accordance with the regulations of the University of Melbourne, I acknowledge that components of the work presented in this thesis were collaborative (percentages refer to the contribution of work to each chapter):

Chapter 3

Scott Reddiex (University of Melbourne) performed some of the RNA processing and library preparation for RNA sequencing (0.5%). Willem Van Der Byl and Fabio Luciani (University of New South Wales) performed RNA sequencing analysis for DDM-reactive, GMM-reactive, NKT and $CD4^+$ T cells (2%). Note that isolation of these T cell subsets was performed in collaboration with Michael Souter (University of Melbourne).

Chapter 4

Shihan Li and Scott Reddiex (University of Melbourne) generated the β_2m-deficient SKW-3 cell line (0.5%) used in transductions to produce CD1a-restricted T cell lines. Tan-Yun Cheng and D. Branch Moody (Brigham and Women's Hospital and Harvard Medical School) performed mass spectrometry and lipid antigen discovery of prepared 17a28 TCR, 27a28 TCR, or 29a28i TCR co-complexes with CD1a-DDM or CD1a-endo (2%).

Zehua Tian facilitated in soluble TCR chain expressions and protein production (0.25%).

Chapter 5

Members of Stephen Kent's Laboratory (University of Melbourne) assisted with the harvesting and processing of pig-tailed macaque tissues, namely Jennifer Juno, Stephen Kent, Kathleen Wragg, Vinca Alcantara, and Thakshila Amarasena (0.5%).

Acknowledgements

Who would have thought that by attending the Faculty of Science's "Speed Date a Scientist" event in 2014, I would lock myself in for a six-year ride of Honours and a PhD? A/Prof. Daniel Pellicci, I am grateful that you took me on after our serendipitous meeting. You saw something in me that I hadn't seen myself and have guided me to become an independent researcher – so much so that my first thought when I got an allergy was "CD1a-restricted T cells!" I know you had not been planning on supervising an Honours student at the time, which makes me all the more grateful that you did take me on. And the rest is history. Thank you to my co-supervisor, Prof Dale Godfrey, for also adopting me as a student and making time for me despite your incredibly busy schedule, especially when COVID-19 hit. Dale, you've always looked out for me, and your attention to detail and scepticism around which cells are "real" have made me constantly work harder to ensure that my science is up to scratch. You're also an incredible mix of a great scientist and good person that I can only hope to aspire to become. Working under both Dan and Dale has been a privilege, as they are both leaders in our niche (hipster/awesome) field. They have both supported my presentations at conferences and seminars, and believed in me. I know that I've stretched this PhD out, but I am really grateful to you both for standing by me.

Thank you to all members past and present of the Godfrey and Pellicci Labs who have contributed immensely to my work and life during the last few years. You've been wonderful colleagues and friends.

Adam, you are researcher goals – incredibly successful with a great work-life balance. You know everything about everything and are a fountain of knowledge. Thank you for all your help over the years and for answering all my questions. Catarina, Chris, Darryl, Fee, Fern, Garth, Janice, Nick, Marc, Rob, and Tom, you have also been great researcher role models for me. Everyone I've seen go in that "postdoc office"/is a postdoc in the lab is a force to be reckoned with in science, and I'm fortunate to have learned a thing or two from you. Thank you for sharing your knowledge and expertise, and for inspiring me to follow in your footsteps as a young researcher. Nick, a special shout out to you for your guidance with a lot of this work: learning how to do PCRs, analyse sequences, trying and trying to get the best tetramer staining possible in macaques with that pesky "molecule X" in the way, writing it all down…this thesis wouldn't be very long without your help.

Marty and Zheng, you keep the lab running smoothly and we simply would not function without you. Marie-Sophie, you were only with us for a year, but you became such a good friend. Sie sind mein bester freund! I can't wait to visit you and Ulli again – and perhaps we can take the trip that we planned now that we're both done with our theses! Speaking of trips, Cat, thank you for sharing such an epic adventure with me in the US and for always being "mother hen". It's nice knowing that someone's got my back. I thoroughly enjoy working with you and I'm glad to have taken my next steps as a researcher under your guidance. Carol, I can't believe you signed on to read this entire thing to ensure that I had all my i's dotted and t's crossed in all the right places. You have been so incredibly generous with your time. You are an absolute legend in the lab, in the kitchen, and just in general. I cannot thank you enough. If this was a race (VERY long distance), it's like I fell flat on my face just before the finish line, but you helped me up and held my hand to the end. This thesis is done thanks to you (and your computer). Calvin, you're a great bench buddy and best desk MAIT I could ask for. C-C is a covalent bond – so it's no

wonder we're so tight! Scott, Marty, Daz, Tom, Ying, Kat, Sam, Rebecca, Keit, Carol, Elena, Kezia, Bella and Becky, you've also been wonderful friends and coffee buddies. (Or should I say "tea buddies?" Daz, you predicted I would start drinking coffee by the end of Honours, and if not then, then certainly during the PhD but alas, I'm still not a fan. Even as I scrambled to get this thesis together – just like then.) It's because of you all that I enjoy working in the Godfrey Lab. *This list keeps getting longer the longer I drag out the thesis!! I now even have to add yet another generation of students – another Kat, Tina and Ryan – who cheered me on through the very final sprint.

Thank you to my PhD Advisory Committee, Frank Carbone, Katherine Kedzierska, Gabrielle Belz, and Jennifer Juno for your guidance and for sharing your expertise. I have always appreciated your take on my research – and Frank, I hope this thesis convinces you that CD1a-restricted T cells exist and are the real deal. Jen, you've not only been a great collaborator and advisor, but also a good friend and someone I look up to as an ECR kicking so many goals.

Thank you also to all the collaborators I've had the pleasure of working with (in no particular order): Jen Juno, Kathleen Wragg and Stephen Kent at The University of Melbourne Willem Van Der Byl and Fabio Lucciani at the Kirby Institute, UNSW; Branch Moody, Ildiko Van Rhijn, Tan-Yun Cheng and Rachel Cotton (a.k.a. my CD1a venting buddy) at Brigham and Women's Hospital and Harvard Medical School; Shelby O'Connor at the University of Wisconsin-Madison and Charles (Chuck) Scanga at the University of Pittsburgh; Graham Ogg and Koshika Yadava at Oxford University; and Stuart Berzins at Federation University (thank you so much for all the samples!). A special thank you to my colleagues in the ARC Centre of Excellence for Advanced Molecular Imaging. Prof. Jamie Rossjohn and Dr Adam Shanine at Monash University, and Prof. Spencer Williams at the University of Melbourne. Thank you also to James Whisstock, Juliana Villa-Ortiz and Annette Wittmann for your encouragement with regards to the Centre's student group and my science singing endeavours. Could a song about MAIT cells, NKT cells and CD1a-restricted T cells just be my thesis? It's an album.

Thank you to the McCluskey, Brooks, Kedzierska, Wakim, Mackay Labs and others for their generous lending of reagents, assistance, their friendly, collegial nature, especially during the long hours, and for not asking me to be quiet if I was singing loudly in the lab on a weekend. Sidonia Eckle, Alex Corbett, Pat Reading and Linda Wakim, in particular, I have regarded as mentors/people I can seek wisdom from when working out what to do in my life.

Many people in the Department of Microbiology and Immunology have been great friends during my years as a student – friendly faces in the corridor, chats while making tea, late-night tunes in the flow lab, all that jazz. Speaking of flow, the Flow Cytometry Core team, Tina, Vanta, Angela, Catherine and Lankesha have all been so helpful, especially when it came to sorting cells. And I sorted a lot of cells throughout my PhD.

Thank you to my Honours buddies, Keit, Miku, Will, Rachel, and (the elusive) Xavier. We've stuck by each other through it all! Keit, you've been a great eighth floor buddy and I knew we would be great friends all those years ago. Pull all-nighters together in Honours, stay together. And Miku 姉ちゃん, I love our chats, jokes, shared meals, and everything about our friendship. 美紅姉ちゃんの作った料理（茶碗蒸しやラーメン

など）はとても美味しい！美紅姉ちゃんは本当に私の最高の親友だよ！美紅姉ちゃんが大好き！

Thank you to the people who gave my science communication a chance to grow. Mike Flattley, Luan Ismahil, Renee Beale, Rena Singh, Rebecca Elliot and Cath Somerville, you all gave me the opportunity to write for you, and I can't thank you enough. If only writing this thesis was as anywhere near as easy or fun as writing articles about other people's science for the general public. The Australia and New Zealand Society for Immunology also gave me a good start in science communication, offering me the chance to be Social Media Ambassador at conferences and write an animation about the immune system. Gabi Khoury and Tyani Chan in particularly, you've been such wonderful supports. Also, Mike, whenever I think I have too much on my plate, I think of you. You are so good at juggling everything and I can only hope that some of that rubs off on me via osmosis or something.

Thank you to the DMI teaching staff (Odilia, Karena, Louise, Jess and Dan) and GTAC for giving me the opportunity to explore my passion for teaching. You teach all the students who come through this department so many core skills that you need as a researcher: the ability to pass the knowledge on. You've also given me so much encouragement over the years – to pursue teaching and science communication…but to also get through this PhD!

Jen, Graham, Linden, Michael and Rosie, the UniMelb SciComm Teaching Team, I cannot emphasise how much you have helped me throughout the past few years. I was so lucky to find such an amazing group of people to work with. You are all wonderful people, great friends, and you've taught me a lot about communicating science. Hopefully some of those lessons have rubbed off on this thesis – I have to 'practice what I preach,' right? I've been "so close" with this thesis for a long time, and you all lifted me up every time I hit a wall. Jen and Linden, you especially helped me out heaps in the leadup to FameLab and other presentations before I was even a team member, so thank you for being so generous with your time. To steal Jen's line: you're the best!! You were also the best motivation for me to actually get this thing written and done.

The UniMelb SciComm Shut Up And Write gang was instrumental in getting me to sit down and do some writing during the lockdowns. You've all supported me so much and I have appreciated our SUAW accountability and the chats in between. In lockdown, it was wonderful to see your faces as we all struggled to get through our work together. Stephanie, you were always a friendly, constant presence, and always looking out for me. Kate and Rosie, you two are two very good friends I now have who I wish I'd had sooner. You are both incredible people and, to me, the epitome of cool. I have so much love for both of you.

Other mentors I've picked up along the way include Anna Lavelle, Maggie Evans-Galea and Michelle Gallaher, three incredible #WomeninSTEM and three of the biggest cheerleaders who lift up other women in STEM. Jess Borger and Kylie Quinn are also incredible forces driving equity, diversity and inclusion in immunology. They are the best role models young people in immunology could hope for and have taught me so much about using my voice to fight for what I believe in and also share my passion for science with others.

To the Sworkers, you're a bunch of nerds, and of course I say that in the most endearing, best possible way. Because I am one of you. I am so glad to be part of such an amazing team and I am constantly in awe and inspired by all the incredible things you do. I always come in to Scienceworks with a smile on my face – even during this final, very sleep-deprived week of thesis-writing – because I know I get to hang out with a great team who really care for each other. You are all a wonderfully caring bunch of people and you've been so supportive, offering me food, naps in the newly refurbished nap zone complete with dinosaur buddies, and helping to lighten my load. Being so entrenched in the world of academia, it blew my mind, this idea of only working for a set number of hours and then completely clocking off for the day. Doug, Nina, and Rosa, I feel like you're teaching me how to have a better work-life balance by telling me to get out of there at the end of a shift. Thank you all for being such great bubbly bundles of energy and a never-ending source of puns (Owen!) and science jokes. Kate, I was "soon-to-be-doctor" when I first joined…and it's finally becoming a reality.

Lastly, my family and friends have held me up over these past several years. Mum & Dad have supported me throughout, especially by flinging food my way – although, I won't be the kind of doctor you initially wanted in the end, Dad. You both see me at my worst and love me anyway. Sasha, you're a fantastic big brother and I very much enjoy our weekly lap of Princes Park. Why have we not done that this whole time? Dorothée, you've been a good friend and I stayed with you and your family in Langenthal at a really crucial time when I had no idea what to do…and what my luck that your mother advises graduate students! My good friends – Alex and Dan, Alice, Bec, Hasini, Himasha, Jenny, Julia, Mahi, Sarah, Vivian, Vivien, Winn and 佳奈ちゃんと私の日本人の家族 – you have all helped me get through and kept me sane. Thank you for hanging out with me, travelling with me, chatting with me, and essentially, giving me a life outside of science. Wanting to spend time with you has forced me to keep *somewhat* of a work-study-life balance.

List of Publications

Publications arising during candidature:

2021

Nicholas A Gherardin, Samuel J Redmond, Hamish EG McWilliam, Catarina F Almeida, Katherin HA Gourley, Rebecca Seneviratna, Shihan Li, Robert De Rose, Fiona J Ross, **Catriona V Nguyen-Robertson**, Shian Su, Matthew E Ritchie, Jose A Villadangos, D Branch Moody, Daniel G Pellicci, Adam P Uldrich, Dale I Godfrey. CD36 family members are TCR-independent ligands for CD1 antigen-presenting molecules. *Science Immunology,* 2021, 25;6(60) doi: 10.1126/sciimunol.abg4176.

Jessica G Borger, **Catriona V Nguyen-Robertson,** James Harris. Trailblazing women immunologists of Australia and New Zealand. *Immunology and Cell Biology,* 2021, 99(4):338-343 doi: 10.1111.imcb.12454.

2020

Catriona V Nguyen-Robertson, Ashraful Haque, Justine Mintern, Anne C La Flamme. COVID-19: searching for clues among other respiratory viruses. *Immunology and Cell Biology,* 2020, 98(4): 247-250 doi: 10.1111/imcb.12336.

Kathleen M Wragg, Hyon-Xhi Tan, Anne B Kristensen, **Catriona V Nguyen-Robertson**, Anthony D Kelleher, Matthew S Parsons, Adam K Wheatley, Stuart Berzins, Daniel G Pellicci, Stephen J Kent, Jennifer A Juno. High CD26 and Low CD94 Expression Identifies an IL-23 Responsive $V\delta2^{+}$ T Cell Subset with a MAIT Cell-like Transcriptional Profile. *Cell Reports,* 2020, 16;31(11):107773 doi: 10.1016/j.celrep.2020.107773.

2017

Erik D Hanson, Eli Danson, **Catriona V Nguyen-Robertson**, Jackson J Fyfe, Nigel K Stepto, David B Bartlett, Samy Sakkal. Maximal exercise increases mucosal associated invariant T cell frequency and number in healthy young men. *European Journal of Applied Physiology*, 2017, 117(11): 2159-2169 doi: 10.1007/s00421-017-3704-z.

List of Awards, Bursaries, and Presentations

Awards

2021 3 Minute Thesis Competition Runner Up, The University of Melbourne

2020 Science Outreach Award, Australia and New Zealand Society for Immunology

2019 Qiagen PhD Achievement Award Runner-Up, Department of Microbiology and Immunology, The University of Melbourne

2019 Second Place, FameLab Australia Victorian Semi-Finals, Melbourne
Finalist in the FameLab Australia Finals, Perth

List of Presentations

Oral Presentations:

2020 Australian Research Council Centre of Excellence for Advanced Molecular Imaging Student Summit, Online **(awarded Best Presentation, Third Place)**

2020 Faculty of Medicine, Dentistry and Health Sciences Graduate Research Conference, The University of Melbourne, Online
(awarded Best Presentation, Immunology, Second Place)

2020 Immunology Group of Victoria Meeting, Online,
(awarded Best Student Presentation)

2019 FameLab Australia (semi-finals, final), Perth **(Runner Up in the Victorian Semi-Finals)**

2018 Australasian Society for Immunology Annual Scientific Meeting, Perth
(awarded BD Science Communication Award)

2018 Australian Research Council Centre of Excellence for Advanced Molecular Imaging Summit, Cape Schanck

2018 Peter Doherty Institute Immunology Theme Meeting, Melbourne

2018 Immunology Group of Victoria Meeting, Werribee Park

2017 3 Minute Thesis Competition (heat, semi-finals, final), The University of Melbourne

2017 Australian Research Council Centre of Excellence for Advanced Molecular Imaging Summit, Torquay

2017 Immunology Group of Victoria Meeting, Yarra Valley

2017 The Doherty Institute Scientific Conference, Macedon Ranges

2016 Australian Research Council Centre of Excellence for Advanced Molecular Imaging Summit, Torquay

2016 International Congress of Immunology, Melbourne

2016 Biomed Link, Melbourne

2016 The Immunology Group of Victoria Roadshow, Melbourne

Poster Presentations:

2020 European Molecular Biology Laboratories (EMBL) Australia Postgraduate Symposium, online **(awarded Best Poster Prize, 4th year)**

2020 Victorian Infection and Immunity Network (VIIN) Symposium, online **(awarded Audience Choice Award)**

2019 Australia and New Zealand Society for Immunology Society for Immunology Annual Scientific Meeting, Adelaide

2018 Australasian Society for Immunology Annual Scientific Meeting, Perth **(awarded ASI Poster Prize)**

2018 Australian Research Council Centre of Excellence for Advanced Molecular Imaging Summit, Cape Schanck

2018 European Congress of Immunology, Amsterdam

2017 CD1 MR1 2017, Napa Valley

2017 Australasian Society for Immunology Annual Scientific Meeting, Brisbane **(awarded the Immunology and Cell Biology Poster Prize)**

2017 Australian Research Council Centre of Excellence for Advanced Molecular Imaging Summit, Torquay

2016 World Life Sciences Conference, Beijing

2016 Australian Research Council Centre of Excellence for Advanced Molecular Imaging Summit, Torquay

2016 Victorian Infection and Immunity Network Young Investigator Symposium, Melbourne

Session Chair:

2021 Faculty of Medicine, Dentistry and Health Sciences ECR Symposium, online

2021 Victorian Infection and Immunity Network (VIIN) Symposium, online

2018 Peter Doherty Institute Immunology Theme Meeting, Melbourne

2018 Australian Research Council Centre of Excellence for Advanced Molecular Imaging Summit, Cape Schanck

2017 Department of Microbiology and Immunology Seminar, The University of Melbourne

2016 Australian Research Council Centre of Excellence for Advanced Molecular Imaging Summit, Torquay

List of Prizes and Bursaries

ASI Travel Bursary 2019

Major Bartlett Domestic Travel Scholarship, 2019

ASI Postgraduate Travel Award, 2018

Major Bartlett International Travel Scholarship, 2017

World Life Science Conference Travel Scholarship, 2016

Immunology Group of Victoria Travel Scholarship, 2016

Melbourne Research Training Program Scholarship, 2016-2020

Australian Research Council Centre of Excellence for Advanced Molecular Imaging PhD Scholarship, 2016-2020

List of Abbreviations

a-GalCer/α-GC	a-galactosylceramide
β2m	β2-microglobulin
5-A-RU	5-amino-6-D-ribitylaminouracil
5-OE-RU	5-(2-oxoethylideneamino)-6-D-ribitylaminouracil
5-OP-RU	5-(2-oxopropylideneamino)-6-D-ribitylaminouracil
6-FP	6-formylpterin
7-AAD	7-aminoactinomycin D
AB	alkyl benzoate
Abexp	alkyl benzoate expressed (in GnTI$^-$ cells)
ABL	alkyl benzoate loaded
Ac-6-FP	acetyl-6-formylpterin
ACD	allergic contact dermatitis
Ag	antigen
AHR	aryl hydrocarbon receptor
AIDS	acquired immunodeficiency
APC	antigen presenting cell/allophycocyanin
ATP	adenosine triphosphate
BAL	bronchoalveolar lavage
BCG	Bacillus Calmette–Guérin
BirA	biotin-[acetyl-CoA-carboxylase] ligase and biotin-operon repressor
BUV	Brilliant Ultraviolet
BV	Brilliant Violet
CCR	chemokine receptor
CD	cluster of differentiation
cDNA	complementary deoxyribonucleic acid
CDR	complementarity determining region
CID	collision-induced dissociation
CLA	cutaneous lymphocyte antigen
CNS	central nervous system
CXCR	C-X-C chemokine receptor
DAG	diacylglyceride
DAMP	danger associated molecular pattern
DC	dendritic cell
DDM	dideoxymycobactin
DEAE	diethylaminoethanol
DMEM	Dulbecco's Modified Eagle's Medium
DMSO	dimethyl sulfoxide
DN	double negative
DNA	deoxyribonucleic acid
DP	double positive
DTH	delayed-type hypersensitivity
DTT	dithiothreitol
EAE	experimental autoimmune encephalomyelitis
EDTA	ethylenediamine-tetraacetic acid
EIS-MS	electrospray ionization mass spectrometry
ELISA	enzyme-linked immunosorbent assay
Endo	endogenous

EpCAM	epithelial cell adhesion molecule
ER	endoplasmic reticulum
FACS	fluorescence activated cell sorting
FCS	fetal calf serum
FGT	female genital tract
FITC	fluorescein isothiocyanate
FPLC	fast protein liquid chromatography
GEM	germline-encoded mycoyl
GFP	green fluorescent protein
GILZ	glucocorticoid-induced leucine zipper
GM-CSF	granulocyte macrophage colony-stimulating factor
GMFG	glia maturation factor gamma
GMM	glucose monomycolate
GnTI	N-acetyl-glucosaminyltransferase I
GSL	glycosphingolipid
HDM	house dust mite
HEK	human embryonic kidney
HEPES	2-hydroxyethylpiperazine-N-2-ethane sulfonic acid
HIV	human immunodeficiency virus
HLA	human leukocyte antigen
HPLC	high performance liquid chromatography
HPLC-QTof2-MS	high-performance liquid chromatography-quadrupole-time of flight mass-spectrometry
HRP	horseradish peroxidase
hu	human
IBP	inclusion body preparation
ICOS	inducible T cell-co-stimulator
IFN	interferon
iGb3	isoglobohexosylceramide
IL	interleukin
ILC	innate lymphoid cell
iLN	inguinal lymph node
IPTG	isopropyl β-D-1-thiogalactopyranoside
KO or -/-	knock out
LA	Luria agar
LB	Luria broth
LPA	lysophosphatidic acid
LPC	lysophosphatidylcholine
LTBI	latent tuberculosis infection
MA	mycolic acid
mAb	monoclonal antibody
MACS	magnetic activated cell sorting
MAIT	mucosal-associated invariant T cell
MFI	mean fluorescence intensity
MHC	major histocompatibility complex
MR1	MHC-I like related protein 1
mLPA	methyl-lysophosphatidic acid
mLN	mesenteric lymph nodes
mRNA	messenger ribonucleic acid
MS	mass spectrometry/multiple sclerosis

MTb	mycobacterium tuberculosis
MW	molecular weight
NHP	non-human primate
NK	natural killer
NKT	natural killer T
PA	phosphatidic acid
PAMP	pathogen associated molecular pattern
PBMC	peripheral blood mononuclear cell
PBS	phosphate buffered saline
PBS-T	phosphate-buffered saline tween-20
PC	phosphatidylcholine
PCA	principle component analysis
PCR	polymerase chain reaction
PE	phosphatidylethanolamine/Phycoerythrin
PG	phosphatidylglycerol
PI	phosphatidylinositol
PLA	phospholipase A
PLZF	promyelocytic leukemia zinc finger
PMA	phorbol 12-myristate 13-acetate
pMHC	peptide-MHC
PTM	pig-tailed macaque
RF-10	RPMI 1640 complete media
RNA	ribonucleic acid
RT	room ttemperature
SAV	streptavidin
SDS-PAGE	sodium dodecyl sulfate polyacrylamide gel electrophoresis
SGL	sulfoglycolipid
SIV	simian immunodeficiency virus
SM	sphingomyelin
SPR	surface plasmon resonance
TB	tuberculosis
TBS	tris-buffered saline
T_{CM}	central memory T
TCR	T cell receptor
T_{EM}	effector memory T
TGF-β	transforming growth factor-β
Th	T helper
TNF	tumour necrosis factor
TRAV	T cell receptor alpha variable
TRBV	T cell receptor beta variable
Treg	regulatory T
UV	ultraviolet
WT	wild type

Table of Contents

ABSTRACT iii

DECLARATION v

PREFACE vi

ACKNOWLEDGEMENTS vii

LIST OF PUBLICATIONS xi

LIST OF AWARDS, PRESENTATIONS AND BURSARIES xii

LIST OF ABBREVIATIONS xv

TABLE OF CONTENTS xviii

FIGURES AND TABLE INDICES xxii

CHAPTER 1. LITERATURE REVIEW 1

1.1 INTRODUCTION 1
1.2 MHC AND RELATED MOLECULES 4
1.2.1 MHC molecules and peptide antigens *4*
1.2.2 MHC-related proteins *6*
1.2.3 The CD1 family *7*
1.2.4 CD1 molecule structure *8*
1.2.5 Localisation of CD1 molecules *9*
1.2.6 Unconventional T cells *10*
1.3 PRESENTATION OF ANTIGENS TO T CELLS BY CD1 12
1.3.1 CD1 Lipid antigens *12*
1.3.2 Recognition of CD1 antigens *15*
1.3.3 CD1-restricted TCR diversity *16*
1.4 ROLE OF CD1-RESTRICTED T CELLS IN HEALTH AND DISEASE 17
1.4.1 CD1-restricted T cell frequency *18*
1.4.2 CD1-restricted T cell effector functions *19*
1.4.3 CD1-restricted T cells in infection *20*
1.4.4 CD1-restricted T cells in cancer *24*
1.4.5 CD1-restricted T cells in autoimmunity *26*
1.4.6 CD1a-restricted T cells in skin immunity and allergy *29*
1.5 SUMMARY, HYPOTHESIS AND AIMS 31
1.5.1 Summary *31*
1.5.2 Overarching Hypothesis *32*
1.5.3 Aims *32*

CHAPTER 2. MATERIAL AND METHODS 34

2.1 MEDIA AND BUFFERS 37
2.2. PRIMARY TISSUE SAMPLES 39
2.3 PRODUCTION OF CD1 TETRAMERS 39
2.3.1 Transfection of 293- GnTI⁻ cells *39*
2.3.2 Purification of CD1 Protein *41*
2.3.3 Sodium dodecyl sulphate (SDS)/ Polyacrylamide Gel Electrophoresis *41*
2.3.4 Biotinylation of CD1 Molecules *41*
2.3.5 Loading of CD1 with lipid antigens *42*
2.3.6 Tetramerisation of CD1 Monomers *42*
2.4 FLOW CYTOMETRY 43
2.4.1 Cell staining for flow cytometry *43*
2.4.2 Intracellular stains *47*

2.4.3 Magnetic enrichment *47*
2.4.4 Flow cytometry data analysis *47*
2.5 TCR SEQUENCING 48
2.5.1 Reverse transcription *48*
2.5.2 Nested Polymerase Chain Reaction (PCR) *48*
2.5.3 DNA Agarose gel electrophoresis *48*
2.5.4 Sequencing reaction *49*
2.6 RNA SEQUENCING 49
2.6.1 Cell lysis and reverse transcription *49*
2.6.2 PCR amplification of cDNA libraries *50*
2.6.3 Assessment and quantification of cDNA *51*
2.6.4 Tagmentation reaction and final PCR amplification *51*
2.6.5 RNA sequencing data analysis *52*
2.7 CELLULAR ASSAYS 53
2.7.1 Production of TCR-expressing and CD1-expressing cell lines *53*
2.7.2 Expansion of primary human T cells *54*
2.7.3 SKW-3 and J.76 activation assays *55*
2.8 PRODUCTION OF SOLUBLE HUMAN AB-TCRS AND CD1A-TCR CO-COMPLEXES 55
2.8.1 Cloning and expression of genes encoding soluble CD1a-restricted TCRs *55*
2.8.2 Production of inclusion bodies *55*
2.8.3 Refolding of soluble TCRs *56*
2.8.4 Purification of refolded human αβ-TCR *56*
2.8.5 Treatment of soluble CD1a for crystallography *56*
2.8.6 Co-complexation of αβ-TCR with CD1a *57*
2.9 ENZYME-LINKED IMMUNOSORBENT ASSAY (ELISA) 57

CHAPTER 3. CHARACTERISATION OF CD1A-RESTRICTED T CELLS THAT RECOGNISE A LIPID ANTIGEN DERIVED FROM M.TUBERCULOSIS 58

3.1 INTRODUCTION 58
3.2 RESULTS 61
3.2.1 Validation of tetramer production *61*
3.2.2. Isolation of CD1a-restricted T cells using magnetic enrichment *61*
3.2.3 Phenotypic characterisation of surface markers expressed by CD1a-restricted T cells *65*
3.2.4 Transcription factor expression and cytokine production in CD1a-restricted T cells *70*
3.2.5 Comparative transcriptomic analysis of CD1a-restricted T cells *76*
3.3 DISCUSSION 89

CHAPTER 4. CHARACTERISATION OF CD1A-RESTRICTED T CELL ANTIGEN RECOGNITION 99

4.1 INTRODUCTION 99
4.2 RESULTS 103
4.2.1 CD1a-restricted T cell receptor diversity *103*
4.2.2 Validation of CD1a reactivity by CD1a-restricted T cell lines *114*
4.2.3 Recognition of multiple lipid antigens by CD1a-restricted T cells *120*
4.2.4 Interaction of CD1a-lipids and TCR *127*
4.2.5 Production of Recombinant Human CD1a-restricted TCRs *135*
4.2.6 Production of Human CD1a for structural studies *143*
4.2.7 Isolation of TCR:CD1a Ternary Complexes *143*
4.2.8 Lipid antigen discovery *150*
4.2.9 Interaction between CD1a and CD4 ..... *170*
4.3 DISCUSSION 174

CHAPTER 5. ISOLATION AND CHARACTERISATION OF MACAQUE CD1-RESTRICTED T CELLS 184

5.1 INTRODUCTION 184
5.2. RESULTS 190
5.2.1 Production of C1R cell lines that express transmembrane ptmCD1 molecules *190*
5.2.2 Production of ptmCD1 molecules for tetramers *193*
5.2.3 Analysis of the soluble ptmCD1 molecules by ELISA *196*

5.2.4 Assessment of trans-species cross-reactivity between ptmCD1 molecules and huCD1-restricted TCRs *198*
5.2.5 Isolation of human and macaque CD1-reactive T cells with ptmCD1 tetramers *206*
5.2.6 Optimisation of tetramer labelling by minimising TCR-independent binding *208*
5.2.7 TCR usage of ptmCD1-tetramer^{+} T cells *215*
5.2.8 Generation of TCR-transduced SKW-3 cell lines expressing selected TCRs from ptmCD1 tetramer^{+} sorted cells *220*
5.2.9 Enumeration of ptmCD1-restricted T cell populations in macaque tissues *223*
5.2.10 Phenotypic characterisation of ptmCD1-restricted T cells in macaque tissues *233*
5.3 DISCUSSION 245

CHAPTER 6. ANALYSIS OF CD1A-RESTRICTED T CELLS IN THE SKIN AND SKIN ALLERGY **254**

6.1 INTRODUCTION 254
6.2 RESULTS 257
6.2.1. Isolation of skin CD1-restricted T cells *257*
6.2.2. Characterisation of skin CD1-restricted T cells *264*
6.2.3. TCR repertoire of skin CD1-restricted T cells *267*
6.2.4 Activation of CD1a-restricted T cells with alkyl benzoate *270*
6.2.5 Production of soluble CD1a in the presence of alkyl benzoate *274*
6.2.6. Recognition of CD1a tetramers loaded with alkyl benzoate by CD1a-restricted T cell lines *276*
6.2.7. Identification of C15 alkyl benzoate loaded in CD1a produced in the presence of C12-15 alkyl benzoate *280*
6.2.8. Isolation of T cells with CD1a-alkyl benzoate tetramers in healthy human blood *286*
6.3 DISCUSSION 288

CHAPTER 7: GENERAL DISCUSSION **295**

APPENDICES 308

BIBLIOGRAPHY 320

Figure and Table Indices

Figures

Figure 1.1. V(D)J recombination gives rise to a diverse repertoire of human αβ-TCRs.
Figure 3.1. Validation of CD1a tetramer loading.
Figure 3.2. Isolation of CD1a-restricted T cell populations directly *ex vivo* from healthy human blood.
Figure 3.3. CD4 and CD8 co-receptor expression by CD1a-restricted T cells in healthy human blood.
Figure 3.4. CD45RO and CD27 expression by CD1a-restricted T cells directly *ex vivo* in healthy human blood.
Figure 3.5. Expression of innate-like T cell markers by CD1a-restricted T cells in healthy human blood.
Figure 3.6. Expression of migratory markers by CD1a-restricted T cells in healthy human blood.
Figure 3.7. Expression of γδ-TCRs by CD1a-restricted T cells in healthy human blood.
Figure 3.8. Transcription factor expression in CD1a-restricted T cells from healthy human blood.
Figure 3.9. Intracellular cytokine staining of CD1a-restricted T cells following stimulation.
Figure 3.10. Isolation of DDM-reactive T cells, type I NKT cells, and conventional $CD4^+$ T cells for single cell RNA sequencing.
Figure 3.11. Transcriptionally distinct populations of "unconventional" T cells.
Figure 3.12. Top differentially expressed genes between the three clusters.
Figure 3.13. Comparison of differentially expressed genes between DDM-reactive T cells and other cell types.
Figure 4.1. MACS-enrichment of CD1a-restricted T cells for TCR sequencing.
Figure 4.2. TCR diversity in CD1a-restricted T cells as determined by multiplex PCR amplification and TCR sequencing.
Figure 4.3. TCR diversity in CD1a-restricted T cells that recognise DDM as determined by multiplex PCR amplification and TCR sequencing.
Figure 4.4. Single cell RNA-sequencing analysis of CD1a-restricted T cells in donor CNR70.
Figure 4.5. TCR diversity in CD1a-restricted T cells as determined by RNA sequencing
Figure 4.6. Labelling of CD1a-$tetramer^+$ T cells with a Vβ3 mAb.
Figure 4.7. Production and validation of CD1a-tetramer binding by CD1a-restricted T cell lines produced.
Figure 4.8. Validation of CD1a-reactivity by CD1a-restricted T cell lines produced.
Figure 4.9. Recognition of multiple lipid antigens by CD1a-restricted TCRs.
Figure 4.10. T cell activation in response to CD1a presenting DDM stereoisomers.
Figure 4.11. Mutational analysis defining key interactions between CD1a-restricted TCRs and CD1a presenting endogenous lipids.
Figure 4.12. Mutational analysis defining key interactions between DDM-specific TCRs and CD1a presenting DDM.
Figure 4.13. Mutational analysis defining key interactions between dual-reactive TCRs and CD1a presenting DDM.

Figure 4.14. Purification of soluble 27a28 CD1a-restricted TCR.
Figure 4.15. Purification of soluble 29a28i CD1a-restricted TCR.
Figure 4.16. Purification of soluble 17a28 CD1a-restricted TCR.
Figure 4.17. Purification of soluble 8-2a2 CD1a-restricted TCR.
Figure 4.18. Endo-H and Thrombin treatment of soluble CD1a for TCR co-complexation.
Figure 4.19. Purification of soluble 17a28 CD1a-restricted TCR co-complexed to CD1a loaded with DDM.
Figure 4.20. Purification of soluble 27a28 CD1a-restricted TCR co-complexed to CD1a loaded with DDM.
Figure 4.21. Purification of soluble 29a28 CD1a-restricted TCR co-complexed to CD1a loaded with DDM.
Figure 4.22. Mass spectrometry analysis of lipids eluted from 27a28 TCR:CD1a-endo co-complex (Run A).
Figure 4.23. Detection of phosphatidylglycerol in analysis of ions at *m/z* 747.3 in 27a28:CD1a-endo, fraction 36.
Figure 4.24. Identification of lipids in analysis of ions at *m/z* 769 and 795 in 27a28:CD1a-endo, fraction 36.
Figure 4.25. Detection of glycosyl diacylglycerol in analysis of ions at *m/z* 795 and 975 in 27a28:CD1a-endo, fraction 36.
Figure 4.26. Detection of DDM in analysis of ions at *m/z* 838 in TCR-CD1a co-complexes.
Figure 4.27. Detection of SM and PC in analysis of ions at *m/z* 847 and 870 in 27a28:CD1a-endo, fraction 37.
Figure 4.28. Detection of PI in analysis of ions at *m/z* 885 in 27a28:CD1a-endo, fraction 39.
Figure 4.29. Assessment of SM, PC and PI eluted from 27a28:CD1a-endo co-complexation fractions.
Figure 4.30. Assessment of bacterial lipids eluted from 27a28:CD1a-endo co-complexation fractions.
Figure 4.31. Nanospray negative mode analysis of lipids eluted from 29a28 TCR:CD1a-endo co-complex.
Figure 4.32. Assessment of lipids eluted from 29a28:CD1a-endo co-complexation fractions.
Figure 4.33. Recognition of PC and SM by CD1a-restricted TCRs.
Figure 5.1. Homology of CD1 molecules between human and macaque species.
Figure 5.2. Transduction efficiency of C1R cell lines following transduction with ptmCD1-encoding plasmids.
Figure 5.3. Macaque CD1 purification using Ni-NTA chromatography followed by gel filtration/size exclusion chromatography.
Figure 5.4. Biotinylation of ptmCD1 followed by gel filtration/size exclusion chromatography purification.
Figure 5.5. ELISA of soluble macaque CD1 proteins.
Figure 5.6. Testing trans-species cross reactivity of macaque CD1a with human CD1a-restricted T cells
Figure 5.7. Testing trans-species cross reactivity of macaque CD1b with human CD1b-restricted T cells.
Figure 5.8. Testing trans-species cross reactivity of macaque CD1c with human CD1c-restricted T cells.

Figure 5.9. Testing trans-species cross reactivity of macaque CD1d with human CD1d-restricted T cells.
Figure 5.10. Isolation of group 1 CD1-restricted T cell populations directly *ex vivo* from healthy human blood using macaque or human CD1 tetramers.
Figure 5.11. Isolation of CD1-restricted T cell populations directly *ex vivo* from healthy macaque blood using ptmCD1 tetramers.
Figure 5.12. Dual tetramer stain of human or macaque blood using ptmCD1 tetramers.
Figure 5.13. Tetramer stain of human or macaque blood using ptmCD1 tetramers with an anti-CD36 blocking antibody.
Figure 5.14. Optimisation of macaque T cell ptmCD1b and ptmCD1c tetramer staining.
Figure 5.15. Preparation of human and macaque CD1-restricted T cells for TCR sequencing.
Figure 5.16. PtmCD1a-restricted TCR variable gene usage.
Figure 5.17. Validation of ptmCD1-restricted TCR sequences.
Figure 5.18. Gating strategy for tetramer staining in healthy macaque tissues.
Figure 5.19. Enumeration of CD1-restricted T cells in healthy macaque peripheral blood and spleen.
Figure 5.20. Enumeration of CD1-restricted T cells in healthy macaque lymph nodes.
Figure 5.21. Enumeration of CD1-restricted T cells in healthy macaque liver and rectum.
Figure 5.22. Enumeration of CD1-restricted T cells in healthy BAL and lung.
Figure 5.23. Macaque splenocytes MACS-enriched with CD1 tetramers.
Figure 5.24. CD4 and CD8 co-receptor expression by CD1-restricted T cells in healthy macaque blood.
Figure 5.25. CD4 and CD8 co-receptor expression by CD1-restricted T cells in healthy juvenile macaque tissues.
Figure 5.26. Phenotypic characterisation of CD1-restricted T cells in healthy macaque blood.
Figure 5.27. Memory phenotypes displayed by CD1-restricted T cells in healthy, juvenile macaque blood.
Figure 5.28. Chemokine receptor expression in CD1-restricted T cells in healthy macaque blood.
Figure 5.29. Phenotypic characterisation of CD1-restricted T cells in healthy juvenile macaque tissues.
Figure 6.1. Labelling of Collagenase P-treated PBMCs with mAbs.
Figure 6.2 Isolation of T cells directly *ex vivo* from skin from abdominoplasty.
Figure 6.3. Dual labelling of CD1-ag and MR1-5-OP-RU tetramers.
Figure 6.4. Frequencies of unconventional T cells isolated directly *ex vivo* from epidermis.
Figure 6.5. Phenotype of CD1-restricted T cells in the epidermis.
Figure 6.6. Isolation of lymphocytes from skin explants cultured *ex vivo*.
Figure 6.7. Identification of potential CD1a allergens in dermatological and cosmetic products.
Figure 6.8. Activation of CD1a-restricted T cells with alkyl benzoate.
Figure 6.9. Production and biotinylation of CD1a in the presence of alkyl benzoate.
Figure 6.10. Labelling of CD1a-restricted T cell lines with alkyl benzoate tetramers.
Figure 6.11. Mass spectrometry analysis of the C12-15 alkyl benzoate standard.

Figure 6.12. Mass spectrometry analysis of lipids loaded in CD1a produced in the presence of alkyl benzoate.
Figure 6.13. Mass spectrometry analysis of alkyl benzoate and CD1a produced in expi293F cells.
Figure 6.14. Isolation of CD1a-restricted T cell populations directly *ex vivo* from healthy human blood.
Figure AIII.I. Comparison of differentially expressed genes between DDM-reactive T cells and type I NKT cells.
Figure AIII.II. Comparison of differentially expressed genes between DDM-reactive T cells and GMM-reactive T cells.

Tables

Table 2.1. General reagents.
Table 2.2. Preparation of buffers.
Table 2.3. Purified CD1 and MR1 antigens.
Table 2.4. Flow cytometry antibodies and viability dyes.
Table 2.5. Primers used in RNA-Sequencing cDNA library preparation.
Table 4.1. Patterns of biases among the CD1a-restricted TCR repertoire.
Table 5.1. Homology of CD1 proteins across different mammalian species.
Table 5.2. Human ptmCD1-restricted TCRs selected for the generation of cell lines.
Table AI.1. Sequences of human and macaque proteins transfected into cell lines.
Table AII.1. Soluble human and macaque protein sequences and expression systems.
Table AIV.1. Human ptmCD1a-restricted TCRs.
Table AIV.2. Human ptmCD1c-restricted, TRAV9-2^{+} TRBV4-1^{+} TCRs.

Chapter 1. Literature Review

1.1 Introduction

The immune system uses a vast multitude of cellular and molecular mechanisms to protect against infection and disease. There are two general arms of the immune system: innate immunity, which acts immediately to broadly prevent pathogen occupation, and adaptive immunity, which is delayed in its response but acts in a highly specific manner against targeted pathogens by recognising antigenic molecules called antigens (Murphy and Weaver, 2020).

Cells and components of the innate immune system are critical for the rapid recognition of pathogens and initiation of inflammatory responses (Pennock et al., 2013). Innate immune cells, such as macrophages, monocytes, neutrophils, natural killer (NK) cells and dendritic cells (DCs) are responsible for initial containment of infectious agents. They use pattern recognition receptors (PRRs) to recognise pathogen-associated molecular patterns (PAMPs), such as bacterial or viral components, or danger-associated molecular patterns (DAMPs) released by damaged cells, such as extracellular DNA, to drive inflammation (Amarante-Mendes et al., 2018). Engagement of PRRs on innate immune cells activate antimicrobial and pro-inflammatory responses to eliminate, or at least contain, infections. Innate immune cells also create an environment that informs and directs the proliferation and differentiation of adaptive immune cells: B and T lymphocytes (Pennock et al., 2013).

T lymphocytes (herein referred to as T cells) are central to adaptive immune responses. They utilise unique, specialised T cell receptors (TCRs) to survey the body for pathogens or abnormalities in the form of antigens (Murphy and Weaver, 2020). TCRs are highly specific to particular antigens and upon recognition of their cognate antigen, they adopt one of two broad functions; “helper” T (Th) cells coordinate the response of other immune cells (both adaptive and innate) and “cytotoxic” T cells kill infected host cells (or tumour cells) to contain infection (Murphy and Weaver, 2020).

Antigen inexperienced, or “naive”, T cells emerge from the thymus and circulate through the blood and secondary lymphoid tissues (Pennock et al., 2013). Their activation

involves coordinated interactions between TCRs and antigen-presenting molecules on the surface of antigen presenting cells (APCs). APCs constantly capture antigens, and if activated by signals such as PAMPs and DAMPs, increase their presentation capacity and migrate to lymph nodes, where naive T cells are housed. Following recognition of their cognate antigen, T cells are activated to proliferate and acquire potent effector functions to control or eliminate pathogenic disease (Pennock et al., 2013). Activated T cells can also differentiate into memory T cells, enabling antigen-experienced T cells to remain in circulation post-infection and protect against previously encountered pathogens by eliciting a more rapid and robust response in the case of subsequent infection (Farber et al., 2014).

TCRs are diverse in nature, allowing T cells to recognise an expansive array of unique antigenic molecules and thus allowing for highly specific responses to the large variety of pathogens we encounter. A TCR's unique specificity for a given antigen is determined by its TCR sequence. During development in the thymus, T cells undergo somatic gene recombination, a process directed by the lymphoid-specific recombination-activating gene (RAG) and DNA repair proteins (Bassing et al., 2002, Oettinger et al., 1990, Schatz et al., 1989). TCRs are typically formed as heterodimers of either α- and β-chains, or γ- and δ-chains, however some δ- and β-TCR chain heterodimers have also been observed (Geisler et al., 1988, Hochstenbach and Brenner, 1989, Saito et al., 1988, Pellicci and Uldrich, 2018).

The somatic recombination of TCR genes occurs during thymic development. RAG genes direct the assembly of variable (V), diverse (D), joining (J), and constant (C) genes by creating double-stranded breaks in the DNA, which is followed by non-homologous end joining to produce a functional TCR chain (Krangel, 2009, Roth, 2014). *Tcrd*, *Tcrg,* and inital *Tcrb* recombination occur early in T cell development at the $CD4^{-}CD8^{-}$ double negative (DN) 2 and DN3 stages in the same manner (Capone et al., 1998). Successful recombination of *Tcrd* and *Tcrg* promotes the assembly of a γδ-TCR, whereas successful recombination of *Tcrb* drives assembly of an αβ-TCR (Capone et al., 1998, Krangel, 2009, Livak et al., 1999).

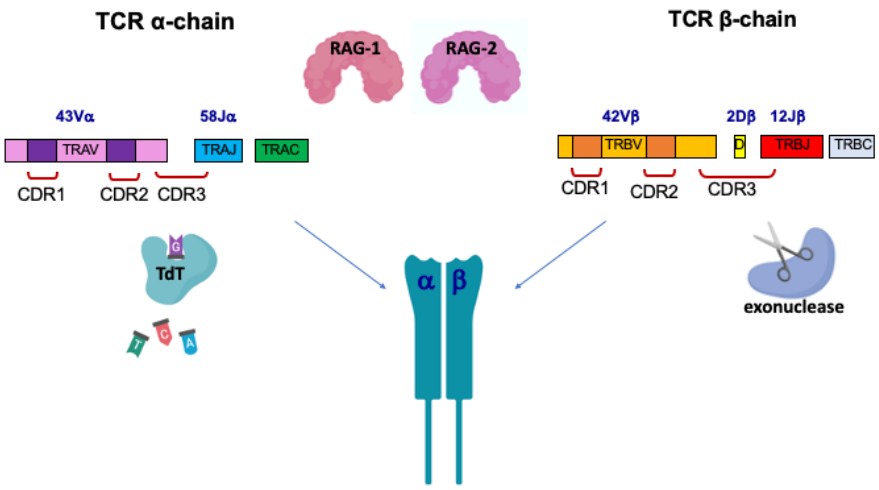

Fig.1.1. V(D)J recombination gives rise to a diverse repertoire of human αβ-TCRs. The process is directed by the recombination activating genes (RAG-1 and RAG-2), which create double-stranded breaks in the DNA to select for a given *TRAV, TRAJ, TRBV, TRBD and TRBJ* gene. Additional diversity is introduced at the junction between genes by terminal deoxynucleotidyl transferase (TdT), which adds random non-templated (N) nucleotides, and the removal of germline bases by exonucleases.

The "mixing and matching" of TCR component genes gives rise to the diversity observed in the human TCR repertoire: a TCR α-chain composed of one of 43 V (*TRAV*) and 58 J (*TRAJ*) genes along with a constant gene, is paired with a β-chain containing one of 42 V (*TRBV*), one of two D (*TRBD*), one of 12 J (*TRBJ*) genes and a constant region (Lefranc et al., 1999, Lefranc et al., 2009, Turner et al., 2006) (*Fig 1.1)*. In addition to V(D)J recombination, the imprecise nature of the non-homologous end joining process introduces further diversity (Rock et al., 1994). Terminal deoxynucleotidyl transferase (TdT), a template-independent DNA polymerase, adds random non-templated (N) nucleotides, and exonucleases may remove germline bases (Cabaniols et al., 2001). These processing events give rise to hypervariable antigen-binding regions, called complementarity determining regions (CDRs), of which there are three per TCR chain (Chothia et al., 1988). The resulting recombined TCR α- and β-chains are randomly paired to give rise to more than 10^{15} potential TCR gene arrangements (Davis and Bjorkman, 1988, Davis, 1990). Following positive and negative selection of T cells during development, based on their ability to recognise MHC but without being highly self-reactive respectively, there are only approximately 3 x 10^{11} naive T cells in circulation with 10^{7} unique TCR clones (Arstila et al., 1999, Jenkins et al., 2010).

One caveat of extensive TCR diversity is that each individual TCR clone exists at a low frequency in the total T cell pool, which limits the magnitude and speed of the initial immune response when challenged with a particular antigen. In contrast to rapidly responding innate immune cells, the proliferation and expansion of T cells in preparation to mount a response to any specific antigen takes several days after the initial recognition of antigen (Bradley et al., 1991, Swain et al., 1996). The identification of "unconventional" T cells with innate-like properties challenges the idea that all T cells have a delayed response and highlights how some T cell subsets can act as a link between innate and adaptive immune responses.

1.2 MHC and related molecules

1.2.1 MHC molecules and peptide antigens

Conventional T cells recognise specific peptide antigens in the context of major histocompatibility complex (MHC) molecules. MHC class I (MHC-I) and class II (MHC-II) molecules are similar in function, presenting peptide antigens at the cell surface of

APCs to $CD8^+$ and $CD4^+$ T cells respectively. MHC-I is ubiquitous on all nucleated cells, while the expression of MHC-II molecules is mostly restricted to professional APCs such as B cells and DCs (Hewitt, 2003). Peptides presented by MHC molecules are sourced from different locations: intracellular for MHC-I and extracellular for MHC-II (Neefjes et al., 2011). There are exceptions with cross-presentation however, whereby exogenous antigens are presented by MHC-I molecules (Amigorena and Savina, 2010), and MHC-II molecules can capture endogenous peptides when the respective proteins are degraded through autophagy (Crotzer and Blum, 2010).

MHC-I molecules are comprised of a transmembrane polymorphic heavy chain, organised into three extracellular domains (α1, α2 and α3) that associates with β_2-microglobulin (β_2m) (York and Rock, 1996). The α1 and α2 domains form an antigen binding cleft that binds a peptide fragment typically between 8-10 amino acids in length (Adams and Luoma, 2013, York and Rock, 1996). Upon successful antigen capture, the peptide-loaded MHC-I ternary complex (pMHC) is transported to the cell surface where it can present antigens to T cells (Williams et al., 2002), and can subsequently be internalised from the membrane for recycling (Neefjes et al., 1992). This cycle of antigen capture, presentation and recycling occurs constitutively, enabling MHC-I-restricted T cells to constantly survey cells for the presence of either self- or pathogen-derived peptide antigens.

MHC-II molecules comprise of transmembrane α- and β-chains (Brown et al., 1993) and capture peptides derived from proteins degraded in the endosomal pathway (Germain, 1994, Lotteau et al., 1990). The peptide-binding cleft of MHC-II is more open compared to that of MHC-I, such that the length of bound peptides is not as constrained; peptides loaded into MHC-II molecules are typically 13-25 amino long (Chicz et al., 1992).

MHC molecules are polymorphic and the biology of their various alleles differ substantially between individuals such that they can have different consequences with regards to the relevant immune responses (Trowsdale, 2011). Notably, many MHC-II alleles are strong genetic markers for autoimmune diseases, possibly due to the repertoire of peptide antigens they capture and present to T cells (Fernando et al., 2008). For example, evidence suggests that HLA-DQ allelic variation is a major type 1 diabetes predisposing locus (Onengut-Gumuscu and Concannon, 2002, Thorsby and Ronningen,

1993). MHC allelic variation therefore has consequences in disease susceptibility, vaccine design and immunotherapy, and means that T cell therapies that target specific MHC alleles or peptide antigens need to be personalised.

1.2.2 MHC-related proteins

In mammals, a number of antigen presentation molecules exist that arose from genomic duplications and subsequent mutations of the classical MHC-I genes (Yu and Milstein, 1989), regarded as nonclassical MHC-I (sometimes referred to as MHC-Ib, although this terminology is contentious as many of these genes sit outside the MHC gene locus). These MHC-related molecules resemble MHC-I in sequence and structural homology but, in general, are non-polymorphic, present different types of antigens, and are typically only expressed at the cell surface under specific conditions or by certain cell types (Balk et al., 1989, Martin et al., 1986). Two such MHC-like molecules are MHC-related protein 1 (MR1) and the CD1 family. These structurally resemble MHC-I molecules in that they are comprised of transmembrane heavy chains consisting of α1, α2 and α3 domains that associate with β_2m (Moody et al., 2005, Krovi and Gapin, 2016, Miley et al., 2003).

MHC and TCR genes evolved simultaneously and are present in all extant jawed vertebrates, including fish, while the CD1 and MR1 genes are absent (Dascher, 2007). Marsupials and mammals typically encode a single functional MR1 gene, which demonstrates the highest conservation among species of all MHC-Ib molecules (Reinink and Van Rhijn, 2016). The human genome encodes one MR1 protein and five different CD1 proteins, called CD1a through to CD1e, all of which lie outside the MHC locus. In humans, the CD1 and MR1 genes are located on chromosome 1, while the MHC locus lies on chromosome 6 (Riegert et al., 1998, Albertson et al., 1988, Reinink and Van Rhijn, 2016, Yamaguchi et al., 1997). In fact, chickens are the only animal in which the CD1 and MHC loci have been found to be linked (Miller et al., 2005, Salomonsen et al., 2005), supporting a model of CD1 gene evolution arising from gene duplication while still linked to the MHC locus.

Genomic sequencing has revealed recognisable CD1 genes from several reptile species (Yang et al., 2015) and marsupials (a single gene in the bandicoot (Baker and Miller,

2007) and thylacine (Cheng and Belov, 2014)), however none of the CD1 sequences from marsupials, chickens, and reptiles are equivalent to any of the five isotypes in placental mammals. Given their evolutionary distribution, CD1 genes most likely arose in a common ancestor of placental mammals from a primordial form of CD1 (Reinink and Van Rhijn, 2016). Subsequent gene duplications, deletions, and inactivations have shaped the composition of the CD1 gene family, resulting in CD1 molecules with similar features across species but with key differences particular to each species that may have arisen due to selection pressure caused by pathogen exposure (Dascher and Brenner, 2003). Evolutionary conservation and similarities between CD1 in different species are important to consider when studying MHC-related proteins in animal models.

1.2.3 The CD1 family

The CD1 protein family is encoded by five monomorphic genes to produce five CD1 isoforms (Martin et al., 1986). The five CD1 proteins are divided into groups based on the homology of their nucleotide and amino acid sequences: Group 1 consists of CD1a, CD1b and CD1c, CD1d belongs to group 2 and CD1e to group 3 (Calabi et al., 1989, Porcelli and Modlin, 1999). The CD1 isoforms differ in their antigen processing and presentation, tissue distribution, intracellular trafficking and structure (Zajonc and Wilson, 2007). Importantly, these differences endow CD1 molecules with the ability to present a broad range of lipids, indicating that T cells restricted to CD1 (CD1-restricted T cells) may be important for a range of human immune responses (Birkinshaw et al., 2015, Van Rhijn et al., 2006, Kasmar et al., 2009). Notably, CD1e remains localised within Golgi compartments and lysosomes, and is not directly involved in antigen presentation to T cells, rather, it is involved in intracellular lipid transfer and loading of endogenous lipids into CD1 (Angenieux et al., 2005, Angenieux et al., 2000, de la Salle et al., 2005). Further discussion will therefore only focus on the four CD1 isoforms that present antigens on the cell surface.

In humans, MHC-I is ubiquitously expressed on all nucleated cells, while CD1 molecule expression is more limited. Group 1 CD1 expression is limited to professional APCs and is mostly induced in a stimulus-dependent manner on various subsets of human DCs, monocytes, and thymocytes (Pena-Cruz et al., 2003, Van Rhijn et al., 2013b). CD1a is

highly abundant on Langerhans cells (Dougan et al., 2007, Fithian et al., 1981, Mizumoto and Takashima, 2004, Caux et al., 1992). It is also expressed by bronchial dendritic cells (Tazi et al., 1993b), and its expression can be modified by stimuli from pathogens, tumours, host immune responses (e.g. cytokines), and the environment (e.g. smoking) (Coventry and Heinzel, 2004, Gogolak et al., 2007, Mollah et al., 2003, Pintarelli et al., 2019). In contrast, CD1d has a wider distribution and is constitutively expressed by cortical thymocytes, B cells, macrophages, and DCs (Dougan et al., 2007, Somnay-Wadgaonkar et al., 1999). It is also expressed by non-haematopoietic-derived cells including hepatocytes, adipocytes, intestinal epithelial cells and skin cells among other cell types (Dougan et al., 2007, Huh et al., 2013).

In contrast to polymorphic classical MHC molecules, CD1 molecules do not display allelic variation that affects antigen presentation (albeit single amino-acid polymorphisms have been identified for CD1a and CD1d that are not located around the antigen-binding cleft) (Han et al., 1999, Oteo et al., 2001). This suggests that, unlike the presentation of peptide antigens by MHC molecules to conventional T cells, the presentation of lipid antigens by CD1 molecules is more universal within the population. Although, single nucleotide polymorphisms (SNPs) in the non-coding and regulatory regions of the human *CD1A* gene result in little to no CD1a expression and a correlated increased susceptibility to tuberculosis (TB), demonstrating both variability within the population and the importance of CD1a (Seshadri et al., 2014).

1.2.4 CD1 molecule structure

MHC-I molecules provide a constrained, anchored binding-cleft for the presentation of short peptides, whereas CD1 molecules provide a groove of a greater overall volume, containing hydrophobic channels that are suitable for accommodating long lipid acyl chains (Zeng et al., 1997, Gadola et al., 2002). In contrast to the exposed nature of peptide antigens in MHC-I and MHC-II for TCR contact, most CD1 ligands are occluded by the CD1 protein itself, buried within the hydrophobic pockets, and only protrude through a narrow opening for TCR interactions (Batuwangala et al., 2004, Gadola et al., 2002, Zajonc et al., 2003). CD1 molecules are formed by A'- and F'-pockets or portals, with

the shape and connectivity between portals differing between each isoform (Moody et al., 2005, Zeng et al., 1997).

Among the CD1 molecules, CD1a has the smallest antigen-binding cleft of approximately 1300Å^3, comprising of two distinct A'- and F'-pockets (Zajonc et al., 2003). The A'-pocket is shaped such that it restricts the length of alkyl chains of lipid antigens it can accommodate to 18-23 carbons (Zajonc et al., 2005b). The A'-roof, however, is versatile, and while small lipids remain buried within the cleft, large head groups can protrude and interact directly with TCRs (Zajonc et al., 2005b). CD1b has the largest antigen-binding cleft, which can accommodate a total of 80 carbons with a total volume of 2200Å^3 (Gadola et al., 2002). Unlike CD1a, it contains multiple interconnected portals to form a hydrophobic, tunnel-like network (Gadola et al., 2002). CD1c and CD1d are more moderate in size (1780 and 1650 Å^3 respectively) (Ly and Moody, 2014, Scharf et al., 2010).

CD1a, CD1c, and CD1d typically bind self-lipids with a 1:1 stoichiometry (Ly and Moody, 2014). However, the crystal structures of some CD1 molecules (namely CD1b, CD1c, and CD1d) have revealed small hydrocarbon chains that act as spacer lipids within the A'- or F'-pockets to provide stability within the groove in the absence of larger lipid antigens (Ly and Moody, 2014, Gadola et al., 2002, Garcia-Alles et al., 2011, Huang et al., 2011, Garcia-Alles et al., 2006, Scharf et al., 2010, Zajonc et al., 2005a). The necessity of spacer lipids is determined by the number of carbons in the acyl chains of lipid antigens. Naturally occurring spacer lipids can "prop up" smaller antigens, thereby enhancing recognition (Huang et al., 2011), but are likely displaced when the CD1 molecules encounter large exogenous lipids (Ly and Moody, 2014).

1.2.5 Localisation of CD1 molecules

The spectra of lipid antigens presented by each CD1 isoform is dependent on where it is localised within the cell. CD1 molecules capture endogenous self-lipids in the endoplasmic reticulum (ER) where they are folded, and then are trafficked along the secretory pathway to reach the cell surface (Moody and Porcelli, 2003). CD1b, CD1c, and CD1d may associate with spacer lipid molecules during assembly in the ER, which

help to stabilise the protein molecules and prevent the binding of self-lipids with long acyl chains, prior to reaching the cell surface (De Libero and Mori, 2007, Ly and Moody, 2014, Garcia-Alles et al., 2006, Zajonc et al., 2005a).

CD1a predominantly remains at the cell surface, where it can capture exogenous lipids, although studies suggest that this is not the main site of loading (Sugita et al., 1999). CD1b, CD1c, and CD1d, on the other hand, enter the recycling pathway by binding adaptor protein (AP) complexes that mediate endocytosis via their cytoplasmic tail tyrosine residues (Barral and Brenner, 2007, Mizumoto and Takashima, 2004). In the endocytic pathway, they encounter increasingly acidic environments, which are optimal for lipid-loading as the CD1 molecules become partially denatured, before returning to the cell surface for presentation: CD1c and CD1d bind AP-2 and capture antigens in early and late endosomes, while CD1b binds both AP-2 and AP-3 to enter late endosomes and lysosomes (Barral and Brenner, 2007, Ernst et al., 1998, Shamshiev et al., 1999). As CD1a lacks an endosomal localisation motif, it is internalised through an AP-independent pathway, similar to MHC-I (Barral et al., 2008), but it can also capture exogenous lipids in the early endosomal compartment (Agea et al., 2005). The varying intracellular localisation of CD1 isoforms allows for presentation of a wide breadth of endogenous and exogenous lipids captured in different cellular compartments.

1.2.6 Unconventional T cells

While most T cell studies have focused on T cell recognition of peptides presented by MHC, "unconventional" T cells are gaining increasing interest. This group comprises various subsets of T cells that are defined by TCR usage, antigen recognition, and restriction element (i.e. non-peptide antigens presented by MHC-Ib molecules). Many unconventional T cell subsets studied to date are present in blood and some non-lymphoid tissues at higher frequencies than antigen-specific MHC-restricted T cells (Godfrey et al., 2015, Legoux et al., 2017, Kawano et al., 1997, Kobayashi et al., 2012, Macho-Fernandez et al., 2014, Morita et al., 1995). Subsets of unconventional T cell include CD1-restricted T cells that recognise lipid antigens, the most well-known of which are natural killer T (NKT) cells, mucosal-associated invariant T (MAIT) cells that recognise vitamin B metabolites, and γδ T cells that recognise phosphoantigens (pAg), lipids and other

antigens (Godfrey et al., 2015). Unlike MHC-restricted T cells, these cells recognise evolutionarily conserved antigens, generally exhibit limited TCR diversity and rapidly acquire effector functions without requiring priming upon activation (Godfrey et al., 2015, Van Rhijn and Moody, 2015). These characteristics enable them to respond rapidly to stimuli at the site of disease and broaden the scope of cellular immunity by responding to non-peptide antigens.

MR1 and MAIT cells

Like CD1, MR1 is an MHC-I-like molecule identified with high sequence homology (40-50%) to MHC-I (Hashimoto et al., 1995). While most cells can express MR1, surface expression of MR1 is tightly regulated and typically low (Huang et al., 2008, Riegert et al., 1998). In comparison to CD1 family members, the solvent-exposed antigen binding cleft of MR1 more closely resembles that of MHC-I, however, it is composed of a mixture of charged, hydrophobic and bulky residues that render it unsuitable for accommodating peptide antigens (Kjer-Nielsen et al., 2012). Instead, MR1 presents vitamin B metabolites to an evolutionarily conserved unconventional T cell population known as mucosal-associated invariant (MAIT) cells (Tilloy et al., 1999, Huang et al., 2009, Kjer-Nielsen et al., 2012). Several stimulatory and inhibitory MR1 ligands have been identified, including drug-like molecules, and folate and riboflavin derivatives (Kjer-Nielsen et al., 2012, Keller et al., 2017, Corbett et al., 2014). The most agonistic ligands known to date are 5-(2-oxopropylideneamino)-6-D-ribitylaminouracil (5-OP-RU) and 5-(2-oxoethylideneamino)-6-D-ribitylaminouracil (5-OE-RU), formed from 5-amino-6-D-ribitylaminouracil (5-A-RU) – a ligand precursor and intermediate metabolite in riboflavin biosynthesis (Corbett et al., 2014).

MAIT cells are innate-like T cells that play a role at the interface of the innate and adaptive immune responses. They become activated via TCR recognition of MR1-ligand complexes, or they can bypass TCR-dependent activation by responding to inflammatory cues from IL-12 and IL-18 signalling (Jo et al., 2014, Treiner et al., 2003, Ussher et al., 2014, Godfrey et al., 2019). These two pathways of activation allow MAIT cells to respond to riboflavin-producing bacteria and yeast, as well as microbes that do not produce MR1 ligands (i.e. viruses or non-riboflavin-producing bacteria) (Provine and Klenerman, 2020). Early studies of MAIT cells demonstrated that they are mostly localised to mucosal sites, hence their name; however, they have since been commonly

found throughout the body, including in the peripheral blood, where they exist at a high precursor frequency (up to 10% all T cells) (Godfrey et al., 2010, Treiner et al., 2005, Corbett et al., 2014). MAIT cells typically express a semi-invariant TCR in humans, which consists of an invariant α-chain composed of TRAV1-2 with TRAJ33, TRAJ20 or TRAJ12 gene segments paired with a less restricted array of β-chains including TRBV6-1, TRBV6-4 and TRBV20 (Tilloy et al., 1999, Reantragoon et al., 2013). MAIT cells are thus an interesting population of unconventional T cells that are innate-like in their function and display a semi-invariant TCR, that can be compared to lipid-reactive T cells.

1.3 Presentation of antigens to T cells by CD1

1.3.1 CD1 Lipid antigens

Lipids play a critical role in immunity, in part by acting as antigens for CD1-restricted T cells. Lipid-reactive T cells recognise a large array of both foreign lipid antigens and self-lipids (Godfrey et al., 2015).

CD1d presents a number of glycosphingolipids (GSLs) to NKT cells, the most well-studied and agonistic of which is α-Galactosylceramide (α-GalCer). Type I NKT cells are classified for their expression of a semi-invariant TCR that endows them with the ability to recognise α-GalCer (Kawano et al., 1997). It was originally isolated from the marine sponge, *Agelas mauritianus*, but more recently and relevantly, a closely related analogue was discovered in *Bacteroides,* a genus of bacteria that comprises greater than 50% of human gut microbiota (Wieland Brown et al., 2013). GSLs (specifically α-glucuronyl- and α-galacturonylceramides) in the cell wall of the ubiquitous *Sphingomonas* bacterial species are closely related to α-GalCer and are also strong agonists for type I NKT cells (Kawasaki et al., 1994, Wu et al., 2005, Kawahara et al., 2000). In addition, a number of GSLs and diacylglycerols (DAGs) isolated from microbial pathogens (e.g. *Streptococcus pneumoniae*, *Aspergillus fumigatus* and *Borrelia burgdorferi*) also activate type I NKT cells (Van Kaer et al., 2015a).

Type I NKT cells typically interact with GSLs that contain an α-anomeric linkage between the carbohydrate moiety and lipid tail (Kawano et al., 1997). Because

mammalian cells were thought to only produce β-anomeric GSLs, endogenous type I NKT cell ligands remained enigmatic for years (Ilan, 2009, Van Kaer and Joyce, 2010). Some β-linked monoglycosylceramides, such as β-glucosylceramides (β-GluCer) and isoglobotrihexosylceramide (iGb3), a β-anomeric lysosomal glycosphingolipid, appeared to be stimulatory (Ortaldo et al., 2004, Brennan et al., 2011, Parekh et al., 2004). iGb3 especially was proposed as a candidate ligand important for NKT development, albeit subsequent studies have indicated that it may not be as critical as once thought (Zhou et al., 2004c, Zhou et al., 2004a, Pellicci et al., 2020). The controversy around lipids recognised by type I NKT cells may stem from contamination issues, as a study found that commercial and in-house β-GluCer was not stimulatory itself, but was in fact contaminated with α-linked GluCer agonists (Kain et al., 2014). A number of mammalian α-anomeric GSLs have since been identified and can activate type I NKT cells, and contamination of α- and β-linked glycolipids are an important consideration for future studies of lipid-reactive T cells (Brennan et al., 2014, Kain et al., 2014).

Another subset of CD1d-restricted cells called type II NKT cells, at least some of which appear to recognise β-anomeric glycolipids, exhibit a more diverse TCR repertoire (Dhodapkar and Kumar, 2017). Type II NKT cells do not recognise α-GalCer, but instead a large proportion of these cells are autoreactive to self-lipids such as sulfatide, phospholipids, and cell membrane lysophospholipids such as LPC (Rossjohn et al., 2012, Dhodapkar and Kumar, 2017). They can also recognise microbial ligands, including glycolipids (phosphatidylglycerol (PG), diphosphatidylglycerol (DPG), and PI) from *Mycobacterium tuberculosis* (Mtb) or *Corynebacterium glutamicum*, α-glucuronosyl diacylglyceride (α-GlcA-DAG) from *Mycobacterium smegmatis*, and PG from *Listeria monocytogenes* (Tatituri et al., 2013, Wolf et al., 2015, Burugupalli et al., 2020). Together, both NKT cell subsets respond to a wide breadth of microbial and self-lipid antigens.

Providing diversity in the scope of lipids presented by T cells, group 1 CD1 molecules capture and present different types of lipids. CD1a presents a variety of self- and non-self-lipids, preferentially loading lipids with acyl chain lengths between C_{18}-C_{23} (Agea et al., 2005, de Jong et al., 2014, Hunger et al., 2004, Moody et al., 2004, Pena-Cruz et al., 2003, Zajonc et al., 2003). Self-lipids, such as gangliosides and sulfatides, are recognised by CD1a-autoreactive T cells (de Jong et al., 2010, de Lalla et al., 2011), and these are

thought to be either permissive or non-permissive to TCR binding depending on their headgroup structure and size (Birkinshaw et al., 2015, de Jong et al., 2014). Squalene and wax esters, present in epidermis and sebum, are headless agonistic lipids presented by CD1a, while membrane lipids in the skin with polar headgroups act as antagonists (de Jong et al., 2014). The best studied CD1a antigen is dideoxymycobactin (DDM), an iron-chelating compound derived from Mtb (Moody et al., 2004). DDM is synthesised as an intermediate in mycobactin production during intracellular infection and contributes to CD1a-DDM-specific T cell activation (Moody et al., 2004).

CD1b and CD1c also present various lipid components of mycobacterial cell walls. These lipids are typically protease-resistant and are usually uncleaved in APCs, and are therefore larger antigens (Beckman et al., 1996, Cheng et al., 2006). Their acyl lipid chains are buried deep within the CD1 antigen-binding grooves and the headgroups of these antigens protrude to be presented to T cells. The larger antigen-binding groove of CD1b makes it suited to present large lipid antigens, such as those from mycobacteria (Gadola et al., 2002). Mycobacterial mycolates that act as CD1b antigens, such as glucose monomycolate (GMM), glycerol monomycolate, and mycolic acid, have a longer carbon chain length (C70-80) compared to other mycobacterial membrane lipids (Batuwangala et al., 2004, Beckman et al., 1994, Garcia-Alles et al., 2011, Moody et al., 1997, Layre et al., 2009, Guiard et al., 2009). CD1b is loaded with self-lipids during folding in the ER, and these pre-bound self-lipids are unloaded in the acidic environment of lysosomes in favour of exogenous lipid antigens (Relloso et al., 2008). CD1b-autoreactive T cell populations are rarely observed (de Lalla et al., 2011), possibly given that CD1b is more geared towards presenting larger, non-self-lipids instead. On the other hand, CD1c present self-lipids such as methyl-lysophosphatidic acids (mLPAs), which accumulate in leukemia (Lepore et al., 2014) in addition to mycoketides from pathogenic mycobacteria (Matsunaga et al., 2004, Moody et al., 2000). The contribution of lipid-reactive T cells in immunity against mycobacteria will be further discussed later in this chapter.

The diverse array of lipid antigens presented by CD1 molecules allows lipid-reactive T cells to mediate a wide range of immunological outcomes, particularly in infection, cancer, autoimmunity, and other diseases. For this reason, the manipulation of lipid-reactive T cells with specific lipid antigens is attractive as a potential immunotherapy strategy.

1.3.2 Recognition of CD1 antigens

Accumulating evidence suggests multiple mechanisms that CD1-restricted TCRs use to interact with CD1-lipid complexes. Three models of antigen recognition have been proposed by Branch Moody and colleagues (Moody and Suliman, 2017):

- *Head group discrimination*: the recognition of lipid antigen head groups involves high specificity for both the lipid and CD1 molecule, such as in the case of CD1b-GMM and CD1d-α-GalCer recognition (Borg et al., 2007, Gras et al., 2016). In both these cases, the head group protrudes above A'-roof of the CD1 molecule, such that the CDR loops of the TCR can interact with both the lipid head group and CD1. This model would likely suit the recognition of CD1a-DDM, however the molecular interactions between CD1a-DDM and a DDM-specific TCR have yet to be determined using structural studies of a ternary complex.
- *Absence of interference*: When the lipid antigen is buried within the hydrophobic antigen-binding cleft without a head group protruding above the A'-roof, TCRs are able to interact directly with the CD1 molecule. This is seen in the case of CD1a-autoreactive TCR clone, BK6, which can only recognise small, headless lipid antigens while large headgroups, such as that of sphingomyelin, protrude and block TCR contact with CD1a and the epitope (Birkinshaw et al., 2015).
- *CD1 remodelling*: the capture of certain lipid antigens induces a conformational change in the CD1 molecules, including remodelling of the TCR binding epitopes, and it is these changes that are recognised by TCRs. Examples include the structural reorganisation exhibited by CD1c when it captures rigid C12-18 cholesteryl esters (Mansour et al., 2016). Similar to the absence of interference model, TCR interaction is primarily with the CD1 molecule itself instead of with the lipid antigen.

These different mechanisms of lipid antigen recognition could explain the large number of both self- and non-self-lipid antigens that are known to activate CD1a-restricted T cells and how autoreactivity may occur. Studies of the interaction between the CD1a-restricted TCR, BK6, and its cognate antigens (i.e., endogenous lipids such as LPC) have revealed that CDRs primarily interact with the CD1a surface, specifically over the A'-roof where the bound ligand is not exposed (Zajonc et al., 2005b, Birkinshaw et al., 2015). Small lipids are only exposed in the F-pocket, towards the C-terminal end of the α1 helix, while larger lipids have exposed, lipophilic head groups that can disrupt the A'-roof (Zajonc et

al., 2005b, Zajonc et al., 2003).

Few studies have assessed the structural and molecular interactions between CD1a-restricted TCRs and antigens, and only one as a ternary complex with TCR:CD1a-lipid. Furthermore, this particular study used an autoreactive TCR that bound CD1a with the absence of interference model, which would not suit DDM and other potent antigens (Birkinshaw et al., 2015). There is therefore a great need to further assess whether different CD1a-restricted TCRs adopt similar or distinct docking modes to interact with CD1a-lipid complexes. CD1a-restricted T cells may interact with foreign lipids that tend to have larger head groups in a different manner, which could be important in the context of infection and allergy.

1.3.3 CD1-restricted TCR diversity

Most studies of CD1-restricted T cells to date have focused on semi-invariant, type I NKT cells. In humans, their TCR contains an invariant Vα24-Jα18 TCR α-chain and a limited set of Vβ11^{+} TCR-β chains, only differing in the CDR3β loop (Dellabona et al., 1994, Lantz and Bendelac, 1994, Porcelli et al., 1993). The invariant TCR α-chain is, in part, one of the reasons that type I NKT cells have been more widely studied than other CD1-restricted T cells; monoclonal antibodies (mAbs) can be used to target Vα24, Jα18, Vβ11, or the invariant CDR3α loop (Exley et al., 2008, Gansuvd et al., 2003, Montoya et al., 2007). It is important to note that some human α-GalCer-reactive NKT cells do not express the semi-invariant TCR, including novel populations that express γδ-TCRs, hybrid δ/αβ-TCRs, and αβ-TCRs with different chain pairings (Uldrich et al., 2013, Le Nours et al., 2016, Pellicci et al., 2014).

The TCR repertoire of group 1 CD1-restricted T cells has not been explored as thoroughly. Evidence so far suggests that, with the exception of type I NKT cells, there is heterogeneity in the V, D, J gene usage of most lipid-reactive αβ-TCRs (Vincent et al., 2005, Cohen et al., 2009, de Jong et al., 2010, de Lalla et al., 2011, Grant et al., 1999). In addition, some γδ-TCRs can recognise CD1-lipid that predominantly express Vδ1 (Uldrich et al., 2013, Spada et al., 2000, Faure et al., 1990, Bai et al., 2012, Zajonc and Girardi, 2014). TCR diversity among group 1 CD1-reactive T cells may permit the

recognition of a vast range of lipid antigens presented in the context of different CD1 isoforms, however, patterns of TCR bias are even emerging within populations of T cells that recognise specific lipid antigens.

For example, two classes of CD1b-restricted T cells that exhibit specificity towards a mycobacterial lipid (GMM), broadly termed LDN5-like T cells and germline-encoded mycolyl lipid-reactive (GEM) T cells, have been found to express biased TCRs with TRAV17 and TRBV4-1, or a semi-invariant TCR α-chain comprised of TRAV1-2 and TRAJ9 respectively (Van Rhijn et al., 2014, Van Rhijn et al., 2013a). In addition, mycobacterial phosphomycoketide (PM)-specific CD1c-restricted αβ-and γδ-TCRs incorporate TRBV7-9 with diverse CDR3 loop sequences, or Vδ1 respectively (Roy et al., 2014, Roy et al., 2016). To date, studies of CD1a-restricted T cells have been limited to few T cell clones and appear to be diverse in humans with no categories existing based on TCR repertoire or antigen recognition. An analysis of skin-infiltrating T cells during CD1a-mediated contact dermatitis in CD1a-transgenic mice exhibited a substantial increase in T cells that expressed Vβ2 (*Trbv1*) or Vβ4 (*Trbv2*) (Kim et al., 2016). These patterns and biases of particular variable TCR genes for antigen-specific CD1-restricted T cells opens up the possibility of biases among CD1a-restricted TCRs that remain unknown, especially within antigen-specific groups.

1.4 Role of CD1-restricted T cells in health and disease

There is a wealth of data on the role of NKT cells in the immune system, mostly focusing on type I NKT cells. Studies of Jα18$^{-/-}$ and CD1d$^{-/-}$ mouse models, which lack type I NKT cells and all NKT cells respectively, have implicated NKT cells in a broad range of immune responses and diseases (Bae et al., 2019, van Puijvelde and Kuiper, 2017, Wu and Van Kaer, 2009). Building on these, human studies have revealed fluctuating patterns in NKT cell frequency in the context of disease (Nair and Dhodapkar, 2017, Simoni et al., 2013). The development of CD1d-α-GalCer tetramers propelled the ability to study type I NKT cells in mice and humans (Benlagha et al., 2000, Matsuda et al., 2000), providing a deeper understanding of their role in the immune system, especially in disease. Studies of group 1 CD1-restricted T cells in disease have progressed to a lesser

extent due to their absence in mice, however they are increasingly being brought into the spotlight in both homeostasis and disease pathology.

1.4.1 CD1-restricted T cell frequency

The use of tetramers and cellular assays have enabled the isolation of CD1-restricted T cells to determine their frequency in blood and other tissues. Type I NKT cells have been isolated at frequencies of up to 2.34% of total blood T cells using CD1d tetramers loaded with α-GalCer or 0.776% with a monoclonal antibody targeting the invariable CDR3β loop (Bienemann et al., 2011, Gumperz et al., 2002). Given the lack of distinct TCR sequence or one uniform and high affinity/highly stimulatory antigen (like α-GalCer) for the other CD1-restricted T cell subsets, it has been more difficult to determine their frequencies.

An *ex vivo* cell-based assay determined that self-reactive CD1-restricted T cells represent between 1/300 to 1/10 of all circulating lymphocytes (de Lalla et al., 2011). This was determined in the second of two studies enumerating the frequency of CD1a-autoreactive T cell populations in human blood, however, there was a discrepancy between the two studies' estimates despite both using a single-cell cloning strategy for limiting dilution assays in which they tested reactivity of individual T cell clones to CD1-expressing APCs (de Jong et al., 2010, de Lalla et al., 2011). This discrepancy illustrates the fact that a focus on a limited number of clones cultured *in vitro* may not provide an accurate representation of all CD1-restricted T cells *in vivo*. Furthermore, the detection of CD1-restricted T cells in these previous studies relied on IFN-γ secretion as a measurement of reactivity, yet CD1-restricted T cells may be heterogeneous in their effector functions and thus produce a wide array of different cytokines upon stimulation, and not necessarily IFN-γ (Li et al., 2011a). Assays detecting secretion of certain cytokines may therefore underestimate the frequency of CD1-restricted T cells. In addition, the discrepancy between frequency estimates may also stem from the use of different CD1-transfected cell lines – C1R cells (de Lalla et al., 2011) and K562 cells (de Jong et al., 2010) – which likely have different lipidomes, thereby influencing the range of endogenous lipid antigens captured by CD1 within these APCs. Like studies of CD1b-, CD1c- and CD1d-restricted T cells, tetramers could be employed to determine the frequencies of CD1-

restricted T cell population directly *ex vivo*, especially those populations that exhibit specificity for exogenous lipid antigens.

1.4.2 CD1-restricted T cell effector functions

As part of the adaptive arm of the immune system, conventional T cells typically require several days to acquire their effector functions. Upon activation, they clonally expand, differentiate into effector cells and then migrate to sites of infection to participate in the immune response – a process that takes days (Pennock et al., 2013). In contrast, unconventional T cells appear to act at the junction of the innate and adaptive immune systems and are hence regarded as "innate-like" (Pereira and Macedo, 2016, Kronenberg and Kinjo, 2009). Type I NKT cells, for example, are capable of immediately responding to activation by producing large quantities of cytokines or directly killing target cells within minutes to hours, thereby having a major impact on immune responses early on (Rossjohn et al., 2012, Crowe et al., 2003). This rapid gaining of effector function is analogous to that of memory T cells, which immediately respond to antigen engagement (van Der Vliet et al., 2000). Accordingly, type I NKT cells express high levels of the memory marker CD45RO, and activation marker CD28 upon maturation and egress from the thymus, while conventional T cells only upregulate expression of these markers upon antigen encounter (Sandberg et al., 2004). Unlike type I NKT cells, group 1 CD1-restricted T cells appear to be spread across the naive and effector/memory compartments as determined by their expression of CD45RA and CD45RO respectively, at least when studied *in vitro* (de Lalla et al., 2011).

The diversity of cytokines and chemokines produced by CD1-restricted T cells confers them with important roles in the immune response. In mice, NKT cells are known to differentiate into multiple effector subsets defined primarily by their expression of transcription factors and cytokines: NKT1, NKT2, NKT17, NKT10 and NKT_{FH} cells, each of which is enriched in distinct tissues (Crosby and Kronenberg, 2018, Pellicci et al., 2020). NKT1 cells are similar to T_h1 cells in that they express high amounts of transcription factor T-bet, secrete IFN-γ upon activation and are cytotoxic, but also secrete IL-4, thus distinguishing them from conventional T_h1 cells (Georgiev et al., 2016, Lee et al., 2013, Lee et al., 2016, Engel et al., 2016). NKT2 cells express high levels of transcription factor PLZF and resemble T_h2 cells in their secretion of type 2 cytokines IL-

4, IL-5 and IL-13 (Georgiev et al., 2016, Lee et al., 2013, Lee et al., 2016, Engel et al., 2016). NKT17 cells are RORγt^{hi} and PLZF^{int}, and produce GM-CSF, IL-17 and IL-22 upon activation (Georgiev et al., 2016, Lee et al., 2013, Lee et al., 2016, Engel et al., 2016). NKT10 cells play a regulatory role by secreting IL-10 and IL-2 (Sag et al., 2014), while NKT_{FH} cells express germinal centre marker, BCL-6, and provide cognate help to antigen-specific B cells (Chang et al., 2011). Accordingly, NKT cells can have a multitude of functions that resemble peptide-reactive helper T cells with an overlap of cytokines produced by each subset, although it is important to note that most knowledge of NKT effector subsets stems from studies of mice, not of human NKT cells.

From what is currently understood, group 1 CD1-restricted T cells appear to be less innate-like compared to NKT cells. Upon *in vitro* activation, CD1-autoreactive T cells exhibit a T_h0 or T_h1 phenotype and produce large quantities of IFN-γ and TNF (de Lalla et al., 2011). Additionally, CD1a-autoreactive T cells have produced IL-22, IL-2 and IFN-γ in response to stimulation, similar to T_h22 cells (de Jong et al., 2010). In combination with expression of the skin-homing marker cutaneous lymphocyte-associated antigen (CLA), the production of IL-22 is indicative of a role of CD1a-restricted T cells in host defence and tissue repair in the skin (de Jong et al., 2010), however these functional studies have been limited to *in vitro*-cultured CD1-autoreactive T cell clones, and may not be reflective of their roles *in situ*. Group 1 CD1-restricted T cells have mostly been studied in the context of self-reactivity rather than stimulation by exogenous lipid antigens, and therefore their full range of effector functions may be unappreciated. Further studies are needed to validate these findings and assess the activity of CD1-restricted T cells *in vivo.*

1.4.3 CD1-restricted T cells in infection

NKT cell activity may either promote or inhibit immune responses to many different microbial pathogens, including viruses, bacteria, fungi and protozoa (reviewed in (Torina et al., 2018, Rossjohn et al., 2012)). These responses to infection occur either via recognition of infection-induced self-antigens or lipids produced directly by the infectious agent (Mattner et al., 2005, Zeissig et al., 2012), or by TCR-independent activation with IL-18 and IL-12, which are often produced in response to PRR sensing (Brigl et al., 2003, Holzapfel et al., 2014, Zeissig et al., 2012). This innate-like, cytokine-

driven activation of type I NKT cells has been observed in bacterial infections and viral infections alike (Tohn et al., 2011, Wesley et al., 2008), and it is unknown whether this also occurs for other CD1-restricted T cells.

Many bacteria utilise glycolipid synthesis pathways that can produce agonists for NKT cells and contain cell wall antigens that have similar chemical structures to that of α-GalCer (Kinjo et al., 2005). For example, *Borrelia burgdorferi*, the causative agent of Lyme disease, produces glycosylated diacylglycerol (DAG), which acts as a weak agonist for type I NKT cells, driving CD1-dependent responses that are required for infection clearance (Olson et al., 2009). Similarly, a lipopeptidophosphoglycan derived from *Entamoeba hystolitica* activates type I NKT cells, which, again, are necessary for effective clearance (Ito et al., 2013).

NKT cells are recruited and respond to microbial pathogens via a number of pathways, depending on the pathogen. The identification of further lipid-based ligands that elicit T cell responses will provide valuable insight into the role that other CD1-restricted T cells subsets play during infection and how they can be manipulated.

Mycobacteria

While there is little evidence of group 1 CD1-restricted T cells playing roles in infection to a diverse range of pathogens, they have had well-studied relationships with mycobacterial lipids. NKT cells, however, do not appear to play a protective role in mycobacterial immunity. Rather, CD1d-deficient mice do not have significantly different TB susceptibility compared to control mice, and a single nucleotide polymorphism (SNP) in the *CD1D* gene (rs859009) significantly decreased pulmonary TB risk an Iranian cohort, rather than being seemingly necessarily for effective immunity (Behar et al., 1999, Taheri et al., 2019).

Mycobacteria species contain unique, lipid-rich cell walls, with lipids comprising 30-60% of their dry weight (Brennan and Goren, 1979, Daffe and Draper, 1998). A large number of lipid antigens derived from mycobacteria are known potent agonists for CD1-restricted T cells (Van Rhijn et al., 2013b). Interestingly, Mtb or its cell wall lipids induce group 1 CD1 (but not CD1d) expression through TLR-2 signalling, further supporting the idea of cross-talk between the innate and adaptive immune systems via CD1d-dependent responses (Roura-Mir et al., 2005b).

As previously discussed in Section 1.3.1, various lipid components of mycobacterial cell walls are presented by group 1 CD1 molecules. Of particular interest are: DDM presented by CD1a (Moody et al., 2004); mycobacterial mycolates, such as GMM and mycolic acid, which are presented by CD1b (Batuwangala et al., 2004, Beckman et al., 1994, Garcia-Alles et al., 2011, Moody et al., 1997, Layre et al., 2009, Guiard et al., 2009); and mycoketides such as mannosyl-β1-phosphomycoketide (MPM) and PM presented by CD1c (Ly et al., 2013, Matsunaga et al., 2004, Moody et al., 2000, de Jong et al., 2007). Mycolic acids, for example, are the hallmark of the cell envelope of Mtb and related species and genera (Daffe and Draper, 1998), raising the question of whether recognition of mycobacterial lipids by CD1-restricted T cells may be protective against infection by multiple mycobacterial species.

Immunisation of guinea pigs with BCG or lipid extracts from Mtb stimulates strong proliferative and cytolytic responses from CD1b- and CD1c-restricted T cells, indicating that they are involved in the response and may play a role in protection (Dascher et al., 2003, Hiromatsu et al., 2002, Watanabe et al., 2006). GMM, for example, is the immunodominant lipid in the response against *M.avium paratuberculosis,* which causes paratuberculosis in animals (Van Rhijn et al., 2009). This suggests that GMM in combination with other mycobacterial lipids may be able to generate cellular responses that target antigens from Mtb and related bacteria. Immunisation of cows with GMM alone resulted in CD1b-restricted T cell responses and the formation of memory T cells, albeit these T cell responses were weak and no B cell response was detected, further supporting the importance of T cell recognition (Nguyen et al., 2011, Nguyen et al., 2009). In addition, MPM is a potent agonist for CD1c-restricted T cells and is produced by pathogenic mycobacteria, including *M.avium*, *M.bovis* (BCG), and Mtb (Moody et al., 2000, Matsunaga et al., 2004). A role for CD1c-restricted T cells in Mtb immunity was first demonstrated by the isolation of T cell clones that respond to CD1c antigens from individuals who documented positive tuberculin (PPD) but were not found in naive individuals (Moody et al., 2000). Populations of CD1c-restricted T cells that recognise mycoketides, such as mannosyl-phosphodolichols, have since been observed in Mtb-infected patients in larger numbers compared to healthy controls (Moody et al., 2000).

Group 1 CD1-restricted T cells have shown strong proliferative and cytolytic responses in response to mycobacterial lipids, however studies demonstrating this have largely used

lipid antigen-pulsed DCs or CD1-expressing transfectant cell lines *in vitro* rather than showing what they do *in situ* (Gilleron et al., 2004, Ulrichs et al., 2003). Human T cell clones have demonstrated cytolytic responses to mycobacterial lipids *in vitro* (Beckman et al., 1996, Hiromatsu et al., 2002, Kawashima et al., 2003, Ulrichs et al., 2003, Watanabe et al., 2006). Cytotoxic activity was demonstrated *ex vivo* by effector T cells isolated from guinea pigs immunised with Mtb lipid antigens against DCs pulsed with the same lipids (Hiromatsu et al., 2002). Although, some of these T cell clones exhibited cytotoxicity towards $CD1^+$ cells even in the absence of mycobacterial antigens, suggesting a level of CD1-autoreactivity that must also be taken into account when determining the role of CD1-restricted T cells in mycobacterial infection (Beckman et al., 1996, Bendelac et al., 1995, Porcelli et al., 1989, Vincent et al., 2002, Balk et al., 1991, Sieling et al., 2000). Furthermore, the proliferation and IFN-γ production by circulating lipid-reactive T cells of individuals with latent tuberculosis infection (LTBI) is greater than those from uninfected healthy donors, and lipid-antigen-specific responses are detectable in patients with active TB at the start of treatment (Ulrichs et al., 2003), suggesting that T cells are involved in the immune response.

Compared to other group 1 CD1-restricted T cells, fewer studies have examined the anti-mycobacterial responses of CD1a-restricted T cells. However, the importance of CD1a in Mtb immunity was highlighted by the identification of *CD1A* polymorphisms that are associated with greater TB susceptibility (Seshadri et al., 2014). Seshadri and colleagues identified two SNPs associated with TB in cohorts of Vietnamese adults: an intronic SNP (rs411089) associated with greater risk of pulmonary and meningeal TB, and another in the regulatory region (rs366316) that was only associated with pulmonary TB in one cohort tested (Seshadri et al., 2014). Both SNPs likely influence CD1a expression independently of each other, leading to a CD1a deficiency in monocyte-derived DCs and thus impaired ability to present lipid antigens to T cells (Seshadri et al., 2013, Seshadri et al., 2014). A subsequent study of an Iranian cohort also found that rs411089 was associated with pulmonary TB, while rs366316 was not (Taheri et al., 2019). These inconsistencies may reflect differences between cohorts and populations, and the association of polymorphisms in *CD1* genes and disease susceptibility therefore warrants further investigation in larger cohorts with different ethnicities and genetic backgrounds.

Further evidence to support an anti-mycobacterial role for CD1-restricted T cells is that DCs that migrate to sites of cutaneous *M.leprae* infection express CD1a, CD1b, and CD1c (Sieling et al., 1999). These $CD1^+$ DCs in dermal granulomas were highly efficient APCs for group 1 CD1-restricted T cells *in vitro*, and group 1 CD1 expression in leprosy lesions correlated with effective immunity, suggesting that CD1-restricted T cell responses play a role in host defence against *M.leprae* (Sieling et al., 1999). Another study isolated CD1a-restricted T cells that respond to *M. leprae* lipids presented by $CD1a^+$ LCs from lesional skin of a *M. leprae* patient (Hunger et al., 2004). Additionally, CD1a is upregulated in bronchoalveolar lavage DCs of TB patients (Buettner et al., 2005), and its expression by monocytes is induced by Mtb infection and/or the presence of Mtb cell wall lipids *in vitro* (Roura-Mir et al., 2005b).

These data suggest that CD1a-restricted T cells play a role in surveillance against mycobacterial infection, however further studies of mycobacterial lipid-reactive CD1a-restricted T cells that assess their activity directly *ex vivo* or in animal models are required to determine their protective capabilities in TB to support *in vitro* assays.

1.4.4 CD1-restricted T cells in cancer

There is growing evidence of CD1-restricted T cells playing a role in tumour surveillance. The potent type I NKT cell agonist, α-GalCer, has demonstrated potent anti-tumour properties (Kawano et al., 1997, Kobayashi et al., 1995, Macho-Fernandez et al., 2014, Morita et al., 1995). It has since been used in over 30 anti-tumour clinical trials to exploit the immunomodulatory functions of NKT cells with variable outcomes (reviewed in Zhang et al., 2019). For example, clinical trials using α-GalCer-pulsed DCs in cancer immunotherapy have been successful in small lung cell cancers by engaging type I NKT cells to mediate crosstalk between the adaptive and innate immune responses (Fujii et al., 2013). A synthetic aminocyclitolic ceramide analogue of α-GalCer, HS44, has also shown promise for clinical therapies as it has fewer TCR contacts, thereby avoiding unrestrained type I NKT cell activation (i.e., cytokine storm) (Kerzerho et al., 2012). There is therefore great potential for α-GalCer and other analogues to be used in cancer immunotherapy to stimulate type I NKT cells (Zhang et al., 2019).

Studies have demonstrated a protective role for NKT cells in tumour surveillance, mostly through the production of Th1 cytokines and recruitment of other cytolytic cell

populations (Terabe and Berzofsky, 2008). Upon stimulation with α-GalCer in combination with IL-12 and IL-18, they contribute to tumour protection by secreting large quantities of IFN-γ and cross-activating NK cells and $CD8^+$ T cells (Kitamura et al., 1999, Smyth et al., 2002, Crowe et al., 2002). They also indirectly enhance tumour immunity by modulating the effects of immunosuppressive cells, such as regulatory T (Treg) cells, myeloid-derived suppressor cells, and suppressive IL-10-producing neutrophils (De Santo et al., 2010, De Santo et al., 2008, Venken et al., 2013, Venken et al., 2014). In addition, lysophospholipids associated with inflammation are presented to type II NKT cells in multiple myeloma patients (Chang et al., 2008), while type I NKT cell frequencies are reduced and anti-tumour effects are hampered, and stimulation with α-GalCer can reverse this, as reviewed in (Favreau et al., 2016).

Group 1 CD1 and their lipid-reactive T cell counterparts have also been implicated in tumour immunology. All four CD1 molecules are expressed by malignant cells in blood and bone marrow samples from acute myeloid leukemia, B-acute lymphoblastic leukemia and T-acute lymphoblastic leukemia patients to varying degrees (Lepore et al., 2014). Evidence also supports a role for CD1c-restricted T cells in tumour surveillance and protection against leukemia via the recognition of specific lipids, such as methyl-lysophosphatidic acids (mPLAs) (Porcelli et al., 1989, Lepore et al., 2014). Self-reactive CD1c-restricted T cells recognise and lyse acute leukemia cells presenting mLPA, which typically accumulates in primary leukemia blasts, and appear to be protective *ex vivo* and in a human leukemia xenograft mouse model (Lepore et al., 2014). The expansion of mLPA-specific leukemia-reactive T cells isolated from patients therefore shows promise as an immunotherapy to augment antitumour responses by targeting this tumour-associated lipid (Lepore et al., 2014, Lepore et al., 2015).

CD1a-restricted T cells have not yet been observed in cancers themselves, but expression of CD1a by cells within the tumour microenvironment is associated with protection in some tumour types, potentially due to the presentation of tumour-specific glycolipids (Coventry and Heinzel, 2004). For example, the leukemia-like disease Langerhans cell histiocytosis (LCH) is characterised by inflammatory lesions containing pathogenic $CD1a^+$ $CD207^+$ DCs (Geissmann et al., 2001, West et al., 2014, Chikwava and Jaffe, 2004). In addition, although CD1a is not typically expressed by circulating T cells as it is downregulated following thymocyte maturation (Sotzik et al., 1993, Res et al., 1997), its

expression can be triggered under certain conditions including cancers. Polyclonal populations of CD1a^{+} T cells have been identified in LCH lesions that are absent in peripheral blood, expressing NK/NKT cell markers, CD16 and CD56, suggestive of an innate-like phenotype (West et al., 2014). Cortical T cells exhibit higher CD1a expression in pre-lymphoblastic lymphomas and leukemias profiles (especially cortical T-ALL), and infiltrating CD3+/TdT+/CD1a+ T cells have been observed in follicular dendritic cell sarcomas, demonstrating that immature CD1a+ T cell infiltration is associated with particular cancers (Kim et al., 2010, Cortelazzo et al., 2011, Craig and Foon, 2008, Han and Bueso-Ramos, 2007). CD1a-restricted T cells may therefore play a role in tumour surveillance and anti-tumour activity by responding to tumour-specific lipids or increased levels of CD1a. The development of a method to study these T cells in tumour tissues would aid the study of them in the context of cancer.

1.4.5 CD1-restricted T cells in autoimmunity

Many inflammatory and autoimmune conditions alter lipid profiles, and therefore CD1-restricted T cells may respond to changes in lipid levels under these conditions. Levels of lysophospholipids that are presented by CD1d, such as LPC, are elevated in multiple myeloma, asthma, allergic and autoimmune inflammation, and are also a major constituent of oxidised low-density lipoprotein (LDL) in atherosclerotic plaques (Mehta et al., 1990, Mills and Moolenaar, 2003, Okita et al., 1997, Sasagawa et al., 1999), suggesting a role for NKT cells in chronic inflammatory states.

Given the ability of NKT cells to recognise autoantigens, they have been studied in a variety of autoimmune diseases. Reduced circulating type I NKT cell frequencies have been observed in conjunction with an increase at the site of inflammation in several autoimmune or inflammatory conditions, suggesting that they traffic to the site of inflammation and play a role in disease (Torina et al., 2018). Their number and function appear altered in autoimmune conditions, such as type 1 diabetes, arthritis and systemic lupus erythematosus (SLE) (reviewed in (Wu and Van Kaer, 2009)). However, seemingly conflicting results have been observed in mouse models and human patients, sometimes dependent on the genetic background of the mouse or stage of disease, thereby complicating our understanding of NKT cells in autoimmunity (Subleski et al., 2011). In addition, some studies of autoimmune conditions, such as rheumatoid arthritis, have also

suggested opposing roles for NKT cell subsets in disease pathogenesis that may stem from the functional differences between type I and type II NKT cells, which appear to be pathogenic and protective respectively (Subleski et al., 2011).

Torina and colleagues proposed a model of time-dependent activation influencing whether NKT cells are pathogenic or protective. They suggest that short exposure (2-4 hours) to ligands shifts the balance towards the production of anti-inflammatory molecules, such as IL-10, while NKT cells that are exposed to their ligands for longer periods of time secrete pro-inflammatory cytokines such as IFN-γ (Torina et al., 2018). This is supported by the induction of a tolerogenic state in type I NKT cells in autoimmune experimental lupus and type I diabetes models following short-term *in vivo* activation with α-GalCer (Yang et al., 2012, Tohn et al., 2011). The stage of disease may also influence type I NKT cell function. They are believed to protect against the development of type 1 diabetes, as their number and function are reduced in patients and non-obese diabetic (NOD) mice, while adoptive transfer, α-GalCer stimulation, or CD1d overexpression prevents diabetes progression (Tard et al., 2015, Van Kaer and Wu, 2018). However, type I NKT cells appear to enhance pathogenesis mediated by diabetogenic $CD8^+$ T cells once they emerge and begin to target pancreatic β-islet cells (Griseri et al., 2005).

Given the abundance of lipids in the central nervous system (CNS) (Hirabayashi, 2012), it would be reasonable to assume that lipid-reactive T cells might play a role in neuroinflammatory diseases. The CNS was historically regarded as immune-privileged as it was thought that immune cells could not pass the blood-brain barrier. Cumulative evidence, however, suggests that recruitment of immune cells and neuroinflammation do occur in neurological diseases (Cui and Wan, 2019, Fung et al., 2017, Skaper et al., 2018).

MS is an autoimmune disorder in which T cells mediate demyelination of CNS neurons (Goverman, 2009). The myelin sheath of neurons is composed largely of lipids (70-85% of myelin's dry weight) (Fewou et al., 2009) and so it may contain lipids that are antigens for lipid-reactive T cells. T cell clones isolated from multiple sclerosis (MS) patients were observed to recognise self-GSL (sulfatides and gangliosides) (De Libero and Mori, 2003, Shamshiev et al., 1999, Shamshiev et al., 2000). Sulfatides derived from myelin can be

carried by apolipoprotein E in cerebrospinal fluid to be captured by APCs and activate type I NKT cells, resulting in auto-reactivity (Stax et al., 2017).

There have been numerous studies assessing NKT cell frequency in MS, with some reporting a decrease (Demoulins et al., 2003, Illes et al., 2000, van der Vliet et al., 2001), others reporting an increase (O'Keeffe et al., 2008, Gigli et al., 2007), and another not observing any difference (Gausling et al., 2001). Again, these conflicting findings may result from studying different forms or stages of disease, or may reflect the various methods used to identify type I NKT cells (i.e. single-stranded conformation polymorphism of TCR chains (Illes et al., 2000), mRNA analysis with Vα24 and Jα18 specific probes (Demoulins et al., 2003), or flow cytometry with TCR antibodies and/or tetramers (O'Keeffe et al., 2008, van der Vliet et al., 2001, Gigli et al., 2007)). Type I NKT cell function appears to be impaired in MS patients (O'Keeffe et al., 2008), and this hypo-responsiveness is restored in patients on type 1 interferon-β therapy, which upregulates CD1d and co-stimulatory molecule (CD28 and CD40) expression on DCs (Gigli et al., 2007). Following *ex vivo* stimulation, patient type I NKT cells secrete large quantities of Th2 cytokines (and IL-10 to a lesser extent), which complements the observation of protective Th2 responses in MS-like experimental autoimmune encephamyelitis (EAE) in mouse models following type I NKT cell stimulation (Jahng et al., 2001, Miyamoto et al., 2001). In addition, type II NKT cells have also been shown to react to sulfatides that are abundant in myelin sheaths, and also may play an immunomodulatory role by suppressing pathogenic T cells that react to myelin oligodendrocyte glycoprotein in the CNS (Jahng et al., 2004). These studies reveal a role for NKT cells in the progression of neurodegenerative disease (reviewed in (Van Kaer et al., 2015b)), and collectively raise the question of whether other CD1-restricted T cell subsets may also play a role, especially given that some lipid antigens (including sulfatides) can be presented by all CD1 molecules (Shamshiev et al., 2002). While there have not yet been any direct studies of this, it does warrant further investigation. Additionally, according to the Human Protein Atlas, cells in the hippocampus, caudate, cerebral cortex and cerebellum – purkinje cells in particular – express CD1a and therefore may present lipid antigens specific to the CNS (Uhlen et al., 2015) (https://www.proteinatlas.org/ENSG00000158477-CD1A/tissue/primary+data).

Taken together, the aberrant frequency and/or function of NKT cells in autoimmune inflammatory diseases suggest that they play a role in the disease pathology. Type I NKT cells appear to be either protective or pathogenic depending on the autoimmune condition, stage of disease and immune microenvironment, and can play an opposing role to type II NKT cells. Group 1 CD1-restricted T cell subsets may also play a role in these diseases by promoting crosstalk between the innate and adaptive immune systems and/or by recognition of autoantigens presented by CD1.

Given that CD1a-restricted T cells have demonstrated autoreactivity to CD1a presenting self-lipids (de Jong et al., 2014, Vincent et al., 2005), CD1a may also be involved in autoimmune diseases. CD1a-expressing APCs and CD1a-restricted T cells infiltrate sites of autoimmune disease and can induce T cell cytotoxicity in the thyroid in Graves' Disease and thyroiditis (Roura-Mir et al., 2005a). Furthermore, there have been numerous studies associating CD1a-reactive T cells with atherosclerotic inflammation, due to CD1a expression by macrophage foam cells and DCs in atherosclerotic lesions leading to T cell responses (Melian et al., 1999, Bobryshev et al., 1996). The lipid triacylglycerol (TAG), in particular, is a risk factor for atherosclerosis and coronary heart disease (Hokanson and Austin, 1996, Sarwar et al., 2007, Schulte et al., 1999) and is presented by CD1a (de Jong et al., 2014), perhaps contributing to pathology. In addition, *in vitro* assays have allowed the identification of other CD1a autoantigens, including skin-specific oils such as squalene, sphingolipid ligands, and phosphatidic acid-containing compounds (de Jong et al., 2014), which leads to the question of whether CD1a-restricted T cells can recognise skin lipids and what maintains tolerance under normal conditions.

1.4.6 CD1a-restricted T cells in skin immunity and allergy

Skin is one of the first barriers that microorganisms must breach to establish an infection. It comprises of a network of innate and adaptive immune cells that form a strong barrier to deter pathogens while maintaining healthy microbiota. Under steady-state conditions, CD1a is abundantly expressed by LCs and dermal DCs (Boltjes and van Wijk, 2014, Mizumoto and Takashima, 2004). Additionally, CD1a-autoreactive T cells isolated by de Jong and colleagues expressed high levels of the skin-homing marker cutaneous leukocyte antigen (CLA), and produced IL-22, which is typically an indicator of $CD4^+$ T

cells that express skin homing receptors (de Jong et al., 2010, Cotton et al., 2021, Duhen et al., 2009, Trifari et al., 2009). Together, these are suggestive of an important role for CD1a-restricted T cells in skin homeostasis and barrier protection.

CD1a expression by epidermal and/or dermal DCs increases as part of lymphoproliferative skin conditions, such as T cutaneous lymphoid hyperplasia, lymphomatoid papulosis, parapsoriasis and mycosis fungoides, the most common form of cutaneous T cell lymphoma (Pigozzi et al., 2006). $CD1a^+$ LCs and $CD1a^+$ dermal DCs are also abundant in contact dermatitis, atopic dermatitis (AD), psoriasis, and lichen planus, with $CD1c^+$ dermal DCs also having been observed in contact dermatitis (Pigozzi et al., 2006, Deguchi et al., 2002, Kim et al., 2016, Bangert et al., 2003, Scibior et al., 2019, Wollenberg et al., 1996). In addition, $CD1a^+$ dermal LCs facilitate T_H17 cell-mediated inflammation in a CD1a transgenic mouse model of contact dermatitis when the skin touches poison ivy, characterised by an infiltration of inflammatory granulocytes and IL-17-producing $CD4^+$ T cells (Kim et al., 2016). The dominant immunogen in poison ivy and poison oak that causes this response is urushiol C15:2, which alone, was sufficient to induce a T_H17 cell response, partially mediated by CD1a-restricted T cells in CD1a-transgenic mice (Kim et al., 2016).

Recent studies have also demonstrated a role for CD1a-restricted T cells themselves in allergy-associated inflammation. Phospholipases present in common allergens such as house dust mite (HDM), and bee and wasp venom, break down self-lipids in the skin to generate free fatty acids and lysophospholipids that can be presented to (and activate) CD1a-restricted T cells as neoantigens (Bourgeois et al., 2015, Jarrett et al., 2016b). Further evidence supports a role for these cells in allergic dermatitis at an elevated frequency due to bee and wasp venom- or HDM-responsive T cells in allergic individuals compared to non-allergic individuals (Subramaniam et al., 2016, Jarrett et al., 2016a), although it is likely that they are responsive to PLA-generated neoantigens.

Similar neoantigens are also produced by phospholipases released by mast cell exosomes, contributing to psoriasis pathogenesis (Kim et al., 2016, Cheung et al., 2016). The discovery of such phospholipases that can generate CD1a neoantigens warrants investigation of whether other skin allergies might be mediated by CD1a and CD1a-restricted T cells, and how this is regulated. In addition, NKT cells, and to a greater extent,

γδ-T cells, infiltrate the dermis 72 hours following positive epicutaneous patch tests and helper $CD3^+$ $CD4^+$ cell numbers also increase in both the dermis and epidermis (Bangert et al., 2003). Given the abundance of inflammatory CD1a- and CD1c-expressing APCs in contact dermatitis, whether CD1-restricted T cells also infiltrate warrants further investigation. Furthermore, benzyl benzoate and benzyl cinnamate, found in balsam of Peru, a tree oil commonly used in cosmetic products, were recently identified as CD1a antigens that activate CD1a-restricted T cell clones *in vitro* (Nicolai et al., 2020). Together, these studies strongly support a role for CD1a-restricted T cells in skin disease and there is great potential to investigate CD1a-restricted T cell responses to other lipids that cause skin allergy.

1.5 Summary, Hypothesis and Aims

1.5.1 Summary

CD1a-restricted T cells – and other unconventional T cells – represent a significant proportion of the T cell pool. They recognise self-lipids, foreign lipids, and neoantigens presented by CD1a, such as the mycobacterial lipid, DDM, cell membrane lipids, and headless cutaneous oils. Evidence suggests that CD1a-restricted T cells and other group 1 CD1-restricted T cell subsets play important roles during infection (particularly with mycobacteria), skin allergy, and autoimmunity, however their exact role(s) in the immune system mostly remain an enigma. Emerging evidence particularly highlights the role of CD1a-restricted T cells in skin inflammation, especially associated with allergic contact dermatitis and psoriasis, and given the abundance of CD1a-expressing LCs in the skin, manipulation of these cells may be key to preventing these pathologies. Based on the wealth of knowledge around type I NKT cell function, the immunomodulatory effects of α-GalCer and analogues have been exploited for therapeutic purposes. Studies of CD1a-restricted T cell biology and function in humans and animal models have been limited, yet the monomorphic nature of CD1a makes it an ideal target in clinical therapies and vaccinations. These cells have been shown to adopt Th1, Th17, or Th22-like responses upon activation, however, much of the data on these cells to date is based on few studies of *in vitro* cultured cells. By gaining a better understanding of CD1a-restricted T cells, the TCRs they use and the antigens they respond to, it may be possible to manipulate

them in infection and also suppress any pathogenic role they may play in allergy and autoimmune disorders.

1.5.2 Overarching Hypothesis

CD1a-restricted T cells represent a functionally unique population of T cells in the human immune system. Their distinct TCR repertoire and antigen specificity imbues them with the ability to recognise a broad range of lipid antigens such that they play specialised roles in infection and inflammatory diseases in humans.

1.5.3 Aims

Aim I – To characterise the phenotype and function of CD1a-restricted T cells

Studies determining the biology and function of CD1a-restricted T cells have largely been of T cell clones grown in culture for long periods. In this chapter, CD1a tetramers were used to isolate CD1a-restricted T cells from human blood directly *ex vivo* to provide a better understanding of how these cells may function *in situ*. RNA sequencing was also used to gain insight into their transcriptome and compare them to other T cell subsets.

Aim II – To characterise TCR diversity and antigen recognition by CD1a-restricted T cells

The TCR repertoire of CD1a-restricted T cells is thought to be diverse, similar to that of conventional T cells. However, other CD1-restricted T cell populations were also once considered diverse in their TCR repertoire before evidence revealed patterns of Vα and Vβ gene biases among antigen-specific groups. The TCR diversity of CD1a-restricted T cells that recognise self-lipids or DDM was therefore examined. Furthermore, structural studies serve as a basis for exploring the key amino acids involved in TCR/CD1a recognition, however only one ternary structure has been solved of an (autoreactive) CD1a-restricted TCR to date. The work presented here aimed to provide insight into the molecular interactions between TCR/CD1a-lipid and determine the breadth of lipid antigens that can be recognised by CD1a-restricted TCR clones.

Aim III – To develop regents for the isolation and characterisation of macaque CD1-restricted T cells

The absence of CD1a and other group 1 CD1 molecules in the murine genome has precluded the use of mouse models to study group 1 CD1-restricted T cells. Non-human primates (NHP), such as macaques, have been identified as good models to study lipid-reactive T cells, as they produce all four CD1 isoforms with high homology to their human counterparts. However, studies have only focused on type I NKT cells to date, using a trans-species cross-reactive human CD1d-α-GalCer tetramer while the cross-reactivity of human and macaque group 1 CD1 remains unexplored. Here, reagents were developed to study CD1-restricted T cells in pig-tailed macaques as a step towards studying lipid-reactive T cells in NHP models of health and disease, especially TB.

Aim IV – To determine whether C12-15 alkyl benzoate is an allergen presented to CD1a-restricted T cells

There is accumulating evidence to suggest a role for CD1a-restricted cells in allergic contact dermatitis and other skin pathologies through the recognition of foreign lipids and neoantigens. The recognition of an oil called alkyl benzoate, commonly found in skincare products, by CD1a-restricted T cells was investigated to determine whether CD1a may play a role in mediating allergy to alkyl benzoate-containing products.

Chapter 2. Material and Methods

Table 2.1. General Reagents

Reagent	Manufacturer/Source	Catalogue no.
2-log DNA ladder	New England BioLabs	N3200S
2X PCR master mix	Promega	M7505
Acetic acid	Chem-Supply	AA009
Adenosine Triphosphate (ATP)	Sigma Aldrich	A7699
AgeI restriction enzyme	New England BioLabs	R0052S
Ampicillin	Sigma Aldrich	A9518
BamHI restriction enzyme	New England BioLabs	R0136S
Benchmark Protein Ladder	Invitrogen	10747012
BglII restriction enzyme	New England BioLabs	R0143S
Bicine buffer (NaOH)	Sigma Aldrich	B8660-100G
BigDye Terminator v3.1 Cycle Sequencing Kit	Applied Biosystems	4337455
Biotin ligase (BirA)	Dr Jie Lin, Department of Microbiology and Immunology, University of Melbourne	N/A
Boric Acid	Chem-Supply	BA031-500G
Bovine serum albumin	Sigma	A7906
Bovine thrombin	Sigma Aldrich	T4646
Brilliant Blue R 250	Sigma	27816
Bromophenol blue	Sigma Aldrich	B5525
Chloramphenicol	Sigma	C0378
Citric acid	AnalaR	100813M
Collagenase P from *Clostridium histolyticum*	Merck	COLLP-RO
Compensation Beads Set Anti-Mouse Ig, κ	BD Biosciences	552843
Compensation Beads Set Anti-Rat/Hamster Ig, κ	BD Biosciences	552845
d-Biotin	Sigma Aldrich	B4501
Dasatinib	Peter MacCallum Cancer Centre	N/A
Dimethyl sulphoxide (DMSO)	Sigma	D-2650
DMEM Media	Gibco	10567014
DNase	Roche	10104159001
Dithiothreitol (DTT)	Invitrogen	R0861
EcoRI restriction enzyme	New England BioLabs	R0101S
Endoglycosidase H (endo H)	New England BioLabs	P0702S
Ethanol	Chem-Supply	EA043-2.5L-J
Ethylenediamine-tetraacetic acid (EDTA)	Ajax	AJA180-500G
ExoSAP-IT	Affymetrix	78201.1.ML
Fc Block	Miltenyi Biotec	130-059-901
Ficoll-Paque PLUS	GE Healthcare	17144003
Foetal Calf Serum (FCS)	Gibco	A31605
Fugene 6 reagent	Promega	E2691
Glutamax	Gibco	35050061
Glycine	Chemsupply	GA0007
Nickel-nitrilotriacetic acid (Ni-NTA) agarose resin	Thermo Fisher Scientific	88223
Hydrochloric acid	Chem-Supply	RP1104-P2.5L
Hydrogen peroxide	Sigma	H1009

Imidazole	Sigma-Aldrich	I2399
Kanamycin sulfate	Sigma	K4000
KpnI restriction enzyme	New England BioLabs	R0142S
L-Arginine	Sigma	A5006-1KG
Luria Agar (LA) plates + 30µg/mL kanamycin	Media Preparation Unit, University of Melbourne	N/A
Luria Agar (LA) plates +100µg/mL ampicillin	Media Preparation Unit, University of Melbourne	N/A
Luria broth	Media Preparation Unit, University of Melbourne	N/A
Magnesium acetate tetrahydrate (MgOAc)	Sigma Aldrich	M5661-250g
Magnesium chloride	Sigma	M8266-100G
Methanol	Univar	A318
MoBio Ultraclean 15 Kit	MoBio	12100-300
Agarose	Biorad	1613101EDU
Anti-Mouse Ig,κ/Negative Control Compensation Plus Particles Set	BD Pharmingen	560497
N-2-hydroxyethylpiperazine-N-2-ethane sulfonic acid (HEPES)	Gibco	11344041
NdeI restriction enzyme	New England BioLabs	R0111S
NEBuffer 2.1 (10x)	New England BioLabs	B7202S
NEBuffer 3.1 (10x)	New England BioLabs	B7203S
Non-essential amino acids	Gibco	11140050
OptiMEM Media	Gibco	31985070
Oxidised glutathione	Sigma	G4376
Paraformaldehyde (PFA)	Electron Microscopy Science	50-980-487
Pepstatin A	Merck	516481
Phenylmethane sulfonyl fluoride (PMSF)	Sigma	P7626
Phosphate buffered saline (PBS)	Microbiology and Immunology Media Preparation Unit	N/A
Phytohemagglutinin-P (PHA)	Sigma-Aldrich	L1668
Polyethylenimine (PEI)	Sigma-Aldrich	408727-100ML
Reduced glutathione	Sigma	C4251
rhIL-15	Peprotech	200-15
rhIL-2	Peprotech	200-02
rhIL-7	eBioscience	RIL75
Roswell Park Memorial Institute (RPMI) 1640 Media	Gibco	61870036
Sodium acetate (anhydrous)	Sigma	S2889
Sodium carbonate	Chem-Supply	3310
Sodium chloride	Chem-Supply	SA046
Sodium dodecyl sulfate (SDS)	Bio-Rad	L5750-500G
Sodium hydrogen carbonate	Chem-Supply	SA001
Sodium phosphate monobasic	Sigma	S0751
Sodium pyruvate	ThermoFisher	11360070
Sterile water for Irrigation	Baxter	PSBX401-1
Streptavidin (unconjugated)	Sigma-Aldrich	189730
Streptavidin-BV421	BioLegend	405226
Streptavidin-PE	BD Biosciences	554061
Streptomycin and penicillin	ThermoFisher	15-140-122
SuperScript VILO cDNA Synthesis Kit and Master Mix	Invitrogen	11755250

SYBER Safe DNA gel stain	Invitrogen	S33102
T4 ligase and buffer	Promega	M1801
Tetramethylbenzidine	Sigma Aldrich	860336-100MG
Tris(hydroxymethyl)methylamine	Chem-Supply	T0377
Trypan blue	Sigma	T8154
Trypsin	Media Preparation Unit, University of Melbourne	N/A
Tryptone	Oxoid	LP0042
Tween20	Sigma	P1379-500ML
Urea	Univar	817/5KG
XhoI restriction enzyme	New England BioLabs	R0146S
Yeast extract	Oxoid	LP0021B
ZymoPURE Plasmid Gigaprep System kit	Zymogen	D4204
ZymoPURE Plasmid Maxiprep System kit	Zymogen	D4202
ZymoPURE Plasmid Miniprep System kit	Zymogen	D4210
RNase inhibitor	Clontech	2313A
dNTP mix (10mM)	Promega	U1515
Triton X-100	Sigma-Aldrich	X100-500ML
Betaine 5M	Sigma	B0300-1VL
SuperScript II Reverse Transcription Kit	Invitrogen	18064-071
Superscript VILO Reverse Transcription Kit	Invitrogen	11755250
KAPA HiFi HotStart ReadyMix	Clontech	KP-KK2602
ERCC Spike-In Mix	ThermoFisher	4456740
Agencourt AM Pure XP Beads	Beckman Coulter	A63881
Quant-iT PicoGreen dsDNA Assay Kit	ThermoFisher	P7589
Glutathione (oxidized)	Sigma	G4376-10G
Glutathione (reduced)	Sigma	G4251-25G
Ionomycin	Sigma	I24222
OptiMEM Media	Gibco	31985-078
Phorbol 12-myristate 13-acetate (PMA)	Sigma	P1585
Polybrene	Sigma	H9268
RPMI 1640 Media	Gibco	61870036
DMEM Media	Gibco	10567014
Tyloxopol	Sigma	T0307
Triton X-100 (BioXtra) for RNA-seq	Sigma-Aldrich, Merck	T9284
Nextera® XT DNA Sample Preparation Kit (96 Samples)	Illumina	FC-131-1096
Nextera® XT Index Kit v2 Set A (96 indices, 384 samples)	Illumina	FC-131-2001
Nextera® XT Index Kit v2 Set D (96 indices, 384 samples)	Illumina	FC-131-2004
FreeStyle 293 Expression Medium	ThermoFisher	1233
GolgiStop	BD Biosciences	554724

2.1 Media and Buffers

RF-10 complete media: Roswell Park Memorial Institute (RPMI)-1640 medium (Gibco) was supplemented with 10% (v/v) heat-inactivated foetal calf serum (FCS) (Gibco), 2 mM Glutamax (Gibco), 0.1 mM non-essential amino acids (NEAA) (Gibco), 1% (v/v) penicillin-streptomycin (Gibco), 1 mM sodium pyruvate (Gibco) and 50 mM β-2-mercaptoethanol (Sigma), and 0.015 M HEPES (Gibco).

Human T cell culture media: a 1:1 (v/v) mix of RPMI-1640 and AIM-V, supplemented with 10% (v/v) heat-inactivated FCS (Gibco), 2% (v/v) human AB serum (Sigma), 100 ug/ml penicillin and streptomycin (Gibco), 2 mM Glutamax (Gibco), 1 mM sodium pyruvate (Gibco), 0.1 mM NEAA (Gibco), 50 μM β-2-mercaptoethanol (Sigma), and 0.015 M HEPES (Gibco). Additionally, recombinant human IL-2 (Peprotech), IL-7 (eBioscience), and IL-15 (Peprotech) were added at 100 U/mL, 50 ng/mL, and 2 ng/mL respectively for T cell expansion as indicated.

Mammalian expression DMEM-10 media: Prior to transfection, cells were cultured in Dulbecco's Modified Eagle Medium (DMEM) (Gibco), which was supplemented with 10% (v/v) heat-inactivated FCS (Gibco), 2 mM Glutamax (Gibco), 0.1 mM NEAA (Gibco), 1% (v/v) penicillin-streptomycin (Gibco), 1 mM sodium pyruvate (Gibco) and 50 mM β-2-mercaptoethanol (Sigma), and 0.015 M HEPES (Gibco). Upon transfection, penicillin-streptomycin and β-2-mercaptoethanol were removed, and FCS concentration was reduced to 1% (v/v).

Table 2.2. Preparation of Buffers

Buffer	Preparation
0.5x Tris/Borate/EDTA (TBE) Buffer	54 g Tris base, 27.8 g boric acid and 20 mL 0.5 EDTA (pH 8.0) made up to 10 L in ddH_2O
10x DNA loading buffer	3.9 mL glycerol, 500 µL 10% (w/v) SDS, 200 µL 0.5 M EDTA and 0.025 g bromophenol blue made up to 10 mL in ddH_2O
10x SDS-PAGE Running Buffer	30.3 g Tris-base, 144 g glycine, 100 mL 20% SDS made up to 1 L in ddH_2O
2x SDS-PAGE Loading Buffer	100 mM Tris (pH 6.8), 200 mM DTT, 4% SDS, 0.2% (w/v) bromophenol blue, 20% (v/v) glycerol in ddH_2O.
5x Big Dye Sequencing Reaction Buffer	200 µL 1 M $MgCl_2$ and 2 mL 1M Tris-HCl (pH7.1) made up to 10 mL in ddH_2O
Biomix A	0.5 M bicine buffer (NaOH) (pH 8.3)
Biomix B	100 mM ATP, 100 mM MgOAc and 500 µM d-biotin
Coomassie Blue Stain	0.25% (w/v) bromophenol blue, 45 mL methanol, 5 mL acetic acid in 50 mL ddH_2O
ELISA Coating Buffer	15 mM sodium carbonate and 35 mM sodium hydrogen carbonate pH 9.6
Fluorescence-activated cell sorting (FACS) Wash Buffer	2% heat-inactivated FCS in PBS
Magnetic-activated cell sorting (MACS) Buffer	0.5% heat-inactivated FCS and 2mM EDTA in PBS
PAGE Destaining Solution	250 mL methanol and 70 mL acetic acid made up to 1 L in ddH_2O
PBS-T Buffer	0.05% (v/v) Tween20 in PBS
PBS_5BSA Buffer	0.5% (w/v) BSA in PBS
PBS_5BSA-T Buffer	0.5% (w/v) BSA and 0.05% (v/v) Tween20 in PBS
TCR Refold Buffer	0.1 M Tris, 2 mM EDTA (pH 8.0), 0.4 M L-Arginine, 0.5 mM oxidised glutathione, 5 mM reduced glutathione, 5 M Urea, 0.2 mM PMSF, 1 ug/mL pepstatin A in MilliQ made to a final pH of 8.0 with HCl.
TMB Buffer	0.2 M sodium phosphate, 0.1 M citric acid, 2 tetramethylbenzidine tablets and hydrogen peroxide in 20 mL
Tris Buffered Saline (TBS)	10 mM Tris-HCl (ph 8.0) and 150 mM NaCl in ddH_2O
IBP lysis buffer	50mM Tris-HCl (pH 8.0), 1% (v/v) Triton X-100, 1% (w/v) sodium deoxycholate, 100mM NaCl, 10mM DTT in MQ
3M Imidazole buffer	204.2g of Imidazole in 1L PBS
10x G5 buffer	3.87g of sodium citrate in 300mL MilliQ H_2O (50mM sodium citrate), pH adjusted to 5.5 with HCl
FACS fix	1% paraformaldehyde in 160mL PBS

2.2. Primary Tissue Samples

Human blood samples

Buffy coats from healthy human blood were obtained from the Australian Red Cross Blood Service. Ethics approval was granted by both the Red Cross and the University of Melbourne Human Research and Ethics Committee (1035100). Peripheral blood mononuclear cells (PBMCs) were isolated by standard density gradient with Ficoll-Paque PLUS (density 1.077 g/mL) (GE Healthcare Life Science) according to manufacturer's instructions.

Human skin samples

Healthy human skin samples were obtained from abdominoplasty surgery, a gift of Professor Stuart Berzins at Federation University. Ethics approval was granted by the Ballarat Health Services and St John of God Health Care Human Research Ethics Committee (HREC/15/BHSSJOG/5). Subcutaneous fat was removed and the epidermal and dermal layers were processed together or separately as indicated. Skin samples were enzymatically digested as 2 x 2 cm^2 pieces in 1 mg/mL Collagenase P (Merck) and RPMI-1640 medium for 90 minutes at 37°C, and passed through a 70 μm filter followed by a 30 μm filter to obtain single cell suspensions. Donor-matched blood (when provided) was processed as per buffy coats.

Macaque samples

Macaque PBMCs and tissues were provided as single cell suspensions by the Kent Laboratory, University of Melbourne. These studies were approved by the Animal Ethics Committee of the CSIRO Australian Animal Health Laboratory, under project numbers 1787 and 1887. Tissue samples obtained include blood (PBMCs), spleen, liver, lung, bronchoalveolar lavage (BAL), rectum, lymph nodes, and thymus.

2.3 Production of CD1 tetramers

2.3.1 Transfection of 293- GnTI$^-$ cells

Human embryonic kidney (HEK) 293-GnTI$^-$(Graham et al., 1977) were used to express soluble CD1/β_2m molecules. This cell line was produced by the transformation of HEK

cells with sheared human adenovirus type 5 DNA, and the E1A adenovirus gene allows these cells to produce high levels of proteins via transactivation of viral promoters (Harrison et al., 1977, Graham et al., 1977). The 293 T cells used here lack N-acetyl-glucosaminyltransferase I (i.e. are GnTI$^-$) and therefore synthesise proteins that lack complex N-glycans (Reeves et al., 2002). Both human and macaque CD1 molecules contained a 6-histidine tag for purification purposes, and a Bir-A tag for biotinylation. Human *CD1* and *β_2m* genes were previously cloned into a pHLsec plasmid expression vector, provided by A/Prof Daniel Pellicci and Dr Adam Uldrich (University of Melbourne) (Birkinshaw et al., 2015, Uldrich et al., 2013). *M.nemestrina CD1* and *β_2m* gene constructs were designed and also cloned into a pHLsec plasmid expression vector in a similar fashion (Appendix I).

Prior to transfection, 293-GnTI$^-$ cells were seeded into 5 x 175 cm^2 multilayered flasks (Cellstar) and maintained in DMEM-10 media at 37°C/ 5% CO_2 to 40% confluency. For each multilayered flask of GnTI$^-$ cells, a mixture of 137.5 µg of *β_2m*-pHLsec plasmid, 137.5 µg of *CD1A, CD1B, CD1C* or *CD1D*-pHLsec plasmid was added to 36 mL OptiMEM media (Gibco) and 425 µL polyethylenimine (PEI) (Sigma-Aldrich) as previously described (Birkinshaw et al., 2015). This mixture was added to 293-GnTI$^-$ cells in the presence of fresh antibiotic-deficient, supplemented DMEM-10 media. Protein-containing supernatant was harvested on days 5 and 8 after transfection and pooled for protein purification. Cell supernatant was filtered using a 0.2 µm Nalgene rapid-flow bottle top filter (Thermo Scientific) and stored at 4°C until ready for purification.

The FreeStyle 293-F cell line (Expi293F) (ThermoFisher) was transfected using the ExpiFectamine 293 Transfection Kit (ThermoFisher) to produce soluble CD1a protein in a non-adherent cell culture with native glycosylation. Expi293F cells were cultured in FreeStyle 293 Expression Medium (ThermoFisher). A total of 80 µg of plasmid DNA (40 µg *CD1A*:pHLSec and 40 µg *β_2m*:pHLSec) was mixed with 5 mL Opti-MEM medium (Gibco) and 216 µL of ExpiFectamine (ThermoFisher) separately, before being added to an additional 5 mL of Opti-MEM medium. These mixtures were added in a dropwise fashion to 200 x 10^6 Expi293F cells in 85 mL expression medium. Cells were cultured at 37°C/ 5% CO_2/ 125RPM overnight. 18 hours post transfection, 500 µL of Enhancer I and 5 mL of Enhancer II solutions (ThermoFisher) were added to make a total transfection

volume of 100 mL. Protein-containing supernatant was collected on day 6, filtered using a 0.2 μm Nalgene rapid-flow bottle top filter (Thermo Scientific) and stored at 4°C.

2.3.2 Purification of CD1 Protein

Filtered solution was spiked with 20 mM imidazole and passed over an Ni-NTA column (Thermo Scientific) by gravity flow. The 6-histidine tag encoded within the CD1 molecules allowed binding to the column resin. NiNTA columns containing bound-CD1 molecules were attached to a ÄKTA fast protein liquid chromatography (FPLC) system (GE Healthcare) and washed with PBS containing 20 mM imidazole before being exposed to an increasing gradient of imidazole (20 to 250 mM) to elute CD1 protein off the column. CD1-containing fractions were assessed by SDS-PAGE, pooled and concentrated to approximately 1 mg/mL in TBS (Table 2.2) using a Vivaspin 15 concentrator (Satorius) with a 10 kDa molecular weight cut-off (MWCO).

2.3.3 Sodium dodecyl sulphate (SDS)/ Polyacrylamide Gel Electrophoresis

To perform electrophoresis, protean precast 12% polyacrylamide gels (BioRad) were placed into a vertical electrophoresis cell (BioRad) in SDS-PAGE running buffer (Table 2.2). A Benchmark protein molecular weight (MW) ladder (Invitrogen) was loaded in at least one lane for all SDS-PAGE gels. 2 μg protein samples were prepared by adding 2 x SDS-PAGE loading buffer (Table 2.2) (and 0.2 M DTT for reduced samples) to a final sample volume of 20 μL and heat-denatured at 95°C for 5 minutes prior to loading. Electrophoresis was conducted at 25 mA per gel for 45 minutes. Following electrophoresis, gels were stained with Coomaisse stain (Table 2.2) for 10-15 minutes while gently rocking. Excess dye was then removed by gently rocking gels in a destaining solution (Table 2.2) overnight.

2.3.4 Biotinylation of CD1 Molecules

For biotinylation, CD1 molecules were buffer exchanged into a 10 mM Tris buffer (pH 8.0) (Table 2.2) using a PD-10 desalting column (GE Healthcare) as per the

manufacturer's instructions. A reaction mix, containing biotin ligase (BirA, a gift of Dr Jie Lin, University of Melbourne) and 440 µL each of Biomix A and Biomix B (Table 2.2), was prepared separately before being added to 3.5 mL of CD1 in Tris buffer (10 mM, pH 8.0). BirA was added to monomeric CD1 at a ratio of 2.5 µg of enzyme/mg protein and incubated overnight at 28 °C.

Biotinylated monomer was concentrated using a Vivaspin 6 concentrator (Satorius) and equilibrated into TBS (Table 2.2). Protein was purified over a HiLoad 16/600 Superdex 200 pg gel filtration column (GE Healthcare) using the ÄKTA fast protein liquid chromatography (FPLC) system (GE Healthcare). Fractions collected were assessed by SDS-PAGE and selected fractions were concentrated. Purified 0.1 mg aliquots of biotinylated protein were stored at -20 °C or at -80 °C for long-term storage.

2.3.5 Loading of CD1 with lipid antigens

Lipid antigens were prepared by dissolving them in 0.5% (v/v) tyloxapol (Sigma) in TBS. Lipids were sonicated in an Ultrasonic Bath (Unisonics Australia) for 15 minutes prior to being added to protein. Each lipid was incubated with protein overnight at room temperature (RT, 21-22°C). Lipids used and their respective presentation molecule are listed in Table 2.3. Most lipid antigens loaded into CD1a were added at a 6:1 lipid:protein molar ratio, unless otherwise stated.

2.3.6 Tetramerisation of CD1 Monomers

To tetramerise monomeric CD1, streptavidin-PE (BD Pharmingen), streptavidin-BV421 (BioLegend), or streptavidin-PE-Cy7 (BD Pharmingen) were added to biotinylated CD1 in a MW ratio of 4:1 CD1:streptavidin. One fifth of the total streptavidin volume was added at a time with a 10-minute incubation between each addition.

Table 2.3. Purified CD1 and MR1 antigens

Antigen	Presentation Molecule	Supplier	Molecular Weight Loading Ratio
Dideoxymycobactin (DDM) – 840 A	CD1a	Janice Cheng, Bio21 Institute, University of Melbourne	6:1
DDM – 840 B	CD1a	Janice Cheng, Bio21 Institute, University of Melbourne	6:1
DDM – 840 C	CD1a	Janice Cheng, Bio21 Institute, University of Melbourne	6:1
DDM – 840 D	CD1a	Gift of Janice Cheng, Bio21 Institute, University of Melbourne	6:1
C15:2 urushiol CAS: 83258-37-1	CD1a	Novachem	15:1
C12-15 alkyl benzoate CAS: 68411-27-8	CD1a	Making Cosmetics	varies as indicated
C16:0 Sphingomyelin (SM) CAS: 6254-89-3	CD1a	Avanti Polar Lipids	6:1
C24:1 SM CAS: 94359-13-4	CD1a	Avanti Polar Lipids	6:1
C42:2 Phosphatidyl choline (PC) CAS: 8002-43-5	CD1a	Avanti Polar Lipids	6:1
Glucose monomycolate (GMM) (C32)	CD1b	Gift of Branch Moody, Brigham and Women's Hospital, Harvard Medical School	6:1
Mannosyl-β1-phosphomycoketide (MPM) (C32)	CD1c	Gift of Branch Moody, Brigham and Women's Hospital, Harvard Medical School	6:1
α-Galactosylceramide (α-GalCer), KRN7000 CAS: 158021-47-7	CD1d	Avanti Polar Lipids	3:1
α-GalCer, PBS-44	CD1d	Gift of Paul Savage, Brigham Young University	3:1
5-(2-oxopropylideneamino)-6-D-ribitylaminouracil (5-OP-RU)	MR1	Gift of David Farlie, University of Queensland *MR1 refolded in house with permission from Jim McCluskey's group	100:1

2.4 Flow Cytometry

2.4.1 Cell staining for flow cytometry

Single cell suspensions were washed in PBS and stained with a surface mAb cocktail and tetramer for 30 minutes at RT in FACS buffer (Table 2.2). All antibodies used in these studies are listed in Table 2.4. Note that prior to staining, PBMC samples were first

incubated with 50 mM dasatinib (gift from the Peter MacCallum Cancer Centre Pharmacy) in PBS for 30 minutes at 37 °C to block TCR recycling (Weichsel et al., 2008).

Following antibody staining, samples were washed in FACS buffer (Table 2.2), fixed with 1% paraformaldehyde for 10 minutes at 4 °C (if not being FACS-sorted) and analysed by flow cytometry on an LSR Fortessa (BD Biosciences). Cells being collected for *in vitro* expansion or single cell sequencing, were sorted using an Aria III (BD Biosciences). Compensation was performed by adding each antibody to anti-mouse or anti-rat/hamster Ig Compensation Beads (BD Biosciences) according to manufacturer's instructions.

Table 2.4. Flow cytometry antibodies and viability dyes

Immunogen	Fluorochrome/ conjugate	Clone	Isotype	Dilution	Manufacturer	Cat. #
7-aminoactinomycin D (7-AAD)	-	-	-	2 µg/mL in DMSO	Sigma	A9400-1MG
CD195 (CCR5)*	BV421	J418F1	Rat IgG_{2b}, κ	1/100	BioLegend	359118
CD196 (CCR6)	BV496	11A9	Ms IgG_1, κ	1/100	BD Horison	564659
CD196 (CCR6)*	BV785	GO34E3	Ms IgG_{2b}, κ	1/100	BioLegend	353422
CD11b	BV711	M1/70	Rat IgG_{2b}, κ	1/200	BioLegend	101241
CD11c	FITC	Bu15	Ms IgG_1, κ	1/50	BioLegend	337214
CD14	APC-Cy7	MΦP9	Ms IgG_{2b}, κ	1/100	BD Pharmingen	557831
CD161	PE-Cy7	HP-3G10	Ms IgG_1, κ	1/50	BioLegend	339918
CD19	APC-Cy7	HIB19	Ms IgG_1, κ	1/30	BioLegend	302218
CD1a	BV421	HI149	Ms IgG_1, κ	1/100	BioLegend	563938
CD1a	APC	HI149	Ms IgG_1, κ	1/100	BioLegend	559775
CD1a	Purified	HI149	Ms IgG_1, κ	1/100	BioLegend	300102
CD1a	PE	SK9	Ms IgG_1, κ	1/100	eBioscience	12-0017-41
CD1b	APC	SN13	Ms IgG_1, κ	1/50	BioLegend	329110
CD1b	Purified	SN13	Ms IgG_1, κ	1/100	BioLegend	329102
CD1c	Purified	L161	Ms IgG_{2b}, κ	1/100	BioLegend	331502
CD1d	Purified	51.1	Ms IgG_1, κ	1/100	BioLegend	350304
CD1c	AF647	L161	Ms IgG_{2b}, κ	1/100	BioLegend	331510
CD1d	PE	42.1	Ms IgG_{2b}, κ	1/100	BD Pharmingen	550255

CD1d	PE-Cy7	51.1	Ms IgG_1, κ	1/100	BioLegend	350309
CD20*	PE-CF594	2H7	Ms IgG_{2b}, κ	1/200	BD Horizon	562295
CD218a (IL-18Ra)	APC	H44	Ms IgG_1, κ	1/50	eBioscience	17-7183-42
CD27*	BV786	O323	Ms IgG_1, κ	1/100	BioLegend	302832
CD27*	BV510	M-T271	Ms IgG_1, κ	1/100	BioLegend	356420
CD28*	BV711	CD28.2	Ms IgG_1, κ	1/50	BioLegend	302948
CD3	APC	UCHT1	Ms IgG_1, κ	1/50	BD Pharmingen	555335
CD3	AF700	UCHT1	Ms IgG_1, κ	1/50	BD Pharmingen	557943
CD3	BUV395	UCHT1	Ms IgG_1, κ	1/50	BD Pharmingen	563546
CD3	BV421	UCHT1	Ms IgG_1, κ	1/50	BD Pharmingen	562426
CD3*	Purified	SP34-2	Ms IgG_1, κ	1/50	BD Pharmingen	551916
CD3 (NA/LE)	Purified	UCHT1	Ms IgG_1, κ	1/500	BD Pharmingen	555329
CD3*	AF700	SP34-2	Ms IgG_1, κ	1/100	BD Pharmingen	557917
CD36	APC	5-217	Ms IgG_{2a}, κ	1/100	BioLegend	336208
CD4	AF700	RPA-T4	Ms IgG_1, κ	1/100	BD Pharmingen	557922
CD4	BV421	RPA-T4	Ms IgG_1, κ	1/50	BD Horizon	562424
CD4	BUV496	SK3	Ms IgG_1, κ	1/50	BD Horizon	564651
CD4*	FITC	L200	Ms IgG_1, κ	1/200	BD Pharmingen	550628
CD4*	BV605	RPA-T4	Ms IgG_1, κ	1/200	BioLegend	300556
CD42b	APC	HIP1	Ms IgG_1, κ	1/50	BD Pharmingen	551061
CD45	AF700,	2D1	Ms IgG_1, κ	1/100	BioLegend	368514
CD45	PE-Cy7	HI30	Ms IgG_1, κ	1/100	BD Pharmingen	557748
CD45	BV510	HI30	Ms IgG_1, κ	1/100	BioLegend	304041
CD45**	BUV395	D058-1283	Ms IgG_1, κ	1/100	BD Horizon	564099
CD45RO	AF700	UCHL1	Ms IgG_{2a}, κ	1/100	BioLegend	304218
CD56	BV605	HCD56	Ms IgG_1, κ	1/30	BioLegend	318333
CD61	APC	VI-PL2	Ms IgG_1, κ	1/100	BioLegend	336422
CD62p	BV650	AK-4	Ms IgG_1, κ	1/100	BD Horizon	564035
CD69	PE	FN50	Ms IgG_1, κ	1/50	BD Pharmingen	555531
CD69*	APC-Fire	FN50	Ms IgG_1, κ	1/50	BioLegend	310946
CD8*	BV650	RPA-T8	Ms IgG_1, κ	1/400	BioLegend	301041
CD8α	BUV805	SK1	Ms IgG_1, κ	1/400	BD Pharmingen	564912
CD95*	FITC	DX2	Ms IgG_1, κ	1/50	BD Pharmingen	556640

CLA	BV421	HECA-452	Rat IgM, κ	1/50	BD Horizon	563961
CLA	FITC	HECA-452	Rat IgM, κ	1/50	BD Pharmingen	555947
EpCam*	PE Dazzle	EBA-1	Ms IgG_1, κ	1/100	BD Horizon	565399
FoxP3	BV421	206D	Ms IgG_{2a}, κ	1/100	BioLegend	320123
FoxP3	AF647	259D	Ms IgG_{2a}, κ	1/100	BioLegend	320214
Goat anti-mouse Ig	PE	Polyclonal	Gt Ig	1/100	BD Pharmingen	550589
Goat anti-mouse Ig	BV421	Poly4053	Gt Ig	1/100	BioLegend	405317
ICOS*	PerCP-Cy5.5	C398.4A	Armenian hamster IgG	1/100	BioLegend	313517
IFN-γ	FITC	4S.B3	Ms IgG_1, κ	1/100	BD Pharmingen	554551
IFN-γ	PE	4S.B3	Ms IgG_1, κ	1/100	BD Pharmingen	554552
IL-10	PE	JES3-9D7	Ms IgG_1, κ	1/50	BioLegend	501404
IL-17A	APC	eBio64DEC17	Ms IgG_1, κ	1/50	eBioscience	17-7179-42
IL-18Ra*	PE-Cy7	H44	Ms IgG_1, κ	1/50	Miltenyi	130-101-723
Live/dead	Near infrared	-	-	1/1000	Invitrogen	L34976
Live/dead	Aqua	-	-	1/1000	Invitrogen	L34966
Ms IgG_1, κ isotype control	PE-Cy7	MOPC-21	Ms IgG_1, κ	1/100	BioLegend	400125
Ms IgG_{2b}, κ isotype control	APC	MPC-11	Ms IgG_{2b}, κ	1/100	BioLegend	400319
PLZF	PE	Mags.21F7	Ms IgG_1, κ	1/50	eBioscience	12-9320-80
RORγ-t	AF647	Q21-559	Ms IgG_{2b}, κ	1/100	BD Pharmingen	563620
SCARB1 (CD36L1)	APC	m1B9	Ms IgG_1, κ	1/100	BioLegend	363207
TCR	PE-Cy7	B1	Ms IgG_1, κ	1/50	BD Pharmingen	655410
TCR γδ	FITC	11F2	Ms IgG_1, κ	1/50	BD Pharmingen	347903
TCR Vα7.2*	BV421	3C10	Ms IgG_1, κ	1/100	BioLegend	351715
TCR Vα7.2*	BV711	3C10	Ms IgG_1, κ	1/100	BioLegend	351732
TCR Vδ2	BV711	B6	Ms IgG_1, κ	1/60	BioLegend	351732
TNF-α	BV421	Mab11	Ms IgG_1, κ	1/50	BD Horizon	562783
Vβ11	FITC	C21	Ms IgG_{2a}, κ	1/10	Beckman Coulter	TCRBV11S1
Vβ3	FITC	JOVI.3	Ms IgG_{2a}, κ	1/20	BD Pharmingen	566432

*Anti-human antibodies that were also used to label macaque samples
**Non-human primate (NHP)-specific

2.4.2 Intracellular stains

For experiments employing intracellular staining, cells were initially stained with a near-infrared fixable viability dye (Invitrogen) in PBS for 15 minutes at RT, washed, and stained with a standard surface mAb and tetramer cocktail for 30 minutes at RT. Once surface marker staining was complete, cells were permeabilised using a Foxp3/Transcription Factor staining buffer set kit (eBioscience) following manufacturer's instructions. Briefly, cells were permeabilised for 1 hour at 4°C, stained with intracellular cytokine or transcription factor mAbs (listed in Table 4) in permwash reagent for a further hour at 4°C, and then washed twice with permwash reagent. Cells were then resuspended in FACS buffer ready for analysis by flow cytometry.

2.4.3 Magnetic enrichment

10^8 cells from a buffy coat donor were initially labelled with tetramer (and no other surface mAbs) for 45 min at RT, rocking periodically. Tetramers used in MACS-enrichment were conjugated to PE, and for samples that were stained with two tetramers, PE-Cy7-conjugated tetramers were used for the dual-stain. Following incubation with tetramer, cells were washed in FACS buffer and then incubated with anti-PE beads (Miltenyi Biotec) in MACS buffer (Table 2.2) for 30 minutes at 4°C, rocking halfway.

Tetramer$^+$ cells were magnetically enriched by passing samples over cold LS MACS columns attached to a magnetic stand (Miltenyi Biotec), which were washed thoroughly with MACS buffer before being removed from the magnetic stand to elute bound tetramer$^+$ cells from the column as per manufacturer's instructions.

2.4.4 Flow cytometry data analysis

All flow cytometry data was analysed using Flowjo Software (Treestar). Unless otherwise stated, FACS plots of primary human cells were gated on CD14$^-$CD19$^-$ lymphocytes after dead cell and doublet exclusion. FACS plots of T cell line samples were gated on GFP^{hi} cells following dead cell and doublet exclusion.

2.5 TCR Sequencing

2.5.1 Reverse transcription

CD1 tetramer^{+}-sorted cells were single cell sorted for sequencing. cDNA was generated by reverse transcription using the Superscript VILO Reverse Transcription Kit (Invitrogen). 2 µL of reaction mix was added to each sample containing 0.2 µL Superscript VILO reverse transcriptase (10x, Invitrogen), 0.4 µL Superscript VILO buffer (5x, Invitrogen), and 0.22 µL TritonX-100 (0.1%, Sigma) in H_2O (Baxter). Samples were incubated at 25°C for 10 min, 42°C for 120 minutes, and 85°C for 5 minutes in a Mastercycler^{TM} thermocycler (Eppendorf).

2.5.2 Nested Polymerase Chain Reaction (PCR)

TCR transcripts from each cell were amplified by two rounds of multiplex nested PCR as previously described (Kedzierska et al., 2004, Uldrich et al., 2013). Briefly, each round of PCR was performed in 25 µL reaction mixtures containing 2 µL DNA template, 2 x GoTaq PCR master mix (Promega) and 0.5 µL of each primer/primer mix (5 µM) as previously described (Uldrich et al., 2013, Wang et al., 2012). To amplify both α- and β-chains, *TRAC* and *TRBC* genes were targeted by the reverse primer and a mixture of forward primers targeted 40 *TRAV* or *TRBV* genes. The first, external round of PCR amplified both chains together while reactions for α- and β-chains were performed separately for the second, internal round. Both rounds of nested PCR were performed under the following conditions: 94°C for 2 minutes followed by 35 cycles of 94°C for 30 sec, 52°C for 30 sec, and 72°C for 1 minute, followed by a final cycle of 95°C for 1 minute, 52°C for 1 minute and 72°C for 7 minutes in a thermocycler (Eppendorf).

2.5.3 DNA Agarose gel electrophoresis

Agarose gel electrophoresis was employed to confirm the presence of PCR products. 1% (w/v) agarose gels were prepared using agarose (BioRad) in TBE with 0.01% SyberSafe (Invitrogen) into a cast (BioRad) lined with 30-well combs (BioRad). Set gels were placed into an electrophoresis gel box (BioRad) with the combs removed and wells were submerged in TBE running buffer (Table 2.2). Samples were prepared by adding 10 x

DNA loading buffer to second round DNA product and loaded into wells. A 2-log DNA ladder (New England BioLabs (NEB)) was added to each row on the gel to determine sample size and concentration. Electrophoresis was conducted at 100 V for 1 hour. Following electrophoresis, the gel was visualised using the GeneSnap software in conjunction with a G:Box gel imaging cabinet (SynGene).

2.5.4 Sequencing reaction

DNA samples that produced a visible band in agarose gel electrophoresis were selected for TCR sequencing. PCR products were purified by adding 5 µL of DNA product to 1 µL of ExoSAP-IT (Affymetrix). This was incubated at 37°C for 15 minutes to degrade remnant primers and nucleotides, followed by 15 minutes at 80°C to inactivate the ExoSAP-IT in a thermocycler (Eppendorf).

Treated PCR products were prepared for TCR sequencing by adding a sequencing reaction mixture containing 1 µL DMSO, 5 µL 5 x Big Dye buffer, 1 µL reverse *TRAC* or *TRBC* internal primer (5 µM), 1 µL Big Dye v3.1 (Applied Biosystems) and 6 µL H_2O (Baxter) to the DNA template for a total reaction volume of 20 µL. Sequencing PCR was conducted by heating samples to 95°C for 5 minutes, followed by 30 PCR cycles of 96°C for 10 sec, 50°C for 5 seconds, and 60°C for 4 minutes. Wells were ethanol-dried and capillary separation was performed by the Centre for Translational Pathology, The University of Melbourne, and the Australian Genome Research Facility. 4Peaks (Nucleobytes) and CLC Main Workbench (Qiagen) were utilised for analysis in conjunction with the IMGT database.

2.6 RNA Sequencing

RNA-seq libraries were generated for sequencing from individual cells using the Smartseq2 protocol, slightly modified from that previously outlined (Picelli et al., 2013).

2.6.1 Cell lysis and reverse transcription

Cells were single cell-sorted directly into wells containing 2 µL of lysis buffer. Cell lysis buffer was prepared by adding 0.05 µL RNase Inhibitor (Clontech), 0.095 µL Triton X-

100 (0.2% v/v, Sigma-Aldrich), 0.5 µL dNTP mix (10 mM, Promega), and 0.5 µL Vir70 oligo-dT primer (5 µM, Sigma, *Table 2.5*). Each plate was placed immediately on dry ice following sorting and transferred to -80°C for storage or used immediately in reverse transcription.

Table 2.5. Primers used in RNA-Sequencing cDNA library preparation

Primer	Supplier	Concentration	Sequence
Vir70	Sigma	10 µM	5'-AAGCAGTGGTATCAACGCAGAGTACT$_{30}$VN-3' where "N" is any base and "V" is either "A", "C" or "G"
Vir54	Exiqon	100 µM	5'-AAGCAGTGGTATCAACGCAGAGTACATrGrG+G-3'
Vir52	Sigma	6.25 µM	5'-AAGCAGTGGTATCAACGCAGAGT-3'

Cells in lysis buffer were incubated at 72°C for 3 minutes and then placed immediately on ice for 2 minutes, prior to the addition of 3 µL reverse transcription reaction mixture. Reverse transcription was performed using the SuperScript II Reverse Transcription kit (Invitrogen) in a final reaction volume of 5 µL. The reaction mixture contained 100 U SuperScript II reverse transcriptase (Invitrogen), 1 x SuperScript II buffer (Invitrogen), 5 U RNase Inhibitor (Clontech), 5 mM DTT (Invitrogen), 1 M Betaine (Sigma), 0.6 M $MgCl_3$ (Sigma Aldrich), 1 µM Vir54 primer (Exiqon, *Table 2.5*), 1:400 million dilution of ERCC Spike-in (ThermoFisher) and nuclease-free water. The reverse transcription reaction was carried out by incubating at 42°C for 90 minutes, followed by 10 cycles of 50°C for 2 minutes and 42°C for 2 minutes. Finally, reverse transcription was inactivated by incubation at 15 minutes at 70°C.

2.6.2 PCR amplification of cDNA libraries

The KAPA HiFi HotStart ReadyMix Kit (ClonTech) was used for PCR amplification of cDNA. All reactions used non-specific primers (ISPCR oligo, Vir52 from Sigma, *Table 2.5*). For a total reaction volume of 12.5 µL, 7.5 µL of PCR mix was added to each sample containing 1 x KAPA HiFi HotStart ReadyMix (KAPA Biosystems) and 50 mM Vir52 primer (*Table 2.5*) in nuclease-free water. Initial denaturation occurred at 98°C for 3 minutes, followed by 28 PCR cycles at 98°C for 20 sec, 67°C for 15 sec, and 72°C for 6 minutes, then a final extension round at 72°C for 5 minutes. PCR products were purified using AMPure XP beads (Beckman Coulter) which were added at a 0.8 bead: sample ratio

by volume and purified over a magnetic stand to collect an 11 µL final eluate in nuclease-free water.

2.6.3 Assessment and quantification of cDNA

Samples quality was assessed using a HT DNA 1k/12k, High Sens LabChip (Perkin Elmer). 2 µL of sample was added to 8 µL of HPLC water, loaded into the Labchip with the HT DNA High Sens Reagent kit (Perkin Elmer) and run on the LabChip GXII Touch (Perkin Elmer) as per manufacturer's instructions. Wells for which the electropherogram revealed few or no peaks, or an over-abundance of very small (< 300 bp) or very large (> 7000 bp) peaks were excluded from further analysis.

PCR products that yielded sufficient quality scores with LabChip assessment were quantified using the Quant-iT PicoGreen dsDNA Assay Kit (ThermoFisher) according to manufacturer's instructions. Briefly, PicoGreen Dye (ThermoFisher) and TE buffer (ThermoFisher) were added to each sample. Fluorescence was measured using the CLARIOstar microplate reader (BMG Labtech) and GraphPad Prism was used to convert raw CLARIOstar RFU data to ng/µL concentrations. Dilutions of samples in HPLC water (Sigma Aldrich) were prepared to achieve concentrations of 0.2 ng/µL for tagmentation.

2.6.4 Tagmentation reaction and final PCR amplification

PCR products were tagmented with unique barcodes using the Nextera XT DNA Library Preparation Kit (Illumina). To 1 µL of 0.2 ng/µL cDNA, 2 µL Tagment DNA Buffer (Illumina) and 1 µL Amplicon Tagment Mix (Illumina) were added, and samples were incubated at 55°C for 5 minutes. Once samples had cooled to 10°C, 1 µL of Neutralize Tagment Buffer (Illumina) was added to each well and samples were incubated at RT for 5 minutes. The whole 5 µL volume of tagmented and neutralised gDNA was then used for limited-cycle enrichment PCR, along with 3 µL Nextera PCR Master Mix (Illumina), 1 µL of each Index 1 adapters (N, i7), and 1 µL of each Index 2 adapters (S, i5). A second amplification round was performed as follows: 72°C for 3 minutes, 95°C for 30 secs, then 13 cycles of 95°C for 10 secs, 55°C for 30 secs, 72°C for 30 secs, followed by a final

incubation at 72°C for 5 minutes. Nextera libraries were purified using AMPure XP beads at a 0.6 bead: sample ratio (i.e. 6 µL: 10 µL). HPLC water was added to elute bound PCR product in a volume of 11 µL, which was collected for LabChip analysis. Following quality assessment using the LabChip, plates were transferred to -80°C for long term storage and then shipped to Fabio Luciani's group at the Kirby Institute, University of New South Wales for sequencing and statistical analyses.

2.6.5 RNA sequencing data analysis

Single cell RNA-seq data was analysed using the software R with libraries: *SingleCellExperiment, scater, scran, SC3, MAST, data.table* and *pheatmap,* available from The Comprehensive R Archive Network (CRAN) (https://cran.r-project.org) and Bioconductor (http://bioconductor.org). Single cell experiment data was loaded into R, removing any genes with no reads from the dataset. Mitochondrial genes and the ERCC spike-ins (ThermoFisher, cat no. 4456740) were used as control features. For cell quality control, total count and total number of genes detected per cell were assessed and low-quality cells ($< 2x10^5$ reads or 600 genes, or > 20% ERCC spike-in transcripts) were excluded. Next, for gene quality control, highly expressed genes were assessed. Three genes, long non-coding RNAs (LincRNAs: FP236383.2, FP671120.3, FP236383.3), accounted for 22% of total expression each, and were removed from the dataset. The relationship between mean expression and dropout rate were compared to ensure reliable detection; genes with mean expression < 5 in fewer than three cells were filtered out. The filtered dataset was normalised using the deconvolution methods from the *scran* package to make expression values comparable between cells for PCA analysis. Next, batch correction was performed to remove variability in gene expression due to donor variation and experimental design. Clustering of the dataset and determination of differential gene expression was performed using the *SC3* package, where three clusters provided the best separation of different cell types. Differential gene expression analysis was also performed using *MAST* to compare cell types in pairs, and NKT cells were set as a base for comparison. Differential genes were reported only with an adjusted p-value <0.01 and an absolute log fold change >1.

2.7 Cellular Assays

2.7.1 Production of TCR-expressing and CD1-expressing cell lines

SKW-3 and Jurkat.76 (J.76) were selected as T cell lines, both of which are derived from T-acute lymphoblastic leukaemia lines (Heemskerk et al., 2003, Shima et al., 1986). They are devoid of endogenous TCR rearrangement and expression, and therefore can be engineered to express a TCR of interest (Burger et al., 1999, Voss et al., 2008). The C1R cell line, an Epstein-Barr virus-transformed B lymphoblast, was selected as an APC line devoid of surface HLA-A and HLA-B antigens (Storkus et al., 1989). All cell lines were cultured in RF-10 complete media at 37°C, 5% CO_2.

Full-length TCR α- and β-chain genes were cloned into a 2A-peptide-linked pMIG expression vector to generate cell lines by the retroviral transduction of αβ-TCR-deficient J.76 or SKW-3 cells using a similar protocol to that described previously (Holst et al., 2006).

Selected TCR sequences (Appendix II) were ordered as Strings™ DNA fragments (Thermo Fischer) and were cut with *EcoRI* and *BglII* restriction enzymes to be ligated into a pMIG expression plasmid vector (gifted by Dr. Dario Vignali (Memphis, Tennessee)) cut with the same restriction enzymes. DNA fragments were ligated into the recipient pMIG vector with T4 DNA Ligase (New England Biolabs) according to the manufacturer's instructions at an insert to vector ratio of 6:1 and incubated overnight at 4°C.

Ligated DNA plasmids were used to transform and select DH5α (*Escherichia coli*) cells so that only properly ligated pMIG vectors with the desired insert were selected for in media containing 100 mg/mL ampicillin (supplied by the Media Preparation Unit, The Doherty Institute). Selected pMIG plasmids were purified with miniprep or maxiprep kits (Zymogen) in accordance with the amount of DNA required and sequence verified.

Purified pMIG expression vector containing full-length TCR constructs and a similar vector encoding CD3ε, δ, γ, and ξ in a 1:1 ratio were transfected into HEK 293T cells using FuGENE-6 transfection reagent (Promega), with packaging vectors pEQ-Pam3(-E) and pVSVg. All expression and packaging vectors were kindly provided by Dr. Dario

Vignali (Memphis, Tennessee). Retroviral supernatant was harvested and then used to transduce WT J.76 or SKW-3 cells daily for six days. For transient transfections, TCR and CD3 pMIG vectors were used to co-transfect HEK 293T cells using FuGENE-6 transfection reagent (Promega). Cells were harvested at 24-36 hours after transfection for analysis.

The appropriate *M.nemestrina* CD1 genes (*CD1A, CD1B, CD1C,* and *CD1D*) were cloned into pMIG expression vectors and used to transfect WT C1R cells in a similar manner to produce antigen-presenting cell lines that express macaque CD1 molecules.

2.7.2 Expansion of primary human T cells

Tetramer$^+$ T cells were FACS-sorted and stimulated *in vitro* for four days with plate-bound anti-CD3 and soluble anti-CD28. A 96-well U-bottom plate (CellStar) was coated with 10 μg/mL purified anti-CD3 mAb (clone UCHT1 [BD Pharmingen] for human T cells or clone SP34-2 [BD Pharmingen] for macaque T cells) and 2μg/mL purified anti-CD28 mAb (clone 28.2, BD Pharmingen) for 4 hours at 37°C. Wells were washed with PBS and samples were cultured in these wells in T cell culture media (refer to Section 2.1) with phytohemagglutinin-P (PHA) (1 μg/mL, Sigma), rhuIL-2 (100 U/mL, Peprotech]), and rhuIL-7 (50 ng/mL, eBioscience]). After 4 days, cells were removed from CD3, CD28 and PHA stimulation and allowed to expand for 2-3 weeks in the presence of rhuIL-2 and rhuIL-7.

Skin explants were trimmed of subcutaneous fat and cut into 2 x 2 cm^2 pieces to be cultured on sterile sponge (GelFoam). Each explant was set on a sponge square cut to the same size in individual wells of a 6-well culture plate (Corning). Sponge and skin explants were bathed in complete human T cell culture media with rhuIL-2 (100 U/mL, Peprotech), rhuIL-7 (50 ng/mL, eBioscience), and rhuIL-15 (2 ng/mL, Peprotech) and cultured for 1-2 weeks to promote the exit of T cells from the tissue into the media. The resulting cell-containing media was then transferred to a new 6-well culture plate to allow for cell growth in the absence of tissue explants.

2.7.3 SKW-3 and J.76 activation assays

2 x 10^4 SKW-3 or J.76 cells TCR cell lines were cultured with 3.33 x 10^3 C1R cells for 18 hours in 200 μL RF10 complete media with or without the addition of lipid antigens: DDM, GMM, MPM, α-GalCer, sphingomyelin, C12-15 alkyl benzoate or 0.5% (v/v) tyloxapol. Cells were harvested, washed once in FACS buffer and stained with CD19, CD69, and 7-AAD for 30 minutes. Cells were then washed once in FACS buffer and immediately analysed using flow cytometry. C1R cells were removed from analysis by $CD19^-$ exclusion and T cell activation was measured by CD69 upregulation.

2.8 Production of soluble human αβ-TCRs and CD1a-TCR co-complexes

2.8.1 Cloning and expression of genes encoding soluble CD1a-restricted TCRs

TCR sequences (Appendix I) were ordered as Strings™ DNA fragments (Thermo Fischer), and were digested with the appropriate restriction enzymes at 37°C for 2 hours. *NdeI* and *HindIII* were used to digest α-chain inserts, and *NdeI* and *BglII* were used for β-chain inserts. Digestion products were added to 10x DNA loading dye (Table 2.2) and were isolated by DNA-electrophoresis on a 1.5% w/v agarose gel in TBE buffer (Table 2.2). Digestion products were excised from the agarose gel and purified using the UltraClean™15 Purification Kit (Mo Bio Laboratories) following manufacturer's instructions. Purified DNA fragments were ligated with T4 DNA Ligase (New England Biolabs) into the recipient pET-30 vector (Novagen) according to the manufacturer's instructions at an insert:vector ratio of 6:1 and incubated overnight at 4°C.

2.8.2 Production of inclusion bodies

Genes encoding truncated human TCR α- and β-chains were cloned into pET30 expression plasmids (Novagen), transformed into *E.coli*, which were then induced to express the protein. Genes were then expressed as inclusion bodies in *E.coli* strain BL21 by recombinant methods as previously described (Boulter et al., 2003)**.** Purified inclusion bodies were solubilised in 8 M Urea, 20 mM Tris-HCl (pH 8.0), 0.5 mM EDTA and 1mM DTT.

2.8.3 Refolding of soluble TCRs

Soluble αβ-TCR complexes were produced by oxidative refolding of α and β proteins in a 1:1 equimolar ratio in TCR refold buffer (Table 2.2). Two injections of the α- and β-TCR protein mix into the TCR refold buffer were performed several hours apart, injecting half at a time. Refold mixtures were incubated overnight at 4°C with gentle stirring. TCR proteins contained an engineered disulphide linkage between the TRAC and TRBC domains as previously described to promote correct refolding (Boulter et al., 2003).

2.8.4 Purification of refolded human αβ-TCR

Refolded αβ-TCR complexes were dialysed for 24 hours prior to purification by size-exclusion and ion-exchange chromatography (GE Healthcare). First, refold mixtures were dialysed using spectra/por dialysis membrane with a 6-8 kDa molecular weight cut-off (MWCO) (Spectrum laboratories), dialysing in 10 mM Tris at 4°C with stirring. Tris buffer was changed every 8 h for 24 h. Dialysed mixture was collected and filtered using a 0.2 μm Nalgene rapid-flow bottle top filter (Thermo Scientific). The filtrate was passed over DEAE sepharose anion exchange columns (GE Healthcare) and eluted by connecting the column to a Äkta Pure FLPC (GE Healthcare) system and increasing NaCl concentration (from 0-200 mM) in 10 mM Tris pH 8.0.

DEAE fractions containing correctly refolded αβ-TCR (assessed with SDS-PAGE under reducing and non-reducing conditions) were pooled, concentrated and equilibrated in TBS pH 8.0 to be passed over a Superdex-75 16/600 (S75) gel-filtration column (GE Healthcare). Gel-filtration fractions of interest were again pooled, concentrated, and buffer exchanged into 10 mM Tris pH 8.0 and passed over a Mono-Q 10/100 GL anion exchange column (GE Healthcare). Proteins were eluted with a buffer gradient with an increasing concentration of NaCl (0-1M) in 10 mM Tris pH 8.0. Active fractions were pooled and concentrated in TBS and stored at -20°C at concentrations of 1-5 mg/mL.

2.8.5 Treatment of soluble CD1a for crystallography

Soluble CD1a was treated with endoglycosidase H (endo H) (NEB) to cleave oligosaccharides from N-linked glycoproteins, and thrombin (Sigma) to remove the

leucine zipper. In brief, CD1a was buffer exchanged into 50 mM sodium bicarbonate ($NaHCO_3$), pH 5.5 to a volume of 5 mL. The sample was subsequently incubated for 1 hour with 1000 units/mg of endo H at 37°C, and then equilibrated into PBS following incubation. Thrombin was added at 5.7 units per mg of CD1a for a 4 hour incubation at 37°C. CD1a was also either left loaded with endogenous lipids or loaded with DDM in a 3:1 CD1a:DDM molar ratio overnight.

2.8.6 Co-complexation of αβ-TCR with CD1a

Soluble αβ-TCR heterodimers and soluble endo H-treated CD1a were passed over a Superdex-200 16/600 (S200) gel-filtration column (GE Healthcare) prior to co-complexation. TCR protein was then mixed with soluble endo H-treated CD1a in a 1:1 mass ratio, concentrated, and passed over an S200 gel-filtration column. Fractions were eluted in TBS and stored as separate fractions at -80°C to be sent to Branch Moody's Laboratory (Brigham and Women's Hospital, Harvard Medical School) for lipid antigen discovery or to Jamie Rossjohn's Laboratory (Monash University) for X-ray crystallography.

2.9 Enzyme-Linked Immunosorbent Assay (ELISA)

ELISA assay plate wells (Falcon) were coated overnight at 4°C with 50 µL protein of interest (CD1a, CD1b and CD1c) in ELISA coating buffer (*Table 2.2)* using 2-fold serial dilutions starting at 10 µg/mL. The proceeding day, wells were washed 4 times with 200 µL PBS-T buffer (Table 2.2) and blocked with 200 µL 0.5% (w/v) BSA in PBS for 2 hours at RT. Wells were washed again and incubated with 50 µL primary antibodies (anti-CD1a, SK9, anti-CD1b, SN13, anti-CD1c, L161, or anti-CD1d, 51.1) at 3 µg/mL in PBS with BSA (PBS_5BSA) *(Table 2.2)* for 2 hours at RT. Wells were washed again and incubated with a 2 µg/mL secondary goat anti-mouse IgG mAb conjugated to horse-radish peroxidase (Abcam) in PBS supplemented with 0.5% (w/v) BSA and 0.05% (v/v) Tween20 for 1 hour at RT. Wells were then washed and incubated with 100 µL tetramethylbenzidine (TMB) buffer *(Table 2.2).* Once colour change developed adequately, 50 µL 2.25 M hydrochloric acid was added to stop the reaction. Colour change was measured on an ELISA plate reader (LabSystems Multiskan) by subtracting emission at 540nm from 450 nm.

Chapter 3. Characterisation of CD1a-restricted T cells that recognise a lipid antigen derived from M.tuberculosis

3.1 Introduction

M.tuberculosis (Mtb) is a highly prevalent pathogen and is the top infectious killer worldwide (World Health Organization, 2019). The bacterium is estimated to infect approximately one third of the global population, but cases and mortality are disproportionally skewed towards countries where it is endemic, with almost two-thirds of cases occurring within seven countries (India, Indonesia, China, Philippines, Pakistan, South Africa and Nigeria) (Floyd et al., 2018). Infection is controlled in the majority of adult cases, resulting in latent TB (Dye et al., 1999). Only 5-10% of those infected will develop active TB (Comstock et al., 1974, Vynnycky and Fine, 2000), predominantly immunocompromised adults, especially (human immunodeficiency virus) HIV^+ individuals or individuals on immunosuppressive treatments (Ai et al., 2016). In contrast, infants and young children are often unable to contain the infection, and are at risk of dissemination and developing severe systemic disease, leading to a high mortality (Dodd et al., 2017). Significant efforts made by the World Health Organisation (WHO) and its partners have reduced the number of TB-related deaths, however the death toll remains high at approximately 1.5 million deaths annually (World Health Organization, 2019)). TB prevention is predominantly through the use of a vaccine which contains a live attenuated strain of *M.bovis*, Bacillus Calmette–Guérin (BCG), which is avirulent in humans (Davenne and McShane, 2016). The BCG vaccine is widely used to prevent against severe disseminated disease in children, but it has variable effectiveness against pulmonary disease in adults (Mangtani et al., 2014, Abubakar et al., 2013, Katelaris et al., 2020, Davenne and McShane, 2016).

While the BCG vaccine has been used globally for decades, TB eradication is not possible without a vaccine that protects the entire population (Lonnroth et al., 2015, Matteelli et al., 2018, Sakamoto et al., 2019). It is clear that the vaccine needs to induce a stronger immune response for better protection, however it is not yet completely clear what constitutes an effective immune response in TB.

Studies of BCG vaccine efficacy have revealed the important role of T cells in establishing protection (Andersen and Scriba, 2019). The BCG vaccine contains a largely

complete set of mycobacterial antigens; including highly immunogenic cell wall lipids (Andersen and Doherty, 2005, Kroesen et al., 2019), some of which can be presented by CD1 molecules (Van Rhijn et al., 2013b). The importance of these lipids in generating an immune response is highlighted by the fact that loss of lipid factors reduces vaccine efficacy. The frequency and functionality of mycobacteria-specific T cells in immunised newborns have not been found to correlate with protection or susceptibility (Kagina et al., 2010), although their immune response may be different to adults, as lipid-reactive T cells differ with age (de Lalla et al., 2011).

Lipid-reactive T cells have not yet been considered in TB vaccine design (Andersen and Scriba, 2019), but evidence suggests that they may augment protective immune responses. CD1a-restricted T cell clones exhibit potent reactivity towards the mycobacterial lipid, DDM (Moody et al., 2004). Furthermore, DCs in sites of cutaneous *M.leprae* infection present lipid antigens via CD1a, and group 1 CD1 expression in leprosy lesions correlates with effective immunity, suggesting a role for CD1a and other CD1 molecules in other mycobacterial infections (Sieling et al., 1999). In addition, mycobacterial cell wall lipids also induce group 1 CD1 expression on monocytes through TLR-2 signalling, indicating that CD1 expression and function can be activated through innate signals (Roura-Mir et al., 2005b). Mycobacterial lipids may therefore function as adjuvants and/or cognate T cell antigens to elicit protective CD1-restricted responses in infection (O'Garra et al., 2013).

CD1a-autoreactive T cells studied to date are predominantly $CD4^+$ and their production of IFN-γ and/or IL-2 has been used as a measure of their activation *in vitro* (de Jong et al., 2010, de Lalla et al., 2011). Some also produce IL-22 in humans, or IL-17 in a CD1a transgenic mouse model (de Jong et al., 2010, Kim et al., 2016). Protection and effective clearance of Mtb rely on $CD4^+$ T cell responses (Andersen and Doherty, 2005, Sakai et al., 2014a). A recent study revealed that vaccination of rhesus macaques induces protective pulmonary Th1 and/or Th17 cells to secrete IFN-γ, TNF, IL-2 and IL-17 (Dijkman et al., 2019). The rapid secretion of Th1 and Th17 cytokines by unconventional T cells, such as CD1a-restricted T cells, may also contribute to the clearance of Mtb (Godfrey et al., 2015).

Many enumeration and functional studies of CD1a-restricted T cells to date have involved culture of these cell *in vitro* and assessing reactivity to self-lipids. CD1a-autoreactive T cells are estimated to constitute 0.1-10% of peripheral blood T cells (de Jong et al., 2010, de Lalla et al., 2011). CD1a tetramers have since been used to isolate small populations of CD1a-restricted T cells that recognise DDM *ex vivo*, but not those that were autoreactive (Kasmar et al., 2013). To date, the capacity to identify CD1a-restricted T cells isolated by *in vitro* culture and tetramer labelling methods has enabled their basic characterisation, providing some important clues into their immunological role, yet further research to investigate these cells direct *ex-vivo* is warranted. Furthermore, their response to mycobacterial lipids, such as DDM, remains poorly understood. To evaluate the phenotype of DDM-reactive T cells in healthy blood donors, we developed an enrichment strategy to clearly isolate and characterise these cells without the need for *in vitro* culture.

3.2 Results

3.2.1 Validation of tetramer production

CD1a molecules were produced in an HEK-293S-GnTI$^-$ mammalian expression system to make tetramers. Briefly, GnTI$^-$ cells were transiently co-transfected with pHL-sec plasmids encoding CD1a and β_2m without cytoplasmic tails and with leucine zippers, as described previously (Aricescu et al., 2006, Birkinshaw et al., 2015). CD1a molecules contained endogenous lipid antigens native to GnTI$^-$ cells and/or media, herein known as CD1a-endogenous (CD1a-endo) tetramers, as used in a previous study (Birkinshaw et al., 2015). To investigate CD1a-restricted T cells with defined lipid specificities, CD1a monomers were loaded with lipid antigens, such as DDM. CD1a protein was loaded with DDM at a 6:1 molecular weight ratio of DDM to CD1a using 0.5% (v/v) tyloxapol as a detergent to aid in lipid transfer in and out of the CD1a antigen-binding cleft. To confirm that DDM had been loaded into CD1a, CD1a-DDM monomer was tetramerised to label J.76 cell lines expressing a CD1a-autoreactive TCR, BK6 (Birkinshaw et al., 2015) or DDM-reactive TCRs, Clone 8 and Clone 15. As a control, the same volume and concentration of tyloxapol buffer alone was added to CD1a monomer prior to tetramerisation.

No staining of the wild type (WT) J-76 cell line was observed with any CD1a tetramers, indicating that neither the DDM lipid nor tyloxapol buffer used for loading caused non-specific binding of CD1a to the J-76 cell line *(Fig.3.1)*. BK6 bound CD1a-endo and CD1a-vehicle tetramers, and tetramer fluorescence intensity correlated with CD3 expression, confirming the TCR-mediated specificity (*Fig.3.1)*. However, as expected, BK6 did not bind CD1a-DDM tetramer, as DDM is "non-permissive" for BK6 binding due to its large headgroup (Birkinshaw et al., 2015). Conversely, Clone 8 and Clone 15 cell lines were labelled with CD1a-DDM tetramer but neither CD1a-endo nor CD1a-vehicle tetramers *(Fig.3.1)*, indicating successful loading of DDM, as CD8-2 does not bind CD1a otherwise (Cheng et al., 2017).

3.2.2. Isolation of CD1a-restricted T cells using magnetic enrichment

Following the validation of lipid antigen loading, we assessed the ability of CD1a tetramers to isolate CD1a-restricted T cells directly *ex vivo* from healthy human blood.

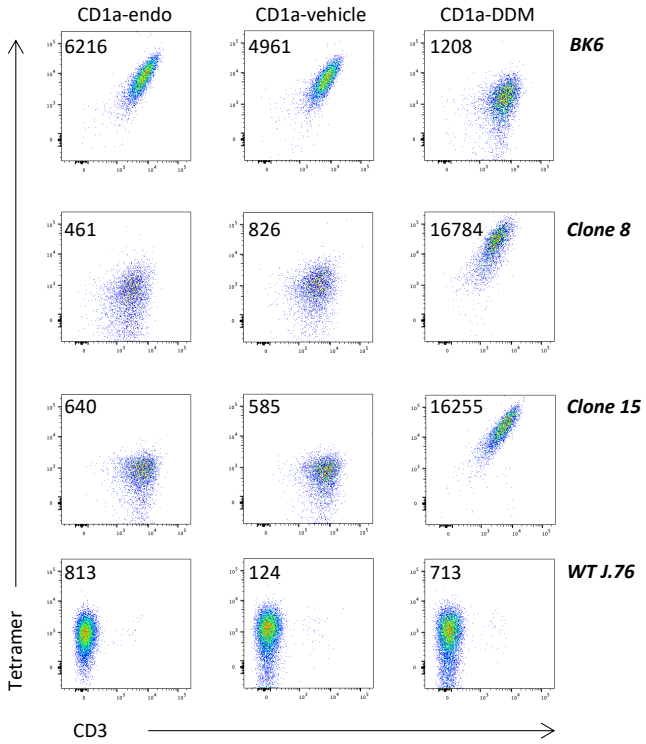

Figure 3.1. Validation of CD1a tetramer loading. CD1a monomer was produced in a GnTI^{-} mammalian expression system and loaded with DDM at a 6:1 molecular weight ratio to CD1a. CD1a containing endogenous lipids (CD1a-endo), or loaded with DDM in 0.5% (v/v) tyloxapol buffer (CD1a-DDM) or 0.5% (v/v) tyloxapol buffer (CD1a-vehicle), were tetramerised and used to label CD1a-restricted TCR-expressing J.76 cell lines BK6, Clone 8, and Clone 15. Plots are gated to represent viable GFP^{high} lymphocytes. Data representative of three independent experiments.

PBMCs were isolated from human buffy coats using Ficoll-Paque gradient centrifugation (De Paoli et al., 1984). To isolate distinct populations of CD1a-restricted T cells and enhance the fluorescence intensity of tetramer staining, we used magnetic enrichment (magnetic activated cell sorting, MACS) similar to previously described protocols for enrichment of peptide antigen-specific T cell populations (Legoux and Moon, 2012). Briefly, PBMCs were sequentially incubated with dasatinib (an inhibitor of TCR internalisation) (Lissina et al., 2009, Schade et al., 2008), CD1a tetramer conjugated to PE or PE-Cy7, and then anti-PE magnetic beads (Miltenyi) before being passed over a magnetic column to collect tetramer$^+$ cells.

To ensure sufficient recovery of tetramer$^+$ T cells, 100 x 10^6 cells of PBMCs were labelled and enriched with each tetramer. PBMCs were labelled with CD1a-vehicle and CD1a-DDM tetramers to compare staining among unenriched cells (taken prior to passing over the magnetic column) and enriched cells. Tetramer$^+$ T cells were present among unenriched cells, however, these were not clearly separated from the tetramer$^-$ cells, did not form distinct populations, and did not isolate sufficient cells for phenotypic analyses *(Fig.3.2a)*. Enriched samples revealed discrete populations of tetramer$^+$ T cells with high fluorescence intensity, suggestive of a skewing towards capturing cells that bound with the highest affinity *(Fig.3.2b)*. Whether the cells that appear to bind to CD1a tetramers with lower affinity in the unenriched samples are genuine CD1a-restricted T cells remains unclear.

In enriched samples, CD3$^-$ CD1a-tetramer$^+$ cells were isolated in several donors for both CD1a-vehicle and CD1a-DDM tetramers, however, the identity of this cell population was not determined. Tetramer binding was unlikely TCR- nor CD36-mediated as CD1a tetramer staining is not affected by anti-CD36 blocking in the same way that other CD1 tetramers are (Gherardin et al., 2021) (discussed further in Chapter 5.2.6). There may be another receptor that binds to CD1a independently of a TCR yet to be discovered, which is a subject of ongoing investigations. It is reassuring, however, that despite TCR-independent tetramer binding among non-T cells, tetramer binding among CD3$^+$ T cells was confirmed to be due to genuine CD1a-recognition as TCR sequences obtained from these cells were later used to generate CD1a-restricted T cell lines (see Chapter 4.2.2).

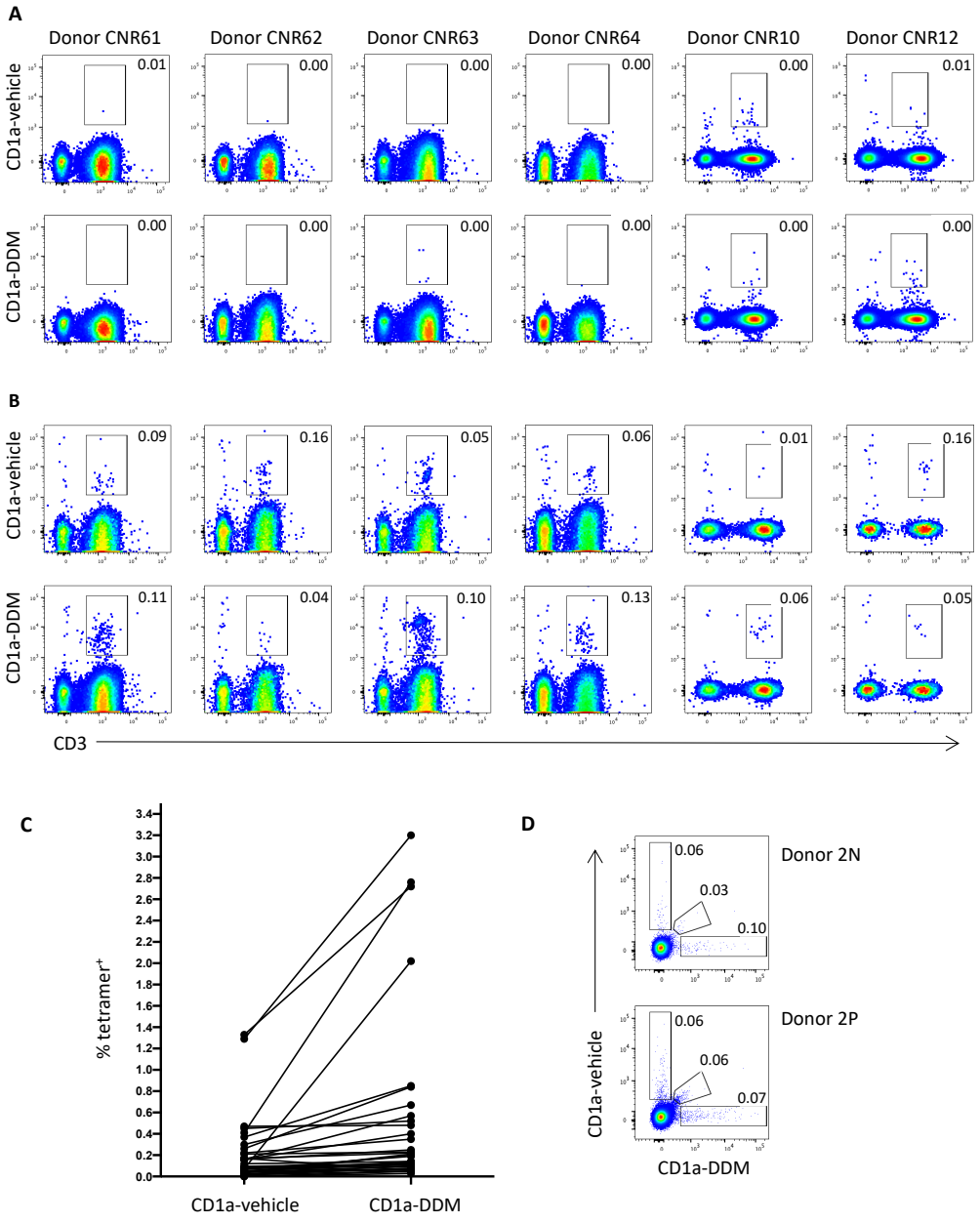

Figure 3.2. Isolation of CD1a-restricted T cell populations directly *ex vivo* from healthy human blood. Each plot represents PBMCs stained with either CD1a-vehicle or CD1a-DDM tetramer and surface antibody stain to obtain CD14$^-$ CD19$^-$ 7-AAD$^-$ single lymphocytes, **A.** without or **B.** with magnetic (MACS) enrichment. Numbers in the top right of each plot indicate the percentage of tetramer$^+$ cells in the total parental population. **C.** Cumulative data of MACS-enriched CD1a-vehicle and CD1a-DDM tetramer$^+$ cell frequencies in 52 donors in 14 independent experiments. **D.** Dual stain with CD1a-vehicle and CD1a-DDM tetramers conjugated to BV421 and PE respectively (without MACS enrichment). Data representative of four donors in two independent experiments.

CD1a-DDM tetramers consistently isolated more cells than the CD1a-vehicle or CD1a-endo tetramers (in 51/52 donors) *(Fig.3.2c)*, reflective of either the nature of the DDM tetramer containing one lipid antigen as opposed to a heterogenous mix of lipids (Birkinshaw et al., 2015), or a greater number of CD1a-restricted T cells targeting a mycobacterial lipid than self-lipids. To ascertain whether the same cells were binding both CD1a tetramers, PBMCs from four donors were stained with both CD1a-DDM and CD1a-vehicle tetramers conjugated to PE and BV421 respectively *(Fig.3.2d)*. Three distinct populations were observed: CD1a-DDM tetramer+, CD1a-vehicle tetramer+ and cells double positive for both *(Fig.3.2d)*. It is unlikely that this was the result of non-specific binding, but rather, potential cross-recognition of both antigens by a population of CD1a-restricted T cells (explored in Chapter 4.2.3). Accordingly, CD1a tetramers were used in combination with MACS-enrichment to isolate unambiguous populations of CD1a-restricted T cells from healthy human blood for further analyses.

3.2.3 Phenotypic characterisation of surface markers expressed by CD1a-restricted T cells

To phenotypically characterise CD1a-restricted T cells, CD1a tetramers were incorporated into a flow cytometry panel designed to measure co-receptor usage (CD4, CD8), memory status (CD27, CD45RO), unconventional T cell markers (IL-18R, CD161), and chemokine receptor expression (CCR7 and CLA). CD1a-autoreactive and DDM-reactive T cells were isolated by magnetic enrichment of CD1a-endo or CD1a-vehicle and CD1a-DDM tetramers respectively, and as a comparison $CD3^+$ $tetramer^-$ T cells were also analysed.

CD1a-$tetramer^+$ cells were first examined for expression of CD4 and CD8 co-receptors in 40 donors. Consistent with previous studies of cultured cells, CD1a-restricted T cells were predominantly $CD4^+$ and in some donors, up to 100% of $tetramer^+$ T cells were $CD4^+$*(Fig.3.3)*. The mean percentage of cells that were $CD4^+$ was 84.2% and 77.5% among CD1a-DDM and CD1a-vehicle $tetramer^+$ cells respectively, with small populations of $CD8^+$ and $CD4^-CD8^-$ double negative (DN) cells (*Fig.3.3)*. These proportions are similar to the co-receptor expression of CD1a-autoreactive T cells previously described (de Lalla et al., 2011, de Jong et al., 2010, Kasmar et al., 2013). The average CD4/CD8 ratio among all T cells was 2.0, which is consistent with the range generally considered normal in humans (1.5-2.5), reflecting wide heterogeneity that is

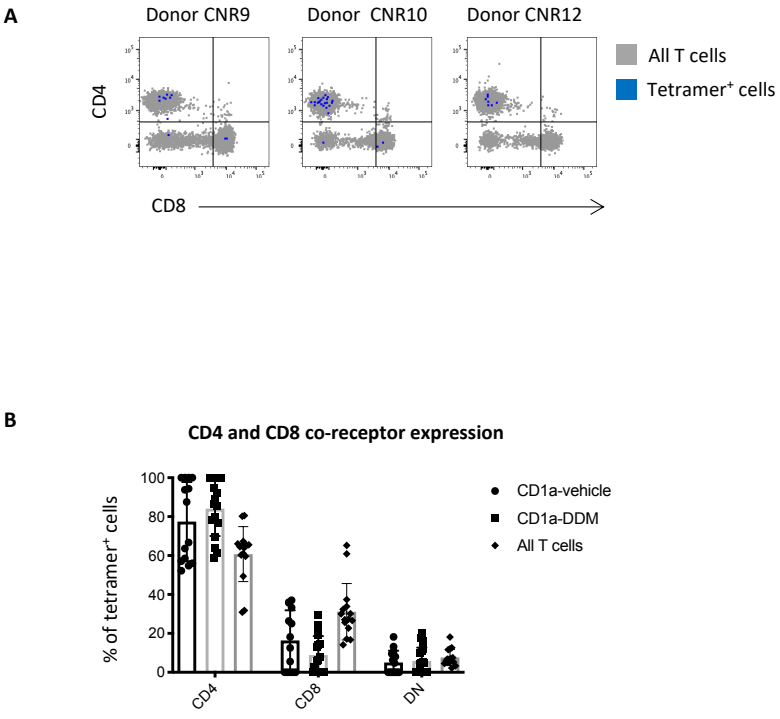

Figure 3.3. CD4 and CD8 co-receptor expression by CD1a-restricted T cells in healthy human blood. A. Gating of $CD4^+$, $CD8^+$ and double negative (DN) populations among $CD3^+$ $tetramer^+$ T cells (blue) compared to the total T cell population (grey). T cells were first identified by gating on $CD14^-$ $CD19^-$ single, live lymphocytes. **B.** Cumulative data for CD4 and CD8 co-receptor expression displaying the percentage of $tetramer^+$ cells that express each or are DN for 40 (CD1-DDM) and 38 (CD1a-endo or CD1a-vehicle) healthy blood donors.

influenced by sex, age, ethnicity, genetics, and microbial exposure (Amadori et al., 1995, McBride and Striker, 2017, Wikby et al., 2008). In contrast, the CD4/CD8 ratio rose to 9.5 and 4.7 among CD1a-DDM and CD1a-vehicle tetramer^{+} T cells respectively, suggestive of an important role of CD4 in interacting with CD1a (investigated in Chapter 4.2.9).

CD1a-restricted T cells were largely positive for the costimulatory T cell marker CD27 and displayed varying levels of the memory marker CD45RO (*Fig.3.4a, 3.4b)*. CD1a-autoreactive T cells are reportedly enriched in the naive CD45RA compartment in both newborns and adults, and the percentage of those that are CD45RO^{+} increases in adults (de Lalla et al., 2011), likely due to further T cell development and antigen exposure. In line with accumulation of the memory phenotype with age, while there was great inter-donor variability, there was a slightly greater trend of increasing frequency of CD45RO^{+} tetramer^{+} T cells compared to all T cells with age among the cohort tested (*Fig.3.4c*). Interestingly, some donors even had clonal populations of CD27^{hi}CD45RO^{+} memory T cells (clonality was verified by TCR sequencing - see *TCR 27a28* isolated from donor CNR2 in Chapter 4.2.1. The proportion of T cells that were CD45RO^{+} varied between individuals, hovering around half, which is consistent with previous quantifications of circulating CD45RO^{+} memory T cells indicating that approximately 50% and 30% are CD4^{+} and CD8^{+} respectively (Hamann et al., 1997, Lanio et al., 2009, Olson et al., 2013, van de Berg et al., 2012, Walton et al., 1998). Expression of CD27 by CD1a-restricted T cells was unsurprising given that many tetramer-negative T cells were also CD27^{+}. CD27 is typically expressed by all naive CD4^{+} T cells and by approximately 80% of the CD4^{+} memory population, as well as most naive and memory CD8^{+} T cells (De Jong et al., 1992, Hamann et al., 1997, Hintzen et al., 1993). CD27^{-} memory populations are less frequent but can include effector cells that display a high antigen recall response (although very few tetramer^{+} cells fell into this category) (Hamann et al., 1997, Schiott et al., 2004).

CD1a-restricted T cells were next interrogated for their expression of CD161 and IL-18R, markers commonly expressed by innate-like T cells such as MAIT and NKT cells (Ussher et al., 2014, Fergusson et al., 2014, Hashimoto et al., 2003). MAIT cells, identified using MR1-5-OP-RU tetramers, were clearly double positive for these markers as expected (*Fig.3.5).* In contrast, CD1a-restricted T cells consistently displayed low levels of CD161

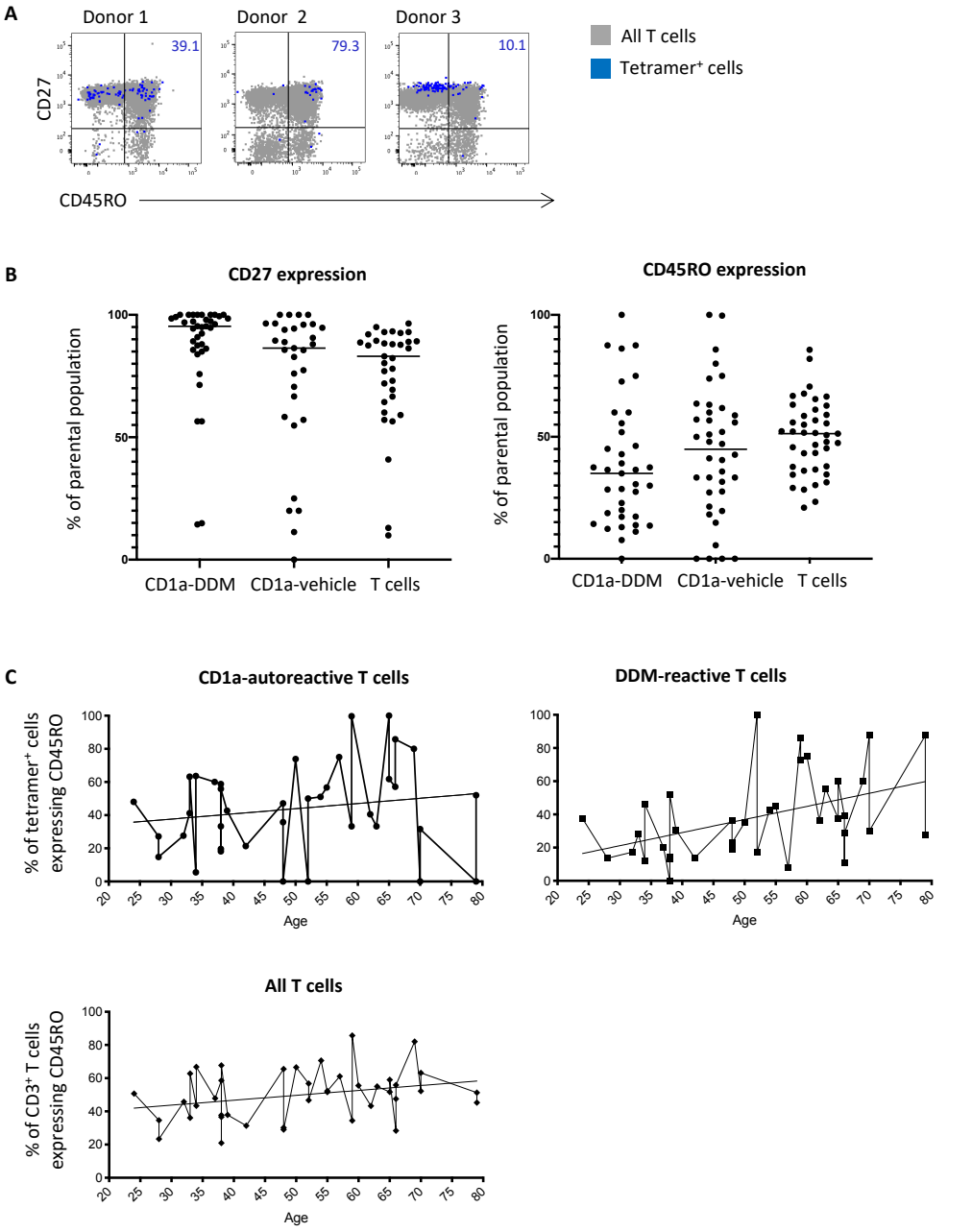

Figure 3.4. CD45RO and CD27 expression by CD1a-restricted T cells directly *ex vivo* in healthy human blood. 38 blood donors were magnetically-enriched for CD1a-DDM tetramer and CD1a-endo or CD1a-vehicle tetramer directly *ex vivo.* **A.** Gating of CD45RO$^+$ and CD27$^+$ populations among CD3$^+$ tetramer$^+$ T cells (blue) was based on the total T cell population (grey) in three donors. CD3$^+$ tetramer$^+$ T cells cells were first identified by gating on CD14$^-$ CD19$^-$ single, live lymphocytes. Numbers indicate percentage of CD27$^+$ CD45RO$^+$ cells. **B.** Percentage of tetramer$^+$ cells that express CD27 or CD45RO among all 38 donors. **C.** Percentage of tetramer$^+$ cells that were CD45RO$^+$ as a function of age, divided into CD1a-autoreactive (CD1a-endo or CD1a-vehicle tetramer$^+$), DDM-reactive (CD1a-DDM tetramer$^+$) and all CD3$^+$ T cells.

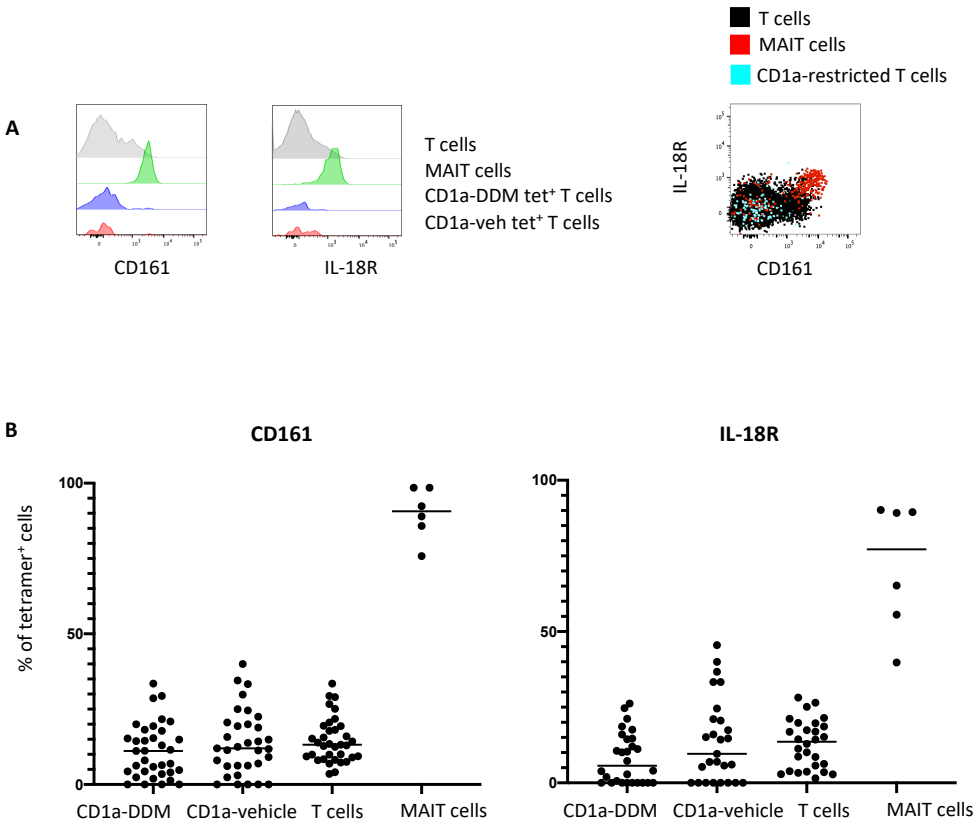

Figure 3.5. Expression of innate-like T cell markers by CD1a-restricted T cells in healthy human blood. Blood donors were magnetically-enriched for CD1a-DDM tetramer and CD1a-vehicle tetramer directly *ex vivo.* 6 donors were also labelled with MR1-5-OP-RU tetramer to isolate MAIT cells as controls. **A.** CD161 and IL-18R expression of CD1a-DDM tetramer$^+$ cells (blue) and CD1a-vehicle tetramer$^+$ cells (red) compared to all T cells (grey) and MR1-5-OP-RU tetramer$^+$ (MAIT) cells (green). **B.** Frequency of CD161$^+$ (n = 35) and IL-18R$^+$ (n = 28) populations among CD1a tetramer$^+$ cells, all T cells, and MAIT cells in all donors.

and IL-18R (*Fig.3.5)*. These data highlight key differences in the phenotype of CD1a-restricted T cells and other unconventional innate-like T cells.

The expression of several homing markers was evaluated on CD1a-restricted T cells isolated directly *ex-vivo* as a previous study revealed that CD1a-autoreactive T cells express a skin homing marker known as cutaneous leukocyte antigen (CLA) (de Jong et al., 2010, Forster et al., 1999). A small number of CD1a-restricted T cells expressed CLA, and some donors revealed a large percentage of tetramer$^+$ cells that were CLA$^+$ (*Fig.3.6)*. CD1a-restricted T cells expressed high levels of the lymphoid organ homing-receptor CCR7 (*Fig.3.6)*, suggesting that they circulate in blood and lymph to secondary lymphoid organs (Forster et al., 1999), but this does not rule out the potential to circulate to skin.

Both αβ- and γδ-T cells are known to recognise lipid antigens presented by CD1 molecules (Luoma et al., 2014, Spada et al., 2000), and therefore whether isolated CD1a-restricted T cells expressed γδ-TCRs was assessed. The frequency of CD1a tetramer$^+$ T cells that expressed γδ-TCRs was lower compared to that of the total T cell pool *(Fig.3.7)*. There was a large degree of inter-donor variation in CD1a-restricted γδ-T cell frequency. Overall, there were more CD1a-autoreactive T cells that were γδ-TCR$^+$ than DDM-reactive T cells, however some donors had higher DDM-reactive γδ-TCR frequencies, ranging up to 12.5% among the 15 donors assessed *(Fig.3.7)*. These results are particularlt interesting as, in comparison with CD1b-, CD1c-, and CD1d-restricted T cells (Bai et al., 2012, Cui et al., 2009, Roy et al., 2016, Russano et al., 2006), fewer studies have identified CD1a-restricted γδ T cells (Agea et al., 2005, Wegrecki et al. 2022).

3.2.4 Transcription factor expression and cytokine production in CD1a-restricted T cells

To gain greater insight into the function of CD1a-restricted T cells, they were analysed for transcription factors PLZF, Rorγt and Foxp3 expression. PLZF is regarded as a master regulator for innate-like responses (Alonzo et al., 2010, Kovalovsky et al., 2010) and is crucial for the development and function of NKT, MAIT, and some γδ-T cells (Das et al., 2010, Kovalovsky et al., 2008, Savage et al., 2008, Pellicci et al., 2020). RORγt is also highly expressed by IL-17-producing innate-like T cells (Leeansyah et al., 2015,

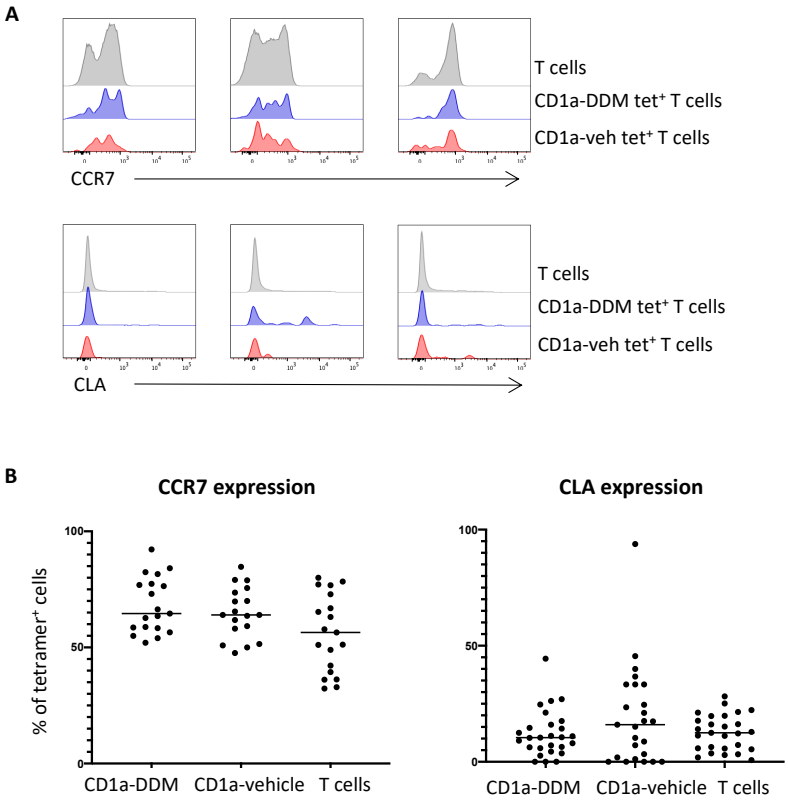

Figure 3.6. Expression of migratory markers by CD1a-restricted T cells in healthy human blood. Blood donors were magnetically-enriched for CD1a-DDM tetramer and CD1a-vehicle tetramer directly *ex vivo.* **A.** CCR7 and CLA expression of CD1a-DDM tetramer$^+$ cells (blue) and CD1a-vehicle tetramer$^+$ cells (red) compared to all T cells (grey) in three donors. **B.** Frequency of CCR7$^+$ (n = 19) and CLA$^+$ (n = 27) cells among CD1a tetramer$^+$ populations and all T cells in all donors.

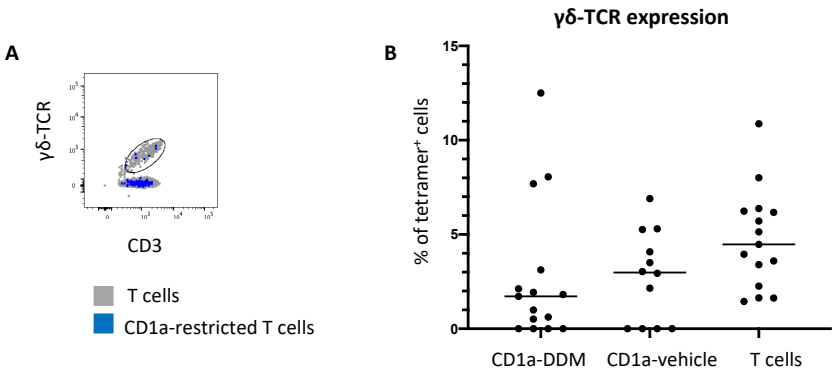

Figure 3.7. Expression of γδ-TCRs by CD1a-restricted T cells in healthy human blood. PBMCs were labelled with CD1a-DDM tetramer (n = 15) and CD1a-vehicle (n = 12) tetramer directly *ex vivo.* **A.** Gating of γδ-TCR$^+$ populations among CD3$^+$ tetramer$^+$ T cells (blue) was based on the total T cell population (grey). CD3$^+$ tetramer$^+$ T cells were first identified by gating on CD14$^-$ CD19$^-$ single, live lymphocytes. **B.** Cumulative γδ-TCR expression shown as a percentage of tetramer$^+$ cells or all T cells.

Rahimpour et al., 2015, Pellicci et al., 2020). Additionally, Foxp3 is a transcription factor expressed by regulatory T cells (Tregs) with potent suppressive activity, particularly when co-expressed with RORγt (Li et al., 2015, Yang et al., 2016).

In this study, MAIT cells were identified using high levels of CD8 and CD161 co-expression as surrogate markers to act as a control to indicate positive transcription factor staining. While the positive shift in mean fluorescence intensity (MFI) for MAIT cells compared to other T cells was minimal, especially for PLZF, MAIT ($CD8^+CD161^+$) cells were consistently double positive for RORγt and PLZF. They displayed MFIs that were on the higher end of PLZF expression among all T cells *(Fig.3.8a)*, albeit they were expected to be more distinctly positive for PLZF like in previous studies (Gherardin et al., 2018). PLZF MFI was also slightly higher among CD1a-tetramer$^+$ T cells compared to both MAIT cell and total T cell populations, while RORγt MFI for DDM-reactive T cells was similar to that of the total T cell population *(Fig.3.8b)*. Fewer donors were examined for Foxp3 expression (n=8), which appeared elevated among some CD1a-tetramer$^+$ cells and MAIT cells compared to T cells *(Fig.3.8b)*. While this transcription factor is not typically associated with MAIT cells, populations of tumour-infiltrating $CD4^+$ $Foxp3^+$ MAIT cells that are positive for other markers typical of regulatory T cells, including CTLA-4, CD25 and Helios, have been identified (Li et al., 2020). Some $Foxp3^+$ CD1a-restricted T cells may therefore play a regulatory role. There was great inter-donor variability, and overall, it appears that CD1a-restricted T cells have higher levels of PLZF, low levels of RORγt and are heterogenous for Foxp3 expression.

Due to the expression of typical transcription factors for unconventional T cells, PLZF, and to a lesser degree, RORγt, the capability of CD1a-restricted T cells to produce Th1 and Th17 cytokines was assessed. Most functional data on CD1a-restricted T cells have been determined using *in vitro* expanded CD1a-autoreactive T cell clones. To assess them *ex vivo,* PBMCs from nine healthy blood donors were non-specifically stimulated with 1 μg/mL phorbol 12-myristate 13-acetate (PMA) and ionomycin for 4 hours in the presence of GolgiStop (BD Biosciences), a protein transport inhibitor. Cells were subsequently labelled with CD1a tetramers (without enrichment), followed by intracellular cytokine staining to examine TNF, IFN-γ, IL-17 and IL-4 production. Within four hours of stimulation, some T cells produced TNF and IFN-γ, but few produced IL-4 or IL-17

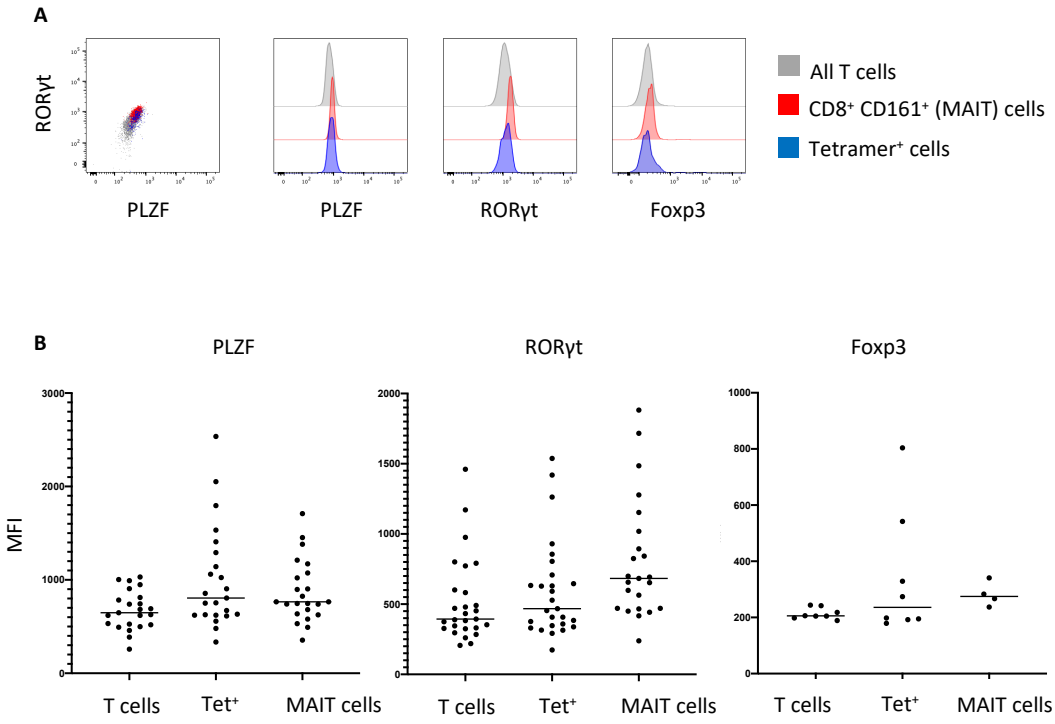

Figure 3.8. Transcription factor expression in CD1a-restricted T cells from healthy human blood. Blood donors were magnetically-enriched for CD1a-DDM tetramer tetramer directly *ex vivo,* fixed and permeabilised, and then labelled for intracellular transcription factors. **A.** PLZF, RORγt and Foxp3 expression of CD1a-DDM tetramer$^+$ cells (blue), CD8$^+$ CD161$^+$ cells (red) and all T cells (grey). **B.** Mean fluorescence intensity (MFI) of PLZF (n = 23), RORγt (n = 23) and Foxp3 (n = 8) among CD1a tetramer$^+$ populations, CD8$^+$ CD161$^+$ T cells (used as pseudo-markers of MAIT cells) and all T cells.

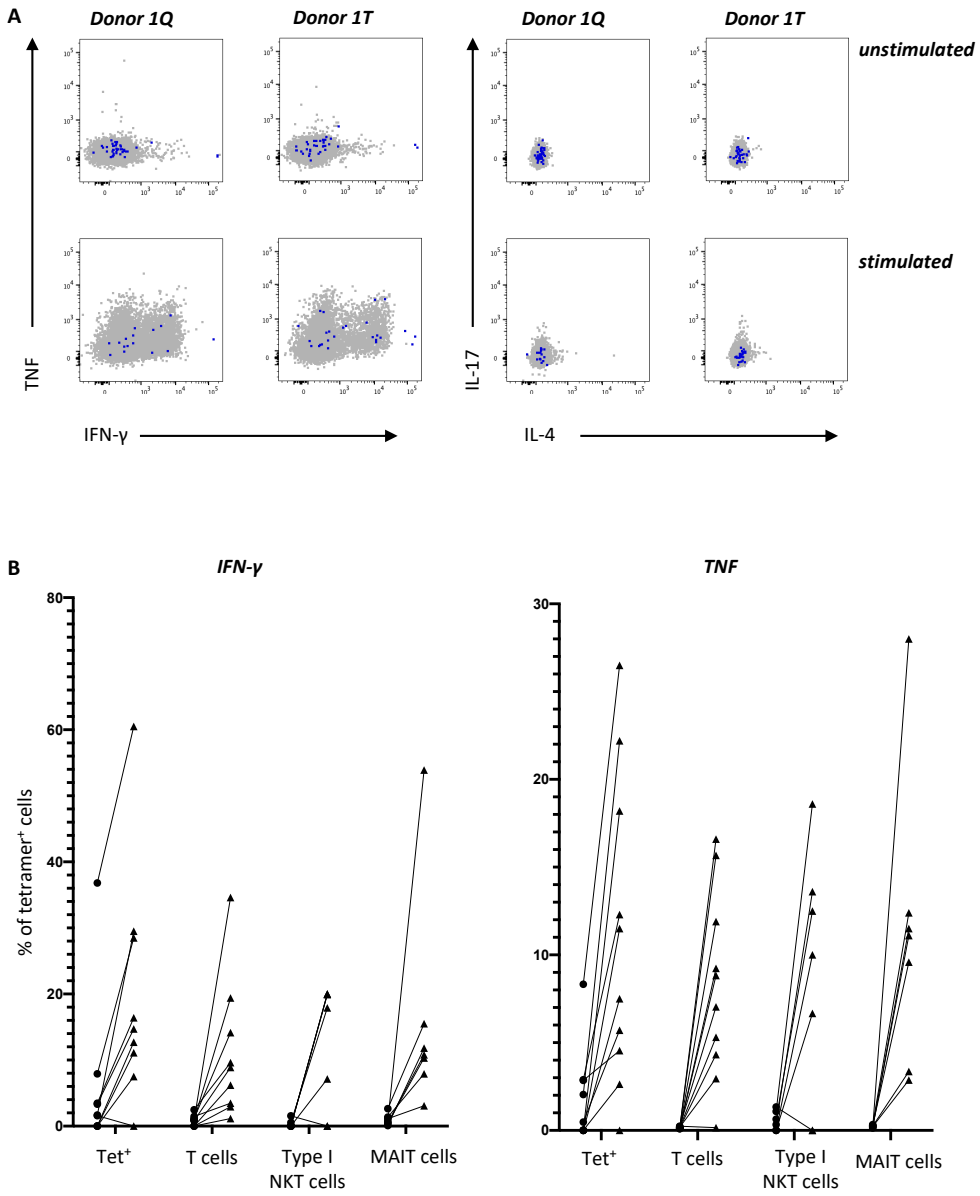

Figure 3.9. Intracellular cytokine staining of CD1a-restricted T cells following stimulation. PBMCs from healthy blood donors were stimulated with 1 µg/mL each of PMA and ionomycin for 4 hours while treated with a protein transport inhibitor. Cells were then fixed and permeabilised for intracellular cytokine staining. **A.** FACS plots depicting TNF, IFN-γ, IL-17 and IL-4 expression of CD1a-DDM tetramer$^+$ cells (blue) and all T cells (grey) with and without stimulation. **B.** Frequency of IFN-γ$^+$ and TNF$^+$ cells among CD1a-DDM tetramer$^+$ populations and all T cells (n = 9), with CD1d-α-GalCer tetramer$^+$ (type I NKT cells) and MR1-5-OP-RU tetramer$^+$ (MAIT) cell populations as controls. Unstimulated cells are depicted in circles (left) and stimulated cells in triangles (right).

(Fig.3.9). Longer stimulation times may be required for Th2 and Th17 differentiation to produce these cytokines given their delayed activation kinetics (Duechting et al., 2017). A small number of CD1a-restricted T cells produced IFN-γ following PMA/ionomycin stimulation, while some produced TNF *(Fig.3.9)*. Type I NKT cells and MAIT cells were identified using CD1d-α-GalCer and MR1-5-OP-RU tetramers respectively, and cells within these populations also did not produce IL-17, consistent with previous studies of peripheral blood MAIT cells following *in vitro* stimulation (Gherardin et al., 2018, Koay et al., 2016). These data provide a glimpse at the potential functional properties of CD1a-restricted T cells upon activation, however further studies are required to study larger populations and determine how these cells would behave when activated *in situ.*

3.2.5 Comparative transcriptomic analysis of CD1a-restricted T cells

Next generation sequencing was performed to gain a greater understanding of the genes that regulate CD1a-restricted T cells. Single cell RNA-sequencing allowed analysis of gene expression across the transcriptome in individual cells (Eltahla et al., 2016). Given that CD1a-DDM tetramer$^+$ cells predominantly express CD4, conventional CD4$^+$ T cells and type I NKT cells were used as controls. CD1a-restricted T cells, type I NKT cells, and conventional CD4$^+$ T cells from four healthy blood donors were index sorted such that each sorted cell could be identified by its location in the plate to match individual cell phenotypes identified by flow cytometry with TCR usage and transcriptome *(Fig.3.10a)*. Donors CNR63, MS28 and MS31 revealed large, distinct CD1d-α-GalCer tetramer$^+$ populations (here on in referred to as type I NKT cells). All four samples labelled with CD1a-DDM tetramer also contained discrete populations of tetramer$^+$ cells, albeit at lower frequencies *(Fig.3.10a)*. From donors CNR63, CNR70, MS28 and MS32 a total of 73, 80, 25 and 34 cells were sorted respectively. From each donor, 80 NKT cells and 80 CD4$^+$ T cells (CD4$^+$ tetramer$^-$ cells in samples labelled with CD1d-α-GalCer tetramer) were sorted. As the cell counts were lower for donors MS28 and MS32, only donors CNR63 and CNR70 progressed for cDNA library preparation and RNA sequencing.

Similar to previous phenotypic analyses of CD1a-restricted T cells by us (*Fig 3.3*) and others, most DDM-reactive T cells were CD4$^+$ (de Jong et al., 2010, de Lalla et al., 2011)

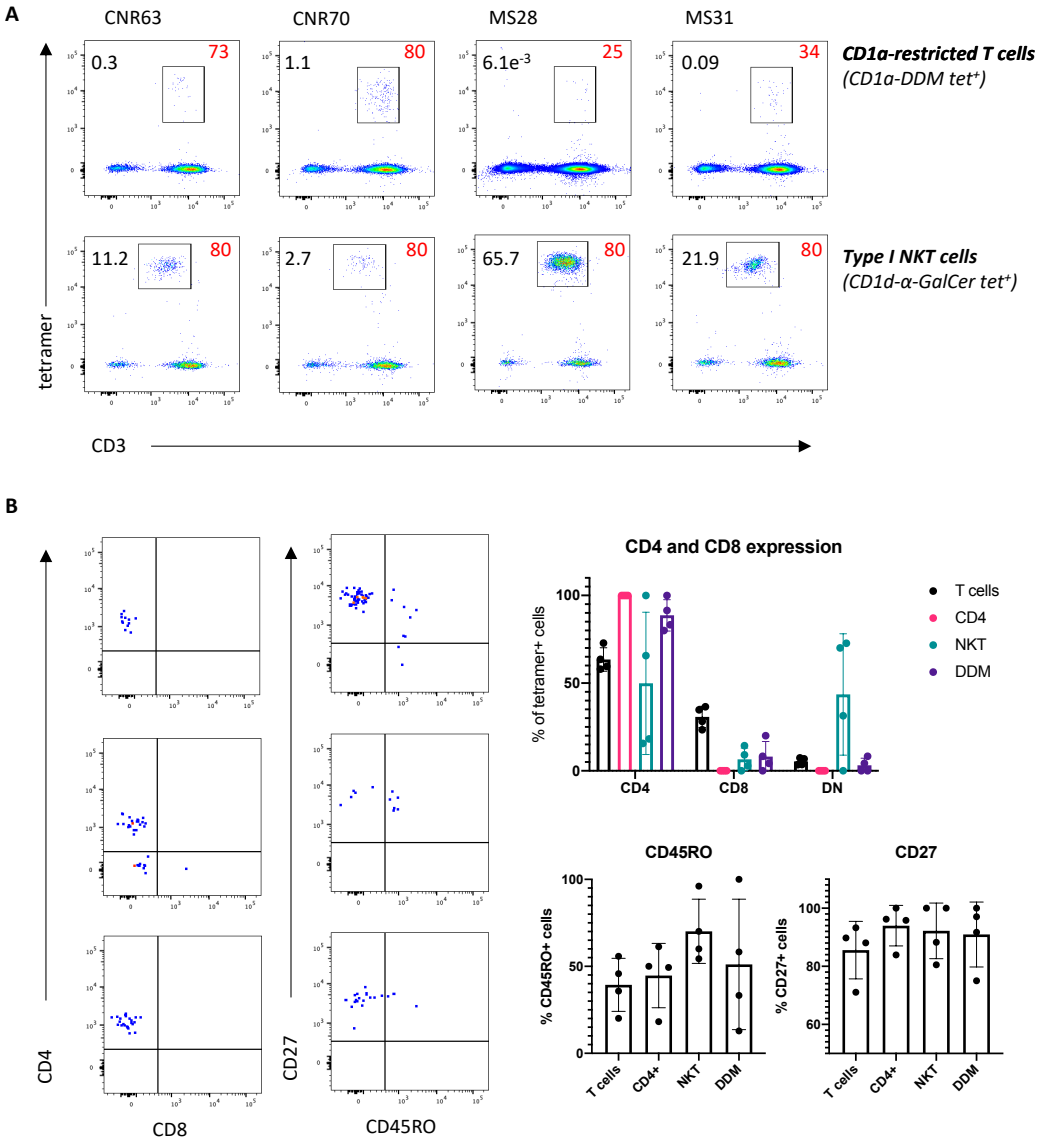

Figure 3.10. Isolation of DDM-reactive T cells, type I NKT cells, and conventional CD4⁺ T cells for single cell RNA sequencing. DDM-reactive T cells and type I NKT cells were MACS-enriched from four healthy blood donors and single cell-sorted for RNA-sequencing. **A.** FACS profiles of all cells acquired for each sample, depicting viable single cells with the exclusion of CD19⁺ B cells. Tetramer⁺ cells were index sorted from within the CD3⁺ tetramer⁺ gate. Black numbers indicate their proportion of the parent population and red numbers indicate number of cells sorted per sample. **B.** Surface phenotype analysis of CD4, CD8α, CD27 and CD45RO expression from donor CNR70 (left) and cumulative data of the percentage of CD4⁺, CD8⁺, DN, CD45RO⁺ and CD27⁺ populations among all T cells, CD4⁺ T cells (CD4+), type I NKT cells (NKT) and DDM-reactive T cells (DDM). Tetramer⁻ cells from the CD4⁺ CD8⁻ quadrant in NKT samples of each donor were also sorted as a CD4⁺ T cell control. Data representative of four donors in two independent experiments.

(Fig.3.10b). Type I NKT cells were either $CD4^+$ or DN for both co-receptors *(Fig.3.10b)*. The majority of type I NKT cells in each donor were $CD45RO^+$ *(Fig.3.10c)*, consistent with their innate-like, activated/memory phenotype (van Der Vliet et al., 2000, Godfrey et al., 2015). DDM-reactive T cells displayed naive/effector T cell dynamics and were varied in their expression of CD45RO between individuals; in some donors, most $tetramer^+$ cells had a $CD45RO^+$ memory phenotype, while other donors had a naïve $CD45RO^-$ phenotype *(Fig.3.10c)*. Similar to previous experiments, most cells were mainly $CD27^+$ *(Fig.3.10c)*. This variation in memory status suggests that some DDM-reactive T cells may be capable of early effector responses following activation, like type I NKT cells, or that some may have previously undergone clonal expansion following antigen-exposure (Golubovskaya and Wu, 2016).

Cells were FACS-sorted directly into a cell lysis buffer for reverse transcription followed by PCR amplification. Samples for which the quality and quantity of DNA product was sufficient, as assessed by LabChip analysis and a Quant-iT PicoGreen dsDNA Assay Kit (see Chapter 2: Materials and Methods), were processed further. cDNA libraries were generated by tagging PCR product with unique barcodes using the Illumina Nextera XT DNA Library Preparation Kit, and sent to Auda Eltahla and William Van De Byl in Fabio Luciani's group (University of New South Wales) for sequencing and data analysis.

A principal component analysis (PCA) was performed on the transcriptomes recovered from each T cell subset. CD1b-restricted GMM-reactive T cells were included as an additional subset for comparison as identified by magnetic enrichment with CD1b-GMM tetramers performed in parallel with Michael Souter (discussed in detail in his PhD thesis, completed at The University of Melbourne). Single cell transcriptomes were normalised to subtract variations between T cell subsets that were caused by experimental conditions, inter-donor differences and variable features that were independent of cell subset. Three separate clusters were observed: type I NKT cells, GMM-reactive T cells, and a third cluster containing both $CD4^+$ T cells and DDM-reactive T cells *(Fig.3.11a)*. A small degree of overlap between cells of different subsets was observed, most notably among type I NKT cells, some of which overlapped with $CD4^+$ T cells (and other subsets). PCA analysis hence suggests that CD1a-restricted T cells were most similar to conventional $CD4^+$ T cells compared to CD1b-GMM-reactive and type I NKT cells, and that the three lipid-reactive T cell populations have distinct transcriptomes.

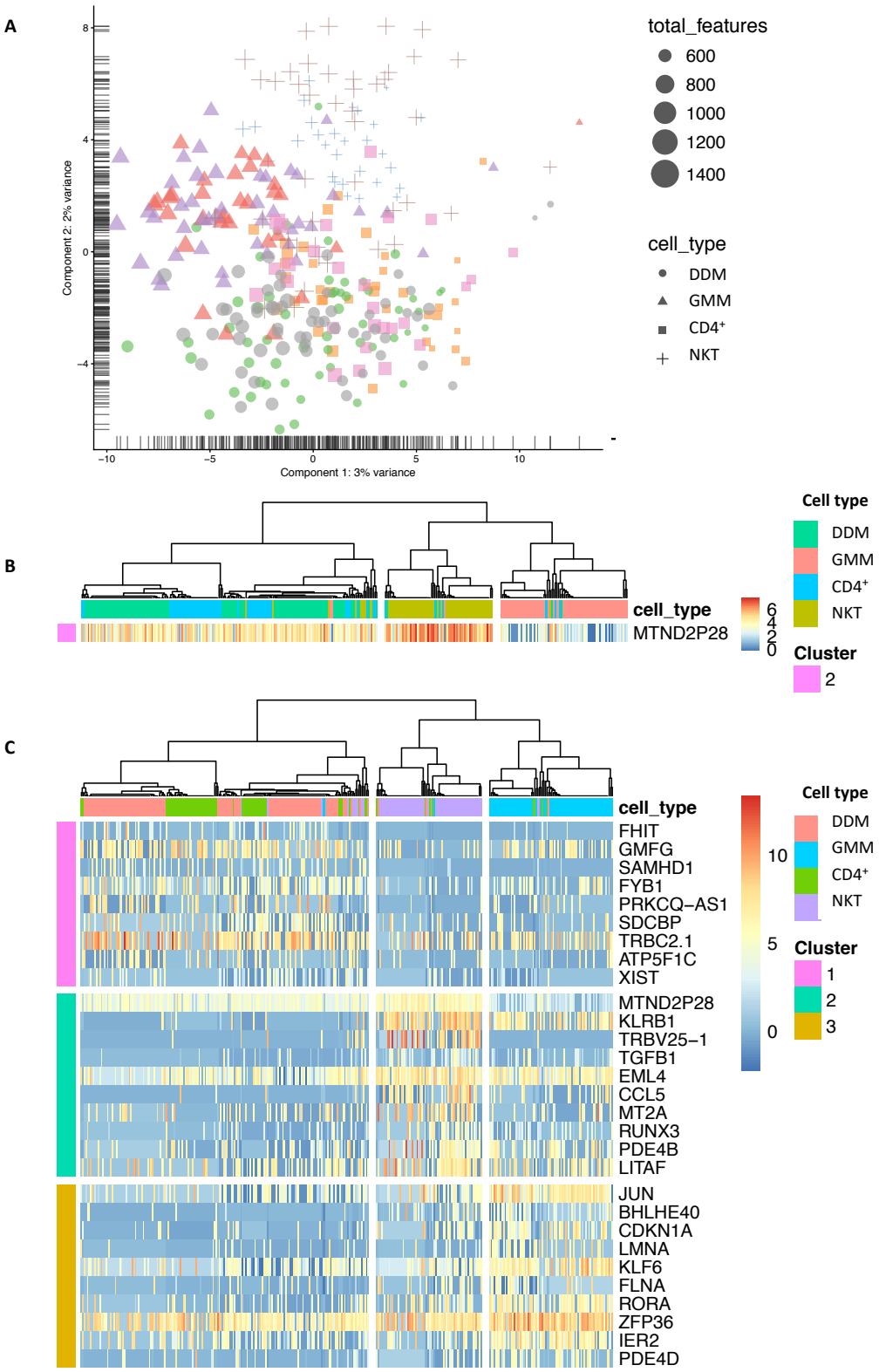
A
total_features
600
800
1000
1200
1400
cell_type
DDM
GMM
CD4+
NKT
Component 2: 2% variance
Component 1: 3% variance
B
cell_type
MTND2P28
Cell type
DDM
GMM
CD4+
NKT
Cluster
2
C
cell_type
FHIT
GMFG
SAMHD1
FYB1
PRKCQ−AS1
SDCBP
TRBC2.1
ATP5F1C
XIST
MTND2P28
KLRB1
TRBV25−1
TGFB1
EML4
CCL5
MT2A
RUNX3
PDE4B
LITAF
JUN
BHLHE40
CDKN1A
LMNA
KLF6
FLNA
RORA
ZFP36
IER2
PDE4D
Cell type
DDM
GMM
CD4+
NKT
Cluster
1
2
3

Figure 3.11. Transcriptionally distinct populations of "unconventional" T cells. Single DDM-reactive and GMM-reactive T cells, type I NKT cells and conventional $CD4^+$ T cells underwent RNA-sequencing after generating cDNA libraries reflective of their transcriptome. **A.** Principal component analysis (PCA) of all cells after normalisation and batch correction showing: CD1a-DDM $tetramer^+$ T cells (circles), CD1b-GMM $tetramer^+$ T cells (triangles), conventional $CD4^+$ T cells (squares), and type I NKT cells (crosses). The size of each cell representation reflects the total number of features (genes) recovered per cell for analysis and its colour is indicative of an individual donor and sample type. **B & C.** Heatmaps displaying each T cell subset segregated based on unsupervised clustering into three clusters and displaying the top marker genes for each cluster: DDM-reactive (DDM) and conventional $CD4^+$ T cells (CD4) (cluster 1), GMM-reactive T cells (GMM) (cluster 2) and type I NKT cells (NKT) (cluster 3). Top marker genes were determined using mean expression values and ranked using a Wilcoxon signed rank test. Marker genes were defined as having an area under the receiver operating characteristic (AUROC) curve of > 0.85 and $p < 0.01$ **(B)** or AUROC of > 0.65 and $p < 0.01$ **(C)**. Dendograms on top of each heat map indicate independent clustering, obtained by measuring similarity between expression patterns across individual cells.

Analysis of transcriptome heat maps for each cell, segregated by similar gene expression between subsets, revealed the same three distinct clusters. Each cluster was mostly homogenous with few cells of each subtype that were scattered among the other clusters (e.g. one DDM-reactive T cell was clustered with type I NKT cells). Top marker genes were determined using mean expression values and ranked using a Wilcoxon signed rank test. When defined as having an area under the receiver operating characteristic (AUROC) curve of > 0.85 and $p < 0.01$ (the default threshold), only one marker gene, *JUN*, was determined *(Fig.3.11b).* The protein encoded by *JUN,* c-Jun, is a leucine zipper and forms part of the AP-1 complex, which is a positive regulator of cellular proliferation, growth and differentiation (Shaulian and Karin, 2002). *JUN* was highly expressed among GMM-reactive T cells while the two other clusters exhibited low-to-intermediate expression of this marker. By relaxing the AUROC to > 0.65, several (9-10) marker genes were determined per cluster *(Fig.3.11c)*. Type I NKT cells were well-defined by their high expression of genes such as *KLRB1,* which encodes CD161; *TGFB1*, which encodes TGF-β; and *TRBV25-1*, aligning with prior knowledge of type I NKT cells being $CD161^+$ (Billerbeck et al., 2010) and expressing a $TRBV25\text{-}1^+$ TCR β-chain (Porcelli et al., 1993, Dellabona et al., 1994, Godfrey et al., 2015), as well as TGF-β being a key regulator of their development and differentiation (Doisne et al., 2009).

Marker genes determined for the DDM-reactive T cell and the $CD4^+$ T cell cluster were *FHIT, GMFG, SAMHD1, FYB1, PRKCQ-AS1, SDCBP, TRBC2.1, ATP5F1C,* and *XIST (Fig.3.11c)*. *FHIT* is a tumour suppressor gene encoding P1-P3-bis(5'-adenosyl) triphosphate, also known as fragile histidine triad protein. *GMFG* (glia maturation factor gamma), is a maintenance factor for haematopoietic stem cells and a regulation factor for lineage commitment (Kawai et al., 2003, Shi et al., 2006). *SAMHD1* encodes a dNTPase that negatively regulates NF-κB and IFN-γ-directed inflammatory responses in viral infections (Chen et al., 2018). *FYB1* encodes FYN binding protein, which augments IL-2 production and is an adaptor protein in TCR signalling cascades (da Silva et al., 1997). *SDCBP* encodes syntenin, a syndecan binding protein involved in cytoskeleton signalling, trafficking of transmembrane proteins, and immunomodulation by enhancing TGF-β signalling (Beekman and Coffer, 2008, Hwangbo et al., 2016). *ATP5F1C* encodes a subunit of the mitochondrial ATP synthase, therefore potentially indicative of the metabolic activity of these cells. The other two marker genes, *PRKCQ-AS1* (PRKCQ

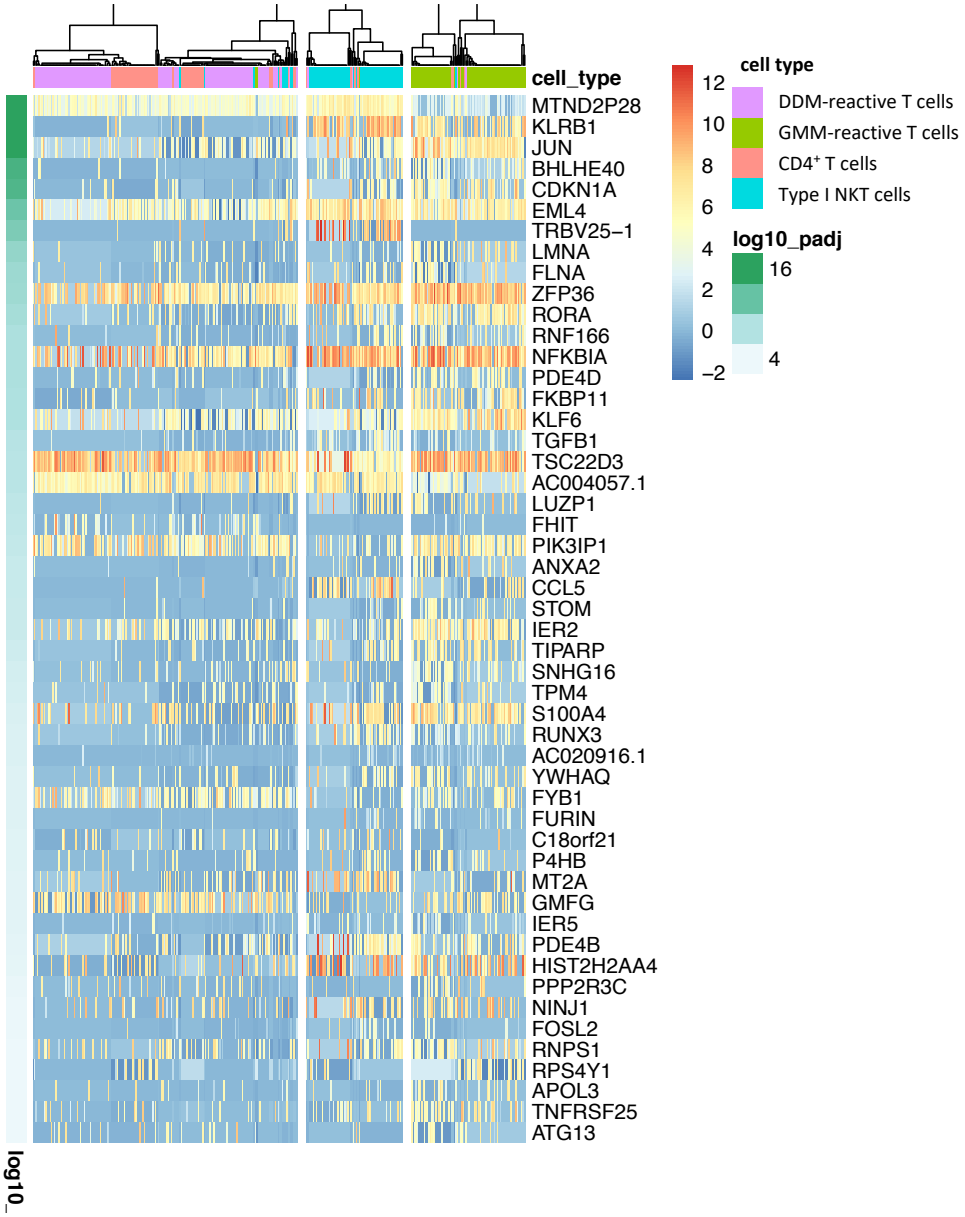

Figure 3.12. Top differentially expressed genes between the three clusters. A gene expression heatmap displaying each T cell subset segregated based on unsupervised clustering into three groups: DDM-reactive and conventional $CD4^+$ T cells (cluster 1), GMM-reactive T cells (cluster 2) and type I NKT cells (cluster 3). Differential expression was calculated using the non-parametric Kruskal-Wallis Test with $p < 0.01$. Dendrograms (top) indicate independent clustering, obtained by measuring similarity between expression patterns across individual cells.

antisense RNA) and *XIST (*X inactive specific transcript)*,* are RNA genes affiliated with long non-coding RNA and may regulate transcription of other genes.

In addition to identifying top marker genes, differential gene expression between clusters was also assessed. Differential expression was calculated using a non-parametric Kruskal-Wallis test and a significant p-value indicates that expression of a given gene in one cluster was dominant over another cluster. Most differentially expressed genes identified had low expression among DDM-reactive T and $CD4^+$ T cells (i.e. were more highly expressed by type I NKT or GMM-reactive T cells) *(Fig.3.12)*. Consistent with flow cytometry data, which revealed no CD161 surface expression (*Fig.3.5)*, DDM-reactive T cells had minimal expression of *KLB1,* while it was highly expressed by NKT cells and some GMM-reactive T cells *(Fig.3.12)*. As expected, DDM-and GMM-reactive T cells were negative for *TRBV25-1*, reflective of their TCR diversity (and bias for other variable genes in the case of GMM-reactive T cells (Van Rhijn et al., 2014, Van Rhijn et al., 2013a)).

Among the top 50 differentially expressed genes, those that were highly expressed by DDM-reactive T and $CD4^+$ T cells include *ZFP36, NFKBIA, TSC22D3*, *AC004057.1*, *PIK3IP1*, and *GMFG (Fig.3.12)*. Genes with anti-inflammatory effects (*ZFP36, NFKBIA,* and *TSC22D3)* were highly expressed across all three clusters (albeit DDM-reactive and $CD4^+$ T cells exhibited relatively lower levels of *ZFP36* and *NFKBIA*, and NKT cells had lower levels of *TSC22D3*). ZFP36, zing finger protein 36, is an RNA-binding protein that regulates inflammation by restraining T cell activation and anti-viral immunity (Moore et al., 2018). *NFKBIA* encodes NFκB inhibitor alpha, the major negative regulator of NFκB (Hayden and Ghosh, 2008). *TSC22D3* encodes a glucocorticoid-induced leucine zipper (GILZ) protein, which also inhibits the expression of pro-inflammatory molecules by preventing translocation of NFκB and AP-1 to the nucleus (Bereshchenko et al., 2019). It has opposing impacts on different T cell subsets, dampening Th1 and Th17 responses while enhancing Th2 responses and TGF-β signalling in Tregs (Bereshchenko et al., 2019). *PIK3IP1* (phosphoinositide-3-kinase interacting protein 1), which suppresses T cell activation (DeFrances et al., 2012), and *GMFG*, were both highly expressed by $CD4^+$ and DDM-reactive T cells as well as GMM-reactive T cells, consistent with *GMFG* being identified as a marker gene for those cells.

DDM-reactive and CD4$^+$ T cells also exhibited intermediate expression of *MTND2P28, EML4, KLF6, IER2, FYB1,* and *S100A4 (Fig.3.12)*.

Subsets were next interrogated for differentially expressed genes between each cell type in a pairwise fashion. Using type I NKT cells as a reference, analysis was performed with the MAST package (Finak et al., 2015) with a calculated threshold to distinguish expressed (≥1) or non-expressed (<1) genes. Only genes that were expressed by both subsets were considered. A total of 21 differentially expressed genes were found between the two control cell types, NKT cells and conventional CD4$^+$ T cells, of which the top 16 are displayed *(Fig.3.13a)*. *KLRB1*, *TRBV25-1* and *CCL5* showed substantial differences in expression *(Fig.3.13a),* which aligns with prior knowledge of type I NKT cells. Production of CCL5 by NKT cells has been observed to be tolerogenic and protective against excessive inflammation (Faunce and Stein-Streilein, 2002, Chen et al., 2019a), and is typically only expressed by conventional T cells following activation (Schall et al., 1988). *GNLY*, encoding granulysin, was expressed by NKT cells but absent in CD4$^+$ cells *(Fig.3.13a)*. Granulysin is located in cytotoxic granules and exhibits anti-microbial activity against a broad range of microbes, including Mtb and therefore is only associated with T cells that have cytotoxic capacity and may be why it was not expressed by CD4$^+$ DDM-reactive T cells (Stenger et al., 1998). *FTH1* and *HLA-B* were the two most highly expressed genes in both subsets, albeit higher in NKT cells *(Fig.3.13a)*. The differential expression of *FTH1*, which encodes the heavy subunit of ferritin (the major intracellular iron storage protein), and the *FTHP10* pseudogene may indicate differences in immunometabolism given that T cell proliferation and effector functions are energy expensive processes that require iron, and ferritin itself can influence cytokine production (Gray et al., 2002, Gray et al., 2001).

Only two differentially expressed genes were found when comparing DDM-reactive T cells and CD4$^+$ T cells, which is likely why they were grouped in the same cluster *(Fig.3.13b).* Expression of *DUSP1* was high in both subsets, but, along with *PNRC1* expression, was comparatively elevated in conventional CD4$^+$ T cells *(Fig.3.13b)*. *DUSP1* encodes MAP kinase (MAPK) phosphatase 1 (MKP1), which dephosphorylates MAPK1/ERK2, considered essential regulators of both innate and adaptive immune responses. MKP1 negatively regulates the production of pro-inflammatory molecules and cytokines, and is required for T cell activation and proliferation (particularly for Th1 and

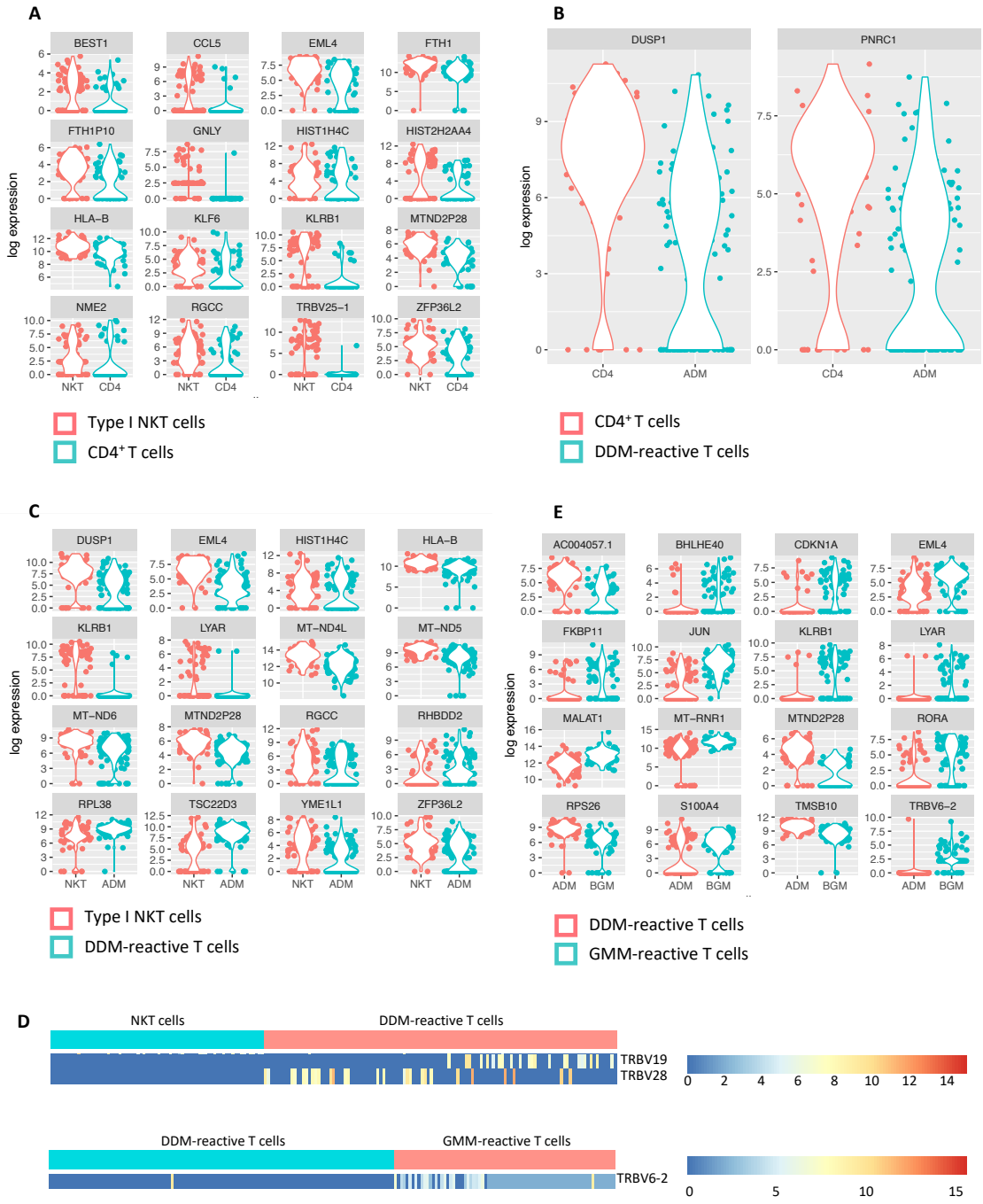

Figure 3.13. Comparison of differentially expressed genes between DDM-reactive T cells and other cell types. Top 16 differentially expressed genes between **A.** Type I NKT cells (red) and CD4⁺ T cells (blue); **B.** CD4⁺ T cells (red) and DDM-reactive T cells (blue); **C.** Type I NKT cells (red) and DDM-reactive T cells (blue); and **E.** DDM-reactive T cells (red) and GMM-reactive T cells (blue). **D.** Differential expression of TRBV genes between DDM-reactive T and NKT cells (top), and DDM-reactive and GMM-reactive T cells (bottom). Differentially expressed genes were determined by p-value <0.01 and absolute log fold change >1.

Th17 responses) (Liu et al., 2007, Noguchi et al., 1993, Sun et al., 1993, Wu et al., 2006, Zhang et al., 2009). *PNRC1* encodes proline rich nuclear receptor coactivator, which is a tumour suppressor gene involved with transcription and maturation of rRNA (Gaviraghi et al., 2018, Wang et al., 2011, Zhou et al., 2007), and a negative regulator of the MAPK/ERK signalling pathway (Zhou et al., 2004b). The identification of only two differentially expressed genes between them highlights the similarity of DDM-reactive T cells to conventional $CD4^+$ T cells, suggesting these subsets share an overlapping phenotype and function, although further experiments are required to validate these findings.

A total of 62 differentially expressed genes were found when comparing DDM-reactive T cells and type I NKT cells, of which the top 16 are displayed *(Fig.3.13c)*. Differentially expressed genes relating to immune function, many of which are inhibitory, include *KLRB1, DUSP1, TSC22D3, RGCC, LYAR* and *ZFP36L2*, all of which were elevated in NKT cells except *TSC22D3* (GILZ – glucocorticoid-induced leucine zipper) *(Fig.3.13c)*. *DUSP1* (MKP1) is immunomodulatory and typically suppressive. RNA-binding protein ZFP36 similarly restrains T cell activation and anti-viral immunity (Moore et al., 2018). *LYAR,* encoding Ly1 antibody reactive protein, also negatively regulates anti-viral innate immunity by impairing the DNA binding capacity of IRF3 and inhibiting NFκB-mediated expression of proinflammatory cytokines (Yang et al., 2019). *RGCC*, regulator of cell cycle, has an inhibitory effect on cell cycle activation induced by TCR/CD28 engagement (Tegla et al., 2015). Hence, many of the genes more greatly expressed by type I NKT cells were immunomodulatory. Other differentially expressed genes included mitochondrially encoded genes*, MT-ND4L, MT-ND5, MT-ND6* and *MTND2P28*, and *YME1L1*, an ATP-dependent metalloprotease located in the mitochondria. *YME1L1* is typically more abundant in tissues with a high mitochondria content (Coppola et al., 2000), suggestive of differences in cellular respiration between these two subsets. Other genes identified are involved in cellular processes and protein metabolism: *RHBDD2,* encoding a membrane-bound protease for intra-membrane proteolysis; *RPL38*, a ribosomal-binding protein; *HIST1H4A (*H4 clustered histone 1), related to protein metabolism; and *EML4,* a microtubule stabilising protein essential for cell proliferation (Houtman et al., 2007, Pollmann et al., 2006). TCR β-chain variable genes *TRBV19* and *TRBV28* were also identified as differentially expressed but were not among the top 16

(Fig.3.13d, Appendix III), suggesting that DDM-reactive T cells may exhibit biases towards these Vβ genes (explored further in Chapter 4.2.1.)

DDM- and GMM-reactive T cells clusters demonstrated a total of 68 differentially expressed genes, of which the top 16 are displayed (*Fig.3.13e)*. Most were comparatively elevated in GMM-reactive T cells, with the exception of *AC004057.1*, *MTND2P28*, *RPS26*, and *TMSB10* (*Fig.3.13e)*. Many of the differentially expressed genes were involved in general cellular functions such as protein synthesis and proliferation. *RPS26* encodes ribosomal protein S26, and *AC004057.1* is a pseudogene for the same protein. *FKBP11* (FKBP19 protein) accelerates protein folding, is involved in the secretory pathway and is therefore particularly elevated in cells/tissues with exocrine properties (Rulten et al., 2006). Thymosin β10, encoded by *TMSB10*, plays an important role in the organisation of the cytoskeleton by inhibiting actin polymerisation, thereby playing a role in cell proliferation and motility (Sribenja et al., 2009, Zhang et al., 2017). *CDKN1A* encodes cyclin dependent kinase inhibitor p21, another regulator of cell proliferation (Georgakilas et al., 2017, Xiong et al., 1993). Collectively, differential expression in these genes, as well as mitochondrial-encoded genes, may indicate differences in cell proliferation, and protein production and secretion. Other differentially expressed genes identified play a role in immune responses. Transcription factors encoded by *BHLHE40* and *ROR* (Bhlhe40 and RORα respectively) influence T cell differentiation and cytokine production (Lin et al., 2014, Miyazaki et al., 2010, Haim-Vilmovsky et al., 2019). GMM-reactive T cells exhibited higher transcription of both *JUN* and *FOS,* which form part of the AP-1 complex that is associated with productive T cell activation, enhanced expansion potential and resistance to exhaustion (Lynn et al., 2019). Note that *FOS* was also elevated in DDM-reactive T cells and therefore, while one of the 68 differentially expressed genes, was not in the top 16 (*Appendix III*). GMM-reactive T cells exhibited low-to-intermediate expression of LYAR, and CD161 was intermediately expressed by GMM-reactive but not DMM-reactive T cells. Lastly, *TRBV6-2* was identified as a differentially expressed gene (*Fig.3.13d)*, reflective of a bias towards this Vβ gene among GMM-reactive T cells, consistent with previous studies (Van Rhijn et al., 2013a).

These data suggest that CD1a-restricted T cells are predominantly $CD4^+$ and have an overlapping phenotype and function to conventional $CD4^+$ T cells. The absence of innate-like T cell marker expression (including CD161, IL-18R, and PLZF) also indicate that

CD1a-restricted T cells play a different role in the immune system to other unconventional T cells like NKT and MAIT cells. Further experiments are required to validate these findings and investigate the role of CD1a-restricted T cells in the immune system.

3.3 Discussion

In comparison to type I NKT cells, which are the most well-characterised CD1-restricted T cell subset, fewer studies have focused on CD1a-restricted T cells. The presence of CD1d in mice, isolation of the strong agonist ligand α-GalCer, and to the development of CD1d-α-GalCer tetramers generated major advances in our understanding of type I NKT cell biology and their potential use as therapeutic agents (Pilones et al., 2012, Simoni et al., 2013, Vivier et al., 2012, Kawano et al., 1997). The monomorphic nature of CD1 molecules similarly allows for the detection of CD1a-restricted T cells with a universal CD1a tetramer. Many studies of CD1a-restricted T cells to date have focused on T cells that react to CD1a presenting self-lipids *in vitro*, however, there is burgeoning interest in those that recognise mycobacterial and other foreign lipids. They appear to play a role in barrier immunity, especially in the skin, and may play a role in immunity to mycobacteria and other bacteria (Colonna, 2010, Van Rhijn et al., 2013b). DDM, a lipid isolated from Mtb is a potent activator of CD1a-restricted T cell clones (Moody et al., 2004), highlighting the importance of studying populations of T cells that recognise such lipids.

Building on previous CD1a tetramer studies (Kasmar et al., 2013), CD1a-restricted T cells were successfully identified from many healthy donors in sufficient numbers to assess their phenotype and function, without the need for *in vitro* culture. Prior to enrichment, it was difficult to isolate many CD1a-restricted T cells with tetramers, especially those that recognise self-lipid antigens (Kasmar et al., 2013). Low-affinity T cells for specific ligands exist at low frequencies and appear negative for CD1a tetramer but may produce robust effector responses upon activation, as has been demonstrated for tetramer-negative pMHC-reactive T cells (Sabatino et al., 2011). Magnetic enrichment of cells labelled with CD1d-α-GalCer tetramer has previously been used to enrich thymic NKT lineage cells by greater than 1,000-fold (Benlagha et al., 2005). Using a similar method, CD1a-tetramer staining was optimised by magnetically enriching samples, which resulted in the isolation of distinct populations of CD1a-restricted T cells. Overall, the frequencies observed here were lower than those observed by previous studies that measured activation of T cells by $CD1a^{+}$ APCs *in vitro*, which may be due to donor variation or a lower sensitivity threshold with tetramers. Another variable that influences tetramer binding could be lipid heterogeneity. CD1a-DDM tetramers were presumably uniformly loaded with a single lipid DDM, and these tetramers consistently isolated more cells, while CD1a-endo/CD1a-vehicle tetramers were loaded with a mixture of

endogenous lipids that differ both within this study, and in other studies of CD1a-restricted T cells. Given that each study used a different CD1a-transfected cell line – HEK cells here, CIR cells (de Lalla et al., 2011) and K562 cells (de Jong et al., 2010) –different lipid repertoires may have been available for antigen loading.

Inter-donor CD1a-restricted T cell variability of frequencies was observed, and all donors consistently had more cells binding DDM-loaded tetramers than endogenous lipid- or vehicle-loaded. This is consistent with the idea that many self-reactive T cells are eliminated during development so that T cells are predominantly non-self-reactive, although self-reactive T cells still do exist in healthy individuals (Walker and Abbas, 2002, Surh and Sprent, 1994). It was typically donors with larger populations of DDM-reactive T cells that also had discernible populations of CD1a-autoreactive T cells, either isolated with CD1a-endo or CD1a-vehicle tetramers. However, when labelled simultaneously with both tetramers, many cells were only single positive for one tetramer, suggesting they were not binding the same cells *(Fig.3.2d)*. The inter-donor variability and correlation between DDM- and endo-reactive frequencies draw parallels to other unconventional T cell subsets, whose frequencies vary markedly (Pellicci et al., 2020) and can be influenced by exposure to microbiota (Constantinides et al., 2019, Koay et al., 2016). For example, given that antigen exposure is a significant contributor of MAIT cell expansion within individuals, similar mechanisms may affect the frequency of CD1a-restricted T cells that recognise non-self-lipids like DDM. Interestingly, one blood donor had a clonal population CD1a-restricted memory T cells. This individual may have received the BCG vaccination to prevent Mtb infection, and therefore has an expanded population of T cells that recognise mycobacterial lipid antigens. CD1a-restricted T cell frequency may also be influenced by variable CD1a expression levels, which can be determined by transcriptional regulators such as the 5' UTR and intronic regions, for which SNPs that influence CD1a expression levels have been determined (Seshadri et al., 2013).

Consistent with previous studies, heterogeneity of CD45RO expression was observed among CD1a-restricted cells (de Jong et al., 2010, de Lalla et al., 2011). CD1a-restricted T cells can have a naive or memory phenotype comparable to conventional T cells in that they are predominantly naive ($CD45RA^{+}$) in newborns and adults, but increase their memory T cells proportions as adults (de Lalla et al., 2011), and indeed, the proportion

of memory CD1a-restricted T cells tended to increase with age. This contrasts with the constitutive effector/memory phenotype observed for other unconventional T cells. For example, MAIT cells transition from a naive phenotype ($CD45RA^+$) early after egress from the thymus and mostly display a memory phenotype ($CD45RO^+$) in circulation (Dusseaux et al., 2011, Martin et al., 2009b), and type I NKT cells acquire a memory-activated phenotype as early as in newborns (van Der Vliet et al., 2000). Also, in contrast to these T cell subsets, CD1a-restricted T cells displayed minimal expression of innate-like markers CD161 and IL-18R (Cosmi et al., 2008, Dusseaux et al., 2011, Martin et al., 2009a). High CD161 and IL-18R expression by MAIT cells and Tc17 cells is linked to IL-17 production and a memory-like phenotype (Fergusson et al., 2011). The absence of this in CD1a-restricted T cells aligns with the observation that they produced IL-22 but not IL-17 in response to stimulation, and exhibit heterogeneity for naive/memory phenotype *(Fig.3.4 and 3.10)* (de Jong et al., 2010), although they also have produced IL-17 in psoriasis pathogenesis (Kim et al., 2016).

Akin to most circulating T cells, only a small number of CD1a-restricted T cells expressed the skin-homing receptor CLA (Fuhlbrigge et al., 1997) (*Fig.2f)*. This contrasts with a previous study that observed CLA expression on cultured memory CD1a-autoreactive T cells (and perhaps the *in vitro* culture conditions induced greater CLA expression) (de Jong et al., 2010). Other skin-homing markers to assess in future studies include CCR4, CCR6 and CCR10, which are particularly integral during inflammation and contact hypersensitivity reactions (Paradis et al., 2008, Tubo et al., 2011), as CD1a-restricted T cells are thought to play a role in these. The low to intermediate expression of CLA may be due to a lack of memory/effector cells in populations assessed. CLA^+ $tetramer^+$ cells were usually also $CD45RO^+$ memory T cells, so CLA may be expressed only by antigen-experienced CD1a-restricted T cells. (CLA expression on epidermal CD1a-restricted T cells is also investigated in Chapter 6.2.2) Like conventional T cells, naive CD1a-restricted T cells may circulate in blood and lymph until they acquire effector functions and traffic to tissues, as antigen-inexperienced T cells typically do not express tissue tropism.

It is unlikely that DDM-reactive T cells isolated from this cohort of healthy blood donors had previously been primed by Mtb or the live-attenuated BCG vaccine, especially among younger Australian blood donors due to the low incidence of TB and targeted

recommendation for BCG vaccination (Faust et al., 2019). Older donors, however, may have received the BCG vaccination as part of the Australian immunisation program that ended in the mid-1980s (Department of Health, 2013). Additionally, it is possible that variability in the frequency of DDM-reactive T cells is also influenced by exposure to similar antigens. DDMs are a family of lipopeptides that were originally identified by their potent antigenicity for CD1a-restricted T cells as an unexpected mycobactin variant (Moody et al., 2004), and this discovery led to the identification of additional monodeoxymycobactins years later (Madigan et al., 2012). There hence may be other mycobacterial lipids structurally similar to DDM that have yet to be described. Mtb synthesises mycobactins, specialised siderophores, to scavenge iron from both extracellular transferrin and the intracellular iron pool (Olakanmi et al., 2002), and actively synthesises deoxymycobactin during iron starvation (Madigan et al., 2012). Other members of the *Mycobacterium* genus produce chemically distinct mycobactins, with small acyl groups and fatty acid tails that make them suitable to fit into CD1a (Snow and White, 1969). CD1a-restricted T cells may therefore respond to a range of mycobacterial lipids.

Other lipids abundant in mycobacterial cell walls include GMM and mycolic acid, both of which are presented to CD1b-restricted T cells (Beckman et al., 1994, Moody et al., 1997). These lipids give insight into the recognition of antigen variants by T cells. GMM-reactive T cell frequencies also vary between healthy individuals, but not between patients with active or latent TB and their uninfected (i.e. healthy) household contacts (Lopez et al., 2020), indicating that factors other than Mtb infection itself may influence these populations. Other mycobacterial pathogens such as *M.ulcerans*, which causes cutaneous skin infection, and *M.avium* are capable of synthesising GMM under glucose-enriched conditions (Deshayes et al., 2013, Matsunaga et al., 2008), and *M.ulcerans* infection cases have been spreading through the Mornington Peninsula and Bellarine Peninsula in Victoria, Australia (Tai et al., 2018). CD1b-GMM-reactive T cells may be cross-reactive with antigenic lipids derived from similar bacteria. LDN5, a prototypical GMM-reactive T cell clone, has found to be reactive with GMM and extracts from *M.leprae* and *M.phlei (Moody et al., 1997)*. Unlike GMM, similar DDM compounds have not been described in other *Mycobacteria* sp. (and closely related bacteria) (Marrakchi et al., 2014), however, this does not rule out the possibility that structurally similar lipids to DDM exist that are also CD1a antigens. Another possibility is that CD1a-DDM-reactive

T cells may cross react with lipids derived from other sources, such as neoantigens generated by phospholipases from house dust mites, bees and wasps, or self-antigens (Bourgeois et al., 2015, de Jong et al., 2014, Jarrett et al., 2016a) (cross-reactivity of CD1a-restricted T cells between lipids will be explored further in Chapter 4).

CD1a-restricted T cells expressed the transcription factor, PLZF, which is an integral transcription factor for the development and innate-like functions of unconventional T cell subsets (Kovalovsky et al., 2008, Savage et al., 2008, Koay et al., 2016). While the processes involved in CD1a-restricted T cell development is unclear, knowledge of MAIT and NKT cell development provides a framework with which to study other unconventional T cell subsets. PLZF is upregulated immediately by NKT cells following positive selection at the DP thymocyte stage to support expansion and lineage fate, and its abundance informs lineage fate and subset differentiation (Lee et al., 2013, Park et al., 2019, Pellicci et al., 2020, Savage et al., 2008). Mature MAIT cells in the thymus express high levels of PLZF while thymic NKT cells tend to downregulate it as they mature (Pellicci et al., 2020, Koay et al., 2018). PLZF is also required for late-stage MAIT cell development and effector function (i.e. cytokine production) and regulates expression of IL-12 and IL-18 receptors on these cell types which provide capacity to be activated in a TCR-independent manner (Fergusson et al., 2014, Ussher et al., 2014, Koay et al., 2016). The data here revealed ambiguous PLZF expression using flow cytometry, but RNA sequencing revealed greater expression of PLZF in type I NKT cells compared to CD1a-restricted T cells. These and other PLZF^{hi} CD161^{hi} subsets, including γδ-T and MAIT cells, share a similar transcriptional profile and can be activated by cytokine in the absence of TCR signalling (Fergusson et al., 2014). It is unlikely that CD1a-restricted T cells are also activated by IL-12 and IL-18 given their lack of expression of IL-18R and CD161. The comparable (and in some cases greater) expression of PLZF by CD1a-restricted T cells to MAIT cells indicates that, while they are functionally similar to conventional CD4^{+} T cells, their development may be closer to that of other unconventional T cells. There are currently no defined subsets of CD1a-restricted T cells based on functionality (unlike mouse NKT cells for example), however they have been observed to produce different cytokines upon activation (de Jong et al., 2010, Kim et al., 2016), which may be driven in part by PLZF. CD1a tetramers could be used to further investigate their expression of TFs, and will provide insight into their regulation and developmental processes, and lineage in the thymus.

Using single cell RNA-sequencing, the transcriptome of CD1a-restricted T cells was determined for the first time. The data revealed key differences between lipid-reactive T cell subsets. Interestingly, DMM-reactive CD1a-restricted T cells appeared most similar to conventional $CD4^+$ T cells in their transcriptome (with only two differentially expressed genes determined between the two populations), suggesting that their functions may overlap. Genes that were highly expressed by DDM-reactive T cells and $CD4^+$ T cells included genes encoding adaptor proteins (*FYB1, SDCBP*) and DNA-binding proteins (*TSC22D3*), suggesting that DDM-reactive T cell function may be regulated by these gene products.

Interestingly, 0several TCR genes were determined as differentially expressed between subsets. *TRBV25-1* was identified as a marker gene for type I NKT cells, consistent with the semi-invariant nature of the TCR (Godfrey et al., 2015). In addition, GMM-reactive T cells had high expression of *TRBV6-2*, for which GEM T cells are known to display a bias (Van Rhijn et al., 2013a), while DDM-reactive T cells had high expression of *TRBV28* and *TRBV19*. CD1a-restricted TCRs have typically been regarded as diverse (Vincent et al., 2005), but this gives an inkling as to the potential bias(es) within the TCR repertoire of DDM-reactive T cells (investigated in greater detail in Chapter 4.2.1). *TRBC2* was also detected as a marker gene for DDM-reactive T cells (although it was not exclusive to this cluster). T cells mutually exclusively express either *TRBC1* or *TRBC2 in their TCR β-chain constant region,* which are highly homologous with no functional differences (Sims et al., 1984, Tunnacliffe et al., 1985). However, there is evidence of skewing for one or the other in T cell malignancies and responses to viruses such as HIV and cytomegalovirus (Kaewpreedee et al., 2019, Maciocia et al., 2017). The higher proportion of DDM-reactive T cells expressing TRBC2 may be due to a similar pattern of skewing among T cells that recognise CD1a and/or DDM.

Some genes that were abundantly expressed by type I NKT cells and GMM-reactive T cells were clearly absent in the transcriptome of DDM-reactive T cells, including *KLBR1* (CD161) and *GNLY* (granulysin). CD161 is abundant on most innate-like immune cells, such as γδ-T cells, NKT cells and MAIT cells, but was not expressed by CD1a-restricted T cells, which may be due to the fact that they are more similar to conventional T cells and do not have the same bridging capacity between adaptive and innate immunity. They

also did not produce granulysin, which contributes to cytotoxic activity (Krensky and Clayberger, 2005), perhaps reflecting more of a helper T cell role as opposed to cells with cytotoxic capacity. Also in contrast to NKT cells and GMM-reactive T cells, CD1a-restricted T cells did not express RORγt or RORα, the signature transcription factors of IL-17-producing T cells (Castro et al., 2017) and innate-like T cells (Leeansyah et al., 2015, Rahimpour et al., 2015, Gherardin et al., 2018, Koay et al., 2016).

CD1a-restricted T cells instead may have a more immunosuppressive role as they exhibited elevated expression of *PIK3IP1, GMFG, GILZ,* and *SDCBP*, all of which are known to inhibit immune responses. PIK3IP1 negatively regulates the PI3K/Akt/mTOR pathway (Zhu et al., 2007), one of the key signalling pathways involved in T cell activation and function, and its deficiency enhances T cell responsiveness (DeFrances et al., 2012, Uche et al., 2018). GMFG is highly expressed in extremely motile cell types and is required for the migration and chemotaxis of T cells (Inagaki et al., 2004, Lippert and Wilkins, 2012, Ikeda et al., 2006). It is additionally a potent inhibitor of MAPK activity by targeting the ERK1/ERK2 MAPK isoform while simultaneously stimulating the p38 isoform, implicating it in cytokine-based stress-activated responses (Lim and Zaheer, 1996, Zaheer and Lim, 1996). The Erk signalling cascade is activated following TCR stimulation, resulting in the activation of several transcriptional factors, including AP1 (c-Fos/c-Jun), that contributes to $CD4^+$ T cell proliferation and differentiation (Lee et al., 2004, Rincon et al., 2001). The regulation of the MAPK signalling pathways plays a key role in determining the balance of Th1/Th2 immune responses: the ERK1/2 pathway typically supports Th2 cells while the p38 MAPK pathway supports Th1 cells, IFN-γ production and immunosuppression by regulatory T cells (Adler et al., 2007, Adler and Steinbrink, 2008, Rincon et al., 2001). The higher expression of GMFG observed by DDM-reactive T cells may therefore be linked to Erk inhibition and limited expression of c-Fos and c-Jun compared to other T cell types, thereby potentially influencing differentiation pathways. GILZ tethers AP1 and NF-κB to also favour immunosuppression (Cannarile et al., 2019). NF-κB and AP-1 contain transcriptional regulator binding sites for most inflammatory mediators (Ji et al., 2019) and by inhibiting them, GILZ inhibits IL-2 production, and consequently, T cell proliferation (Ayroldi et al., 2001). GILZ has been shown to promote Th2 differentiation and TGF-β signalling for regulatory T cell differentiation, while negatively regulating Th17 transcriptional

programs (Cannarile et al., 2019, Bereshchenko et al., 2019), and SDCBP also enhances TGF-β signalling (Hwangbo et al., 2016). In combination, GILZ, SDCBP, GMFG, and PIK3IP1 along with other regulators may provide CD1a-restricted T cells with immunomodulating functions.

The immunosuppressive or anti-inflammatory effects of some genes highly expressed by CD1a-restricted T cells may be important in the context of disease and therapeutics. Recently, PIK3IP1 was identified as an inhibitory checkpoint marker target in cancer immunotherapy to enhance T cell anti-tumour activity (Chen et al., 2019c). Erk inhibition also has therapeutic potential against tumours as the MAPK pathway is aberrantly regulated in cancer (Smalley and Smalley, 2018). As both GILZ and GMFG inhibit MAPK/ERK activation (Ayroldi et al., 2002, Zaheer and Lim, 1996), CD1a-restricted T cells may be protective during transformation processes and/or tumour development and growth. *DUSP1* and *TSC22D3* expression triggered by glucocorticoids, playing a key role in their anti-inflammatory and immunosuppressive effects (Liu et al., 2007). GILZ acts similarly to glucocorticoids, which are widely used as treatments for inflammatory disease to exert immunosuppressive effects by preventing the translocation of NF-κB and AP-1 to the nucleus (Bereshchenko et al., 2019). In addition, GILZ skews $CD4^+$ T cells towards a Th2 phenotype by upregulating GATA3 and STAT6 expression while reducing T-bet expression and inhibiting IL-17A production (Bereshchenko et al., 2019). Interestingly, despite skewing towards Th2 responses, GILZ has been found to be protective in allergic airway disease, as its deficiency exacerbates airway inflammation (Doerner et al., 2014). The expression of these immunomodulatory genes should be noted when considering CD1a-restricted T cells in immunotherapies for diseases of immune overactivation.

The role of CD1a-restricted T cells in TB immunity is not well understood, however, mycobacterial lipids may function as adjuvants and/or cognate T cell antigens. $CD4^+$ T cells play a dominant role in protective immunity during Mtb infection, as $CD4^+$ T cell deficiency (e.g. in mice or HIV^+ individuals) leads to uncontrolled bacterial growth (Cooper, 2009, Markowitz et al., 1997, North and Jung, 2004, Orme et al., 1993). CD1a-restricted T cells, which were revealed to be close in phenotype to conventional $CD4^+$ T cells, were anticipated to also have an important role to play in Mtb control. Following Mtb infection, the local response is defined by an initial burst of pro-inflammatory

cytokines followed by release of anti-inflammatory and immunomodulatory cytokines (e.g. IL-10 and TGF-β) to regulate tissue damage (Sasindran and Torrelles, 2011). CD1a-restricted T cells that have immunosuppressive properties may therefore help to reduce the harmful inflammatory and cell-mediated immunity effects associated with Mtb infection control. On the other hand, production of IFN-γ and, to a lesser extent TNF, by CD1a-restricted T cells upon activation was shown here and by others *in vitro* (de Jong et al., 2010, de Lalla et al., 2011). IFN-γ production, which is essential for resistance to Mtb infection, stimulates infected macrophages to eliminate the bacteria through production of reactive nitrogen intermediates, phagosome-lysosome fusion and autophagy (Green et al., 2013, Sakai et al., 2014b, Kumar, 2017). Antigen-specific $CD4^+$ T cell responses to Mtb infection are delayed compared to responses to other respiratory pathogens (Gallegos et al., 2008, Reiley et al., 2008, Wolf et al., 2008). They are activated in the lung-draining mediastinal lymph node and rapidly proliferate before migrating to the lung, where they produce IFN-γ, TNF, and IL-17 (Wolf et al., 2008). The delay of effector T cell responses is due to a combination of delayed antigen presentation, trafficking, and differentiation, attributed to the action of $Foxp3^+$ regulatory $CD4^+$ T cells and IL-10 (O'Garra et al., 2013). Regulatory mechanisms thus inadvertently assist pathogen persistence. CD1a-restricted T cells may therefore play dual roles in this process as some may be protective (IFN-γ-producing Th1 cells), while others are suppressive. It will be important to better understand their role(s) in TB pathogenesis and protection to best utilise them in vaccine design and treatment.

In summary, this work here presents an in-depth phenotypic analysis of CD1a-restricted T cells isolated from healthy blood donors. Isolation was achieved using an optimised magnetic enrichment strategy with CD1a tetramers, revealing distinct populations of CD1a-restricted T cells whose frequencies varied widely between donors. The surface phenotype of CD1a-restricted T cells observed *ex vivo* was consistent with published findings from cultured CD1a-autoreactive T cells in their skewing towards CD4 co-receptor expression and heterogeneity in memory T cell phenotype (de Lalla et al., 2011, de Jong et al., 2010). A comprehensive transcriptomic analysis of DDM-reactive T cells provided a comparison between GMM-reactive T cells, type I NKT cells and conventional $CD4^+$ T cells. DDM-reactive T cells were most comparable to conventional $CD4^+$ T cells, suggesting that they may be a subset of $CD4^+$ T cells that recognise CD1a-lipid instead of pMHC with overlapping functions (although the functions of $CD4^+$ T cells

are quite broad). Other unconventional T cell subsets appear to be innate-like and are poised to respond rapidly, especially with Th1- or Th17-like responses, while in contrast CD1a-restricted T cells may have widely varying, context-dependent responses. These data provide the groundwork for studying DDM-reactive T cells following BCG vaccination and Mtb-infection alike, and further studies are currently underway to compare these cells in individuals with active and latent TB.

Chapter 4. Characterisation of CD1a-restricted T cell antigen recognition

4.1 Introduction

Conventional αβ T cells exhibit a diverse repertoire of TCR sequences owing to their regions of hyper variability. TCR diversification relies on the use of germline-encoded CDR1 and CDR2 sequences, the juxtaposition of different V, (D) and J germline segments to form combinatorial and junctional variation in CDR3, and the pairing of already diverse TCR α- and β-chains. Most studies have suggested that group 1 CD1-restricted T cells exhibit broad TCR diversity, with emerging subsets of antigen-specific CD1-restricted T cells that display restricted TCR repertoires (Van Rhijn et al., 2013a, Ogg et al., 2019).

It is not uncommon for particular conditions of antigen exposure, like in the case of infectious diseases, to drive TCR biases (reviewed in (Wang et al., 2016)). TCR bias falls within three categories based on the extent of bias: preference for TCR variable genes with little conservation in their CDR3 sequence (type 1), conservation of CDR3 regions (type 2), or identical TCR α- or TCR β-clonotypes (same V, CDR3 and J regions) (type 3) (Turner et al., 2006). Accumulating evidence suggests recurring patterns of variable gene usage among TCRs that bind conserved lipid antigens presented by monomorphic CD1 molecules.

The best-known TCR bias among CD1-restricted T cells is the type 3 bias observed among type I NKT cells. These semi-invariant NKT cells express an invariant Vα24-Jα18 TCR α-chain including a conserved CDR3α sequence, and a limited set of $V\beta11^{+}$ TCR-β chains (Dellabona et al., 1994, Lantz and Bendelac, 1994, Porcelli et al., 1993). Patterns of variable gene biases among CD1b- and CD1c-restricted T cells that recognise certain mycobacterial lipid antigens have also emerged. CD1b-restricted T cell subsets, LDN5-like T cells and GEM cells, both of which recognise the mycobacterial lipid GMM, exhibit a bias for TRAV17 and TRBV4-1 TCR variable genes, or a TCR α-chain comprised of TRAV1-2 and TRAJ9 respectively (Van Rhijn et al., 2014, Van Rhijn et al., 2013a). Additionally, PM-specific CD1c-restricted αβ- and γδ-TCRs utilise conserved gene segments (e.g. β-chains containing TRB7-9*)* (Roy et al., 2014, Van Rhijn et al., 2014). The TCR repertoire of lipid-reactive CD1a-restricted T cells, however, remains

not well described, especially for TCRs that recognise defined mycobacterial lipid antigens.

To date, most studies of CD1a-restricted T cells have been limited to few T cell clones generated *in vitro*, which have so far indicated a diverse TCR repertoire (de Jong et al., 2010, Vincent et al., 2005). However, an analysis of skin-infiltrating T cells during CD1a-mediated contact dermatitis in CD1a-transgenic mice exhibited a substantial increase in $V\beta2^+$ or $V\beta4^+$ T cells, while CD1a-reactive T cells were diverse during homeostasis (Kim et al., 2016), which could be indicative of CD1a antigen driven bias.

TCR biases may have implications in the structural biology of how CD1a-restricted TCRs interact with CD1a and lipid antigens. TCR-pMHC docking geometry has been extensively studied in an effort to understand the restriction of conventional T cells to specific peptide antigens (Marrack et al., 2008, Adams et al., 2011). Most conventional T cells interact with MHC in a loosely conserved diagonal docking orientation (Garcia and Adams, 2005, Rudolph et al., 2006). In contrast, semi-invariant (type I) NKT TCRs interact with CD1d-α-GalCer by binding approximately parallel with the antigen-binding cleft (Borg et al., 2007). They dock over the F'-pocket of the CD1d molecule at the extreme end of the cleft, which is not typically observed in TCR-pMHC complexes (Borg et al., 2007). Given that the rigid structure provided by the restricted type I NKT TCR repertoire is considered to reflect their conserved recognition of the monomorphic CD1d molecule, it is surprising that group 1 CD1-restricted T cells do not follow a similar pattern of conservation given that they also recognise monomorphic molecules.

There is emerging evidence that some CD1-autoreactive TCRs may broadly interact with CD1a molecules themselves but have little contact with the lipid presented (Moody and Cotton, 2017, Cotton et al., 2018, Moody and Suliman, 2017). The only CD1a-autoreactive TCR investigated in structural studies to date, BK6, fits this "absence of interference" model, in which the TCR only binds CD1a when it presents non-protruding lipids that are buried within the antigen-binding cleft (Birkinshaw et al., 2015). In addition, TCRs that interact promiscuously with CD1b presenting self-phospholipids but not sphingolipids also have little interaction with the phospholipid head group as it is shunted sideways along a lateral escape channel in the CD1b molecule (Shahine et al., 2019). Instead, these TCRs interact with a small portion of the lipid that is common to all

major self-phospholipids but absent in sphingolipids, explaining how these TCRs can be broadly cross-reactive yet discriminatory between the two major classes of lipids (Shahine et al., 2019). These findings suggest that there are particular molecular mechanisms that may allow CD1-restricted TCRs to have either promiscuous or specific recognition of lipid antigens.

Lipid antigens that are captured and presented by CD1a can be described as "permissive" (agonistic), or "non-permissive" (antagonistic) depending on their headgroup structure and size (Birkinshaw et al., 2015, de Jong et al., 2014). Permissive antigens, such as LPC, appear to lack direct contact with CD1a-restricted TCRs, and thus TCR autoreactivity is determined by an antigen-free interaction with CD1a (Birkinshaw et al., 2015). Lipids that interfere with the TCR-CD1a binding site by disrupting the A'-roof of CD1a, such as sulfatide and SM, are considered non-permissive (Birkinshaw et al., 2015). LPC and SM contain the same polar head group, but are permissive and non-permissive ligands respectively, likely due to a SM's longer chain length (C_{23} as opposed to C_{18}), which causes it to protrude into the A'-roof (Birkinshaw et al., 2015). This is similar to how CD1b-restricted T cells distinguish between phospholipids and sphingolipids (Shahine et al., 2019). Squalene and wax esters, which are present in epidermis and sebum, are headless autoantigens presented by CD1a, while membrane lipids with polar headgroups in the skin act as antagonists (de Jong et al., 2014), further supporting the absence of interference model. The most well-studied CD1a antigen to date is DDM, a mycobacterial lipid that acts as a potent agonist for many CD1a-restricted T cell clones (Moody et al., 2004). However, it too is a non-permissive lipid for CD1a-autoreactive TCR named BK6, owing to its large headgroup (Birkinshaw et al., 2015, Cheng et al., 2017). Hence CD1a-restricted T cells appear to use multiple structural mechanisms to interact with CD1a, however, the mechanisms have only been described for one CD1a-autoreactive TCR (BK6), and their lipid antigens are not yet definitively categorised.

The recognition of antigens by TCRs is often in concert with CD4 and CD8 co-receptors. It is well established that CD4 and CD8 engagement with MHC-II and MHC-I respectively are crucial in potentiating TCR signalling, and augmenting T cell activation and responses (Janeway, 1992). Early evidence of MHC-Ib molecules also interacting with these TCR co-receptors was the observation that CD8 binds murine thymus leukemia antigen on intra-epithelial lymphocytes with high affinity (12 μM) and an

interface similar to that of CD8 with MHC-I (Leishman et al., 2001, Liu et al., 2003). Some observations also support a role of CD8 engagement with MR1, another MHC-I-like molecule, independently of TCR interactions (Gold et al., 2013, Kurioka et al., 2017), which correlates with a significant bias of $CD8^+$ MR1-restricted MAIT cells in human blood (Corbett et al., 2014). Given the high homology between the α3 domains of MR1 and MHC-I, which is where CD8 interacts with MHC-I (Riegert et al., 1998), it is likely that CD8 also interacts with MR1 to increase the avidity of TCR engagement and fine-tune functional responses, particularly given that CD8-deficient MAIT cells are less associated with typical innate-like T cell markers (CD56, NKG2D, NKG2A) and have low cytotoxic potential (Gherardin et al., 2018, Kurioka et al., 2017). Similar to its crucial role in the activation of MHC II-restricted $CD4^+$ T cells, CD4 facilitates activation of $CD4^+$ type I NKT cells by interacting with CD1d. It may also direct functional responses as CD4 is necessary for cytokine production in $CD4^+$ type I NKT cells (Chen et al., 2007, Thedrez et al., 2007), and NKT cells with and without CD4 display different patterns of Th cytokine production and perforin expression (Gumperz et al., 2002, Lee et al., 2002). Like type I NKT cells, phenotypic analyses of CD1a-restricted T cells in Chapter 3 as well as studies by others have revealed that most express CD4 (de Jong et al., 2010, de Lalla et al., 2011). It is possible that CD4 co-receptor expression may be correlated to the ability of CD4 to interact with CD1a and may facilitate TCR engagement with CD1a-lipid ligands similar to both CD4 and CD8 aiding binding and activation of CD1b-restricted T cells with CD1b-mycolipid (James et al., 2022). The molecular interactions between TCR, CD4 and CD1a-lipid complexes therefore solicit further investigation.

4.2 Results

4.2.1 CD1a-restricted T cell receptor diversity

To explore the TCR repertoire expressed by CD1a-restricted T cells, PBMCs were labelled with CD1a tetramers conjugated to streptavidin-phycoerythrin (PE) and then enriched using magnetic beads reactive against PE for MACS-enrichment (similar to in Section 3.2.2). CD1a tetramers used to isolate T cells were loaded with endogenous lipids, DDM, LPC, urushiol, or 0.5% (v/v) tyloxapol buffer alone (vehicle). MACS-enriched $CD3^+$ CD1a-$tetramer^+$ cells from 20 donors were single cell-sorted using flow cytometry for TCR sequencing (*Fig.4.1*). In some donors, such as donor CNR2, a large discreet population of $tetramer^+$ cells was visible, possibly a consequence of clonal expansion of these cells. In the case of donor CNR2, clonal expansion was confirmed with a dominant TCR clone identified with identical CDR3α and CDR3β sequences, complimented by an enrichment for memory marker CD45RO expression in $tetramer^+$ cells in these donors (Chapter 4.2.3).

4.2.1.1 Determination of TCR diversity using multiplex PCR sequencing for all CD1a-restricted T cells

Paired TCR-α and TCR-β gene sequences were determined by nested multiplex PCR amplification followed by sequencing (Uldrich et al., 2013, Wang et al., 2012). Briefly, cDNA from single cells served as a template for two rounds of nested PCR using a panel of multiplex primers against 40 Vα and 40 Vβ genes. PCR products were sequenced by the Sanger sequencing method with primers against the TCR α- and β-constant domains, followed by capillary separation performed by the Centre for Translational Pathology, The University of Melbourne. Each TCR α- or β- sequence with a different CDR3 sequence was defined as a distinct TCR clonotype.

Among all CD1a-restricted T cells (irrespective of lipid loaded in tetramers), many TRAV and TRBV genes were incorporated into their diverse TCR repertoire (*Fig.4.2)*, albeit with some patterns of bias. Of note were genes TRAV1-2 and TRAV8-2/TRAV8-4, which were both used by 8/73 of TCRs (*Fig.4.2a)*. TRAV1-2 is notably also the Vα gene used by GEM T cells, MAIT cells, and other unconventional T cell subsets (Van Rhijn et al., 2013a, Porcelli et al., 1993, Tilloy et al., 1999). Using sequence primers for TCR sequencing as established by (Wang et al., 2012), it was unclear as to whether these

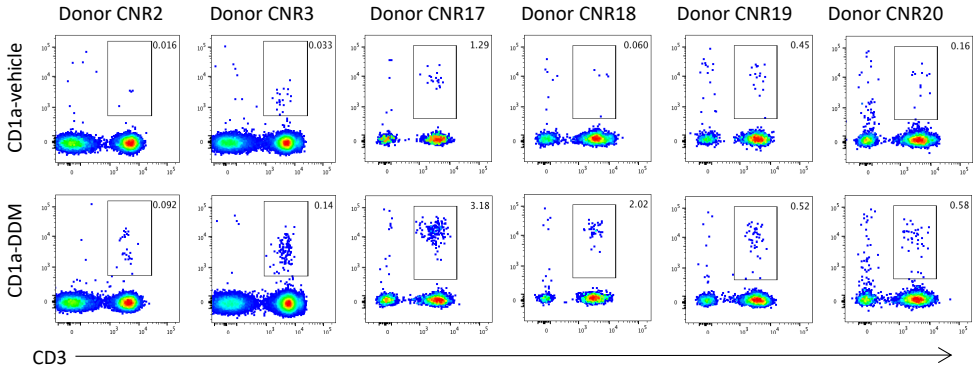

Figure 4.1. MACS-enrichment of CD1a-restricted T cells for TCR sequencing. PBMCs were harvested from blood and 100 x 10^6 cells per donor were stained with either CD1a-DDM or CD1a-vehicle tetramer. Cells labelled with tetramer were enriched using magnetic activated cell sorting (MACS) enrichment. Cells in the gates indicated were single-cell sorted by flow cytometry into 96-well plates for reverse transcription and nested multiplex PCR amplification. Data representative of 20 donors that were FACS-sorted for single-cell TCR sequencing.

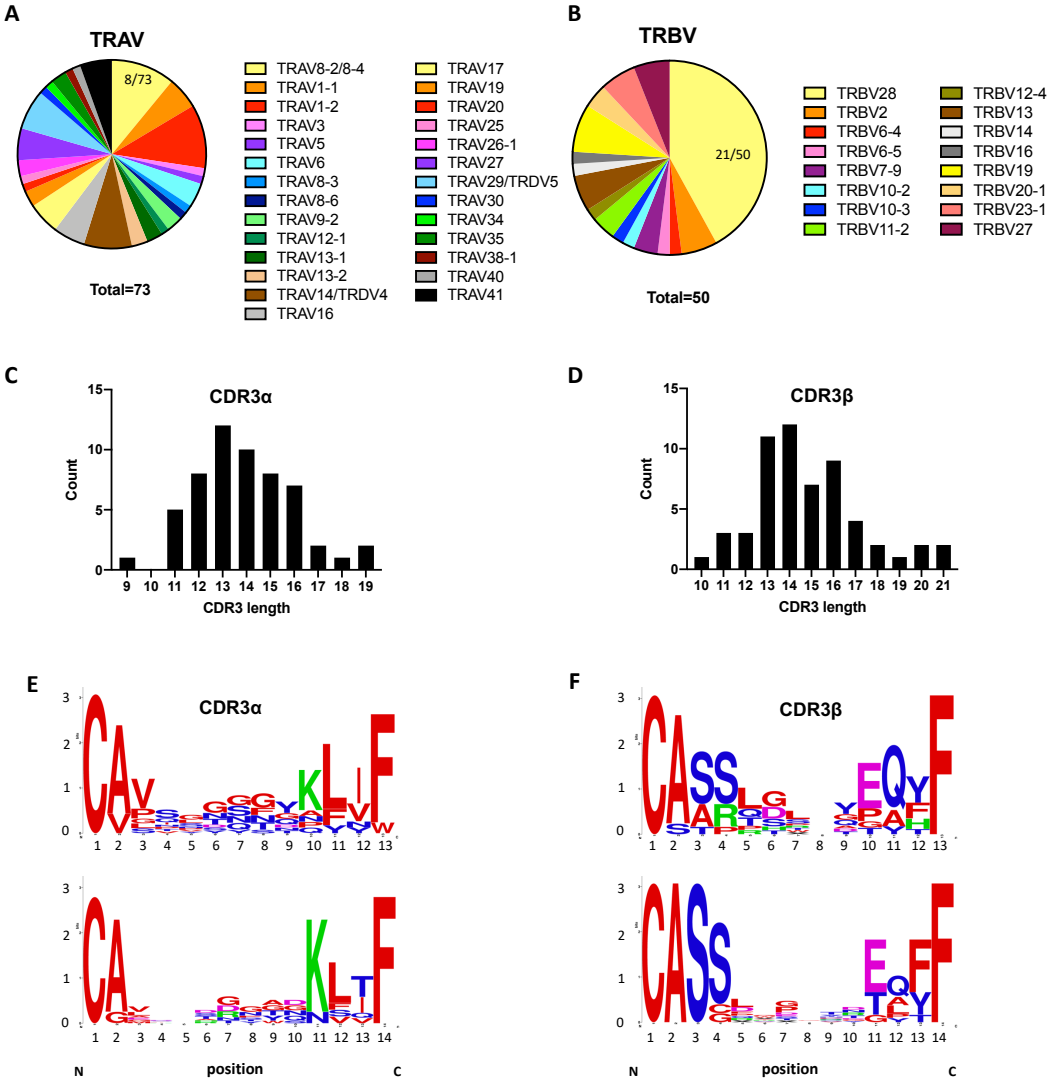

Figure 4.2. TCR diversity in CD1a-restricted T cells as determined by multiplex PCR amplification and TCR sequencing. MACS-enriched CD1a tetramer^{+} T cells (CD1a tetramers loaded with any lipid) were FACS-sorted directly *ex vivo* for reverse transcription, followed by two rounds of nested PCR amplification. Multiplex primers were used to amplify 40 TCR Vα or Vβ gene segments as described by (Wang et al. 2012, Uldrich et al. 2013). Sanger sequencing was performed on amplified DNA products.

A and B. Pie charts displaying the TRAV gene usage of 73 TCR clones in 20 donors (**A**) and TRBV gene segment usage of 50 TCR clones in 15 donors (**B**) as determined by comparing identified sequences against the IMGT database. Only fractions above 10% are shown. **C and D.** Comparison of CDR3α amino acid length (n=56) (**C**) and CDR3β amino acid length (n=57) (**D**) where a CDR3 sequence was obtained. **E and F.** Sequence logos displaying consensus amino acid sequences for CDR3α loops that were 13 or 14 amino acids in length (**E**) and for CDR3β loops that were 13 or 14 amino acids in length. Polar, charged (acidic), charged (basic), and non-polar resides are coloured in blue, pink, green, and red, respectively. Sequence logos were created using Weblogos (Crooks, 2004).

TCRs used TRAV8-2 or TRAV8-4, two paralogous genes, as they differ in regions outside the region captured by the primers for PCR amplification. An alignment of the amino acid sequences encoded by these two genes revealed that they differ in the germline-encoded CDR1 loop, and in one allele of the CDR2 loop (*Appendix IV)*. All TRAV8-2 alleles encode SSYSPS in their CDR1 region, while TRAV8-4 encodes SSVPPY. Both genes encode the sequence YTSAATLV in their CDR2 region except for the allele TRAV8-4*03, which encodes YTTGATLV. These differences in amino acid residues may impact how a TCR would contact CD1a. TCR β-chain analysis also revealed diversity in Vβ gene usage (*Fig.4.2b*). Among 50 TCR clones for which a TCR β-chain was identified, 21/50 contained TRBV28 (*Fig.4.2b*). This is the first instance of a TCR bias described for CD1a-restricted T cells.

In addition to variable amino acid composition, the imprecise joining process during TCR recombination leads to diversity of CDR3 loop size. As amino acid length is critical in the formation of the CDR3 loop structure and specific lengths facilitate the interaction between a TCR and its ligand (Wang et al., 1998, Hughes et al., 2003, Day et al., 2011), the length of CD1a-restricted TCR CDR3 regions were also assessed. CDR3β lengths among naive T cells typically follow a Gaussian distribution (Bousso et al., 1998, Lin and Welsh, 1998, Pannetier et al., 1993, Sourdive et al., 1998), while antigen-induced selection of TCRs with particular antigen-specificities results in the expansion of TCRs with skewed CDR3β length diversity (Day et al., 2011, Turner et al., 2003). The CDR3α sequences were typically 11-16 amino acids in length, with some instances occurring outside this range (*Fig.4.2c*). While these results did not observe a Gaussian distribution, this may have been an artefact of the small sample size. The length of the CDR3β regions was less constrained than CDR3α regions, ranging from 10-21 amino acids in length, albeit most falling within a range of 13-16 (*Fig.4.2d*). A study on CDR3 loop polymorphism revealed that murine TCRs with particular Vβ genes and Vβ-Jβ combinations prefer different CDR3 lengths (Pannetier et al., 1993). However, the CDR3β sequences determined for TRBV28^{+} TCRs ranged from 11-21 amino acids in length, suggesting that these TCRs can accommodate different CDR loop architecture.

Sequence logo analysis (Crooks et al., 2004) for CDR3α and CDR3β regions 13 and 14 amino acids in length (chosen as the modes of each) revealed low amino acid conservation

(Fig.4.2e, Fig.4.2f), indicating that many amino acids in the CDR3 loops were not germline encoded. CDR3α sequences typically started with CAV or CVV, which are germline-encoded in TRAV1-2 and TRAV8-2/TRAV8-4 respectively (*Fig.4.2e)*. They appeared to have a preference for another non-polar residue in the third position, which was often V, P, G, or L (*Fig.4.2e)*. CDR3α sequences 13 amino acids in length displayed high polymorphism in the middle with G, S, N, and T frequently incorporated, whereas this trend was not observed in sequences 14 amino acids in length (*Fig.4.2e)*. KLXF was the most common motif observed in the last four amino acids of the sequence, which is reflective of germline-encoded amino acid residues in the TRAJ genes (*Fig.4.2e)*. Among the 15 donors examined for CDR3β sequences 14 amino acids in length, there was little variation from the CASS motif that is germline-encoded in TRBV28, however there was slightly greater variation in CDR3β sequences 13 amino acids in length (*Fig.4.2f)*. There was no discernible pattern among the middle amino acids, and the CDR3β sequences commonly ended with the motif EQYF or EQFF (*Fig.4.2f)*.

4.2.1.2 Determination of CD1a-restricted T cells intra- and inter-donor variable gene biases

Table 4.1 lists paired (or individual where the pair was not obtained) TCR α- and TCR β-chain sequences as determined in independent experiments from multiple donors using multiplex PCR sequencing. The high frequency of particular TCR clones within a given donor (i.e. 2N, 2V and CNR2) suggests clonal expansion of these cells, which is consistent with many of the CD1a tetramer$^+$ cells in donor CNR2 displaying a CD45RO$^+$ memory T cell phenotype (as seen in Section 3.2.3). The inter-donor biases for TRAV1-2, TRAV8-2/4, and TRBV28 were also observed on an intra-donor level, with multiple donors containing several TCRs with these genes, indicative of slight type 1 TCR biases.

There were intra-donor biases of particular Vα and Vβ gene pairings, in that some donors had two or more CD1a-restricted TCRs with the same variable gene segment pairs in both α- and β-chains, with different CDR3 sequences. Blood donor CNR1 had three different TRAV29$^+$ TRBV28$^+$ T cell clones, isolated with CD1a-vehicle, CD1a-DDM, or CD1a-LPC tetramers (*Table 4.1)*. One of these T cell clones appeared to have been expanded, as it was present in 2/5 cells isolated using the CD1a-vehicle tetramer, and also in one cell isolated using the CD1a-DDM tetramer, suggesting cross-reactivity between lipids.

Table 4.1. Patterns of biases among the CD1a-restricted TCR repertoire. Paired TCR α- and β-chain sequences from single cell-sorted MACS-enriched $CD3^+$ CD1a-tetramer$^+$ cells. The lipid antigens loaded into the tetramers used to isolate each CD1a-restricted T cell are indicated (note that one TCR clone from donor CNR1 was isolated using two independent tetramers). Cells were FACS-sorted directly *ex vivo* for reverse transcription, followed by two rounds of multiplex nested PCR and Sanger sequencing. TRAV, TRAJ, TRBV and TRBJ gene usage was determined by comparing identified sequences against the IMGT database. Frequency is displayed based on the number of clones determined for each donor with each tetramer. Those TCR sequences used to make cell lines are indicated by their cell line name. Colours highlight interesting patterns of TCR variable gene usage in both α- and β-chains.

Donor	TRAV	CDR3α	TRAJ	TRBV	CDR3β	TRBJ	Tetramer	Freq.	Cell line
2N *	29/DV5	CAASALSNQFYF	49	28	CASRFTGWAFF	1-1	endo	5/10	29a28ii
2N	29/DV5	CAASGGYSTLTF	11	10-1	CASSEDTGELFF	2-2	endo	4/10	
2V	8-2/8-4	CVVIGTMFSGYNKLIF	4	19	CAARTDSNQPQHF	1-5	endo	7/17	CNR1
2V	17	CATGNAGNMLTF	39	6-4	N.D.	2-1	endo	1/17	
2V ^	17	CATTNRDDKIIF	30	11-2	CASSLTAPELNNEQFF	2-1	endo	1/17	
2V	17	CATDAEETSGSRLTF	58	N.D.	N.D.	N.D.	endo	1/17	
2V	14	CAMREDRFTNTDKLIF	34	19	CASSLTAPELNNEQFF	2-1	endo	1/17	
2V	10	CVVSRGREYGNKLVF	47	19	CASSILDRSYNEQFF	2-1	endo	1/17	
2V	38-1	CAFHSREDXWGKLQF	24	19	N.D.	N.D.	endo	1/17	
2V	4	CVVSRGREYGNKLVF	24	10-2	CXXXXXXXXXLSEQXF	2-1	endo	1/17	
4A	29/DV5	CAASIXXLRGGSEKLVF	57	28	CASSILGSSGNTIYX	1-3	LPC	1/4	
4A	1-2	CAVVSYNTDKLIF	34	20-1	CSARGSGPXPTDTQYF	2-3	LPC	1/4	
4A	8-2/8-4	CAVSVGSSYKLIF	12	13	CASSPTEWTSGDSSYEQYF	2-7	DDM	1/7	
4A	17	CASSSGGTYKYIF	40	28	CASSLDLTDTQYF	2-3	DDM	1/7	17a28
4A	27	CAGAGTDNTDKLIF	34	6-5	CASRQGWAYEQYF	2-7	DDM	1/7	
4A	35	CAGQSGSKMKTSYDKVIF	50	16	CASSLWDRYTEAFF	1-1	DDM	1/7	35a16
4A	41	WVIQGAQKLVF	54	28	CASSLSLTGTAEYTIYF	1-3	DDM	1/7	
1	1-1	CAVKGTYKYIF	40	28	CASSFPGLAGGRTGELFF	2-2	DDM	1/7	1-1a28
CNR1 *	29/DV5	CAASAWSNQFYF	49	28	CASSFGGPTRELFF	2-2	vehicle/ DDM	2/5, 1/10	29a28i
CNR1	29/DV5	CAASIXXLRGGSEKLVF	57	28	CASSILGSSGNTIYX	1-3	LPC	1/4	
CNR1	29/DV5	CAVXLXXXXXGGXNQLIF	4	28	CASSFGGPTRELFF	2-2	LPC	1/4	
CNR1 #	8-2/8-4	CAVSVGSSYKLIF	12	13	CASSPTEWTSGDSSYEQYF	2-7	DDM	1/10	
CNR1 ^	17	CVVSDRGHNNNDMRF	43	11-2	CASSLKGLYTDXQYF	1-1	vehicle	1/5	
CNR2	27	CAGGSNYKLTF	52	28	CASSQFLAGGTEQYF	2-7	DDM	9/10	27a28
CNR2	16	CALSGTGFQKLVF	8	35	CASGXXGLNTEAFF	1-1	vehicle	1/1	16a28
CNR2	6	CALVRLNDMRF	43	19	CAARTDSNQPQHF	1-5	DDM	1/10	
CNR3 #	8-2/8-4	CVVTGTYGQNFVF	26	13	CASSLEDETQYF	2-5	DDM	1/7	8-2a13i
CNR3 #	8-2/8-4	CAVSLGSGYALNF	41	13	CASSWTSXXSYNEQFF	2-1	DDM	1/7	
CNR3	8-2/8-4	N.D.	42	28	CASSPXXXSNEQFF	2-1	DDM	1/7	
CNR3 ~	8-2/8-4	CVVVSGTYKYIF	40	2	CASSEALLLAGDQETQYF	2-5	DDM	1/7	8-2a2
CNR3	1-2	CAVMDXXXXLIF	12	6-4	N.D.	2-2P	endo	1/8	
CNR3	1-2	CAVLVDTNAGKSTF	27	20-1	CSAIEGEQFF	2-1	endo	2/8	1-2a20-1
CNR3	1-2	CAVMDSNYQLIW	33	6-4	CASSDSTETDTQYF	2-3	endo	1/8	1-2a6-4
CNR3	1-2	CAVMDXXXXLIF	12	6-4	N.D.	2-2P	endo	1/8	
CNR3	1-2	CVPIYNQGGKLIF	23	15	CATSRSLQAEAFF	1-1	urushiol	1/3	1-2a15
CNR7 ~	8-2/8-4	CAVSLRGGGNKLTF	10	2	CASCRGSAYNEQFF	2-1	endo	1/2	

TRAV29/DV5
TRAV8-2/8-4
TRAV17
TRAV1-2 + TRBV6-4, TRBV15 or TRBV20-1
TRBV19
TRBV28
Symbols (* ^ # ~) indicate matching TRAV and TBV gene pairs except pairs with TRAV1-2

Secondly, TCRs isolated from donor CNR6 also exhibited a preference towards TRAV1-2 expression among CD1a-restricted T cells labelled with both vehicle and urushiol-loaded tetramers (*Table 4.1)*. Interestingly, many of those TCRs from donor CNR6 appeared to have similar TCR α- and β-chain pairings to those of MAIT cells (i.e. TRAV1-2 paired with TRBV6-4, TRBV15, or TRBV20-1) (Porcelli et al., 1993, Reantragoon et al., 2013, Tilloy et al., 1999). In addition, TRAV1-2 is the preferential Vα gene in GMM-reactive GEM cells (Van Rhijn et al., 2014). This suggests that perhaps TRAV1-2 may be preferentially used among unconventional T cell subsets.

There were also inter-donor biases of particular Vα and Vβ gene pairings, in that TRAV17$^+$/TRBV11-2$^+$ TCRs were isolated from donors CNR1 and 2V using CD1a-vehicle and CD1a-endo tetramers respectively, and TRAV8-2$^+$/TRBV13$^+$ TCRs were isolated from donors CNR1 and CNR3 using CD1a-DDM tetramers (*Table 4.1)*. Together these data indicate that individual donors may have biases towards particular variable genes and/or gene pairings in the TCR α- and β-chains to form CD1a-restricted T cells.

4.2.1.3 Determination of TCR diversity using multiplex PCR sequencing of CD1a-DDM tetramer$^+$ T cells

Given that previous studies that revealed TCR biases among group 1 CD1-restricted T cells have focused on cells that recognise mycobacterial lipids (CD1b-GMM and CD1c-MPM), DMM-reactive T cells were examined for any antigen-driven bias. Analysis of TCRs isolated with CD1a-DDM tetramers revealed similar patterns within the TCR repertoire to all CD1a-restricted T cells. While the sample size was limited, both TCR α- and β-chains incorporated a number of different variable genes. TRAV8-2/TRAV8-4 was the most common Vα gene, observed in 6/26 TCRs, and TRAV1-1 was used in 4/26 TCRs *(Fig.4.3a)*. The bias for TRBV28 in the TCR β-chain was similarly pronounced among DDM-tetramer$^+$ cells than all CD1a-restricted T cells with 15/32 TCRs being TRBV28$^+$ *(Fig.4.3b)*.

As the CDR3 loop architecture is critical for determining the ability of a TCR to interact with its ligand and antigen-specificity reduces CDR3 length polymorphism (Day et al., 2011, Turner et al., 2003), it was expected that those TCRs that recognise DDM would

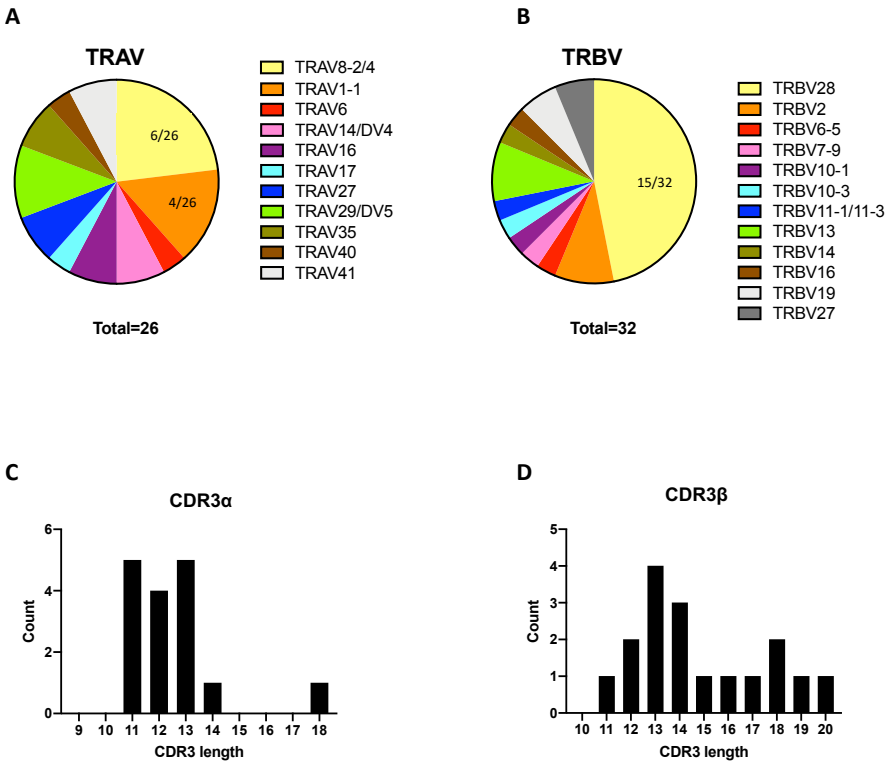

Figure 4.3. TCR diversity in CD1a-restricted T cells that recognise DDM as determined by multiplex PCR amplification and TCR sequencing. MACS-enriched CD1a-DDM tetramer^{+} T cells were FACS-sorted directly *ex vivo* for reverse transcription followed by two rounds of nested PCR. Multiplex primers were used to amplify 40 TCR Vα or Vβ gene segments as described by (Wang et al. 2012, Uldrich et al. 2013). Sanger sequencing was performed on amplified DNA products.

A and B. Pie charts displaying the TRAV gene usage of 26 TCR clones in 10 donors (**A**) and TRBV gene segment usage of 32 TCR clones in 8 donors (**B**) as determined by comparing identified sequences against the IMGT database. Only fractions above 10% are shown. **C and D.** Comparison of CDR3α amino acid length (n=16) (**C**) and CDR3β amino acid length (n=17) (**D**) where a CDR3 sequence was obtained.

have a more restricted CDR3 length diversity than all CD1a-restricted T cells. Most CDR3α regions were between 11-13 amino acids in length, but one was 14 and another was 18 amino acids in length *(Fig.4.3c)*. This range was more restricted than the full range of CD1a-restricted TCRs, however the sample size was also considerably smaller, which should be factored in. The CDR3β region lengths of DDM-reactive TCRs were just as diverse as all CD1a-restricted TCRs, with a mode of 13 amino acids in length *(Fig.4.3d)*.

4.2.1.4 Determination of TCR diversity using single cell RNA sequencing of CD1a-DDM tetramer$^+$ T cells

To account for any biases that may be inherent in the multiplex PCR sequencing method for particular variable genes, TCR repertoire analysis was also derived from single cell RNA-sequencing transcriptomic analysis (as performed in Chapter 3.2.5). CD1a-DDM tetramer$^+$ T cells were single cell-sorted *(Fig.4.4a)* for cDNA library generation and sequencing. Using the bioinformatics tool VDJPuzzle (Rizzetto et al., 2018), full-length TCR α- and TCR β-chain sequences were reconstructed from the transcriptomic data and indexed to each single cell (Eltahla et al., 2016, Rizzetto et al., 2018). Paired and unpaired TCR α- and β-chain sequences from four donors were determined by RNA-sequencing and the relative tetramer MFI during the cell sort for each TCR clone was assessed *(Fig.4.4b, Fig.4.4c)*. Interestingly, in donor CNR70, TRBV28$^+$ T cell clones often had the highest tetramer MFI compared to T cell clones with other Vβ genes *(Fig.4.4b, Fig.4.4c)*, which supports previous single cell TCR sequencing data that implicates a beneficial role of TRBV28.

The bias for TRAV8-4 was much more evident among RNA-sequenced TCRs (26/57), and a large proportion of TCRs also used TRAV14/DV4 (14/57) *(Fig.4.5a)*. The bias for TRBV28 in the TCR β-chain (27/82) was concordant with multiplex PCR sequencing results, and TRBV19 also emerged as a common Vβ gene used among DDM-reactive T cells (22/82) *(Fig.4.5b)*. This result was consistent with these two genes being identified as differentially expressed when compared to other T cell subsets (Chapter 3.2.5). The RNA sequencing method did not reveal many patterns of particular Vα and Vβ pairings due to the small sample size, however, one pairing observed frequently was a TRAV16$^+$ TRAJ20$^+$ α-chain with a TRBV19$^+$ TRBJ2-6$^+$ β-chain (*Fig.4.5c)*.

A

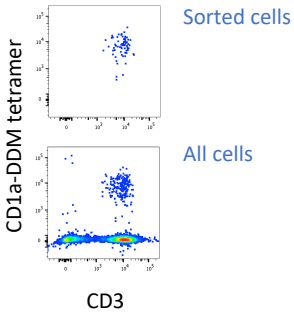

B

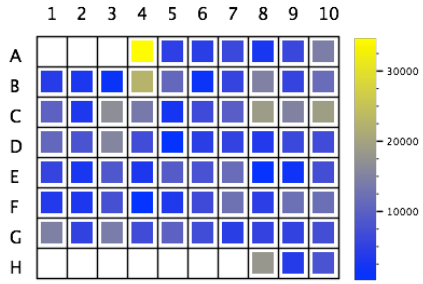

C

Position	TRAV	CDR3a	TRAJ	TRBV	CDR3b	TRBJ
A4	TRAV26-1	CIVNRPDTGNQFYF	TRAJ49	TRBV28	CASSIYGGGRRGYTF	TRBJ1-2
A4	TRAV30	CGTEIPNYGGATNKLIF	TRAJ32	TRBV5-1	CASSPWDRGGNSPLHF	TRBJ1-6
A5				TRBV11-2	CASSSGLTSTDTQYF	TRBJ2-3
A6				TRBV6-5	CASTDPAVNTEAFF	TRBJ1-1
A7				TRBV7-6	CASSPSDRDNEAFF	TRBJ1-1
A10	TRAV8-4	CAVSLSSGYALNF	TRAJ41			
B1				TRBV28	CASSDRGLEQFF	TRBJ2-1
B3				TRBV28	CASSFSTNEQFF	TRBJ2-1
B4				TRBV28	CASSFKYEQYF	TRBJ2-7
B5	TRAV8-4	CAVMAANSGYALNF	TRAJ41	TRBV28	CASSWSQEQFF	TRBJ2-1
B6				TRBV11-3	CASSLDKGLQPGETQYF	TRBJ2-5
B10				TRBV11-1	CASSLESFRGSGANVLTF	TRBJ2-6
C1				TRBV28	CASSSIGLAGGPIPRWTGELFF	TRBJ2-2
C3				TRBV28	CATPGSPGGYTF	TRBJ1-2
C4	TRAV38-1	CARQFDYKLSF	TRAJ20	TRBV28	CASQGGDTGELFF	TRBJ2-2
C6				TRBV28	CASSFGLAGPETQYF	TRBJ2-5
C8	TRAV40	CLLSSNYQLIW	TRAJ33	TRBV28	CASSLGLYNEQFF	TRBJ2-1
C9				TRBV28	CASSTTTGAENYGYTF	TRBJ1-2
D1	TRAV12-3	CAMSYYGQNFVF	TRAJ26			
D3				TRBV13	CASSSEYEQFF	TRBJ2-1
D4				TRBV28	CASIPGTSGTSYEQYF	TRBJ2-7
D6				TRBV28	CASSFVQPYEQYF	TRBJ2-7
D7	TRAV4	CLVGDGYNKLIF	TRAJ4			
D8				TRBV2	CATAREDEQFF	TRBJ2-1
D10	TRAV12-3	CAMSGSGSARQLTF	TRAJ22			
E2	TRAV12-3	CAMTPSGGSYIPTF	TRAJ6			
E3	TRAV17	CGNAGGTSYGKLTF	TRAJ52			
E5	TRAV10	CGTSGTYKYIF	TRAJ40	TRBV28	CASSQELAGFYNEQFF	TRBJ2-1
E8	TRAV12-3	CAMSSVNTNAGKSTF	TRAJ27	TRBV6-2	CASSYGLEAFF	TRBJ1-1
E9				TRBV28	CASSLSVLNEQFF	TRBJ2-1
E10				TRBV28	CASSPASTGELFF	TRBJ2-2
F1				TRBV12-4	CASSYDTGELFF	TRBJ2-2
F2	TRAV16	CDNNNDMRF	TRAJ43	TRBV24-1	CATSDSSGQDPYEQYF	TRBJ2-7
F3				TRBV28	CASSLMIVPNPNYGYTF	TRBJ1-2
F4				TRBV5-1	CASSLTGQGLVSYNEQFF	TRBJ2-1
F7				TRBV13	CASSFPTGYEQYF	TRBJ2-7
F10				TRBV28	CASNRGTPNEKLFF	TRBJ1-4
G2	TRAV8-4	CAAQNQAGTALIF	TRAJ15			
G3				TRBV28	CASSLGTGGSPLHF	TRBJ1-6
G4				TRBV10-3	CAIGGSYEQYF	TRBJ2-7
G6				TRBV13	CASSQQGYTGELFF	TRBJ2-2
G7	TRAV27	CAGPGTYKYIF	TRAJ40	TRBV28	CASSLALGAGDNEQFF	TRBJ2-1
G8	TRAV26-1	CIVSPSNDYKLSF	TRAJ20	TRBV7-6	CASSPSWTGYNEQFF	TRBJ2-1
G9				TRBV28	CASPDTLTGELFF	TRBJ2-2
H10				TRBV28	CASSQDRGRYF	TRBJ2-7

Figure 4.4. Single cell RNA-sequencing analysis of CD1a-restricted T cells in donor CNR70. A. FACS profiles of cells sorted for CD1a-DDM tetramer compared to all acquired cells. **B.** Tetramer mean fluorescence intensity (MFI) of individual sorted CD1a-tetramer$^+$ T cells as they sit in a standard 96 well plate, with blue indicating low intensity and yellow indicating high (note that columns 11 and 12 were not used as they were kept as negative control wells during PCR amplification). One cell was present per well except in position A4, which contained 10 cells. **C.** Paired and unpaired TCR α- and TCR β-chain sequences corresponding to their plate position.

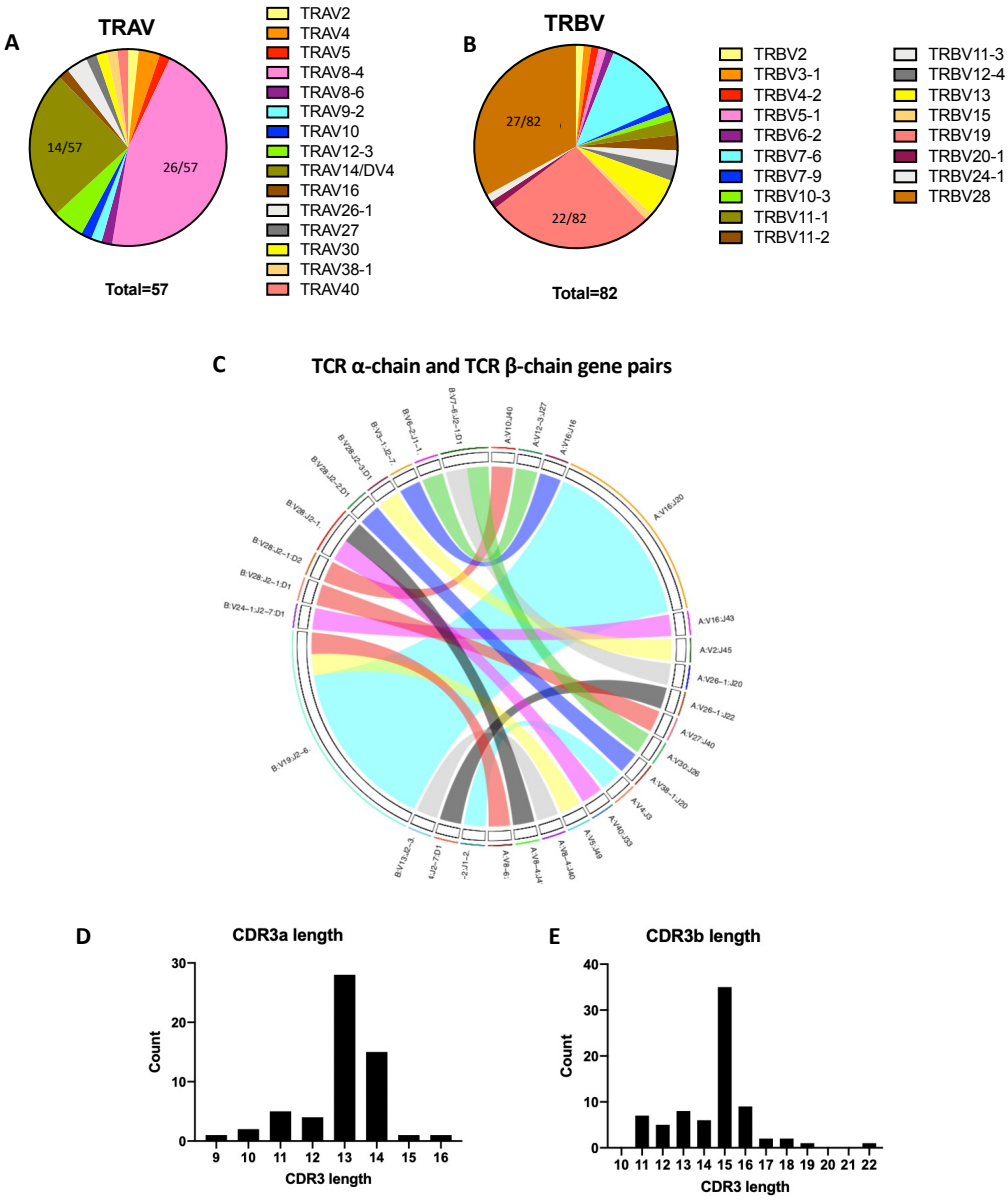

Figure 4.5. TCR diversity in CD1a-restricted T cells as determined by RNA sequencing. MACS-enriched CD1a-DDM tetramer^{+} T cells were FACS-sorted directly *ex vivo* for RNA sequencing. Paired TCR α- and TCR β-chain sequences were reconstructed from single cell RNA-sequencing reads using the VDJPuzzle tool (Rizzetto, 2018).
A and B. Pie charts displaying the TRAV gene usage of 57 TCR clones in 2 donors (**A**) and TRBV gene segment usage of 82 TCR clones in 2 donors (**B**) as determined by comparing identified sequences against the IMGT database. Only fractions above 10% are shown. **C.** Circos map of TCR heterodimer α- and β-chains from DMM-reactive T cells, depicting paired TRAV and TRBV gene segment usage from 19 unique pairs. Nomenclature outlines A/B (TCR-α or TCR-β): Variable gene: Joining gene. **D and E.** Comparison of CDR3α amino acid length (n=56) (**D**) and CDR3β amino acid length (n=82) (**E**).

The length of CDRα sequences among these T cells ranged from 9-16 amino acids (*Fig.4.5d)*. The mode remained 13 amino acids in length (*Fig.4.5d)*, which may be the optimal length for the CDR3α loop to interact with CD1a-DDM. The CDR3β length diversity was similar, with a range from 11-22 amino acids in length, with a mode of 15, two amino acids longer than that obtained using the multiplex PCR sequencing technique (*Fig.4.5e*). This could be reflective of donor variation, as this work focused on cells from only four donors.

The preferential usage of the TRBV gene presents the potential of isolating CD1a-restricted T cells using an antibody that targets Vβ3 (the protein of the TRBV28 gene). A pilot stain of PBMCs with CD1a tetramer and an α-Vβ3 mAb was performed, in which a small population of tetramer$^+$ Vβ3$^+$ cells was observed *(Fig.4.6)*. However, this technique requires further optimisation, especially given that both tetramer and antibody would be expected to bind in close proximity on the cell, and thus may interfere with each other. In two donors, just under two-thirds of CD1a-vehicle tetramer$^+$ cells were also Vβ3$^+$, and around one-third of CD1a-DDM tetramer$^+$ cells were Vβ3$^+$. The semi-invariant TCR of type I NKT cells and MAIT cells can be targeted with antibodies targeting their variable genes (Vα24 and Vβ11, or Vα7.2 respectively). While it would be useful to have an equivalent for CD1a-restricted T cells, an antibody that specifically targets Vβ3$^+$ may exclude many cells. Nonetheless, these TCR biases are worthy of further exploration, especially regarding their structure and molecular interaction with CD1a-lipid.

4.2.2 Validation of CD1a reactivity by CD1a-restricted T cell lines

A series of CD1a-restricted TCR-transduced cell lines were generated to further understand the factors that govern antigen recognition by CD1a-restricted T cells and to validate TCR sequencing approaches. Several sequences determined using single cell multiplex PCR sequencing were selected to generate TCR-transduced J.76 and/or SKW-3 cell lines to confirm CD1a-reactivity, particularly those that were TRAV8-2$^+$ or TRBV28$^+$ (indicated in Table 5.1 with cell line names*)*.

DNA constructs containing a full-length TCR α-chain linked to a paired TCR β-chain (see *Appendix I* for sequences) were cloned into a pMIG retroviral vector immediately

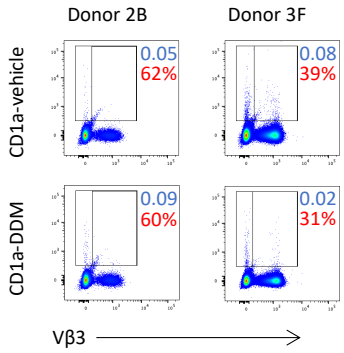

Figure 4.6. Labelling of CD1a-tetramer$^+$ T cells with a Vβ3 mAb. PBMCs from healthy blood donors were co-labelled with CD1a-vehicle or CD1a-DDM tetramer with a mAb targeting Vβ3. Cells are gated on CD3$^+$ T cells. Numbers in blue indicate proportion of T cells that were CD1a tetramer$^+$ and numbers in red indicate the percentage of tetramer$^+$ cells that were also Vβ3$^+$. Data representative of two independent experiments.

upstream of an IRES-GFP cassette as previously described (Birkinshaw et al., 2015). As a result, GFP fluorescence acted as an indicator of TCR expression and transduction efficiency. CD3 and TCR pMIG vectors were co-transfected into HEK 293T cells for retrovirus production (Holst et al., 2006, Szymczak et al., 2004) and retroviral supernatant was used to transduce TCR-deficient J.76 or SKW-3 $\beta_2m^{-/-}$ cells (Hirano et al., 1979, Schneider et al., 1977). Following five days of transduction, cells were assessed and FACS-sorted for high GFP fluorescence, before being expanded *in vitro* to ensure that all cell lines had consistent levels of TCR expression.

All TCR transduced J.76 cell lines showed similar levels of GFP expression, and to ensure tetramer binding results were not influenced by varying levels of TCR on the cell surface, cells were gated on a similar level of GFP and TCR β-chain or CD3 expression for all analyses *(Fig.4.7a)*. Each cell line was labelled with CD1a-endo and CD1a-DDM tetramers, and CD1d-endo was used as a negative control to ensure all tetramer binding was specific to CD1a *(Fig.4.7b)*

The first cell line generated in this study used a CD1a-autoreactive TCR found by sequencing *in vitro*-expanded CD1a-endo tetramer$^+$ FACS-sorted T cells prior to optimisation of tetramer staining with MACS-enrichment (data not shown). This cell line, CNR1, unexpectedly was able to bind both CD1a tetramers, albeit with higher affinity to CD1a-DDM (*Fig.4.7b*). In contrast, BK6, a published CD1a-autoreactive TCR, bound CD1a-endo tetramer but not CD1a-DDM as previously reported (Cheng et al., 2017).

Other TCR sequences for cell line generation were determined from cells MACS-enriched for CD1a tetramer and sorted for sequencing directly *ex vivo*. 29a28i and 29a28ii cell lines were also isolated using endogenous lipids, and displayed cross-reactivity to both CD1a-endo and CD1a-DDM, similar to CNR1 *(Fig.4.7b)*. CD1a-urushiol was used to isolate clone 1-2a20, and interestingly, it bound DDM, another exogenous antigen, but not CD1a-endo *(Fig.4.7b)*. The remaining T cell clones were isolated using CD1a-DDM tetramers, and displayed reactivity to either CD1a-DDM only, or were cross reactive with both DDM and self-lipids. 8-2a2 and 17a28, bound CD1a-DMM tetramers but were negative for CD1a-endo tetramer *(Fig.4.7b)*, similar to previously established DDM-reactive T cell clones, CD8-2, Clone 8 and Clone 15 (Cheng et al., 2017). 1-1a28 and 35a16 showed a high degree of binding to CD1a-DDM and bound CD1a-endo to a much

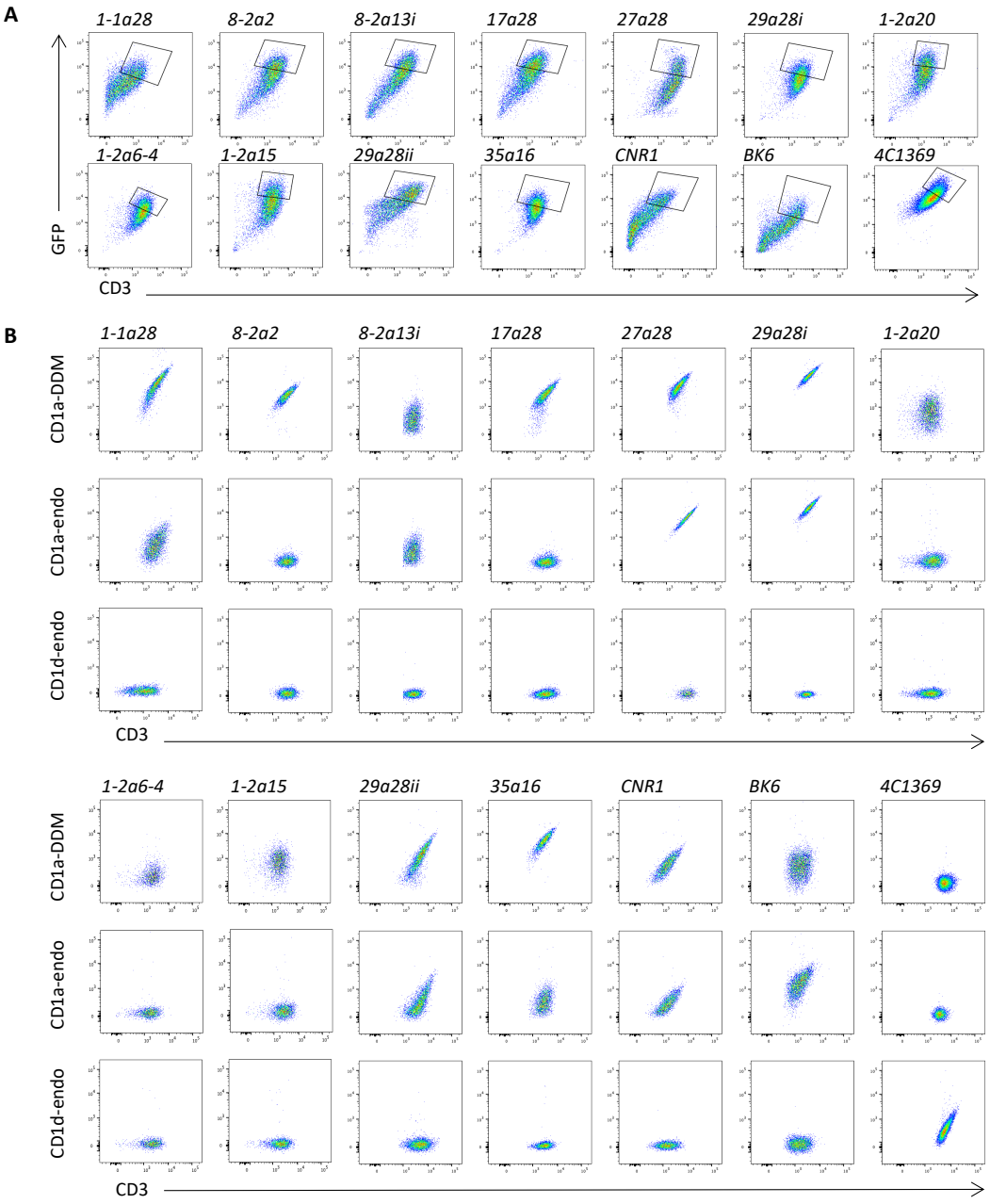

Figure 4.7. Production and validation of CD1a-tetramer binding by CD1a-restricted T cell lines produced. TCR-deficient Jurkat.76 cells were transduced with pMIG vectors containing either CD3 or a full-length TCR α-chain linked to a TCR β-chain and GFP as a reporter. **A.** GFP expression following transduction. All further cell line analyses focused on GFP^{hi} cells. **B.** Cell lines were labelled with CD1a-DDM and CD1a-endo tetramers, with a CD1d-endo tetramer used as a negative control.

Tetramer used for isolation of each TCR clone: 1-1a28, DDM; 8-2a2, DDM; 8-2a13i, DDM; 8-2a13ii, DDM; 17a11-2ii, vehicle; 17a28, DDM; 27a28, DDM; 29a28i, vehicle; 1-2a20, urushiol; 1-2a6-4, endo; 1-2a15, endo; 29a28ii, DDM; 35a16, DDM; CNR1, endo. The autoreactive NKT cell clone, 4C1369, isolated in Matulis et al. 2010, was used as a negative control.

lesser extent, but were still weakly positive *(Fig.4.7b)*, indicating that DDM contributes a substantial part of their CD1a reactivity. 8-2a13i, 27a28, 29a28i and 29a28ii displayed even greater cross-reactivity between CD1a-DDM and CD1a-endo with less discrepancy in staining levels between the two tetramers. However, 8-2a13i appeared to bind both to a lesser degree overall compared to the other TCRs *(Fig.4.7b)*, indicative of a low affinity but broadly reactive TCR. Furthermore, the three TRAV1-2$^+$ cell lines (1-2a6-4, 1-2a15 and 1-2a20) exhibited weak binding to CD1a-DDM tetramer akin to BK6 with CD1a-endo, confirming that they were not MAIT cells and thus validating these sequences *(Fig.4.7b)*.

Interestingly, multiplex PCR sequencing did not discriminate between TRAV8-2 and TRAV8-4 genes due to limited primer coverage, and TRAV8-2 was selected in the generation of these TCR cell lines (initially CNR1, followed by 8-2a2, 8-2a13i, and 8-2a13ii TCR cell lines), which were verified to be CD1a-reactive. Due to the initial reactivity of CNR1, TRAV8-2 was in all subsequent TCR gene constructs. Given that TRAV8-2$^+$ TCRs were not detected by RNA-sequencing, which instead revealed a bias for TRAV8-4, it is possible that the primary T cell clones these cell lines were originally based on were TRAV8-4$^+$ and not TRAV8-2$^+$. If this was the case, it is particularly interesting that the TRAV8-2$^+$ TCR constructs also bound CD1a, given that these Vα genes differ in their CDR loops.

To complement tetramer binding data, T cell activation of these TCRs by CD1a-expressing C1R cells was also assessed. As a co-culture, 3.3×10^3 WT or CD1a$^+$ C1R cells were mixed with 2.0×10^4 CD1a-restricted J.76 cell lines and were incubated overnight with or without the addition of DDM in a 3:1 molecular weight ratio. Upregulation of CD69 was used as a measure of T cell activation. All CD1a-restricted T cell lines tested had greater CD69 MFI following culture with CD1a$^+$ C1R cells compared to WT C1R cells *(Fig.4.8)*. As expected, the activation of BK6 was diminished in the presence of DDM, while for all other cell lines produced here, activation levels were enhanced by the addition of DDM *(Fig.4.8)*. This is consistent with a study reporting CD1-restricted TCRs conferring reactivity to both self-lipids and foreign antigens, for which microbial antigens acted as the more potent agonists (Vincent et al., 2005). However, if CD69 upregulation was already at its maximum with CD1a$^+$ C1R cells alone, this may have masked the effects of DDM addition.

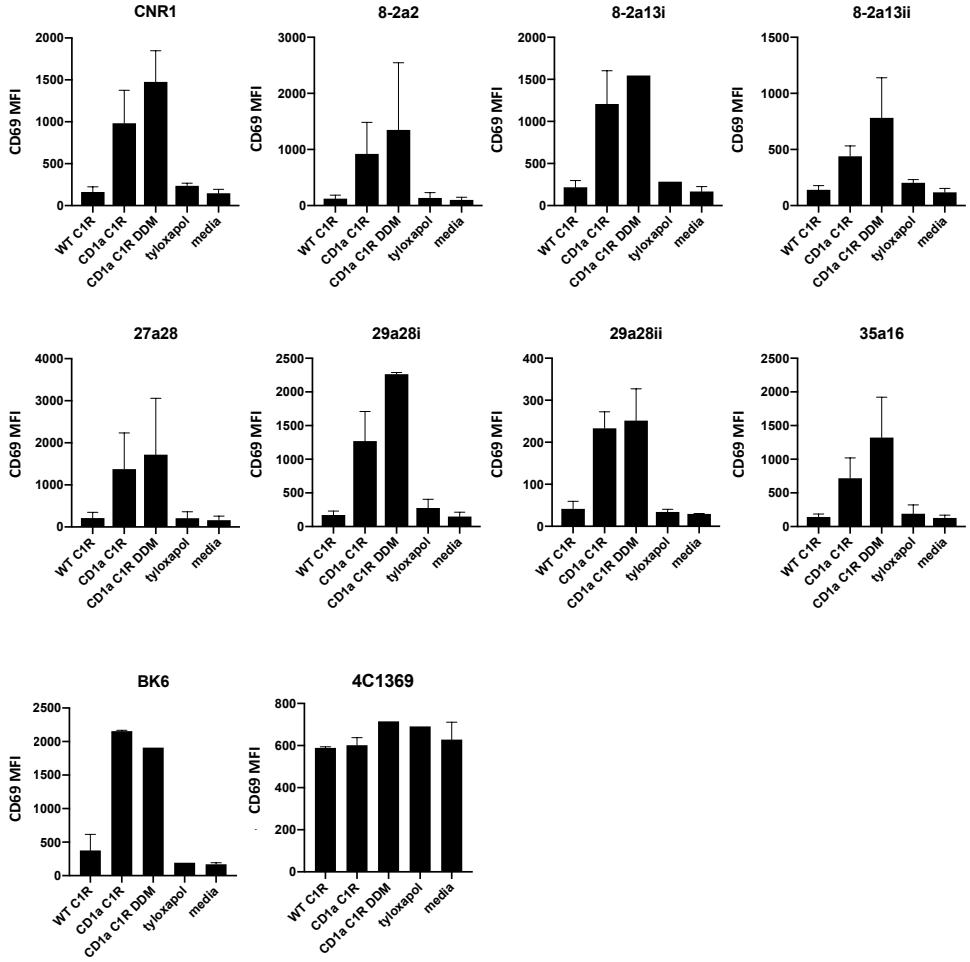

Figure 4.8. Validation of CD1a-reactivity by CD1a-restricted T cell lines produced. Activation assays were performed by co-culturing J.76 CD1a-restricted T cell lines with either wild type (WT) or $CD1a^{+}$ C1R cells with the addition of 3 µg/mL DDM or the equivalent volume of 0.5% (v/v) tyloxapol. Samples were gated on GFP^{hi} cells to ensure transduction efficiency levels were comparable and CD69 upregulation was used as a measure of T cell activation after 18 hours. Data are represented as mean and SEM of three independent experiments, except in samples BK6 and 4C1369 for which DDM and tyloxapol conditions were only performed once.

A human autoreactive CD1d-restricted T cell line, clone 4C1369 (Matulis et al., 2010), was used as a negative control for CD1a tetramer staining and activation by $CD1a^+$ C1R cells. Clone 4C1369 was negative for both CD1a tetramers but positive for the CD1d-endo tetramer, confirming that the absence of CD1a-restricted TCRs binding to the CD1d-endo tetramer was due to CD1 isoform specificity *(Fig.4.7b)*. The 4C1369 cell line also failed to be activated by $CD1a^+$ C1R cells, showing similar CD69 MFI across all conditions *(Fig.4.8)*.

Many of the CD1a-restricted T cell lines generated both bound CD1a tetramers and were activated by $CD1a^+$ APCs, thus confirming their specificity for CD1a, providing cell lines to use as tools in further studies, and validating our TCR sequencing results. Initially all cell lines were produced using J.76 cells and used for tetramer staining and activation assays. Eight CD1a-restricted TCRs (CNR1, 8-2a2, 17a28, 27a28, 29a28i, 29a28ii, and 35a16) were subsequently selected to be transduced into TCR-deficient SKW-3 $\beta_2m^{-/-}$, produced in house by fellow PhD student, Shihan Li (The University of Melbourne). Activation of SKW-3 $\beta_2m^{-/-}$ cell lines provided greater CD69 upregulation with $CD1a^+$ C1R cells and more pronounced distinction between WT and $CD1a^+$ C1R cells compared to J.76 cell lines (data not shown). The differences in activation levels between the two cell lines may have been due to the elimination of any endogenous presentation molecules on the surface of the T cells that could provide background levels of stimulation in addition to that induced by presentation molecules on the C1R cells. While C1R is an MHC class I-A and class I-B negative cell line (Storkus et al., 1989), the total absence of β_2m ensures that no CD1 or other presentation molecules can be expressed. These eight CD1a-restricted TCR clone produced with the TCR-deficient SKW-3 $\beta_2m^{-/-}$ backbone were hence used in all subsequent assays.

4.2.3 Recognition of multiple lipid antigens by CD1a-restricted T cells

When examining tetramer staining and activation of CD1a-restricted T cell lines to confirm CD1a-reactivity, there were several dual-reactive with CD1a-endo and CD1a-DDM (*Fig.4*.7 and *Fig.4.8).* This was surprising as many published CD1a-restricted T cell clones recognise either self-lipids or exogenous lipids (e.g. DDM) (Birkinshaw et al., 2015, Cheng et al., 2017). These results led to the question of how broad their cross-reactivity is between different lipids. The ability of different CD1a-restricted TCRs to

recognise multiple lipid antigens and/or CD1a alone was therefore assessed to determine whether different patterns arose between different TCRs.

CD1a-restricted T cells have been observed to recognise a broad range of lipid antigens, including endogenous self-lipids, neoantigens and foreign lipid antigens. CD1a can present a variety of self-lipids and foreign lipids derived from bacteria and plants to T cells, and favourably loads lipids with acyl chain lengths between C_{18}-C_{23} (Agea et al., 2005, de Jong et al., 2014, Hunger et al., 2004, Moody et al., 2004, Pena-Cruz et al., 2003, Zajonc et al., 2003). The cross-reactivity of CD1a-restricted T cells for some of these known lipid antigens was therefore tested.

To determine whether CD1a-restricted TCRs, isolated with tetramers loaded with one particular lipid (DDM for most TCRs), could bind other lipid antigens, a suite of TCR cell lines were assessed for tetramer binding. CD1a was loaded overnight with 0.5% tyloxapol (CD1a-vehicle), DDM, LPC, urushiol, or left loaded with lipids from the expression system (CD1a-endo) and used to make tetramers. Of these, based on data for clone BK6, DDM were expected to be non-permissive to any CD1a-autoreactive T cells due to its protruding head group (Birkinshaw et al., 2015).

All eight TCRs, including those identified using CD1a-vehicle or CD1a-endo tetramers, had a higher MFI when bound to the CD1a-DDM tetramer compared to CD1a-endo (*Fig.4.9)*. Three TCRs – 8-2a2, 17a28, and 35a16 – only bound CD1a-DDM but not CD1a-endo, consistent with previous results (*Fig.4.7)*. Nor did they bind CD1a-LPC, CD1a-urushiol or CD1a-vehicle *(Fig.4.9)*, suggesting specificity for DDM or preference for large headgroups that protrude above the A'-roof (Zajonc et al., 2005b). TCRs that previously displayed cross-reactivity between CD1a-endo and CD1a-DDM tetramers – 27a28, 29a28i, and 29a28ii – also bound to CD1a loaded with LPC, urushiol, and tyloxapol to similar degrees (*Fig.4.9).* This data suggests that these TCRs are broadly CD1a-reactive and may have a different mechanism of binding to BK6.

4.2.3.1 CD1a interaction with DDM isomers

DDM was initially discovered as an activating lipid antigen for CD1a-restricted T cells using the CD8-2 cell line, and remains the most extensively characterised type of foreign

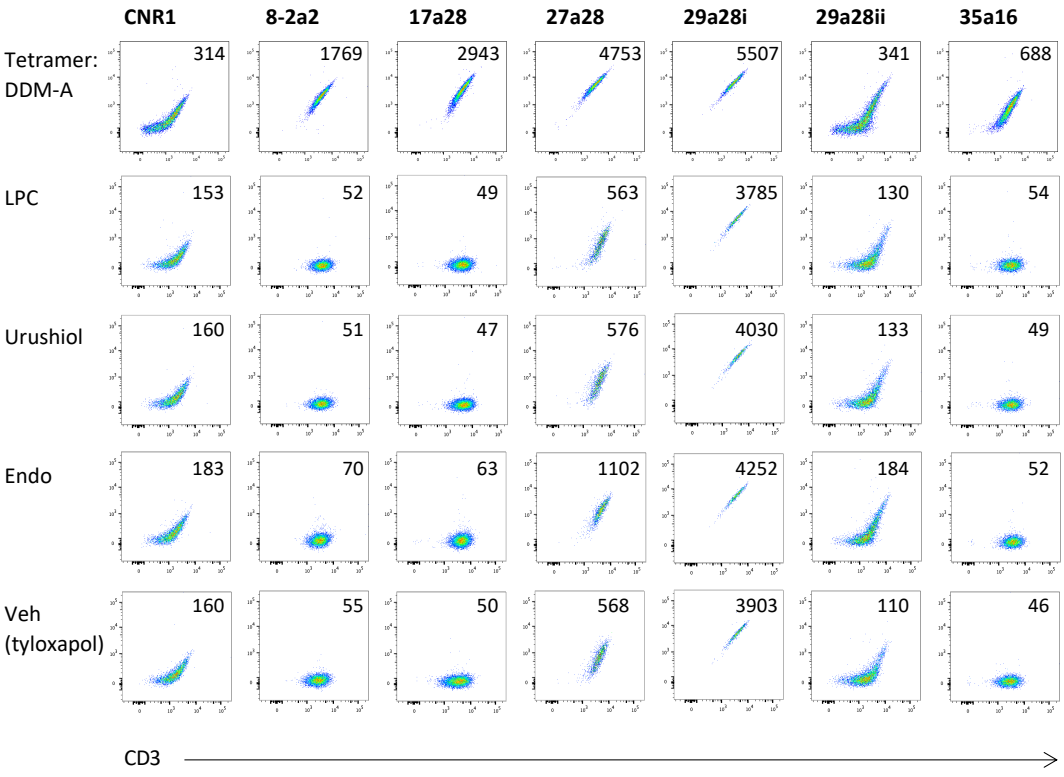

Figure 4.9. Recognition of multiple lipid antigens by CD1a-restricted TCRs. CD1a-restricted TCR SKW-3 $\beta_2m^{-/-}$ cell lines were labelled with a panel of CD1a tetramers loaded with various lipid antigens. CD1a was loaded with a panel of lipids: DDM-A, lysophosphatidylcholine (LPC) or urushiol with 0.5% tyloxapol as a loading agent. "Unloaded" endogenous CD1a and tyloxapol vehicle-loaded CD1a were included as controls. GFP^{hi} cells were gated on to ensure transduction levels were comparable. FACS plot show the relationship between CD3/TCR levels and tetramer staining. Numbers in the top right of each plot indicate tetramer mean fluorescence intensity. Data representative of three independent experiments.

lipid antigen that activates CD1a-restricted T cells (Moody et al., 2004, Rosat et al., 1999). Studies of CD1a and DDM have typically used synthesised lipid molecule DDM-838, as isolation in high yield from natural sources remains impractical (Young et al., 2009, Moody et al., 2004).

Naturally-occurring lipopeptides (DDM variants) isolated from Mtb with slight variation in alkyl chain length and saturation can be recognised by CD1a-restricted T cell clone CD8-2, but the addition of a single unsaturation at the C_2–C_3 position or extension of the acyl chain length from C_{18}-C_{20} increases DDM's antigenic potency (Moody et al., 2004). This suggests that minor structural alterations to the DDM molecule can influence how well it is recognised by CD1a-restricted TCRs. Three stereoisomers of DDM-838 have been described, each with different structure-activity relationships in antigen recognition by DDM-reactive T cell clone CD8-2, clone 8 and clone 15 (Cheng et al., 2017). Assessing the ability of these stereoisomers to interact with CD1a-restricted TCRs may provide insight as to how the DDM head group may be recognised by TCRs.

In a test of Clone 8, Clone 15, and CD8-2, the natural form of DDM-838 (DDM-A) was the most potent, while DDM-C and DDM-D compounds resulted in minimal reactivity (whereas CD1a-autoreactive TCR BK6 weakly bound these) (Cheng, Liu et al. 2017). It was hypothesised that several TCRs identified here would have a different mode of DDM recognition to those established TCRs given that they also cross-react with self-lipids.

Eight CD1a-restricted TCRs were tested for their ability to bind CD1a loaded with different DDM stereoisomers. Similar to CD8-2, clone 8 and clone 15, cell lines 8-2a2, 8-2a13ii, 17a28, and 35a16 bound DDM-A to the greatest degree and had partial binding to DDM-B, while binding to DDM-C and DDM-D tetramers was reduced to that of CD1a-endo/vehicle *(Fig.4.10a)*. CNR1 and 27a28 also had slightly reduced tetramer staining with DDM-C and DDM-D, but still retained high affinity staining, indicating that these TCRs are more broadly reactive to lipids presented by CD1a and are less sensitive to structural changes in lipid antigens (*Fig.4.10a)*. In contrast, 29a28i had slightly greater binding to CD1a-DDM-C, and 29a28ii bound tetramers loaded with DDM-D with an MFI around 2-fold greater than other DDM stereoisomers *(Fig.4.10a)*. The pairing of TRAV29 and TRBV28 may result in a TCR conformation that provides a CDR loop

architecture that can interact better with the stereoisomers, but there was no apparent pattern observed in recognition between all TRBV28^{+} TCRs.

To complement tetramer-binding data and confirm antigen cross-reactivity, T cell activation of each TCR was also assessed in the presence of different DDM stereoisomers *in vitro*. 3.3×10^3 WT or CD1a^{+} C1R cells were incubated with 2×10^4 SKW-3 $\beta_2m^{-/-}$ cells overnight with media alone or each DDM isomer at a 3:1 molecular weight ratio to CD1a. Consistent with previous results, T cell activation was enhanced by the addition of any DDM stereoisomer (*Fig.4.10b*). There were minor differences in activation levels between DDM stereoisomers across the eight TCRs. DDM-C induced the lowest levels of activation in all T cells except 27a28, for which it was the most potent agonist. Similar to DDM-specific T cell clones previously assessed, the addition of DDM-A resulted in the greatest levels of activation for 8-2a2 and 35a16 (*Fig.4.10b*). Surprisingly, three TCRs, 17a28, 29a28i, and 29a28ii, had the greatest CD69 upregulation with DDM-D, the first of which is a DDM-specific TCR (*Fig.4.10b*). CNR1 and 8-2a13ii appeared to be the most indifferent to the chemical alteration between stereoisomers but had slightly enhanced activation with DDM-D and DDM-A respectively (*Fig.4.10b*). It is possible that measuring CD69 upregulation as an outcome of activation may not be sensitive enough to capture larger differences between DDM isomers as the TCRs may have reached maximum CD69 expression with even the least effective isomer.

While DDM-A was the most potent agonist for CD1a-restricted TCRs that recognise DDM specifically, cross-reactive TCRs may have alternate docking onto the CD1a-DDM complex and hence display variable recognition for each DDM stereoisomer. These results highlight the importance of assessing multiple CD1a-restricted TCRs when endeavouring to understand the interaction between TCRs and CD1a-lipid. TCRs with different reactivity (autoreactive, DDM-reactive or cross-reactive) may have different modes of TCR docking onto CD1a-lipid complexes, which have so far been relatively unexplored. Structural studies (i.e. X-ray crystallography of TCR-CD1a-lipid co-complexes), especially exploring TCRs with particular variable genes (TRAV8-2 and TRBV28), and site-directed TCR mutagenesis experiments are required to determine the docking mode of these newly isolated CD1a-restricted TCRs.

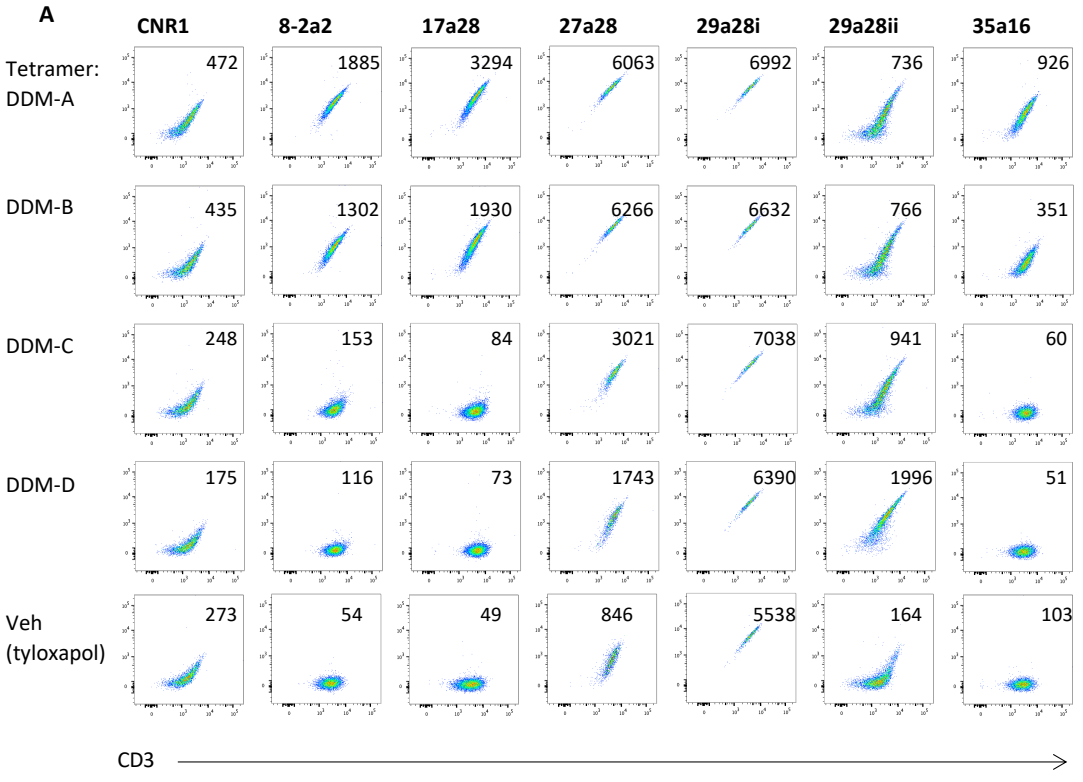
A
CNR1
8-2a2
17a28
27a28
29a28i
29a28ii
35a16
Tetramer:
DDM-A
472
1885
3294
6063
6992
736
926
DDM-B
435
1302
1930
6266
6632
766
351
DDM-C
248
153
84
3021
7038
941
60
DDM-D
175
116
73
1743
6390
1996
51
Veh
(tyloxapol)
273
54
49
846
5538
164
103
CD3

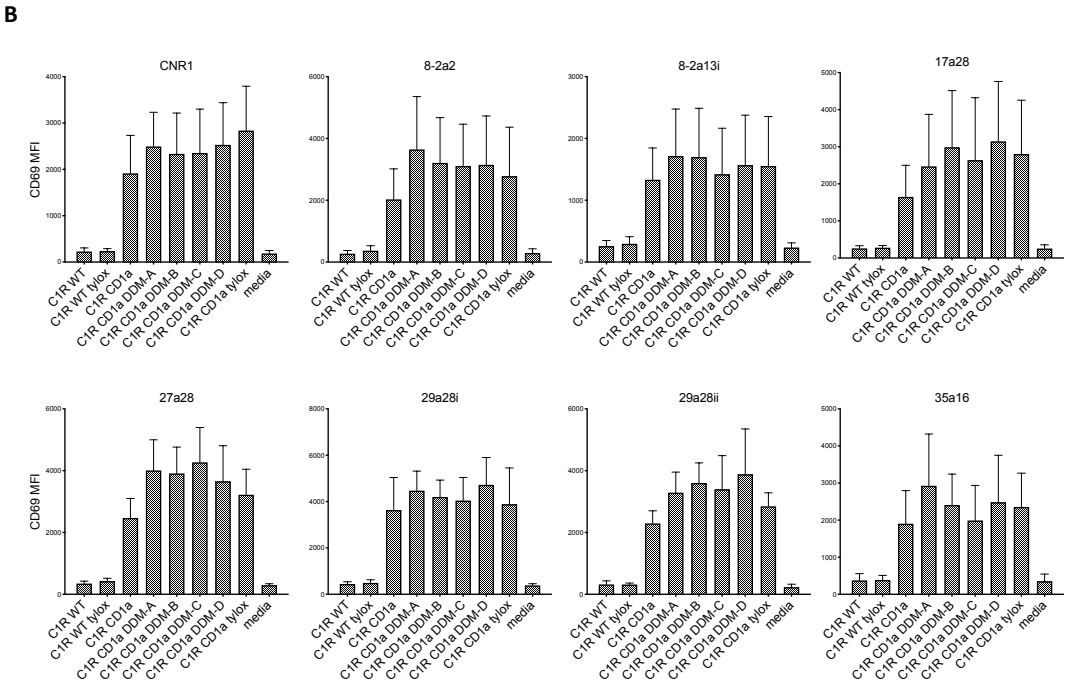
B
CNR1
8-2a2
8-2a13i
17a28
27a28
29a28i
29a28ii
35a16
CD69 MFI
C1R WT
C1R WT tylox
C1R CD1a
C1R CD1a DDM-A
C1R CD1a DDM-B
C1R CD1a DDM-C
C1R CD1a DDM-D
C1R CD1a tylox
media

Figure 4.10. T cell activation in response to CD1a presenting DDM stereoisomers. A. CD1a-restricted TCR SKW-3 $\beta_2m^{-/-}$ cell lines were labelled with a panel of CD1a tetramers loaded with DDM stereoisomers (DDM-A, DDM-B, DDM-C or DDM-D) or 0.5% tyloxapol. Samples were gated on GFP^{hi} cells to ensure transduction efficiency levels were comparable. Numbers in the top right of each plot indicate tetramer mean fluorescence intensity. **B.** CD1a-restricted SKW-3 $\beta_2m^{-/-}$ cell lines were cultured for 18 hours with wild-type (WT) or $CD1a^{hi}$ C1R cells with the addition of DDM stereoisomers or 0.5% (v/v) tyloxapol. Samples were gated on GFP^{hi} cells to ensure transduction efficiency levels were comparable and CD69 upregulation was used as a measure of T cell activation. Data are represented as mean and SEM of three independent experiments.

4.2.4 Interaction of CD1a-lipids and TCR

Three groups of CD1a-restricted T cell reactivity were identified: CD1a-autoreactive, which preferentially bind CD1a loaded with small headless lipid antigens (de Jong, Cheng et al. 2014, Birkinshaw, Pellicci et al. 2015); those that more specifically bind DDM or antigens with large headgroups (Cheng et al., 2017, Moody et al., 2004) (hereon in referred to as DDM-reactive); and those that broadly react to CD1a regardless of the specific lipid (Vincent et al., 2005). The mechanisms by which they do this remain unclear as only the CD1a-autoreactive clone BK6 has been investigated in structural studies (Van Rhijn et al., 2014).

A study of BK6 revealed that the narrow A'-pocket, which holds alkyl chains between C_{18}-C_{23} in length, dominates the interaction at the antigen-binding cleft. Meanwhile, the F'-pocket contains protruding polar head groups and most of the fatty acid chain of the lipid to be directly accessible to TCRs (Birkinshaw et al., 2015, Zajonc et al., 2003). The TCR's CDR loop-CD1a mediated interactions are well established for the BK6 TCR and CD1a, however, whether these interactions are consistent with other CD1a-restricted TCR interactions is yet to be determined.

It was hypothesised that TCRs that only recognise small, endogenous lipids, like BK6, would interact with the antigen-free A'-roof; DDM-reactive TCRs would interact with large, headgroups that protrude from the F'-portal; and broadly reactive CD1a-restricted TCRs would bind somewhere such that larger lipids can facilitate rather than block TCR binding.

The basis of TCR interactions with CD1a-lipid antigen was explored by using C1R cells that were transduced to express either WT CD1a or 12 single site mutants in "hot spot residues" (Birkinshaw et al., 2015). The impact of each amino acid mutation was assessed based on their activation of CD1a-restricted SKW-3 $\beta_2m^{-/-}$ cell lines compared to WT CD1a, allowing the elucidation of the TCR "footprint" on CD1a. A published dataset for the structure of huCD1a-endo available in the Protein Data Bank (PDB) (PDB code 4XBD) was used as a reference to generate a surface map depicting the molecular binding footprint of CD1a-restricted TCR clones on CD1a. This CD1a mutant activation assay for BK6 previously indicated that the BK6 TCR docks over the A'-roof in a manner

that precludes interactions with any protruding lipid out of the F'-portal (Birkinshaw et al., 2015).

Here, the same panel of huCD1a mutants of key residues spanning the F'-pocket and A'-pocket in both the α1 and α2 helices were assessed for their impact on TCR interactions. Each selected residue was mutated to alanine such that the mutants were defined as E61A, E62A, E65A, L69A, I72A, R76A, R83A, K146A, Q150A, H153A, N160A, and D164A (Birkinshaw et al., 2015). Each mutant CD1a was expressed by C1R cells, which were sorted for high CD1a expression by flow cytometry to ensure each line expressed similar levels of CD1a. For each CD1a-restricted T cell line, 3.33×10^3 $CD1a^+$ C1R cells (WT or mutant) were incubated with 2×10^4 SKW-3 $\beta_2m^{-/-}$ cells overnight.

Activation of $CD3^+$ CD1a-restricted TCR SKW-3 $\beta_2m^{-/-}$ cells was assessed by CD69 upregulation, and the impact of each mutation on CD1a-restricted T cell activation was represented as a percentage-fold difference compared to activation by WT CD1a. Amino acids altered in CD1a mutants that resulted in activation levels comparable to WT CD1a (80% or above) were regarded as having no impact on TCR binding. When the CD1a mutants produced activation levels that were 40-80% of WT CD1a, the amino acids were regarded as having moderate importance in TCR binding. When activation levels were reduced to below 40%, which was around the same level as baseline CD69 levels with $CD1a^-$ WT C1R cells, the amino acids were regarded as critical for TCR binding.

Using this approach, TCRs containing TRAV8-2, namely CNR1, 8-2a2 and 8-2a13ii, appeared to have different patterns of binding, suggesting that TRAV8-2^+ CD1a-restricted TCRs do not necessarily interact with the CD1a surface in the same manner *(Fig.4.11)*. Substitutions at the centre of and around the A'-roof (L69 and N160) and at the edge of the F'-pocket (H153) greatly diminished activation of CNR1, which expresses a TRAV8-2^+ $TRBV19^+$ TCR *(Fig.4.11)*. Substitutions around the other A'-roof residues (E61A, E62A, E65A, and D164) also moderately reduced T cell activation *(Fig.4.11)*. There appeared to be minimal impact of I72, Q150, K164 substitutions around the F'-pocket and only moderate impact of others that surround it *(Fig.4.11)*. These data suggest that CNR1 docks over the A'-roof and one side of the F'-portal, through which antigens protrude, similar to BK6 for which mutations in the centre of the A'-roof completely

CNR1

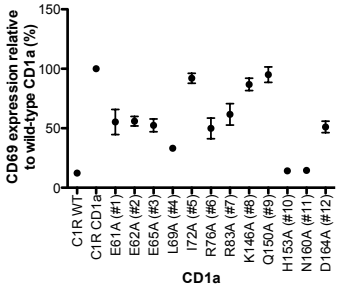

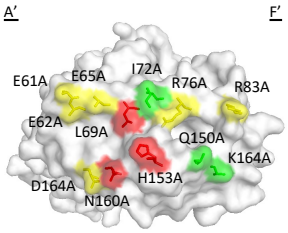

8-2a2

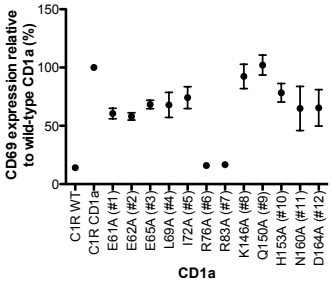

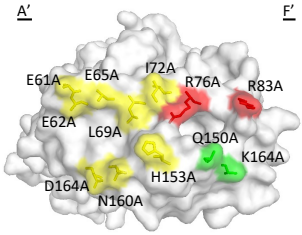

8-2a13ii

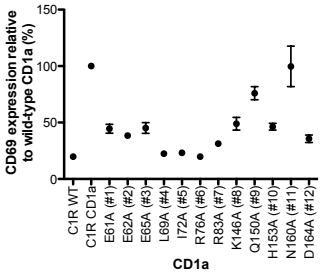

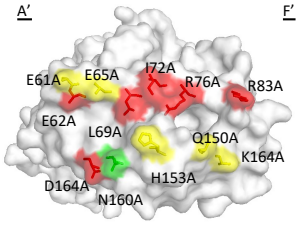

35a16

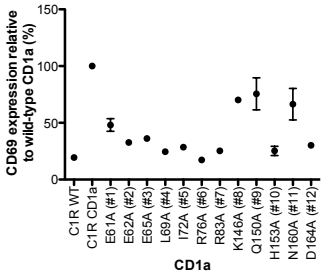

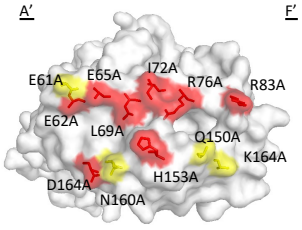

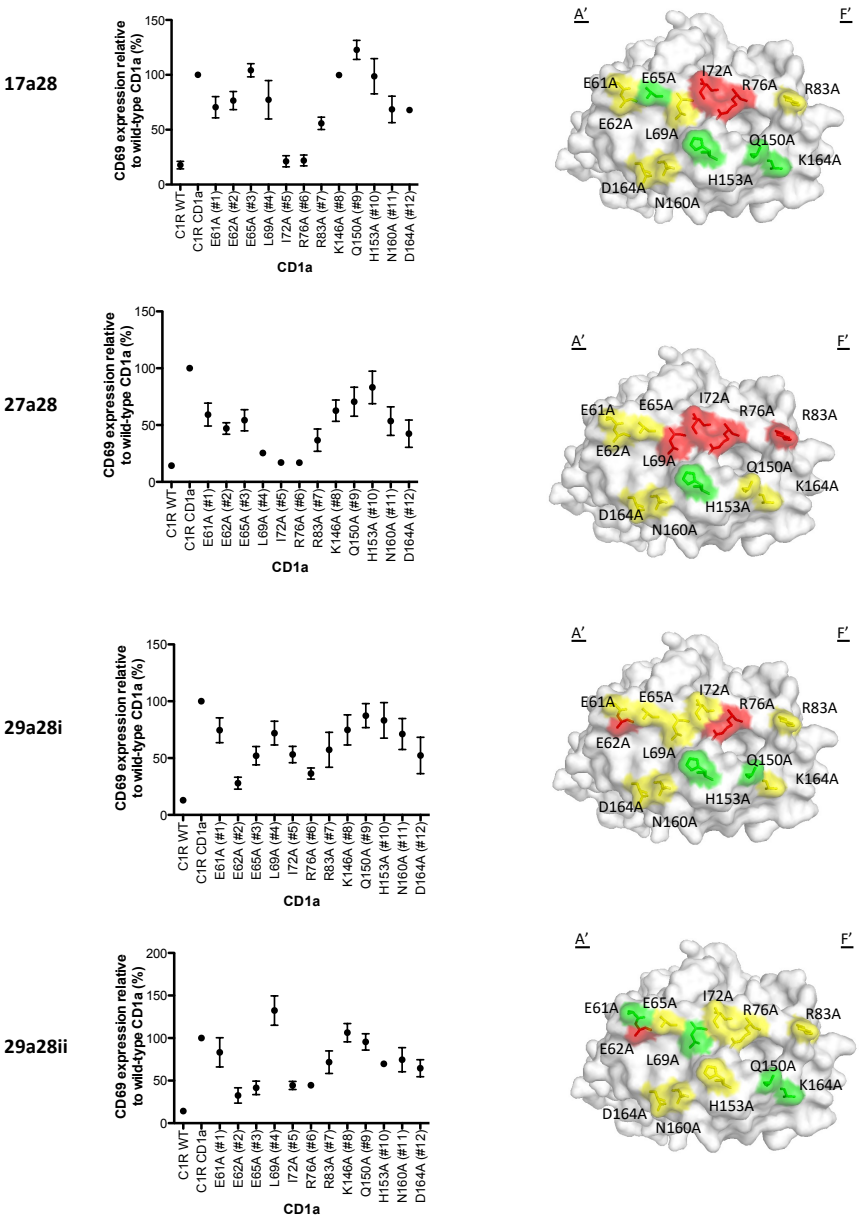

Figure 4.11. Mutational analysis defining key interactions between CD1a-restricted TCRs and CD1a presenting endogenous lipids. C1R cells were transduced with either WT CD1a or a series of mutant CD1a molecules where surface exposed amino acids lining the antigen-binding groove were mutated to alanine. These were co-cultured with CD1a-restricted TCR SKW-3 $\beta_2m^{-/-}$ cell lines and activation was measured by CD69-upregulation after 18 hours. Data is shown as a percentage of CD69 up-regulation relative to CD1a WT (left). On the right are corresponding surface maps of CD1a (PDB code 4XBD) with alanine mutations of CD1a surface residues coloured according to TCR-CD1a interactions relative to WT with no impact on binding (≤80%) (green), partial binding (40-80%) (yellow), and no binding (≤40%) (red). Data are represented as mean and SEM, and are representative of three experiments.

diminish TCR interactions (Birkinshaw et al., 2015), although its binding is not perturbed by the presence of DDM in the same way as BK6.

Activation of DDM-specific TCR, 8-2a2, was most impaired by mutations in residues R76 and R83 around the F'-pocket, while mutations in residues around the A'-pocket only had a moderate impact, indicating that its TCR binding footprint is towards the F'-pocket *(Fig.4.11)*. Substitutions to two other residues around the F'-pocket had minimal impact on TCR activation, suggesting that the TCR may only interact with residues on one side of the pocket through which lipids protrude *(Fig.4.11)*. Given that the only accessibility of lipids is from the F'-pocket, the TCR may interact with the large, protruding head-group of DDM and residues immediately around it.

Multiple amino acid residues across the CD1a molecule appear critical for 8-2a13ii TCR binding, given that 6 out of 12 mutants, negatively impacted T cell activation when mutated *(Fig.4.11)*. All substitutions around both the A'- and F'-pockets either critically or moderately reduced T cell activation except for N160A, which is also on the outer edge of the A'-roof *(Fig.4.11)*. Similarly, 35a16 was also sensitive to changes in most amino acid residues, with 8 out of 12 mutants reducing activation levels to below 40% of WT CD1a and the remaining 4 being reduced to between 40-80% *(Fig.4.11)*. This suggests that these TCRs might adopt a parallel docking mode over the CD1a antigen-binding cleft, rather than interacting with one particular portal.

Overall, TRBV28^{+} TCRs revealed fewer key amino acid residues that, when mutated, reduced T cell activation to below 40% of WT CD1a. 17a28 and 27a28 had similar footprints on CD1a: substitutions to residues lining the edge of the F'-pocket (I72 and R76, as well as L69 and R83 for 27a28) completely impaired T cell activation *(Fig.4.11)*. Residues over the A'-roof of CD1a also moderately reduced activation when mutated *(Fig.4.11)*. 29a28i and 29a28ii TCRs, which displayed the greatest tetramer binding and activation in response to CD1a of all TCRs tested and are broadly CD1a-reactive, were the least affected by mutations in CD1a (*Fig.4.11)*. Activation of TCR 29a28ii was only critically reduced with one amino acid, namely E62A, which surrounds the A'-pocket *(Fig.4.11)*. TCR 29a28i was also critically impacted by the same substitution as well as R76 around the F'-pocket *(Fig.4.11)*. This finding provides further evidence that the pairing of TRAV29 with TRBV28 may allow for particular CDR loop confirmations that

provide a distinct docking mechanism. It also may be that their key CD1a contact residues were not among the 12 initially identified by Birkinshaw and Pellicci (Birkinshaw et al., 2015).

Substitution of R76, a residue around the F'-portal, had minimal impact on BK6 binding (Birkinshaw et al., 2015), while it abrogated binding ability for 7/8 TCRs tested here, and had moderate impact for the remaining TCR (29a28ii) (*Fig.4.11*). This indicates that it may be critical as a contact residue for TCRs that recognise larger, non-self-lipids. The differences in key CD1a contact residues between the TCRs tested here and BK6 indicate multiple docking mechanisms of CD1a-restricted TCRs onto CD1a-lipid complexes, which could be reflective of their antigen reactivities and might be further investigated.

To account for differences in the amino acids engaged when the DDM headgroup protrudes out of the F'-pocket, CD1a mutant C1R cells were cultured with CD1a-restricted T cell lines in the presence of DDM to determine whether it made a difference to the TCR footprint on CD1a (*Fig.4.12).* TCRs 8-2a2, 17a28 and 35a16 exhibit greater binding to CD1a when loaded with DDM rather than endogenous lipids and therefore were expected to interact predominantly with F'-pocket residues and the DDM headgroup, and not the antigen-free zone above the A'-pocket. 8-2a2 was moderately sensitive to mutations around the F'-pocket (R76 and R83) without DDM, and these two residues became critical for T cell activation when DDM was present, suggesting that the TCR might interact with these residues around the DDM headgroup *(Fig.4.12)*. Conversely, substitutions to residues around the F'-portal (I72, R76 and R83) were not as critical for 17a28 TCR contact and activation when DDM was added *(Fig.4.12),* possibly because DDM may obscure contact with this residue. 35a16 had the greatest sensitivity to alterations in the CD1a structure, which became more pronounced with the addition of DDM *(Fig.4.12)*. This was consistent with the previous results, indicative of it docking across the entire CD1a groove.

CD1a-autoreactive TCR, BK6, predominantly docks above the A'-roof and the large head-group of DDM disrupts this TCR-CD1a interaction (Birkinshaw et al., 2015). Given that DDM protrudes out of the F'-pocket, it was therefore expected that TCRs that bind CD1a-endo and CD1a-DDM dock in such a way that access to key contact residues is not blocked by DDM. Indeed, when the CD1a mutant activation assay was performed with

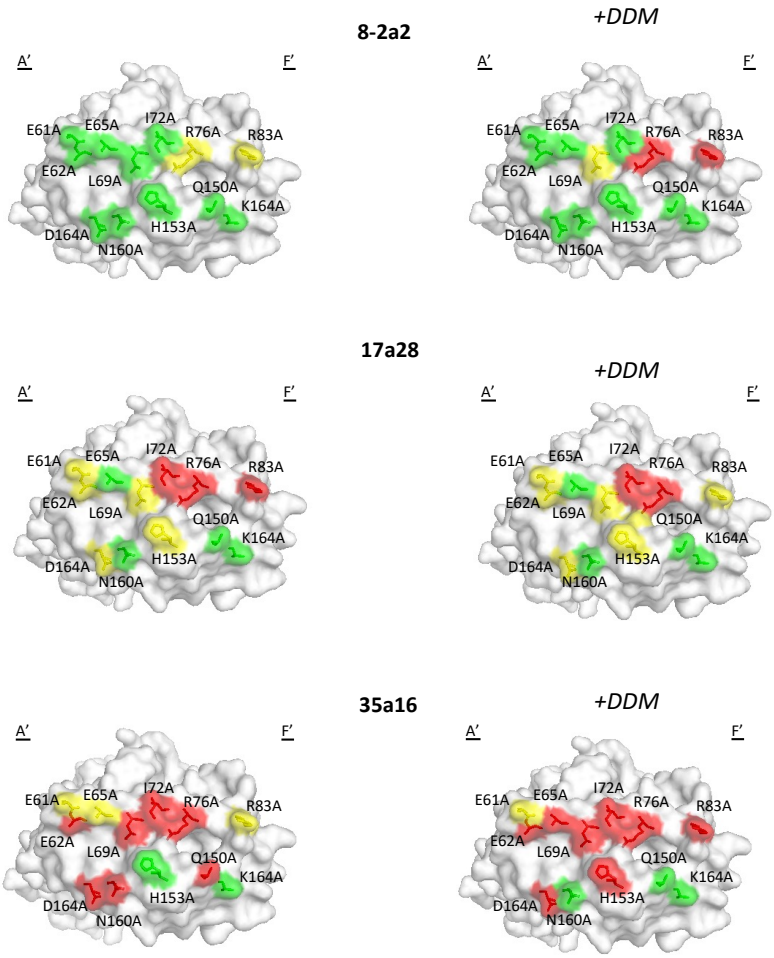

Figure 4.12. Mutational analysis defining key interactions between DDM-specific TCRs and CD1a presenting DDM. C1R cells were transduced with either WT CD1a or a series of mutant CD1a molecules where surface exposed amino acids lining the antigen-binding groove were mutated to alanine. These were co-cultured with CD1a-DDM-reactive TCR SKW-3 $\beta_2m^{-/-}$ cell lines with and without the addition of 3 µg/mL DDM (right and left respectively) and activation was measured by CD69-upregulation after 18 hours. Surface maps of CD1a (PDB code 4XBD) with alanine mutations of CD1a surface residues coloured according to TCR-CD1a interactions relative to WT with no impact on binding (≤80%) (green), partial binding (40-80%) (yellow), and no binding (≤40%) (red). Data are represented as mean and SEM, and are representative of two experiments.

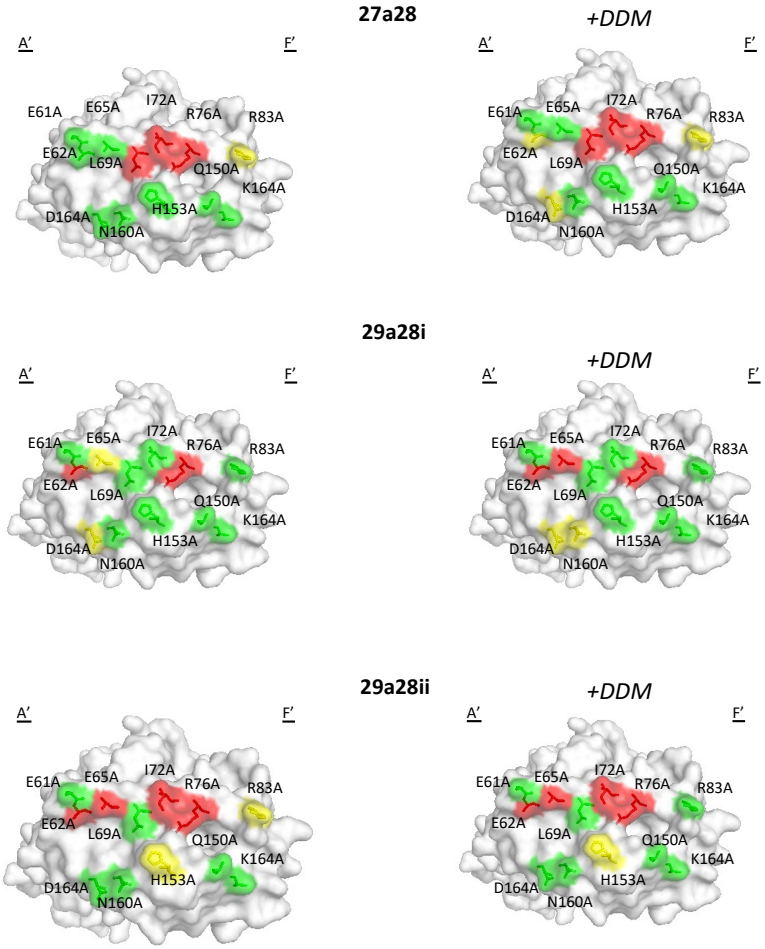

Figure 4.13. Mutational analysis defining key interactions between dual-reactive TCRs and CD1a presenting DDM. C1R cells were transduced with either WT CD1a or a series of mutant CD1a molecules where surface exposed amino acids lining the antigen-binding groove were mutated to alanine. These were co-cultured with CD1a-DDM-reactive TCR SKW-3 $\beta_2m^{-/-}$ cell lines with and without the addition of 3 µg/mL DDM (right and left respectively) and activation was measured by CD69-upregulation after 18 hours. Surface maps of CD1a (PDB code 4XBD) with alanine mutations of CD1a surface residues coloured according to TCR-CD1a interactions relative to WT with no impact on binding (≤80%) (green), partial binding (40-80%) (yellow), and no binding (≤40%) (red). Data are represented as mean and SEM, and are representative of two experiments.

and without DDM, there appeared to be little difference in the key contact residues between the two conditions *(Fig.4.13)*. A critical residue for all three dual-reactive TCRs was R76A on the edge of the F'-pocket, and it may be that these TCR CDR loops are shaped in such a way that they can reach around any bulky antigen head that protrudes *(Fig.4.13)*.

In summary, the key amino acid residue contacts identified for the CD1a-restricted TCRs studied here are spread across the CD1a molecule, and the loss of one particular amino acid did not elicit the same effect across all TCRs. These differences may be due to CDR loop configuration and how they interact with both CD1a and lipids. These findings thus indicate variability in TCR docking modes onto CD1a-lipid complexes, which could be validated with further structural studies of ternary TCR-CD1a-lipid co-complexes.

4.2.5 Production of Recombinant Human CD1a-restricted TCRs

Soluble TCRs were produced for X-ray crystallography and lipid antigen discovery to provide further insight into the interactions between CD1a-lipids and TCRs and to identify high affinity CD1a lipids respectively. Four CD1a-restricted TCRs were selected for expression and soluble TCR production: two were broadly CD1a-reactive (27a28 and 29a28i) and two were DDM-reactive (8-2a2 and 17a28). The final amino acid sequences for each TCR chain can be found in Appendix II.

Similar to gene constructs generated for T cell line production, DNA constructs were generated, encoding TCR α- and β-chain sequences that were truncated immediately prior to the 7 transmembrane domain and contained "Avidex" cysteine residues, described in patent: Avidex WO 03/020763, A2, 2003 *(Appendix II).* Final TCR gene segments were cloned into pET30 expression vectors and expressed in BL-21 E-coli cells as inclusion body preparations (IBPs). Each IBP was analysed by SDS-PAGE to determine expression levels and concentration based on a control TCR of known concentration (data not shown).

Soluble CD1a-restricted TCRs were generated by oxidative refolding of TCR α- and β-chain IBPs using a method similar to that previously described (Garboczi et al., 1996).

Briefly, α- and β-chain proteins were injected in a 1:1 equimolar ratio in a urea refold buffer. TCR proteins contained an engineered disulphide linkage between the TRAC and TRBC domains as previously described to promote refolding (Boulter et al. 2003). Refolded TCR was purified using 24-hour dialysis followed by sequential chromatography involving DEAE anion exchange, S-75 gel filtration and MonoQ anion exchange. DEAE purification separates proteins based on molecular charge and efficiently removes the majority of the non-refolded TCR as it is retained on the DEAE sepharose following elution with 200mM NaCl. Gel filtration separates proteins based on size and is used to exclude aggregated and monomeric TCR. Mono-Q anion exchange also separates proteins based on charge for the small-scale enrichment of highly pure proteins.

Fig.4.14a shows the DEAE chromatogram trace of 27a28 TCR (left) and SDS-PAGE of fractions under reducing and non-reducing conditions (right). Coomassie Blue staining revealed two bands of approximately 50 kDa under non-reducing conditions in all fractions, representative of an αβ-heterodimer and ββ-homodimer, which was slightly larger. Under reducing conditions, two bands representing a β-chain and α-chain were present at 30 and 20 kDa respectively at increasingly equivalent ratios across the fractions as the ratio of homodimer to heterodimer equilibrated. All fractions were pooled, concentrated, and passed over a gel filtration column. *Fig.4.14b* shows the HiLoad Superdex 75 pg (S75) gel filtration chromatogram trace of the 27a28 TCR (left) and SDS-PAGE of fractions under reducing and non-reducing conditions (right). The chromatogram revealed an expected peak at around 56 mL, which corresponded to one major band at 50 kDa on SDS-PAGE and two bands for α- and β-chains of equal thickness under reducing conditions in fraction 19. Fractions in this peak (15-21) were pooled, concentrated, and passed over Mono-Q. *Fig.4.14c* show the Mono-Q chromatogram trace of the 27a28 TCR (left) and SDS-PAGE of fractions under reducing and non-reducing conditions (right). One major peak was observed from the Mono-Q trace, which corresponded to fraction 73 on the gel containing one major band at 50 kDa under non-reducing conditions and two bands under reducing conditions. Fraction 68, which was in the first peak, contained a ββ-homodimer, as indicated by a single band under non-reducing conditions for the β-chain protein but not the smaller α-chain protein. Fractions 71-75 were pooled and concentrated in TBS for storage at -20 °C.

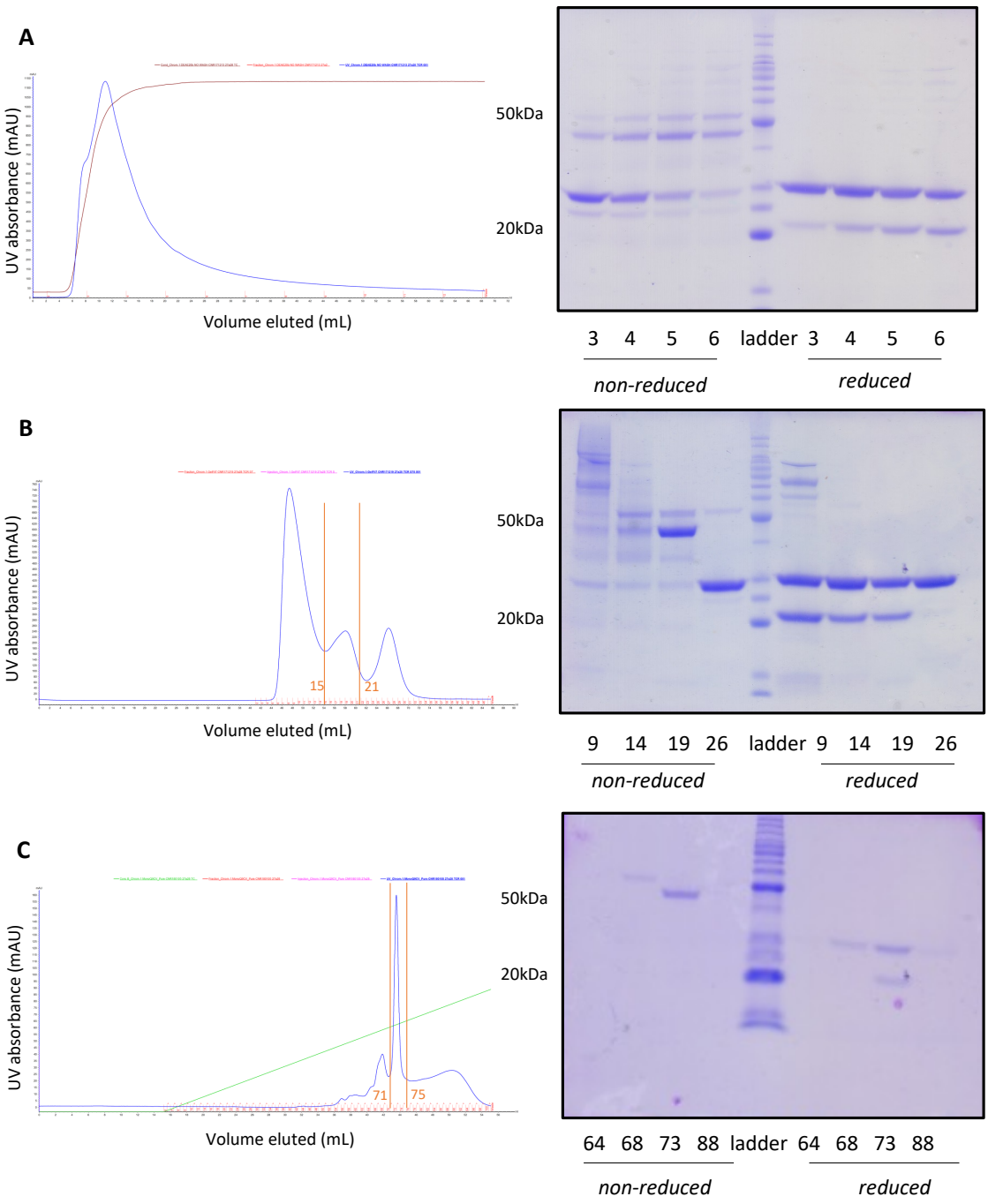

Figure 4.14. Purification of soluble 27a28 CD1a-restricted TCR. A. DEAE anion exchange chromatography of refolded 27a28 TCR (left). Fractions were assessed by SDS-PAGE under reducing and non-reducing conditions (right). Fractions containing TCR (3-12) were pooled for gel filtration. **B.** Gel filtration chromatography of refolded TCR (left). Fractions were assessed by SDS-PAGE under reducing and non-reducing conditions (right). Fractions containing TCR (15-21) were pooled for Mono-Q. **C.** Mono-Q anion exchange chromatography of refolded TCR (left). Fractions were assessed by SDS-PAGE under reducing and non-reducing conditions (right). Fractions 71-75 were collected and concentrated in TBS for storage.

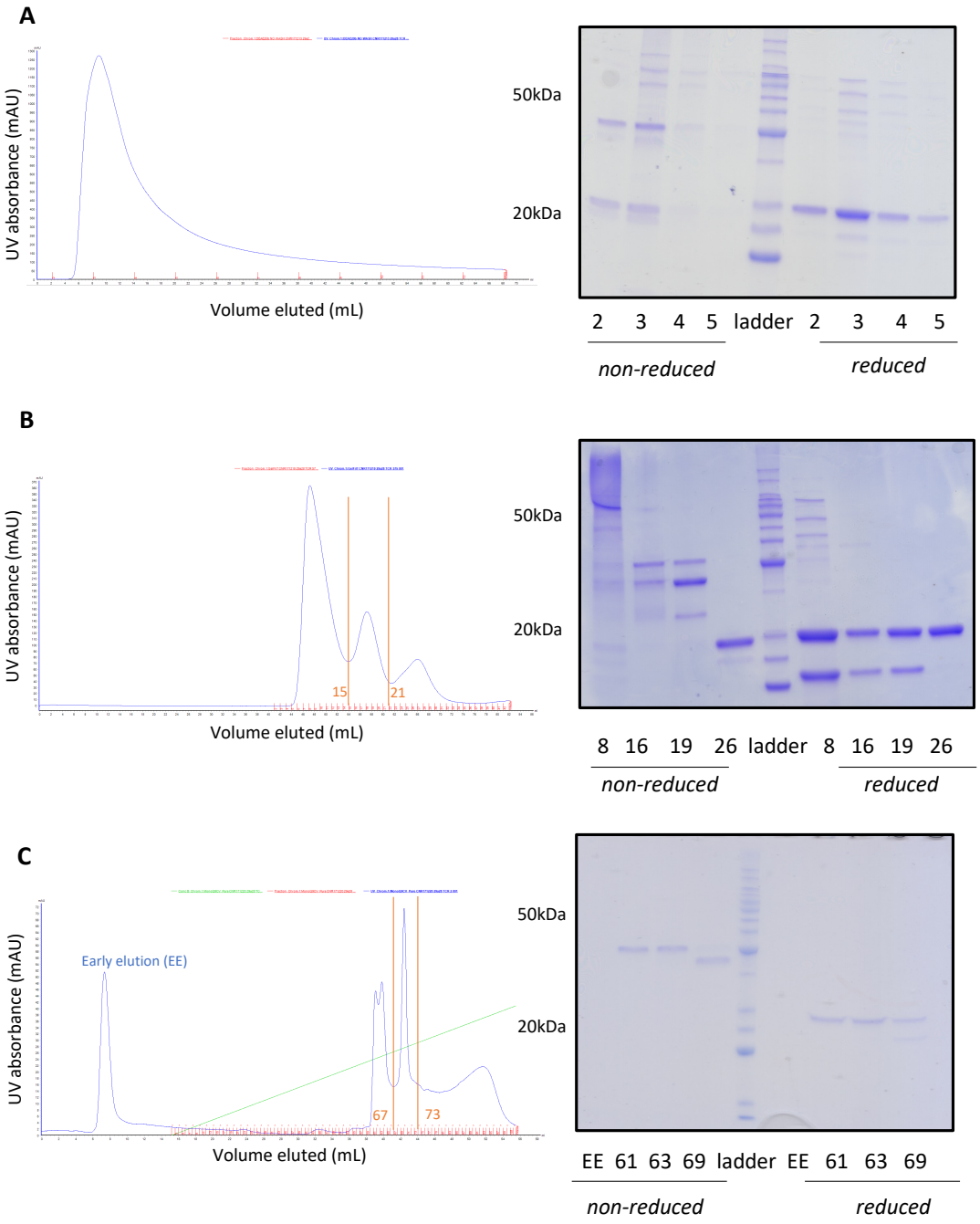

Figure 4.15. Purification of soluble 29a28i CD1a-restricted TCR. A. DEAE anion exchange chromatography of refolded 29a28i TCR (left). Fractions were assessed by SDS-PAGE under reducing and non-reducing conditions (right). Fractions containing TCR (3-12) were pooled for gel filtration. **B.** Gel filtration chromatography of refolded TCR (left). Fractions were assessed by SDS-PAGE under reducing and non-reducing conditions (right). Fractions containing TCR (15-21) were pooled for Mono-Q. **C.** Mono-Q anion exchange chromatography of refolded TCR (left). Fractions were assessed by SDS-PAGE under reducing and non-reducing conditions (right) and fractions 67-73 were collected and concentrated in TBS for storage.

The 29a28i TCR was also refolded, collected using DEAE and assessed by SDS-PAGE (*Fig.4.15a).* There was a band at approximately 50 kDa under non-reducing conditions (an αβ-heterodimer), and two bands (α- and β-chains) under reducing conditions, and fractions containing these bands were pooled and concentrated (*Fig.4.15a)*. Reducing conditions indicated the presence of more β-chain, and thus, the presence of ββ-homodimer in addition to αβ-heterodimer. S75 pg gel filtration was used for further purification (*Fig.4.15b).* The chromatogram revealed an expected peak at around 57 mL, which corresponds to one major band at 50 kD on SDS-PAGE and two bands of equal thickness under reducing conditions in fraction 16. Fractions in this peak (15-21) were pooled, concentrated, and passed over Mono-Q. One major peak was observed in the Mono-Q trace, which corresponded to one major band at 50 kD under non-reducing conditions and two bands under reducing conditions (*Fig.4.15c)*. An early elution was detected prior to the introduction of a salt gradient, suggesting that the protein may have passed straight through the column without binding the positively charged resin, however, when a sample of this flow through was assessed by SDS-PAGE, no protein was visible (*Fig.4.15c)*. Fractions 61 and 63 appeared to contain ββ-homodimer as they produced a single, slightly larger band than expected for a TCR at around 50 kDa under non-reducing conditions and only a single band under reducing conditions, whereas fraction 69, which corresponds to the second main peak, contained both α- and β-chain proteins in equal amounts. Fractions 67-73 were collected as soluble αβ-TCR protein for structural studies.

The DDM-reactive TCR 17a28 was refolded, collected using DEAE and assessed by SDS-PAGE (*Fig.4.16a).* Reducing conditions revealed the presence of predominantly β-chain protein and a very faint band representing the smaller α-chain protein in the earlier fractions (*Fig.4.16a)*. These results indicate that the efficiency of α- and β-chain dimerisation was relatively low. Nonetheless, fractions corresponding to the chromatogram peak were collected and concentrated for further purification by S75 pg gel filtration. The gel filtration chromatogram revealed an expected peak at around 56 mL (fraction 17), corresponding to two bands under reducing SDS-PAGE (*Fig.4.16b)*. These bands were not of equal intensity when stained with Coomassie Blue, again indicating the presence of ββ-homodimer in the same elution volume as αβ-TCR (*Fig.4.16b)*. Fraction 26 revealed the presence of a large amount of remaining β-chain monomer as seen by a single band at approximately 30 kDa under both reduced- and non-reduced conditions (*Fig.4.16b)*. Fractions in the middle peak (13-21) were pooled,

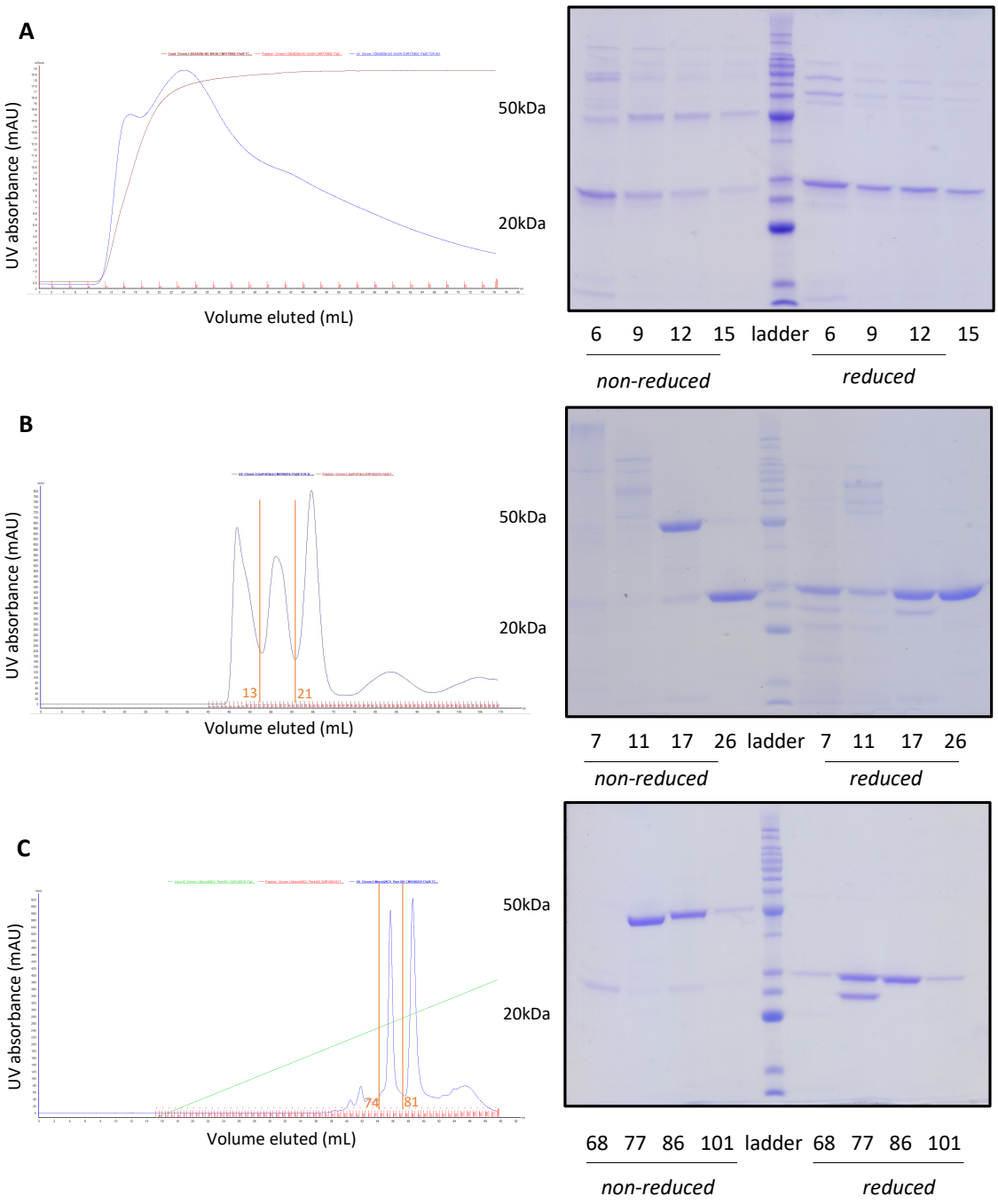

Figure 4.16. Purification of soluble 17a28 CD1a-restricted TCR. A. DEAE anion exchange chromatography of refolded 17a28 TCR (left). Fractions were assessed by SDS-PAGE under reducing and non-reducing conditions (right). Fractions containing TCR (5-20) were pooled for gel filtration. **B.** Gel filtration chromatography of refolded TCR (left). Fractions were assessed by SDS-PAGE under reducing and non-reducing conditions (right). Fractions containing TCR (13-21) were pooled for Mono-Q. **C.** Mono-Q anion exchange chromatography of refolded TCR (left). Fractions were assessed by SDS-PAGE under reducing and non-reducing conditions (right) and fractions 74-81 were collected and concentrated in TBS for storage.

concentrated, and passed over Mono-Q (*Fig.4.16c).* The first major peak in the Mono-Q trace corresponds to one major band at 50 kDa under non-reducing conditions and two bands under reducing conditions in fraction 77. Fraction 86, in the second main peak, contained only β-chain protein (*Fig.4.16c)*. While the elution volume of TCR heterodimer was similar to the elution of TCRs 27a28 and 29a28i, it was unexpectedly the first peak, and not second, that contained heterodimer and not homodimer (*Fig.4.16c)*. Fractions 74-81 were collected as soluble αβ-TCR protein for structural studies.

The final TCR, 8-2a2, was also refolded, passed over a DEAE column and assessed by SDS-PAGE *(Fig.4.17a).* Bands at 50 kDa were faintly visible in fractions 8 and 11 under non-reducing conditions, which were divided into two, smaller bands under reducing conditions. The low staining intensity for TCR protein bands suggested that the amount of protein was low, albeit present. Fractions corresponding to the chromatogram peak (2-20) were collected and further purified by S75 pg gel filtration. Fractions in the second peak (4-11), corresponding to one band at 50 kDa on SDS-PAGE and two bands under reducing conditions *(Fig.4.17b)*, were collected and passed over Mono-Q. UV absorbance values and band staining intensity on SDS-PAGE gels were relatively low compared to other TCRs *(Fig.4.17c)*. The second major peak in the Mono-Q trace corresponds to one major band at 50 kDa under non-reducing conditions and two bands under reducing conditions in fraction 73. The last major peak was the highest and corresponded to a band at 30 kDa in fraction 80 indicating the presence of β-chain monomer. Fractions 71-79 were hence collected as soluble αβ-TCR protein for structural studies.

Overall, the yields of soluble CD1a-restricted TCRs were moderate; approximately 664 μg and 992 μg of purified 17a28 and 27a28 TCRs were generated respectively from a 2 L refold containing 20 mg of each α- and β-chain IBPs. 73.8 μg and 46 μg of purified 8-2a2 and 29a28i TCRs were generated respectively from a 400 mL refold containing 15 mg of each α- and β-chain IBPs. Additional 2 L refolds of 8-2a2, 17a28, and 29a28i TCRs were performed in a similar fashion to produce more αβ-TCR given that SDS-PAGE indicated low quantities of TCR αβ-heterodimer produced compared to ββ-homodimer following refold. Subsequently, sufficient quantities (approximately 1 mg of each) of αβ-heterodimer were obtained for structural studies, specifically, for co-complexation with soluble CD1a-lipid.

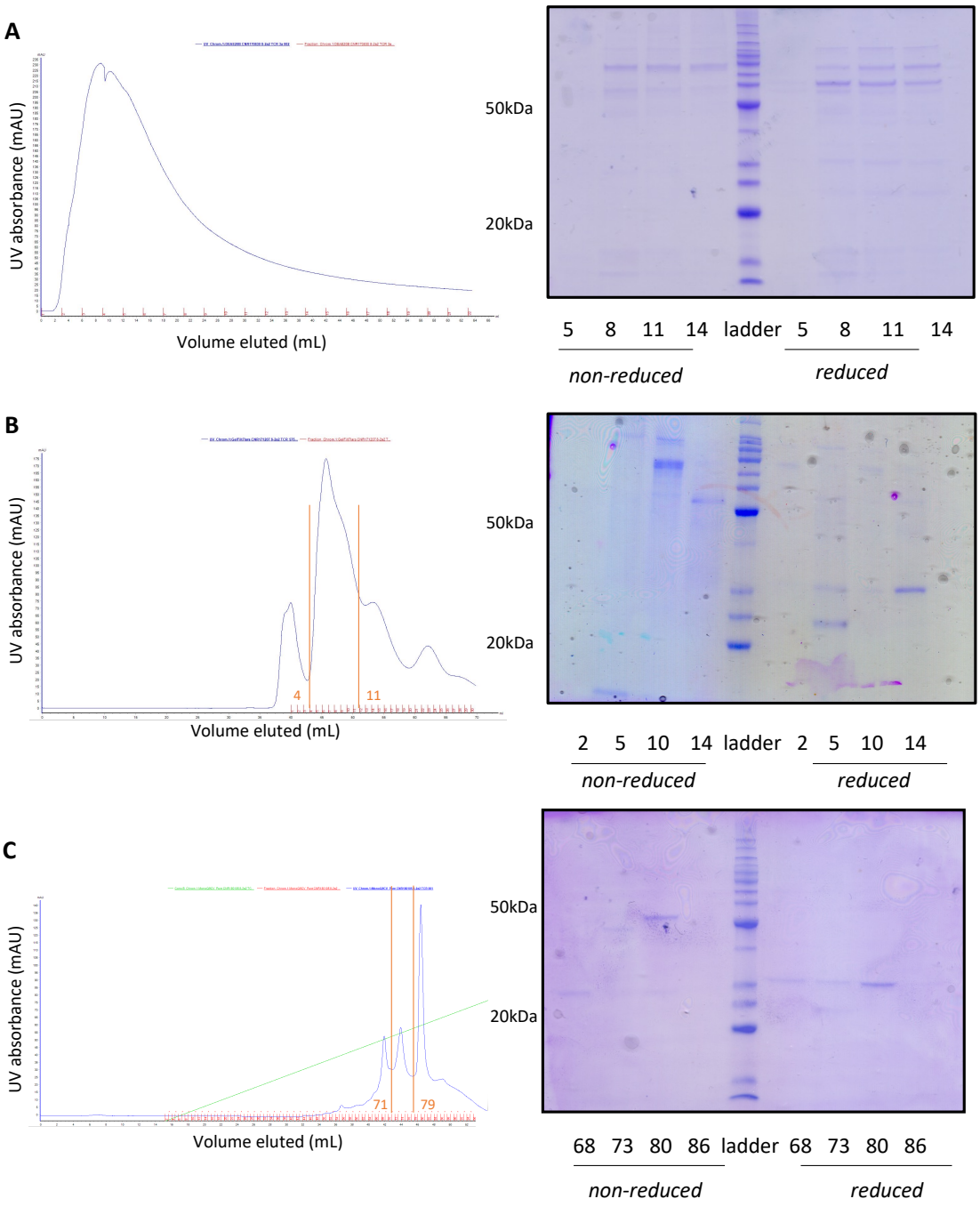

Figure 4.17. Purification of soluble 8-2a2 CD1a-restricted TCR. A. DEAE anion exchange chromatography of refolded 8-2a2 TCR (left). Fractions were assessed by SDS-PAGE under reducing and non-reducing conditions (right). Fractions containing TCR (2-20) were pooled for gel filtration. **B.** Gel filtration chromatography of refolded TCR (left). Fractions were assessed by SDS-PAGE under non-reducing conditions (right). Fractions containing TCR (4-11) were pooled for Mono-Q. **C.** Mono-Q anion exchange chromatography of refolded TCR (left). Fractions were assessed by SDS-PAGE under reducing and non-reducing conditions (right) and fractions 71-79 were collected and concentrated in TBS for storage.

4.2.6 Production of Human CD1a for structural studies

Soluble human CD1a was generated using the GnTI$^-$ mammalian expression system and His-tagged CD1a was purified by Ni-NTA agarose, in the same method as production of CD1a monomer for tetramers. Purified CD1a was sequentially treated with endoglycosidase H (endo-H) (New England BioLabs) and thrombin (Sigma) for removal of N-linked sugars and C-terminal leucine zippers that may interfere with crystallography, respectively. The decreasing size of CD1a after each successive treatment was visible by SDS-PAGE (*Fig.4.18a)*. Following endo-H treatment, CD1a protein decreased slightly in size (*Fig.4.18a)*. Due to the dilution of CD1a in progressive steps, a lower amount of fully treated CD1a was assessed by SDS-PAGE, however the shift in size was evident following removal of C-terminal leucine zippers on the heavy chain while the size of β_2m remained consistent (*Fig.4.18a)*.

Treated CD1a was divided into 5 mg for CD1a-endo and 4 mg for CD1a-DDM binary complexes, the latter of which was loaded overnight with DDM in a 3:1 molecular weight ratio (CD1a:DDM). These were then purified using gel filtration (*Fig.4.18b)*. The chromatogram trace for CD1a-DDM was uniform, while CD1a-endo revealed a small shoulder prior to the main peak on its chromatogram trace, suggestive of a minimal amount of untreated CD1a, which was not collected.

4.2.7 Isolation of TCR:CD1a Ternary Complexes

Soluble 17a28 TCR, 27a28 TCR, and 29a28i TCR, and CD1a cleaved with enzymes endoglycosidase H and thrombin were purified using gel filtration with a Superdex-200 16/60 (S200) size-exclusion column in preparation for complexation.

To produce a TCR:CD1a-DDM co-complex, 17a28 was added to CD1a-DDM at a 1:2 mass ratio (750 μg TCR: 1500 μg CD1a). The co-complex was purified by passage over an S200 size-exclusion column (0.5 ml/min flow rate). The chromatogram trace revealed two distinct peaks: one at the same elution volume as TCR and CD1a-DDM alone, and the other at an earlier elution corresponding to the larger 17a28:CD1a-DDM co-complex (*Fig.4.19*). Fractions eluted in the first peak were deemed to contain the 17a28:CD1a-DDM co-complex based on assessment by SDS-PAGE (*Fig.4.19*). Under non-reducing

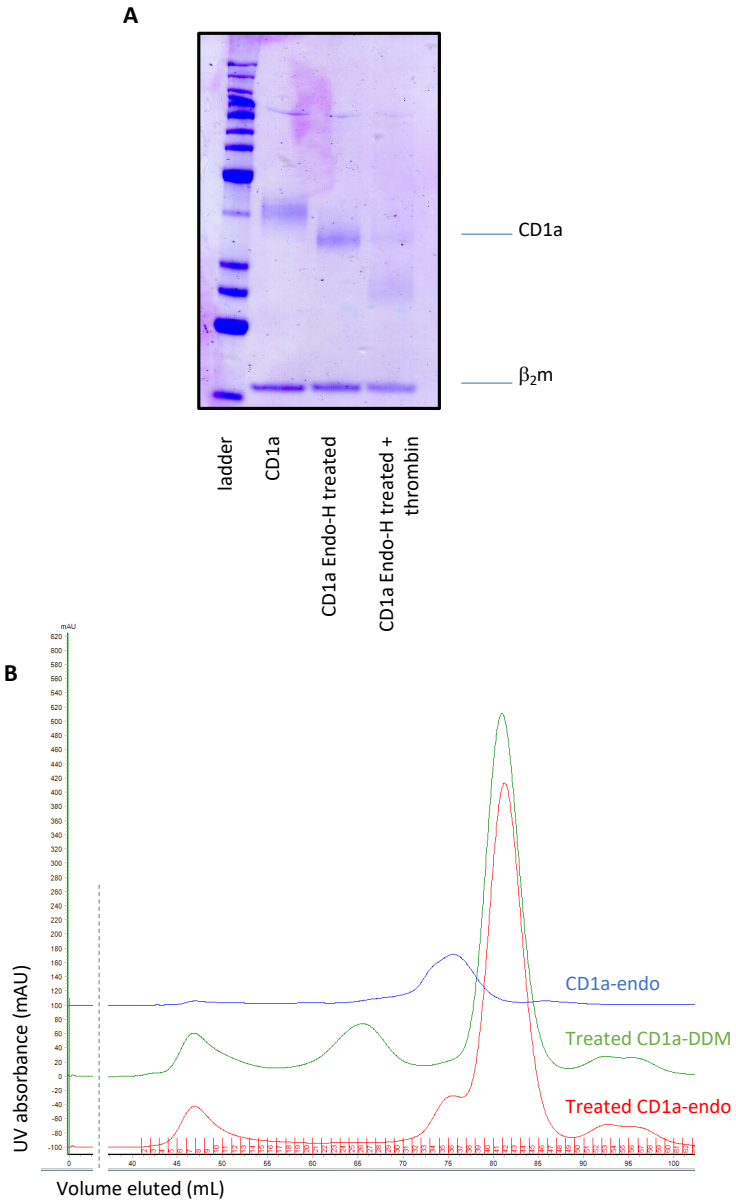

Figure 4.18. Endo-H and Thrombin treatment of soluble CD1a for TCR co-complexation. Soluble CD1a was treated with endoglycosidase H (endo H) to cleave oligosaccharides from N-linked glycoproteins, and thrombin to remove the leucine zipper. The sample was first incubated with endo H for 1h, followed by thrombin for 4h. **A.** Untreated CD1a, Endo-H-treated CD1a and thrombin-treated CD1a were assessed by SDS-PAGE. **B.** Chromatograms of treated and untreated CD1a-endo run over an S200 column.

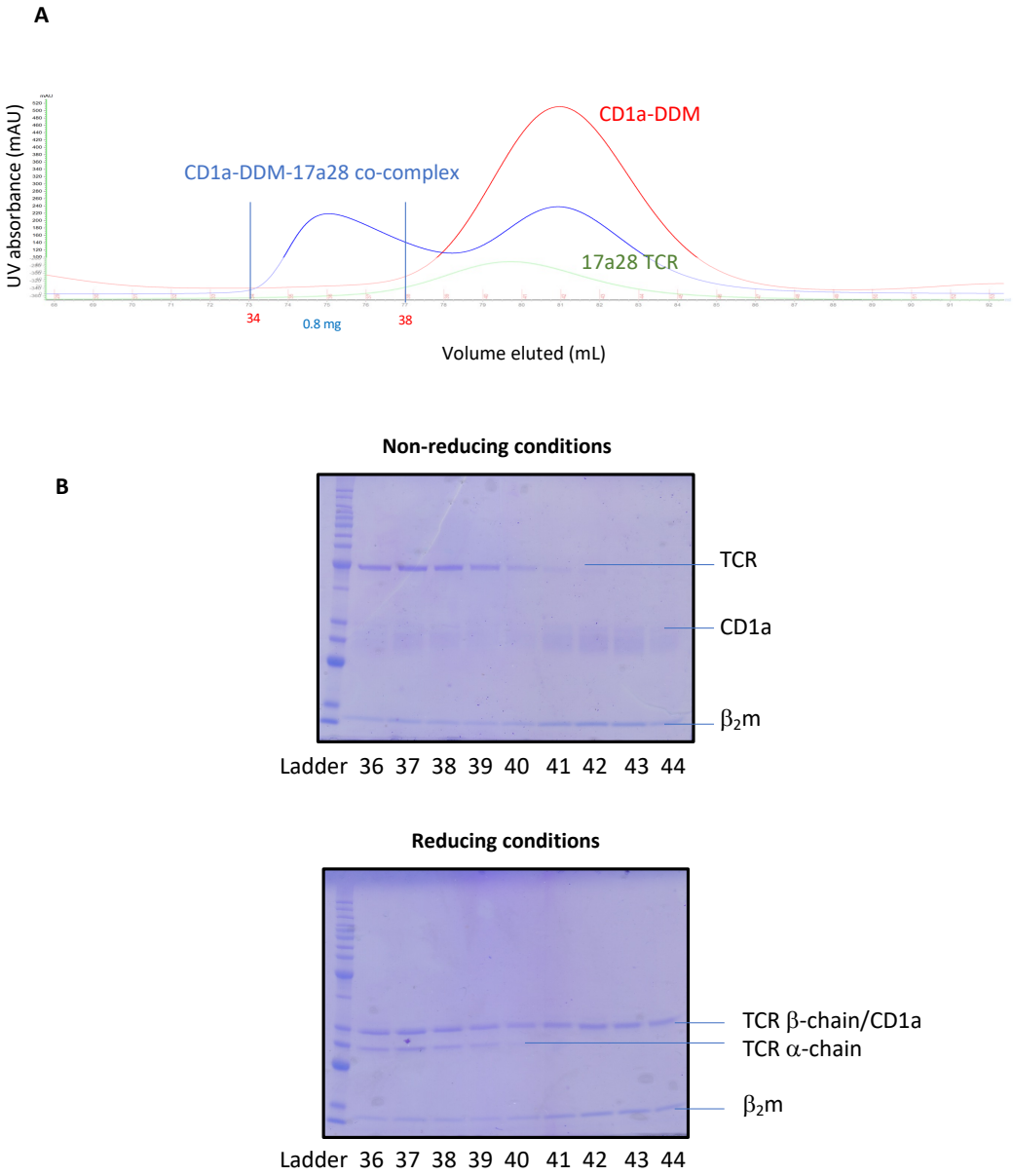

Figure 4.19. Purification of soluble 17a28 CD1a-restricted TCR co-complexed to CD1a loaded with DDM. A. CD1a-DDM was added to TCR in a 2:1 mass ratio and loaded onto an S200 column for gel filtration chromatography at flow rate 0.5 mg/mL. **B.** Fractions were assessed by SDS-PAGE under non-reducing (top) and reducing conditions (bottom).

conditions, it was difficult to determine whether CD1a and TCR were present at a 1:1 ratio given the heterogeneity of CD1a glycosylation. In later fractions, however, the bands representative of TCR were no longer present while unbound CD1a and β_2m remained, which was expected as it was added in excess. Under reducing conditions, it was easier to determine that bands representative of TCR α- and β-chains and β_2m were of equal band staining intensity in the early fractions (36-39), clearly indicating the presence of co-complex. Fractions 34-38 were pooled and concentrated in TBS to a final amount of 0.8 mg of protein. Of the total, 100 µg was sent to Dr Tan-Yun Cheng in Branch Moody's Laboratory at Brigham and Women's Hospital as a control for lipid antigen discovery and 0.7 mg of co-complex was sent to Jamie Rossjohn's Laboratory at Monash University for future X-ray crystallography work.

To produce a TCR:CD1a-endo co-complex, 27a28 TCR was added to Endo H- and thrombin-treated CD1a at a 1:1 mass ratio. The co-complex was purified by passage over a Superdex-200 16/60 size-exclusion column. No distinct early peak was detected on the chromatogram obtained by passing CD1a-endo and 27a28 TCR over a gel filtration column, however there was a slight shift of the peak towards earlier fractions (*Fig.4.20a*). When fractions were assessed by SDS-PAGE under non-reducing conditions, Coomassie Blue staining of the early fractions (fractions 35 and 37) revealed three proteins matching the apparent molecular weights of CD1a, β_2m, and TCR with similar band intensity, consistent with 1:1:1 stoichiometry (*Fig.4.20a*). The lack of two distinct peaks, as observed in the chromatogram trace of 17a28 and CD1a-DDM co-complexation, is typical following co-complexation given that some excess smaller TCR or CD1a-endo should remain. This suggests that the TCR had low-affinity binding to CD1a or that co-complexation was unsuccessful. A repeat co-complexation experiment was performed by again loading CD1a-endo and 27a28 TCR at a 1:1 mass ratio over a size-exclusion column. Similar to the first experiment, a single peak was observed at a slightly earlier elution volume compared to each of CD1a-endo and 27a28 TCR alone but not two distinct peaks (*Fig.4.20b*). SDS-PAGE analysis revealed that CD1a and TCR were present together in fractions 36 to 39 (*Fig.4.20b*), and it is possible that all protein co-complexed to form TCR:CD1a-lipid complexes uniform in size. Fractions from Run A and Run B were concentrated individually for lipid antigen discovery by mass spectrometry, so that lipids identified in CD1a that bound TCR in earlier fractions (permissive) could be distinguished from those lipids loaded into CD1a that did not bind TCR (non-permissive).

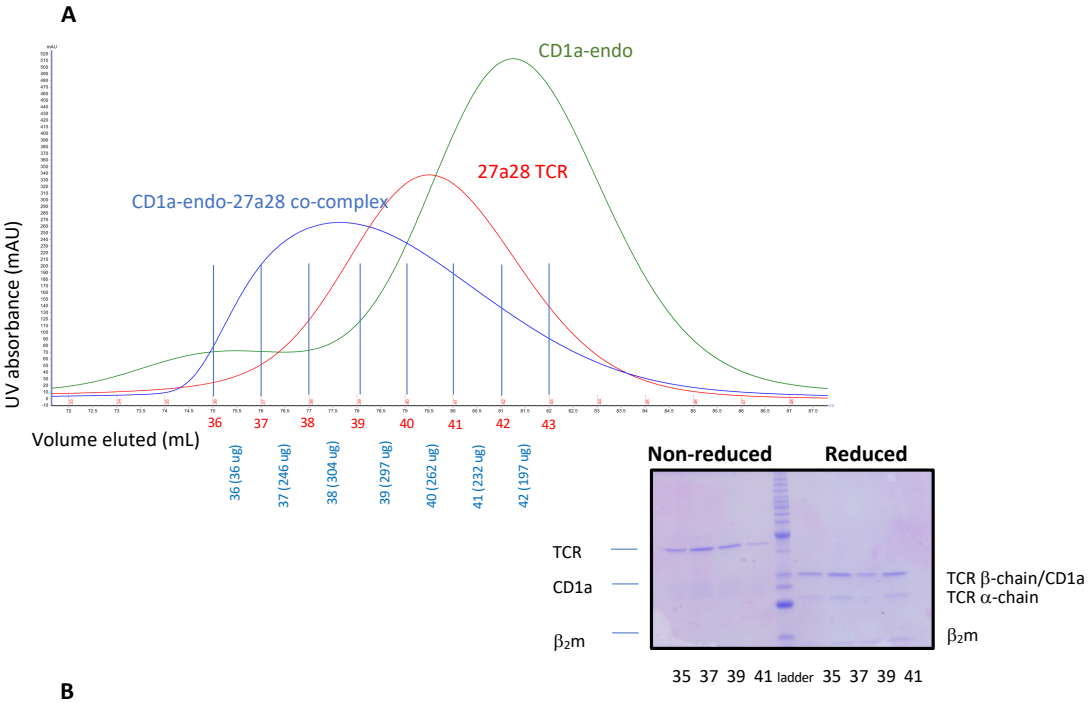
A
CD1a-endo
27a28 TCR
CD1a-endo-27a28 co-complex
UV absorbance (mAU)
Volume eluted (mL)
36 37 38 39 40 41 42 43
36 (36 ug)
37 (246 ug)
38 (304 ug)
39 (297 ug)
40 (262 ug)
41 (232 ug)
42 (197 ug)
Non-reduced
Reduced
TCR
CD1a
β2m
TCR β-chain/CD1a
TCR α-chain
β2m
35 37 39 41 ladder 35 37 39 41

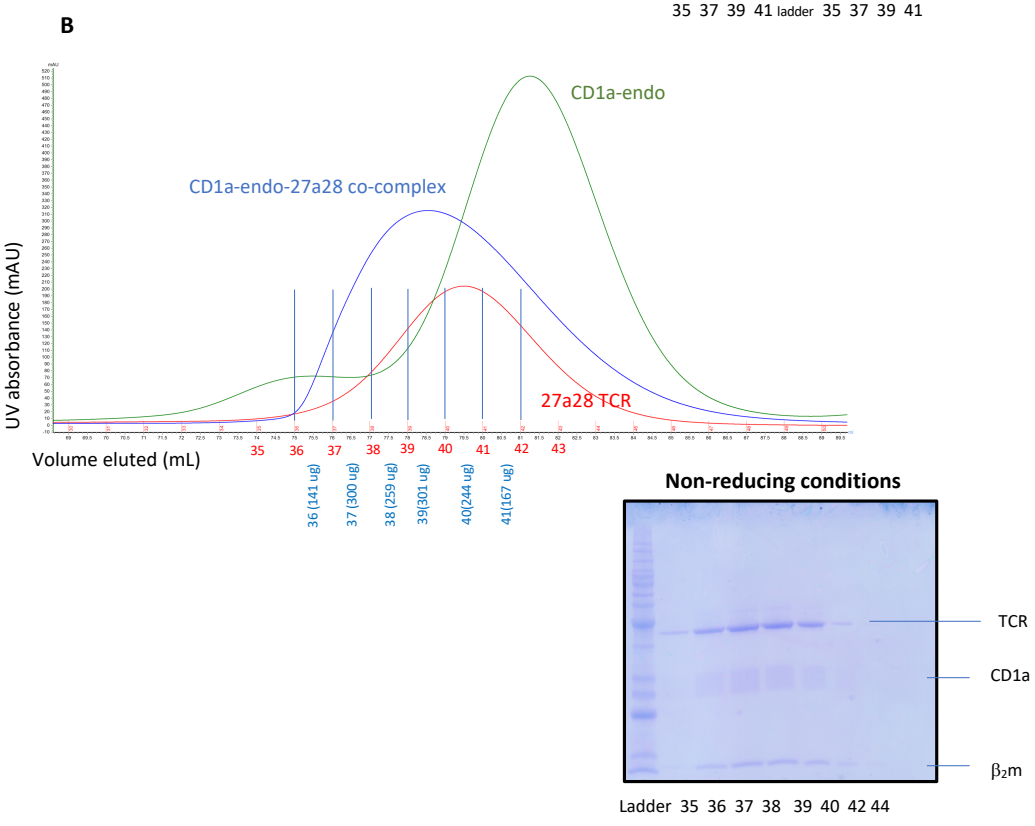
B
CD1a-endo
CD1a-endo-27a28 co-complex
27a28 TCR
UV absorbance (mAU)
Volume eluted (mL)
35 36 37 38 39 40 41 42 43
36 (141 ug)
37 (300 ug)
38 (259 ug)
39(301 ug)
40(244 ug)
41(167 ug)
Non-reducing conditions
TCR
CD1a
β2m
Ladder 35 36 37 38 39 40 42 44

Figure 4.20. Purification of soluble 27a28 CD1a-restricted TCR co-complexed to CD1a loaded with DDM. A. CD1a was added to TCR in a 1:1 mass ratio and loaded onto an S200 column for gel filtration chromatography at flow rate 0.5 mg/mL. Selected fractions were assessed by SDS-PAGE under reducing and non-reducing conditions. **B.** In a repeat experiment, CD1a-DDM was again added to TCR in a 1:1 mass ratio and loaded onto an S200 column for gel filtration chromatography. Fractions were assessed by SDS-PAGE under non-reducing conditions.

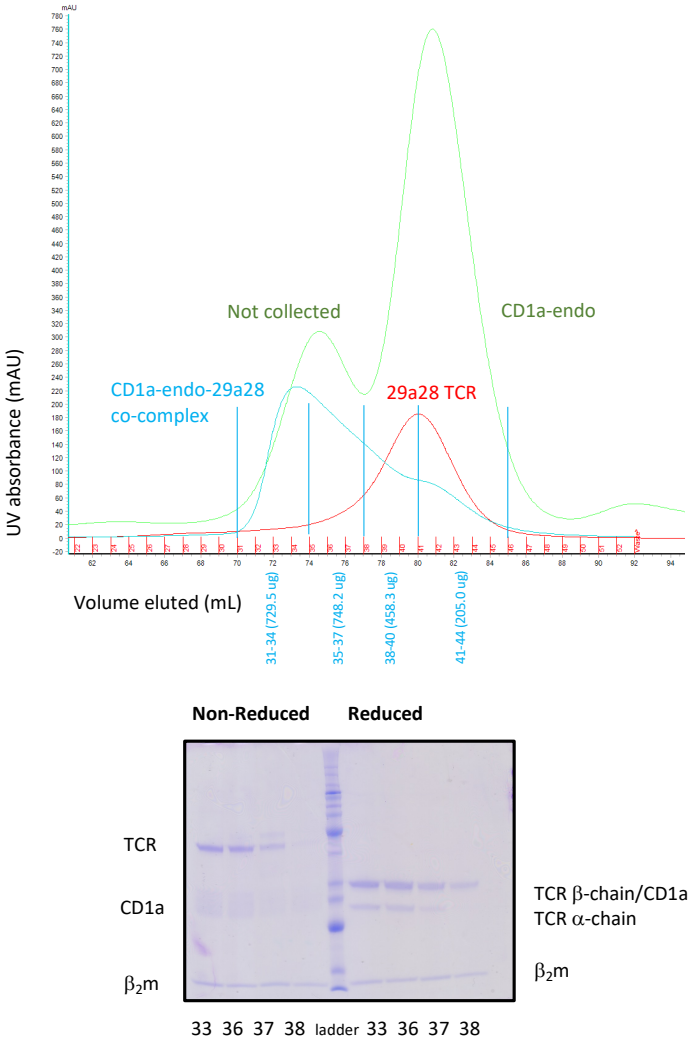

Figure 4.21. Purification of soluble 29a28 CD1a-restricted TCR co-complexed to CD1a loaded with DDM. A. CD1a was added to TCR in a 1:1 mass ratio and loaded onto an S200 column for gel filtration chromatography at flow rate 0.5 mg/mL. Selected fractions were assessed by SDS-PAGE under reducing and non-reducing conditions. Fractions were pooled and concentrated as indicated.

Co-complexation of the 29a28 TCR with CD1a-endo was performed in a similar manner by adding them together at a 1:1 mass ratio and passing them over a size-exclusion column. The gel filtration chromatogram revealed a distinct peak that eluted at an earlier volume to TCR and CD1a alone (*Fig.4.21*). Analysis by SDS-PAGE revealed the presence of both CD1a and TCR proteins in the earlier fractions that correspond to the first peak, while unbound CD1a was present in the later fraction (fraction 38) (*Fig.4.21*). Fractions 31-34, 35-37, 38-40, and 41-44 were pooled as representative of two early, one middle, and one late-eluting fractions. A comparison of CD1a lipids in the later and earlier fractions will therefore indicate permissive and non-permissive lipids for this TCR.

The fractions of both co-complexes were collected and concentrated individually to be analysed for lipid antigen discovery by mass spectrometry, and 36-301 μg of co-complex was obtained for each fraction. These yields were not sufficient for X-ray crystallography and were therefore used solely for lipid antigen discovery.

4.2.8 Lipid antigen discovery

The TCR trap method of lipid antigen discovery is a cell-free assay to identify antigenic lipids that mediate higher affinity binding of TCRs to CD1a than nonantigenic lipids (Birkinshaw et al., 2015). Given that CD1a-endo contains a mixture of endogenous lipids from the lipidome of GnTI$^-$ cells, CD1a-restricted TCRs, 27a28 and 29a28i, would be expected to selectively bind those CD1a-endo complexes that present permissive lipid antigens, forming a TCR-CD1a co-complex, hence "trapping" permissive lipids. Conversely, CD1a-endo complexes presenting non-permissive lipids for these TCRs are expected to remain in the unbound CD1a fraction. This approach has been used to identify a number of permissive (agonistic) and non-permissive (non-agonistic) endogenous antigens that can be presented by CD1a to the CD1a-autoreactive TCR BK6, and subsequently for other CD1 molecules (Birkinshaw et al., 2015, Brennan et al., 2017). The use of multiple TCRs allows for the discovery of a broader range of lipids, given that results so far suggest that CD1a-restricted TCRs use multiple docking methods onto CD1a and therefore may have different antigen specificities. Soluble 27a28 and 29a28i TCR:CD1a co-complexes were produced to identify self-lipid antigens that can be recognised by CD1a-restricted T cells that are more broadly reactive.

Soluble 27a28 and 29a28i TCRs were complexed with soluble CD1a-endo and passed over a column for gel filtration chromatography. A subset of CD1a proteins bound the TCR heterodimers, leading to the formation of a higher molecular weight ternary complex, which was eluted in earlier fractions before separate CD1a and TCR monomers *(Fig.4.20, Fig.4.21)*. Mass spectrometry (MS) analysis of selected TCR-CD1a-endo co-complex fractions was performed by Dr Tan-Yun Cheng, Branch Moody's Laboratory at Brigham and Women's Hospital to compare the identity of lipids in the earlier and later elutions. Among the many ligands, we focused on MS signals with correspondence of molecular ions to the expected exact mass of carbon-rich molecules, high intensity signals, and mass values that matched those of known membrane lipids from human cells and/or permissive lipids for BK6.

CD1a from collected fractions was eluted from the TCR-CD1a co-complex using a mixture of chloroform, methanol and water according to a modified Bligh and Dyer method as previously described (de Jong et al., 2014). Lipids were subsequently separated from the aqueous phase and collected for MS analysis. Extracted lipids were analysed using high performance liquid chromatography MS (HPLC-MS), nano-electrospray ionization mass spectrometry (EIS-MS) and collision-induced dissociation tandem MS (CID-MS-MS). Lipid identification was based on the co-elution of unknown products with standards that matched the *m/z* values reported in the literature and by detection of component structures in CID-MS-MS.

4.2.8.1 27a28 TCR

Positive-mode EIS-MS analysis of lipids eluted from the 27a28 TCR:CD1a co-complex identified numerous ions, and the mass intervals among the most abundant ions were diverse (*Fig.4.22)*, suggesting the presence of structurally diverse lipids from a broad range of classes loaded into CD1a. Lipid ligands that were either trapped-in or excluded-from TCR-CD1a complexes were identified using shotgun nano-electrospray with multistage ion-trap MS, allowing for a broad detection of lipid compounds. The early fractions (36 and 37) containing TCR-CD1a complexes revealed fewer elution ions, suggesting that the 27a28 TCR bound only a small subset of CD1a-lipid complexes among all CD1a-lipid present in the starting CD1a-endo mixture (*Fig.4.22)*. In

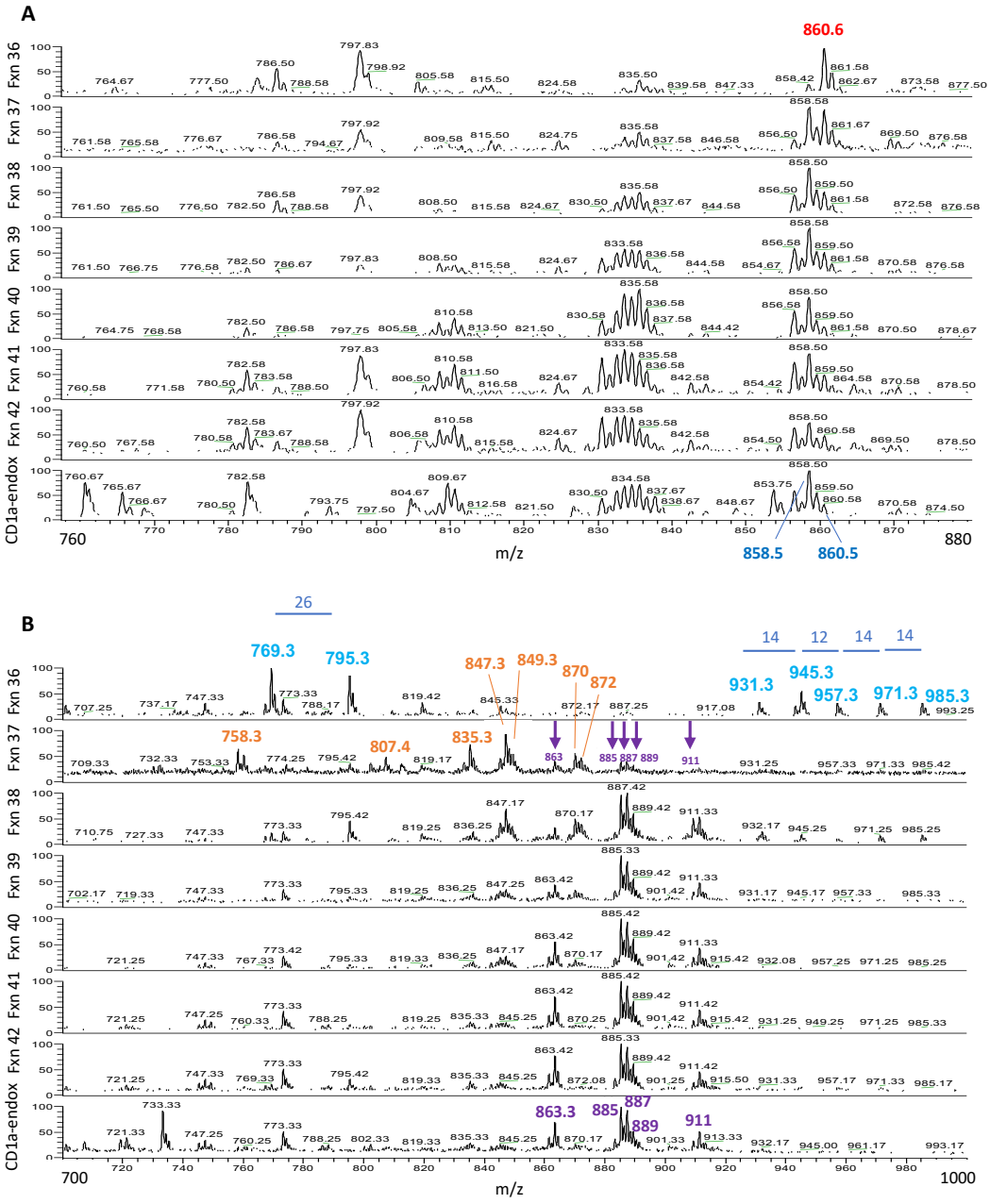

Figure 4.22. Mass spectrometry analysis of lipids eluted from 27a28 TCR:CD1a-endo co-complex (Run A). Soluble 27a28 TCR protein was complexed with CD1a-endo and passed over an S200 column for gel filtration chromatography and lipids eluted from CD1a in selected fractions were assessed by mass spectrometry. **A.** Nanospray positive mode analysis **B.** Nanospray negative mode analysis. Mass spectrometry was performed by Dr Tan-Yun Cheng, Brigham and Women's Hospital.

Relative ion intensities indicated in blue were enriched in fraction 36 but not present in CD1a-endo. Relative ion intensities indicated in orange boxes were enriched in fraction 37. The presence of relative ion intensities indicated by purple arrows was decreased in fraction 37 compared to CD1a-endo alone.

comparison, later fractions (40-42), containing CD1a and TCR monomer, revealed MS profiles more similar to that of the CD1a-endo control (*Fig.4.22)*.

In co-complex fraction 36, both positive and negative-mode ESI-MS analysis identified prominent ion signals at *m/z* ratios of 769, 795, 931, 945, 957, 971, and 985, which were not present in the CD1a-endo control (*Fig.4.22)*. These ions therefore may not correspond to CD1a auto-antigens and could be contaminating lipids from GnTI$^-$ culture media and preparations. Nanospray negative mode CID-MS was used to determine the identity of these lipids. CID of *m/z* 747.3 revealed a mass and collisional pattern that matches that of phosphatidylglycerol (PG) (*Fig.4.23)*. CID of *m/z* 769.3 revealed a lipid containing C16:0 and C18:1 fatty acids (*Fig.4.24a)*. The head group was not determined, but PG, phosphatidylinositol (PI), sphingomyelin (SM), phosphatidylcholine (PC), phosphatidylethanolamine(PE) and phosphatidylserine (PS) were excluded as candidate lipids. Similarly, CID of *m/z* 795.3 revealed a lipid that was also neither PG, PI, SM, PC, PE, nor PS, consisting of two C18:1 fatty acids (*Fig.4.24a)*. High-performance liquid chromatography-quadrupole-time of flight mass-spectrometry (HPLC-QTof2-MS), which provides more accurate molecular weight information, confirmed that there was no phosphate present in these lipids, but they did contain a ring structure and carboxylate (*Fig.4.24b)*. These molecules are likely to be anionic glycosyl (glucuronosyl) diacylglycerols, with molecular formulae $C_{43}H_{77}O_{11}$ and $C_{45}H_{79}O_{11}$, consistent with mass and collisional patterns similar to lipids reported in gram-negative bacteria (Wolucka et al., 1993). In addition, the mass and collision pattern of ions at 957.3 were consistent with hexosyl-glucuronyl diacylglyercol, and only differed to the ion at *m/z* 795.3 by one, hexosyl sugar (*Fig.4.25)*. Thus, ions at *m/z* 931, 945, 957, 971, and 985 appear to represent a series of glycosyl diacylglycerols like those found in gram-negative bacteria (Tatituri et al., 2007) whose fatty acyl chains differ in carbon length and saturation. More information would be required to confirm these ions, however, given that these lipids did not appear to be loaded in CD1a-endo, we did not endeavour to determine their identity as they may be a source of contamination. It is tempting to speculate that the contaminating lipids were within the culture media (e.g. in the FCS), however, they were not present in the eluents from CD1a alone. They were either not preferentially "trapped" in the absence of a TCR or they came from elsewhere. Nonetheless, these results reveal the identities of potential bacteria derived CD1a antigens.

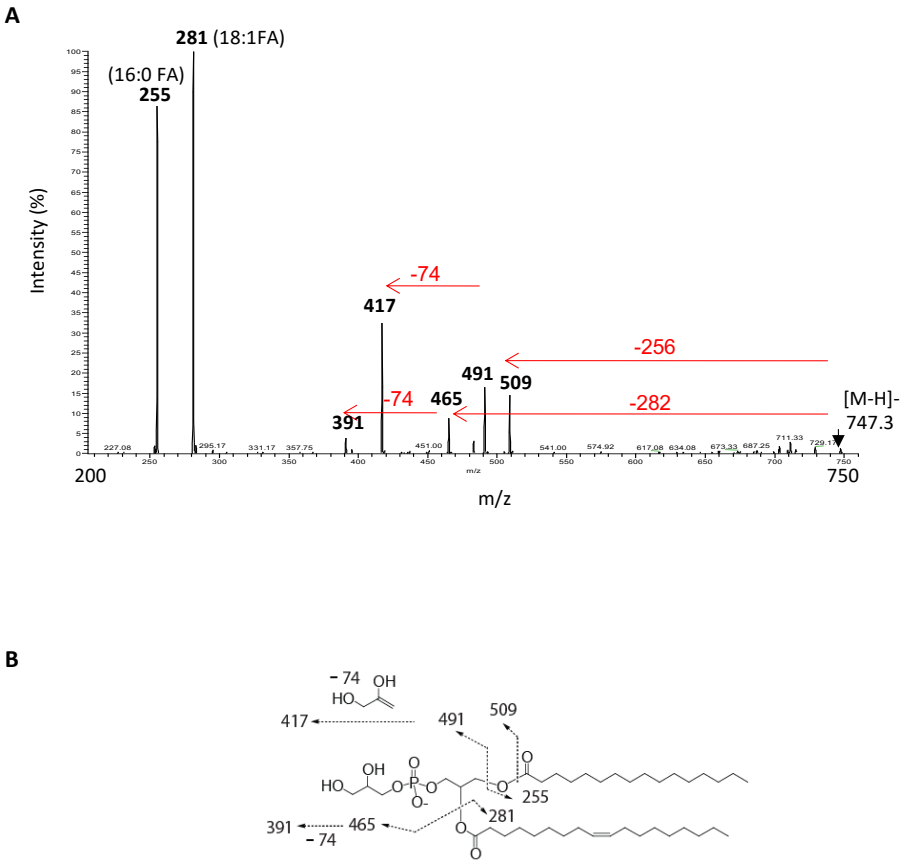

Figure 4.23. Detection of phosphatidylglycerol in analysis of ions at *m/z* 747.3 in 27a28:CD1a-endo, fraction 36. A. Collision-induced dissociation (CID) of (negative mode, nanospray) of *m/z* 747.3 in fraction 36 from gel filtration of 27a28 TCR co-complexed to CD1a-endo Run A. Lipids were eluted from CD1a in this fraction and assessed by using mass spectrometry by Dr Tan-Yun Cheng, Brigham and Women's Hospital. **B.** Mass and collisional patterns match to phosphatidylglycerol.

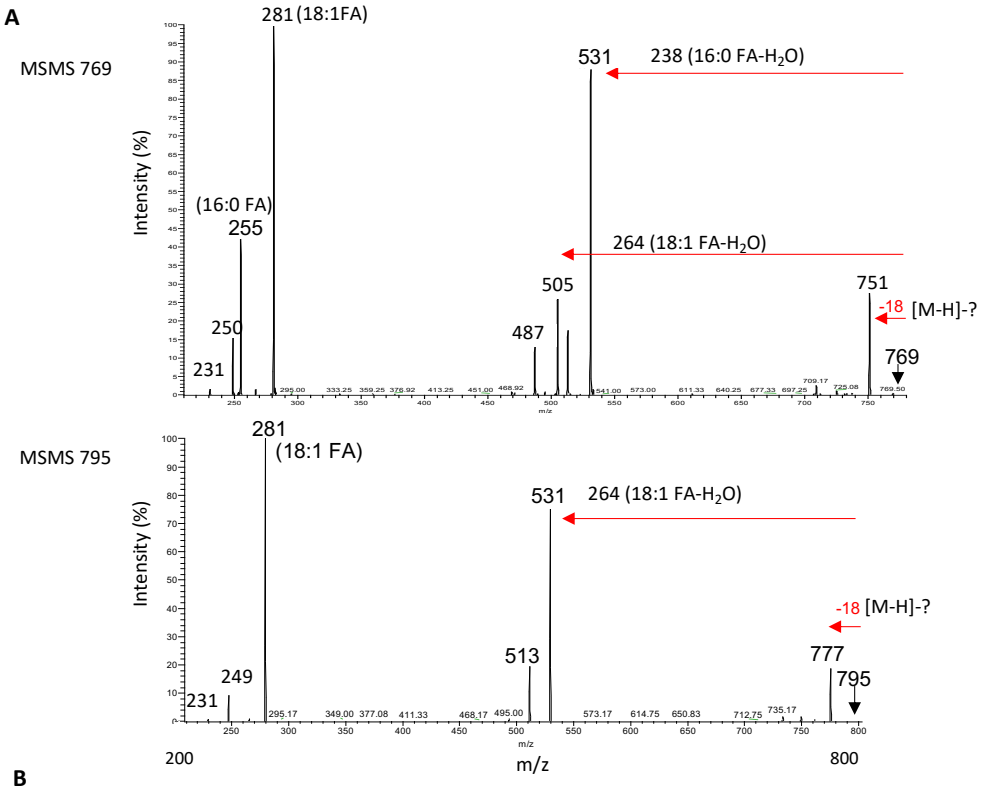

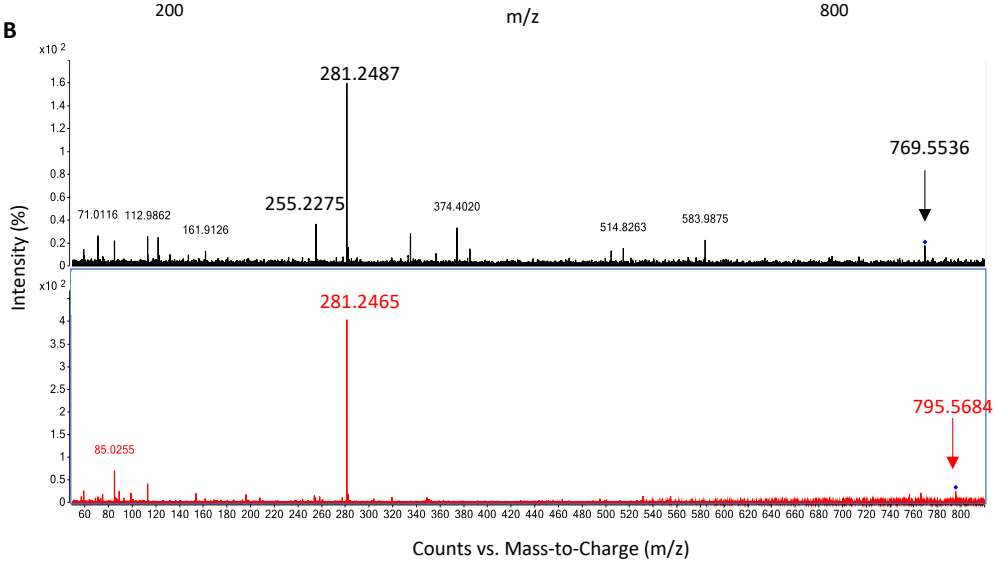

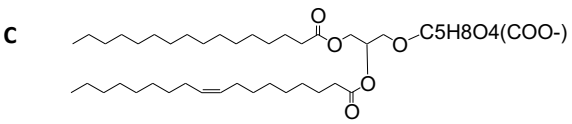

$C_{43}H_{77}O_{11}^-$

Exact Mass: 769.5466

Figure 4.24. Identification of lipids in analysis of ions at *m/z* 769 and 795 in 27a28:CD1a-endo, fraction 36. A. CID (negative mode, nanospray) of *m/z* 769.3 and 795.3 in fraction 36 from gel filtration of 27a28 TCR co-complexed to CD1a-endo Run A. **B.** CID (negative mode, HPLC-QTof2-MS) of *m/z* 769.3 (rt: 10.572-10-689 min, 3 scans) and 795.3 (rt:10.639-10.874,5 scans). Lipids were eluted from CD1a in fraction 36 and assessed by using mass spectrometry by Dr Tan-Yun Cheng, Brigham and Women's Hospital. **C.** Mass and collisional patterns identify a ring structure and carboxylate.

A

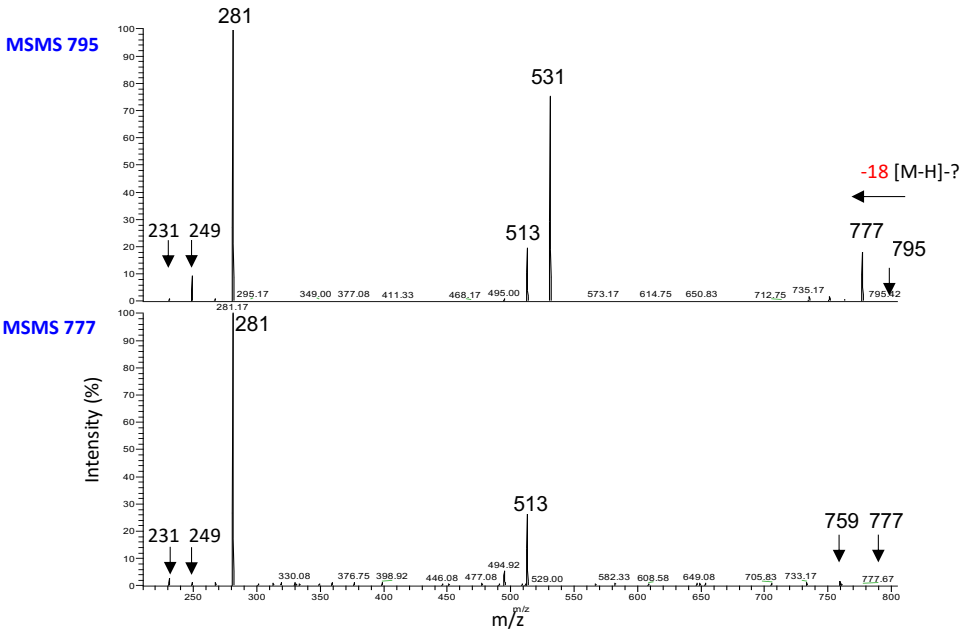

B

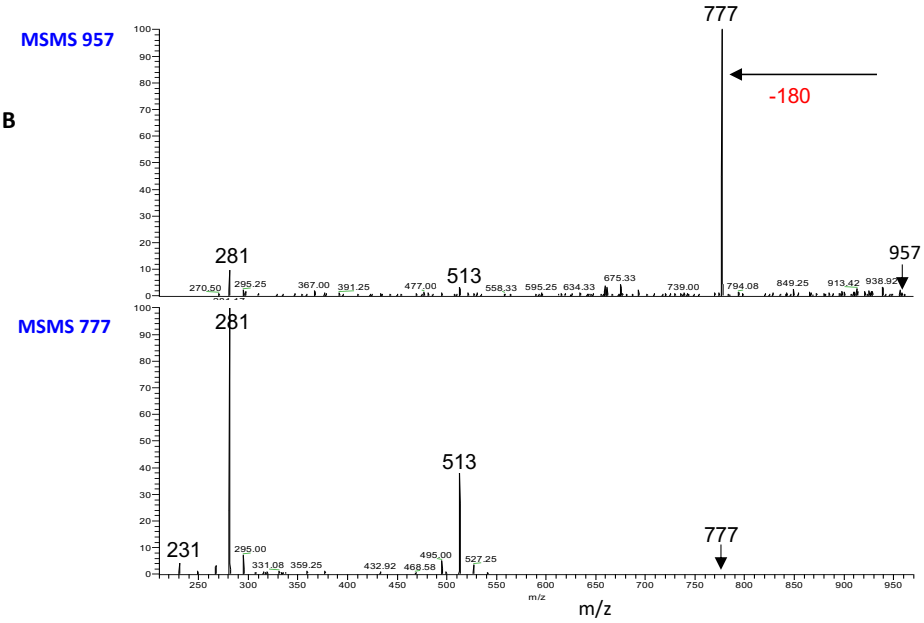

C

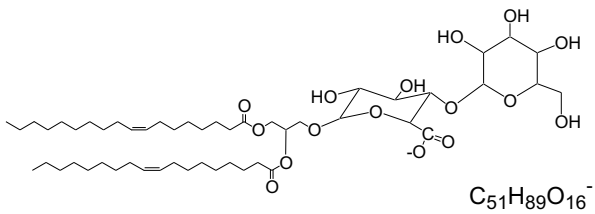

$C_{51}H_{89}O_{16}^-$

Exact Mass: 957.6151

Figure 4.25. Detection of glycosyl diacylglycerol in analysis of ions at *m/z* 795 and 975 in 27a28:CD1a-endo, fraction 36. CID (negative mode, nanospray) of *m/z* **A.** 795 and **B.** 975 in fraction 36 from gel filtration of 27a28 TCR co-complexed to CD1a-endo Run A. Lipids were eluted from CD1a in this fraction and assessed by using mass spectrometry by Dr Tan-Yun Cheng, Brigham and Women's Hospital. **C.** Mass and collisional patterns match to glycosyl diacylglycerol.

To avoid lipids in fraction 36 confounding TCR-trap analysis of 27a28, fraction 37 was selected to represent early elution of the TCR-trap. Fraction 37 contained an enrichment of ions at *m/z* 758, 807, 835, 847, 849, 870, and 872 compared to CD1a-endo alone and later fractions, reflective of lipid antigens that mediate high-affinity TCR binding to CD1a (i.e. permissive lipids) (*Fig.4.22)*. In contrast, ions at *m/z* 863, 885, 887, 889, and 911, were decreased in earlier fractions compared to CD1a-alone and later fractions, indicative of non-permissive lipids that do not bind this TCR (*Fig.4.22)*.

As a control, eluent from 17a28 TCR-CD1a DDM co-complex was analysed and compared to the lipid eluent from 27a28 and 29a28i TCR traps. Lipid eluted from 17a28 TCR-CD1a-DDM revealed a signal at *m/z* 860.6 with ESI-MS and CID, providing a similar MS profile to that previously observed for DDM (Moody et al., 2004) (*Fig.4.26a)*, thus confirming the presence of DDM. The ion at *m/z* 860 detected in 27a28 TCR:CD1a-endo fraction 36 (positive mode analysis) had the same collision pattern as DDM, *m/z* 860 indicating carry-over of DDM (*Fig.4.26b)*. This may have been a result of column contamination and may have been present in only the earliest eluted fraction as 27a28 has previously displayed greater affinity for CD1a loaded with DDM compared to endogenous lipids, as seen with tetramer staining and activation assays.

Considering lipids eluted from fraction 37, negative mode CID-MS analysis of selected ions at *m/z* 847 and 870 identified sphingomyelin (SM) and phosphatidylcholine (PC) respectively (*Fig.4.27)*. Fragments from the ion at *m/z* 847 corresponded to SM with a saturated C18 fatty acyl chain and C22 chain with five unsaturations (molecular formula $C_{46}H_{90}N_2O_6P$) (*Fig.4.27a,b)*. Fragments from the ion at *m/z* 870 were identified as PC with C16:1 and C24:1 fatty acyl chains (molecular formula $C_{47}H_{83}NO_8P$) (*Fig.4.27b)*. Chloromethane was identified as an adduct ion in both by the loss of 50 atomic mass units such that their true masses were 797 and 820 (*Fig.4.27c)*. Nanospray negative mode CID analysis of fraction 39 identified PI at *m/z* 885, with a molecular formula of $C_{47}H_{82}NO_{13}P$ and two fatty acyl chains of C18:0 and C20:4 (*Fig.4.28)*.

An analysis across individual fractions was used to determine the relative levels of SM, PC, and PI, as these have been previously determined as lipids of interest for the BK6 TCR (Birkinshaw et al., 2015). In CD1a-endo alone, a number of SM, PC, and PI lipid

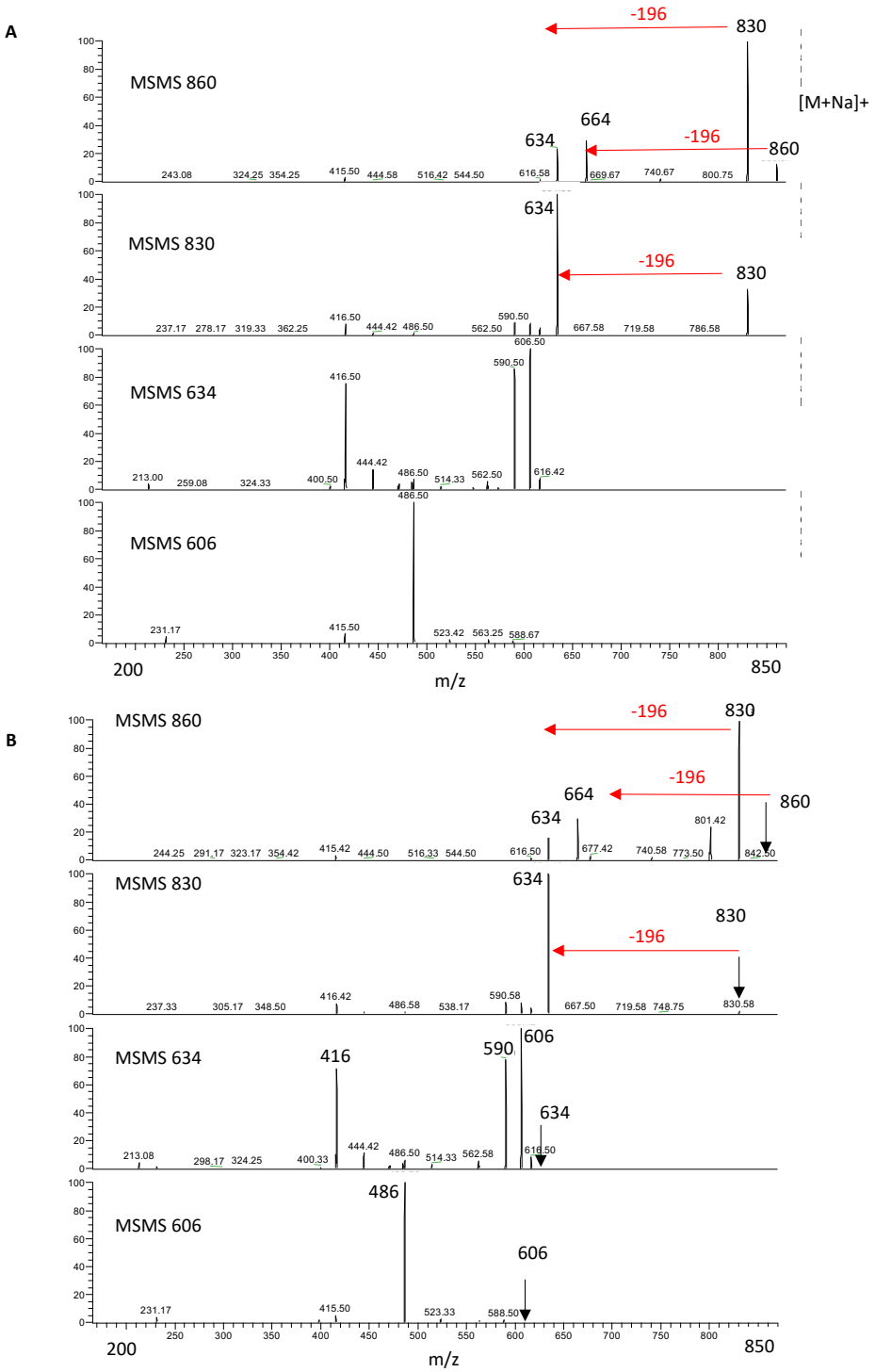

Figure 4.26. Detection of DDM in analysis of ions at *m/z* 838 in TCR-CD1a co-complexes. CID (positive mode, nanospray) of *m/z* 838 in **A.** 17a28 TCR:CD1a-DDM co-complex and **B.** fraction 36 from gel filtration of 27a28 TCR co-complexed to CD1a-endo Run A. Lipids were eluted from CD1a in this fraction and assessed by using mass spectrometry by Dr Tan-Yun Cheng, Brigham and Women's Hospital.

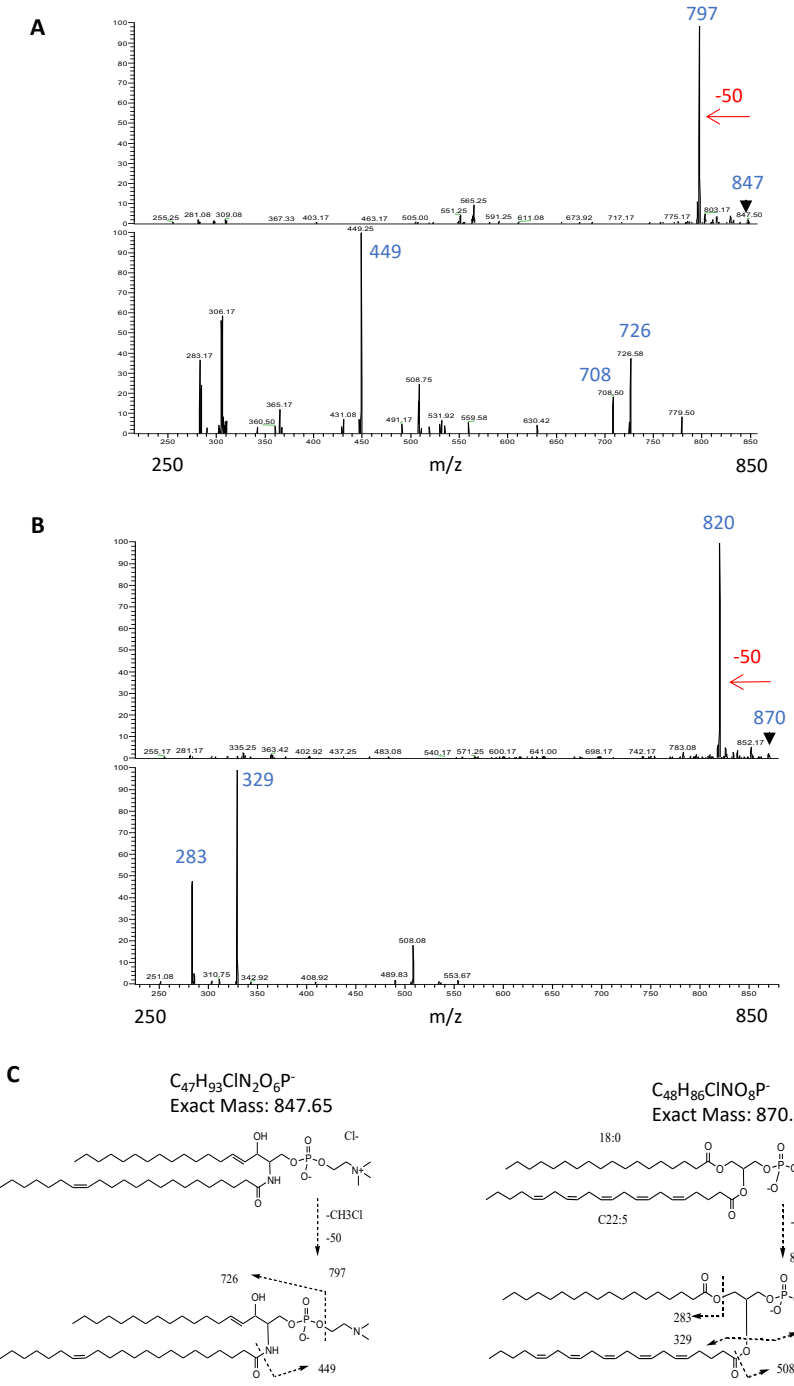

Figure 4.27. Detection of SM and PC in analysis of ions at *m/z* 847 and 870 in 27a28:CD1a-endo, fraction 37. CID (negative mode, nanospray) of *m/z* **A.** 847 and **B.** 870 in fraction 37 from gel filtration of 27a28 TCR co-complexed to CD1a-endo Run A. Lipids were eluted from CD1a in this fraction and assessed by using mass spectrometry by Dr Tan-Yun Cheng, Brigham and Women's Hospital. **C.** Mass and collisional patterns match to C42:2 SM and C32:5 PC.

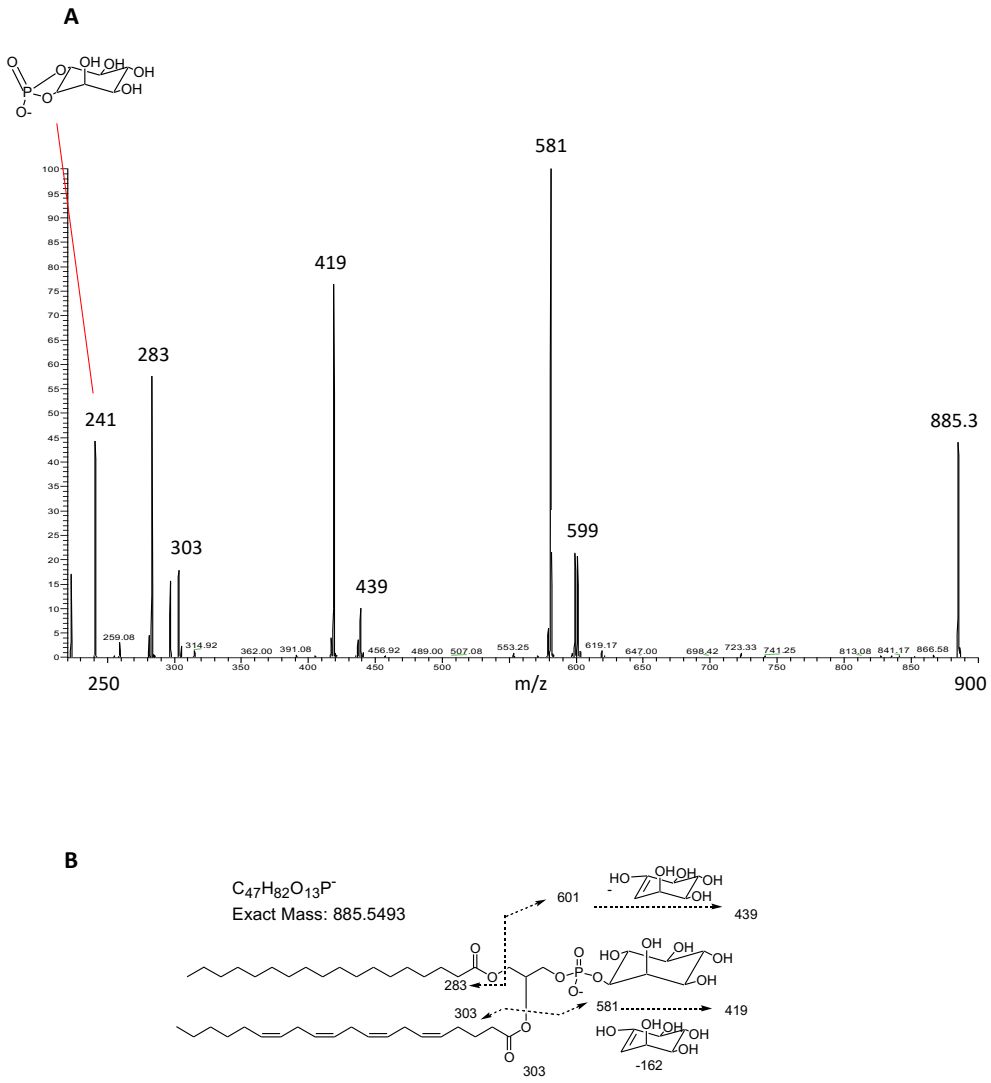

Figure 4.28. Detection of PI in analysis of ions at *m/z* 885 in 27a28:CD1a-endo, fraction 39. **A.** CID of (negative mode, nanospray) of *m/z* 885 in fraction 39 from gel filtration of 27a28 TCR co-complexed to CD1a-endo Run A. Lipids were eluted from CD1a in this fraction and assessed by using mass spectrometry by Dr Tan-Yun Cheng, Brigham and Women's Hospital. **B.** Mass and collisional patterns match to C38:4 phosphatidylinositol (PI).

antigens were present with differences in fatty acid chain length and saturation. Analogues of SM included C40:2, C41:2, C42:3, C42:2, and C42:1, of which C42:2 was the most abundant analogue captured by CD1a as determined by the area under the ion peak in MS (*Fig.4.29a)*. PC analogues present in CD1a included C34:1, C36:1, C38:4, C40:6, C40:5, and C40:4, of which C40:5 was the most abundant (*Fig.4.28a)*. PI analogues were the same as those for PC, of which C38:4 was the most abundant (*Fig.4.29a)*. Each fraction from both runs A and B were assessed for the most abundant analogue in each lipid class as a comparison to CD1a-endo. SM 42:2 (*m/z* 857) and PC C40:5 (*m/z* 880) were enriched in fractions 38-40 of Run A and 37-39 of Run B compared to CD1a-endo alone (*Fig.4.29b)*, suggesting that these lipid antigens are permissive for 27a28 TCR binding to CD1a. Conversely, PI C38:4 (*m/z* 885) was present at higher levels in the later fractions (*Fig.4.29b)*, indicating that PI is a non-permissive lipid for this TCR.

Surprisingly, the earliest fractions in both runs A and B of the 27a28 TCR-trap were contaminated with ions consistent with DDM (*Fig.4.30)*. The presence of DDM was not tested for in fraction 36 of Run A as the sample had been depleted, however it was present in other earlier fractions (*Fig.4.30)*. It was also found in fraction 35 of Run B, as well as smaller amounts in the later fractions (*Fig.4.30)*. PG, which is produced by both bacterial and mammalian cells, was enriched in fraction 36 of Run A, and undetected in fraction 37 with a gradual increase through the later fractions, and Run B showed a similar increase in PG amount across the fractions (*Fig.4.30)*. The earliest fractions in both runs A and B of the 27a28 TCR-trap (fractions 36 and 35 for Runs A and B respectively) were also contaminated with ions consistent with bacterial hexosyl-glucuronyl diacylglycerols and glucosyl diacylglycerols, indicating that these bound the TCR with very high affinity (*Fig.4.30)*.

The results suggest differing permissive and non-permissive lipids for TCR 27a28 to those previously determined for BK6, for which PC and PI are regarded as permissive while SM is non-permissive (Birkinshaw et al., 2015), thus highlighting the importance of investigating multiple CD1a-restricted TCRs. They also reveal several bacterial lipid antigens that may be recognised by CD1a and interact with this particular TCR with high affinity, similar to DDM. Although the results were indicative of a contamination, they also provided potentially valuable data and this experiment should be repeated outside of this thesis.

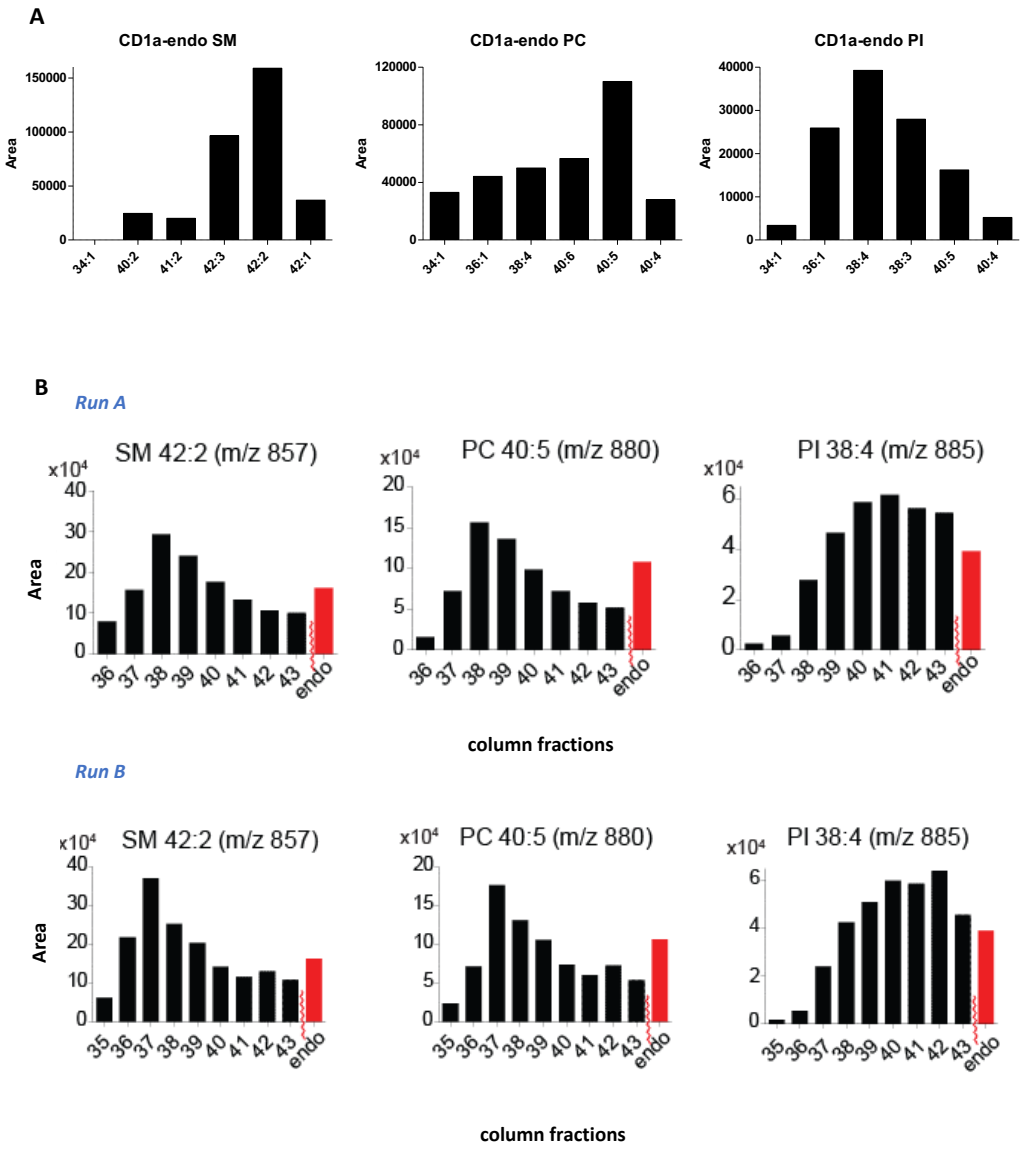

Figure 4.29. Assessment of SM, PC and PI eluted from 27a28:CD1a-endo co-complexation fractions. A. Determination of chain length and saturation of SM, PC and PI in binary CD1a-endo control. The most abundant analogs were investigated in further analyses. **B.** Relative abundance SM C42:2 (m/z 857) , PC C40:5 (m/z 880), and PI C38:4 (m/z 885) in fractions collected from 27a28:CD1a-endo co-complex gel filtration Run A (top) and Run B (bottom). Lipids were eluted from CD1a and TCR-CD1a co-complex and assessed by using mass spectrometry (positive mode) by Dr Tan-Yun Cheng, Brigham and Women's Hospital.

SM, sphingomyelin; PC, phosphatidylcholine; PI, phosphatidylinositol

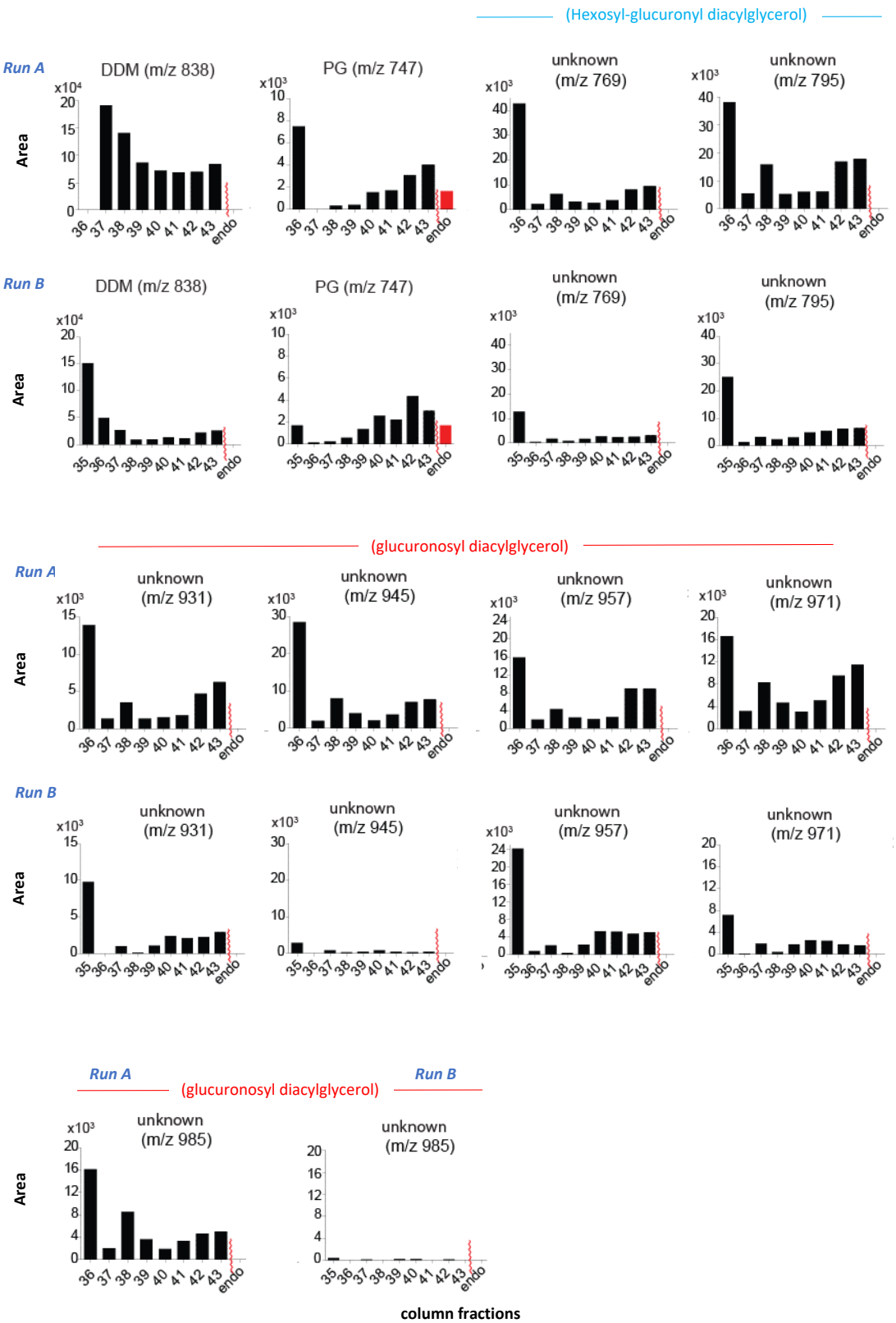
(Hexosyl-glucuronyl diacylglycerol)
Run A
DDM (m/z 838)
PG (m/z 747)
unknown (m/z 769)
unknown (m/z 795)
Area
Run B
DDM (m/z 838)
PG (m/z 747)
unknown (m/z 769)
unknown (m/z 795)
Area
(glucuronosyl diacylglycerol)
Run A
unknown (m/z 931)
unknown (m/z 945)
unknown (m/z 957)
unknown (m/z 971)
Area
Run B
unknown (m/z 931)
unknown (m/z 945)
unknown (m/z 957)
unknown (m/z 971)
Area
Run A
(glucuronosyl diacylglycerol)
Run B
unknown (m/z 985)
unknown (m/z 985)
Area
column fractions

Figure 4.30. Assessment of bacterial lipids eluted from 27a28:CD1a-endo co-complexation fractions. Relative abundance of bacterial lipids identified in fractions collected from 27a28:CD1a-endo co-complex gel filtration Run A (top) and Run B (bottom). Lipids assessed were DDM (detected in positive mode nanospray analysis at m/z 838), PG (m/z 747), two hexosyl-glucuronyl diacylglycerols (m/z 769 and 795), and a series of glucuronosyl diacylglycerols (m/z 931, 945, 957, 971, and 985) all in negative mode nanospray analysis. Lipids were eluted from CD1a and TCR-CD1a co-complex and assessed by using mass spectrometry (positive mode) by Dr Tan-Yun Cheng, Brigham and Women's Hospital.

DDM, dideoxymycobactin; PG, phosphatidylglycerol

4.2.8.2 29a28 TCR

Nanospray negative mode ESI-MS analysis of lipids eluted from the 29a28i TCR:CD1a co-complex revealed different profiles across the different fractions (*Fig.4.31)*, indicating the presence and absence of particular lipids in the early TCR-trap fractions. In the early fractions (31-34) PCs were relatively enriched compared to PIs, and in the late fractions (41-45) PGs were relatively enriched compared to PIs (*Fig.4.31).*

HPLC-MS lipidomic analysis and negative mode reverse phase HPLC were utilised to identify specific lipid analogues that differ between fractions. After excluding the solvent front and isotope ions, nine ions were identified by mass as enriched in the early fractions compared to later fractions and CD1a-endo that are candidate ligands for permitting or promoting binding of 29a28i onto CD1a: DAG C36:2, DAG C36:1, DAG C34:2, DAG C34:1, PC C40:5, deoxyceramide C42:2, deoxyceramide C42:1, and ceramide C42:1 (*Fig.4.32)*. In addition, PC C34:1 was relatively equally present across all fractions (*Fig.4.32)*, suggesting that it could be a low-affinity lipid antigen for this TCR. Non-permissive lipids were identified by enrichment in the later fractions compared to fractions 31-34: PI C38:4, SM C42:2, PG C36:2, PI C36:1, and to a lesser extent, SM C40:2 and PG C34:1 (*Fig.4.32)*. These results suggest that the 29a28i TCR traps several headless antigens and PC, which has a medium-sized head group, consistent with the absence of interference type recognition first outlined by (Moody and Suliman, 2017, Moody and Cotton, 2017) and the known permissive lipids for the BK6 TCR (Birkinshaw et al., 2015)

Interestingly, while the same stock of treated CD1a-endo was prepared and used in all three TCR-trap experiments, DDM was only associated with 27a28 (both runs) and not 29a28i (even though they were completed in the order: 27a28 Run A, 29a28i, 27a28 Run B and TCR protein used in each run was produced separately). It will be important to ascertain which lipids are truly permissive for these TCRs as opposed to those that are contaminants. The contaminants do, however, provide some insight into bacterial lipids that can be presented by CD1a to T cells. Furthermore, analysis of only the endogenous

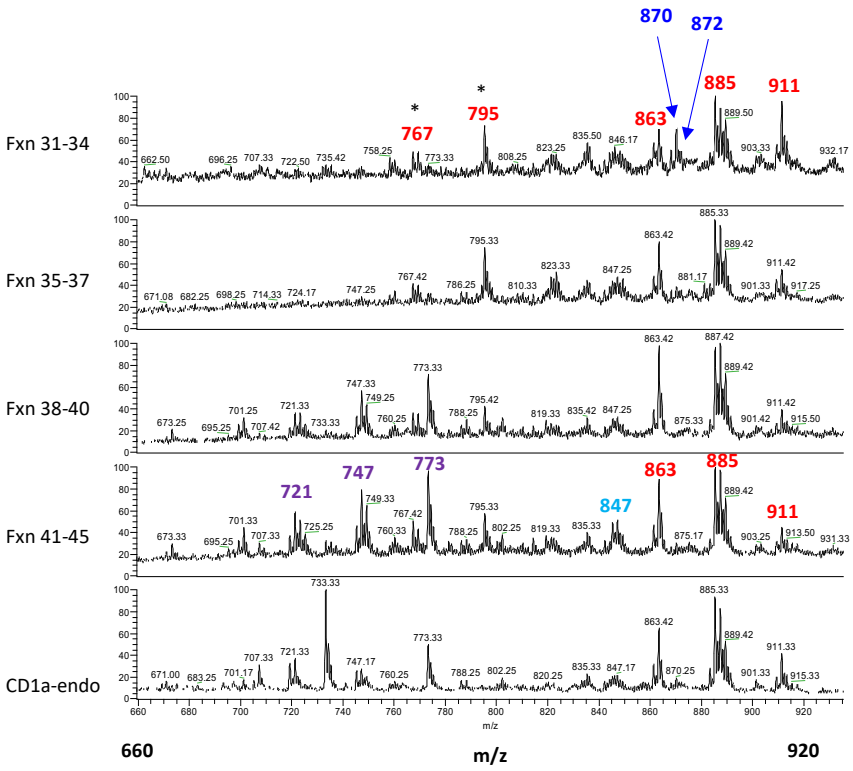

Phosphatidylcholine (PC) Phosphatidylinositol (PI) Sphingomyelin (SM) Phosphatidylglycerol (PG)

* contaminants

Figure 4.31. Nanospray negative mode analysis of lipids eluted from 29a28 TCR:CD1a-endo co-complex. Soluble 29a28i TCR protein was complexed with CD1a-endo and passed over an S200 column for gel filtration chromatography and lipids eluted from CD1a in selected fractions were assessed by mass spectrometry. Mass spectrometry was performed by Dr Tan-Yun Cheng, Brigham and Women's Hospital.

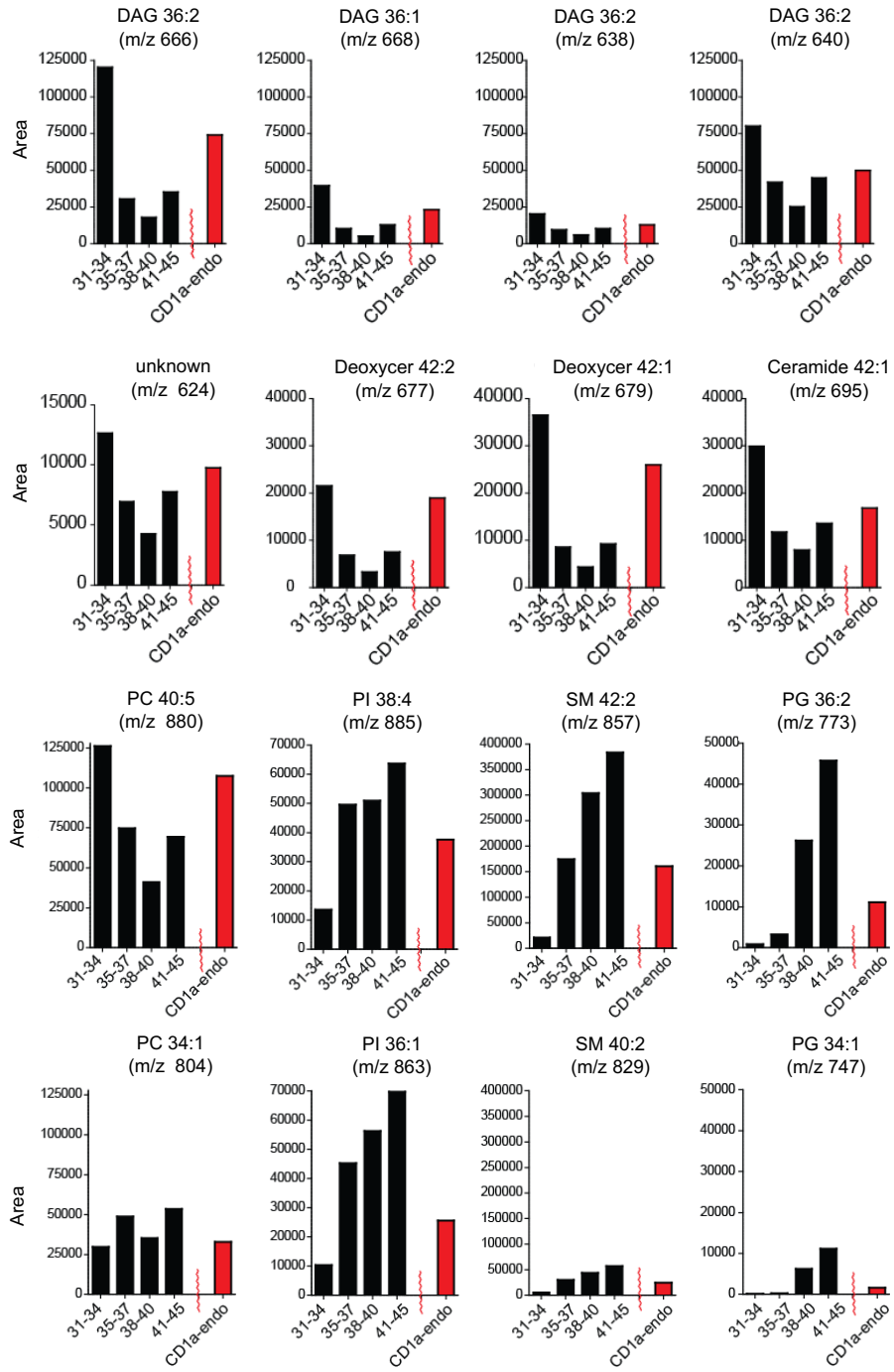

Figure 4.32. Assessment of lipids eluted from 29a28:CD1a-endo co-complexation fractions. Abundance of all predominant lipids identified in fractions collected from 27a28:CD1a-endo co-complex gel filtration Run B. Lipids were eluted from CD1a and TCR-CD1a co-complex and assessed by using mass spectrometry (positive mode) by Dr Tan-Yun Cheng, Brigham and Women's Hospital.

DAG, diacylglycerol; deoxycer, deoxyceremide; SM, sphingomyelin; PC, phosphatidylcholine; PI, phosphatidylinositol; PG, phosphatidylglycerol

lipids revealed different preferences for binding and permissive lipids for TCRs 27a28 and 29a28i.

4.2.8.3 Confirming lipid trap analysis results

The results of the lipid trap mass spectrometry revealed several lipids that are permissive for the TCRs 27a28 and 29a28i, some of which were originally thought to have been non-permissive (as they are non-permissive specifically for the canonical BK6 TCR (Birkinshaw et al., 2015)). As such, the ability of four TCRs to bind PC and SM presented by CD1a-tetramers was tested. The PC and SM analogues used in this preliminary tetramer staining were PC 24:1, SM 16:0 and SM 24:0 (Avanti Polar Lipids) (nomenclature equivalent to PC 48:2, SM 34:1 and SM 40:1) as these were readily available.

CD1a-endo was loaded with SM or PM at RT (21-22°C) overnight in a 3:1 ratio and tetramerised. SKW-3 β_2m CD1a-restricted T cell lines were subsequently assessed for their ability to bind the resulting tetramers. As expected, DDM-specific TCRs 8-2a2 and 17a28 bound tetramers loaded with DDM the best and had little variation in staining with SM and PC-loaded tetramers, and the vehicle and endogenous controls (*Fig.4.33*). The 27a28 and 29a28i TCRs used in TCR trap analyses revealed marginally greater tetramer binding with either CD1a-SM or CD1a-PC when compared to CD1a-vehicle or CD1a-endo (*Fig.4.33*). The small difference between CD1a loaded with SM and PC, and endogenous lipids may be due to the fact that SM and PC comprise part of the lipid repertoire presented by CD1a-endo, resulting in only a small preferential binding to CD1a-PC or CD1a-SM alone. While this experiment should be repeated using the SM and PC analogues with a greater degree of unsaturation identified by MS (SM 42:2 and PC 40:5) in addition to PI, it suggests that SM and PC are indeed permissive lipids for these two TCRs.

4.2.9 Interaction between CD1a and CD4

While previous analyses of T cell and CD1a-lipid interactions focused on TCR docking onto the CD1a molecules, the CD4 and CD8 co-receptors typically play important roles as part of the TCR complex. CD4 and CD8 engagement with MHC-II and MHC-I respectively augment T cell signalling, activation and responses (Janeway, 1992),

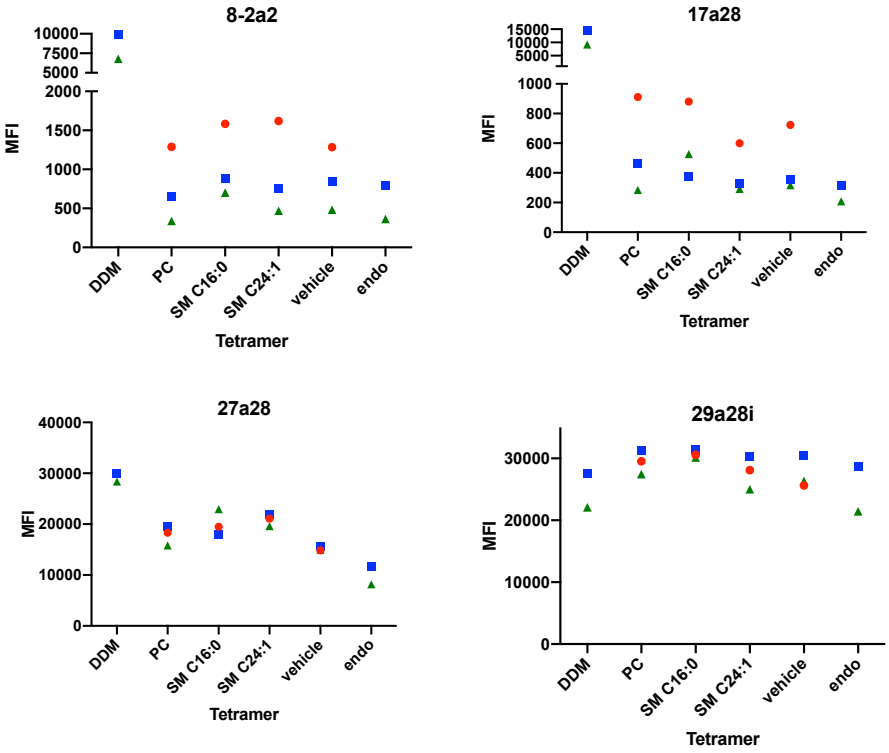

Figure 4.33. Recognition of PC and SM by CD1a-restricted TCRs. CD1a-restricted TCR SKW-3 $\beta_2m^{-/-}$ cell lines 8-2a2 and 17a28 (DDM-specific), and 27a28 and 29a28i (cross-reactive) were labelled with a panel of CD1a tetramers loaded with C24:1 PC, C16:0 SM, or C24:1 SM. Samples were gated on $CD3^{hi}$ GFP^{hi} cells to ensure TCR levels were comparable. Data are representative of three independent experiments, except for staining with CD1a-DDM and CD1a-endo tetramers, which were used in only two experiments. Different colours and shapes are indicative of independent experiments.

however, their interaction with CD1a is less well understood. Because $CD4^+$ CD1a-restricted cells constituted the majority of CD1a-restricted T cells in most individuals here and in studies performed by others (de Jong et al., 2010), it was hypothesised that the CD4 co-receptor may facilitate CD1a recognition.

To assess the interaction of CD4 and CD8 with CD1a, CD1a tetramers were tested for their ability to bind TCR-deficient SKW-3 $\beta_2m^{-/-}$ cells transduced with CD4 or CD8αβ (gift of Dr Michael Souter, The University of Melbourne) *(Fig.4.34)*. TCR-deficient $CD4^+$ cells bound CD1a-DDM, CD1a-vehicle, and CD1a-endo tetramers, but did not bind PE-conjugated streptavidin alone, MR1-5-OP-RU, or other CD1 tetramers (*Fig.4.34a*). This suggests that CD4 has some degree of interaction with CD1a independently of the TCR. In contrast, TCR-deficient $CD8^+$ cells were labelled with the same tetramers and only bound MR1-5-OP-RU (*Fig.4.34a. Fig.4.34b*), consistent with previous observations of TCR-independent binding of CD8 to MR1 tetramers presenting 5-OP-RU, 6-FP and Ac-6-FP (presented as part of Michael Souter's PhD Thesis, submitted to The University of Melbourne in 2020). To account for the possible effect of the detergent tyloxapol in CD1a-vehicle and CD1a-DDM tetramers interacting with J.76.CD4, tyloxapol was added to CD1a-endo tetramer and streptavidin alone, but this had no effect on tetramer binding ability (*Fig.4.34b*).

These results suggest that CD4 may mediate binding to CD1a. The possibility that CD1a is able to bind to CD4 is worthy of further exploration because this interaction may enhance CD1a avidity and augment the functional outcome of antigen recognition by CD1a-restricted T cells. An association between CD1a and CD4 may explain why most CD1a restricted T cells are $CD4^+$ and not $CD8^+$, in contrast to MAIT cells that are conversely predominantly $CD8^+$ and display an important interaction between their CD8 co-receptor and MR1. These results provide a basis to warrant further investigation, and studies such as an interrogation of which CD1a amino acid residues contribute to the CD4-CD1a interaction with CD1a mutant cell lines, and a comparison with MHC-I, may provide additional insight.

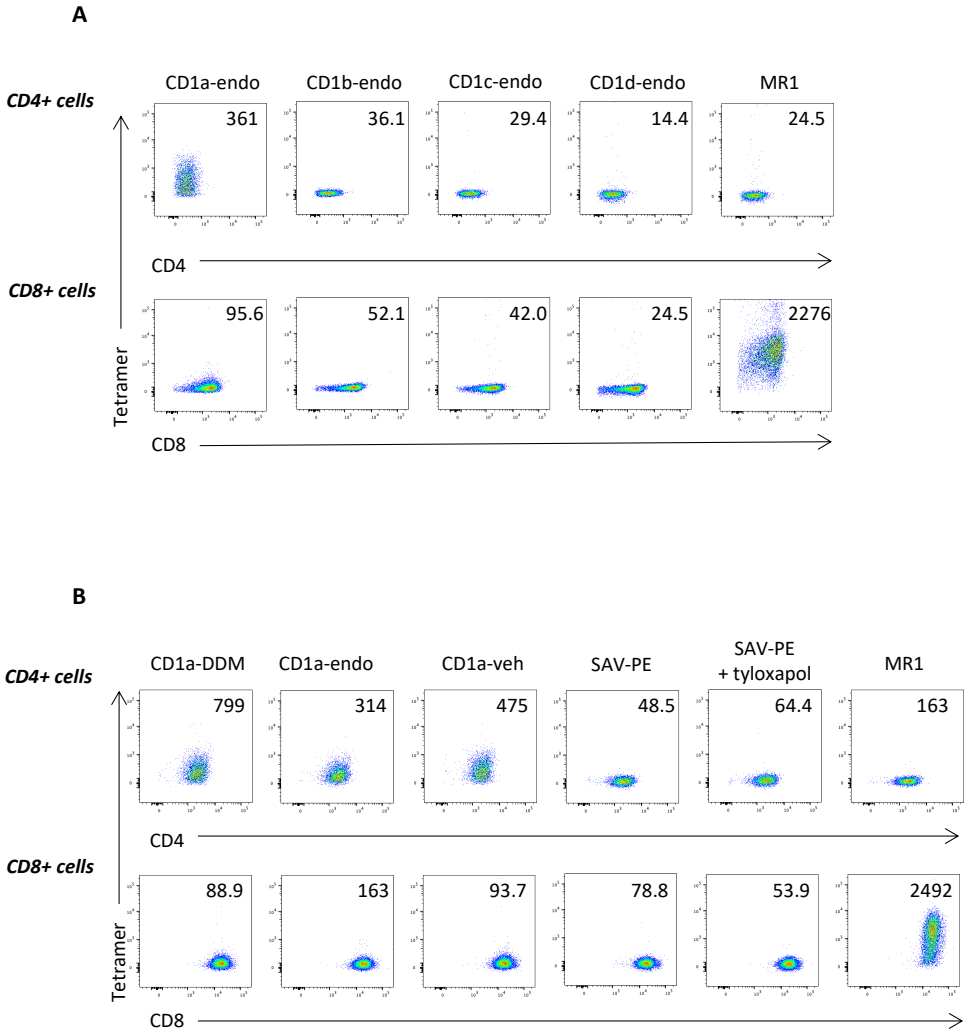

Figure 4.34. Binding of CD1a to CD4 in a TCR-independent manner. TCR-deficient cell lines expressing either CD4 or CD8 co-receptor were assessed for their ability to bind **A.** CD1a-endo, CD1b-endo, CD1c-endo, CD1d-endo, or MR1-5-OP-RU tetramers or **B.** a panel of CD1a tetramers loaded with DDM, endogenous lipids, or 0.5% (v/v) tyloxapol, streptavidin tetramers controls with the equivalent concentration of SAV-PE in TBS as CD1a-tetramers with and without 0.5% (v/v) tyloxapol, and MR1-5-OP-RU. Samples were gated on GFP^{hi} cells to ensure CD4 or CD8 levels were comparable. Data are representative of three independent experiments.

4.3 Discussion

Using CD1a tetramers, CD1a-restricted T cells in healthy blood donors were successfully identified in sufficient numbers to assess their TCR repertoire. Using multiplex nested PCR (Wang et al., 2012) and single cell RNA-sequencing (Rizzetto et al., 2018), we revealed, for the first time, patterns of intra- and inter-donor variable gene bias in the repertoire of CD1a-restricted TCRs. Furthermore, many of the TCRs isolated were broadly reactive to CD1a presenting lipids antigens with different structures and others were DDM-specific, suggestive of multiple binding mechanisms of TCRs onto CD1a. With the TCR sequences determined from these analyses, transmembrane and soluble CD1a-restricted TCRs were generated to explore the interaction between TCRs and CD1a-lipid complexes. To date, studies investigating the structural biology of these interactions have focused on either CD1a presenting DDM alone (Zajonc et al., 2005b), or one CD1a-autoreactive T cell clone (Birkinshaw et al., 2015).

Both multiplex nested PCR sequencing and RNA sequencing methods revealed a diverse TCR repertoire, consistent with the literature (Cohen et al., 2009, Grant et al., 1999, Vincent et al., 2005). However, consistent with the emerging patterns of TCR biases among other group 1 CD1-restricted T cells (Roy et al., 2014, Van Rhijn et al., 2014, Van Rhijn et al., 2013a), there were notable patterns of TCR variable gene bias among CD1a-restricted TCRs. Both α- and β-chains of CD1a-restricted TCRs frequently incorporated particular V genes. The TCR diversity of naive human αβ T cells is estimated to be 2.5×10^7, and that of memory cells is estimated to be 100-fold less (Arstila et al., 1999). Given that many peripheral CD1a-restricted T cells isolated from human blood were $CD45RO^+$, and unconventional T cells are generally thought to be innate-like and can predominately display a memory phenotype (van Der Vliet et al., 2000, Martin et al., 2009b, Koay et al., 2016), it was possible that the TCR repertoire could have been limited, especially among the $CD45RO^+$ fraction.

Using two independent methods of TCR sequencing, nearly half of the CD1a-restricted T cells identified were $TRBV28^+$. Co-labelling of a population of T cells with CD1a tetramers and an anti-Vβ3 (TRBV28) mAb among PBMCs, confirmed that this bias was not an effect of the sequencing process (i.e. primers targeting various variable genes working better than others in PCR amplification) but rather, a true bias for TRBV28 that may be beneficial for the TCR-CD1a interaction. Interestingly, a MAIT-like population

has recently been described that expresses a public TRAV36^{+} TRBV28^{+} TCR (Koay et al., 2019), which is an example of similar TCR bias patterns between unconventional T cells. Further structural studies (e.g. X-ray crystallography) of the TRBV28^{+} TCRs may provide insight into the role of TRBV28 in the TCR-CD1a interaction with the soluble 27a28 and 29a28i TCR proteins produced here.

Multiplex PCR sequencing revealed that the variable genes TRAV8-2 and/or TRAV8-4 were frequently expressed by CD1a-restricted TCRs but did not discriminate between the two, as the regions covered by the primers used are identical in sequence. Single cell RNA-sequencing subsequently revealed a slight bias for TRAV8-4 while TRAV8-2 was not observed among any of the CD1a-restricted cells sequenced, suggesting that the bias among CD1a-restricted T cells is for TRAV8-4, not TRAV8-2. Prior to RNA-sequencing, TRAV8-2 was selected to produce TCR cell lines, which were confirmed to be reactive to CD1a-tetramers. This is an interesting outcome in itself, as if the original CD1a-restricted TCR isolated from primary cells were indeed TRAV8-4^{+}, it suggests that despite amino acid differences in CDR1α and CDR2α sequences, both TRAV8-2 and TRAV8-4 are structurally similar enough to produce a TCR with the capacity to bind CD1a-lipid complexes. In addition, TRAV14/DV4 and TRAV1-2 genes were frequently observed among CD1a-restricted TCRs sequenced, albeit not to the same extent as TRAV8-4. TRAV1-2 is the preferential Vα gene in GEM cells and MAIT cells (Van Rhijn et al., 2013a, Porcelli et al., 1993, Treiner et al., 2003), suggestive of the preferential use of TRAV1-2 among multiple unconventional T cell subsets. These TCR biases were only further exemplified when only examining DDM-reactive T cells, consistent with more distinct variable gene patterns observed among other antigen-specific T cells (Gras et al., 2008).

Similar TCR structures seemed to be utilised to recognise CD1a-lipid complexes, particularly among broadly CD1a-reactive T cells, which may bind directly to the monomorphic CD1a molecule (Martin et al., 2009b). CD1a-autoreactive T cells appeared to have a diverse TCR repertoire, but a large proportion of TCRs examined in this study used the variable gene TRBV28.

It is important to understand the TCR repertoire of CD1a-restricted T cells as patterns of TCR bias can play a role in infectious disease, T cell malignancies, autoimmunity and

allergy (Miles et al., 2011a, Miles et al., 2011b). For example, CD1c-restricted T cells that display a TCR variable gene bias can recognise abnormal lipids expressed in tumours (Lepore et al., 2014)). Analysis of TCR sequences from a greater number of individuals will develop our understanding of the CD1a-restricted TCR repertoire and if patterns emerge that are associated with disease-related antigens, they may be useful in diagnosis and treatment. Nonetheless, TCR biases may become more prevalent in a disease state or when investigating reactivity to particular antigens, as they have here when comparing all CD1a-restricted T cells to DDM-reactive T cells, which could be exploited.

The CDR3 length distribution of CD1a-restricted TCRs was examined. CDR3 loop architecture is critical for determining the ability of a TCR to interact with its ligand, and antigen-specificity generally reduces CDR3 length polymorphism (Day et al., 2011, Turner et al., 2003). Most conventional T cell clones that bind the same pMHC complex have the same CDR3 length of 6-12 amino acids (Yao et al., 2007, Rock et al., 1994). It was therefore possible that recognition of monomorphic CD1a may also limit CDR3 length. CDR3α sequences of CD1a-restricted T cells (independent of antigen) were typically 11-16 amino acids in length, with some instances occurring outside this range. The length of the CDR3β regions was less constrained, ranging from 10-21 amino acids in length, most falling within the smaller range of 13-16. RNA-sequencing of DDM-reactive T cells, revealed a similar CDR3 length diversity, ranging from 9-16 amino acids for CDRα sequences and 11-22 amino acids for CDR3β sequences. CDR3 region sequences determine TCR structure and specificity, making this diversity in CDR3 loop architecture among TCRs that bind CD1a-lipid complexes interesting. CD1a-restricted TCR CDR3 loops were typically longer and span a greater range in length compared to MHC-restricted αβ-TCRs (Rock et al., 1994, Yao et al., 2007), which may compensate for biases in variable genes used.

Selected TCR sequences were used to generate CD1a-restricted TCR cell lines to be used in further studies. The resulting cell lines bound CD1a tetramers, thereby validating the isolation and sequencing processes. Both multiplex PCR sequencing and RNA-sequencing yielding similar results with regards to the TCR repertoire, provides confidence that most – if not all – cells isolated using the methods described here were truly CD1a-restricted.

As part of their validation, cell lines were tested for their ability to bind CD1a tetramers presenting endogenous self-lipids and exogenous lipids, and some displayed a level of cross-reactivity, despite the hinderance usually observed by CD1a-restricted T cell clones that bind either one or the other. The idea of antigen cross-reactivity conferred by a single TCR clone is reasonable given that there are more potential TCR possibilities than TCRs in the body, and this limitation allows only a fraction of the potential TCR repertoire to be expressed in each individual. For this reason, it is estimated that a single conventional TCR may recognise more than 1 x 10^6 pMHC complexes (Mason, 1998), however, it was unknown whether this level of cross-reactivity between antigens would also carry over to T cells that are restricted to CD1.

CD1a-autoreactive T cell clone BK6 does not bind CD1a tetramers loaded with DDM (Birkinshaw et al., 2015), while CD8-2 (Grant et al., 1999), Clone 8, and Clone 15 fail to bind CD1a tetramers loaded with endogenous lipids permissive for BK6, but do bind CD1a-DDM tetramers (Cheng et al., 2017, Moody et al., 2004, Young et al., 2009). Consistent with the findings of Vincent et al., multiple CD1a-restricted TCRs identified were both self-reactive and microbial antigen-reactive, albeit the recognition of self-antigens was weaker (Vincent et al., 2005). Each dual-reactive TCR displayed greater tetramer binding and activation with DDM compared to self-lipids, suggesting that these T cells preferentially target exogenous foreign antigens but do have an inherent level of autoreactivity. In fact, there is evidence that each isoform of CD1 (CD1a, CD1b, CD1c and CD1d) can activate some T cells in the absence of added foreign antigen, highlighting that this phenomenon is not unique to CD1a (Balk et al., 1991, Beckman et al., 1996, Bendelac et al., 1995, Porcelli et al., 1989, Vincent et al., 2002, Sieling et al., 2000).

We investigated the interactions between TCR-CD1a-lipid to determine the structural nuances that influence recognition, activation, and suppression of CD1a-restricted T cells. There is little observable difference in the binary structure of CD1a presenting DDM and sulfatide despite the difference in alkyl chain number (one and two respectively) and the chemical nature of the hydrophilic head groups between these two antigens (Zajonc et al., 2005b, Zajonc et al., 2003). This suggests that the difference in TCR recognition therefore lies in the head groups exposed through the F'-portal and is dependent on whether or not they interfere with recognition of the A'-roof (Zajonc et al., 2005b, Birkinshaw et al., 2015, Zajonc et al., 2003).

Multiple TCRs were investigated for their ability to recognise various lipid antigens including endogenous lipids, and analogues of DDM. None followed the same recognition pattern as BK6, which is only autoreactive to endogenous lipids presented by CD1a, as large antigen headgroups perturb the TCR-CD1a interface. Instead, they either appeared to recognise DDM, or display dual reactivity to self and foreign lipid. The TCRs investigated here appeared to bind preferentially to lipids with larger headgroups, but many could also recognise CD1a presenting endogenous self-lipids with small headgroups, suggesting that there might be another mechanism of interaction between CD1a-lipid complexes and TCRs not yet considered. A possible mechanism for recognition of multiple lipid antigens by one TCR is the direct binding of the TCR to CD1a in a lipid-independent manner as it binds in a different location that is neither affected by protrusion of a lipid headgroup nor the dynamics of the A'-roof.

Such broad cross-reactivity between structurally different lipids has not yet been observed for CD1a-restricted T cells. For example, analogues of DDM that vary slightly in alkyl chain length and saturation state can all be recognised by CD1a-restricted T cell clone CD8-2, but C20:1 DDM-838, so named due to its mass, is the analogue that acts as the most potent agonist (Moody et al., 2004). This finding, while only based on one T cell clone, highlights that minor structural alterations to the DDM molecule can impact its recognition and agonistic potential as a CD1a lipid. The ability of CD1a-restricted T cell lines developed here to recognise four DDM stereoisomers revealed the stereoisomers exhibited varying agonistic potency depending on the T cell clone. In an initial study by Cheng and colleagues, three T cell clones, Clone 8, Clone 15, and CD8-2 all bound best to DDM-A, the naturally occurring stereoisomer (Cheng et al., 2017). Here, however, these three T cell clones that bound better to DDM-C or DDM-D, highlighting the need to study multiple CD1a-restricted T cell clones to gain insight into their structural biology.

Notably, whilst LPC and SM contain the same polar head group, they are permissive and non-permissive ligands respectively, and it is the longer chain length of SM (C_{23} as opposed to C_{18}) that causes it to protrude into the A'-roof (Birkinshaw et al., 2015). There therefore may be different patterns in chemical structure of these CD1a antigens that influence whether they are permissible to TCR docking onto CD1a. Albeit while longer SM and PC were determined to be permissive to 27a29 and 29a28i binding with lipid trap analyses, they bound CD1a tetramers loaded with shorter, more saturated SM and PC

analogues. Nevertheless, small differences in the alkyl chains of lipids may affect headgroup exposure at the TCR-CD1a-lipid interface.

To assess the binding footprint of the TCRs on the CD1a molecule, the ability of C1R cells expressing CD1a with single amino acid substitutions in key "hot spot" residues to activate CD1a-restricted T cells was measured. The footprint of BK6, a CD1a-autoreactive T cell clone, for which lipids with large headgroups are non-permissive for TCR recognition and activation, is predominantly over the A'-roof (Birkinshaw et al., 2015). It was this study that lead to the absence of interference model of recognition by CD1a-autoreactive T cells; their TCRs recognise CD1a-lipid complexes provided the lipid antigen head group does not interfere with the interaction between the TCR and key contact residues on the A'-roof (Cotton et al., 2018, Moody and Suliman, 2017).

Interestingly, TCRs that had the lowest affinity for CD1a (as determined by activation assays and tetramer-binding), being CNR1, 35a16 and 8-2a13ii, had the greatest sensitivity to alterations in the CD1a structure overall. Their binding footprint was predominantly over the A'-roof, spreading to surround the F'-portal in some cases, which is a similar pattern to BK6. In contrast the higher affinity TCRs were less sensitive to changes in CD1a. This was unexpected, as they were hypothesised to have greater interactions with the CD1a molecule itself. The low number of critical CD1a amino acid residues determined in the interaction with these TCRs could be either because they interact with fewer CD1a residues, or because they bind to other key residues not assessed in this assay. It is important to note that the observed reduction in activation may have been a consequence of an indirect effect of any given mutation on the CD1a conformation (i.e. impacting on neighbouring residues or antigen loading). Nonetheless, collectively these data reveal that there are multiple footprints that CD1a-restricted TCRs can assume onto CD1a, allowing for different antigen-specificities and cross-reactivity. Soluble CD1a-restricted TCRs and CD1a were produced for future SPR analyses, and ternary complexes of TCR with CD1a-endo or CD1a-DDM for X-ray crystallography, which will provide further insight into the molecular interactions between these TCRs and CD1a-lipid complexes.

Ternary TCR-CD1a-lipid complexes were used in "TCR trap" analyses with two broadly CD1a-reactive TCRs to identify antigenic lipids that mediate high affinity binding to

CD1a-lipid complexes. By using two TCRs with seemingly different lipid antigen specificity to the previously studied BK6, they would potentially reveal a different repertoire of permissive lipids. For BK6, permissive antigens appear to lack direct contact with the TCR, and thus autoreactivity is determined by contacts with CD1a itself, while lipids that interfere with the TCR-CD1a binding site by disrupting the A'-roof of CD1a, such as sulfatide and SM, are considered non-permissive (Birkinshaw et al., 2015).

Mass spectrometry of the lipids eluted from 27a28 TCR:CD1a-lipid ternary complexes that bound with high affinity revealed a different pattern of permissive and non-permissive lipids to what was established for BK6. PC (C16:1-24:1) and SM (C18:0-22:0) were permissive lipids for this TCR, and PI (C18:0-20:4) was non-permissive. In contrast, PC and PI are permissive and SM is non-permissive for BK6 (Birkinshaw et al., 2015), highlighting the importance of investigating multiple CD1a-restricted TCRs. Furthermore, contamination with bacterial lipids allowed for the discovery of CD1a antigens derived from bacteria. In addition to DDM, two uronic acid-containing bacterial compounds were revealed as high-affinity CD1a antigens.

Glucuronosyl diacylglcerols that have previously been isolated in *M.smegmatis*, one of a few known glucuronic acid-containing compounds found in mycobacteria (Wolucka et al., 1993) were loaded into CD1a. While *M.smegmatis* is not generally considered a human pathogen (Brown-Elliott and Wallace, 2002), its glucuronosyl diacylglcerol displays broad immunological cross-reactivity with anti-*M.avium* and anti-Mtb sera, suggesting the presence of similar glucuronic acid-containing compounds in these pathogenic mycobacterial species (Wolucka et al., 1993). Glucuronosyl diacylglycerols have also been described in Streptomyces spp. (Batrakov and Bergelson, 1978, Bergelson et al., 1970), *Bacillus cereus* (Minnikin et al., 1971), Pseudomonas spp. (Wilkinson, 1968, Wilkinson, 1969), and two halotolerant bacteria species (Peleg and Tietz, 1971, Stern and Tietz, 1973).

A mannosylated variant of glucuronosyl diacylglycerol, hexosyl-glucuronyl diacylglyercol, that was first described in *Corynebacterium glutamicum* (Tatituri et al., 2007) was also identified. This compound is similar to Mtb lipoglycans (Tatituri et al., 2007), which is unsurprising given the similar array of cell wall-associated glycolipids displayed by cornybacteria and mycobacteria, such as phosphatidyl-*myo*-inositol

(PI) mannosides (PIMs) and lipoglycans (Besra et al., 1997, Brennan and Ballou, 1967, Brennan and Ballou, 1968, Hill and Ballou, 1966, Brennan and Nikaido, 1995, Morita et al., 2004, Tatituri et al., 2007). Given that these glucuronosyl diacylglycerols were detected in ternary complexes bound with high affinity, it will be interesting to determine whether there are additional antigens from these species that induce cross-protective responses mediated by CD1a-restricted T cells.

Mass spectrometry of the lipids eluted from 29a28i TCR:CD1a-lipid ternary complexes that bound with high affinity revealed a repertoire of permissive lipids more in line with that of the BK6 TCR (Birkinshaw et al., 2015). PCs were permissive for this TCR while PGs were non-permissive. Furthermore, nine candidate ligands were identified as having high-affinity binding to the 29a28i TCR: diacylglycerol (DAG) C36:2, DAG C36:1, DAG C34:2, DAG C34:1, PC C40:5, deoxyceramide C42:2, deoxyceramide C42:1, and ceramide C42:1. These results suggest that the 29a28i TCR preferentially binds lipid antigens with small-to-medium sized head groups, which is consistent with BK6 and absence of interference type recognition (Moody and Suliman, 2017, Moody and Cotton, 2017).

While the same stock of soluble CD1a-endo was prepared and used in all three TCR-trap experiments, DDM contamination was only associated with 27a28 (both runs) and not 29a28i (even though they were completed in the order: 27a28 Run A, 29a28i, 27a28 Run B with the same equipment and the 27a28 TCR protein for the second run was produced independently). Due to the bacterial lipid contaminants, it was difficult to ascertain which self-lipids were truly permissible for these TCRs, especially 27a28. While the source of these contaminating bacterial lipids is unclear, one possible source is mycobacterial contamination of the FCS used in cell culture for CD1a production. The contaminants do, however, provide some insight into bacterial lipids that may be presented by CD1a to T cells.

Lastly, whether CD4 may facilitate interaction of the TCR complex with CD1a was assessed. Phenotypic studies, performed here and by others, show that most CD1a-restricted T cells express CD4 (de Jong et al., 2010), suggesting that the CD4 co-receptor may be important for CD1a binding. CD8 binds the mouse thymus leukemia antigen (a mouse MHC-Ib molecule) on intra-epithelial lymphocytes with high affinity with an

interface similar to that of CD8 with MHC-I (Leishman et al., 2001, Liu et al., 2003). CD8 has been demonstrated to bind MR1 independently of TCR interactions (presented as part of Dr Michael Souter's PhD Thesis, submitted to The University of Melbourne in 2020) which correlates with a significant bias of CD8 expression among MR1-restricted MAIT cells in human blood (Corbett et al., 2014, Riegert et al., 1998). There is also evidence to suggest that there is a skewed expression of CD4 and CD8 co-receptors among lipid-reactive T cells. For example, a guinea pig immunisation model with mycobacterial lipid extract revealed that the CD1b- and CD1c-restricted mycobacterial lipid-reactive T cells were mostly $CD8^+$ and/or DN T cells with cytotoxic capacity (Hiromatsu et al., 2002). NKT cells predominantly fall within $CD4^+$ or DN T cell subsets (with an additional $CD8\alpha^+$ subset in humans) (Apostolou et al., 2000, Bendelac et al., 1994, Lantz and Bendelac, 1994, Ohteki and MacDonald, 1994, Takahashi et al., 2002), highlighting differences of CD4 and CD8 co-receptor expression between species.

Consistent with the results here, another study determined that circulating lipid antigen-reactive T cells in TB patients were predominately $CD4^+$ (Ulrichs et al., 2003). A TCR-deficient cell line transduced with CD4 demonstrated the ability to bind to CD1a, supporting the hypothesis that CD4 may facilitate, or even augment, TCR binding to CD1a. Although, this is surprising given that CD1a is more closely related to MHC-I in structure compared to MHC-II (Zeng et al., 1997). The interaction between CD1a and CD4, and how it complements TCR-CD1a binding, hence requires further investigation.

These studies collectively revealed that CD1a-restricted T cells can interact with CD1a-lipid complexes in multiple ways that permit variability in lipid antigen reactivity. It will be interesting to examine how self-reactivity is suppressed or avoided under normal conditions if some CD1a-restricted T cells are autoreactive, although it appeared that foreign lipid antigens, such as DDM, were more potent agonists. Other overtly self-reactive T cells, such as type I NKT cells, are typically quiescent, but have immediate innate-like effector functions under inflammatory conditions or infection, even in the absence of specific foreign lipid antigen recognition (Mempel et al., 2002, Nieuwenhuis et al., 2002, Brigl et al., 2003). In addition, self-reactive MHC-restricted T cells, such as $CD4^+$ $CD25^+$ regulatory T cells are important for the maintenance of homeostasis and autoreactivity (Jordan et al., 2001, Sakaguchi et al., 1995), and self-reactive CD1a-restricted T cells may play a similar role.

These studies also highlight that the difference in TCR-CD1a interactions may mean that anti-CD1a blocking mAbs may fail to neutralise all CD1a-dependent T cell responses because they are binding to a site that does not block TCR engagement. Interestingly, in a preliminary study of the two TCRs with the greatest levels of activation in the presence of $CD1a^{+}$ C1R cells and CD1a-tetramer binding, 27a28 and 29a28i, the anti-CD1a blocking mAb had little effect (data not shown). This suggests that their TCR docking to the CD1a molecule is unperturbed by the positioning of this antibody on its epitope, which is not necessarily surprising if they have different binding sites on the CD1a-lipid complex to self-reactive or DDM-reactive TCRs. A greater understanding of TCR-CD1a interactions will therefore aid in the development of therapeutics that target CD1a-restricted T cells.

Chapter 5. Isolation and characterisation of macaque CD1-restricted T cells

5.1 Introduction

To gain a greater understanding of the role of group 1 CD1-restricted T cells in the context of homeostasis and disease *in vivo*, animal models are essential. Murine models have been extensively used to study type I NKT cells, however the absence of group 1 CD1 genes in mouse and rat genomes has precluded the use of murine models for functional *in vivo* analyses of these cells (Dascher and Brenner, 2003, Strominger, 2010, Van Rhijn et al., 2013b, Bradbury et al., 1988). To date, transgenic mice for human group 1 CD1 molecules (Felio et al., 2009) or humanised severe combined immunodeficient (SCID), which have been engineered to develop a functional human CD1 compartment (Lockridge et al., 2011), have been used for *in vivo* function studies. Recently, a transgenic mouse model was produced to express human CD1a to study the role of CD1a in skin inflammation (Kim et al., 2016). However, given that it is still unclear how CD1a-restricted T cells develop, CD1a-restricted T cells in these mice may not necessarily be completely reflective of their human counterparts. It is therefore ideal to study group CD1-restricted T cells in animals in which all CD1 molecules are naturally expressed.

As mycobacterial cell wall lipids can be potent lipid antigens as well as contributors to persistence and virulence (Ghazaei, 2018), CD1-restricted T cells have been of great interest in animal models of tuberculosis. Guinea pigs, which have orthologs of CD1b, CD1c, and CD1d, have been used in studies of immunisation strategies with mycobacterial lipids to assess the response of lipid-reactive T cells (Dascher et al., 2003, Hiromatsu et al., 2002, Watanabe et al., 2006). Cows, a natural host for *M.bovis*, are used as another model of TB and have CD1a, CD1b and CD1d orthologs (Nguyen et al., 2009, Nguyen et al., 2013, Van Rhijn et al., 2006), however working with bovine models can be cumbersome. Disadvantages of using guinea pigs and cows are that neither contain all four CD1 molecules and only exhibit 61-74% homology with human group 1 CD1 molecules (*Table 5.1*). Guinea pigs also have additional variations of CD1b and CD1c not seen in humans, which may conflict results when translating the findings of these studies to humans. In addition, there are fewer reagents to explore immunity in these animals making working with them particularly challenging.

	Macaca mulatta	*Macaca nemestrina*	*Macaca fascicularis*	*Mus musculus*	*Cavia porcellus*	*Bos taurus*
CD1a	85/90	85/90	86/90	N/A	N/A	62/76
CD1b	95/97	94/97	94/97	N/A	B1: 67/82 B2: 68/80 B3: 69/77 B4: 62/76	74/84
CD1c	90/93	91/93	91/93	N/A	C1: 65/75 C2: 61/73 C3: 66/77	N/A
CD1d	81/93	90/93	89/93	61/74	69/78	65/79

Table 5.1. Homology of CD1 proteins across different mammalian species. Protein sequences were obtained from the National Center for Biotechnology Information protein database and compared to each respective *Homo sapiens* CD1 sequence. The first number indicates percentage of identical amino acids, and second indicates percentage of identical or similar property amino acids.

The most closely related CD1 molecules to humans are those in non-human primates (NHP). Marmoset and rhesus monkeys have recently been identified as good models to study lipid-reactive T cells, particularly in the context of mycobacterial infection (Barouch et al., 2002, Sharpe et al., 2017). Yu et al. constructed a phylogeny tree detailing the conservation of the CD1 primate locus (Yu et al., 2019). *CD1D* is likely to be the oldest CD1 gene with the most conservation among species, which is expected given its presence in mice, followed by *CD1A* and then a divergence of *CD1B* and *CD1C* through additional gene duplication events, all of which remain highly conserved (Yu et al., 2019). In a comparison of CD1 homologs in select species (*Table 5.1*), the most closely related macaque species to humans in terms of homology of CD1 proteins is pig-tailed macaque (*Macaca nemestrina*), which was not assessed by Yu and colleagues. Pig-tailed macaques (PTM) have 85% amino acid conservation for CD1a, 94% for CD1b, 91% for CD1c, and 90% for CD1d, which is above the level of conservation between human and rhesus macaque (*M.mulatta)* or crab-eating macaque *(M.fascicularis)* (*Table 5.1*). An alignment of each CD1 protein sequence was also performed for these species to determine conserved regions *(Fig.5.1).* CD1a and CD1b had few amino acid differences between the three macaque species and humans, while CD1c and CD1d had larger areas of difference at the C-terminal and N-terminal ends respectively, with a deletion of amino acids in human CD1d. This may not reflect differences in the areas exposed to T cells but may impact membrane anchoring and association with β_2m *(Fig.5.1).*

The similarities between CD1d and NKT cells across mammalian species are well documented for CD1d loaded with α-GalCer and type I NKT cells. Trans-species cross-reactivity is established between human and mouse type I NKT cells and CD1d-α-GalCer (Brossay et al., 1998), despite the lower conservation of CD1d (61% homology (*Table 5.1*)). This cross-reactivity may be enabled by their conserved TCR (17 of the 25 amino acid residues in the TCR α-chain that mediate contact between CD1d or α-GalCer are conserved) and TCR footprint onto the lipid-antigen complex (Borg et al., 2007, Pellicci et al., 2009). For this reason, previous studies have used murine CD1d-α-GalCer tetramers to isolate type I NKT cells from rhesus, cynomolgus, and pig-tailed macaques (Fernandez et al., 2009, Gansuvd et al., 2003, Motsinger et al., 2003, Fernandez et al., 2012, Liu et al., 2006) and more recently, human CD1d-α-GalCer tetramers have been used in sooty mangabeys, rhesus macaques and pig-tailed macaques (Rout et al., 2010a, Rout et al., 2012, Yu et al., 2019, Rout et al., 2010b, Li et al., 2012b). Experiments *in*

Figure 5.1. Homology of CD1 molecules between human and macaque species. Protein sequences for *Macacata mulatta, Macaca fascicularis and Macacca nemestrina* were obtained from the National Center for Biotechnology Information protein database and compared to each respective *Homo sapiens* CD1 sequence. The order of each species' sequence is outlined in blue. Red highlighted residues indicate those that differ from the consensus sequence as determined with CLC Main Workbench.

vitro have also confirmed recognition and activation of macaque type I NKT cells by human or murine CD1d-transfected dendritic cells with the addition of α-GalCer (Rout et al., 2010b, Motsinger et al., 2003).

Like in mice, macaque type I NKT cells express a semi-invariant TCR that closely resembles its human counterpart. When testing for cross-reactivity of anti-human mAbs typically used to isolate type I NKT cells, both rhesus and cynomolgus monkey type I NKT cells bound the Vα24 mAb (Gansuvd et al., 2003, Motsinger et al., 2003), suggestive of a conserved epitope. Additionally, rhesus macaques display a conserved epitope for the anti-human mAb 6B11, which is specific for the type I Vα24-Jα18 CDR3α (Gansuvd et al. 2003). Indeed, rhesus macaque type I NKT TCRs incorporate TRAV10 (Vα24) and TRAJ18 into their TCR α-chain (Kashiwase et al., 2003) and their CDR3α sequence is nearly identical to that of human type I NKT cells, with one single amino acid difference (Yu et al., 2019). In contrast, the 6B11 mAb does not bind $V\alpha24^+$ cells derived from PTMs, despite the 98% homology of PTM and human CD1d (Kashiwase et al., 2003). Initially, it was hypothesised that macaque type I NKT cells are not $V\beta11^+$ ($TRBV25^+$) given their inability to bind the anti-human Vβ11 mAb (Gansuvd et al., 2003, Motsinger et al., 2003), however a later study observed a dominant rearrangement of TRBV25 and TRBJ2 among NKT TCRs (Yu et al., 2019). While this is the same TCR β-chain rearrangement observed in humans, there is an amino acid substitution in the CDR2β loop and shorter CDR3β loops (Yu et al., 2019), which may explain the lack of conservation in the Vβ11 mAb binding epitope. Note that the CDR2β loop amino acid substitution was not in the two tyrosines that are key for interacting with CD1d-α-GalCer, but an aliphatic amino acid residue to aromatic (L60F, denoting the human then rhesus macaque residue) (Borg et al., 2007, Yu et al., 2019). These findings illustrate the highly conserved nature of type I NKT cells between macaques and humans. In fact, an alignment of simian primate type I NKT TCR sequences revealed that their CDR1α and CDR3α are highly conserved between seven primate clades (including monkeys, apes and humans), indicative of a "pan-primate" type I NKT TCR rearrangement (Yu et al., 2019).

Given the lack of cross-reactivity with human mAbs targeting the semi-invariant NKT TCR, tetramers are an ideal reagent to identify NHP type I NKT cells without relying on the anti-Vα24 mAb, which may also target $V\alpha24^+$ conventional T cells, or clone 6B11

mAb, which does not work across all NHPs. Nonetheless, the existence of a consistent type I NKT TCR arrangement across primate species implies that we may therefore expect similar patterns of variable gene usage and biases observed in humans among macaque group 1 CD1-restricted T cells, which will be explored in this study. In addition to CD1d conservation and trans-species cross-reactivity, group 1 CD1-restricted T cells also appear to have minimal trans-species reactivity between rhesus macaque CD1b and human GMM-reactive T cell clone, LDN5 (Morita et al., 2008). Macaque-specific tetramers will provide tools to further explore the possibility of using NHPs to study lipid-reactive T cells and evaluate their similarity to humans.

Models of human infectious disease in NHPs have been a valuable tool for investigating pathogenesis, and developing vaccines and therapies against infections such as HIV and TB (Barouch et al., 2002, Sharpe et al., 2017). Due to the high conservation between human and macaque CD1 (*Table 5.1*), PTM were selected as a candidate to study all CD1-restricted T cells. We produced multiple tools to study pigtailed macaque CD1 (ptmCD1) and ptmCD1-restricted T cells, including APC cell lines expressing transmembrane ptmCD1 molecules, soluble ptmCD1 tetramers, and T cell lines expressing ptmCD1-restricted TCRs. Elucidation of the phenotypic and functional characteristics of ptmCD1-restricted T cells will provide insight into how these cells participate in the immune system during health and disease.

5.2. Results

5.2.1 Production of C1R cell lines that express transmembrane ptmCD1 molecules

A suite of APCs that express transmembrane ptmCD1 molecules was produced to provide a tool to explore the interaction between CD1-restricted T cells and CD1 *in vitro* using PTM primary cells or cell lines. DNA constructs encoding transmembrane ptmCD1a, ptmCD1b, ptmCD1c, or ptmCD1d heavy chains were cloned into a pMIG retroviral vector immediately upstream of an IRES-GFP cassette using EcoRI and XhoI restriction enzyme sites as previously described and used for retroviral transduction (Holst et al., 2006).

Active retrovirus was produced by co-transduction of CD1-encoding pMIG vectors with two helper plasmids (pEQ-Pam-E and pVSV-g) into HEK 293T cells. Cells were transduced with 4 μg of pMIG plasmids encoding each of *CD1A, CD1B, CD1C* or *CD1D* to be produced as proteins and paired with endogenous huβ$_2$m. To produce a C1R cell line that expresses all four CD1 molecules, WT cells were also co-transduced with 1 μg of all four pMIG plasmids, and the resulting cell line was termed: ptmCD1abcd$^+$. Retroviral supernatant was harvested every 12 hours and used to transduce C1R cells, an Epstein-Barr Virus transformed HLA-A- and HLA-B-deficient lymphoblastoid line (Storkus et al., 1989, Zemmour et al., 1992). Following four days of transduction, the transduction efficiency was analysed by flow cytometry for GFP expression. The spread of GFP$^+$ cells indicated successful transduction of all C1R cell lines *(Fig.5.2a)*. However, the transduction efficiency appeared lower when compared to huCD1$^+$ C1R cell lines, given that GFP expression was lower in ptmCD1$^+$ C1R cells *(Fig.5.2a)*.

To assess expression of CD1 molecules, transduced C1R cells were labelled with anti-human CD1a, CD1b, CD1c, and CD1d mAbs. Two anti-huCD1a mAb clones were tested to find one that binds a conserved epitope between human and PTM: clone HI149 was cross-reactive while clone SK9 was not (*Fig.5.2b*). Anti-human CD1b and CD1c mAbs bound ptmCD1b and ptmCD1c molecules respectively on the surface of C1R cells. In contrast, neither anti-huCD1d mAbs tested (clones R3G1 and 51.1) bound ptmCD1d while they bound huCD1d (*Fig.5.2b)*, despite the 90% conservation between human and

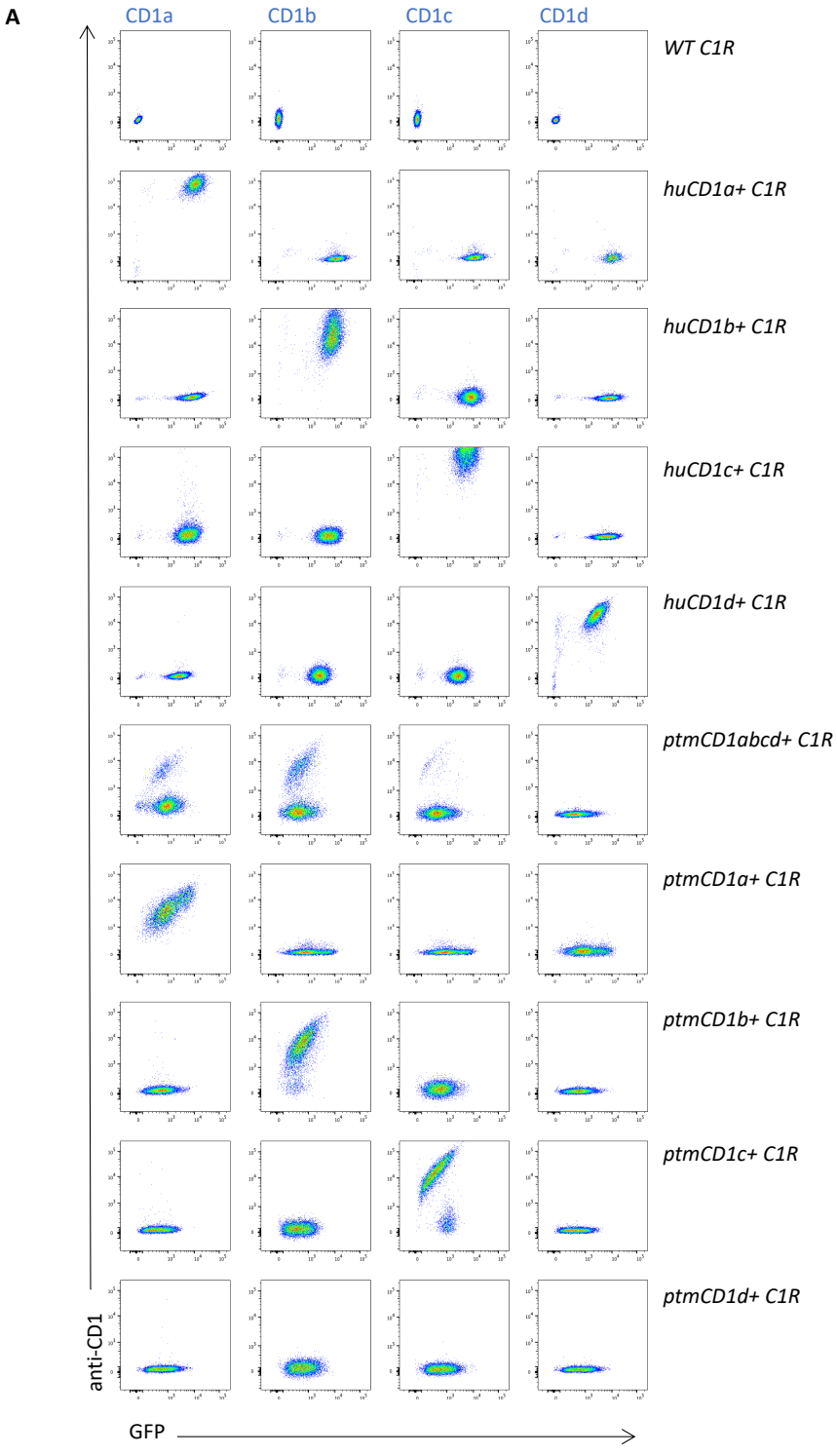
A
CD1a
CD1b
CD1c
CD1d
WT C1R
huCD1a+ C1R
huCD1b+ C1R
huCD1c+ C1R
huCD1d+ C1R
ptmCD1abcd+ C1R
ptmCD1a+ C1R
ptmCD1b+ C1R
ptmCD1c+ C1R
ptmCD1d+ C1R
anti-CD1
GFP

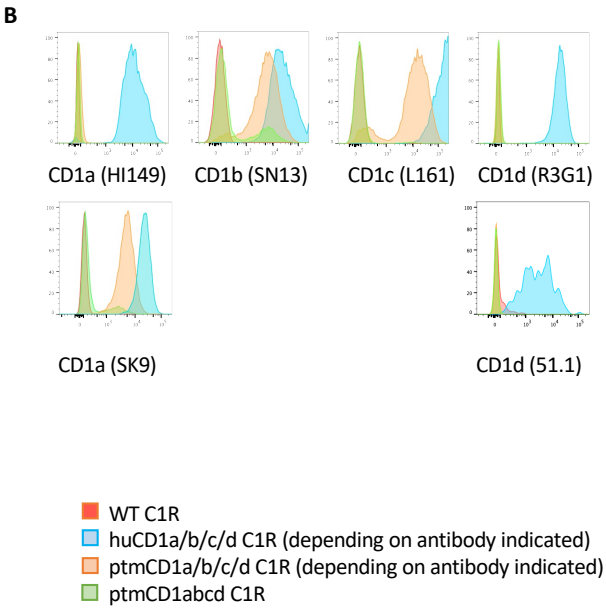

Figure 5.2. Transduction efficiency of C1R cell lines following transduction with ptmCD1-encoding plasmids. A. WT C1R cells were transduced with plasmids encoding macaque or human CD1, or co-transduced with all four macaque CD1 isoforms. Cells were assessed for transduction efficiency using the GFP reporter gene and labelled with anti-human CD1a (clone SK9), CD1b, CD1c and CD1d mAbs as indicated above each column. Data is representative of three independent experiments.

B. Histograms depicting expression of each CD1 molecule to assess transduction efficiency and trans-species interaction of anti-human mAbs with ptmCD1. WT, huCD1a$^+$, pCD1a$^+$, and pCD1abcd$^+$ C1R cells were labelled with anti-human CD1a mAbs (clones HI149 and SK9). WT, huCD1b$^+$, pCD1b$^+$, and pCD1abcd$^+$ C1R cells were labelled with anti-human CD1b mAb (clone SN13). WT, huCD1c$^+$, pCD1c$^+$, and pCD1abcd$^+$ C1R cells were labelled with anti-human CD1c mAb (clone L161). WT, huCD1d$^+$, pCD1d$^+$, and pCD1abcd$^+$ C1R cells were labelled with anti-human CD1d mAb (clones R3G1 and 51.1). All transduced cell lines shown are gated on GFP^{hi} cells, while WT cells were not due to their absence of GFP expression. Data is representative of three independent experiments.

ptm, pig-tailed macaque; hu, human

PTM CD1d. Expression of ptmCD1d in transduced C1R cells was therefore unable to be confirmed by flow cytometry. CD1a, CD1b, and CD1c were expressed by C1R cells and we identified anti-human mAbs that are cross-reactive with group 1 CD1 molecules from PTM.

5.2.2 Production of ptmCD1 molecules for tetramers

Soluble macaque CD1 tetramers were produced for use in studies of CD1-restricted T cells in macaque models. In order to generate tetramers, soluble ptmCD1 molecules were produced in a mammalian HEK-293S-GnTI$^-$ cell expression system identical to that used to produce human CD1 (huCD1) molecules such that they were loaded with endogenous lipids native to this (human) cell line.

GnTI$^-$ cells were co-transfected with a pHL-sec plasmid containing *PTTM CD1A*, *CD1B*, *CD1C,* or *CD1D* genes and another pHL-sec plasmid encoding *β_2m* without cytoplasmic tails*,* as has been previously described (Aricescu et al., 2006). The *CD1A* gene and its associated *β_2m* gene had additional leucine zippers to be consistent with soluble huCD1a molecules produced earlier in this thesis in order to provide strong association between the CD1a heavy chain and β_2m (Birkinshaw et al., 2015). Transfected GnTI$^-$ cells produced soluble heterodimeric CD1/β_2m molecules which were then purified.

Purification of CD1 molecules was achieved by nickel-agarose chromatography. The CD1 proteins contained a carboxy-terminal BirA 6 x histidine tag (Birkinshaw et al., 2015), which bound to a nickel-agarose column, allowing separation from contaminants. As per human CD1a, bound CD1 molecules were subsequently eluted from the column with an increasing concentration of imidazole (not shown). Collected protein was pooled and then passed over S200 gel filtration column for further purification (*Fig.5.3 left)* and assessed for purity by 12% SDS-PAGE (*Fig.5.3 right)*. SDS-PAGE analysis of CD1a, CD1b, and CD1c revealed multiple bands of ~37 kDa, which correspond to differentially glycosylated CD1 proteins (*Fig.5.3 right)*. CD1a revealed four bands, CD1b revealed two bands, while CD1c revealed four as well as the presence of a dimer between 80-90 kDa (*Fig.5.3 right)*. This was analogous to human CD1 proteins produced in the same expression system which form four, two and three differentially glycosylated products

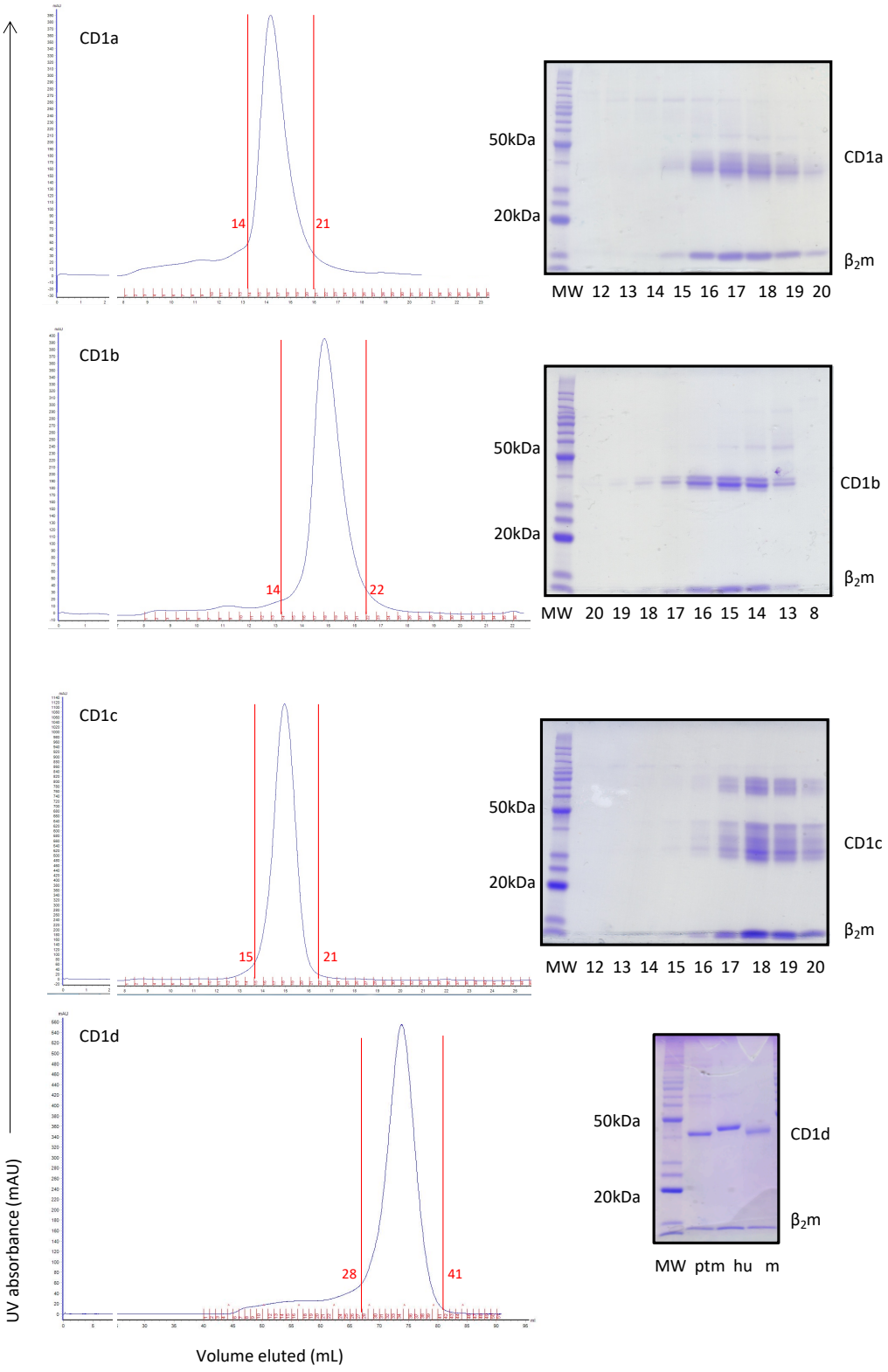
CD1a
14
21
50kDa
20kDa
CD1a
β2m
MW 12 13 14 15 16 17 18 19 20
CD1b
14
22
50kDa
20kDa
CD1b
β2m
MW 20 19 18 17 16 15 14 13 8
CD1c
15
21
50kDa
20kDa
CD1c
β2m
MW 12 13 14 15 16 17 18 19 20
CD1d
28
41
50kDa
20kDa
CD1d
β2m
MW ptm hu m
UV absorbance (mAU)
Volume eluted (mL)

Figure 5.3. Macaque CD1 purification using Ni-NTA chromatography followed by gel filtration/size exclusion chromatography. A. Chromatograms obtained from the final purification step of each macaque CD1 protein using a nickel-nitriloacetic acid agarose (Ni-NTA) and Superdex 200 pg gel filtration/size exclusion chromatography, representing absorbance during the elution off the column. Eluted fractions were assessed by 10% SDS-PAGE (right). **B.** Comparison of macaque (ptm), human (hu) and mouse (m) CD1d produced in the GnTI$^-$ expression system. Data representative of three independent expression experiments.

ptm, pig-tailed macaque; hu, human; m, mouse; SAV, streptavidin; MW, molecular weight marker; kDa, kilodaltons

respectively (data presented as part of Catriona Nguyen-Robertson's Honours Thesis, submitted to The University of Melbourne in 2015). CD1c was further purified using MonoQ chromatography and subsequent ELISA and flow cytometry analyses confirmed the presence of CD1c in the correct conformation (see Sections 6.2.3 and 6.2.4). CD1a protein and its associated β_2m had a marginally larger molecular weight compared to the other CD1 and β_2m molecules as they both contained an additional leucine zipper (*Fig.5.3 right)*. PtmCD1d was produced separately, purified and assessed by SDS-PAGE. The heavy chain of CD1d only revealed one band, indicating that in contrast to the group 1 CD1 molecules, the CD1d molecules had uniform glycosylation. It was comparable in size to huCD1d and mCD1d, both between 37-39 kDa (*Fig.5.3 right)*.

The CD1-containing fractions were pooled and biotinylated overnight with BirA. Biotinylated CD1 monomers were separated from free biotin using a S75 gel filtration column (*Fig.5.4a*). The peaks corresponding to the elution of each biotinylated CD1 isoform were observed at a volume of approximately 80 mL (*Fig.5.4a*). A second peak was observed at approximately 100 mL, corresponding to the elution of excess biotinylation biomix reagents (*Fig.5.4a*). Fractions 30-42, 37-47, 38-48 and 34-42 were collected for CD1a, CD1b, CD1c, and CD1d respectively, corresponding to the first major peak of the chromatograms (*Fig.5.4a*).

Biotinylation efficiency was determined by running tetramerised CD1 on an 12% SDS-PAGE gel *(Fig.5.4b)*. In brief, streptavidin was added at a 4:1 molecular weight ratio to heat-denatured monomeric huCD1 and ptmCD1, which were subsequently assessed for the ability to form tetrameric complexes by observing a shift in their molecular weight. The presence of monomer at around 37 kDa was observed in lanes containing CD1 protein alone. CD1a, CD1b, CD1c, and CD1d proteins were successfully tetramerised as indicated by the absence of a monomer band on SDS-PAGE and the formation of a larger-sized complex when streptavidin was added *(Fig.5.4b)*.

5.2.3 Analysis of the soluble ptmCD1 molecules by ELISA

The conformational integrity of the soluble ptmCD1 molecules produced was tested by reactivity towards anti-huCD1 antibodies. Anti-huCD1a (SK9), anti-huCD1b (SN13) and anti-huCD1c (L161) mAbs bind to a conserved conformational epitope on their respective

B

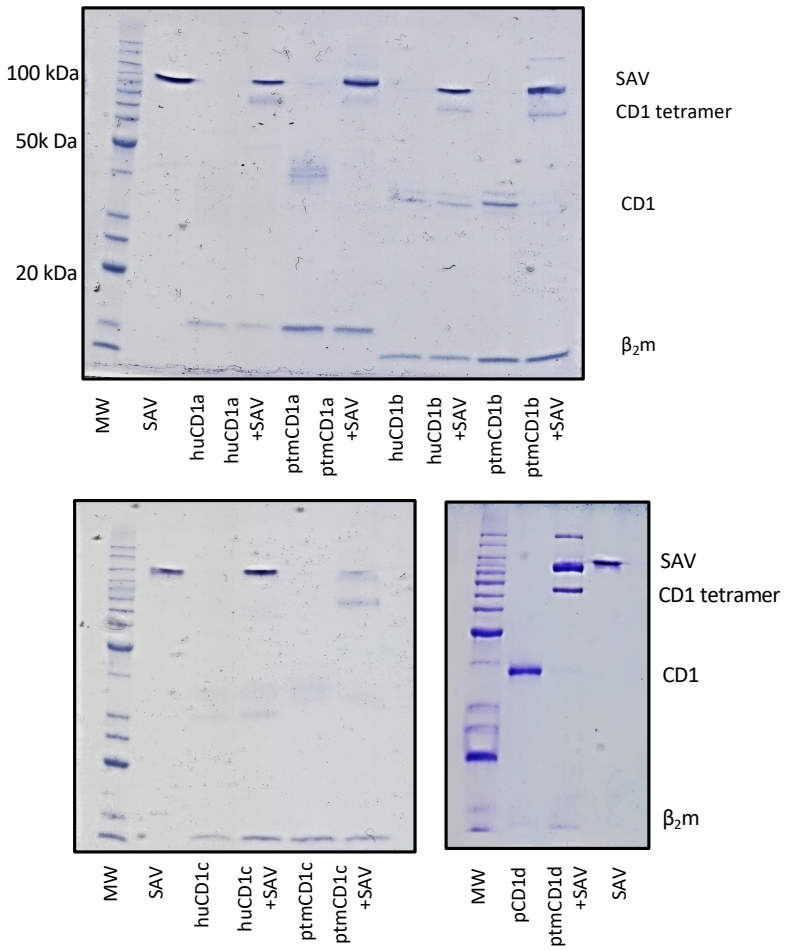

Figure 5.4. Biotinylation of ptmCD1 followed by gel filtration/size exclusion chromatography purification. A. Chromatograms obtained from the final purification step of each macaque CD1 protein following overnight biotinylation with BirA using Superdex 200 gel filtration/size exclusion chromatography, representing absorbance during the elution off the column. Fractions containing biotinylated macaque CD1 protein were pooled and concentrated. **B.** Biotinylation efficiency was tested by tetramerising monomeric CD1 molecules. 2 µg of each CD1 protein was denatured at 95°C , allowed to cool, and then incubated with streptavidin at a 1:1 weight ratio. Samples were assessed by 10% SDS-PAGE. Data representative of three independent expression experiments.

ptm, pig-tailed macaque; hu, human; SAV, streptavidin; MW, molecular weight marker; kDa, kilodaltons

CD1 molecules *(Fig 5.2)*. As an anti-huCD1d mAb has not yet been identified to cross-react with ptmCD1d, only group 1 CD1 molecules were assessed by ELISA. HuCD1d and ptmCD1d were used as negative controls for each antibody to confirm that results were CD1 isoform specific.

Wells were coated with decreasing concentrations of soluble human or macaque CD1 protein by performing a serial dilution starting at 2 mg/mL and incubated overnight. Wells were then incubated with the same concentration of their corresponding antibody: huCD1a and ptmCD1a were labelled with anti-huCD1a, huCD1b and ptmCD1b were labelled with anti-huCD1b, and huCD1c and ptmCD1c were labelled with anti-huCD1c *(Fig.5.5)*. PtmCD1a bound the anti-huCD1a mAb at levels comparable to huCD1a *(Fig.5.5a)*. Surprisingly, ptmCD1b consistently bound the anti-huCD1b mAb to a greater degree than huCD1b across the serial dilution *(Fig.5.5b)*. Similarly, ptmCD1c bound the anti-huCD1c mAb at levels slightly below those of huCD1c at most concentrations, but well above those of the negative control anti-huCD1d mAb *(Fig.5.5c)*. These results suggest that the soluble group 1 ptmCD1 molecules produced in the mammalian expression system have intact antibody-binding epitopes and thus, their correct conformational shape.

5.2.4 Assessment of trans-species cross-reactivity between ptmCD1 molecules and huCD1-restricted TCRs

Once confirmed by ELISA to be in the correct conformational shape, biotinylated CD1 monomers were tetramerised and used to label established SKW-3 cell lines expressing human CD1a-, CD1b-, CD1c, and CD1d-restricted TCRs to both evaluate human-macaque cross-reactivity and confirm the reactivity of these tetramers towards CD1-restricted TCRs. To ensure a comparison of only TCR-expressing cells, and to compare similar TCR levels between cells, only GFP^{hi} cells were included in the analyses as GFP was a reporter of TCR transduction efficiency.

The ability of huCD1a-restricted TCRs to bind ptmCD1a was first assessed. Seven huCD1a-restricted T cell lines: 8-2a2, 17a28, 27a28, 29a28i, 29a28ii, 35a16 and CNR1, were assessed for their ability to bind huCD1a-endo, huCD1a-DDM, ptmCD1a-endo, and ptmCD1a-DDM tetramers (*Fig.5.6)*. The CD1b-restricted 'Fee1' cell line was used as a

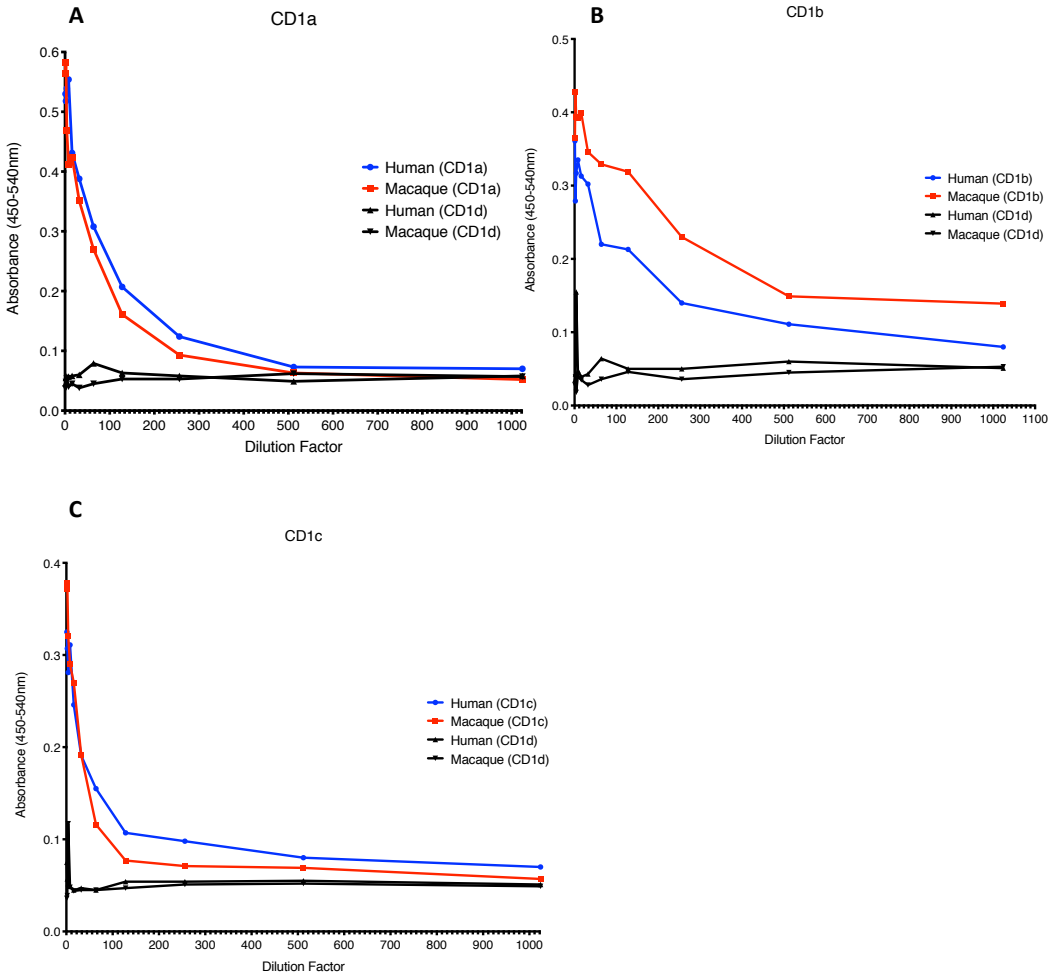

Figure 5.5. ELISA of soluble macaque CD1 proteins. Plates were coated with a decreasing concentration of **A.** human or macaque CD1a, **B.** human or macaque CD1b, or **C.** human or macaque CD1c using 2-fold serial dilutions starting at 10 µg/mL such that 11 concentrations were measured in addition to a control without protein. Samples were subsequently labelled with their respective anti-human mAb, or an anti-human CD1d mAb as a negative control (black). Bound antibody was visualised using a secondary goat anti-mouse IgG mAb conjugated to horse-radish peroxidase and tetramethylbenzidine. Absorbance at 540 nm was subtracted from absorbance at 450 nm. Data representative of three experiments.

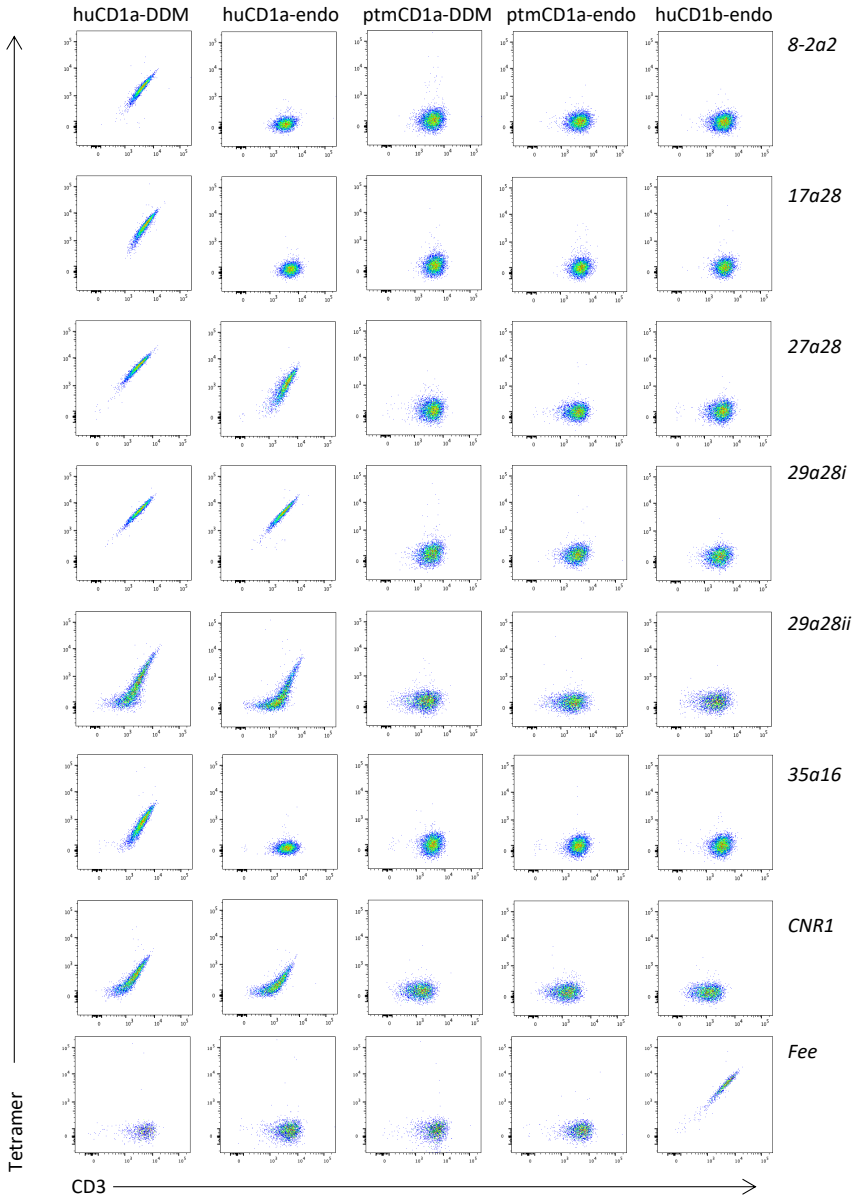

Figure 5.6. Testing trans-species cross reactivity of macaque CD1a with human CD1a-restricted T cells. CD1a-restricted TCR SKW-3 $\beta_2m^{-/-}$ cell lines were labelled with a panel of tetramers: human CD1a loaded with DDM (huCD1a-DDM), or with endogenous lipids (huCD1a-endo), macaque CD1a loaded with DDM (ptmCD1a-DDM) or endogenous lipids (ptmCD1a-endo), and human CD1b with endogenous lipids (huCD1b-endo). The CD1b-restricted Fee1 T cell clone was used as a negative control. Samples were gated on GFP^{hi} cells to ensure transduction efficiency levels were comparable. Data are representative of three independent experiments.

negative control to account for the possibility of non-specific binding of tetramers. HuCD1a-restricted TCRs bound huCD1a tetramers following the same patterns of antigen specificity observed previously. However, they bound neither ptmCD1a tetramers loaded with endogenous lipids nor DDM (whether they were CD1a-autoreactive, DDM-specific or broadly CD1a-reactive) (*Fig.5.6),* consistent with a previous study investigating trans-species activation of clone CD8-2 with rhmCD1a (Morita et al., 2008). As a positive control for huCD1a tetramers, 8-2a2, 17a28 and 35a16 bound huCD1a-DDM, and 27a28, 29a28i, 29a28ii and CNR1 bound both huCD1a-DDM and huCD1a-endo (*Fig.5.6)*.

Five huCD1b-restricted T cell lines: Fee1, LDN5, and TCR 4.17, TCR 4.27 and TCR 4.41 (provided by Dr Michael Souter, The University of Melbourne), were assessed for their ability to bind huCD1b-endo, huCD1b-GMM, ptmCD1b-endo, and ptmCD1b-GMM tetramers (*Fig.5.7)*. CD1a-restricted TCR 17a28 acted as a negative control and did not bind any tetramer. The GMM-specific T cell clone LDN5 bound both huCD1b-GMM and ptmCD1b-GMM (*Fig.5.7a),* consistent with trans-species activation seen by Morita et al. with this cell line (Morita et al., 2008). Two CD1b-autoreactive T cell clones, TCR 4.17 and TCR 4.41, only bound huCD1b tetramer loaded with either endogenous self-lipids or GMM and neither ptmCD1b tetramer (*Fig.5.7a)*. The other two CD1b-autoreactive T cell clones, Fee1 TCR and TCR 4.27, bound both human and macaque CD1b regardless of which lipid antigen was present (*Fig.5.7a)*. This suggests that the docking of these TCRs is slightly different to 4.17 and 4.41 such that they are interacting with different parts of the CD1b molecules, in that Fee1 TCR and TCR 4.27 may bind a region that is conserved between macaque and human CD1b. Positive tetramer staining was observed for all tetramers on the TCR 4.27 cell line, but it did not bind ptmCD1a-endo tetramer, confirming its specificity for CD1b *(Fig.5.7b)*. This is the first instance where human CD1b-restricted T cells have been shown to bind macaque CD1b without the addition of GMM, albeit with lower tetramer MFI with ptmCD1b tetramers compared to huCD1b, suggestive of lower binding affinity.

Three huCD1c-restricted T cell lines: 1C4, 1C9 and 3C4 (provided by Dr Adam Uldrich, The University of Melbourne) were assessed for their ability to bind huCD1c-endo and ptmCD1c-endo tetramers (*Fig.5.8)*. 1C9 and 3C4 bound ptmCD1c tetramer in a TCR-dependent manner, as indicated by the correlation between CD3 expression and tetramer

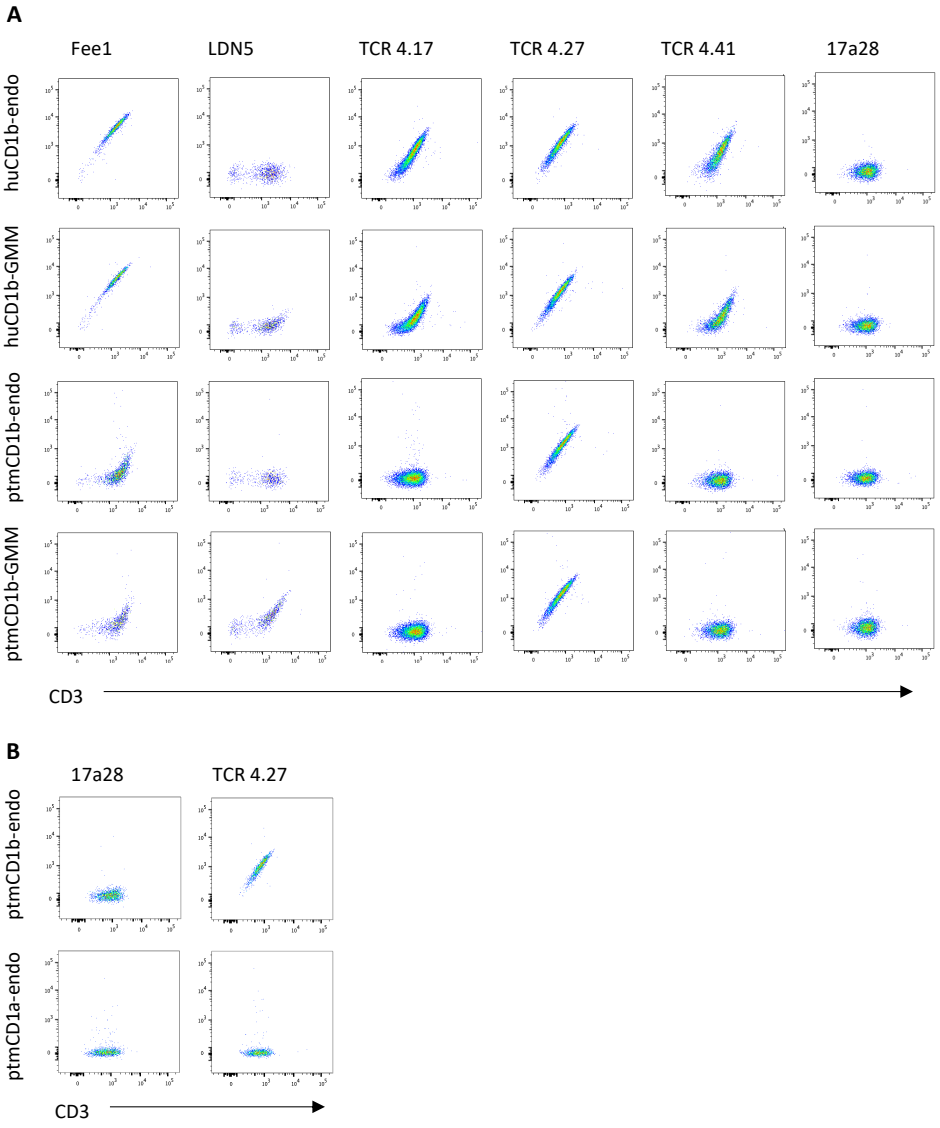

Figure 5.7. Testing trans-species cross reactivity of macaque CD1b with human CD1b-restricted T cells. A. Human CD1b-restricted TCR SKW-3 cell lines, Fee1, LDN5, TCR 4.17, TCR 4.27 and TCR 4.41, were labelled with a panel of tetramers: human CD1b loaded with GMM (huCD1b-GMM) or endogenous lipids (huCD1b-GMM), or macaque CD1b loaded with GMM (ptmCD1b-GMM) or endogenous lipids (ptmCD1b-endo). **B.** TCR 4.27 and CD1a-restricted T cell line 17a28 were labelled with ptmCD1b-endo and ptmCD1a-endo tetramers. All samples were gated on GFP^{hi} cells to ensure transduction efficiency levels were comparable. Data are representative of three independent experiments.

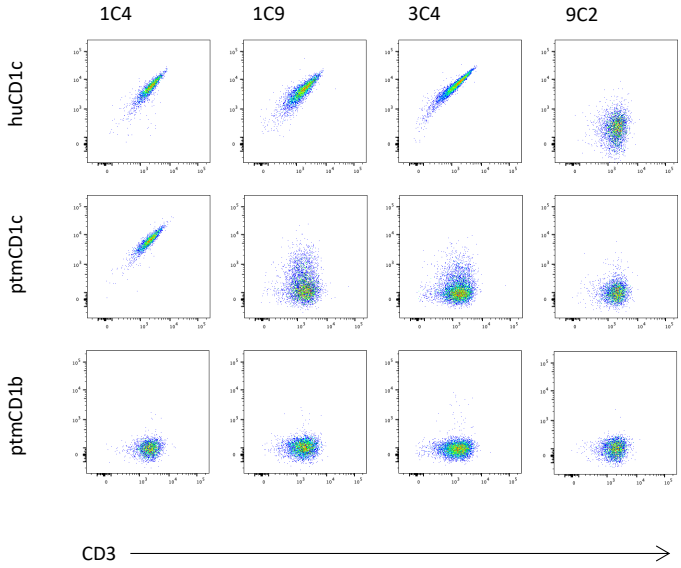

Figure 5.8. Testing trans-species cross reactivity of macaque CD1c with human CD1c-restricted T cells. Human CD1c-restricted TCR J.76 cell lines, 1C4, 1C9 and 3C4, were labelled with either human CD1c loaded with endogenous lipids (huCD1c) or macaque CD1c loaded with endogenous lipids (ptmCD1c) tetramers. Samples were gated on GFP^{hi} cells to ensure transduction efficiency levels were comparable. Data are representative of three independent experiments.

binding. The CD1d-restricted T cell line 9C2 was used as a negative control and did not bind either CD1c tetramer. Interestingly, TCR clone 1C4 bound both human and macaque CD1c tetramers (*Fig.5.8),* so while not interchangeable with huCD1c, ptmCD1c exhibits some cross-reactivity for at least one TCR. This suggests that these TCRs also may bind different regions of the CD1c molecule and that 1C4 binds a conserved region, given that huCD1c and ptmCD1c are 91% homologous. These cell lines all express a γδ-TCR and therefore may dock in an unconventional manner onto CD1c-lipid complexes. This is the first instance where trans-species cross-reactivity has been observed between macaque CD1c and huCD1c-restricted T cells, as it was not observed in a previous study with clone CD8-1 (Morita et al., 2008).

The human type I NKT TCR cell line NKT15 was assessed for its ability to bind mouse, PTM, and human CD1d tetramers (*Fig.5.9a)*. As expected, it bound all three CD1d variants loaded with PBS44 (α-GalCer) but not CD1d loaded with endogenous lipids (*Fig.5.9a),* consistent with previous observations of human and PTM NKT cross-reactivity (Li et al., 2012b). Four NKT cell lines with different specificities were subsequently assessed for their ability to bind human and macaque CD1d tetramers: NKT15 (type I), TRAV-26A (atypical), TRAV-26B (atypical), and Vδ3 (type II) (provided by Dr Catarina Almeida, The University of Melbourne) (*Fig.5.9b)*. Interestingly, while the typical type I NKT cells bound ptmCD1d-α-GalCer, TRAV-26A and TRAV-26B did not, despite their positive staining with huCD1d-α-GalCer (*Fig.5.9b),* potentially due to different mechanisms of TCR docking onto CD1d-α-GalCer (Le Nours et al., 2016). No huCD1d-restricted T cell line bound ptmCD1d loaded with endogenous lipids, thus requiring the presence of α-GalCer to be cross-reactive (*Fig.5.9b)*. These results indicate a lack of trans-species reactivity between macaque CD1d and human atypical NKT cell lines, highlighting the need to use ptmCD1d molecules when studying atypical or type II NKT cells in this particular animal model.

Taken together, these data demonstrate that soluble ptmCD1 molecules were successfully produced for the study of group 1 and group 2 CD1-restricted T cells in macaques, which will be vital for understanding their role in macaque models of human diseases.

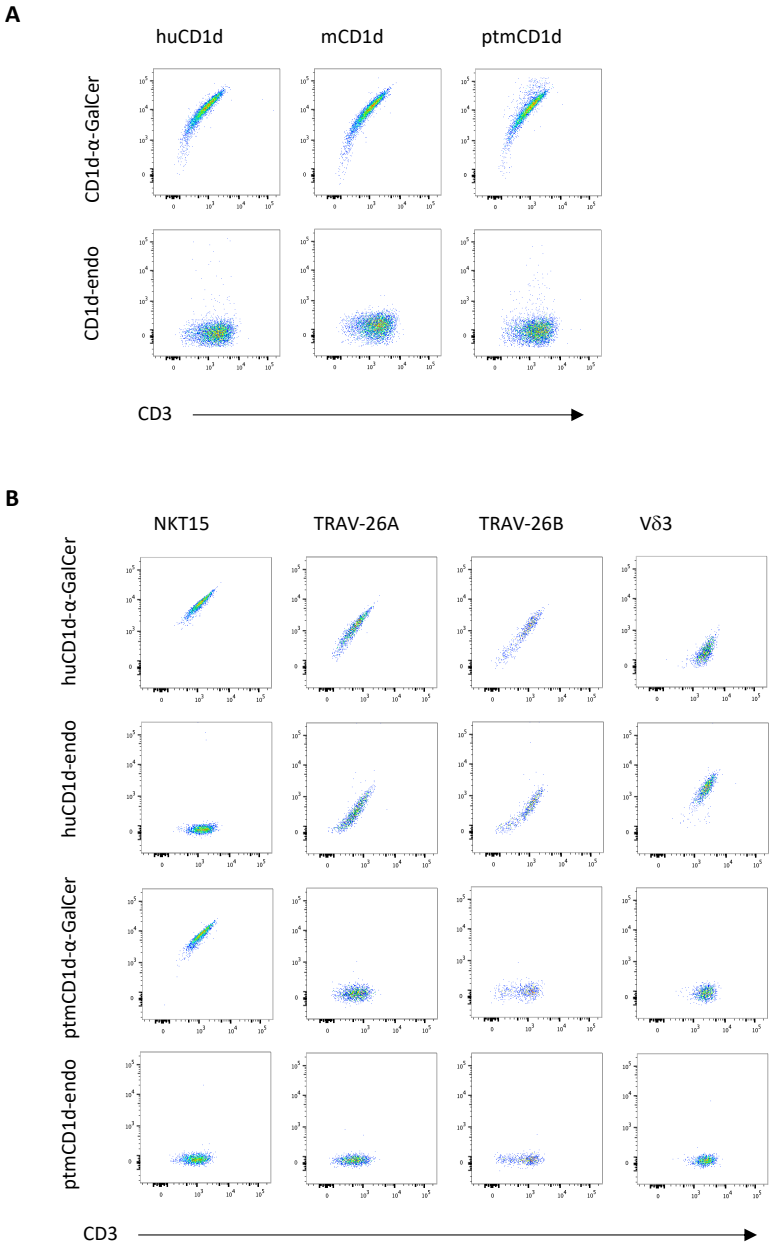

Figure 5.9. Testing trans-species cross reactivity of macaque CD1d with human CD1d-restricted T cells. A. Human type I NKT TCR J.76 cell line NKT15 was labelled with human CD1d (huCD1d), mouse CD1d (mCD1d), or macaque CD1d (ptmCD1d) loaded either with α-GalCer (PBS44) or endogenous lipids. **B.** Human CD1d-restricted TCR J.76 cell lines: NKT15 (type I NKT), TRAV-26A, TRAV-26B and Vδ3, were labelled with human or macaque CD1d tetramers loaded with α-GalCer (PBS44) or endogenous lipids. Samples were gated on GFP^{hi} cells to ensure transduction efficiency levels were comparable. Data are representative of three independent experiments.

5.2.5 Isolation of human and macaque CD1-reactive T cells with ptmCD1 tetramers

Validated ptmCD1 tetramers were used to isolate ptmCD1-reactive T cells in human PBMCs (huPBMCs) due to their greater availability over PTM samples for optimisation of tetramer labelling. HuPBMCs were labelled with human and PTM group 1 CD1 tetramers loaded with endogenous lipids and produced similar staining profiles for CD1a (*Fig.5.10a)*. Surprisingly, ptmCD1b tetramers bound a greater number of both $CD3^+$ and $CD3^-$ cells compared to the huCD1b tetramer, producing a similar staining pattern to huCD1c and ptmCD1c tetramer staining (*Fig.5.10a)*. HuCD1c, ptmCD1b and ptmCD1c tetramers revealed high $tetramer^+$ cell frequencies and $CD3^-$ $tetramer^+$ staining, which is suggestive of TCR-independent tetramer binding (*Fig.5.10a)*. HuCD1c, huCD1d, and to a lesser extent, huCD1b molecules are known to bind other molecules on cells, including NK cell receptors, and (immunoglobulin-like transcript) ILT-2 and ILT-4 on monocytes (Carbone et al., 2000, Li et al., 2012a, Li et al., 2009), and this phenomenon may be also seen in macaques. As ILT-4 is exclusively expressed on APCs and not T cells, there may be other ligands expressed on subsets of T cells that bind CD1 tetramers.

CD36 family members CD36, scavenger receptor class B type 1 (SR-B1) and lysosomal integral membrane protein-2 (LIMP-2) have recently been identified as ligands for huCD1 proteins CD1b, CD1c and CD1d but not CD1a (Gherardin et al., 2021). These ligands are responsible for non-TCR-mediated tetramer binding that confound tetramer staining analyses of CD1b-, CD1c- and CD1d-restricted T cells (Gherardin et al., 2021). As human platelets express high levels of CD36 and can contaminate lymphocytes during PBMC preparation (Gherardin et al., 2021, Hui et al., 2015, McFarland et al., 2006), it was possible that platelets were contributing to non-TCR-mediated labelling with ptmCD1b and ptmCD1c tetramers. HuPBMCs were co-stained with ptmCD1a, ptmCD1b, or ptmCD1c tetramers and a mAb targeting platelet receptor CD42b to determine whether $tetramer^+$ cells were indeed platelets. Many cells positive for huCD1c, ptmCD1c and ptmCD1b tetramers were also positive for CD42b, whereas both huCD1a and ptmCD1a $tetramer^+$ cells were $CD42b^-$ (*Fig.5.10b).* The exclusion of $CD42b^+$ $tetramer^+$ cells that bind tetramer independently of a TCR is explored further in Section 5.2.6.

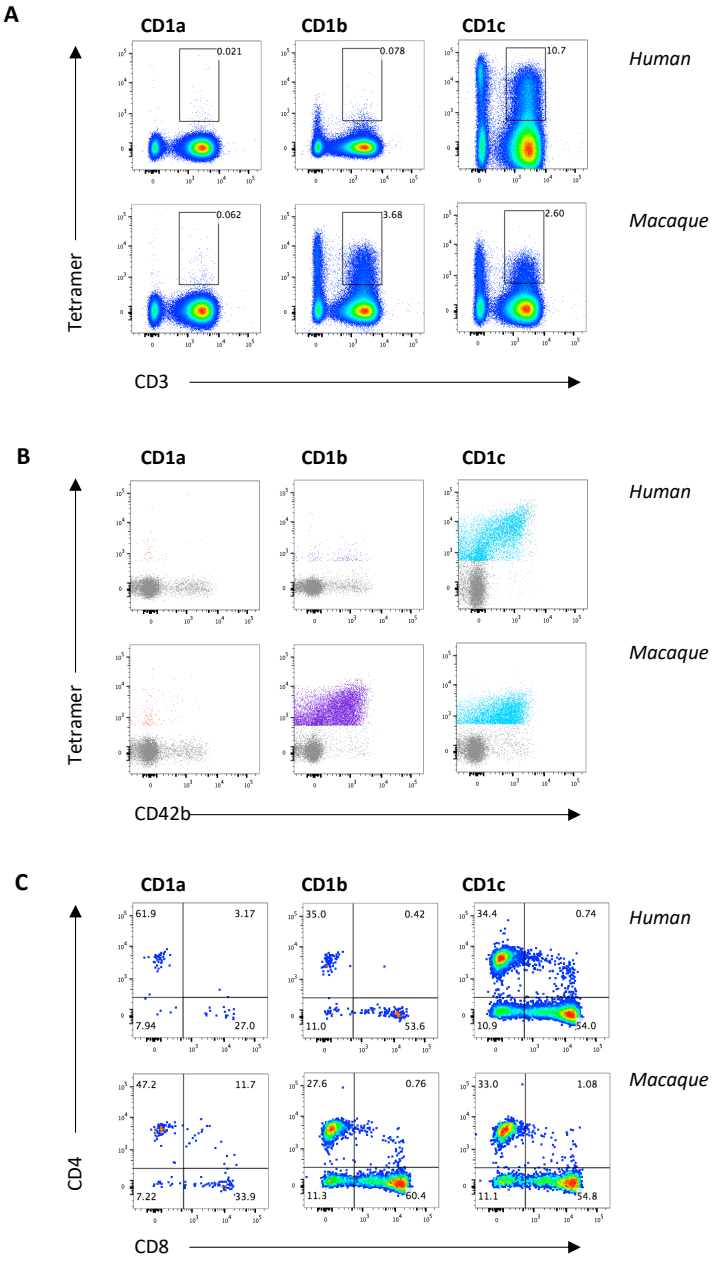

Figure 5.10. Isolation of group 1 CD1-restricted T cell populations directly *ex vivo* from healthy human blood using macaque or human CD1 tetramers. A. Human and macaque CD1-endo tetramer staining of human T cells (CD1a, CD1b, and CD1c as indicated). **B.** Correlation between CD42b and tetramer labelling among tetramer$^+$ cells (coloured) and all T cells (grey). **C.** CD4 and CD8 co-receptor expression profile of tetramer$^+$ cells. Data reflective of six donors across two independent experiments.

Nonetheless, a preliminary analysis of CD4 and CD8 co-receptor expression among tetramer$^+$ cells revealed a greater proportion of CD8$^+$ ptmCD1a tetramer$^+$ cells while, in keeping with our previous findings, huCD1a-tetramer$^+$ cells were predominantly CD4$^+$ (*Fig.5.10c)*. The percentage of DN cells were consistent between huCD1a and ptmCD1a tetramer$^+$ cells, indicating a clear shift from CD4 expression to CD8 with the ptmCD1a tetramer (*Fig.5.10c)*, raising the question of whether ptmCD1a may bind CD8 or does not interact with CD4 in the same way as huCD1a. Conversely, ptmCD1b and ptmCD1c tetramer$^+$ cells revealed similar CD4 and CD8 expression profiles to their human tetramer$^+$ counterparts (*Fig.5.10c)*, which may be an effect of the same T cells being captured due to trans-species cross-reactivity and/or contaminating cells binding both tetramers independently of their TCR.

Having shown that the ptmCD1 tetramers could successfully label human T cells, they were used to stain ptmPBMCs. Populations of CD1-autoreactive T cells were discerned from peripheral blood as CD3$^+$ cells with the ability to bind to CD1 tetramers presenting endogenous lipids (*Fig.5.11)*. Interestingly, compared to huPBMC samples *(Fig.5.10)*, tetramer$^+$ cell frequencies and tetramer staining of the CD3$^-$ population were reduced, indicative of a reduction of TCR-independent tetramer binding. This may be due to variation in the receptor(s) that bind these tetramers, or variation in expression levels between the two species. Samples labelled with CD1a and CD1d tetramers exhibited low background staining of CD3$^-$ cells, while CD1b and CD1c tetramer staining resulted in a larger population of tetramer$^+$ cells, especially in donor BABA, similar to staining profiles seen in human samples (*Fig.5.11)*. Optimisation of tetramer staining was therefore neededd to ensure that only cells that bound CD1 molecules in a TCR-dependent manner were isolated.

5.2.6 Optimisation of tetramer labelling by minimising TCR-independent binding

To assess the specificity of CD1 binding to human and PTM T cells, a dual tetramer stain was performed in which PBMCs were stained with a combination of ptmCD1 tetramers (i.e. CD1a with CD1b, CD1c or CD1d, etc.). To account for variability in fluorophore brightness, each combination was performed twice, alternating which tetramer was conjugated to PE and BV421. Donor GC2 (human) revealed a population of double positive cells when labelled with ptmCD1b and ptmCD1c tetramers, and to a lesser

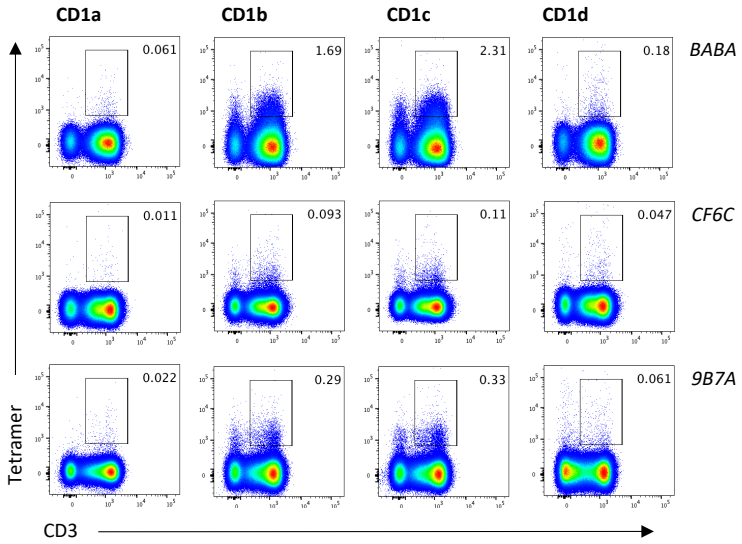

Figure 5.11. Isolation of CD1-restricted T cell populations directly *ex vivo* from healthy macaque blood using ptmCD1 tetramers. Macaque PBMCs were labelled with ptmCD1a, ptmCD1b, ptmCD1c, or ptmCD1 (all endo) tetramers as indicated. Cells are gated on $CD3^+$ $CD20^-$ 7-AAD^- single lymphocytes. Data reflective of nine donors across three independent experiments.

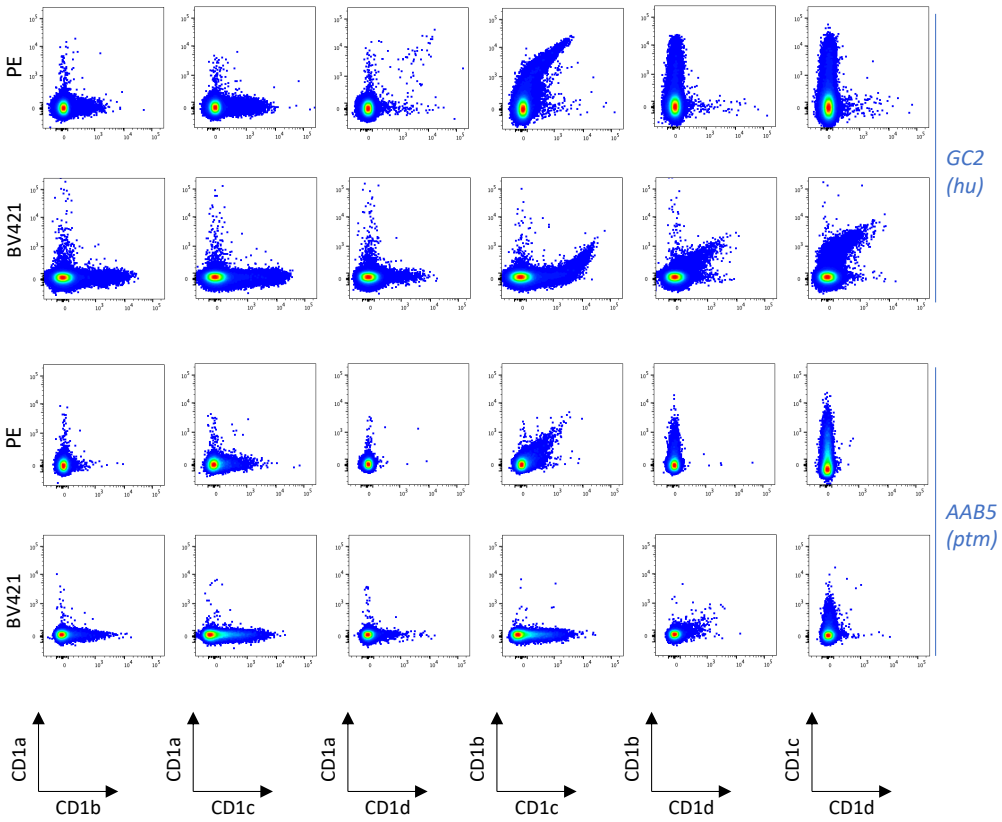

Figure 5.12. Dual tetramer stain of human or macaque blood using ptmCD1 tetramers. $CD20^-$ $CD3^+$ T cells from macaque (ptm) and $CD14^-$ $CD19^-$ $CD3^+$ T cells from human (hu) donors were labelled with a combination of ptmCD1a, ptmCD1b, ptmCD1c or ptmCD1d tetramers simultaneously, conjugated to either BV421 or PE fluorophores. Each combination was repeated such that both tetramers were tested with boh BV421 and OPE fluorophores. Data representative of four donors across two independent experiments.

extent, ptmCD1d with either ptmCD1b or ptmCD1c tetramers *(Fig.5.12)*. This was consistent with both these tetramers co-labelling CD42b in previous analyses, suggesting that they may bind the same cells by engaging with a receptor in a TCR-independent manner. A similar trend was seen in ptmPBMCs, for which samples including CD1b and CD1c tetramers revealed a population of double positive cells, and again only slightly for CD1d in combination with either. Because TCRs are not expected to bind two different CD1 restriction elements, the labelling of the same population of cells with two different CD1 tetramers suggests that the molecule responsible for TCR-independent binding interacts with CD1b, CD1c and CD1d (to a lesser extent), but not CD1a. There were, however, $CD3^+$ cells that were single positive for either tetramer, that indicate that the tetramers can also bind genuine CD1-restricted T cells by gating out DP cells.

Given that CD36 family members bind huCD1b, huCD1c and huCD1d, use of an anti-huCD36 mAb can block TCR-independent tetramer staining (Gherardin et al., 2021). Here, a similar blocking step with an anti-huCD36 mAb prior to incubating ptmPBMCs with tetramer was attempted to ascertain whether this would also optimise tetramer staining in PTMs based on the method previously described (*Fig.5.13)* (Gherardin et al., 2021). Briefly, samples were incubated with 3 μg/mL anti-CD36 for 15 minutes at RT, after which tetramers were added directly to samples for a further 30-minute incubation.

$Tetramer^+$ populations were reduced in huPBMC samples labelled with ptmCD1b and ptmCD1c tetramers with the anti-huCD36 block as seen previously (Gherardin et al., 2021). CD1b-$tetramer^+$ populations were reduced with the blocking antibody from 1.37% of the parental population to 0.05%, and 2.46% to 0.05% for human donors 3F and 5A respectively (*Fig.5.13)*. Similarly, CD1c-$tetramer^+$ populations were also reduced from 1.17% of the parental population to 0.05%, and 1.23% to 0.03% for human donors 3F and 5A respectively (*Fig.5.13)*. As expected, CD36 blocking had little impact on ptmCD1a tetramer staining as CD1a tetramers are not subject to this issue (Gherardin et al., 2021) (*Fig.5.10-5.13*), nor did blocking affect ptmCD1d tetramer staining, suggesting that ptmCD1d may not be a ligand for CD36 family members *(Fig.5.13)*.

Notably, the same anti-huCD36 mAb that blocked TCR-independent binding of ptmCD1b and ptmCD1c tetramers in human samples did not block TCR-independent

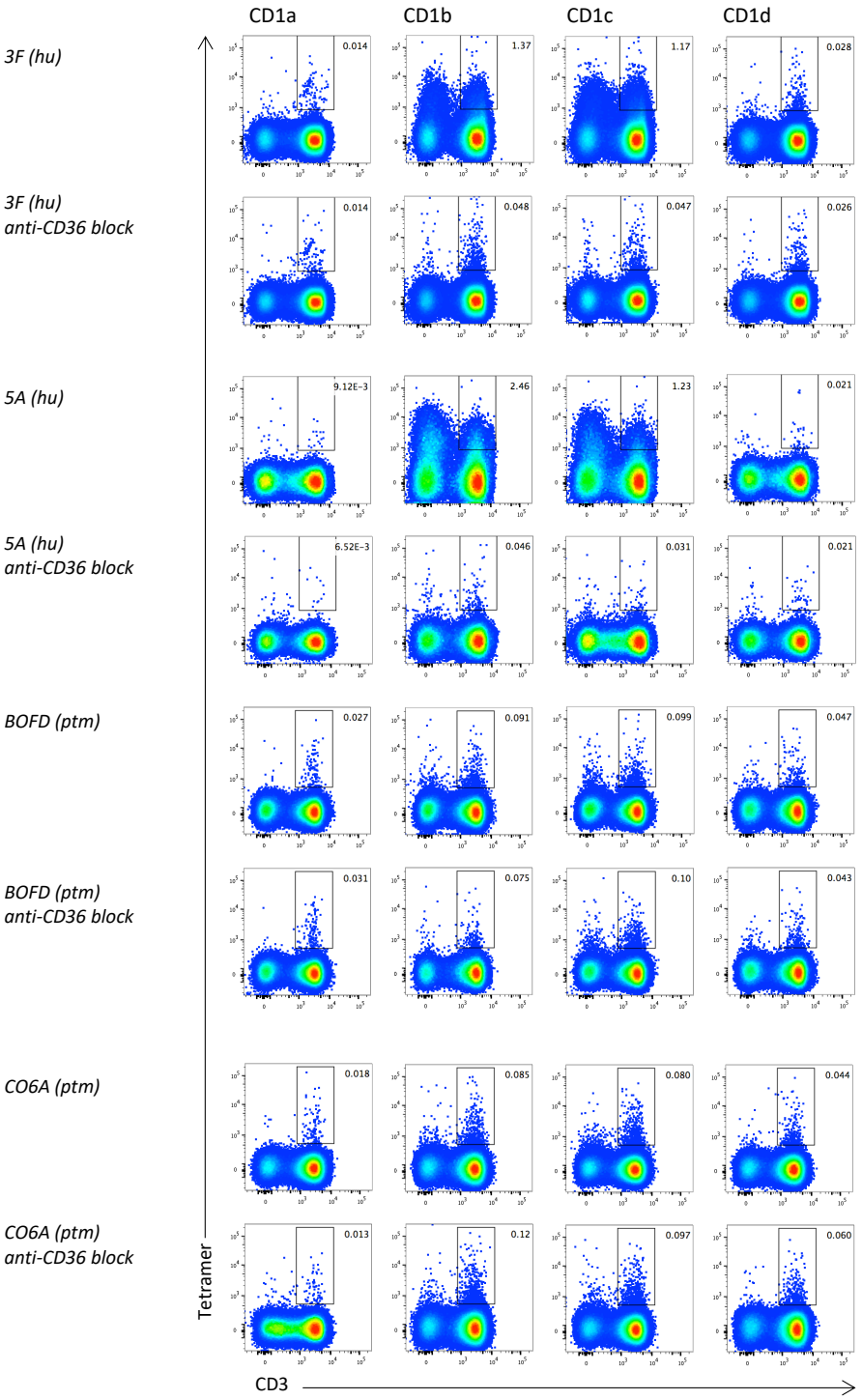

Figure 5.13. Tetramer stain of human or macaque blood using ptmCD1 tetramers with an anti-CD36 blocking antibody. PBMCs from human (hu) donors and macaque (ptm) were incubated with an (anti-human) anti-CD36 antibody for 15 minutes prior to incubation with ptmCD1 tetramers. Data representative of 10 donors (4 human and 6 macaque) across 3 independent experiments.

binding in macaque samples *(Fig.5.13)*. All four tetramers produced similar staining patterns with and without the addition of the anti-huCD36 mAb, and a similar percentage of cells were positive for tetramer, ranging from 0.01-0.1% of the parental population *(Fig.5.13)*. This suggests that the anti-huCD36 mAb may not be cross-reactive with ptmCD36 and a different method is required for blocking TCR-independent staining.

Given that an anti-huCD36 mAb reduced TCR-independent binding in huPBMCs but not ptmPBMCs, alternative platelet markers that may contribute to TCR-independent binding and could be targeted with a blocking antibody were assessed. CD36 and SCARB1 (CD36L1) were both tested, both of which are capable of binding lipids (reviewed in (Kaczmarek et al., 2017)), and other platelet markers CD42b, CD62p and CD61. PtmPBMCs from four donors were labelled with ptmCD1c tetramer and co-stained with one of anti-human CD36, CD42b, CD61, CD62p, and SCARB1 mAbs to determine whether these antibodies are cross-reactive between human and PTM cells, and in particular, whether ptmCD1c-tetramer$^+$ cells were positive for any of these markers.

Consistent with TCR-independent binding, samples labelled with anti-CD36 and anti-SCARB1 mAbs revealed many ptmCD1c-tetramer$^+$ cells that were also positive for these markers (*Fig.5.14a)*. However, there were also small populations of CD1c-tetramer$^+$ cells that were negative for these markers, which may be genuine CD1c-restricted T cells (*Fig.5.14a)*. Interestingly, the anti-CD36 mAb conjugated to APC used here was the same clone as the unconjugated mAb used for blocking in *Fig.5.13,* indicating that the antibody might weakly bind ptmCD1c but does not block TCR-independent TCR binding. Following the exclusion of SCARB1$^+$ cells, there were fewer tetramer$^+$ cells compared to the parental population, which may be more representative of the true frequencies of CD1c-restricted T cells in PTM (*Fig.5.14b)*. Platelet markets CD42b and CD62p were also targeted with mAbs but did not successfully label any macaque cells (*Fig.5.14a)*, including non-T cells, indicating that their binding epitopes are not conserved between PTMs and humans. The anti-CD61 mAb bound a small population of macaque cells, but these cells did not bind tetramer (*Fig.5.14a)* and may therefore be a population of contaminating cells (e.g. CD51/61$^+$ cells (Clemetson K.J., 2019, Lowin and Straub, 2011)). These results suggest that blocking or eliminating cells that co-label with SCARB1 and CD36 may provide optimal staining by eliminating TCR-independent tetramer staining.

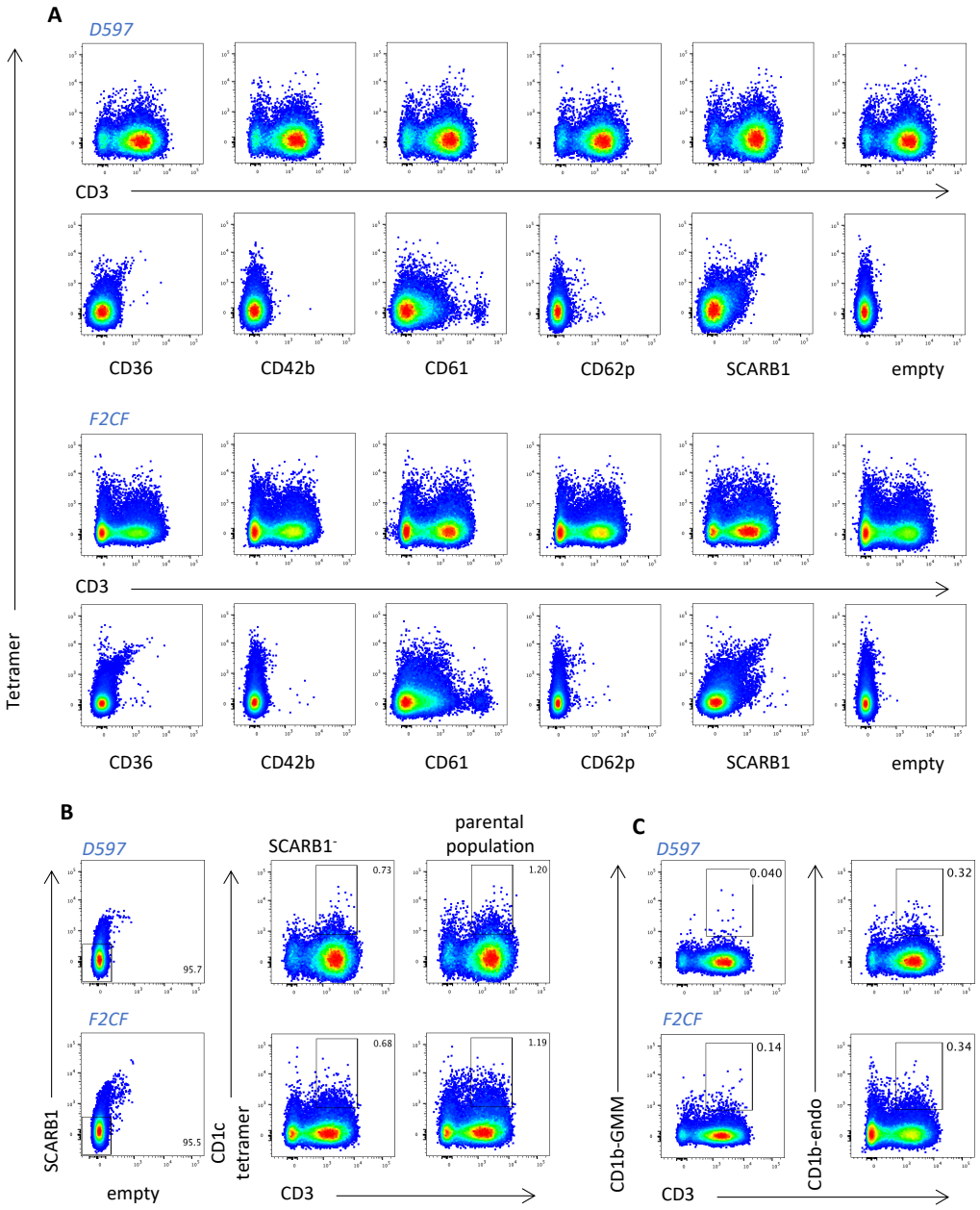

Figure 5.14. Optimisation of macaque T cell ptmCD1b and ptmCD1c tetramer staining. A. PtmPBMCs from two donors were labelled with ptmCD1c-endo tetramers in addition to anti-CD36, anti-CD42b, anti-CD61, anti-CD62p or anti-SCARB1 (anti-human) mAbs. The top row depicts tetramer staining of T cells and the bottom row shows the relationship between tetramer staining and the chosen mAb staining. **B.** SCARB1$^-$ cells were gated and assessed for cleanliness of ptmCD1c tetramer staining when compared to the parental population. **C.** PtmPBMCs from two donors were labelled with either ptmCD1b-GMM or ptmCD1b-endo tetramers. Data representative of four donors across two independent experiments.

Interestingly, labelling ptmPBMCs with ptmCD1b-GMM tetramers appeared to reduce TCR-independent staining without the need for SCARB1 or CD36 blocking *(Fig.5.14c)*. The same macaque donor samples were stained with either CD1b-endo or CD1b-GMM tetramers and the tetramer staining profile appeared cleaner and more distinct in the sample stained with CD1b-GMM tetramer compared to CD1b-endo tetramer *(Fig.5.14c)*. This may be due to the presence of the detergent tyloxapol in the tetramer, by nature of the GMM lipid being solubilised in 0.5% (v/v) tyloxapol, or due to a conformational change akin to CD1d with α-GalCer or sulfatide that minimises TCR-independent binding (Gherardin et al., 2021, Li et al., 2009). Given that GMM and other exogenous lipids will likely be more relevant as lipid antigens in further macaque studies looking at CD1b, this may prove beneficial. Unfortunately, this effect was not observed with CD1c with comparing CD1c-endo and CD1c-MPM tetramers (data not shown).

Thus, similar to human samples, the use of mAbs targeting CD36 family members, or loading of defined lipid antigens may aid in reducing TCR-independent tetramer-binding. Using a combination of the methods discussed, it may be possible to confidently label and isolate macaque T cells that are restricted to CD1a, CD1b, CD1c, and CD1d.

5.2.7 TCR usage of ptmCD1-tetramer$^+$ T cells

The TCR repertoire of macaque CD1-restricted T cells remains undefined. Given the absence of a set of multiplex primers that specifically target PTM TCR genes, the TCR repertoire of human T cells that bind ptmCD1 was examined. This also enabled the generation of TCR-expressing cell lines that bind ptmCD1 for tetramer development and functional studies. This is especially important for ptmCD1a, which is not trans-species cross-reactive with any of the human TCR cell lines tested (*Fig.5.6*).

Tetramer$^+$ T cells from a total of five human donors were single cell-sorted by flow cytometry for multiplex PCR and sequencing. Cells from two donors were isolated after *in vitro* expansion: cells positive for each ptmCD1 tetramer were bulk sorted *(Fig.5.15a),* stimulated, and then expanded for two weeks *in vitro.* Cells were stimulated with plate-bound anti-CD3 (10 μg/mL) and anti-CD28 (2 μg/mL) mAbs, in the presence of PHA (1 μg/mL), IL-2 (100 U/mL) and IL-7 (50 ng/mL) for four days, and then were placed in fresh media containing IL-2 and IL-7. Following expansion, samples were re-labelled

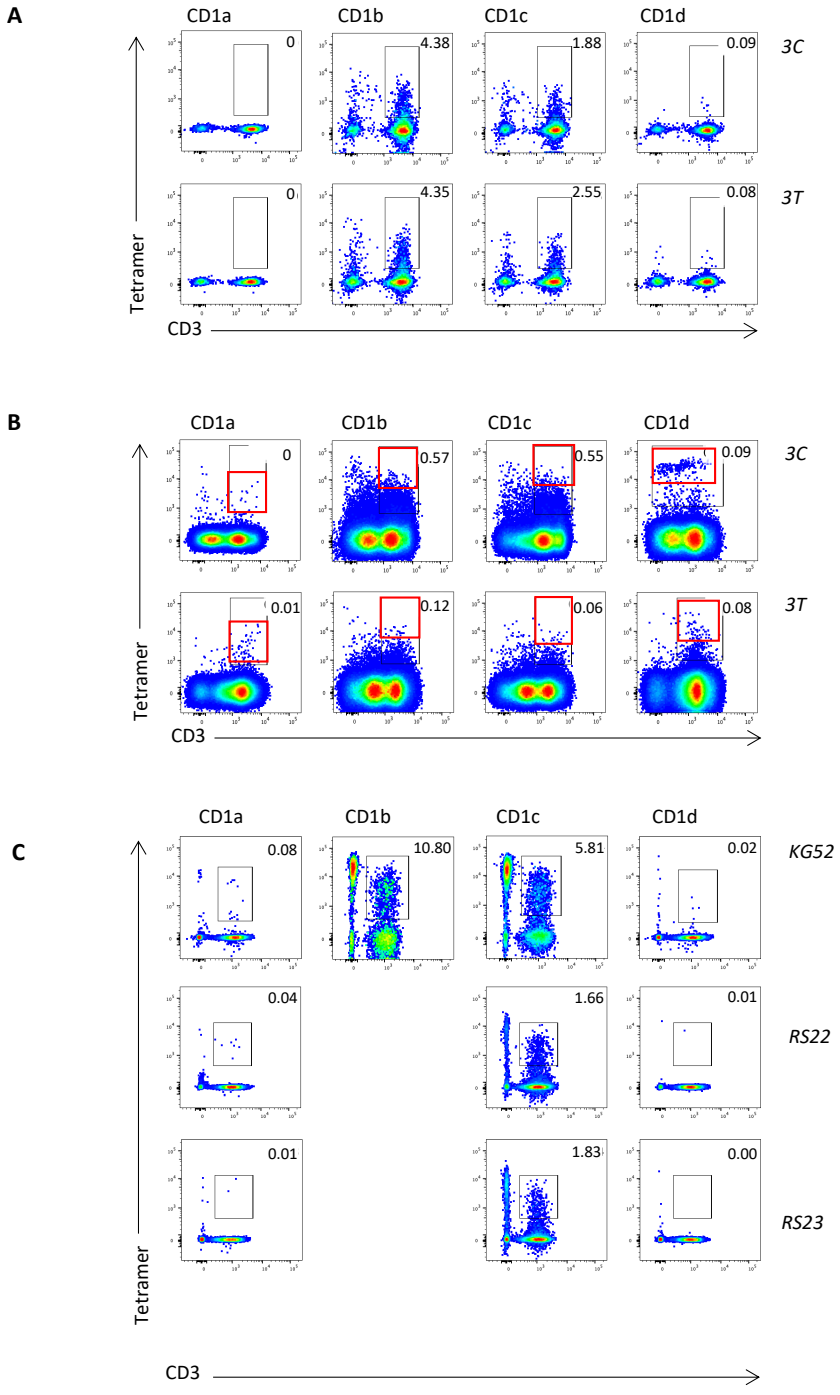
A
CD1a
CD1b
CD1c
CD1d
0
4.38
1.88
0.09
3C
0
4.35
2.55
0.08
3T
Tetramer
CD3
B
CD1a
CD1b
CD1c
CD1d
0
0.57
0.55
0.09
3C
0.01
0.12
0.06
0.08
3T
Tetramer
CD3
C
CD1a
CD1b
CD1c
CD1d
0.08
10.80
5.81
0.02
KG52
0.04
1.66
0.01
RS22
0.01
1.83
0.00
RS23
Tetramer
CD3

Figure 5.15. Preparation of human and macaque CD1-restricted T cells for TCR sequencing. A. Two huPBMC donors were labelled with CD1a-endo, CD1b-endo, CD1c-endo, or CD1d-endo tetramers directly *ex vivo* to FACS-sort $CD3^+$ $tetramer^+$ cells in bulk. The frequency of $CD3^+$ $tetramer^+$ cells is indicated in black. **B.** Sorted cells were stimulated with plate-bound anti-CD3 (10 µg/mL) and anti-CD28 (2 µg/mL) mAbs, and PHA (1 µg/mL) in the presence of IL-2 (100 U/mL) and IL-7 (50 ng/mL) for four days, and cultured for another two weeks in IL-2 and IL-7 without stimulatory agents. Expanded lymphocytes were re-labelled with the same tetramers to identify CD1-restricted T cell populations. The frequency of $CD3^+$ $tetramer^+$ cells is indicated in black with comparable gates to pre-expansion. Red boxes indicated cells sorted for TCR sequencing. Data representative of three independent experiments. **C.** HuPBMCs MACS-enriched for CD1a-endo, CD1b-endo, CD1c-endo or CD1d-endo tetramers directly *ex vivo* following anti-CD36 mAb block. $CD3^+$ $tetramer^+$ cells were single-cell FACS-sorted for TCR sequencing. CD1b-endo tetramer was only used for donor KG52 but not donors RS22 and RS23.

with ptmCD1 tetramers. Some expansion of CD1-restricted T cells was observed after culture for some donors (but not all), particularly in donor 3C there was evidence of expansion of CD1a- and CD1d-restricted T cells *(Fig.5.15b)*. This likely suggests that the sort gates used included some T cells that non-specifically bound to some tetramers *(Fig.5.15a)*. Therefore, another approach was used to isolate genuine ptmCD1-restricted T cells for sequencing, whereby huPBMCs were first blocked with an anti-CD36 mAb to minimise non-specific ptmCD1 tetramer staining, followed by MACS-enrichment. Magnetically enriched $CD3^+$ $tetramer^+$ cells from three donors were single cell-sorted using flow cytometry via the same enrichment protocol used for huCD1a tetramers in Chapter 3.2.1 (*Fig.5.15c*).

A total of 11 TCR α-chain and 7 TCR-β chain sequences were obtained from human T cells stained with ptmCD1a tetramer (*Fig.5.16a)*. Among the 11 TCR α-chains, 10 different TRAV genes were identified and 2/11 sequences contained TRAV26-2 (*Fig.5.16a)*. While only a small number of TCR β-chains were obtained, 3/7 sequences were $TRBV28^+$, suggesting a similar variable gene usage bias for TRBV28 that is observed among huCD1a-restricted TCRs that bind huCD1a tetramers (*Fig.5.16a)*. These three $TRBV28^+$ TCR clones were all derived from one donor, and interestingly, two had identical non-germline encoded CDR3β sequences but were paired to different TCR α-chains (*Appendix IV).* This intra-donor bias suggests that, despite little cross-reactivity observed for ptmCD1a by huCD1a-restricted T cells, there may be similarities in the molecular interactions between CD1a and TCRs between the two species that result in a bias towards TRBV28. As the number of clones obtained with ptmCD1a tetramer was low, further donors with a greater number of TCR sequences would need to be tested to further explore this pattern.

A total of 39 TCR α-chain and 43 TCR-β chain sequences (from paired and unpaired TCRs) were obtained from ptmCD1b $tetramer^+$ cells in three donors (*Fig.5.16b)*. PtmCD1b-reactive human TCRs exhibited diversity in both their TCR α- and β-chain genes (*Fig.5.16b)*. While there was diversity of TRAV genes, TRAV6 occurred in 5/39 TCR clones (*Fig.5.16b)*. The TCR β-chain also showed recurring patterns of variable gene usage with 12/43 TCRs and 5/43 TCRs expressing TRBV20 and TRBV14, respectively (*Fig.5.16b)*.

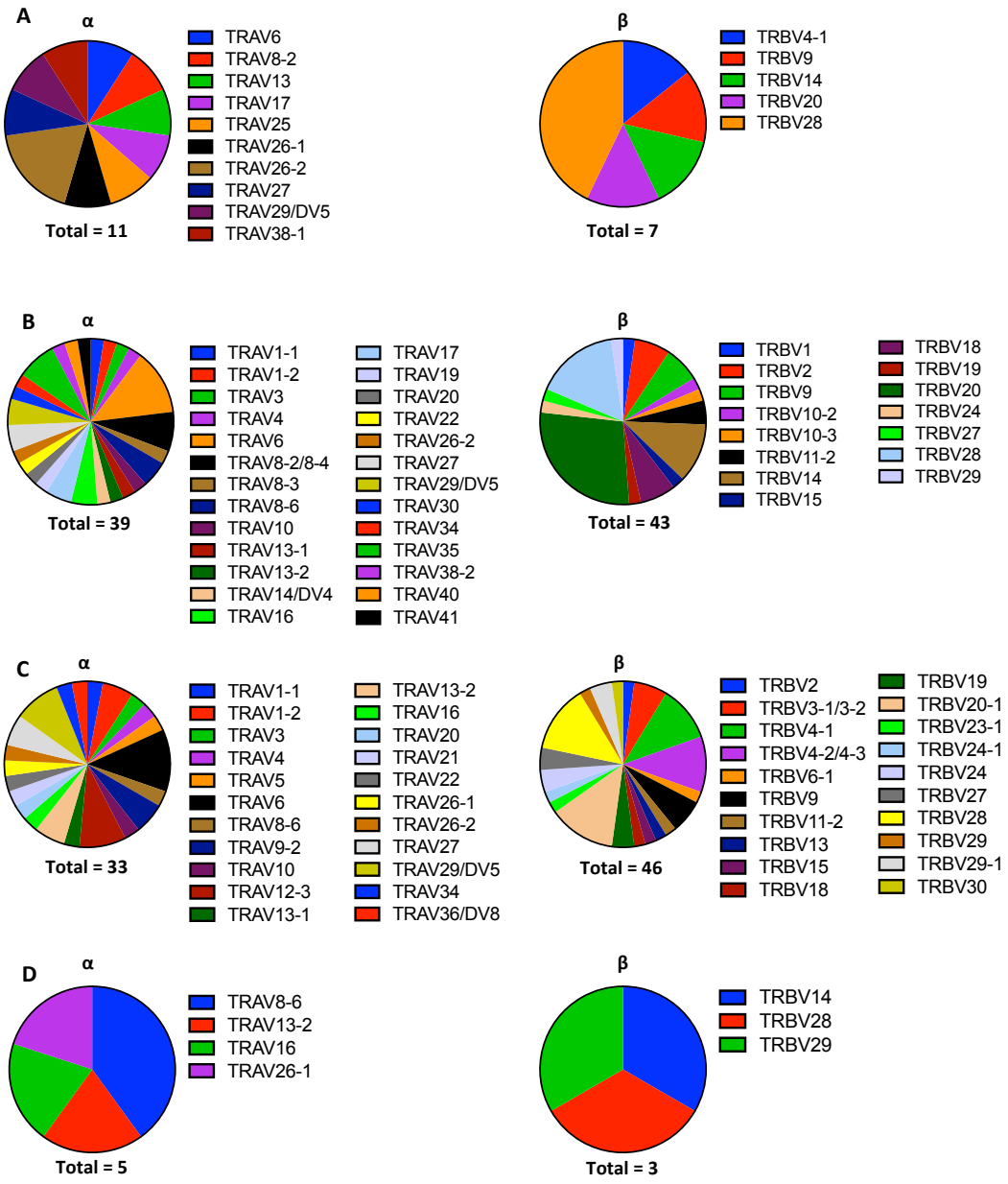

Figure 5.16. ptmCD1a-restricted TCR variable gene usage. CD1a tetramer^{+} T cells were FACS-sorted directly *ex vivo* for reverse transcription, followed by two rounds of nested PCR. Multiplex primers were used to amplify all TCR variable gene segments. Sanger sequencing was performed on amplified DNA products. TRAV (left) and TRBV (right) gene usage was determined by comparing identified sequences against the IMGT database. **A.** Variable gene usage of TCRs from T cells isolated using ptmCD1a-endo tetramer. Data indicative of 11 TCR α-chain and 7 β-chain genes from three donors. **B.** Variable gene usage of TCRs from T cells isolated using ptmCD1b-endo tetramer. Data indicative of 39 TCR α-chain and 43 β-chain genes from three donors. **C.** Variable gene usage of TCRs from T cells isolated using ptmCD1c-endo tetramer. Data indicative of 33 TCR α-chain and 46 β-chain genes from six donors. **D.** Variable gene usage of TCRs from T cells isolated using ptmCD1d-endo tetramer. Data indicative of five TCR α-chain and three β-chain genes from one donor.

Across six donors, 33 TCR α-chain and 46 TCR-β chain sequences (from paired and unpaired TCRs) were obtained from cells sorted with ptmCD1c tetramer (*Fig.5.16c)*. Human ptmCD1c-restricted TCRs also exhibited diversity in both their TCR α- and β-chains (*Fig.5.16c)*. TRBV4-1, TRBV4-2/4-3, TRBV20-1 and TRBV28 were most frequent among T cell clones (*Fig.5.16c)*. Interestingly, there were two ptmCD1c-restricted T cell clones identified with TRAV9-2^{+} TRBV4-1^{+} with unique CDR3α and CDR3β sequences *(Appendix IV)*, suggesting that this variable gene pairing may be advantageous in the interaction between the TCR and ptmCD1c.

Few sequences were obtained from ptmCD1d-restricted T cell clones due to their lower frequency among huPBMCs. Furthermore, only one donor yielded enough cells for single cell-sorting and sufficient DNA following PCR amplification for sequencing. The five TCR α-chains and three β-chains included variable genes found to be more common among T cells restricted to the other CD1 molecules: TRBV28 (CD1a) and TRBV14 (CD1b) (*Fig.5.16d)*.

This work provided a basis with which to generate cell lines that recognise ptmCD1 molecules. While it also provided interesting patterns regarding variable gene usage, a much greater number of T cell clones would need to be sequenced to determine whether any patterns or biases do exist. Furthermore, sequencing of ptmCD1-restricted T cells isolated from macaque blood and tissues would be of greater value. A similar multiplex PCR amplification and sequencing protocol is yet to be established for macaques, however work is currently underway to develop a method of sequencing macaque TCRs.

5.2.8 Generation of TCR-transduced SKW-3 cell lines expressing selected TCRs from ptmCD1 tetramer^{+} sorted cells

To validate TCRs obtained from single cell sequencing analysis, HEK 293T cells were transiently transfected to express these TCRs and confirm reactivity to CD1 tetramers. DNA constructs encoding paired TCR α- and β-chains linked by a 2A-peptide-linker, were cloned into a pMIG retroviral vector that contained the huTRBC gene (from previous cloning) with GFP as a reporter, similar to the generation of human CD1a-restricted T cell lines in Chapter 4.2.2. HEK 293T cells were transiently co-transfected

with TCR- and huCD3-encoding pMIG vectors and cells were harvested after 36 hours for flow cytometry analysis.

Sequences used for transduction were selected based on either frequency or patterns of particular variable gene usage in the TCR α- or β-chains as outlined in Table 5.2. Following transient transfection, each sample was labelled with their respective huCD1 and ptmCD1 tetramer: 13-1pa4-1 with CD1a, 16pb28 with CD1b, 6pc4-1 and 8-6pc4-1 with CD1c, and 26pd29 with CD1d.

Table 5.2. Human ptmCD1-restricted TCRs selected for the generation of cell lines. Paired TCR α- and β-chain sequences from single cell-sorted $CD3^+$ ptmCD1 $tetramer^+$ cells. TCR genes were amplified with two round of multiplex nested PCR prior to Sanger sequencing. TRAV, TRAJ, TRBV and TRBJ gene usage was determined by comparing identified sequences against the IMGT database. Frequency is displayed based on the number of clones determined for each donor with each tetramer.

Cell line	Donor	Restriction	TRAV	CDR3α	TRAJ	TRBV	CDR3β	TRBJ	Freq.
13-1pa4-1	3T	CD1a	13-1	CAASKYSTLTF	11	4-1	CASSQGVLDGYTF	1-2	12/12
16pb28	3C	CD1b	16	CALSHTGNQFYF	49	28	CASRLRGRREETQYF	2-5	3/11
8-6pc4-1	KG52	CD1c	8-6	CAVSDRWGYQKVTF	13	4-1	CASSQDRTGTPYEQYF	2-7	6/22
6pc4-1	KG52	CD1c	6	CALIGYQKVTF	13	4-1	CASSQLGTDTNYGYTF	1-2	14/22
26pd29	3C	CD1d	26-1	CIVRVTQGSNQLIW	33	29-1	CSATYRDRGLGTEAFF	1-1	3/4

Analysis of transiently transfected cells revealed that 13-1pa4-1 bound ptmCD1a but not huCD1a tetramers, and similarly, both 6pc4-1 and 8-6pc4-1 bound ptmCD1c but not huCD1c tetramers *(Fig.5.17)*. All three TCRs appeared to bind specifically to ptmCD1 but not huCD1. Conversely, 16pb28 and 26pd29 did not result in positive tetramer staining, suggesting that the TCR sequences were incorrect, or the sequences obtained were not truly CD1-restricted *(Fig.5.17)*.

To generate stable T cell lines that bind ptmCD1 molecules, TCR-deficient SKW-3 cell lines were engineered to express 13-1pa4-1, 6pc4-1 and 8-6pc4-1 TCRs. The same TCR- and CD3-encoding pMIG constructs were used to again transiently co-transfected HEK

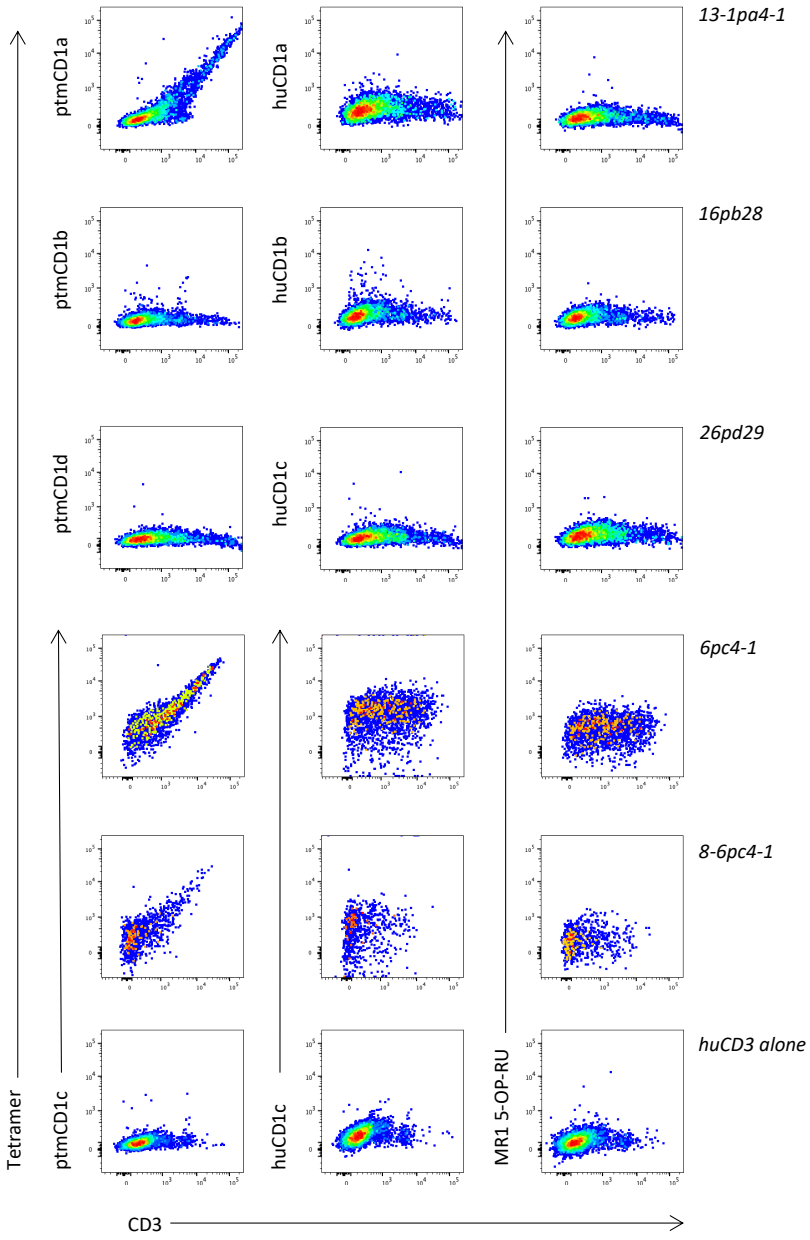

Figure 5.17. Validation of ptmCD1-restricted TCR sequences. Tetramer staining of 293T cells 36 hours following co-transfection with pMIG vector plasmids containing huCD3 and each TCR construct: 13-1pa4-1, 16pb28, 26pd29, 6pc4-1 or 8-6pc4-1, or huCD3 alone. Cells were examined for positive ptmCD1 tetramer staining using the tetramer they were isolated with (indicated by the second letter of their name, e.g. 13-1pa4-1 was isolated with ptmCD1a tetramer). Data is representative of 3 independent experiments.

293T cells, along with pEQ-Pam-E and pVSV-g helper plasmids to produce retrovirus. Retroviral supernatant was harvested every 24 hours for five days and used to transduce SKW-3 $\beta_2m^{-/-}$ cells. The same tetramer binding patterns were observed when the resulting T cell lines were labelled with the same tetramers (data not shown).

Including previously identified trans-species cross-reactive T cell lines, Fee1 and TCR 4.27 for CD1b, 1C4 for CD1c and NKT15 for CD1d, the generation of 13-1pa4-1 as a stable SKW-3 cell line means that there are now T cell lines that recognise each of the ptmCD1 molecules. These cell lines will be particularly useful to verify ptmCD1 tetramer assays and in activation assays with APCs in future work.

5.2.9 Enumeration of ptmCD1-restricted T cell populations in macaque tissues

Following validation of new ptmCD1 tetramers, they were then employed to enumerate populations of lipid-reactive T cells in peripheral blood and tissues of 12 healthy juvenile PTMs that were necropsied following SIV and influenza vaccination (considered as healthy controls for the purpose of this study). Macaque tissues were harvested by Professor Stephen Kent and processed in collaboration with members of the Kent Laboratory (The University of Melbourne). Tissues collected include inguinal lymph nodes (iLN), mesenteric lymph node (mLN), thymus, spleen, blood, liver, rectum, lung, and bronchoalveolar lavage (BAL). Blood was processed using Ficoll-Paque centrifugation; LNs, thymus and spleen were processed mechanically; and lung, liver and rectum were digested enzymatically with collagenase D to obtain cell suspensions for FACS analysis. Non-lymphoid tissues were stained with different antibody cocktails to blood and lymphoid tissue to help identify T cells in tissues in which they are not as abundant (e.g. cells expressing the epithelial cell adhesion molecule (EpCAM) were removed from the analysis) *(Fig.5.18a)*.

Tissues from each donor were divided into three samples to be stained with CD1a-DDM or CD1d-α-GalCer tetramers independently, or dual-stained with CD1b-GMM and CD1c-MPM tetramers in PE and BV421 respectively. At the time of these experiments, there was no anti-CD36 or anti-SRB1 blocking mAb that could be used to reduce contamination by cells that bound in a TCR-independent manner. As another approach to optimise tetramer staining, cells that were double positive for both CD1b and CD1c

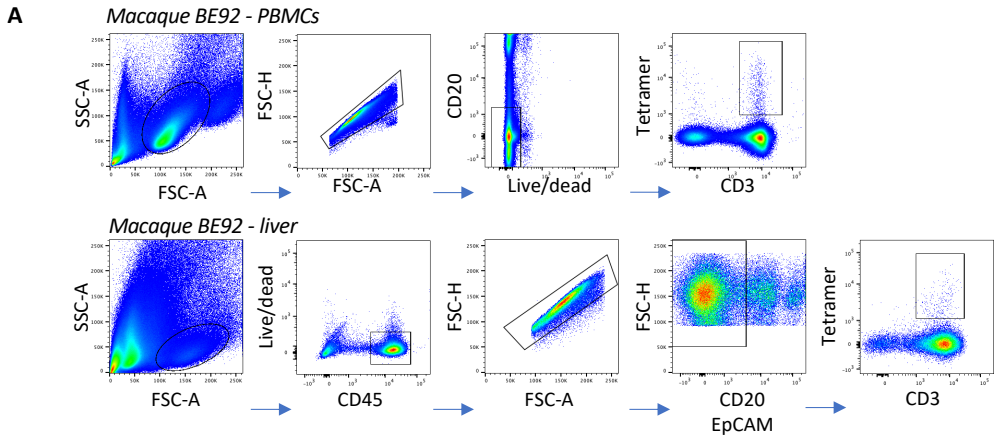
A
Macaque BE92 - PBMCs
SSC-A
FSC-A
FSC-H
FSC-A
CD20
Live/dead
Tetramer
CD3
Macaque BE92 - liver
SSC-A
FSC-A
Live/dead
CD45
FSC-H
FSC-A
FSC-H
CD20
EpCAM
Tetramer
CD3

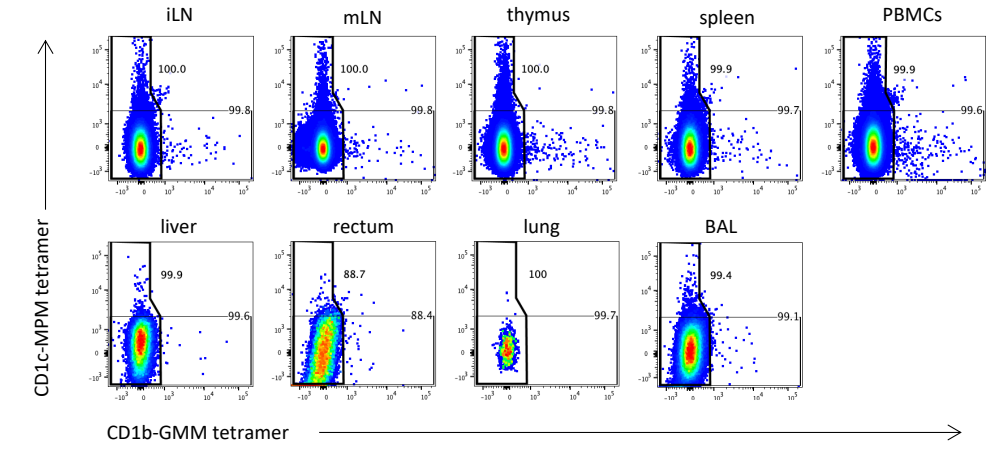
B
Macaque AA93
iLN
mLN
thymus
spleen
PBMCs
100.0
99.8
100.0
99.8
100.0
99.8
99.9
99.7
99.9
99.6
liver
rectum
lung
BAL
99.9
99.6
88.7
88.4
100
99.7
99.4
99.1
CD1c-MPM tetramer
CD1b-GMM tetramer

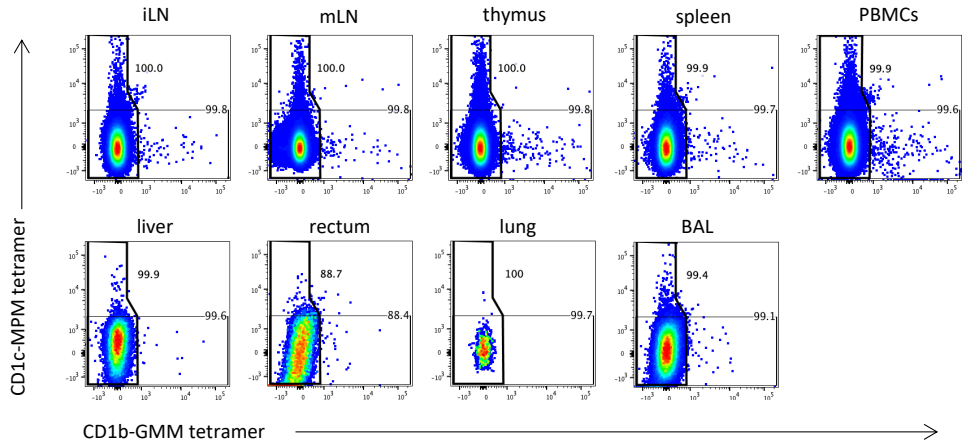
Macaque BE92
iLN
mLN
thymus
spleen
PBMCs
100.0
99.8
100.0
99.8
100.0
99.8
99.9
99.7
99.9
99.6
liver
rectum
lung
BAL
99.9
99.6
88.7
88.4
100
99.7
99.4
99.1
CD1c-MPM tetramer
CD1b-GMM tetramer

Figure 5.18. Gating strategy for tetramer staining in healthy macaque tissues. 12 juvenile macaque donors were necropsied for the harvesting of tissues: iLN, mLN, thymus, blood (PBMCs), spleen, BAL, liver, lung, and rectum. **A.** General gating strategy for all tetramers. For LN, thymus, PBMC and spleen samples, cells were identified by gating on $CD3^+$ $CD20^-$ single, live lymphocytes (top). Non-lymphoid tissues, BAL, liver, lung, and rectum were additionally gated on $EpCAM^-$ $CD45^+$ cells (bottom). **B.** Dual CD1-GMM and CD1c-MPM tetramer staining was used to exclude non-TCR-mediated tetramer binding from these analyses. Samples were co-stained with CD1b-GMM tetramer in PE, CD1c-MPM tetramer in BV421. Thicker gates denote CD1b-GMM $tetramer^-$ cells that were used to analyse CD1c-restricted T cells. Thinner gates denote CD1c-MPM $tetramer^-$ cells that were used to analyse CD1b-restricted T cells. Percentages of the parental population are shown. Data representative of 12 donors across two independent experiments (except three donors for which lung samples were excluded).

iLN, inguinal lymph node; mLN, medistinal lymph node; BAL, bronchoalveolar lavage

tetramers were excluded from the analysis, as these cells likely represented cells that were binding in a TCR-independent manner. Cells that were positive for CD1b tetramer were excluded from the CD1c tetramer analysis and vice versa (*Fig.5.18b)*. There were not many samples with double-positive populations *(Fig.5.18b)*, potentially given that CD1b-GMM tetramer appears to reduce confounding non-TCR-mediated staining compared to CD1b-endo tetramer *(Fig.5.14)*.

Among peripheral blood T cells, CD1-Ag tetramer$^+$ T cells were relatively low in frequency, ranging from <0.01-0.65% *(Fig.5.19)*. CD1a-restricted T cells comprised up to 0.22% of the T cell population (mean = 0.13%) *(Fig.5.19)*. CD1b-restricted T cells were the rarest subset, with the highest frequency detected among all donors being 0.04% of T cells *(Fig.5.19)*. CD1c-restricted T cells ranged up to 0.65% of the blood T cell pool *(Fig.5.19)*. The frequency of type I NKT cells was an average of 0.06% *(Fig.5.19)*. CD1-restricted T cells were generally more frequent in the spleen, with tetramer$^+$ population frequencies averaging 0.20%, 0.04%, 0.40% and 0.07% for CD1a, CD1b, CD1c, and CD1d tetramers respectively *(Fig.5.19)*. CD1-restricted T cells were less prevalent in LNs compared to the blood and spleen, representing up to 0.46% of T cells. The average frequencies of CD1a-restricted T cells were 0.09% and 0.07% in iLN and mLN respectively *(Fig.5.20)*. CD1b-restricted T cells were again observed at the lowest frequencies, comprising an average of 0.04% and 0.03% of T cells in iLN and mLN respectively. Type I NKT cells similarly had an average of 0.04% in cells isolated from both LNs *(Fig.5.20)*. CD1c-tetramer$^+$ cells were again the greatest in frequency, reflective of a greater spread of the population into the tetramer$^+$ gate, comprising an average of 0.21% and 0.22% in iLN and mLN respectively *(Fig.5.20)*. Lymph node, spleen and PBMC type I NKT cell frequencies were hence consistent with the findings of Yu et al, for which most donors had fewer than 0.1% of T cells as tetramer$^+$ cells in these tissues while some donors had a maximum of 0.5% (Yu et al., 2019).

Liver, rectum, and BAL samples revealed higher frequencies of CD1-restricted T cells compared to lymphoid tissues and blood. CD1a-restricted T cells were the predominant CD1-restricted T cell population in the liver, ranging between 0.25-2.28% of T cells with a mean of 0.83% *(Fig.5.21)*. Type I NKT cells, CD1b- and CD1c-restricted T cells represented 0.29%, 0.12% and 0.18% of liver T cells respectively *(Fig.5.21)*. The rectum

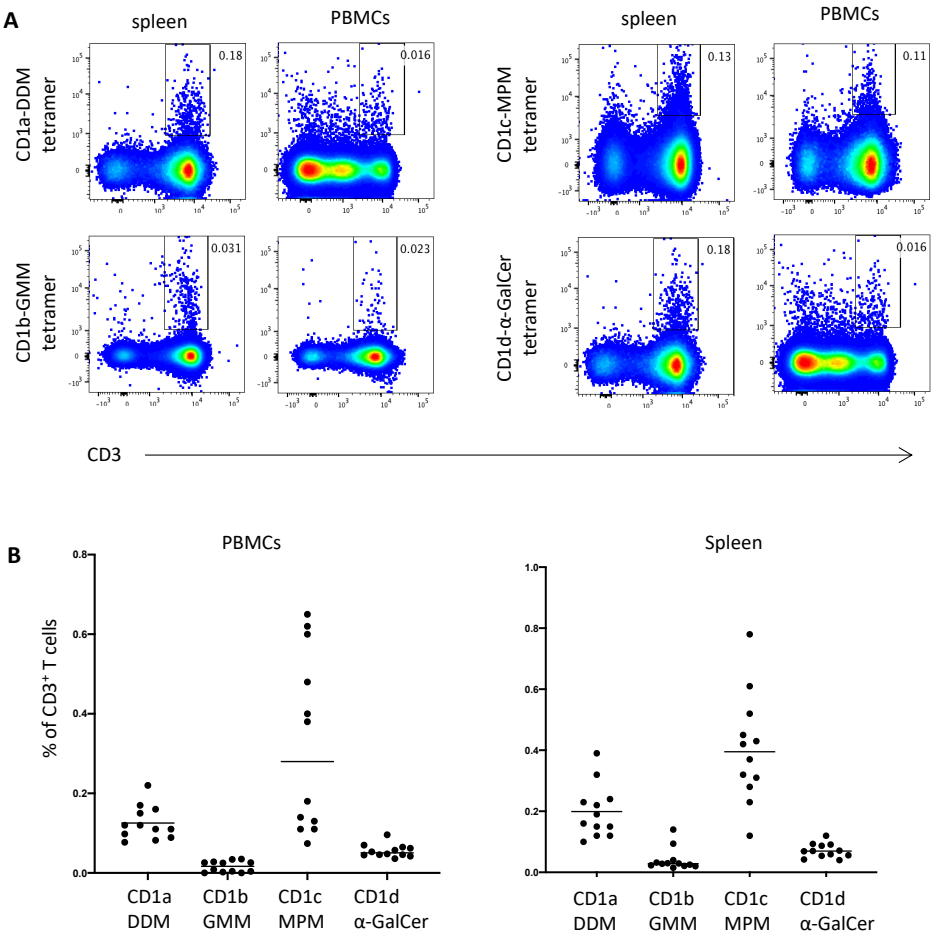

Figure 5.19. Enumeration of CD1-restricted T cells in healthy macaque peripheral blood and spleen. 12 juvenile macaque donors were necropsied, and PBMCs and splenocytes were harvested for staining. **A.** Samples were labelled with ptmCD1a-DDM, ptmCD1b-GMM, ptmCD1c-MPM or ptmCD1d-α-GalCer tetramers to isolate CD1-restricted T cell populations. **B.** Tetramer$^+$ cells as a proportion of all CD3$^+$ T cells after being gated on CD20$^-$ viable, single lymphocytes using the strategy shown in *(Fig.5.18a)*. Each of the 12 macaques is represented by an individual dot and the mean tetramer$^+$ cell frequency for each tetramer is displayed.

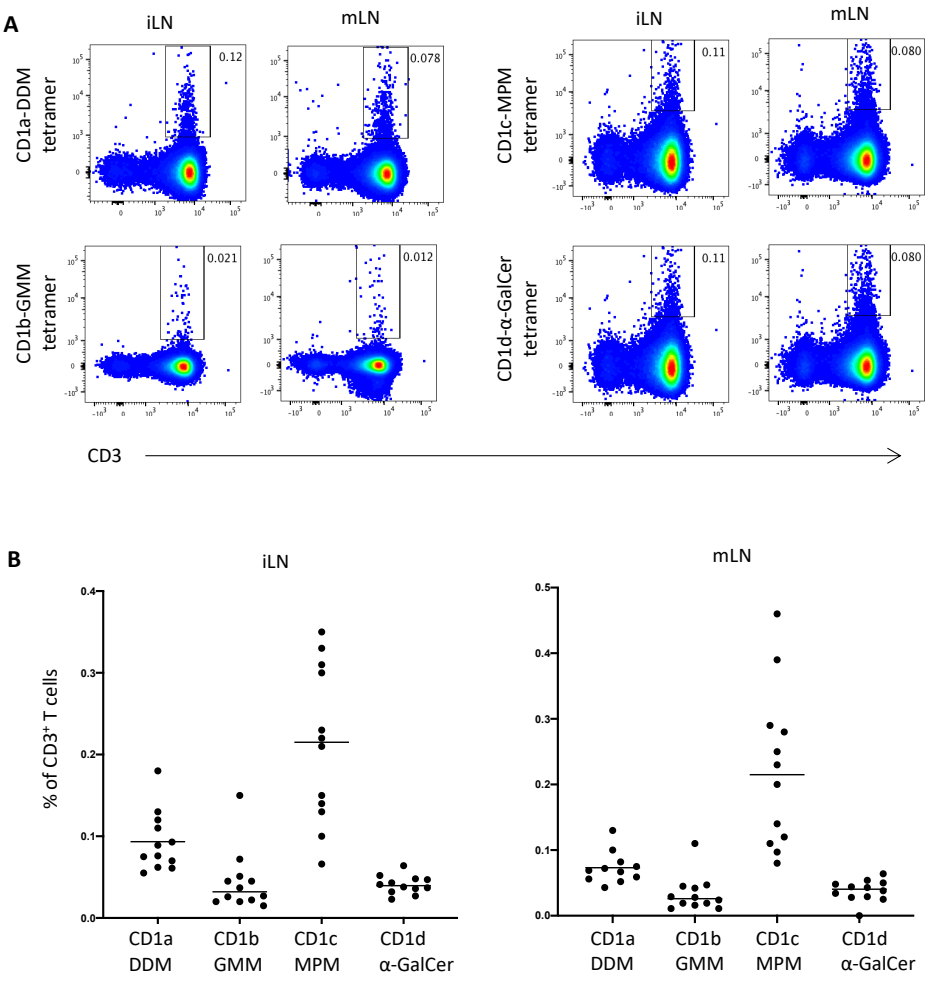

Figure 5.20. Enumeration of CD1-restricted T cells in healthy macaque lymph nodes. 12 juvenile macaque donors were necropsied, and their inguinal LN (iLN) and mesenteric LN (mLN) were harvested and processed to form single cell suspensions. **A.** Samples were labelled with ptmCD1a-DDM, ptmCD1b-GMM, ptmCD1c-MPM or ptmCD1d-α-GalCer tetramers to isolate CD1-restricted T cell populations. **B.** Tetramer$^+$ cells as a proportion of all CD3$^+$ T cells after being gated on CD20$^-$ viable, single lymphocytes using the strategy shown in *(Fig.5.18a)*. Each of the 12 macaques is represented by an individual dot and the mean tetramer$^+$ cell frequency for each tetramer is displayed.

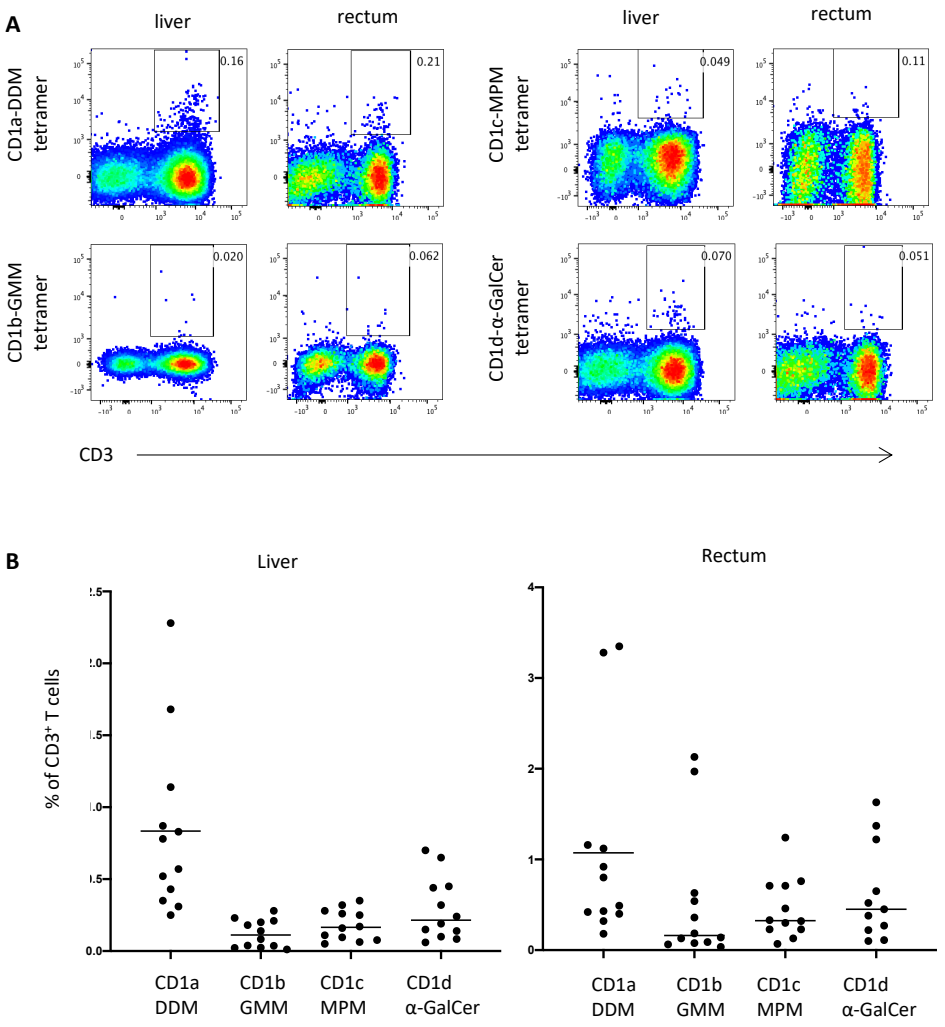

Figure 5.21. Enumeration of CD1-restricted T cells in healthy macaque liver and rectum. 12 juvenile macaque donors were necropsied, and their liver and rectum were harvested and digested to form single cell suspensions. **A.** Samples were labelled with ptmCD1a-DDM, ptmCD1b-GMM, ptmCD1c-MPM or ptmCD1d-α-GalCer tetramers to isolate CD1-restricted T cell populations. **B.** Tetramer$^+$ cells as a proportion of all CD3$^+$ T cells after being gated on CD45$^+$ EpCAM$^-$ CD20$^-$ viable, single lymphocytes using the strategy shown in *(Fig.5.18a)*. Each of the 12 macaques is represented by an individual dot and the mean tetramer$^+$ cell frequency for each tetramer is displayed.

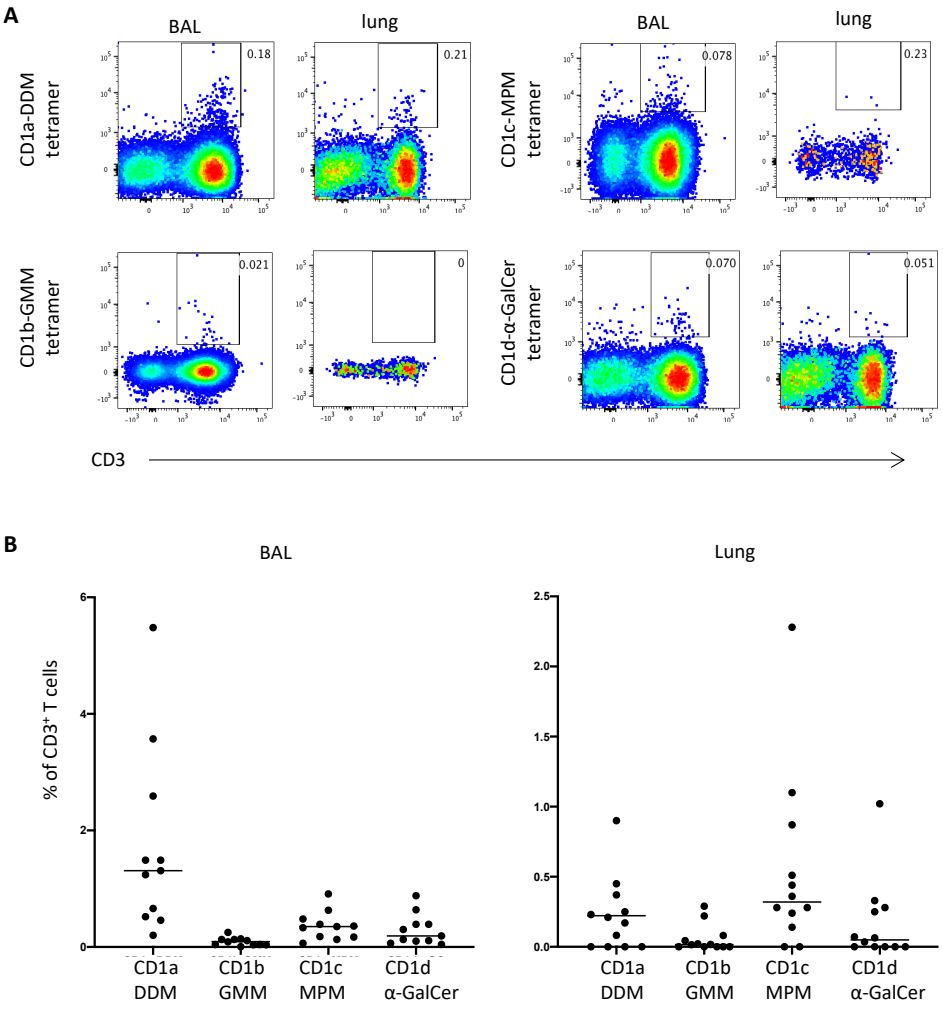

Figure 5.22. Enumeration of CD1-restricted T cells in healthy BAL and lung. 12 juvenile macaque donors were necropsied, and their BAL and lung samples were harvested. **A.** Samples were labelled with ptmCD1a-DDM, ptmCD1b-GMM, ptmCD1c-MPM or ptmCD1d-α-GalCer tetramers to isolate CD1-restricted T cell populations. **B.** Tetramer$^+$ cells as a proportion of all CD3$^+$ T cells after being gated on CD45$^+$ EpCAM$^-$ CD20$^-$ viable, single lymphocytes using the strategy shown in *(Fig.5.18a)*. Each of the 12 macaques is represented by an individual dot and the mean tetramer+ cell frequency for each tetramer$^+$ is displayed.

had even higher frequencies of CD1a-restricted T cells, reaching 3.35% of T cells with a mean of 1.07% *(Fig.5.21)*. CD1b-restricted T cells ranged from 0.04-2.13% (mean = 0.52%), CD1c-restricted T cells ranged from 0.07-1.24% (mean = 0.46%), and type I NKT cells ranged from 0.10-1.63% (mean = 0.63%) *(Fig.5.21)*.

Both lung tissue and BAL fluid were assessed for the presence of airway CD1-restricted T cells. Three lung samples were excluded from the analysis as there were too few cells for adequate staining by flow cytometry. These three lung samples were mechanically digested and the samples did not resuspend well during staining with tetramers and mAbs, thereby confounding the results. Populations of lymphocytes (i.e. $CD3^+$, $CD4^+$, and $CD8^+$ T cell subsets) in the BAL are generally expected to be reflective of those in peripheral blood (Harbeck, 1998). However, CD1a-, CD1b- and CD1d-$tetramer^+$ T cell populations were consistently higher in BAL *(Fig.5.22)* than in blood *(Fig.5.19)* for each donor. CD1a-restricted T cell populations in the BAL ranged from 0.20%-5.48% (mean = 1.73%) *(Fig.5.22)*, while CD1b-restricted T cells frequencies were virtually undetectable. CD1c-restricted T cells comprised a mean of 0.36% of T cells in BAL *(Fig.5.22)*, which was similar to blood *(Fig.5.19)*. Type I NKT cells comprised a mean of 0.29% of BAL T cells *(Fig.5.22)*. In the lungs, all CD1-restricted T cell subsets were low in frequency in most samples *(Fig.5.22)*, consistent with a previous report that examined type I NKT cell populations in rhesus macaque lung tissue (Yu et al., 2019).

Given the low frequency of T cells that bound the CD1-antigen (CD1-Ag) tetramers, magnetic enrichment was employed as a secondary approach to enhance detection of these cells for further analysis. Splenocytes were MACS-enriched with CD1a-DDM or CD1d-α-GalCer tetramers conjugated to PE, or CD1b-GMM-PE and CD1c-MPM-PE-Cy7 tetramers stained simultaneously. As seen with human samples, $tetramer^+$ populations were better separated from $tetramer^-$ cells following enrichment due to a greater MFI *(Fig.5.23)*. Comparable to results in human PBMCs, MACS-enrichment with CD1a-DDM tetramer isolated distinct populations ranging from 1.85-2.39% of T cells (*Fig.5.23a)*. Enrichment of CD1b-GMM and CD1d-α-GalCer tetramer staining also revealed large populations of similar frequencies (ranging 1.38-2.42% and 1.78-1.98% of T cells respectively) (*Fig.5.23b, Fig.5.23c)*. CD1c-MPM tetramer from the spleen was enhanced following MACS-enrichment, however $CD3^-$ $tetramer^+$ cells were also

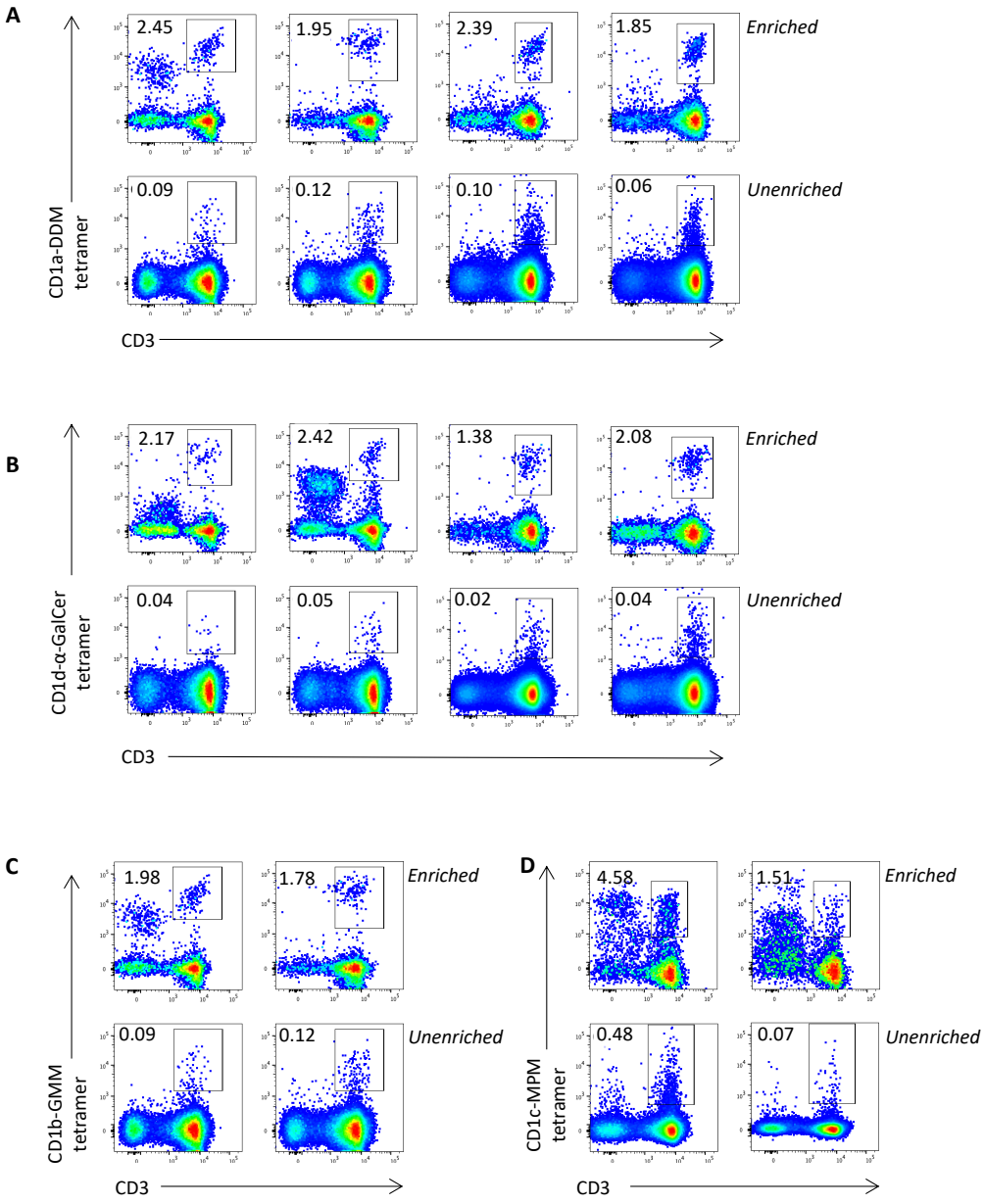

Figure 5.23. Macaque splenocytes MACS-enriched with CD1 tetramers. 100 x 10^6 splenocytes were labelled with **A.** CD1a-DDM (PE) **B.** CD1b-GMM (PE) **C.** CD1c-MPM (PE-Cy7) **D.** CD1d-α-GalCer (PE) tetramers, co-labelled with anti-PE magnetic beads, and then MACS-enriched over a magnetic column. MACS-enriched samples and unenriched spleen were then labelled with an antibody cocktail to identify $CD20^-$ $CD3^+$ live, single lymphocytes. Plots for each tetramer show MACS-enriched sample (top) and unenriched sample (bottom) for each donor. Each tetramer was used to MACS-enrich four donor samples in two independent experiments and CD1b tetramer in PE and CD1c tetramer in PE-Cy7 were used simultaneously.

prevalent (*Fig.5.23d)*, which might indicate TCR-independent staining. Overall, MACS-enrichment resulted in a more defined staining profile of CD1-reactive T cells.

The use of blocking antibodies towards CD36 and SCARB1, if available, or co-labelling with tetramer, may further enhance tetramer staining by preventing TCR-independent binding. As determined by tetramer staining profiles above, CD1c tetramer staining profiles were more likely to be affected by non-TCR-mediated tetramer staining, whereas CD1a and CD1d tetramers often yielded clearer populations of tetramer$^+$ cells. Therefore, while tetramer staining methods are yet to be optimised, this study provides a glimpse at CD1-restricted T cell populations found in PTM tissues. CD1-restricted T cells appear the most abundant in liver, rectum and BAL, and exist at lower frequencies in the blood and lymphatic tissues. MACS-enrichment following tetramer stain aided in the isolation of distinct tetramer$^+$ populations in the spleen and is worth pursuing in future phenotypic analyses of ptmCD1-restricted T cells in all tissues for which it is feasible (i.e. sufficient cells can be harvested). Collectively, these studies represent an important step forward for the analysis of CD1-restricted T cells in macaque tissues.

5.2.10 Phenotypic characterisation of ptmCD1-restricted T cells in macaque tissues

Given the lack of clarity on whether all ptmCD1 tetramer staining above was TCR-mediated, phenotypic analyses were performed on tetramer$^+$ cells with two aims. Firstly, to determine whether tetramer$^+$ cells were distinct to tetramer$^-$ T cells as a way of validating tetramer staining. Secondly, provided tetramer staining was indeed TCR-mediated, to characterise CD1-restricted T cell subsets in PTM for the first time. Based on tetramer staining above, cells labelled with CD1a and CD1d tetramers, and CD1b-GMM to a lesser extent, appeared more likely to be an accurate reflection of CD1a-, CD1d- and CD1b-reactive T cells respectively.

Due to the restriction of flow cytometry markers to those that cross-react between human and PTM epitopes, an initial phenotypic analysis of CD1-restricted T cells in ptmPBMCs assessed CD4, CD8, CD27 IL-18R and chemokine receptor expression in six animals. Subsequently, to investigate tissue-specific differences, CD1 tetramers were incorporated into a flow cytometry panel designed to measure co-receptor usage (CD4, CD8), memory

status (CD27, CD28, CD95), activation (CD69, ICOS), and chemokine receptor expression (CCR5 and CCR6) in 12 macaque macaques in blood, spleen, and LNs.

Fig.5.24a shows the gating of tetramer$^+$ T cells for each CD1 tetramer in three macaques. Consistent with previous tetramer staining, CD1a and CD1d tetramers produced the cleanest tetramer staining profile while CD1b and CD1c tetramers produced a spread of cells in the CD3$^+$ tetramer$^+$ cell gate, in line with non-TCR-mediated staining *(Fig.5.24a)*. Despite differences in their tetramer staining profiles, CD4 and CD8 co-receptor expression was consistent for T cells restricted across CD1 isoforms (*Fig.5.24b*). The frequency of CD4$^+$ cells among tetramer$^+$ T cells ranged between 28.0-75.0% and 0.0-60.0% for CD8$^+$ cells (*Fig.5.24c*). Unlike human CD1a-restricted T cell populations, the majority of which are predominantly CD4$^+$, CD4 co-receptor expression was less frequent among ptmCD1a-restricted T cells (*Fig.5.24c*). CD1b-, CD1c- and CD1d-restricted T cells were similarly variable in their co-receptor expression. Macaque B0399 was the only macaque in which all CD1-restricted T cells were mostly CD4$^+$ (*Fig.5.24c*). As a control, MR1-5-OP-RU tetramer was included in three macaques, and as expected, the MAIT cells were enriched for CD8$^+$ (*Fig.5.24c*) (Reantragoon et al., 2013, Chen et al., 2019b). Type I NKT cells were also assessed with CD1d-α-GalCer tetramer and were predominately CD8$^+$ in the same two macaques, which is similar to previous findings in rhesus macaques that were primarily CD8α$^+$, however, the distribution was not as clear-cut in this case (*Fig.5.24c*) (Yu et al., 2019).

To determine whether there was variability between different tissue types, CD4 and CD8 co-receptor expression was assessed in different lymphoid tissues. Interestingly, MACS-enrichment of splenocytes labelled with all four tetramers also appeared to enrich for CD4$^-$ CD8$^-$ (DN) T cells regardless of tetramer binding (not seen to the same extent among unenriched splenocytes) (*Fig.5.25).* It is possible that the enrichment process is biased towards selecting DN T cells, at least among splenocytes. Excluding MACS-enriched samples, all CD1 tetramer$^+$ T cells followed a similar pattern of having the highest CD4$^+$ frequencies in LNs, then PBMCs, and fewer in the spleen due to a rise in DN or CD8$^+$ T cell frequencies, consistent with the total T cell population (*Fig.5.25).*

Next, CD27 was investigated as a pseudo-indicator of memory and activation status, being expressed more so by activated and memory T cells compared to naive cells (Ahlers

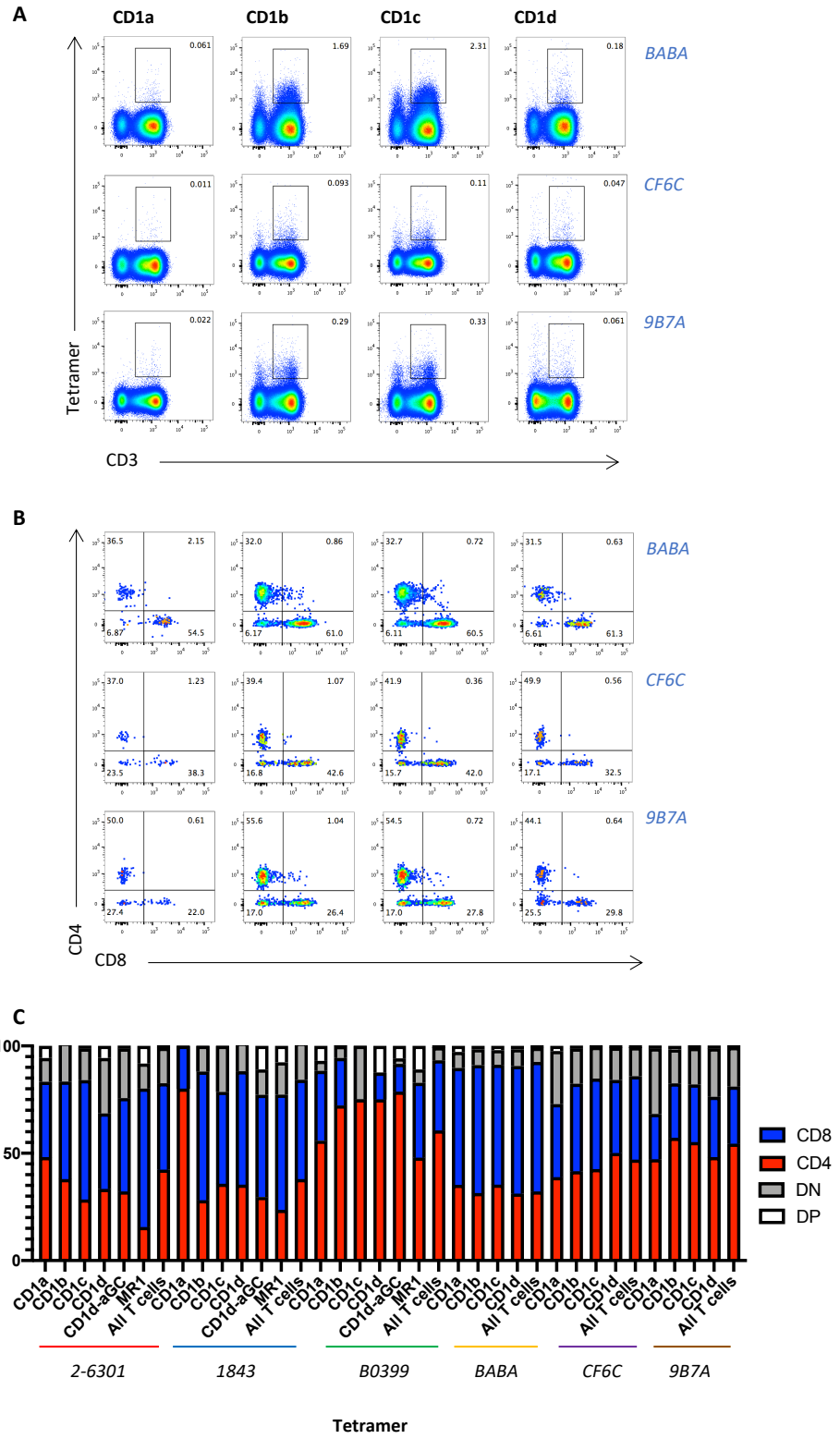
A
CD1a
CD1b
CD1c
CD1d
BABA
CF6C
9B7A
Tetramer
CD3
B
CD4
CD8
C
% of CD1-tetramer+ cells
100
50
0
CD8
CD4
DN
DP
CD1a
CD1b
CD1c
CD1d
CD1d-aGC
MR1
All T cells
2-6301
1843
B0399
BABA
CF6C
9B7A
Tetramer

Figure 5.24. CD4 and CD8 co-receptor expression by CD1-restricted T cells in healthy macaque blood. A. CD1 tetramer staining of macaque T cells. Three macaque blood donors were labelled with CD1a-endo, CD1b-endo, CD1c-endo or CD1d-endo tetramers directly *ex vivo*, and $CD3^+$ $tetramer^+$ T cells were identified by gating on $CD20^-$ single, live lymphocytes. **B.** CD4 and CD8 expression profile of $tetramer^+$ cells as gated in A. **C.** Co-receptor usage (CD4, red; CD8, blue; DN, grey; or DP, white) expressed as a percentage of all $tetramer^+$ cells or all T cells (average across all tetramer samples) in six donors. Three additional donors were analysed in a separate experiment and also labelled with CD1d-α-GalCer and MR1-5-OP-RU tetramers as control populations. Each donor is represented individually.

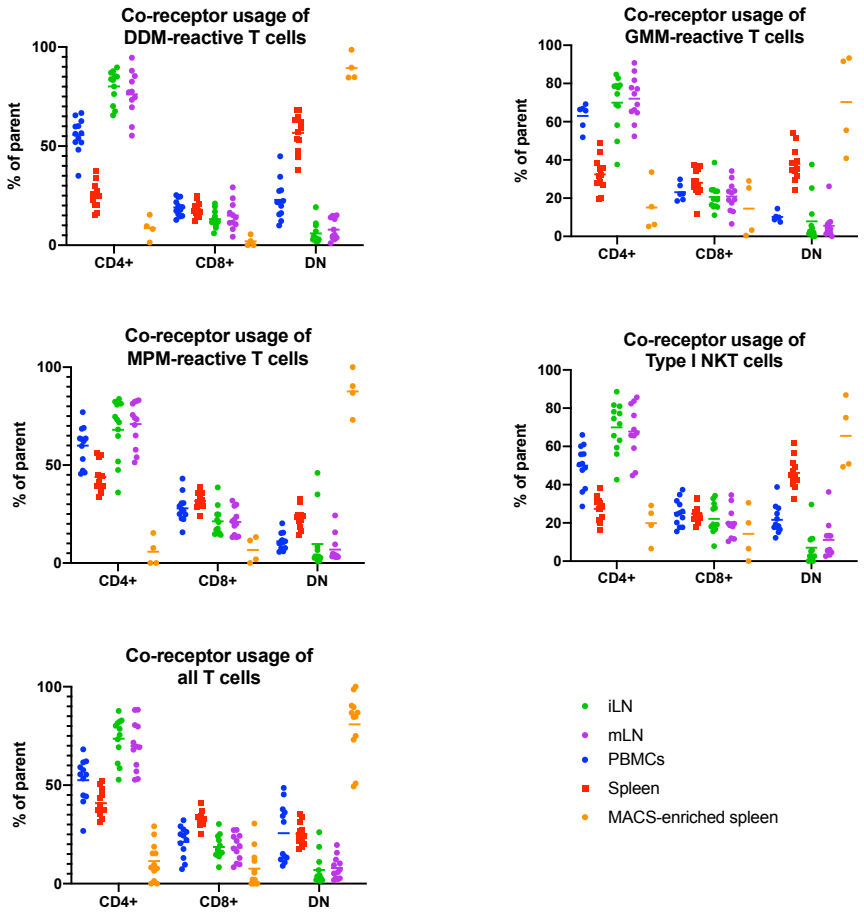

Figure 5.25. CD4 and CD8 co-receptor expression by CD1-restricted T cells in healthy juvenile macaque tissues. 12 juvenile macaque donors were necropsied and iLN (green), mLN (purple), peripheral blood (PBMCs) (purple) and spleen (red) were harvested. Samples were labelled with CD1a-DDM, CD1b-GMM, CD1c-MPM or CD1d-α-GalCer tetramers directly *ex vivo*, and splenocytes were also MACS-enriched for each tetramer (orange). $CD3^+$ $tetramer^+$ T cells were identified by gating on $CD20^-$ single, live lymphocytes. Frequencies of $CD4^+$, $CD8^+$, and double negative (DN) cells were plotted as a percentage of $tetramer^+$ cells or total T cells (average for each donor across all tetramer samples). Note that CD1b-restricted T cell populations were only analysed in six PBMC donors and only four donors were MACS-enriched for each tetramer.

and Belyakov, 2010). Most tetramer$^+$ cells were CD27$^+$, especially for CD1a-tetramer$^+$ and CD1d-tetramer$^+$ populations (*Fig.5.26)*, similar to human CD1a-restricted T cells. Macaque 1843 was the only outlier, for which the majority of tetramer$^+$ cells were CD27$^-$ and T cells from this macaque were CD27^{low} overall (*Fig.5.26b)*. This may have been an artefact of the macaque's response to influenza and SIV vaccination given that CD27$^-$ CD4$^+$ effector memory T cells display a high antigen recall response (Schiott et al., 2004).

The anti-human IL-18R mAb did not provide as clear separation between positive and negative populations, but positive cells were still discernible (*Fig.5.26)*. The greatest frequency of IL-18R$^+$ were among MAIT cells followed by type I NKT cells (*Fig.5.26)*, which is consistent with previous literature describing high IL-18R expression by innate-like T cells (Billerbeck et al., 2010, Hashimoto et al., 2003, Ussher et al., 2014). Comparatively high frequencies of IL-18R$^+$ cells were also observed among type II NKT cells and MAIT cells in some macaque donors (*Fig.5.26)*. Group 1 CD1-restricted T cells were variable but consistently lower compared to NKT cells and MAIT cells. CD1a-DDM tetramer$^+$ cells were expected not to express IL-18R as huCD1a-restricted T cells were consistently negative for innate-like T cell markers, IL-18R and CD161 in Chapter 3.2.3.

Memory phenotypes of CD1-restricted T cell populations from the blood of 12 macaques was delineated using CD95 and CD28 (*Fig.5.27a)*, as has been used in other NHP models (Pitcher et al., 2002, Messaoudi et al., 2011). Naive CD4$^+$ T cells are defined as CD95^{low} CD28^{high}, T effector memory (T_{EM}) as CD95^{hi} CD28$^-$, and T central memory (T_{CM}) as CD95^{hi} CD28$^-$ (Pitcher et al., 2002). Among all four CD1-restricted T cell subsets, T_{EM} was the least abundant population, comprising an average of 6.33-11.32% of all tetramer$^+$ cells (reflective of a low number of T_{EM} cells among all T cells) (*Fig.5.27b)*. Overall, CD1a- and CD1c-restricted T cells were predominantly naive with means of 52.2% and 65.7% respectively. CD1b-restricted T cells were predominantly T_{CM} cells (mean = 54.1%), and type I NKT cells had the most even distribution across T_{CM} and naive populations (means of 39.3% and 45.5% respectively) (*Fig.5.27b)*. In general, naive CD4$^+$ T cells had lower expression of inducible co-stimulator (ICOS) compared to T_{CM} subsets (*Fig.5.27c)*, consistent with its upregulation following activation (Hutloff et al., 1999). Interestingly, naive CD4$^+$ tetramer$^+$ cells had greater MFI for ICOS compared to all naive CD4$^+$ T cells among CD1a- and CD1d-tetramer$^+$ cells, while they were lower

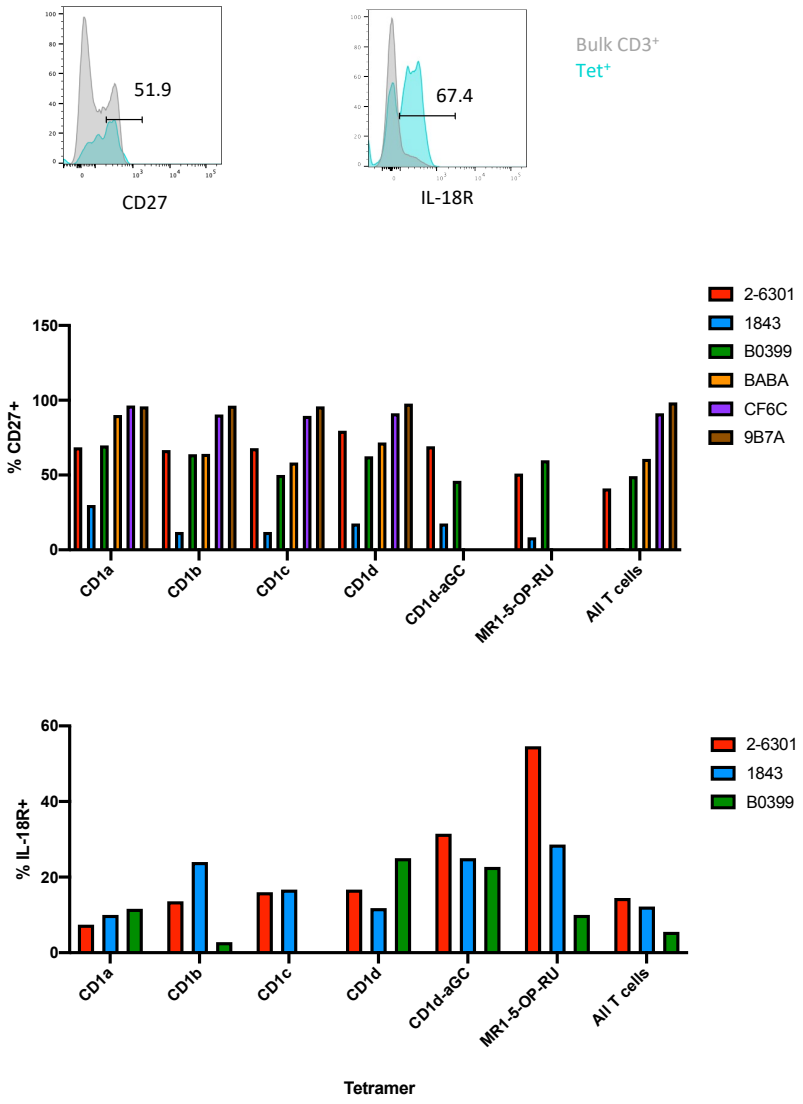

Figure 5.26. Phenotypic characterisation of CD1-restricted T cells in healthy macaque blood. Six macaque blood donors were labelled with CD1a-endo, CD1b-endo, CD1c-endo or CD1d-endo tetramers directly *ex vivo* in two separate experiments. Three donors analysed in a separate experiment were also labelled with CD1d-α-GalCer and MR1-5-OP-RU tetramers as control populations. $CD3^+$ $tetramer^+$ T cells were identified by gating on $CD20^-$ single, live lymphocytes. Gating strategy (top) and CD27 and IL-18R expression as a percentage of all $tetramer^+$ cells or all T cells (average for each donor across all tetramer samples) in six/three donors as represented by different coloured bars (bottom).

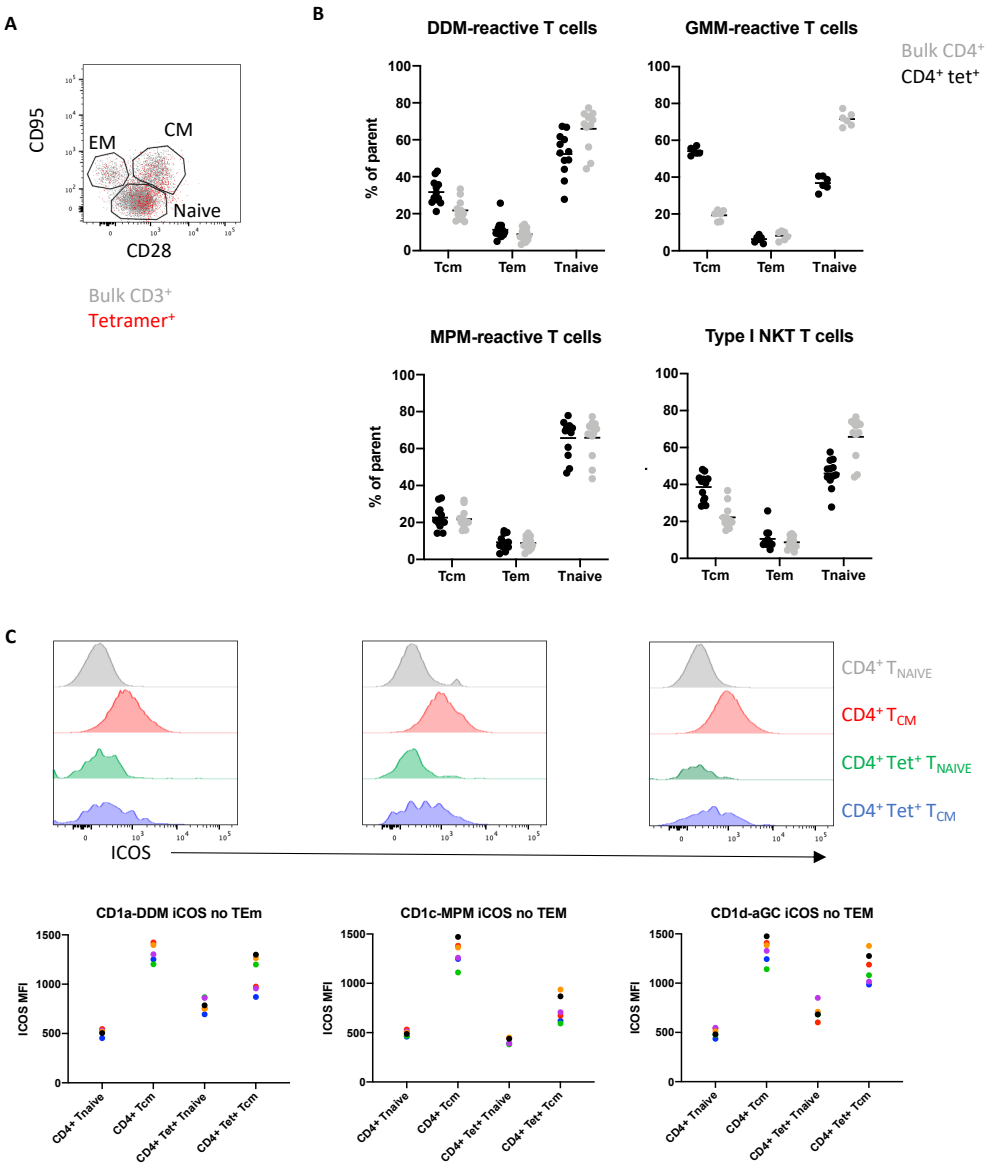

Figure 5.27. Memory phenotypes displayed by CD1-restricted T cells in healthy, juvenile macaque blood. Peripheral blood from 12 juvenile macaque donors was collected and processed to obtain PBMCs in two separate experiments. Samples were labelled with CD1a-DDM, CD1b-GMM (6 donors only), CD1c-MPM or CD1d-α-GalCer tetramers directly *ex vivo*, and $CD3^+$ $tetramer^+$ T cells were identified by gating on $CD20^-$ single, live lymphocytes. To determine memory phenotypes, samples were stained with anti-human CD95 and CD28 mAbs, and using the gating strategy indicated **(A)**, frequencies of Tcm, Tem and Tnaive were plotted as a percentage of $tetramer^+$ cells (black) or all CD4+ T cells (grey) **(B)**. **C.** CD4+ Tcm, Tem and Tnaive cells in 6 donors were assessed for their expression of inducible T cell co-stimulator (ICOS) with and without CD1a-DDM, CD1c-MPM and CD1d-α-GalCer tetramers. Each donor is represented as a separate colour.

Tcm, central memory T cells; Tem, effector memory T cells; Tnaive, naïve T cells; ICOS, inducible T cell co-stimulator

for comparative T_{CM} subsets (*Fig.5.27c)*. CD1c-MPM tetramer$^+$ CD4$^+$ T_{CM} cells also exhibited a lower ICOS MFI compared to all CD4$^+$ T_{CM} cells (*Fig.5.27c)*. The number of T_{EM} cells recovered was too low to accurately gauge ICOS expression levels (*Fig.5.27b)*.

Expression of chemokine receptors CCR5, CCR6 and CXCR3 among CD1-restricted T cells was also assessed. Some macaques, particularly BABA (CD1a) and 9B7A (CD1a, CD1b and CD1c), had distinct populations of CCR5$^+$ tetramer$^+$ T cells (*Fig.5.28)*. Other CD1-restricted T cell populations exhibited low-to-intermediate expression of CCR5 (*Fig.5.28)*. Many type I NKT cells and, to a lesser extent, MAIT cells were also CCR5$^+$, consistent with the literature (Chen et al., 2019b, Kim et al., 2002, Dusseaux et al., 2011). While CXCR3 and CCR6 are typically expressed by innate-like T cells (Kim et al., 2002, Thomas et al., 2003, Voillet et al., 2018), type I NKT cells had the lowest frequencies of CCR6$^+$ cells compared to other CD1-restricted T cell subsets (*Fig.5.28)*. The discrepancy between these results may be due to different ratios of CD4 and CD8 expression, as CCR6 is typically expressed by CD8+ and DN type I NKT cells (Kim, Johnston, and Butcher 2002). CD1-endo tetramer$^+$ cells expressed greater levels of CCR6 compared to type I NKT cells but lower than those of MAIT cells, ranging up to 12.00% (*Fig.5.28).* Consistent with previous observations, MAIT cells had high CCR6 expression without a strong positive correlation to CCR5 (Chen et al., 2019b, Kondo et al., 2007). In contrast, CXCR3 expression was high for all T cell subsets examined: averaging 34.57%, 39.00%, 40.50%, 44.10%, 55.30% and 41.23% of CD1a-, CD1b-, CD1c- restricted T cells, type II NKT cells, type I NKT cells, and MAIT cells respectively (*Fig.5.28)*.

The expression of these chemokine receptors was similarly investigated in different tissues to gain a sense of the behaviour of CD1-restricted T cells in these locations. CCR5 expression levels were consistent between tissues, apart from slightly greater expression in the spleen, which was seen among all T cells (*Fig.5.29a)*. Expression among peripheral blood CD1-restricted T cells was generally lower than what was previously observed (*Fig.5.28)*. For example, CCR5$^+$ subsets averaged below 10% for group 1 CD1-restricted T cells, but were higher and more comparable to previous observations for type I NKT cells (*Fig.5.29a)* (Hashimoto et al., 2003). CD1a-DDM tetramer$^+$ splenocytes also exhibited greater CCR5 expression compared to all T cells (*Fig.5.29a)*. CCR6 expression levels were generally highest in peripheral blood for CD1b-restricted T cells and type I NKT cells (*Fig.5.29b)*. An enrichment of CCR6 has not yet been reported for CD1b-

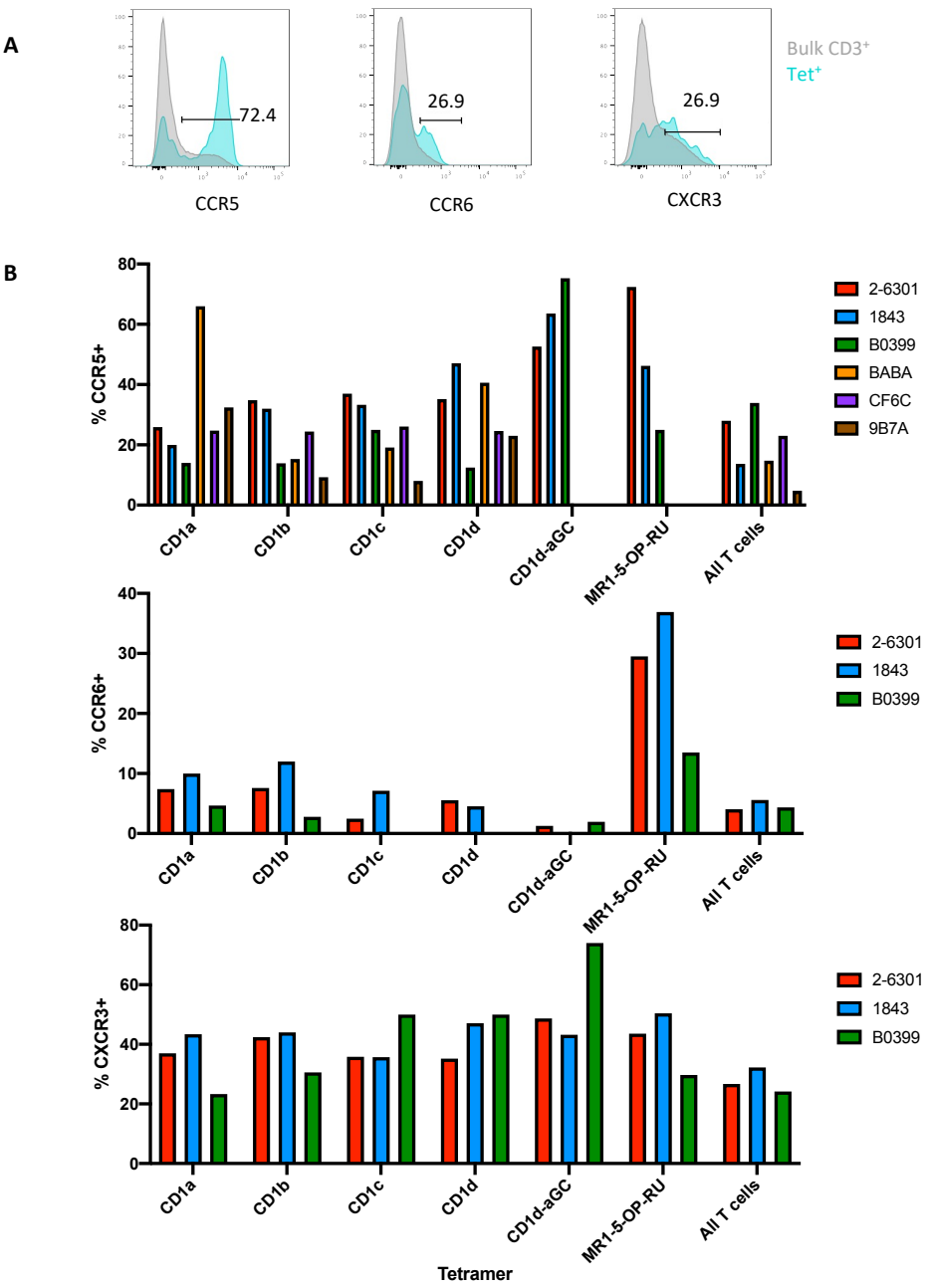

Figure 5.28. Chemokine receptor expression in CD1-restricted T cells in healthy macaque blood. Six macaque blood donors were labelled with CD1a-endo, CD1b-endo, CD1c-endo or CD1d-endo tetramers directly *ex vivo* in two separate experiments. Three donors analysed in a separate experiment were also labelled with CD1d-α-GalCer and MR1-5-OP-RU tetramers as control populations. $CD3^+$ $tetramer^+$ T cells were identified by gating on $CD20^-$ single, live lymphocytes. **A**. Representative gating strategy and **B.** CCR5, CCR6 and CXCR3 expression as a percentage of all $tetramer^+$ cells or total T cells (average across all tetramer samples) in six/three donors as represented by different coloured bars.

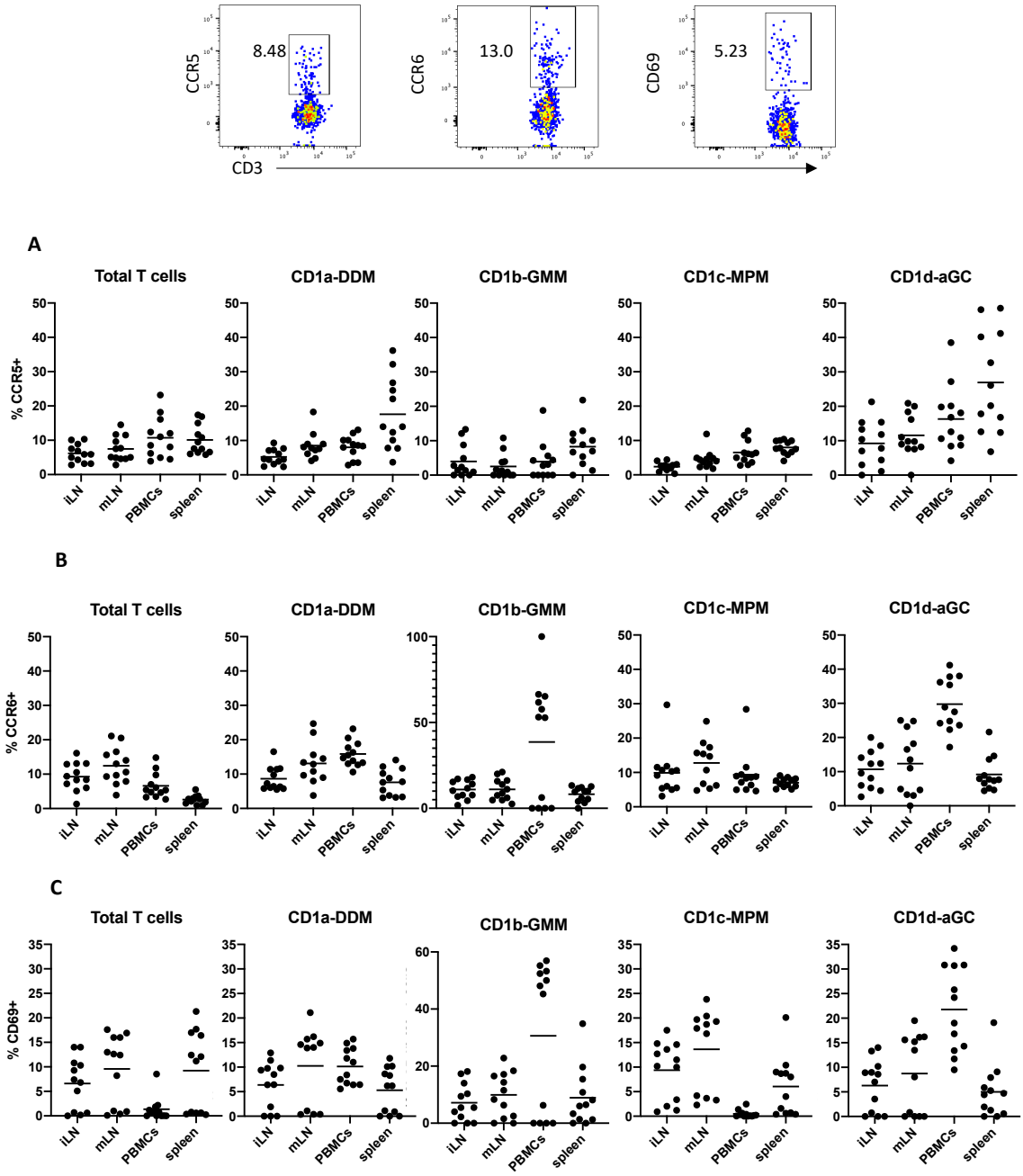

Figure 5.29. Phenotypic characterisation of CD1-restricted T cells in healthy juvenile macaque tissues. 12 juvenile macaque donors were necropsied and peripheral blood (PBMCs), spleen, thymus, iLN and mLN were harvested. Samples were labelled with CD1a-DDM, CD1b-GMM, CD1c-MPM or CD1d-α-GalCer tetramers directly *ex vivo*, and $CD3^+$ $tetramer^+$ T cells were identified by gating on $CD20^-$ single, live lymphocytes. **A**. CCR5, **B**. CCR6 and **C.** CD69 expression is displayed as a percentage of all $tetramer^+$ cells or the total T cell population. Gating for all three markers is represented above panel A.

restricted T cells, although, huCD1a-autoreactive memory T cells have been observed to express CCR6 (de Jong et al., 2010). CCR6 expression was consistently intermediate for CD1a- and CD1c-restricted T cells in all tissues, ranging up to 24.7% and 29.7% respectively (*Fig.5.29b).* The activation state of CD1-restricted T cells was assessed by CD69 expression. Peripheral blood CD1b-restricted T cells had $CD69^+$ T cell frequencies ranging from 45.30-56.90%, and type I NKT cells had similarly high frequencies compared to all T cells, indicating high levels of activation among these cells (*Fig.5.29c).* In other tissues, CD1-restricted T cells exhibited low to moderate CD69 expression (*Fig.5.29c).* These data are indicative of small populations of CD1-restricted T cells that are memory or activated T cells. Importantly, because $tetramer^+$ populations followed distinct phenotypic trends from the total T cell pool, especially with the CD1b-GMM tetramer, this suggests that tetramer staining was predominantly TCR-dependent.

Collectively, these data provide some insight into the phenotypes of CD1-restricted T cells in different macaque tissues. CD4/CD8 co-receptor expression varied between CD1-restriction and tissue type, however all CD1-restricted T cells appeared enriched for CD4 expression in LNs. NKT and MAIT cell populations exhibited high IL-18R expression. However, group 1 CD1-restricted T cells lacked expression of this innate-like T cell marker and many were naive, although memory populations were observed, particularly for CD1b-GMM reactive cells. Chemokine receptor expression also varied between the different populations, suggestive of functional diversity, although further experiments to validate this are warranted. Despite the need to further optimise ptmCD1 tetramer staining, this work provides the framework for more detailed analysis of CD1-restricted T cells in healthy macaque animals and in models of disease.

5.3 Discussion

NHP models, including macaques, are frequently used in pre-clinical testing due to their phylogenetic proximity to humans. To date, type I NKT cells have been studied in various monkeys, including sooty mangabeys and rhesus, cynomolgus, and pig-tailed macaques (Gansuvd et al., 2008, Gansuvd et al., 2003, Kashiwase et al., 2003, Motsinger et al., 2003, Yu et al., 2019, Fernandez et al., 2012, Fernandez et al., 2009, Liu et al., 2006, Rout et al., 2010b, Rout et al., 2010a, Rout et al., 2012). Due to the limitations of using murine models to study group 1 CD1-restricted T cells and CD1d-restricted type II NKT cells, novel reagents were developed for the study of all CD1-restricted T cells in PTM, including CD1 tetramers, CD1-restricted T cell lines and CD1-expressing APC lines.

Trans-species cross-reactivity of huCD1d-α-GalCer tetramer with mouse and NHP type I NKT cells is well-established. Here, cross-reactivity was only observed for TRAV10-TRAJ18-TRBV25^{+} NKT cells, and not atypical NKT cells that also recognise α-GalCer. These results suggest that the structural and molecular basis for CD1d–Ag recognition between type II and atypical NKT cells are fundamentally distinct between humans and macaques, as cross-reactivity likely relies on the conservation of key contact regions for both the TCR and CD1d.

Mammalian type I NKT TCRs use a conserved docking mode to recognise CD1d-Ag complexes (Rossjohn et al., 2012, Borg et al., 2007, Brossay et al., 1998, Pellicci et al., 2009). By using parallel docking over the F'-pocket of CD1d, they can recognise a range of lipid antigens (Le Nours et al., 2016, Girardi and Zajonc, 2012). Conversely, type II and atypical NKT TCRs can adopt distinct docking modes over CD1d-Ag complexes (Almeida et al., 2019, Le Nours et al., 2016, Pellicci and Uldrich, 2018). It hence may be differences in the way these individual TCRs engage CD1d that influence whether they are cross-species-reactive.

In addition, variable cross-reactivity was observed among group 1 CD1-restricted T cells. Like NKT cells, CD1b-restricted T cells exhibited varying levels of trans-species cross-reactivity between macaque and human CD1b that was somewhat antigen-dependent, consistent with a previous study revealing cross-reactivity in the presence of GMM (Morita et al., 2008). Here, for the first time, cross-reactivity was observed independently of GMM. CD1b-restricted TCRs might therefore also adopt different mechanisms of

binding CD1b-Ag complexes, with some docking in a conserved manner onto human and macaque CD1b. CD1b has the greatest homology between humans and PTM compared to other CD1 isoforms (*Table 5.1)*, which may contribute to its higher degree of trans-species reactivity. This is also the first instance of cross-reactivity observed between ptmCD1c and a huCD1c-restricted TCR, in this case presenting endogenous self-lipids. Cross-reactivity was not tested in the presence of a mycobacterial lipid, such as MPM, and a previous study did not reveal any reactivity of CD1c-restricted clone CD8-1 in the presence of mycobacterial lipid extracts (Morita et al., 2008). In contrast, huCD1a-restricted T cells did not recognise ptmCD1a, consistent with the previous lack of activation of a huCD1a-restricted T cell clone with rhesus macaque CD1a (Morita et al., 2008). CD1a has the least conservation between humans and PTMs, which may explain the inability of huCD1a-restricted TCRs to dock onto ptmCD1a in a way analogous to huCD1a (albeit human and macaque CD1a molecules were similar enough that one mAb clone targeting huCD1a also bound ptmCD1a).

After confirming their binding reactivity, ptmCD1 tetramers were employed to label healthy human peripheral blood for T cells restricted to ptmCD1. HuPBMCs labelled with ptmCD1d tetramer revealed small populations of tetramer^{+} cells, which may have been a result of binding independent of CD1-restriction, or alloreactivity due to the monomorphic nature of CD1 in both species. Human T cells labelled with ptmCD1b and ptmCD1c tetramers revealed evidence of TCR-independent binding akin to that seen with huCD1b, huCD1c and huCD1d tetramers (Gherardin et al., 2021). A large proportion of T cells were positively labelled for ptmCD1b and ptmCD1c tetramers, which likely included cells that bound these tetramers in a TCR-independent manner.

CD36 and SCARB1 were assessed as potential markers to target for tetramer staining optimisation. CD36, important for the recognition and endocytic uptake of oxidised phospholipids (Asch et al., 1987, Stewart et al., 2010), can bind lipidic molecules such as oxidised low-density lipoproteins, phospholipids, long-chain fatty acids, and bacterial diacylated lipopeptides including mycobacterial lipids (Park, 2014). Documented CD1 lipid antigens reported include lipopeptides and phospholipids (reviewed in (Kaczmarek et al., 2017)), thereby providing potential interaction sites should CD36 capture the same lipid antigens as CD1 molecules. SCARB1, also binds low-density and high-density lipoproteins with high affinity (Acton et al., 1996, Acton et al., 1994), and therefore may

display a similar phenomenon. CD36 is highly conserved across mammals (Holmes, 2012), which may explain TCR-independent binding to CD1 tetramers being observed across species (humans, mice (data not shown) and macaques). When comparing CD1c tetramer staining in human and macaque samples, TCR-independent staining appears more prominent in human samples, which may be reflective of the human *CD36* gene containing transcription factor binding sites contributing to a high gene expression level (6.6 times higher) (Holmes, 2012), thereby providing more potential receptors.

The findings here suggest that CD36 and SCARB1 may bind ptmCD1b and ptmCD1c molecules, and that blocking these scavenger receptors prior to tetramer staining may minimise TCR-independent staining. There may also be a way to manipulate CD1 tetramer staining to exclude cells that do not bind via their TCR, by loading CD1 molecules with specific lipid antigens (and removal of lipids that act as ligands for CD36 and SCARB1). Lipid-dependent reduction in TCR-independent staining was first seen with huCD1d-α-GalCer, which cannot bind ILT-4, presumably due to conformational changes to CD1d caused by α-GalCer compared with CD1d containing endogenous lipids (Li et al., 2009). A similar phenomenon was observed with ptmCD1b-GMM, which resulted in a reduction in tetramer^{+} cells compared to CD1b-endo. This suggests that the addition of GMM (in the detergent tyloxapol) alters the CD1b conformation, GMM and/or the detergent interfere with the interaction, or the detergent removes lipids that act as CD36 and SCARB1 ligands from CD1b. Notably, the addition of MPM did not reduce tetramer-independent staining for CD1c, but it may be possible to optimise tetramer staining with defined lipid antigens.

Prior to this study, the TCR repertoire of macaque CD1-restricted T cells remained ill-defined. While this was merely a preliminary study including a small number of T cell clones, the sequences determined revealed a diverse TCR repertoire with some hints of recurring variable gene usage patterns, similar to biases among human CD1-restricted T cells reported in this thesis and by others (Van Rhijn et al., 2014, Vincent et al., 2005, Cohen et al., 2009, de Jong et al., 2010, de Lalla et al., 2011, Grant et al., 1999). Studies of macaque type I NKT cells suggest the presence of a "pan-primate" type I NKT TCR rearrangement, incorporating the same TCR α- and β-chain variable genes and exhibiting high conservation among residues that mediate contacts between the TCR and CD1d-α-GalCer (Gansuvd et al., 2003, Kashiwase et al., 2003, Motsinger et al., 2003, Yu et al.,

2019). It is therefore unsurprising that there may be pan-primate patterns of variable gene usage among CD1-restricted T cells, especially among those T cells that recognise mycobacterial lipid antigens, such as the TRBV28 gene bias observed among CD1a-DDM-reactive T cells. Analysis of ptmCD1a-restricted TCRs revealed an intra-donor bias for TRBV28, which is the same variable gene bias determined earlier in this study among huCD1a-restricted TCRs. There were other regularly occurring variable genes among ptmCD1b-, ptmCD1c-, and ptmCD1d-restricted TCRs, however with the small number sequences, it is difficult to determine whether these were true biases.

A number of ptmCD1-restricted SKW-3 T cell lines were generated for use in tetramer labelling and activation assays, along with a suite of ptmCD1 transfectant C1R cells lines. Both rhesus macaque and murine type I NKT cells respond to huCD1d transfectants in the presence of α-GalCer (Ishihara et al., 2000, Nicol et al., 2000, Nieda et al., 1999, Yu et al., 2019), but given the limited trans-species cross-reactivity between CD1 molecules and group 1 CD1-restricted T cells or type II NKT cells, the cell lines produced here will be useful tools in studying all macaque CD1-restricted T cells *in vitro*. Such CD1-expressing C1R cell lines could be used in characterisation and functional studies of CD1-restricted T cells. They could also be employed to expand CD1-restricted T cells *in vitro* to use in adoptive immunotherapies as has previously been done for type I NKT cells (Bagnara et al., 2009), which are particularly of interest given the monomorphic nature of CD1 molecules.

No study has yet enumerated CD1-restricted T cell populations in macaques other than type I NKT cells. Lipid-reactive populations were assessed in several tissues using CD1a-DDM, CD1b-GMM, CD1c-MPM and CD1d-α-GalCer tetramers. One study of rhesus macaque type I NKT cells reported a small percentage of type I NKT cells by labelling Vα24$^+$ T cells, isolating 0.27% among PBMCs and 0.15% in spleen, the majority of which were also 6B11$^+$ (Gansuvd et al., 2003). Another study reported type I NKT cells occurring within <0.01-0.35% of splenocytes anti-Vα24 with mCD1d-α-GalCer tetramers (Motsinger et al., 2003). More recently, huCD1d-α-GalCer tetramers have been used to isolate rhesus macaque type I NKT cells, which occur at varying frequencies, typically <0.1% of CD3$^+$ T cells (Yu et al., 2019), comparable to the results here. In the current study, CD1-restricted T cells were generally more frequent in the spleen compared to LNs, and were present at similar frequencies to type I NKT cells enumerated

previously (Yu et al., 2019). CD1c-restricted T cells were consistently the most abundant population in each lymphoid tissue, while CD1b-restricted T cells were the least abundant, which is consistent with autoreactive CD1-restricted T cell populations identified in humans (de Lalla et al., 2011).

In concordance with previous observations for CD1-autoreactive T cell subsets among huPBMCs using tetramers (data presented as part of Catriona Nguyen-Robertson's Honours Thesis, submitted to The University of Melbourne in 2015), CD1-restricted T cell subsets were relatively low in frequency among PTM peripheral blood T cells, ranging from <0.01-0.65%. CD1c-restricted T cells were consistently the most abundant in ptmPBMCs, which is in line with the observation that huCD1c-autoreactive T cells were the most abundant CD1-autoreactive T cell subset (de Lalla et al., 2011). The frequencies of CD1-restricted T cells determined here were more in line with those of de Jong et al., who estimated that the frequency of huCD1a-autoreactive T cells among peripheral blood memory T cells is between 0.02-0.4% (de Jong et al., 2010). The variability between these results may be due to different lipid specificities, as the two studies used different cell lines to produce CD1 molecules that may have had different endogenous lipid repertoires, and here, mycobacterial lipid antigens were used. Lymph node, spleen and PBMC type I NKT cell frequencies were consistent with the findings of Yu et al., for which most donors had fewer than 0.1% of T cells as tetramer^{+} cells in these tissues while some donors had frequencies up to 0.5% (Yu et al., 2019), emphasising the variability between donors.

Liver, rectum, and BAL samples exhibited higher frequencies of CD1-restricted T cell subsets compared to lymphoid tissues and blood. CD1a-restricted T cells were the most predominant population in the liver, followed by CD1d-, CD1c- and then CD1b-restricted T cells. Murine NKT and MAIT cells are enriched in the liver and thought to play an important role there (Huang et al., 2018), and these data suggest that other CD1-restricted T cells, especially CD1a-restricted T cells, may be similarly enriched in macaques (albeit similar enrichments are not observed in humans). The rectum had even higher frequencies of CD1a-resricted T cells. Liver, rectum, BAL and lung tissues were more difficult to process compared lymphoid tissues and blood, and as a result fewer cells were obtained, potentially leading to an inaccurate estimate of frequencies. It is therefore imperative to optimise tissue harvesting and tetramer staining techniques to obtain clear, distinct

populations of CD1-restricted T cells in these tissues for further enumeration and characterisation. Magnetic-enrichment of tetramer staining in splenic samples produced the most distinct populations of tetramer$^+$ cells, albeit appeared to also enrich for a CD4$^-$ CD8$^-$ DN T cell population, highlighting that this method is worth pursuing for tissues that have enough cells.

A preliminary phenotypic analysis of CD1-restricted T cell populations in lymphoid tissues and peripheral blood was performed, with the assumption that tetramer$^+$ cells were indeed CD1-restricted T cells. CD4 and CD8 expression was heterogenous among CD1-autoreactive T cell populations, which was surprising given the predominant expression of CD4 by huCD1-restricted T cell populations shown here and by others (de Jong et al., 2010, de Lalla et al., 2011). The proportions of DDM-, GMM-, MPM- and α-GalCer-reactive T cells that were CD4$^+$ were typically higher in the LNs and lowest in the spleen, reflecting an increase in DN cell frequencies. Previous findings suggest that while human type I NKT cells are typically CD4$^+$ or DN, their rhesus and cynomolgus counterparts contrastingly predominately express CD8 (Motsinger et al., 2003, Yu et al., 2019). Here, however, ptmCD1-restricted T cells (recognising bacterial lipids) mirrored their human counterparts and were mostly CD4$^+$ albeit with greater variability. As lipid-reactive CD8$^+$ T cells mediate responses in BCG immunisation (Kawashima et al., 2003, Chen et al., 2009) and CD4$^+$ T cells are critical for control of Mtb infection (Boom et al., 2003), the existence of both these subsets among CD1-restricted T cells is likely to be beneficial.

Mouse and human NKT cells are known to express innate-like and memory T cell markers such as CD161 (Exley et al., 1997, Exley et al., 1998), but interestingly, macaque type I NKT cells have previously been found to be low or negative for this marker, the exception being within tissues such as spleen and liver (Gansuvd et al., 2003, Yu et al., 2019). IL-18R expression was investigated, which is typically positively correlated with CD161 in NKT cells, MAIT cells and T_h17 cells (Cosmi et al., 2008, Dusseaux et al., 2011, Martin et al., 2009b). CD1a-restricted T cells were consistently low for IL-18R expression compared to the other populations, similar to huCD1a-restristed T cells, which are consistently negative for IL-18R and CD161 (Chapter 3). Meanwhile, type II NKT cells and CD1c-restricted T cells in PTM displayed higher levels of IL-18R expression similar to MAIT cells and type I NKT cells.

Memory phenotypes among blood CD1-restricted T cell populations were delineated using CD95 and CD28 as done in other NHP models (Pitcher et al., 2002, Messaoudi et al., 2011). Few T_{EM} cells were detected in the blood, consistent with other studies of pig-tailed and rhesus macaques (Mason et al., 2008, Pitcher et al., 2002), and naive T cell were more abundant given that the macaques studied were juveniles (Saule et al., 2006, Thome et al., 2014, van Gent et al., 2009). CD1a-, and to a greater extent, CD1c-restricted T cells, were predominantly naive, which is similar to a previous observation that human CD1-autoreactive T cells develop naive/memory dynamics but remain mostly naive in adult peripheral blood (de Lalla et al., 2011). More than half of GMM-reactive T cells displayed a T_{CM} phenotype, aligning with the memory phenotype of CD1b-GMM and CD1b-mycolic acid-reactive T cells seen in humans (Lopez et al., 2020). There were also many type I NKT cells that displayed a memory phenotype, and donors tended to have a more even distribution across T_{CM} and naive populations, reflective of circulating type I NKT cells displaying an activated/effector memory phenotype in rhesus macaques and humans (D'Andrea et al., 2000, Gansuvd et al., 2003, Rout et al., 2010b, Yu et al., 2019, Sandberg et al., 2004), however the majority were still naive. The difference between studies may be explained by the use of different markers used to identity T cells with an activated/effector memory phenotype (e.g. CD45RO/CD45RA, CCR7 and CD28), or species differences. $CD4^+$ T_{CM} cells were assessed for ICOS which upregulated on $CD4^+$ T cells following antigenic stimulation and typically expressed by cells with prior activation. Among $tetramer^+$ $CD4^+$ T_{CM} subsets ICOS expression was lower compared to all $CD4^+$ T_{CM} cells. Given that ICOS expression levels are correlated with the type of cytokines produced by cells (e.g. high expression is linked to IL-10 and intermediate expression to T_h2 cytokines), the lower expression of ICOS compared to other T_{CM} cells may be reflective of the inflammatory potential of CD1-restricted T cells (Lohning et al., 2003).

The activation status of CD1-restricted T cells was assessed by CD27 and CD69, which is transiently expressed on mature T cells (Cosulich et al., 1987, Hara et al., 1986, Testi et al., 1989). Most CD1-restricted T cells were $CD27^+$, particularly within CD1a- and CD1d-restricted T cell populations. CD69 levels were high among peripheral blood GMM-reactive T cells, which may correlate to a higher expression of T_{CM} cell markers here and the memory phenotype of human GMM-reactive T cells, suggesting prior *in vivo* activation of such cells (Lopez et al., 2020). Circulating type I NKT cells also had

high expression of CD69, in contrast to a rhesus macaque study that found CD69 expression to be higher in lymphoid tissues compared to the blood (Yu et al., 2019). These differences may be an artefact of age or the fact that CD69 may not always be reflective of activation. This is in line with another study that found human type I NKT cells to be negative for HLA-DR and CD69 in neonates, but were still considered active due to high CD25 expression (D'Andrea et al., 2000). It will therefore be interesting to investigate the balance of activating and inhibitory markers on CD1-restricted T cell subsets in human and macaques.

Distinct populations of $CCR5^+$ CD1-restricted T cells were identified, and consistent with previous studies indicating abundant CCR5 expression, with type I NKT cells and MAIT cells exhibiting the highest expression levels (Chen et al., 2019b, Kim et al., 2002, Dusseaux et al., 2011, Hashimoto et al., 2003). CCR5 is the main receptor used by HIV for virus entry into the cell and cell-to-cell spread in humans, and is also the major co-receptor for simian immunodeficiency virus (SIV) pathogenesis in macaques (Littman, 1998, Unutmaz et al., 1998). Given the susceptibility of $CCR5^{hi}$ $CD4^+$ T cells to HIV infection (Motsinger et al., 2002) and the predominant expression of CD4 by macaque lipid-reactive T cells, their expression of CCR5 may influence the impact of SIV/HIV on lipid-reactive T cell populations. In rhesus macaques, while the majority of $V\alpha24^+$ NKT cells are $CD4^-$, they exhibit high expression of CCR5 and are more susceptible to SIV infection than conventional $CD4^+$ T cells (Motsinger et al., 2003). With many ptmCD1-restricted T cells being $CCR5^+$ in this study, these cells warrant further investigation in the context of SIV immunopathology.

As peripheral blood MAIT and type I NKT cells are associated with CCR5, CCR6 and CXCR3 (Chen et al., 2019b, Kim et al., 2002, Thomas et al., 2003, Voillet et al., 2018), expression of these chemokine receptors by ptmCD1-restricted T cells was investigated. There was no correlation between CCR5 and CCR6 expression as observed by others among human innate-like T cells (Chen et al., 2019b, Kondo et al., 2007). CCR6 expression levels were generally highest in peripheral blood compared to other tissues for CD1b-restricted T cells and type I NKT cells, and were consistently intermediate among CD1a- and CD1c-restricted T cells. CCR6 is involved in both inflammatory and homeostatic roles in the immune system (Baba et al., 1997, Cook et al., 2000), suggesting that CD1-restricted T cells, especially GMM-reactive T cells and NKT cells, may play a

role in these processes. CXCR3 expression levels were also high, suggesting that these T cell subsets are equipped to respond to proinflammatory chemotactic cues, such as IFN-γ sensed by CXCR3 (Loetscher et al., 1996). It was reassuring that CD1-Ag tetramer$^+$ populations did not simply mimic expression of these markers for the whole T cell population, indicating that tetramer staining, especially for CD1a-DDM, CD1b-GMM and CD1d-α-GalCer tetramer$^+$ cells were likely staining in a TCR-dependent manner.

In summary, this is the first study to demonstrate the production and use of ptmCD1 tetramers loaded with mammalian endogenous lipids or mycobacterial lipid antigens in order to identify and isolate CD1-restricted T cell populations in macaque tissues. These T cells exhibited cell surface phenotypes somewhat similar to other unconventional T cells and therefore may also play a role in coordinating adaptive and innate immune responses like they do in humans and mice. Cell lines that express ptmCD1-restricted TCRs or transmembrane ptmCD1 molecules were generated and will be useful tools to study these cells *in vitro*. Thus, this work forms a basis to build upon knowledge of lipid-reactive T cells in NHP models. This is particularly important as CD1-restricted T cells have been implicated to play a role in many diseases, and therefore may represent important targets for T cell immunotherapy approaches that are not possible or more cumbersome with polymorphic antigen-presenting molecules. Given that some immunotherapies have been demonstrated to directly cross-react with both their human and macaque targets, use of macaque models will allow rapid translation of new laboratory discoveries into clinical trials (Miller et al., 2010, Rhode et al., 2016, Weaver et al., 2009). Studying CD1-restricted T cells in macaques will hence provide great insight into diseases in which lipids play a large role, including mycobacterial infections and autoimmune diseases such as multiple sclerosis. Furthermore, as many studies of COVID-19 are now being carried out in macaques (Munoz-Fontela et al., 2020, Salguero et al., 2021), these reagents may provide some insight into the role that these cells play in different infections. Collectively, these data represent a major step forward in understanding lipid-reactive T cells in macaques to provide a basis for studying these cells in NHP models of disease.

Chapter 6. Analysis of CD1a-restricted T cells in the skin and skin allergy

6.1 Introduction

Accumulating evidence from numerous studies suggests a role for CD1a and CD1a-restricted T cells in skin immunity. CD1a is predominantly found in human skin and is highly abundant on epidermal Langerhans cells where it can capture and present lipids in skin oils (de Jong et al., 2014, Meunier et al., 1996). Previous studies suggest that CD1a-autoreactive T cells are also present in the dermis (de Jong et al., 2010, Cotton et al., 2021). Additionally, peripheral blood CD1a-autoreactive T cells with a memory phenotype have been observed to express cutaneous lymphocyte antigen (CLA), a marker identifying T cells that participate in skin immunity (Fuhlbrigge et al., 1997, Berg et al., 1991, Picker et al., 1990), in addition to CCR4, CCR6, and CCR10, which together enable skin-homing (de Jong et al., 2010, Duhen et al., 2009).

Supporting the notion of CD1a-restricted T cells playing a role in the skin, they can recognise small, headless autoantigens in skin (de Jong et al., 2014). These oily lipids found in skin are stimulatory given that they do not interfere with TCR-CD1a contact, at least for TCRs that have been interrogated to date (de Jong et al., 2014). Apolar lipids, such as squalene, triacylglycerols (TAGs), free fatty acids and wax esters, which lack bulky and/or polar headgroups are considered agonistic. Meanwhile CD1a self-lipids with charged or large headgroups (e.g. sphingolipids and phosphatidic acid-containing compounds with varying headgroups, chain length and saturation) tend to be antagonistic for CD1a-restricted T cells (de Jong et al., 2014). This is in line with the "absence of interference" model of recognition. However, there still appear to be restrictions on CD1a recognition of small oily autoantigens, as cholesterol and cholesterol esters, which are similarly hydrophobic to the aforementioned apolar lipids, are not recognised by CD1a-autoreactive T cells (de Jong et al., 2014). Understanding the reactivity of CD1a-restricted T cells to these self-lipids is important as the epidermis has a greater enrichment of TAGs than any other tissue, and squalene, a component of sebum, is enriched in the sebaceous glands (Nicolaides, 1974).

The presence of CD1a-expressing Langerhans cells, CD1a autoantigens, and CD1a-restricted T cells that express skin-homing markers suggest roles for CD1a in skin

homeostasis, tissue repair and immunity, particularly when the barriers between the dermis and epidermis break down. A number of studies discuss CD1a-autoreactive T cells in the context of immunopathological conditions (e.g. allergy or autoimmunity) (Agea et al., 2005, Roura-Mir et al., 2005a, Shamshiev et al., 1999). Upon activation, some CD1a-autoreactive T cells adopt a skin-homing T_h22 phenotype, producing IL-22 sometimes together with IFN-γ and IL-2 (de Jong et al., 2010, Duhen et al., 2009, Eyerich et al., 2009, Nograles et al., 2009, Cotton et al., 2021). IL-22 acts on non-hematopoietic epithelial cells in the skin, such as keratinocytes (Wolk et al., 2004), to trigger the production of antimicrobial peptides and gene expression promoting cellular differentiation and survival (Boniface et al., 2005, Wolk and Sabat, 2006). IL-22 participates in many chronic inflammatory conditions, including those in the skin, and is a target in psoriasis treatment (Zhang et al., 2011). Psoriatic lesions are known to contain T_h22 cells, and the over-production of IL-22 promotes acanthosis (epidermal thickening) associated with psoriasis (Lowes et al., 2014, Boniface et al., 2007), with CD1a-restricted T cells thought to play a role. CD1a-restricted T cells have also been observed to produce IL-17 upon activation, another cytokine implicated in psoriasis pathogenesis (Kim et al., 2016, von Stebut et al., 2019). CD1a-dependent production of IL-17 and IL-22 by $CD4^+$ T cells have since been implicated in psoriatic skin inflammation, providing evidence for CD1a-restricted T cells in its pathogenesis (Kim et al., 2016).

There is also evidence of CD1a-mediated contact hypersensitivity and allergic reactions. Unlike other CD1 isoforms, surface CD1a molecules rapidly capture extracellular lipid antigens without requiring antigen processing within the endosomal/recycling network (Manolova et al., 2006, Sugita et al., 1999) and could therefore potentially rapidly respond to lipids within or absorbed by the skin. Neoantigens that are presented by CD1a can be generated by the cleaving of self-phospholipids by phospholipases in bee and wasp venom, and house dust mites, contributing to the allergies individuals exhibit towards these creatures (Bourgeois et al., 2015, Jarrett et al., 2016b). Further evidence supporting a role for these cells in allergic dermatitis is an elevated frequency of bee and wasp venom-responsive T cells in allergic individuals compared to non-allergic individuals (Subramaniam et al., 2016). In fact, similar neoantigens are also produced by phospholipases released by mast cell exosomes, contributing to psoriasis pathogenesis (Kim et al., 2016, Cheung et al., 2016). Changes in the lipid repertoire, and subsequently,

lipids captured and presented by CD1a, may therefore contribute to skin inflammation and allergy.

LCs themselves also initiate and regulate contact hypersensitivity (Bennett et al., 2005). CD1a-restricted T cells express the aryl hydrocarbon receptor (AHR) (de Jong et al., 2010), which is expressed by skin cells and is involved in LC maturation, IL-22 production and contact hypersensitivity. Hence, CD1a-restricted T cells may play a role in facilitating IL-22 production via AHR or other forms of signalling (Quintana et al., 2008, Trifari et al., 2009, Veldhoen et al., 2009). In addition, CD1a-restricted T cells have been shown to contribute to the allergic response to poison ivy by mediating IL-17 inflammatory responses via the recognition of C15:2 urushiol in a similar manner to psoriasis pathogenesis (Kim et al., 2016).

More recently, CD1a contact allergens have been identified in cosmetic products, specifically those that contain balsam of Peru, which is commonly used in skincare products and is a contact allergen seen in medical practice (Fransway et al., 2013, Wolf et al., 2013, Nicolai et al., 2020). A number of small, hydrophobic compounds in balsam of Peru such as C15 farnesol, benzyl benzoate and benzyl cinnamate, were observed to trigger CD1a-mediated contact hypersensitivity reactions and CD1a-restricted T cell IFN-γ production (Nicolai et al., 2020). Most known contact allergens in cosmetic products are nonpeptidic small molecules, such as cations or metals, that interfere with TCR recognition of HLA-peptide complexes (Kaplan et al., 2012, Peiser et al., 2012), while these act as independent antigens presented by CD1a. The aforementioned study hence provided an example of tree oils in dermatological products that are known to initiate potent contact hypersensitivity also functioning as CD1a antigens (Nicolai et al., 2020).

To further evaluate the role of CD1a-restricted T cells in skin immunity and homeostasis, they were isolated and phenotypically characterised from healthy skin donors and compared to other unconventional T cell subsets. In addition, following a personal allergic reaction to sunscreen, this study aimed to determine whether the causative agent of the reaction was also a CD1a allergen that similarly activates CD1a-restricted T cells.

6.2 Results

6.2.1. Isolation of skin CD1-restricted T cells

CD1a-restricted T cells have been implicated to play a role in skin immunity, especially given their expression of skin-homing markers among circulating memory cells (de Jong et al., 2010), yet remain relatively uncharacterised in this tissue. Building on previous work interrogating these cells in skin (Cotton et al., 2021), they were isolated from healthy human skin samples for characterisation. Skin samples were obtained following abdominoplasty surgery and donor-matched blood was processed to obtain PBMCs when available. Subcutaneous fat was trimmed off all skin samples, and the dermal and epidermal layers were either processed together or separately. Epidermis was separated from dermis by scraping the top layers of skin, and either whole skin or separate layers were enzymatically digested in 1 mg/mL Collagenase P.

As the use of collagenase in tissue digestion can impact surface marker epitopes targeted by mAbs for identification and characterisation, mAbs used were first tested with PBMCs treated with or without Collagenase P under the same conditions (*Fig.6.1).* In most cases, staining profiles with CD45, CD3, CLA, αβ-TCR, and γδ-TCR remained similar with and without Collagenase P. The most striking difference was that the anti-CD4 mAb binding epitope remained intact for clone RPA-T4 but not SK3 following Collagenase P digestion, determined by the absence of $CD4^+$ cells in the sample stained with clone SK3. There was also a reduction in $CD1a^+$ cell populations using the H149 anti-CD1a mAb clone, which was not apparent with the SK9 clone. These staining profiles informed the antibodies used in phenotypic analyses of skin T cells digested with Collagenase P to ensure intact mAb binding epitopes.

Whole skin, epidermis and dermis samples were compared in three donors to determine which processing method would yield the highest T cell recovery. Samples containing epidermis only yielded the most T cells ($CD45^+$ $CD3^+$), while fewer cells in total were recovered from whole skin and dermis samples *(Fig.6.2a)*. $Tetramer^+$ cells were difficult to isolate in whole skin and dermis samples given the low frequency of T cells, while small populations of CD1a-restricted T cells and MAIT cells were observed *(Fig.6.2b)*, albeit they were observed at lower frequencies than in donor-matched PBMCs. Given that LCs predominantly reside in the stratum spinosum layer of the

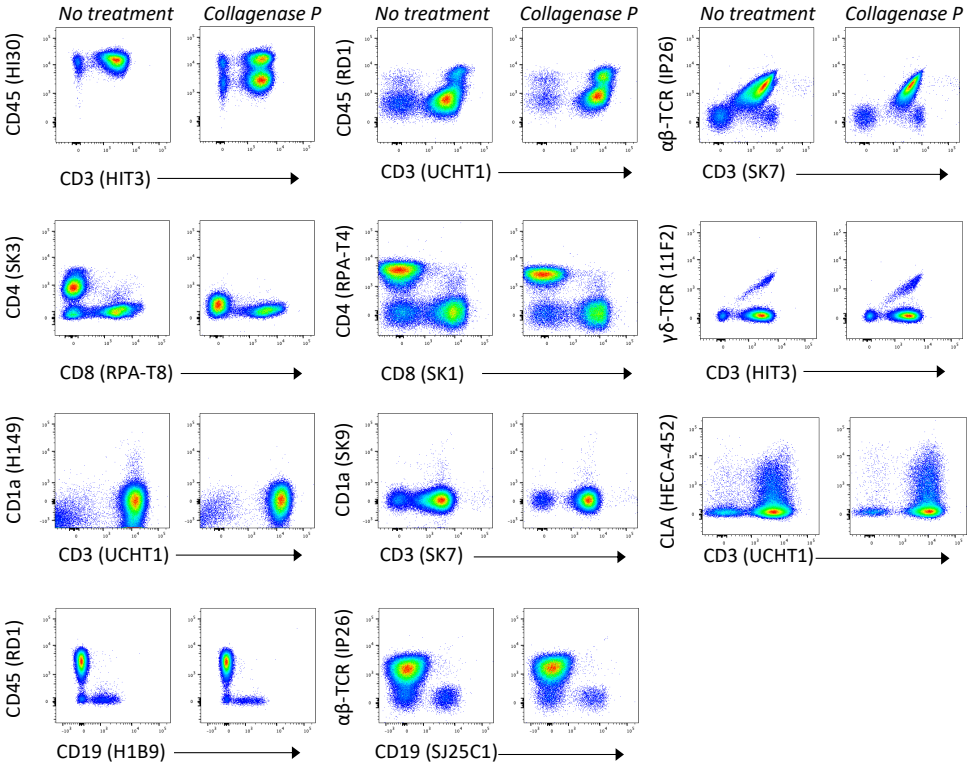

Figure 6.1. Labelling of Collagenase P-treated PBMCs with mAbs. PBMCs were incubated with 1 mg/mL Collagenase P in RF-10 media (right) or RF-10 alone (left) at 37°C for 90 minutes. Following which, they were labelled with mAbs targeting CD45, CD3, αβ-TCR, γδ-TCR, CD4, CD8, CD1a, CLA, and CD19. Cells shown are already gated on 7-AAD$^-$ single lymphocytes. Data are representative of three donors in three independent experiments.

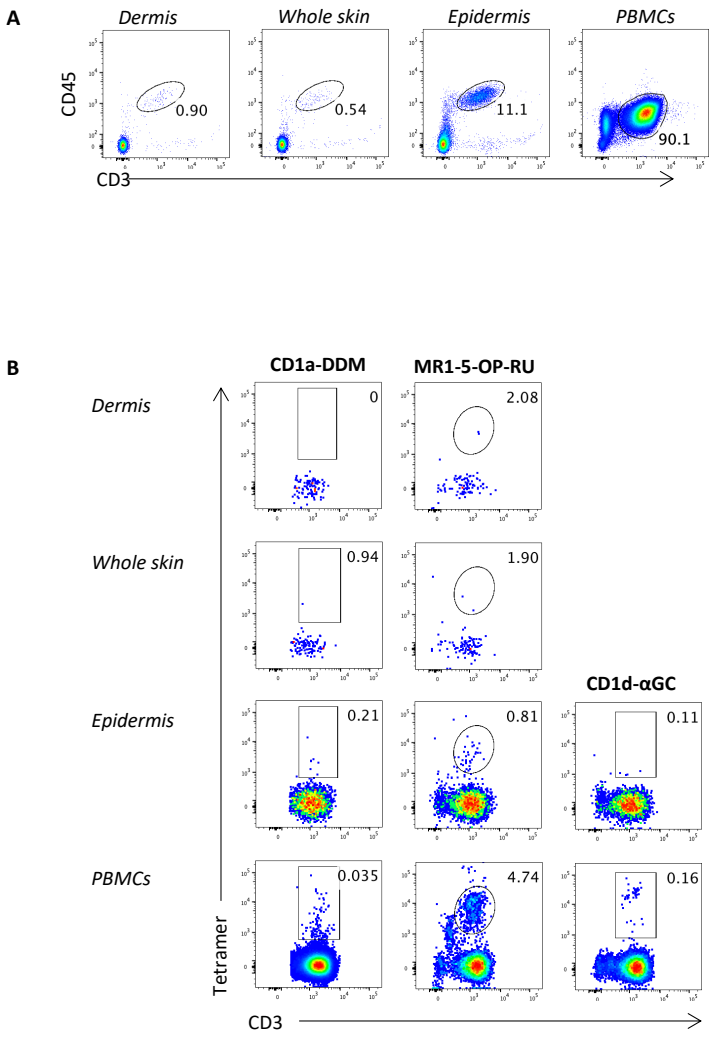

Figure 6.2 Isolation of T cells directly *ex vivo* from skin from abdominoplasty . A. Isolation of T cells from 20 cm^2 (5 x 2 cm x 2 cm squares) of epidermis, dermis and whole skin and donor-matched PBMCs. T cells were identified by expression of CD45 and CD3. **B.** T cells were labelled with CD1a-DDM, MR1-5-OP-RU, and CD1d-α-GalCer (α-GC) tetramers. Note that CD1d-α-GC was only used in epidermis and PBMC samples due to insufficient cells obtained from dermis and whole skin samples. Data representative of three donors in three independent experiments.

epidermis, and isolation from epidermis was the most fruitful (whole skin and dermal samples did not yield many T cells *(Fig.6.2a)*), further flow cytometry analyses focused only on epidermal samples.

Epidermal cells from 15 donors were labelled with CD1a-endo (lipids endogenous to GnTI$^-$ cells), CD1b-endo, CD1c-endo, CD1d-endo, CD1d-α-GalCer or MR1-5-OP-RU tetramers. To verify that tetramer labelling was specific for each CD1 molecule, epidermal cells and PBMCs were co-labelled with two, independent tetramers: CD1a-endo with CD1b-endo, CD1c-endo with MR1-5-OP-RU, and CD1d-endo with CD1d-α-GalCer *(Fig.6.3)*. Very few cells bound both tetramers, indicating that tetramer$^+$ cells in the epidermis were more likely to be true CD1-restricted T cells or MAIT cells rather than being the result of non-specific tetramer binding.

Identification of CD1-restricted T cells from human skin cells using flow cytometry proved challenging, and while all tetramers revealed small populations, more distinct populations were only observed for NKT cells and MAIT cells *(Fig.6.4a, b)*. The proportion of CD1a-, CD1b- and CD1d-restricted T cells was typically higher in skin compared to blood, while CD1c-restricted T cells and MAIT cell populations were lower in skin compared to blood. Overall, MAIT cell frequencies were the highest for both tissues in these donors, reaching as high as 3% and 6% of T cells in skin and blood respectively. This is similar to a previous report of MAIT cells constituting a small percentage of the total T cell population with little difference between skin and blood (Li et al., 2017). Type II NKT cells (CD1d-endo tetramer$^+$ cells) were the second most abundant population in the skin – more abundant than type I NKT cells – followed by CD1c- and CD1a-restricted T cells. Epidermal CD1a-restricted T cell frequencies varied between donors, demonstrating that there are measurable populations of CD1a-restricted T cells in the skin of some donors, although all donors had fewer than 3% within the total T cell pool *(Fig.6.4a, b)*. It may be that they were in the dermis instead of epidermis, but the processing of skin samples to interrogate these tissues requires optimisation.

Frequencies of γδ-T cells were lower in the epidermis compared to blood *(Fig.6.4a, c)*, which was surprising given that they are typically more abundant in non-lymphoid tissues including skin (Dupuy et al., 1990, Nielsen et al., 2017). However, within individual

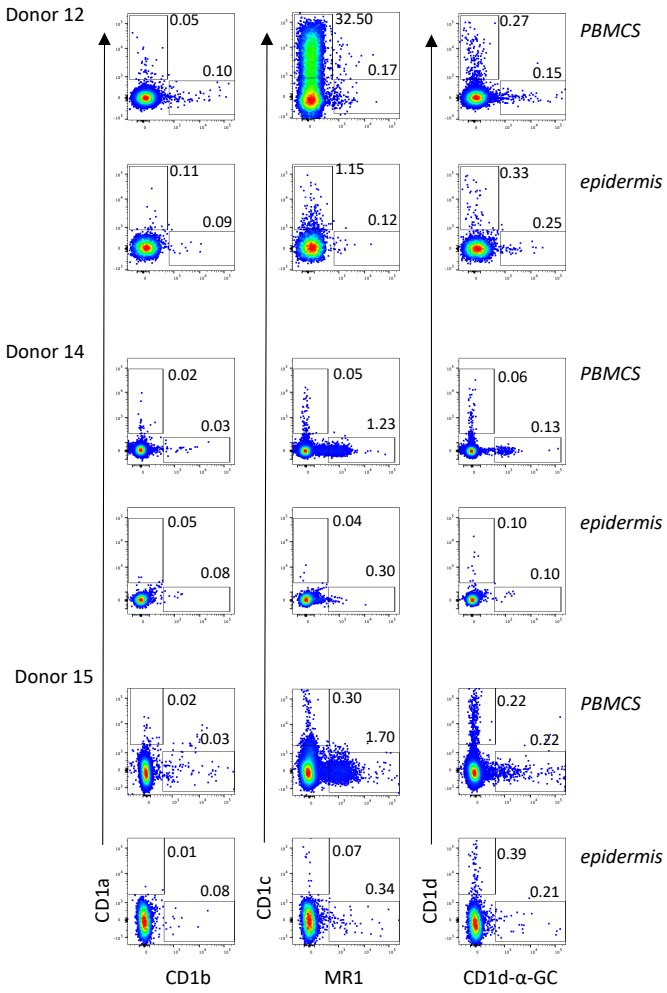

Figure 6.3. Dual labelling of CD1-ag and MR1-5-OP-RU tetramers. Epidermal cells and PBMCs from matched blood were co-stained with two different tetramers simultaneously: CD1a-endo with CD1b-endo, CD1c-endo with MR1-5-OP-RU, and CD1d-endo with CD1d-α-Galcer. Cells are gated on $CD45^{+}$ $CD3^{+}$ $CD14^{-}$ $CD19^{-}$ $7\text{-}AAD^{-}$ lymphocytes. Data are representative of five donors, each in independent experiments.

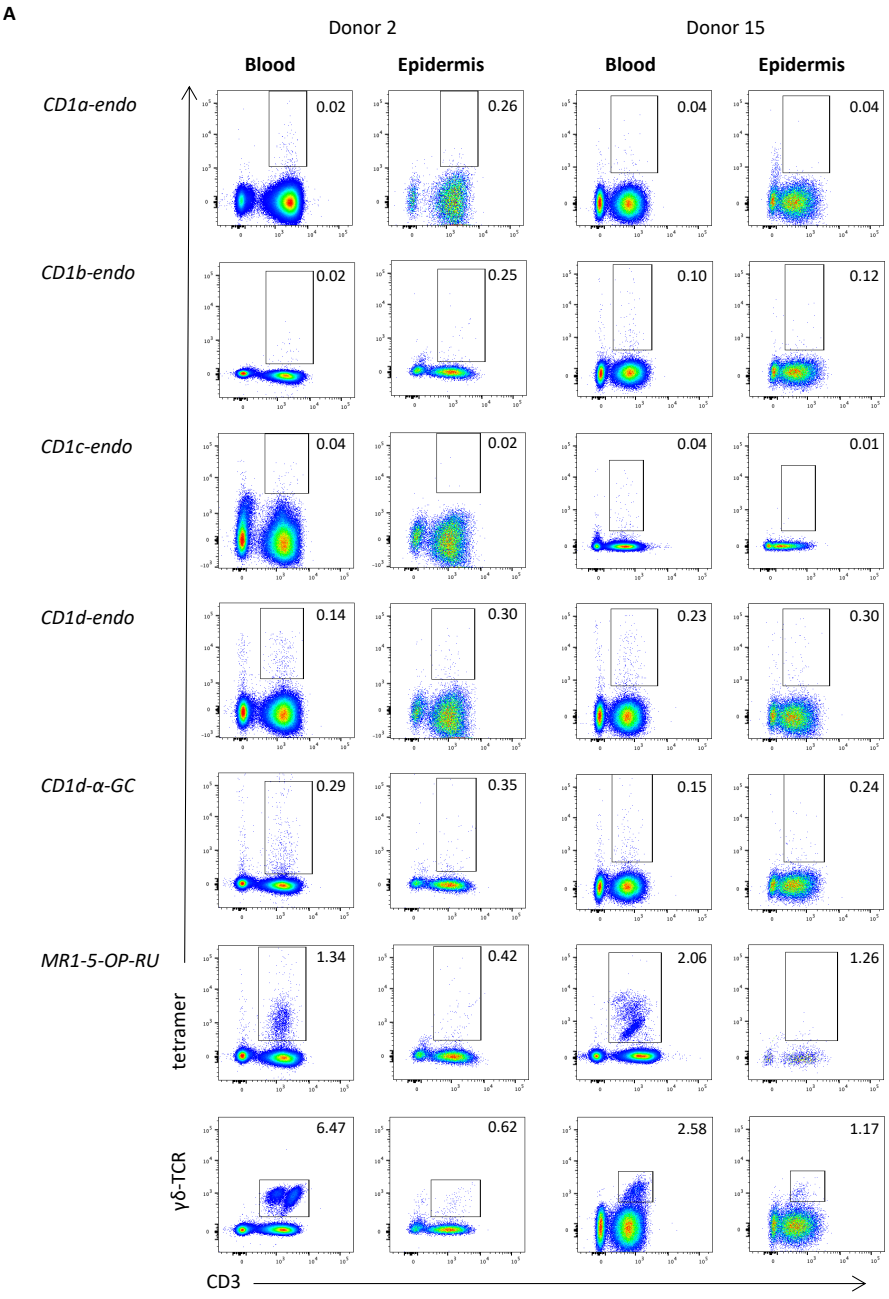
A
Donor 2
Donor 15
Blood
Epidermis
Blood
Epidermis
CD1a-endo
0.02
0.26
0.04
0.04
CD1b-endo
0.02
0.25
0.10
0.12
CD1c-endo
0.04
0.02
0.04
0.01
CD1d-endo
0.14
0.30
0.23
0.30
CD1d-α-GC
0.29
0.35
0.15
0.24
MR1-5-OP-RU
1.34
0.42
2.06
1.26
tetramer
6.47
0.62
2.58
1.17
γδ-TCR
CD3

B

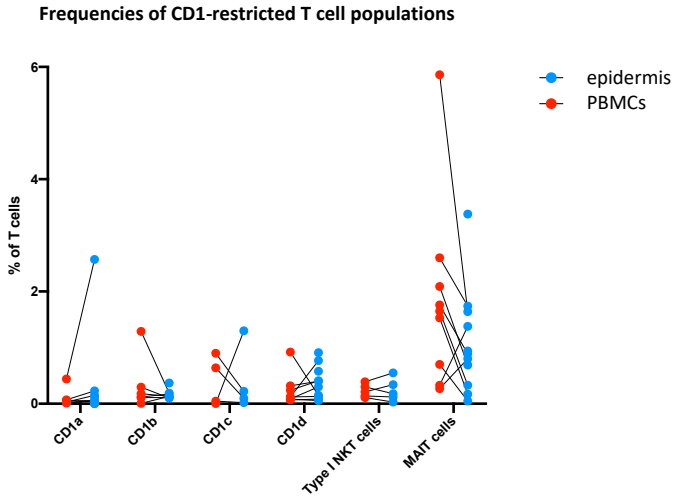

C

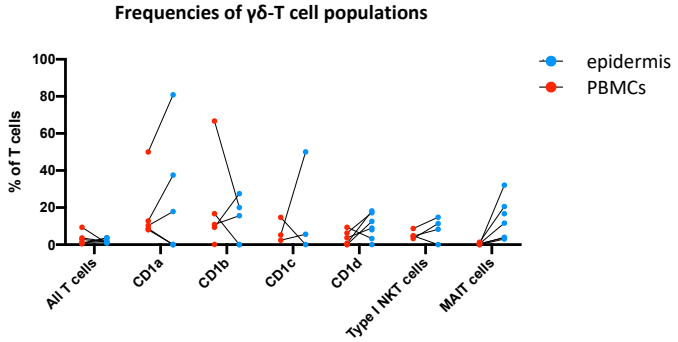

Figure 6.4 Frequencies of unconventional T cells isolated directly *ex vivo* from epidermis. Skin from abdominoplastic surgeries was processed to produce a single cell suspension of epidermal cells for flow cytometry. **A.** Isolation of T cell populations labelled with CD1a-endo, CD1b-endo, CD1c-endo, CD1d-endo, CD1d-α-GalCer or MR1-5-OP-RU tetramers, or an anti-δγ-TCR mAb within the epidermis and PBMCs in two donors. Cells are gated on $CD45^+$ $CD14^-$ $CD19^-$ 7-AAD^- lymphocytes. **B.** Frequencies of CD1-restricted T cell populations and MAIT cells from peripheral blood (red) and epidermis (blue) in 11 donors. Note that each tetramer was not used in all donors and the number of donors are indicated: CD1a-endo (n = 11), CD1b-endo (n = 7), CD1c-endo (n = 4), CD1d-endo (n = 11), CD1d-α-GalCer (n = 5), and MR1-5-OP-RU (n = 11). One donor did not have matched blood provided. **C.** Frequencies of γδ-TCR^+ T cells in 7 donors. The number of donors assessed for each subset of $tetramer^+$ cells are as indicated: CD1a-endo (n = 6), CD1b-endo (n = 5), CD1c-endo (n = 3), CD1d-endo (n = 7), CD1d-α-GalCer (n = 4), and MR1-5-OP-RU (n = 7).

CD1-restricted T cell populations and MAIT cells, γδ-T cell frequencies increased overall in the skin compared to blood (with the exception of CD1b-restricted T cells). Among epidermal CD1a-restricted T cells, γδ-TCR$^+$ T cell frequencies ranged from undetected to 81%. As a comparison, γδ-TCR$^+$ frequencies ranged up to 32% and 18% of MAIT cells and CD1d-α-GalCer reactive T cells respectively. These data suggest that lipid-reactive and metabolite-reactive T cells are found in the epidermis, some of which are γδ-T cells, and these populations may play various roles in maintaining skin homeostasis and barrier tissue immunity.

6.2.2. Characterisation of skin CD1-restricted T cells

To phenotypically characterise epidermal unconventional T cells, CD1a, CD1b, CD1c, CD1d, and MR1 tetramers were incorporated into a flow cytometry panel designed to measure co-receptor usage (CD4, CD8), memory status (CD45RO), and skin-homing marker receptor expression (CLA). Phenotypic analyses were limited due to the use of Collagenase P in enzymatic tissue digestion as it can impact mAb epitopes *(Fig.6.1)*. As a comparison, tetramer$^-$ CD3$^+$ T cells were also analysed to ensure phenotypic profiles were as expected for skin-localising T cells.

Epidermal tetramer$^+$ cells were first examined for expression of CD4 and CD8 co-receptors. Among all T cells, CD4$^+$ and CD8$^+$ T cell proportions were approximately matched between blood and skin, albeit CD4$^+$ T cell populations were slightly lower in skin compared to blood in favour of CD8$^+$ T cells *(Fig.6.5a)*. Consistent with analysis of magnetically enriched CD1a tetramer$^+$ cells isolated from PBMCs *(Chapter 3.2.3)*, CD1a-restricted T cells were predominantly CD4$^+$ in both blood and skin. Overall, the percentage of T cells that expressed CD4 was slightly higher in the epidermis compared to blood among CD1b-endo, CD1c-endo, and CD1d-endo tetramer$^+$ cells *(Fig.6.5a)*. Percentages of both CD4$^+$ and CD8$^+$ type I NKT cells were lower in the epidermis compared to blood, in favour of a CD4$^-$ CD8$^-$ DN population *(Fig.6.5a)*. Peripheral blood MAIT cells were predominantly CD8$^+$, consistent with previous observations (Reantragoon et al., 2013, Gherardin et al., 2018), however they appeared to shift towards greater CD4 expression in the skin. This contrasts a study that demonstrated the presence of CD8$^+$ MAIT cells in psoriatic plaques (Teunissen et al., 2014), albeit there may be infiltration of different T cell subsets during pathology.

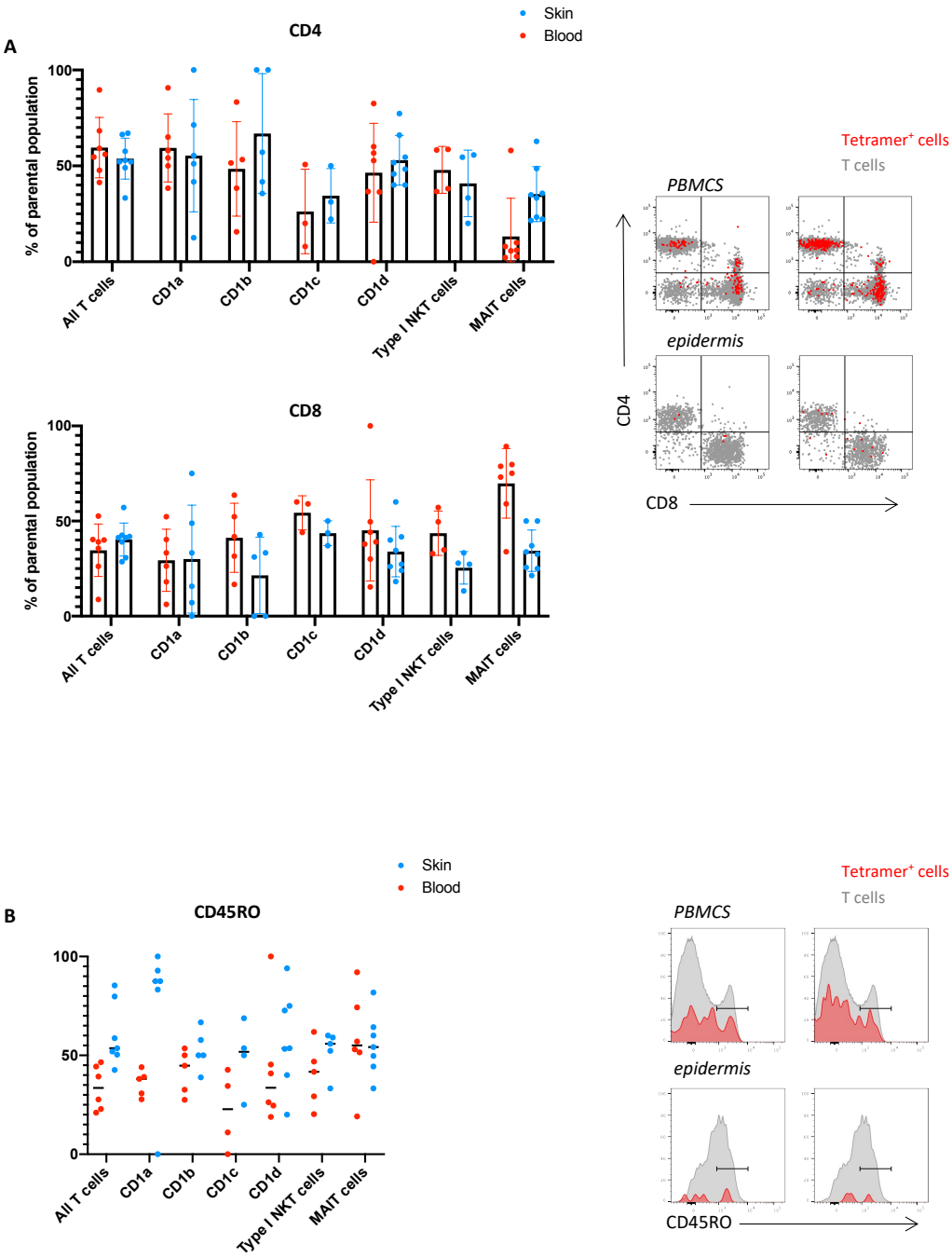
A
CD4
Skin
Blood
% of parental population
100
50
0
All T cells
CD1a
CD1b
CD1c
CD1d
Type I NKT cells
MAIT cells
CD8
Tetramer+ cells
T cells
PBMCS
epidermis
CD4
CD8
B
CD45RO
CD45RO

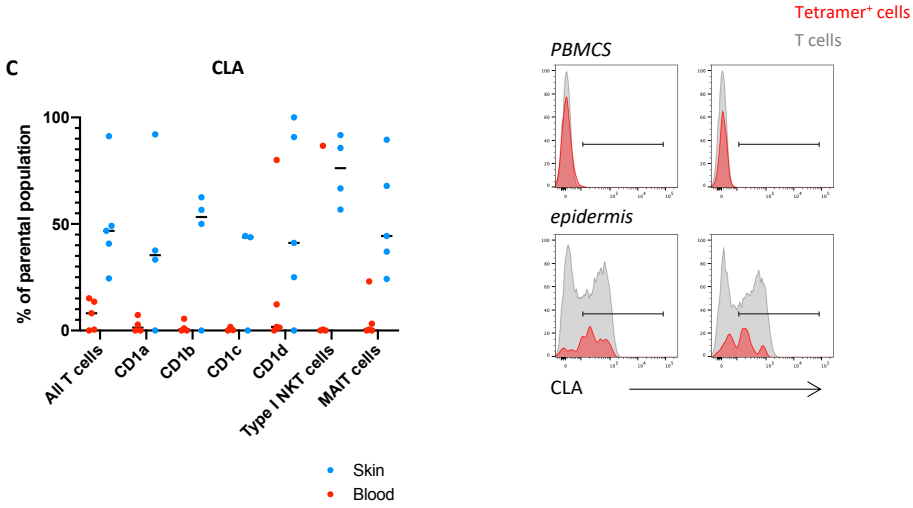

Figure 6.5 Phenotype of CD1-restricted T cells in the epidermis. Gated CD45$^+$ CD3$^+$ T cells isolated from peripheral blood (red) and epidermis (blue) were labelled with cell surface markers for phenotypic analysis. Cell groups analysed include all CD3$^+$ cells (T cells), and tetramer$^+$ cells with CD1a-endo, CD1b-endo, CD1c-endo, CD1d-endo, CD1d-α-GalCer (type I NKT cells), and MR1 5-OP-RU (MAIT cells) tetramers. Graphs indicate percentage of the parental population that were **A.** CD4$^+$ and CD8$^+$, **B.** CD45RO$^+$ and **C.** CLA$^+$. FACS plots on the right of each graph show an example of the gating strategy used for each phenotype with tetramer$^+$ cells (red) compared to all T cells (grey). Data collectively representative of 8 donors, however some donors were not labelled with all six tetramers, thereby reducing the number of donors for each tetramer: CD1a-endo (n = 6), CD1b-endo (n = 5), CD1c-endo (n = 3), CD1d-endo (n = 7), CD1d-α-GalCer (n = 4), and MR1-5-OP-RU (n = 6).

Given that only antigen-experienced T cells typically gain access to non-lymphoid tissues (Miyawaki et al., 1990, Sanders et al., 1988), memory phenotype of epidermal CD1-restricted T cells was assessed. Expression of the memory marker, CD45RO, by all T cells and all individual lipid-reactive T cell subsets was enhanced in the skin *(Fig.6.5b)*, which was expected. $CD45RO^{hi}$ cells ranged from 83-100% among CD1a-restricted T cells, a higher proportion than other CD1-restricted T cell subsets. Greater expression of CLA was observed in the skin across all T cell subsets compared to blood (where CLA expression was minimal) *(Fig.6.5c)*. Indeed, T cells in the skin typically express skin-homing memory T cell markers (CD45RO/CLA/CCR4) (Clark et al., 2006a, Seneschal et al., 2012). Expression of CLA allows these cells to migrate to the skin and the disparity between CLA expression seen here and among CD1a-restricted T cells in other studies may be due to the different techniques used for cell isolation, tissues used, or donor variation. Importantly, these phenotypic data are based on samples from individuals who are likely obese, and therefore may not be completely representative of T cells in healthy individuals. Together, these data suggest that epidermal CD1-restricted T cells are antigen-experienced and primed to respond to environmental stimuli and potentially microbiota, although more detailed analyses are required to determine their effector/resident memory phenotypes and their role in skin homeostasis and immunosurveillance.

6.2.3. TCR repertoire of skin CD1-restricted T cells

While isolation of T cells from enzymatically digested whole skin proved challenging, T cells have been previously observed to spontaneously migrate from human skin explants cultured *ex vivo* by taking advantage of their tendency to migrate to sites of wound healing and tissue repair (Clark et al., 2006b). T cells isolated from *ex vivo* cultures may adopt different phenotypes to those *in vivo* and therefore could not be reliably used for surface phenotype characterisation but were instead used for TCR sequencing. However, it is important to note that the TCR repertoire determined might not be reflective of *in vivo* frequencies as some T cell clones may expand, die, or not migrate when in culture.

T cells were isolated from the skin using an adapted culture method based on that previously described (Clark et al., 2006b). Briefly, 2x2 cm^2 explants were cut from donor skin and placed on an absorbable gelatin sponge in 6-well culture plates. The subcutis

(i.e. subcutaneous fat) was trimmed such that the reticular layer of the dermis lay on the gelatin sponge. Sponges were submerged in T cell culture media such that the surface of the explants (i.e. the epidermal layers) were exposed to receive oxygen. Explants were cultured for two weeks in media containing exogenous cytokines, IL-2 and IL-15, to encourage T cell growth and migration from the skin into culture media. Cells isolated in the media following culture were labelled with CD1 tetramers to determine whether T cells that recognise lipid antigens could be isolated in the skin.

Most cells isolated following culture were $CD3^+$ $CD45^+$ *(Fig.6.6a)*, indicating the successful isolation of T cells from skin explants using this method. Additionally, $CD4^+$, $CD8^+$ and $CD4^-CD8^-$ cells were observed among T cells isolated *(Fig.6.6a).* Samples were labelled with CD1a-endo, CD1b-endo, CD1c-endo, CD1d-endo, or CD1d-α-GalCer tetramers from three donors, and small populations of $tetramer^+$ cells were observed *(Fig.6.6b)*.

Populations of CD1a-endo, CD1c-endo and CD1d-endo $tetramer^+$ T cells from two donors were single cell-sorted for multiplex nested PCR to amplify TCR genes and sequencing was performed using the method described in Chapter 4.2.1. Sequences were obtained for six CD1a-restricted TCRs, nine CD1c-restricted TCRs and ten CD1d-restricted TCRs. The variable gene commonly incorporated into CD1a-restricted TCR β-chains as previously observed with TCR and RNA sequencing, TRBV28, was utilised by a CD1a-restricted TCRs sequenced *(Fig.6.6c)*, consistent with a bias for TRBV28 observed in TCR sequencing of peripheral blood CD1a-restricted T cells (Chapter 4.2.1). Surprisingly, 5/9 CD1d-restricted TCRs were also $TRBV28^+$, and 2/10 and 3/9 CD1c- and CD1d-restricted T cells respectively expressed TRAV8-2 or TRAV8-4 *(Fig.6.6c)*. These variable genes were identified as commonly used among CD1a-restricted T cells in Chapter 4.2.1, suggesting that there may be structural benefits endowed by these variable genes (e.g. in CDR1 and CDR2) for T cells that recognise self-lipids in the skin. However, this was a preliminary analysis and more T cells from more donors would have to be sequenced to make any conclusive remarks.

This study of cutaneous unconventional T cells was preliminary and few $tetramer^+$ cells were recovered. It was therefore difficult to make conclusions regarding the phenotype of these cells. However, together with a recent study that investigated CD1a-autoreactive

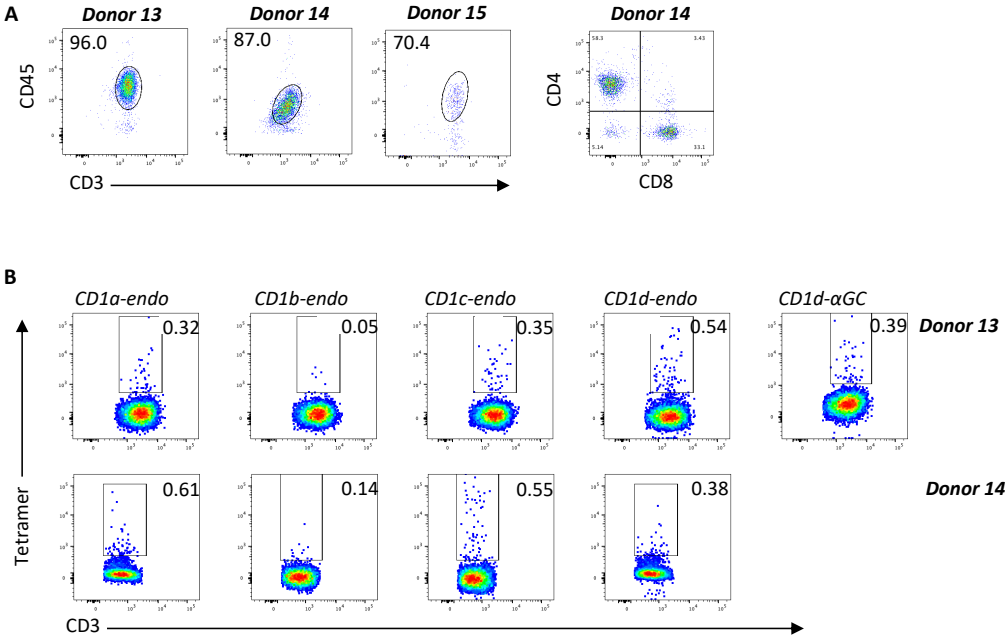

C

TCR sequences derived from CD1a-endo tetramer⁺ primary T cells			
TRAV	**TRAJ**	**TRBV**	**TRBJ**
4*01	31*01	28*01	2-3*01
4*01	23*01	-	-
29/DV5*01	13*02	-	-
6*03	20*01	9*01	1-2*01

TCR sequences derived from CD1d-endo tetramer⁺ primary T cells			
TRAV	**TRAJ**	**TRBV**	**TRBJ**
8-2/8-4	13*02	-	-
8/2-8/4	21*01	28*01	-
8/2-8/4	13*02	28*01	1*01
13-2	42*01	28*01	1-1*01
25*01	37*01	28*01	25*01
3*01	17*01	2	1-5*01
1-2*01	12*01	20-1	2-7
4*01	23*01	27*01	2-5*01
13*02	34*01	28*01	2-7*01

TCR sequences derived from CD1c-endo tetramer⁺ primary T cells			
TRAV	**TRAJ**	**TRBV**	**TRBJ**
21	26*01	-	-
8-2/8-4	48*01	-	-
27*03	33*01	-	-
13-2	41*01	-	-
26-2*01	45*01	2	2-7*01
1-1*02	5*01	12-3/12-4	2-4*01
3	17	2	2-7*01
8-2/8-4	20*01	1-2*01	12*01
1-2*01	12*01	27*01	
29/DV5*02	42*01	27*01	2-1*01

Figure 6.6 Isolation of lymphocytes from skin explants cultured *ex vivo*. Skin tissue without subcutaneous fat (2 cm x 2 cm squares) was cultured in T cell media on GelFoam sponges to encourage migration of T cells into the media. **A.** Recovery of CD45⁺ CD3⁺ T cells from three donors, donor 14 revealed a typical CD4/CD8 co-receptor expression profile. **B.** Isolation of CD1-restricted T cells from two donors (donors 13 and 14) with CD1a-endo, CD1b-endo, CD1c-endo, CD1d-endo and CD1d-α-GalCer tetramers. FACS plots represent cells gated as CD45⁺ CD3⁺. **C.** TCR sequences derived from primary T cells sorted based on binding to CD1a-endo, CD1c-endo or CD1d-endo tetramers. Tetramer⁺ cells were single cell-sorted and TCR Vα and Vβ domain gene segments were amplified by multiplex nested PCR. TCR genes were determined by Sanger sequencing and analysed using the IMGT database.

T cells in the skin (Cotton et al., 2021), these experiments represent a basis upon which future studies may characterise lipid-reactive T cells in the skin both directly ex vivo and following in vitro culture to determine TCR repertoire.

6.2.4 Activation of CD1a-restricted T cells with alkyl benzoate

Following a preliminary analysis of cutaneous CD1a-restricted T cells, they were further investigated in the context of skin pathologies. The recent identification of ingredients in balsam of Peru, benzyl benzoate and benzyl cinnamate, that are presented by CD1a as agonists for T cells, opens up the idea that other oils in skincare products may also trigger CD1a-restricted T cell-mediated allergies (Nicolai et al., 2020). Following a delayed-type hypersensitivity (DTH) reaction to a sunscreen experienced by myself (so-determined by the delay in local inflammation following contact sensitisation) *(Fig.6.7a)*, I sought to identify whether the causative ingredient was acting through the CD1a pathway. The allergy was caused by the Cancer Council Sports Spray sunscreen, while the Cancer Council Sports Lotion had not previously triggered any allergic reactions. A comparison of the ingredients in these products identified C12-15 alkyl benzoate, dipropylene glycol dibenzoate, PPG-15 stearyl ether benzoate, bis-ethylhexyloxyphenol, and methoxyphenol triazine as present within the spray but not in the lotion *(Fig.6.7b)*.

C12-15 alkyl benzoate (CAS no. 68411-27-8) has previously been reported to cause an allergic reaction in a case study of a 27 year-old male, who presented with similar symptoms to those in my case: itchy skin rash on neck, arms, armpits, knee-folds, and eyelids after application of sunscreen and exposure to sunlight (Werbrouck et al., 2015). The case study reported possible photo-allergic contact dermatitis seen towards C12-15 alkyl benzoate, benzyl benzoate, benzyl salicylate, and products containing C12-15 alkyl benzoate (Werbrouck et al., 2015), suggesting immune responses to these benzyl compounds.

C12-15 alkyl benzoate was of interest due to its structural similarities to other CD1a allergens previously identified: benzyl cinnamate, benzyl benzoate and, particularly, C15 urushiol *(Fig.6.7c)* (Kim et al., 2016, Nicolai et al., 2020). It is highly soluble in oil and oil-like solvents, which helps keep active ingredients dispersed through the formula,

A

B

Cancer Council – Sports [Lotion]	Cancer Council – Sports [Spray]
INCI Name	INCI Name
Water	Water
Homosalate	C12-15 Alkyl Benzoate (and) Dipropylene Glycol Dibenzoate (and) PPG-15 Stearyl Ether Benzoate
Isopropyl Palmitate	Beeswax
Octocrylene	Butyl Methoxydibenzoylmethane
Ethylhexyl Salicylate	Cocoglycerides
Cocoglycerides	Isopropyl Palmitate
Beeswax	4-Methylbenzylidene Camphor
Butyl Methoxydibenzoylmethane	Dimethicone
Dimethicone	Octocrylene
4-Methylbenzylidene Camphor	Butylene Glycol
Butylene Glycol	PEG-15 Cocamine
PEG-15 Cocamine	PEG-40 Stearate
PEG-40 Stearate	Bis-Ethylhexyloxyphenol Methoxyphenol Triazine
Phenoxyethanol	Phenoxyethanol
Methylparaben	Methylparaben
Acrylates/C10-30 Alkyl Acrylate Crosspolymer	Propylparaben
Propylparaben	Acrylates/C10-30 Alkyl Acrylate Crosspolymer
Triethanolamine	Ethylparaben
Ethylparaben	Triethanolamine
Acrylates/C10-30 Alkyl Acrylate Crosspolymer	Disodium EDTA
Tocopheryl Acetate	Tocopheryl Acetate
BHT	BHT
Disodium EDTA	
Aloe Barbadensis Leaf Extract	

C

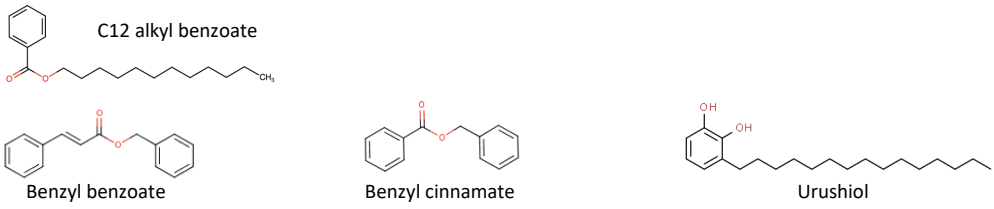

Figure 6.7 Identification of potential CD1a allergens in dermatological and cosmetic products. A. The subject (CNR)'s face and neck two days following a delayed type hypersensitivity reaction to the Cancer Council Sport Sunscreen aerosol spray. **B.** List of ingredients in the Cancer Council Sport Sunscreen lotion and aerosol spray with those ingredients exclusively in the spray indicated in red. Ingredients are listed in order of predominance. **C.** Chemical structures of benzyl ring-containing CD1a antigens used in cosmetic products and/or known CD1a allergens: C12 alkyl benzoate structure compared to benzyl benzoate, benzyl cinnamate, and urushiol.

leading to its wide use in a variety of products (Becker et al., 2012). It is used as an emollient and texture enhancing (skin conditioning) agent in baby-care, hygiene, cosmetic and sun-care products. A higher percentage of individuals with contact dermatitis are sensitive to alkyl benzoate compared to benzyl benzoate (Goossens, 2016). The ability of CD1a-restricted T cells to recognise and be activated by alkyl benzoate was therefore tested.

To determine whether C12-15 alkyl benzoate activates CD1a-restricted SKW-3 $\beta_2m^{-/-}$ cells, they were co-cultured with $CD1a^+$ C1R cells with increasing concentrations of C12-15 alkyl benzoate. Commercially available C12-15 alkyl benzoate (hereon in referred to simply as alkyl benzoate) is a mixture of alkyl benzoates with varying chain length (C12-15), rather than a single compound. It was unclear which, if any, may act as a CD1a antigen. The oil is typically added to skincare/hygiene product formulae at 0.5-5.0% (v/v), however, following application, it would undoubtedly reach a lower concentration once absorbed through skin. C12-15 alkyl benzoate was added to cells at a range of concentrations to evaluate impact on activation as well as toxicity.

The CD1a-autoreactive T cell line BK6, CD1a-DDM-reactive T cell line 17a28, and cross-reactive T cell line 27a28, were each assessed for activation by measuring CD69 upregulation *(Fig.6.8)*. In three independent experiments, alkyl benzoate was added at 1%, 5%, or 10% of the total culture media volume. The proportion of cells that were 7-AAD^+ was assessed to determine whether increasing concentrations of alkyl benzoate were toxic in the cell culture *(Fig.6.8a)*. For all cell lines, the least amount of cell death occurred when cells were cultured in media alone (i.e. no C1R cells were added), and there was little change with or without the addition of alkyl benzoate. For all three CD1a-restricted T cell lines, increasing concentrations of alkyl benzoate correlated with greater CD69 MFI *(Fig.6.8b)*. The minimal difference in cell death following the addition of alkyl benzoate suggests that this was not an artefact of increased toxicity *(Fig.6.8a)*.

For 17a28 and 27a28 T cell lines, which both recognise the large headgroup of DDM, the addition of alkyl benzoate resulted in levels of activation greater than with $CD1a^+$ C1R cells alone. The CD1c-restricted, negative control T cell line 3C4 was not activated by $CD1a^+$ C1R cells or the addition of alkyl benzoate. It was difficult to determine the exact impact of alkyl benzoate on activation of CD1a-restricted T cells, especially given that,

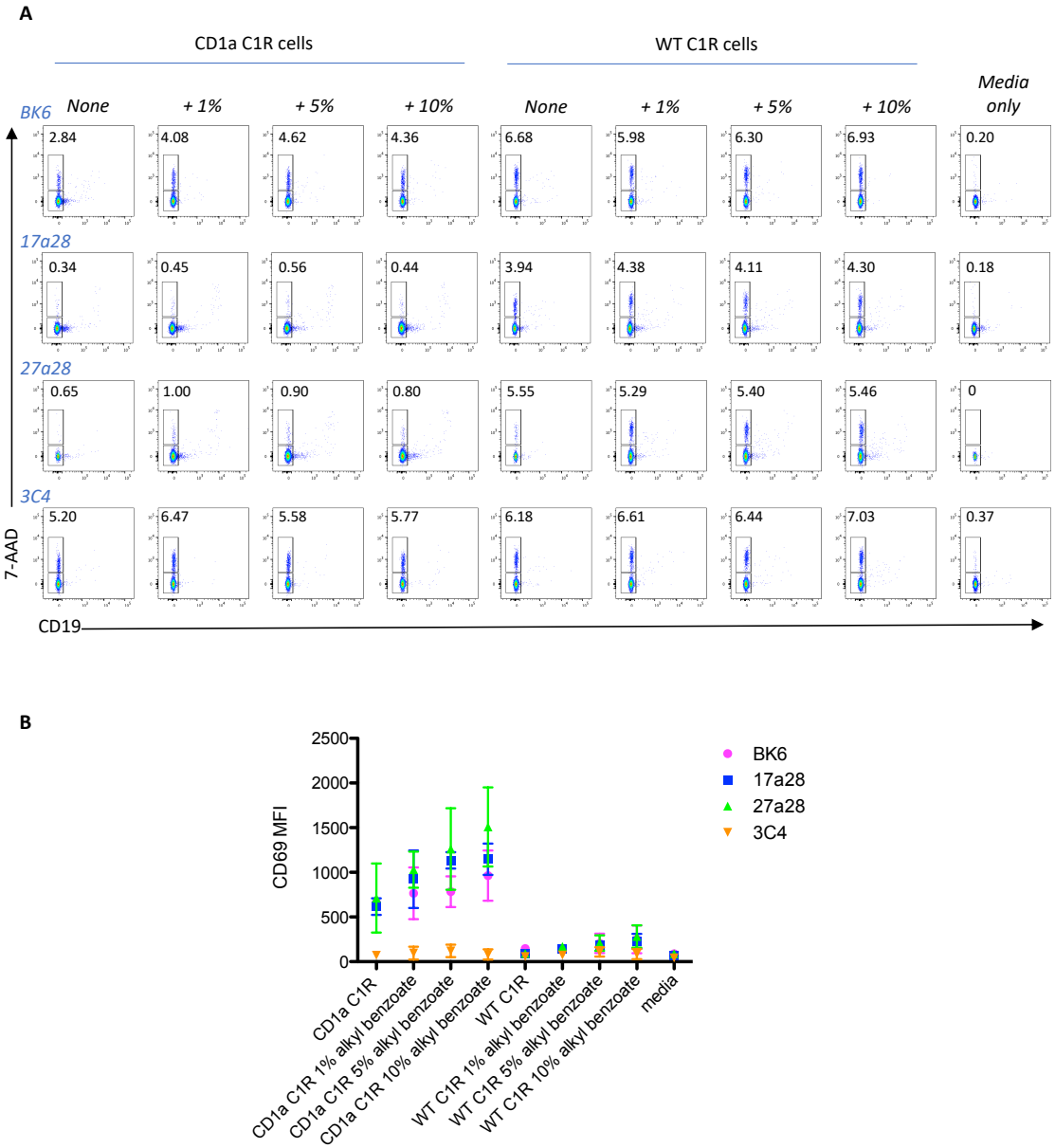

Figure 6.8. Activation of CD1a-restricted T cells with alkyl benzoate. CD1a-restricted TCR SKW-3 $\beta_2m^{-/-}$ cell lines, BK6, 17a28, and 27a28, or CD1c-restricted T cell line 3C4, were co-cultured with CD1a+ or WT C1R cells. Alkyl benzoate was added at 1%, 5% or 10% (v/v) to the culture media. **A.** Exclusion of dead and B cells using 7-AAD and anti-CD19 respectively. Toxicity was determined by the percentage of cells that were 7-AAD$^+$, indicated by the number in the top left of each plot. **B.** Activation was measured by CD69-upregulation after 18h, assessed on 7-AAD$^-$ CD19$^-$ cells. Data representative of three independent experiments.

as seen in this assay and by others, CD1a-autoreactive T cells typically show baseline reactivity towards endogenous self-lipids, leading to background levels of activation (Vincent et al., 2005). This phenomenon can mask the response to potential exogenous antigens, in this case, alkyl benzoate. Nevertheless, these results indicated that alkyl benzoate may activate CD1a-restricted T cells or is metabolised by C1R cells to form an antigen that is presented to CD1a-restricted T cells.

6.2.5 Production of soluble CD1a in the presence of alkyl benzoate

To determine whether alkyl benzoate itself was acting as a CD1a lipid antigen, or whether it had been metabolised as part of the activation assay by C1R cells, CD1a was produced in the presence of alkyl benzoate for tetramer studies and mass spectrometry. Soluble CD1a molecules were produced in a mammalian HEK 293S-GnTI$^-$ cell expression system identical to that used previously here and in (Aricescu et al., 2006, Birkinshaw et al., 2015). GnTI$^-$ cells were co-transfected with *pHLSec-CD1A* and *pHLSec-β_2m* plasmids in normal transfection media or media spiked with alkyl benzoate so that it comprised 0.5% (v/v) of the total media volume. Notably, it remained partially insoluble and oil droplets were visible in the culture media. Cell viability was reduced with the addition of alkyl benzoate as observed by GnTI$^-$ cells – an adherent cell line – detaching from the flask surface and a change in media colour. The production of soluble CD1a was repeated using the Expi293F expression system, again, co-transfecting Expi293 cells with plasmids encoding the CD1a heavy chain and β_2m with and without alkyl benzoate. Similar to production in GnTI$^-$ cells, at 0.5% (v/v) of total media volume alkyl benzoate remained partially insoluble and the survival rate of cells was diminished.

Soluble heterodimeric CD1a/β_2m molecules were harvested by collecting pooled supernatant and passing it through a 0.2 μm filter. Oil was observed in the filter from samples containing alkyl benzoate, highlighting its insolubility. Ni-NTA chromatography was used to purify CD1a molecules, which contained a carboxy-terminal BirA 6 x histidine tag (Birkinshaw et al., 2015). Harvested protein was passed over an Ni-NTA column and eluted with increasing concentrations of imidazole. The presence of CD1a protein in both samples was confirmed with 12% SDS-PAGE analysis *(Fig.6.9a, Fig.6.9b)*. Given that CD1a was present in both samples, albeit less protein was produced

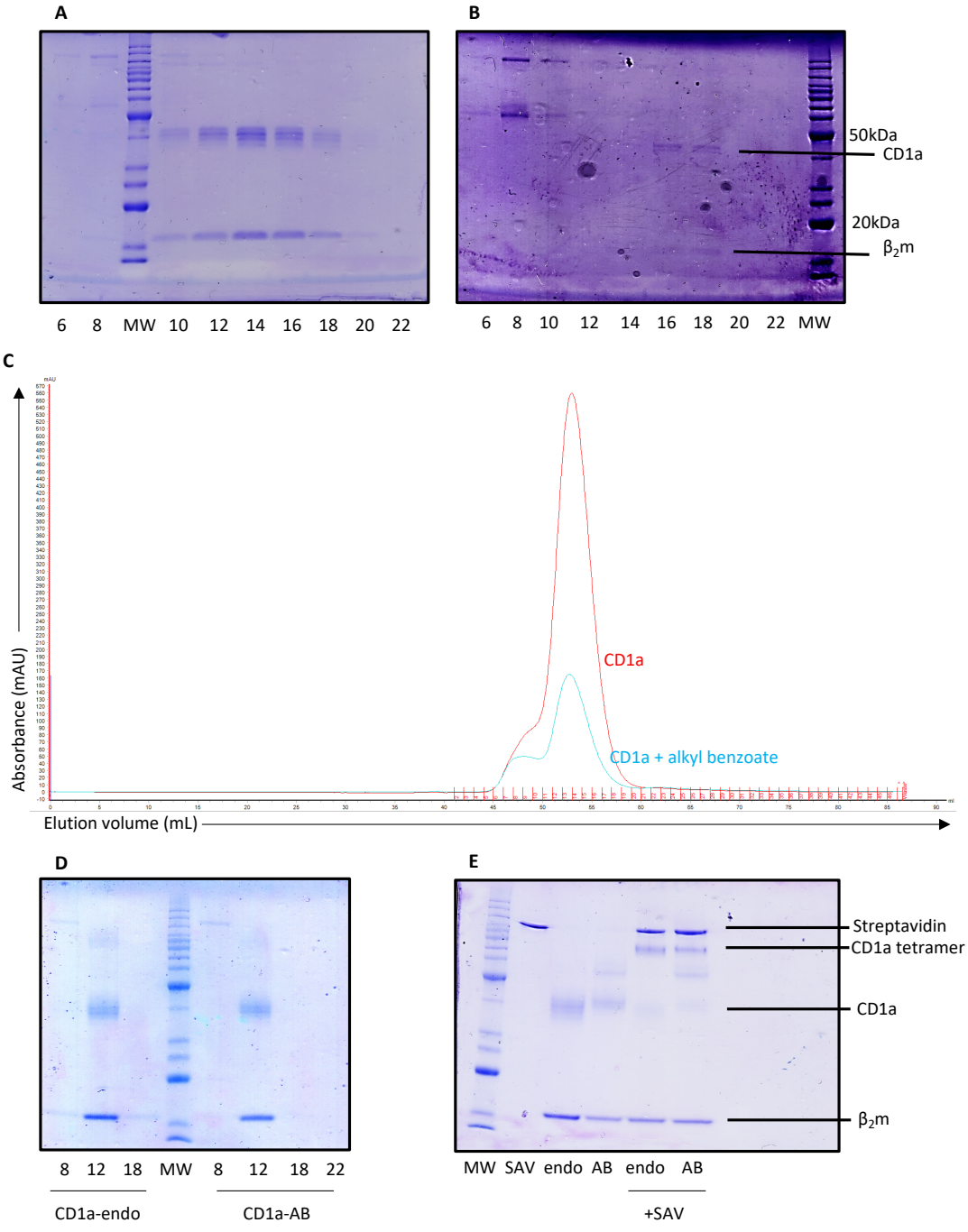

Figure 6.9. Production and biotinylation of CD1a in the presence of alkyl benzoate. Soluble CD1a was produced in GnTI$^-$ cells and supernatant was passed over a Ni-NTA column for purification. Fractions were collected under increasing imidazole concentrations and assessed by 10% SDS-PAGE. CD1a was produced as normal **(A)** or in the presence of C12-15 alkyl benzoate at 0.5% (v/v) of the total media volume **(B)**. **C.** Chromatogram trace of CD1a produced with and without alkyl benzoate run over an S200 gel filtration column. **D.** Fractions following gel filtration were assessed by SDS-PAGE. **E.** Biotinylation efficiency was tested by tetramerising monomeric CD1 molecules. 2 µg of each CD1 protein was denatured at 95 °C , allowed to cool, and then incubated with streptavidin (SAV) at a 1:1 weight ratio.

in the presence of alkyl benzoate, fractions containing CD1a were pooled and biotinylated overnight with BirA *(Fig.6.9a, b)*.

Biotinylated CD1a monomer was separated from free biotin using a 75 pg gel filtration column (*Fig.6.9c*). SDS-PAGE analysis of CD1a following gel filtration revealed multiple bands of approximately 37 kDa, which correspond to differentially glycosylated CD1a protein and one major peak on the chromatogram at an elution volume of approximately 53 mL (fraction 13) *(Fig.6.9c, d)*. The amount of CD1a obtained from GnTI$^-$ culture with alkyl benzoate was lower, which is likely due to toxicity from the insoluble oil in the culture media, resulting in fewer protein-producing cells. CD1a produced in the presence of alkyl benzoate appeared similar in size to standard CD1a and also displayed variable glycosylation as indicated by multiple bands *(Fig.6.9a, d)*. Fractions 11-19 and 11-20 were collected for CD1a produced with and without alkyl benzoate respectively, corresponding to the major peak in each chromatogram (and excluding the smaller, earlier shoulder, which contained larger aggregate protein) (*Fig.6.9c, d*).

Biotinylation efficiency was determined by running tetramerised CD1a on a 12% SDS-PAGE gel *(Fig.6.9e)*. Streptavidin was added at a 1 µg: 1 µg mass ratio to heat-denatured CD1a, which was assessed for its ability to form tetrameric complexes by observing a shift in molecular weight *(Fig.6.9e)*. The presence of monomer at around 37 kDa was observed in lanes containing CD1a alone, but these bands were fainter following the addition of streptavidin in favour of a larger band, indicating successful biotinylation and production of multimeric CD1a.

6.2.6. Recognition of CD1a tetramers loaded with alkyl benzoate by CD1a-restricted T cell lines

CD1a monomer was directly loaded with C12-15 alkyl benzoate and tetramerised to determine the ability of CD1a-restricted T cell lines to recognise it as an antigen. To improve the chance of successful CD1a loading, rather than loading at the typical antigen:CD1a MW ratio of 3:1 or 6:1, alkyl benzoate was diluted in TBS to facilitate loading and added in excess at a MW ratio of 10:1 (CD1a-alkyl benzoate loaded, ABL). Loading was also performed at MW ratios of 50:1 and 100:1, but a 10:1 ratio yielded the

best tetramer labelling, potentially due to oversaturation resulting in a highly oily tetramer mixture (data not shown.) In addition to directly loading CD1a-endo with AB, CD1a monomer expressed in the presence of alkyl benzoate was also tetramerised (CD1a-alkyl benzoate expressed, ABexp). TBS buffer dilutions were performed such that the total volume and overall CD1a concentration were consistent between all tetramers. It was hypothesised that CD1a expressed in the presence of alkyl benzoate might yield a different lipid repertoire to those endogenous self-lipids normally captured by CD1a expressed in GnTI$^-$ cells.

As controls, CD1a-monomer was also treated with either the same volume of 0.5% (v/v) tyloxapol, a common surfactant used to load antigens in soluble CD1 molecules *in vitro* and used for DDM loading (Paletta et al., 2015), or loaded with DDM in a 6:1 MW ratio. Loading took place overnight at RT, and all monomers were left at RT for consistency. All monomer samples were tetramerised the following day to label CD1a-restricted T cell lines: BK6 (CD1a-autoreactive), 17a28 (DDM-reactive), 27a28 (CD1a-crossreactive), and NKT-15 (type I NKT).

CD1a-ABexp labelling of all three CD1a-restricted T cell lines tended to result in greater tetramer MFI compared to CD1a-endo tetramer, while this was not apparent with CD1a-ABL tetramers (*Fig.6.10)*. It is perhaps unexpected that all three cell lines revealed similar patterns for alkyl benzoate tetramers given that they display different antigen reactivity: BK6 is autoreactive, 27a28 is cross-reactive (with a preference for DDM), and 17a28 is DDM-specific. The binding of CD1a-ABexp tetramers may be due to the alteration of the GnTI$^-$ cells' lipid repertoire by replacing the mixture of endogenous lipids that can be either permissive or non-permissive for a single or group of antigen(s) that is more permissive for TCR binding. CD1d-α-GalCer tetramer was used to label cells as a control to ensure that any tetramer binding observed was CD1a-dependent. Overall, results with alkyl benzoate-loaded tetramers suggest that CD1a-restricted T cells may recognise and bind CD1a loaded with alkyl benzoate and/or a derivative lipid antigen.

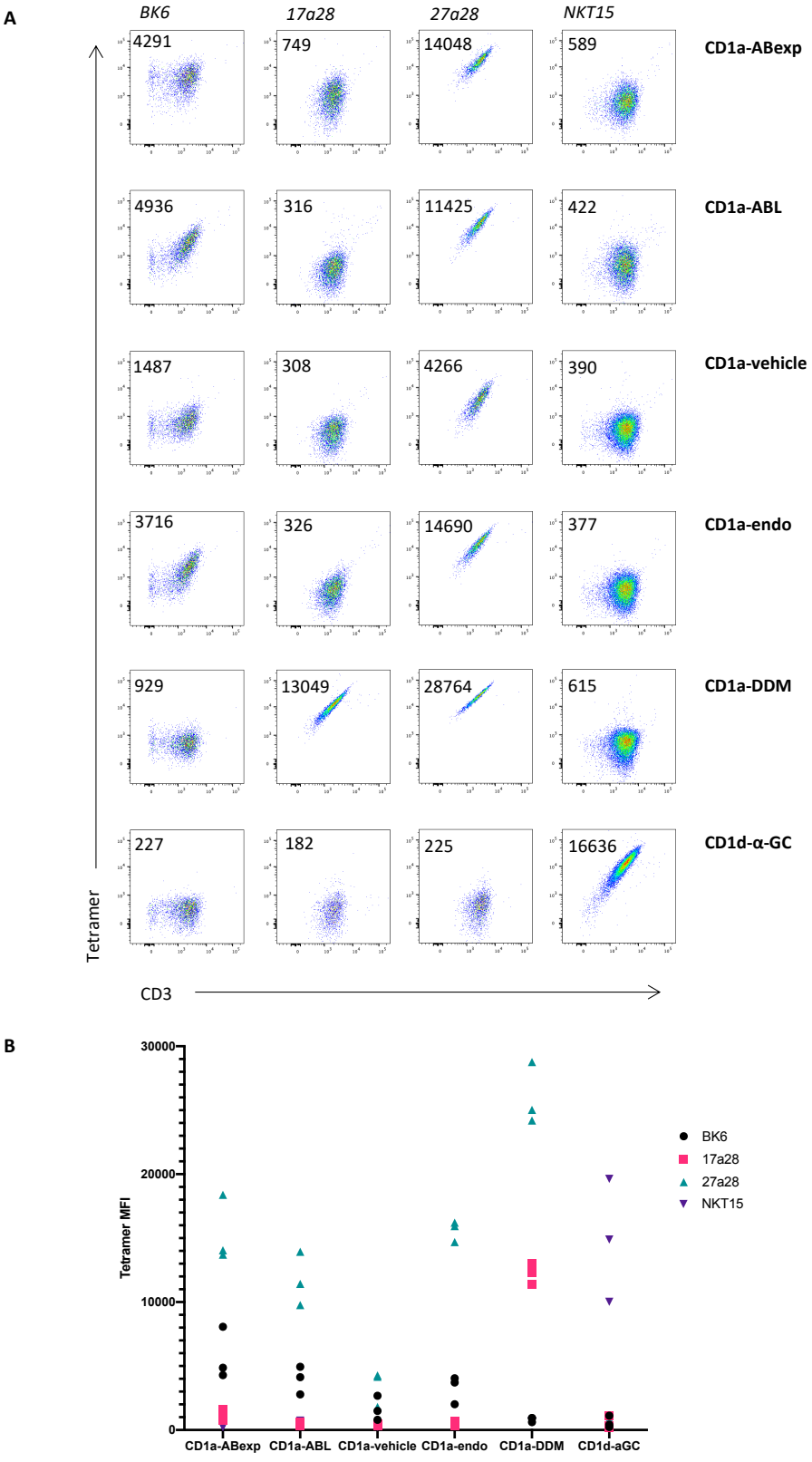
A
BK6
17a28
27a28
NKT15
4291
749
14048
589
CD1a-ABexp
4936
316
11425
422
CD1a-ABL
1487
308
4266
390
CD1a-vehicle
3716
326
14690
377
CD1a-endo
929
13049
28764
615
CD1a-DDM
227
182
225
16636
CD1d-α-GC
Tetramer
CD3
B
30000
20000
10000
0
Tetramer MFI
CD1a-ABexp
CD1a-ABL
CD1a-vehicle
CD1a-endo
CD1a-DDM
CD1d-aGC
BK6
17a28
27a28
NKT15

Figure 6.10. Labelling of CD1a-restricted T cell lines with alkyl benzoate tetramers. Soluble CD1a was produced in the presence of 0.5% alkyl benzoate (v/v) and then used for the production of tetramers (CD1a-ABexp). CD1a produced as per normal (CD1a-endo) was also loaded overnight with alkyl benzoate at a 10:1 MW ratio (CD1a-ABL). Cell lines BK6, 17a28, 27a28, and 3C4 were labelled with CD1a-ABexp, CD1a-ABL, CD1a-vehicle (tyloxapol only), CD1a-endo, CD1a-DDM, or CD1d-αGC tetramers. **A.** Representative plots from one experiment with tetramer MFI indicated in the top right corner. **B.** Data representative of three independent experiments.

6.2.7. Identification of C15 alkyl benzoate loaded in CD1a produced in the presence of C12-15 alkyl benzoate

Mass spectrometry was used to identify the lipid antigen(s) loaded in CD1a expressed in the presence of alkyl benzoate. Aliquots of gel-filtration purified CD1a produced in GnTI$^-$ cells in the presence or absence of alkyl benzoate (200 µg of each in TBS) were sent to Dr Tan-Yun Cheng in Branch Moody's Laboratory (Brigham and Women's Hospital, Harvard Medical School) for mass spectrometry to identify the repertoire of lipids loaded in the different CD1a samples.

Lipids were extracted from CD1a using a mixture of chloroform and methanol and analysed using HPLC-MS according to a method previously described (Cheng et al., 2006). Reverse phase HPLC-MS of protonated ions confirmed that the commercial alkyl benzoate standard contained C12, C13, C14, and C15 analogues with increasing retention time and mass-to-charge ratios (m/z 291.2, 305.2, 319.3, and 333.3 respectively) *(Fig.6.11a, b)*. The mass spectra of eluted ions each had two major peaks: a greater signal representing the protonated ion and a smaller signal representing the ion paired with Na^+ *(Fig.6.11b)*.

Lipid identification was based on the co-elution of unknown products from CD1a-AB eluent with matching *m/z* values in the C12-15 alkyl benzoate reagent standard *(Fig.6.12)*. In the eluents of CD1a produced in the presence of alkyl benzoate, a peak at the same retention time and m/z ratio as C15 alkyl benzoate was detected, and no other alkyl benzoates were present *(Fig.6.12a, b)*. The C15 alkyl benzoate eluted from CD1a-AB was confirmed by the retention time, accurate mass, and collisional pattern match to the standard. This not only indicates that alkyl benzoate is indeed loaded into and presented by CD1a, but that C15 is selectively loaded out of four chain length analogues.

The different lipid repertoire of antigens presented by CD1a produced in the presence and absence of alkyl benzoate was compared. Analysis focused on certain CD1a eluents: C15 benzoate, PC, SM and PI. PC, SM and PI were selected as known agonistic and antagonistic lipid antigens presented by CD1a (Birkinshaw et al., 2015). C15 alkyl

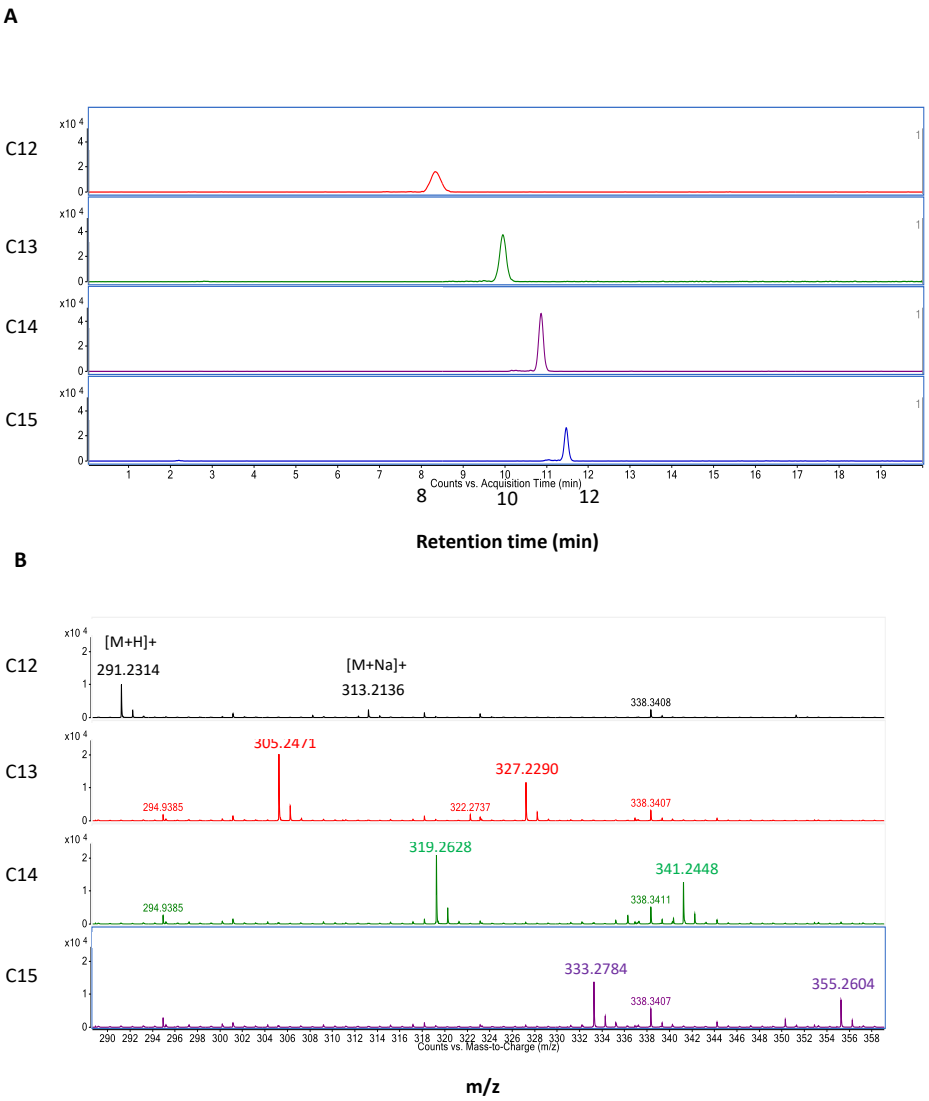

Figure 6.11. Mass spectrometry analysis of the C12-15 alkyl benzoate standard. A. Extracted-ion chromatograms (EIC) from reverse phase HPLC-MS (positive mode) analysis of 3.3 µM C12-15 alkyl benzoate reagent, depicting counts vs acquisition time (retention time). C12, C13, C14, and C15 alkyl benzoates revealed m/z ratios of 291.2324 , 305.2481, 319.2637, and 333.2785 respectively. **B.** Mass spectra for the same four ions. Counts vs mass-to-charge ratio for C12 alkyl benzoate (Rt 8.110-8.556 min, 55 scans), C13 (Rt 9.772-10.111, 42 scans), C14 (Rt 10.715-11.004 min, 36 scans), C15 (11.351-11.558 min, 26 scans). For each alkyl benzoate, the first big peak correlates with an [M+H]+ ion and the second big peak correlates with an [M+Na]+ ion. Mass spectrometry was performed by Dr Tan-Yun Cheng, Brigham and Women's Hospital.

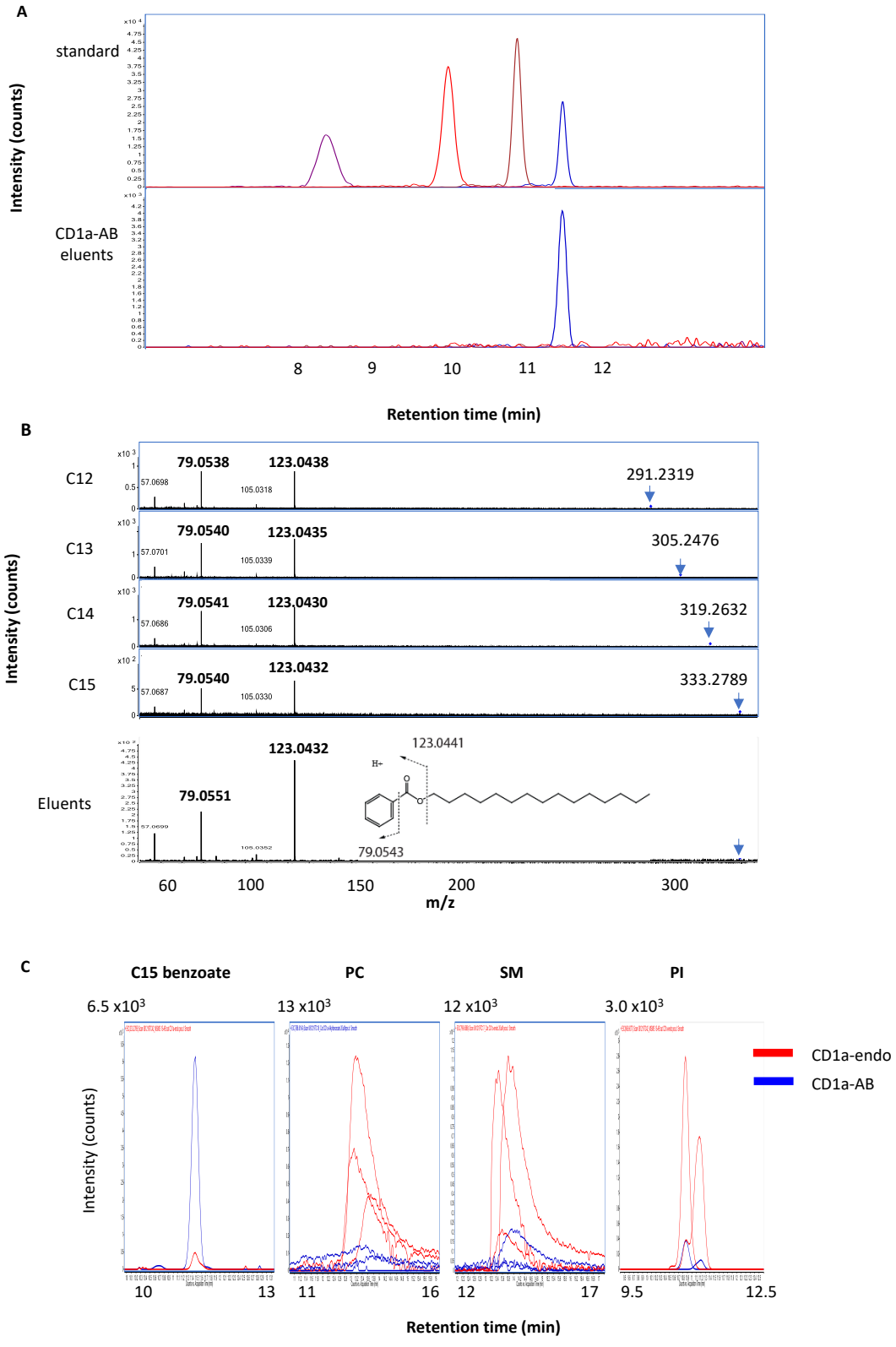
A
standard
CD1a-AB eluents
Intensity (counts)
8
9
10
11
12
Retention time (min)
B
C12
C13
C14
C15
Eluents
79.0538
123.0438
291.2319
79.0540
123.0435
305.2476
79.0541
123.0430
319.2632
79.0540
123.0432
333.2789
123.0432
123.0441
79.0551
79.0543
Intensity (counts)
60
100
150
200
300
m/z
C
C15 benzoate
PC
SM
PI
6.5 x10³
13 x10³
12 x10³
3.0 x10³
CD1a-endo
CD1a-AB
Intensity (counts)
10
13
11
16
12
17
9.5
12.5
Retention time (min)

Figure 6.12. Mass spectrometry analysis of lipids loaded in CD1a produced in the presence of alkyl benzoate. A. EIC of reverse phase HPLC (positive mode) analysis of C12-15 alkyl benzoate standard (top) and lipid eluents from CD1a expressed by GnTI$^-$ cells cultured with alkyl benzoate (CD1a-AB) (bottom) depicting counts vs retention time. **B.** Tandem mass spectrometry counts vs mass-to-charge ratio for C12-15 alkyl benzoate standard (top) and lipid eluents from CD1a (below). Product ions shown from top to bottom are rt 8.186-8.467 min, 12 scans, m/z 219.2324; rt 9.908-10.111 min, 7 scans, m/z 305.2481; rt 10.810-10.996 min, 6 scans, m/z 319.2637; rt 11.409-11.545 min, 5 scans, m/z 333.2785; and rt 11.414-11.515 min, 5 scans, 333.2785. The breakdown of individual product ions from alkyl benzoate is depicted. **C.** Detection of C15 alkyl benzoate (EIC 369.2764), PC (EIC 836.6164), SM (EIC 815.7001), and PI (EIC 906.6067) in CD1a produced as per normal (CD1a-endo, red) and CD1a produced in the presence of alkyl benzoate (CD1a-AB, blue). Mass spectrometry was performed by Dr Tan-Yun Cheng, Brigham and Women's Hospital.

benzoate was present in CD1a produced in the presence of alkyl benzoate but importantly it was not found when it was not added to the culture media *(Fig.6.12c)*, confirming that the presence of alkyl benzoate within CD1a was specifically due to the addition of C12-C15 alkyl benzoate. Untreated CD1a eluents revealed the presence of endogenous lipids PC, SM and PI as expected, but surprisingly, they were minimally present or absent in the alkyl benzoate treated CD1a *(Fig.6.12c)*, suggesting displacement of self-lipids with C15 alkyl benzoate.

This experiment was repeated with CD1a expressed in non-adherent Expi293F cells, which were expected to have a similar lipid repertoire to GnTI$^-$ cells. As with the GnTI$^-$ expression system, cell viability was reduced (30%) in the presence of 0.5% (v/v) alkyl benzoate but sufficient protein was produced.

Consistent with previous results, HPLC-MS analysis revealed strong signals reflecting the elution of alkyl benzoate from CD1a cultured in the presence of alkyl benzoate paired with a loss of self-lipids *(Fig.6.13)*. Interestingly, while labelled as "C12-15 alkyl benzoate", there were small traces of a C16 analogue detected in the standard (a different batch of the same commercial alkyl benzoate used in dermatological products) when assessed by reverse phase HPLC *(Fig.6.13a)*. This difference in the reagent standard was reflected in treated CD1a eluents, as the apparent preference for the larger C15 alkyl benzoate seen in the previous experiment (*Fig.6.12)* also now included C16 alkyl benzoate (to a small degree) *(Fig.6.13a)*. When more protein was examined, a preference for C14 alkyl benzoate was also observed, while the presence of smaller chain length analogues remained minimal. Importantly, the relative abundance of C14 alkyl benzoate in the second experiment was only slightly increased in the CD1a eluent compared to the standard, whereas the relative abundance of C15 alkyl benzoate was greatly increased, suggesting that it is the more preferential analogue *(Fig.6.13c)*. The observation of C14 as an eluent when the protein amount was doubled from 10 μM to 20 μM could hence be due to a higher chance of it being detected as part of the commercial product rather than preferential loading.

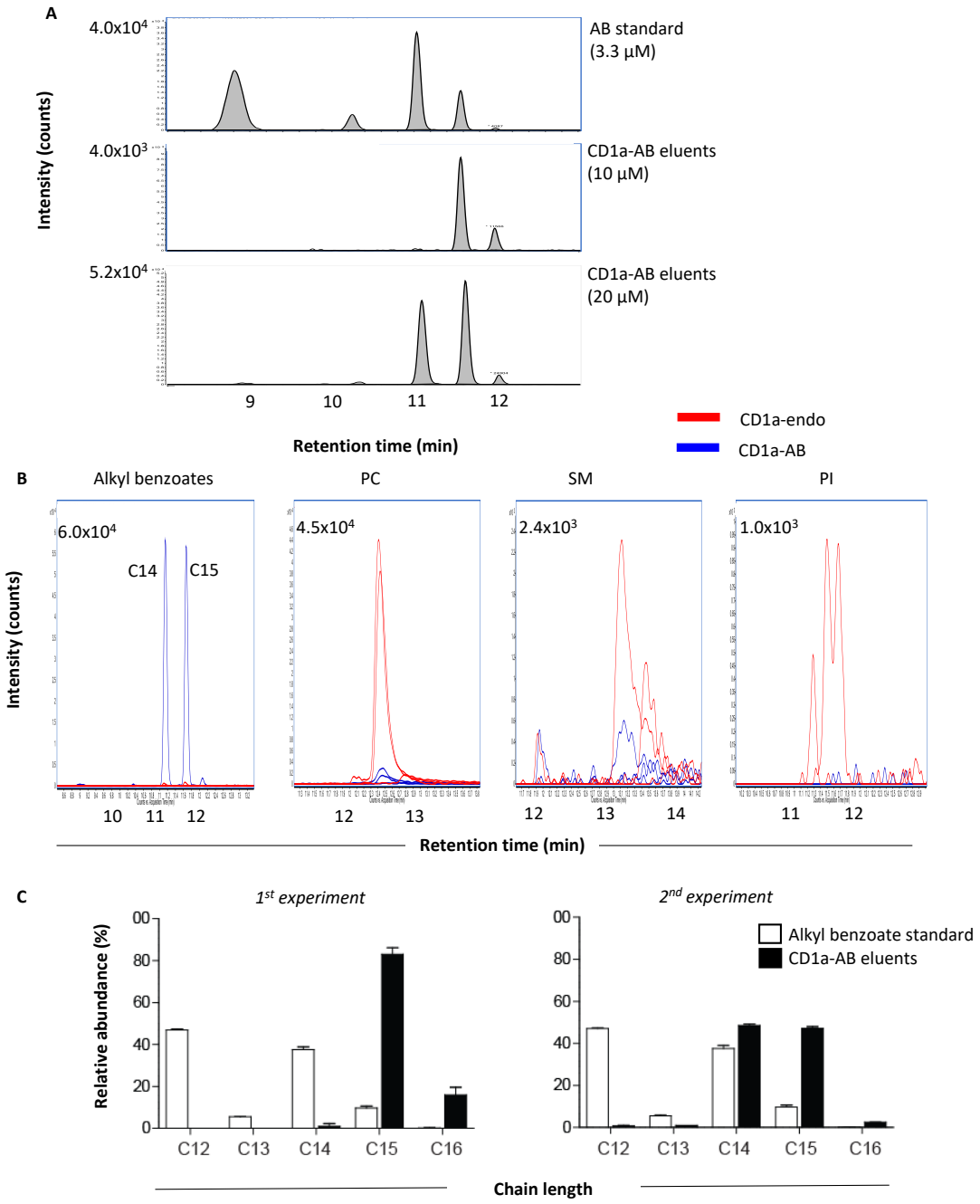

Figure 6.13. Mass spectrometry analysis of alkyl benzoate and CD1a produced in expi293F cells. Reverse phase HPLC, positive mode analyses of CD1a produced in the presence of alkyl benzoate. **A.** Comparison of alkyl benzoate standard and lipid eluents from CD1a produced by expi293F cells cultured with alkyl benzoate using tandem mass spectrometry showing counts vs retention time for EIC (347.2945). **B.** Detection of C15 alkyl benzoate, PC, SM, and PI in CD1a produced as per normal (CD1a-endo, red) and CD1a produced in the presence of alkyl benzoate (CD1a-AB, blue). **C.** Relative abundance of each alkyl benzoate analogue in the first (10 µM eluents) and second (20 µM eluents) experiment. Mass spectrometry was performed by Dr Tan-Yun Cheng, Brigham and Women's Hospital.

These results indicate that, among the chain length variants, CD1a preferentially binds longer (~C15) chain alkyl benzoate compounds. These data strongly support that alkyl

benzoate is indeed a CD1a lipid antigen, and this supports the hypothesis that this antigen can be presented to T cells. Collectively, these findings suggest that C14-16 alkyl benzoates are recognised by CD1a-restricted T cells and may therefore represent a new class of CD1a-restricted allergens.

6.2.8. Isolation of T cells with CD1a-alkyl benzoate tetramers in healthy human blood

Following confirmation of alkyl benzoate loading into CD1a, CD1a tetramers were used in a magnetic enrichment process to isolate CD1a-restricted T cells from healthy human blood that recognise alkyl benzoate as an antigen. Two versions of the alkyl benzoate tetramer were assessed: CD1a-ABexp and 10:1 CD1a-ABL. CD1a-endo monomer was loaded with alkyl benzoate overnight at RT. CD1a-endo and CD1a-ABexp monomer were also left at RT to ensure similar treatment of protein, and all three were tetramerised the following day. CD1a-ABexp, CD1a-ABL, and CD1a-endo tetramers conjugated to PE were used to label 100 x 10^6 PBMCs, that were subsequently incubated with anti-PE magnetic beads, and passed over a magnetic column for magnetic enrichment, as with the method described for CD1a tetramers in Chapter 3.2.2. Two donors were not labelled with CD1a-endo tetramer and only the two alkyl benzoate tetramers of interest.

Fewer cells bound tetramers loaded or expressed with alkyl benzoate compared to CD1a-endo tetramer, suggesting fewer T cells recognise CD1a presenting alkyl benzoate compared to the diverse endogenous lipids loaded in CD1a-endo *(Fig.6.14)*. This makes it difficult to determine whether the tetramer$^+$ cells labelled with the two alkyl benzoate tetramers truly recognised alkyl benzoate, or are more autoreactive to CD1a regardless of the lipid presented. Additionally, the number of cells labelled with tetramer in the unenriched samples were similar to enriched samples – and sometimes more tetramer$^+$ cells were recovered without enrichment, although with less separation between tetramer$^+$ and tetramer$^-$ cells *(Fig.6.14)*. Consistent with previous phenotypic analyses of CD1a-

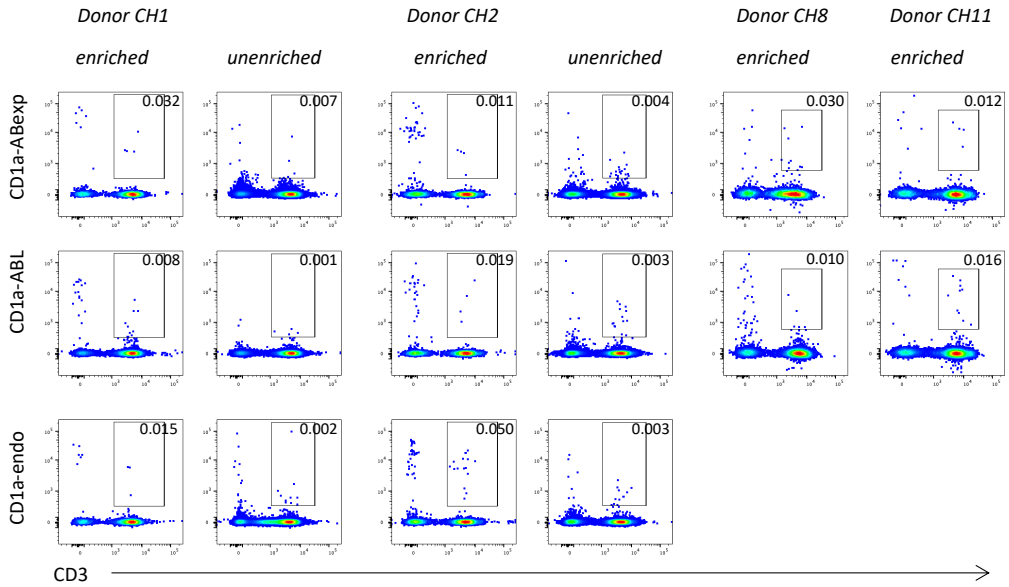

Figure 6.14. Isolation of CD1a-restricted T cell populations directly *ex vivo* from healthy human blood. $CD3^+$ cells labelled with CD1a tetramers among $CD14^-CD19^-7\text{-}AAD^-$ single lymphocytes. Each plot represents PBMCs stained with either CD1a expressed with alkyl benzoate (CD1a-ABexp), CD1a-alkyl benzoate loaded at a 10:1 MW ratio (CD1a-ABL) or CD1a-endo tetramer (in PE), labelled with anti-PE beads, and then $tetramer^+$ cells were enriched over a magnetic column. For two donors, a small number of cells were not passed over the column to compare unenriched samples. Numbers in the top right of each plot indicate the percentage of $tetramer^+$ cells in the total parental population. Data are representative of 4 donors in two independent experiments.

autoreactive T cells in Chapter 3.2.3, tetramer$^+$ cells in these experiments were also predominantly CD4$^+$ (data not shown). The staining with these alkyl benzoate tetramers has yet to be optimised, but nonetheless, as a preliminary assessment of PBMCs from healthy human blood, these experiments suggest that CD1a-restricted T cells that recognise alkyl benzoate may be present in healthy blood. Furthermore, tetramers could be used to assess frequencies of these cells in individuals with ADC to oils like alkyl benzoate in cosmetic/dermatological products to determine whether they have a greater number of CD1a-restricted T cells.

Overall, these experiments, while preliminary and with a small sample size, indicate a possible role for CD1a-restricted T cells in immunological processes of the skin, especially with regards to ADC and other skin pathologies. Furthermore, this data builds upon recent work of others, identifying benzyl benzoate, benzyl cinnamate, or farnesol as CD1a allergens in cosmetic products that are presented by CD1a as T cells agonists (Nicolai et al., 2020), suggesting that alkyl benzoate (particularly C15), is another oil that activates CD1a-restricted T cells.

6.3 Discussion

The skin continually faces numerous challenges such as wounds, infections, inflammatory disorders and cancer. Skin immunity plays a critical role in preventing infection following skin punctures and abrasions as this breach of the first line of defence requires a rapid and potent immune response. To this end, mammals have evolved specialised immune cells that form a barrier in the skin. It has been estimated that human skin contains approximately 1 million T cells/cm^2 and that T cells are more frequent in the skin than in the blood (Clark et al., 2006a).

Unconventional T cells such as γδ-T cells, MAIT cells and NKT cells, also reside in the skin and especially infiltrate under inflammatory conditions such as contact hypersensitivity, allergic contact dermatitis (ACD) and psoriasis (Constantinides et al., 2019, Gober et al., 2008, Kono et al., 2014, Zhao et al., 2008). Consistent with previous studies indicating that γδ-T cells populate non-lymphoid tissues such as skin at high frequencies (Dupuy et al., 1990, Nielsen et al., 2017), populations of γδ-T cells were isolated from the epidermis. Subsets of epidermal lipid-reactive T cells restricted to each of the CD1 molecules expressed γδ-TCRs, and these may represent a group of cells that respond to lipid molecule cues, similar to dendritic epidermal T cells in mice (Li et al., 2011b, Martin et al., 2009a).

The role of lipid-reactive T cells in maintaining skin homeostasis remains relatively unexplored. Previous observations have described human resident T cells in skin being mainly either memory $CD8^+$ T cells in the epidermis and CLA^+ $CD4^+$ or $CD8^+$ T cells in the dermis (Cai et al., 2012). Here, $CD4^+$ and DN T cells were isolated in the epidermis but separating epidermal and dermal layers is not an exact process so some crossover may have been possible. Epidermal T cells were fairly evenly distributed between $CD4^+$ and $CD8^+$ fractions, rather than being predominantly $CD8^+$. Indeed, $CD4^+$ cells were prominent among epidermal CD1b-, CD1c- and CD1d-restricted T cell populations similar to blood. In addition, epidermal CD1-restricted T cells also exhibited elevated expression of CD45RO and CLA, particularly among type I NKT cells. Further studies are required to determine whether these are effector or resident memory T cells and to determine their functional characteristics.

Accumulating evidence implicates a role for CD1a-mediated responses in skin immunity. LCs, which exhibit high expression of CD1a, are thought to interact with skin resident and effector memory T cells, inducing their activation and proliferation in a steady state (Seneschal et al., 2012), and may have a similar relationship with CD1a-restricted T cells. Previous studies suggest that CD1a-autoreactive T cells are present in the skin (de Jong et al., 2010, Cotton et al., 2021), where Langerhans cells can capture and present lipids derived from skin oils (de Jong et al., 2014, Meunier et al., 1996). Upon activation, CD1a-restricted T cells have been known to produce IFN-γ, IL-17 and IL-22, and studies have particularly focused on their recognition of self-antigens in the skin (Cotton et al., 2021, de Jong et al., 2014, de Jong et al., 2010, Kim et al., 2016). The data in this thesis further supports the exploration of epidermal CD1a-restricted T cells and their phenotype using tetramers *ex vivo*.

The isolation of CD1a-restricted T cells that recognise self-lipids in skin here and by others (Cotton et al., 2021) raises the question of how autoreactivity is avoided. One of the challenges of skin immunity is the balance of protecting against a constant threat of pathogens while suppressing unnecessary and harmful inflammation (Nestle et al., 2009). Sebaceous lipids, such as triglycerides, wax esters and squalene are primarily non-polar lipids, and epidermal lipids produced by keratinocytes are a mixture of ceramides, free fatty acids and cholesterol (Pappas, 2009), some of which act as CD1a autoantigens (de Jong et al., 2014). These autoantigens can be recognised promiscuously by an individual CD1a-autoreactive T cell clone (BC2), despite their substantial difference in size (squalene, C30; wax esters, C36; triacylglycerides, C51; and fatty acids, C16) (de Jong et al., 2014). They also lack headgroups to form hydrogen- or charge-based contacts with TCRs, consistent with the non-interference model of interaction observed by a CD1a-autoreactive TCR (BK6) with CD1a-Ag and suggesting that skin oils are similarly permissive to TCR binding (Birkinshaw et al., 2015, de Jong et al., 2014). Given the cross-reactivity and different CD1a docking modes exhibited by TCRs discussed in Chapter 4, it is likely that many CD1a-restricted T cell clones may have the potential to respond to self-antigens in the skin.

One mechanism for preventing autoimmunity could be spatial separation: oily autoantigens are largely concentrated in human sebaceous glands and cornified epithelia (Nicolaides, 1974), while CD1a is largely confined to epidermal LCs and a small

population of CD1a-expressing dermal DCs ($CD14^-$ $CD207^-$ $CD1a^+$) that can also activate cellular immunity (Klechevsky et al., 2008, Nestle et al., 1993, Santegoets et al., 2008). Furthermore, inflammatory skin diseases such as atopic dermatitis and psoriasis are associated with changes in ceramide or other skin lipid composition (Di Nardo et al., 1998, Motta et al., 1993), therefore supporting a role for lipid-reactive T cells that sense these changes in the lipid repertoire in disease pathogenesis. For example, ointments that contain lipids (including ceramide, which can be presented by CD1a (de Jong et al., 2014)) used in treatments can influence T cell responses (Kircik et al., 2011). Thus, the physical separation of CD1a, CD1a-restricted T cells and CD1a antigens, in addition to the accessibility of certain lipids, likely helps prevent excessive activation of these T cells in a healthy state.

Furthermore, when skin is damaged through puncture or abrasion, these may come together to elicit CD1a-dependent immune responses. A degree of CD1a autoreactivity may even be beneficial in barrier repair and skin healing. Human skin contains T cells that conduct immunosurveillance and maintain tissue integrity by providing immune protection and immunoregulation based on their recognition of cognate antigens or epithelial stress-induced antigens (Mueller et al., 2014, Strid et al., 2009). It may be that barrier breaches, such as trauma and infection, transfer surface or sebaceous oils to deeper layers to promote barrier repair by CD1a-restricted T cells (Colonna, 2010, de Jong et al., 2010), whereas CD1a-restricted T cells, CD1a, and potential agonists usually remain segregated under normal conditions.

Conversely, a highly responsive T cell population in the skin can pose problems when the skin is penetrated or breached by other antigens that elicit CD1a-mediated responses. Autoreactivity can contribute to allergies, for example, ACD, a common T cell-mediated inflammatory skin disease (Gober and Gaspari, 2008). CD1a-restricted T cells, specifically, have been implicated in ACD responses due to the recognition of neoantigens or foreign lipids (Cheung et al., 2016, Jarrett et al., 2016b, Kim et al., 2016, Nicolai et al., 2020).

ACD is caused by a DTH response in the skin, in which the immune system reacts to environmental substances that are typically considered harmless. The response is mainly orchestrated by allergen-specific T cells that recognise neoantigens created by reactive chemicals that modify non-immunogenic self-proteins (Vocanson et al., 2009, Mraz et

al., 2020), and self-lipid recognition could contribute to pathology too. Immunopathology is characterised by inflammation and leukocyte infiltration driven by effector T cells (Vocanson et al., 2009).

The first link between CD1a and allergic responses was made in the context of bee and wasp venom, and subsequently, house dust mites due to the introduction of PLA enzymes into the skin that generate neoantigens (Bourgeois et al., 2015, Jarrett et al., 2016b, Subramaniam et al., 2016). A subsequent study investigated DTH responses to common contact dermatitis allergens in consumer products: benzyl benzoate, benzyl cinnamate, farnesol, and coenzyme-Q (Nicolai et al., 2020). While haptens, drugs, or cations are widely known to influence MHC-peptide recognition by T cells that mediate DTH by modifying self-peptides (Gefen et al., 2015), these studies demonstrate that the direct presentation of lipid antigens by CD1a can also contribute to contact dermatitis (Nicolai et al., 2020).

Due to a DTH response following application of a particular sunscreen, I decided to investigate the role of CD1a-restricted T cells in mediating ACD triggered by dermatological products. Interestingly, a survey of European populations revealed that nearly half of those with prolonged rashes (lasting more than three days), attributed their rash to exposure to daily use products including cosmetics, soaps, shampoos, or other household products (Naldi et al., 2014). Two earlier surveys also highlighted the magnitude of skin problems among the general population due to scented or cosmetic products (Johansen et al., 2000, Trattner et al., 2009). Coincidentally, I experienced a DTH reaction to a particular sunscreen, as indicated by immunopathological damage occurring 24–72 hours after initial sensitisation (Mak and Saunders, 2006). A candidate causative agent was identified as C12-15 alkyl benzoate, which is similar in structure to urushiol, a compound found in plants of the *Toxicodendron* genus (e.g. poison ivy and poison oak) that can trigger urushiol-specific T cell reactions and severe inflammation (Kalish, 1990, Kalish and Johnson, 1990, Kalish et al., 1994). Because C15:2 urushiol was previously identified as a CD1a antigen, C12-15 alkyl benzoate was interrogated for its potential to activate CD1a-restricted T cells. It had previously been reported as a trigger for contact dermatitis in a similar-presenting case study, along with benzyl benzoate and benzyl salicylate (Werbrouck et al., 2015). Additionally, AHR, which is expressed by CD1a-restricted T cells (de Jong et al., 2010), may allow these cells to

respond to environmental cues such as UVB (Esser et al., 2013), which may have contributed to the photosensitivity-driven DTH response to alkyl benzoate in the aforementioned case.

A number of studies have assessed the acute dermal toxicity of benzyl-containing compounds in dermatological products, such as benzyl alcohol, benzoic acid, benzyl benzoate, and alkyl benzoates. While they have been declared safe, many were evaluated using rats or rabbits (Becker et al., 2012, Johnson et al., 2017, Nair, 2001). Studies of C12-15 alkyl benzoate, specifically, revealed that it was not toxic to rats or mice when administered orally or as an aerosol, nor was it an irritant in a dermal toxicity study of rabbits (data submitted by the Personal Care Products Council as reported in (Becker et al., 2012)). Like mice, rats do not possess CD1a, while two CD1a genes have been identified in rabbits (Hayes and Knight, 2001) that may present different lipid antigens. The species difference could be similar to the milder IFN-γ response to urushiol observed in mice (Wakabayashi et al., 2005), while in humans and CD1a-transgenic mice with high levels of CD1a in skin tissue, urushiol triggers a greater inflammatory reaction (Kim et al., 2016). The equivalent CD1a-restricted responses in humans may therefore not be observed in these animals. An irritation study in which C12-15 alkyl benzoate was applied to the backs of participants did not result in irritation, however with n = 21 (Becker et al., 2012), it may be that none of the participants tested were susceptible to this allergy. Here, C12-15 alkyl benzoate was confirmed to be loaded into CD1a, with a preference for the longer chain analogue, and could activate CD1a-restricted T cells.

These experiments not only identify a novel CD1a allergen, they also highlight a novel method of selectively loading a CD1a molecule with a lipid molecule. It is unclear whether alkyl benzoate was endocytosed by GnTI$^-$ cells and loaded endogenously or whether loading occurred exogenously. CD1a is typically located at the cell surface *in vivo,* and the lack of transmembrane and cytoplasmic domains in soluble CD1a limits or eliminates endosomal recycle, making exogenous loading plausible (Barral et al., 2008, Sugita et al., 1999). Furthermore, alkyl benzoate displaced endogenous self-lipids loaded in CD1a, thereby potentially displacing non-permissive lipids and resulting in T cell activation (and contributing to allergic responses) in a similar manner to wax esters and other headless skin oils (de Jong et al., 2014).

A wide range of antigenic structures presented by CD1a may contribute to ACDD. The size of the carbon skeletons of oily antigens presented by CD1a identified here and by others, including alkyl benzoate (C14 to C16), are substantially smaller than known antigens presented by other CD1 molecules (C20 to C40) (Zajonc et al., 2005b, Zajonc et al., 2003, Nicolai et al., 2020). Interestingly, benzyl benzoate and benzyl cinnamate lack carbon chains and are thought to be buried within the groove so as to not perturb contact with TCRs and allow for cross-reactivity (Nicolai et al., 2020). In contrast, the binary structure of a CD1a-urushiol complex revealed that a region of the antigen is accessible for direct TCR contact, and the CD1a molecule undergoes a conformational change to accommodate it, potentially impacting TCR binding (Kim et al., 2016). Given the structural similarity of alkyl benzoate to urushiol, it may also have contacts with CD1a-restricted TCRs that are yet to be determined.

A future direction of this work would be to collect blood samples from individuals with known ACD that is triggered by dermatological products containing alkyl benzoate, or similar compounds, and assess their CD1a-restricted T cell frequencies. For reasons that are not entirely clear, some individuals become sensitised to neoantigens and environmental oils (e.g. in plants or in cosmetic products) that can be presented by CD1a, therefore triggering CD1a-dependent inflammatory responses. Alkyl benzoate, an oil found in around 50% of children and adult sun creams (International Nomenclature Cosmetic Ingredient Beauty), is one such novel antigen identified in this thesis that activates CD1a-restricted T cells. Targeting CD1a with inhibitors, including an anti-CD1a mAb or non-permissive lipids that block TCR-CD1a binding (e.g. SM), may therefore be beneficial in therapies to prevent inflammatory skin diseases like psoriasis, eczema and ACD.

There is a growing amount of evidence to support a role for CD1a-restricted T cells in skin – both in homeostasis and disease pathogenesis – and the present study observed populations of epidermal T cells restricted to each CD1 isoform. The data here hence support the idea that γδ-T cells and CD1-restricted T cells are found in the skin and may contribute to an immune network that responds to environmental stimuli. These studies thus highlight the importance of understanding the biology of CD1a and CD1a-restricted T cells in the skin. The modulation of CD1a-restricted T cells may provide opportunities to better understand and treat skin-based allergic reactions.

Chapter 7: General Discussion

Our understanding of "unconventional" T cell populations, including CD1-restricted T cells, has improved substantially over the past two decades. The development of tools such as CD1d-α-GalCer tetramers, which specifically identify type I NKT cells, has led to thousands of studies exploring these cells. Unconventional T cells represent abundant populations of cells within the immune system, comprising up to 10% of circulating T cells – and even more in some organs – and are poised to provide rapid, robust immune responses (de Lalla et al., 2011, Godfrey et al., 2015). The monomorphic nature of CD1 molecules and unique biology of lipid-reactive T cells make them attractive novel cellular targets for immunotherapy and vaccine design that will not be limited by the same inter-donor variability as conventional MHC-restricted T cells.

Despite increasing evidence that they play important roles in infection, allergy, cancer, and autoimmunity, studies of group 1 CD1-restricted T cells that recognise lipid antigens are limited. For example, the role of CD1a-restricted T cells is not well understood, and they may be either protective or pathogenic under different circumstances. The recognition of mycobacterial lipids by CD1a-restricted T cells observed here and by others (reviewed in Van Rhijn et al., 2013b, Van Rhijn and Moody, 2015) suggests that they may be protective against mycobacteria, while their recognition of allergens, such as alkyl benzoate, appears to contribute to allergic reactions in skin. However, their phenotype and functions, their TCR repertoire, and their cognate lipid antigens are not yet fully understood.

CD1a is expressed by epithelial DCs in the skin, respiratory tract, gingiva and salivary gland, conjunctiva, and vagina and cervix (Crawford et al., 1989, Tazi et al., 1993a, Yoshida et al., 1997, Uhlen et al., 2015, van Blokland et al., 2000, Rodriguez-Garcia et al., 2018, Rodriguez-Garcia et al., 2017). This tissue distribution suggests that CD1a may play a role in antigen presentation at sites constantly exposed to environmental stimuli and external pathogens, thereby contributing to barrier immunity by sampling lipid antigens and carrying them to draining lymph nodes.

Lipid-reactive T cells are thought to bridge innate and adaptive immune responses upon recognition of certain lipids, whose levels are perturbed under inflammatory conditions

(Godfrey et al., 2015). In this thesis, populations of CD1a-autoreactive T cells were identified in most donors using tetramers presenting endogenous mammalian lipids, indicating that CD1a-restricted T cells can also respond to self-lipids. Using mass spectrometry, the lipids presented by CD1a that bound CD1a-restricted TCRs in a ternary co-complex were mostly SM and PC, although results varied for different TCR clones and this experiment was limited to the GnTI$^-$ cell lipidome. Identifying self-lipid antigens that are recognised by CD1a-restricted T cells is important to understand their role in inflammatory disease. Serum lipid levels, such as TAG and other potential CD1a antigens, tend to be elevated in chronic inflammatory diseases, such as rheumatoid arthritis, psoriasis, and inflammatory bowel disease (Birkinshaw et al., 2015, de Jong et al., 2014, de Jong et al., 2010, Feingold and Grunfeld, 2000). Self-lipid-reactive CD1a-restricted T cells may hence play a role in allergy and autoimmune responses associated with aberrant lipid profiles to either drive or suppress pathology.

Conventional CD4$^+$ T cells play a key role in adaptive immune responses and polarise immune cells towards the appropriate pathway depending on the nature of the immunological challenge. Consistent with previous studies, CD1a-restricted T cells isolated in this thesis were predominantly CD4$^+$ (de Lalla et al., 2011, de Jong et al., 2010, Kasmar et al., 2013). Not only did most CD1a-restricted T cells express CD4, but a preliminary study assessing whether CD1a tetramers bind CD4 in the absence of a TCR revealed promising results suggesting that there might be an important interaction between CD1a and CD4. This is not too dissimilar to CD4 binding MHC class II molecules to aid TCR recognition and enhance cytokine production (Janeway, 1992, Li et al., 2013). In addition, transcriptomic analysis of CD1a-restricted T cells in this study revealed that their gene expression was more similar to that of conventional CD4$^+$ T cells compared to other lipid-reactive T cell populations such as NKT cells and CD1b-restricted T cells. Furthermore, CD1a-restricted T cells exhibited distinct gene expression from T cells with cytotoxic capacity (i.e. they did not display cytotoxic markers). This is suggestive of CD1a-restricted T cells playing roles more similar to those of existing CD4$^+$ T helper cell subsets, further supported by their production of different cytokine profiles upon activation in different contexts (e.g. IL-22, IL-17, IFN-γ, and IL-13) (de Jong et al., 2010, Kim et al., 2016, Cotton et al., 2021).

Analysis of CD1a-restricted T cells revealed that highly expressed genes encode immunomodulatory effectors, such as *PIK3IP1, GMFG, GILZ,* and *SDCBP*, all of which are known to inhibit immune responses, suggestive of a possible role in regulating immune responses. It is likely that CD1a-restricted T cells are not a homogenous population, but rather, like conventional $CD4^+$ T cells, NKT cells and MAIT cells, can be further divided into subsets and play different roles depending on the immune context. As such, it is important that future studies of CD1a-restricted T cells take this into account, even though there has been little evidence of functional diversity among peripheral blood NKT cells and MAIT cells in humans to date. In a PCA analysis of transcriptomic data, not all CD1a-restricted T cells fell within a single cluster, suggesting that CD1a-restricted T cells may be heterogenous and perform different functions depending on their context of activation.

The limited TCR diversity and antigen repertoire of unconventional T cells mean that their precursor frequency can vastly outnumber pMHC-specific conventional T cells (Godfrey et al., 2015). Evidence to date has indicated that CD1a-restricted TCRs are heterogenous in their V, D, J gene usage (Vincent et al., 2005, Cohen et al., 2009, de Jong et al., 2010, de Lalla et al., 2011, Grant et al., 1999), however, here, discernible patterns of TCR variable gene biases were observed in both TCR α- and β-chains. Many CD1a-restricted TCRs used TRAV8-4, TRAV19 and TRBV28, with a bias for TRBV28 seen in nearly half of all TCRs sequenced. CDR loops encoded by these TCR variable genes may be optimal for CD1a-lipid interactions. In order to test this hypothesis and identify TCR-CD1a/lipid contacts, the soluble CD1a and CD1a-restricted TCR proteins produced in this thesis could be used in future biophysical and structural studies (e.g., surface plasmon resonance analysis and X-ray crystallography to assess affinity, CD1a-lipid contacts and molecular interactions). The incorporation of particular Vα and Vβ genes may also reflect bias caused by thymic selection, or may reflect prior antigen exposure given that many CD1a-restricted TCRs appear to recognise a variety of both self- and non-self-lipid antigens. Like other T cells they may expand upon encountering antigens, thus altering the TCR repertoire within this subset, similar to long-term exposure to aerosols and pollutants altering the pulmonary T cell repertoire (Yurovsky et al., 1996).

CD1a-restricted T cells isolated here and by others have been found to interact with CD1a irrespective of the lipid antigens presented, that is to say they appear autoreactive to CD1a

itself or may bind to the antigen-binding cleft in such a way that allows promiscuous binding between different antigens (Cotton et al., 2021). The exact identity of lipid antigens may therefore not be the main determinant of CD1a-dependent responses, but rather, the lipid headgroup structure may be more important in determining whether T cell activation occurs. One study suggested that antigens are either permissive or non-permissive to TCR binding depending on whether they interfere with the TCR-CD1a interaction, particularly around the CD1a A'-roof (Birkinshaw et al., 2015). However, this thesis has revealed that different TCRs exhibit different binding specificities with regards to permissive or non-permissive lipids. For example, prior studies have indicated that certain lipids with bulky or charged headgroups (e.g. SM) prevent CD1a-dependent T cell activation for certain clones (Birkinshaw et al., 2015, de Jong et al., 2014, Cotton et al., 2021). In this thesis, however, SM was found to be a permissive lipid for a CD1a-restricted TCR that binds a broad range of CD1a-lipid tetramers. It may be that CDR loops encoded by a particular TCR's variable genes enable promiscuous binding to CD1a regardless of lipid content. Additional x-ray crystallography and TCR mutagenesis assays, together with further CD1a mutant activation assays, will provide definitive data regarding TCR recognition of CD1a presenting different antigens.

The TCR biases observed for CD1a restricted T cells were detected using both multiplex nested PCR TCR sequencing and RNA sequencing of CD1a-restricted T cells, giving confidence in the reproducibility of results. Furthermore, similar patterns of variable gene usage were observed among T cells isolated with CD1a-endo, CD1a-vehicle, and CD1a-DDM tetramers. It will be important to sequence CD1a-restricted TCRs that recognise a host of lipid agonists, including squalene, TAG, and lysophospholipids, as well as known antagonist, SM, to determine whether CD1a-restricted T cells with reactivity to different lipid antigens retain the same variable gene biases. Identification of additional CD1a-restricted TCR sequences will help to establish the requirements of TCR-CD1a/lipid antigen recognition.

The contribution of CD1a-restricted TCR responses to antigens in the immune response is of increasing interest in skin homeostasis and disease. CD1a is abundant in the skin, is highly expressed by epidermal LCs, and to a lesser extent, dermal DCs. The former localises at the barrier between the skin immune system and microbiome, making them ideally situated to detect barrier breaches and changes in the external environment

(Mizumoto and Takashima, 2004, Yoshida et al., 2014). The tendency of CD1a to remain at the cell surface where it is able to capture exogenous antigens (Sugita et al., 1999, Barral and Brenner, 2007), suggests that it may present lipids reflective of various environmental factors and antigen exposures in the skin. For example, the lipid repertoire is often altered under inflammatory skin conditions (Di Nardo et al., 1998, Imokawa et al., 1991, van Smeden et al., 2014), and lipid-modifying enzymes that increase levels of lipids known to activate CD1a-restricted T cells have also been implicated in inflammation (Murakami et al., 2016). For example, levels of PLA2 enzymes, which cleave phospholipids to produce lysophospholipids and fatty acid neoantigens that are presented by CD1a, are elevated in some inflammatory skin diseases, allergy, and chronic inflammation (Chiba et al., 2004, Mahil et al., 2017, Murakami et al., 2016, Cheung et al., 2016). This is supported by recognition of neoantigens generated by PLA2 released from mast cell-derived exosomes by psoriatic T cells (Cheung et al., 2016).

Similarly, PLA2 derived from HDM, bee or wasp venom cleaves endogenous skin phospholipids to create neoantigens that activate CD1a-restricted T cells (Bourgeois et al., 2015, Jarrett et al., 2016a). In addition, CD1a-expressing type-2 innate lymphoid cells (ILC2s) produced PLA2 following HDM exposure in an *in vivo* skin model, making them suited to present neoantigens to CD1a-restricted T cells and promote skin inflammation (Hardman et al., 2017). Given that ILC2s are a potent source of immune effector cytokines that have been implicated in allergic diseases and that many CD1a-mediated allergic inflammatory responses appear to be triggered by phospholipid cleavage that generates neoantigens (McKenzie, 2014, de Jong and Ogg, 2020), therapeutic strategies that regulate CD1a expression and PLA2 activity should be further explored. The method of isolating cells from skin suction blisters following *in vivo* antigenic challenge developed by Graham Ogg's research group (Hardman et al., 2017) in combination with CD1a tetramers described here may aid further investigations.

In addition to responses to neoantigens, the recognition of non-self-lipid allergens by CD1a-restricted T cells has been observed in response to C15:2 urushiol (found in poison ivy and poison oak) and small, hydrophobic compounds in cosmetic products (Kim et al., 2016, Nicolai et al., 2020). In these cases, lipid antigens were presented in the CD1a binding groove such that they were minimally exposed for TCR recognition, supporting the hypothesis of indirect recognition rather than antigen-specific responses to these lipids

(Moody and Suliman, 2017, Cotton et al., 2018, Kim et al., 2016, Nicolai et al., 2020). In this thesis, C15 alkyl benzoate was identified as an additional lipid in cosmetic products that is likely presented by CD1a to T cells. Tetramer binding and activation assays suggested that alkyl benzoate is a permissive lipid for CD1a-restricted T cells. Like the previously identified CD1a allergen urushiol, which has a similar structure, it may also be indirectly recognised via the absence of interference model (i.e. it does not hinder crucial TCR interactions with CD1a and therefore can elicit responses) (Kim et al., 2016).

Given the monomorphic nature of CD1a, factors besides HLA genetic variability must explain why not all individuals experience the same allergic responses mediated by CD1a-restricted T cells. One determinant of CD1a-mediated allergy may be basal frequency of CD1a-restricted T cells, as hypersensitive individuals tended to have elevated frequencies of peripheral blood CD1a-restricted T cells that are responsive to CD1a-expressing APCs in the presence of bee/wasp venom and HDM compared to those without allergies (Jarrett et al., 2016a, Subramaniam et al., 2016). This hypothesis is supported by greater frequencies of CD1a-autoreactive T cells in psoriasis patients, and increased $CD1a^+$ cell populations with altered migratory patterns in lesions of inflammatory skin pathologies, including psoriasis, AD, and contact dermatitis (Pigozzi et al., 2006, Deguchi et al., 2002, Kim et al., 2016, Bangert et al., 2003, Scibior et al., 2019, Wollenberg et al., 1996, Cheung et al., 2016, He et al., 2020, Langeveld-Wildschut et al., 2000). Indeed, in this thesis, varying levels of CD1a-restricted T cells were identified using CD1a tetramers loaded with different lipid antigens. Elevated frequencies of $CD1a^+$ cells and CD1a-restricted T cells in individuals with skin allergies and pathologies could be assessed using tetramers loaded with urushiol, alkyl benzoate and other small allergens on blood, blister fluid, and skin biopsies.

CD1a-restricted T cells have also been implicated in airway hypersensitivity reactions to aerosolised allergens such as plant pollen particles. Expression of CD1a by bronchial APCs and respiratory epithelial cells (Soler et al., 1989, Tazi et al., 1993a) suggests that these airway inflammatory responses may be partially mediated by CD1a. CD1a- and CD1d-expressing pulmonary DCs capture and present a number of lipids from cypress pollen, particularly PC and PE, which have stimulated T cell clones from hypersensitive individuals in a CD1-dependent manner (Agea et al., 2005). Lipids derived from olive pollen also trigger CD1d upregulation by monocytes and macrophages, causing NKT cell

activation *in vitro* (Abos Gracia et al., 2017). In another *in vitro* study, NKT cell deficient mice experienced reduced hypersensitivity responses following intranasal administration of ragweed pollen compared to WT mice (Bilenki et al., 2004). Conversely, mice pre-sensitised with α-GalCer exhibited exacerbated responses (Bilenki et al., 2004), implicating NKT cells as drivers of hypersensitivity. CD1a-restricted T cells may also contribute to hypersensitivity to pollen lipids that are presented by CD1a, which could be tested in macaques or CD1a-transgenic mouse models. They may even play a protective role as IL-22, one of the key cytokines known to be produced by CD1a-restricted T cells (de Jong et al., 2010, Hardman et al., 2017), has been observed to attenuate IFN-γ-mediated allergic inflammation in asthmatic patients (Hirose et al., 2018, Hirose et al., 2013, Pennino et al., 2013). IL-22-producing CD1a-restricted T cells may therefore be protective in some cases of airway inflammation, which would be in line with the expression of immunosuppressive genes determined by RNA sequencing in this thesis.

The mechanisms that maintain tolerance to self-lipids under normal conditions in the skin (and airways) despite the presence of CD1a-autoreactive T cells remain unknown. One mechanism for CD1a-restricted T cell tolerance could be spatial separation of T cells, APCs, and lipid agonists, as known CD1a autoantigens are largely concentrated in human sebaceous glands and cornified epithelia (Nicolaides, 1974). Peripheral tolerance of conventional T cells is regulated by both cell-extrinsic (Tregs and tolerogenic DCs) and cell-intrinsic (e.g. transcriptional and epigenetic) mechanisms (Nurieva et al., 2011), and perhaps similar mechanisms are also partly responsible for tolerance of CD1a-restricted T cells. Interactions between costimulatory molecules on APCs with receptors on T cells (e.g. CD28, CD40L and ICOS) is critical for mounting conventional $CD4^+$ T cell responses, while inhibitory signals, such as engagement of receptors CTLA-4 and PD-1, regulate the induction of T cell tolerance (Nurieva et al., 2006, Chen and Flies, 2013). Further studies should therefore investigate the presence of these stimulatory and inhibitory receptors on CD1a-restricted T cells in peripheral blood and skin.

Another possibility is that the abundance of antagonistic lipids, such as SM, under homeostatic conditions prevent CD1a-autoreactive responses. SM has been regarded as a non-permissive lipid antigen that does not activate the CD1a-restricted T cell clone BK6 (Birkinshaw et al., 2015), however, mass spectrometry of lipids eluted from CD1a-lipid-TCR traps performed in this thesis revealed that it did bind a different TCR clone, 27a28,

highlighting the differing reactivities of TCR clones. Furthermore, mass spectrometry of lipids eluted from CD1a expressed in the presence of alkyl benzoate revealed that endogenous lipids, including SM, had been displaced in favour of C14 or C15 alkyl benzoate. This suggests that typical "non-permissive" lipids may be displaced by CD1a allergens, thereby increasing the chance of CD1a-restricted T cells becoming activated. It may be that the ratio of permissive to non-permissive (agonistic to antagonistic) lipids influence CD1a-restricted T cell responses, rather than the presence of specific lipids, and that this balance is perturbed in skin pathologies or by the introduction/generation of specific lipid antigens in the case of allergies.

Understanding how CD1a-restricted T cell tolerance is maintained during steady state may inform the drivers of CD1a-mediated allergy. SM and phospholipids can be cleaved into ceramides and small fatty acid chains respectively, which activate CD1a-restricted T cells (de Jong et al., 2014, Kraft, 2016), and the balance of agonistic and antagonistic lipids may contribute to tolerance. SM appears to be the most promising antagonistic CD1a antigen to date (Birkinshaw et al., 2015, de Jong et al., 2014, Cotton et al., 2021), however, it did not always appear non-permissive to TCR binding in the studies performed as part of this thesis. SM chain length may play a role in determining how the antigen sits in the CD1a antigen binding groove, and therefore SM antigens of varying chain length should be examined for their capacity to impair CD1a-mediated responses. If a universal inhibitory ligand can be identified for CD1a-restricted T cells, or a way to inhibit CD1a-restricted T cell-mediated pathologies is developed (e.g. with an anti-CD1a blocking antibody), it may be possible to prevent CD1a-mediated allergies and skin disorders.

Highlighting the importance of CD1a in the immune response, at least one SNP in the non-coding region of the *CD1A* gene is associated with greater risk of pulmonary TB, likely by reducing CD1a expression in DCs (Seshadri et al., 2013, Seshadri et al., 2014). It is not yet known whether *CD1A* SNPs also influence the development and frequency of CD1a-restricted T cells, however, lower CD1a expression appears to increase disease susceptibility, suggesting a role for CD1a-restricted T cells in mycobacterial lipid antigen recognition.

As further evidence of a role in mycobacterial infections, populations of T cells that bound CD1a tetramers loaded with the TB lipid antigen DDM were isolated in every blood donor assessed in this thesis. Furthermore, while the isomer DDM-A was previously identified as the most agonistic DDM isomer (Cheng et al., 2017), T cell clones assessed here demonstrated different reactivity: some clones showed greater binding and activation with other DDM isomers. Mycobactins that are structurally similar to DDM that have not yet been identified may also be recognised by CD1a-restricted T cells, as elements of the mycobactin biosynthesis pathway are still being discovered (Madigan et al., 2012), and therefore other mycobactin pathway derivates may be CD1a antigens.

Mycobactin production is common among mycobacterial species, and those from the TB group (Mtb*, M.bovis,* and *M.africanum)* are identical (Barclay and Ratledge, 1988), suggesting that DDM and structurally similar lipids from species within this group may also play a role in immunity against a range of mycobacterial species. Supporting this hypothesis, CD1a-restricted T cells have been observed to undergo clonal expansion following the presentation of antigens from *M.leprae*, and these cells were cross-reactive with antigens from Mtb*, M.smegmatis* and *M.phlei* (as well as weakly cross-reactive with ones from additional bacterial species) (Hunger et al., 2004). In this thesis, cross-recognition between CD1a antigens was observed with DDM and less bulky lipids for several CD1a-restricted T cell clones, and therefore it may be possible for DDM-reactive T cells to also recognise and be cross-protective against lipid antigens from related bacteria species. A future direction of this study is to assess whether mycobacterial lipids from other species can also be directly loaded into CD1a, and if so, to assess their capacity to activate different CD1a-restricted T cell clones.

Despite accumulating evidence that lipid-reactive T cells respond to mycobacterial lipids, they have not yet been considered in TB vaccine design as the focus has mostly been on conventional peptide-reactive T cells (Andersen and Scriba, 2019). However, the recognition of immunogenic lipids, such as DDM and GMM, by CD1-restricted T cells may augment protective memory immune responses. The BCG vaccine contains a largely complete set of highly immunogenic cell wall lipids, but these are absent from recently developed, less effective subunit vaccines (Andersen and Doherty, 2005, Rhoades et al., 2005). This negative correlation could highlight the importance of immunogenic lipids.

Furthermore, high frequencies of CD1b-restricted T cells that recognise glycolipids from pathogenic mycobacteria have been found in both healthy donors and LTBI patients (Busch et al., 2016, Stenger et al., 1998, Stenger et al., 1997). Their production of perforin, granzyme B and granulysin upon activation demonstrates a role for these cells during Mtb infection. In addition, some TB-infected individuals have clonally expanded GMM-reactive T cells, termed GEM T cells, that express the highly conserved TRAV1-2/TRAJ9 TCR α-chain (Van Rhijn et al., 2013a, DeWitt et al., 2018). One study showed that populations of TRAV1-2$^+$ GMM-reactive T cells were frequent in South African adolescents with and without LTBI, but not healthy donors in the US, suggestive of TB mediated immunity in areas where TB is endemic (Layton et al., 2018). While CD1a-restricted T cell populations have not been as well studied in the context of TB infection and/or BCG vaccination, clonally expanded populations of DDM-reactive T cells were isolated in some donors in this thesis, and their age is suggestive that they may have received the BCG vaccine, although vaccination status was unconfirmed. Future studies should assess CD1a-restricted T cell frequencies following vaccination and/or infection, as mycobacterial lipids may function as adjuvants and/or cognate T cell antigens to elicit protective CD1-restricted responses.

TB is the leading cause of death among people living with HIV, who are around 19 times more likely to develop active disease than HIV- individuals (World Health Organization, 2019). CD4$^+$ T cells play a dominant role during Mtb infection, and their depletion in people co-infected with HIV leads to the absence of protective immunity and uncontrolled bacterial growth (Cooper, 2009, Markowitz et al., 1997, North and Jung, 2004, Orme et al., 1993). One study found that patients with HIV-TB co-infection have reduced numbers of GMM-reactive T cells compared to HIV- individuals with latent or active TB (Kasprowicz et al., 2016). A reduction of CD1b-restricted T cells that recognise mycobacterial lipids, which are typically CD4$^+$ CCR5$^+$ (and are therefore also potential targets of HIV), may contribute to the increased incidence of TB among HIV+ individuals (Kasprowicz et al., 2016). Furthermore, Type I NKT cells, which also express high levels of CCR5, are similarly depleted in HIV+ individuals (Fernandez et al., 2014, Motsinger et al., 2002, Fleuridor et al., 2003, Mureithi et al., 2011, Sandberg et al., 2002, van der Vliet et al., 2002). Given that most CD1a-restricted T cells here expressed CD4, especially those that bound DDM, their susceptibility to HIV and what this means for HIV/TB co-infection should be thoroughly investigated as their expression of CD4 may

make them targets for HIV infection. Since Mtb-derived DDM is highly antigenic for these cells (Moody et al., 2004), their depletion may impair mycobacterial immunity in HIV-TB co-infection. The role of group 1 CD1-restricted T cells in TB and HIV infection thus warrants further investigation.

Independently of TB, CD1a-restricted T cells may also play a role early in the response to HIV infection. $CD1a^+$ LCs in the vaginal mucosa and endocervix are well placed to sample antigens in the female genital tract (FGT), a critically important site for defence against microbes as a key point of entry for pathogens including HIV (Rodriguez-Garcia et al., 2018, Rodriguez-Garcia et al., 2017, Monin et al., 2020). Unconventional T cells in the FGT, such as MAIT cells and γδ-T cells, have been observed to produce IL-17 and/or IL-22 upon activation (Gibbs et al., 2017, Anipindi et al., 2019). These two cytokines are known to be produced by CD1a-restricted T cells (de Jong et al., 2010, Kim et al., 2016) and therefore, these cells may also interact with lipids sampled from the FGT lumen and contribute to homeostasis and barrier immunity. They may especially play a role in augmenting Th17 responses early in HIV (and other pathogen) infections given that virus-specific IL-17-producing $CD4^+$ T cells induce early pro-inflammatory responses (Yue et al., 2008). In this thesis, CD1a-restricted T cells were not observed to produce IL-17 following 4-hour, non-specific stimulation with PMA and ionomycin, although this may be because they require longer activation times to produce cytokines, or may require a specific microenvironment to induce IL-17 expression. However, a transcriptomic analysis of CD1a-restricted T cells revealed expression of *SAMHD1* (encoding sterile alpha motif (SAM) and histidine/aspartic acid (HD) domain-containing protein 1). SAMHD1, a deoxynucleoside triphosphate (dNTP) triphosphohydrolase, is a key restriction factor that inhibits HIV-1 viral replication by inhibiting reverse transcription in resting $CD4^+$ T cells (Descours et al., 2012, Lahouassa et al., 2012, Lim et al., 2012, Baldauf et al., 2012). Future studies should explore the breadth and magnitude of innate-like immune responses and protection offered by CD1a-restricted T cells, which, unlike GMM-reactive T cells and type I NKT cells, displayed high levels of SAMHD1, and how these cells are impacted by HIV infection.

Compared to other groups of unconventional T cells, CD1a-restricted T cell populations have not been as well studied in the context of TB and HIV infections, and the tetramers generated in this thesis provide valuable tools to study all CD1-restricted T cell subsets

in patients or macaque models of TB and HIV/AIDS. NHP are frequently used in pre-clinical testing due to their phylogenetic proximity to humans. Macaques, specifically, contain similar repertoires of immune cells and exhibit remarkable similarities to humans in their immunological and pathological responses. Researchers can monitor the course of TB disease using nearly identical parameters to those tested in humans, and infection of Asian macaques with simian immunodeficiency virus (SIV) or simian-human immunodeficiency virus (SHIV) is widely regarded as the current best model for AIDS research given that it results in $CD4^+$ T cell depletion (Hatziioannou and Evans, 2012, Pena and Ho, 2015, Thippeshappa et al., 2020). In this thesis, the southern PTM (*M.nemestrina),* found throughout Southeast Asia, was selected as they can successfully model infection with simian-tropic HIV-1 and are increasingly being studied as an NHP model for AIDS (Hatziioannou et al., 2009). Examining T cells that bind CD1a-tetramer from the skin, lungs, reproductive tract, draining LNs, and peripheral blood will provide insight into the role of CD1a-restricted T cells during bacterial and viral infections. Here, tetramers were used to interrogate these tissues in healthy juvenile PTM and showed potential for future studies of lipid-reactive T cells in NHPs.

In this thesis, ptmCD1-restricted T cell populations were isolated from healthy PTM at frequencies aligned with previous estimates of type I NKT cells in rhesus macaques and CD1-autoreactive T cell populations in humans (de Lalla et al., 2011, Yu et al., 2019). The identification of macaque NKT cells has major implications for delineating their role in NHP disease models of TB, HIV, autoimmunity, and other pathological conditions. Type I NKT cells have already been studied in NHP models such as rhesus macaques, particularly in the context of mycobacterial infection (Barouch et al., 2002, Sharpe et al., 2017), and designing tools to study group 1 CD1-restricted T cells in macaques allows us to study these cells in a way we simply cannot in humans. In this thesis, trans-species cross-reactivity was observed between some but not all T cells restricted to different CD1 isoforms. CD1d-α-GalCer and NKT trans-species cross-reactivity had been previously observed for mice, humans and macaques, however this was the first instance the phenomenon was observed for CD1b and CD1c presenting endogenous lipids.

Immunophenotyping of healthy ptmCD1-restricted T cells here revealed expression of CCR5, a key receptor used by HIV/SIV for virus entry into cells and pathogenesis in humans and macaques (Littman, 1998, Unutmaz et al., 1998). Given the susceptibility of

$CCR5^{hi}$ $CD4^+$ T cells to HIV infection (Motsinger et al., 2002) and the predominant expression of CD4 by macaque lipid-reactive T cells, lipid-reactive T cell populations may be specifically targeted by HIV, dependent on their expression of CCR5. In rhesus macaques, while the majority of $V\alpha24^+$ NKT cells are $CD4^-$, they exhibit high expression of CCR5 and are more susceptible to SIV infection than conventional $CD4^+$ T cells (Motsinger et al., 2003). This suggests that CCR5 is a greater determinant than CD4 for susceptibility and that $CD4^-$ unconventional T cells may also be targets. With many ptmCD1-restricted T cells being $CCR5^+$ in this thesis, these cells require further investigation in the context of HIV/SIV immunopathology. Further studies should profile type II NKT and group 1 CD1-restricted T cells in these species to determine whether they also share their TCR repertoire – like the "pan-primate" ($TRAV10\text{-}TRAJ18^+$) semi-invariant NKT TCR (Gansuvd et al., 2008, Gansuvd et al., 2003, Yu et al., 2019), to further elucidate their phenotype, and to establish their role in immunity.

Like NKT and MAIT cells, CD1a-restricted T cells are an attractive target for immunotherapy and vaccine design due to the monomorphic nature of CD1a. Interestingly, the CD1a antigen, squalene, is used as a component of immunologic adjuvants in several vaccines, including seasonal, pandemic and avian influenza, and some COVID-19 vaccine candidates (Lippi et al., 2010, Mirzaei et al., 2020). Commercial squalene used in vaccines is primarily sourced from shark liver oil, or more recently, plants (Kim and Karadeniz, 2012, Wolosik et al., 2013). It is possible that this may activate CD1a-autoreactive T cells in a similar manner to human-derived squalene given that the chemical structure is the same (de Jong et al., 2014). Adjuvants containing squalene (predominantly MF59 and AS03) induce transcriptional responses related to chemokines, cytokines, and pro-inflammatory transcription factors for strong, localised inflammatory responses and recruitment of DCs, monocytes, neutrophils and eosinophils (Harandi, 2018). MF59-based influenza vaccines induce enhanced, longer lasting immune responses and greater efficacy compared to non-adjuvanted vaccines (Esposito et al., 2011, Vesikari et al., 2009, Vesikari et al., 2011, Zedda et al., 2015). This is attributed to enhanced APC recruitment and activation of antigen-specific $CD4^+$ T cells (Galli et al., 2009), of which CD1a-restricted T cells may be included. Rats and mice, which are both CD1a-deficient, respond to squalene as an adjuvant, albeit there are slight variations in the human and murine response to AS03- and MF59-adjuvanted vaccines (Wilkins et al., 2017). Whether there is a contribution of CD1a-restricted T cells to the

immune response following vaccination in humans requires investigation. For example, this could be done using CD1a tetramers to study them at the injection site and in circulation before and after vaccination, and loading tetramers with squalene to assess the ability of T cells to recognise it as an antigen.

Overall, this thesis provides fundamental insight into the biology of CD1a-restricted T cells and lays the foundation for new investigations of these and other lipid-reactive T cells. Specifically, studies focused on examining the molecular mechanisms that govern the recognition of numerous lipid antigens presented by CD1a, as well as the study of CD1-restricted T cells in NHP models and human tissue samples using CD1 tetramers described here. The constitutive high expression of CD1a on skin-resident APCs and studies of CD1a-restricted T cells to date support the notion that CD1a-mediated T cell responses play a central role in skin homeostasis and immunity, as well as skin pathologies. However, the interaction between lipids, APCs and CD1a-restricted T cells requires further exploration. An understanding of exactly how CD1a-restricted T cells respond to different immune challenges and behave *in situ* may advise therapeutic interventions and aid in the development of vaccines that specifically target lipid-reactive T cell responses. The knowledge from such studies will contribute to our understanding of the biology and behaviour of CD1a-restricted, their role in the immune system, and in turn, will provide valuable clues as to how to best manipulate these cell types to protect against infectious disease and unwanted inflammatory immune responses.

Appendices

Appendix I: Transfected protein sequences

Table AI.1. Sequences of human and macaque proteins transfected into cell lines.

Protein	Transfection vector	Protein sequence
CNR1 TCR	pMIG-II	EAIKLGNEFATMLLLLVPVLEVIFTLGGTRAQSVTQLDSHVSVSEGTPVLLRCNYSS SYSPSLFWYVQHPNKGLQLLLKYTSAATLVKGINGFEAEFKKSETSFHLTKPSAHM SDAAEYFCVVIGTMFSGGYNKLIFGAGTRLAVHPYIQNPDPAVYQLRDSKSSDKSV CLFTDFDSQTNVSQSKDSDVYITDKTVLDMRSMDFKSNSAVAWSNKSDFACANAF NNSIIPEDTFFPSPESSCDVKLVEKSFETDTNLNFQNLSVIGFRILLLKVAGFNLLMTL RLWSSGSGATNFSLLKQAGDVEENPGPMSNQVLCCVVLCFLGANTVDGGITQSPK YLFRKEGQNVTLSCEQNLNHDAMYWYRQDPGQGLRLIYYSQIVNDFQKGDIAEGY SVSREKKESFPLTVTSAQKNPTAFYLCAARTDSNQPQHFGDGTRLSILEDLLTIPHNI
1-1a28 TCR	pMIG-II	EAIKLGNEFATMLLLLVPVLEVIFTLGGTRGQSLEQPSEVTAVEGAIVQINCTYQTS GFYGLSWYQQHDGGAPTFLSYNALDGLEETGRFSSFLSRSDSYGYLLLQELQMKD SASYFCAVKGTYKYIFGTGTRLKVLANIQNPDPAVYQLRDSKSSDKSVCLFTDFDS QTNVSQSKDSDVYITDKTVLDMRSMDFKSNSAVAWSNKSDFACANAFNNSIIPEDT FFPSPESSCDVKLVEKSFETDTNLNFQNLSVIGFRILLLKVAGFNLLMTLRLWSSGSG ATNFSLLKQAGDVEENPGPMSNQVLCCVVLCFLGANTVDVKVTQSSRYLVKRTGE KVFLECVQDMDHENMFWYRQDPGLGLRLIYFSYDVKMKEKGDIPEGYSVSREKK ERFSLILESASTNQTSMYLCASSFPGLAGGRTGELFFGEGSRLTVLEDLLTIPHNI
8-2a2 TCR	pMIG-II	EAIKLGNEFATMLLLLVPVLEVIFTLGGTRAQSVTQLDSHVSVSEGTPVLLRCNYSS SYSPSLFWYVQHPNKGLQLLLKYTSAATLVKGINGFEAEFKKSETSFHLTKPSAHM SDAAEYFCVVVSGTYKYIFGTGTRLKVLANIQNPDPAVYQLRDSKSSDKSVCLFTD FDSQTNVSQSKDSDVYITDKTVLDMRSMDFKSNSAVAWSNKSDFACANAFNNSIIP EDTFFPSPESSCDVKLVEKSFETDTNLNFQNLSVIGFRILLLKVAGFNLLMTLRLWSS GSGATNFSLLKQAGDVEENPGPMSNQVLCCVVLCFLGANTVEPEVTQTPSHQVTQ MGQEVILRCVPISNHLYFYWYRQILGQKVEFLVSFYNNEISEKSEIFDDQFSVERPD GSNFTLKIRSTKLEDSAMYFCASSEALLLAGDQETQYFGPGTRLLVLEDLLTIPHNI
8-2a13i TCR	pMIG-II	EAIKLGNEFATMLLLLVPVLEVIFTLGGTRAQSVTQLDSHVSVSEGTPVLLRCNYSS SYSPSLFWYVQHPNKGLQLLLKYTSAATLVKGINGFEAEFKKSETSFHLTKPSAHM SDAAEYFCVVTGTYGQNFVFGPGTRLSVLPYIQNPDPAVYQLRDSKSSDKSVCLFT DFDSQTNVSQSKDSDVYITDKTVLDMRSMDFKSNSAVAWSNKSDFACANAFNNSI IPEDTFFPSPESSCDVKLVEKSFETDTNLNFQNLSVIGFRILLLKVAGFNLLMTLRLW SSGSGATNFSLLKQAGDVEENPGPMSNQVLCCVVLCFLGANTVAAGVIQSPRHLIK EKRETATLKCYPIPRHDTVYWYQQGPGQDPQFLISFYEKMQSDKGSIPDRFSAQQF SDYHSELNMSSLELGDSALYFCASSLEDETQYFGPGTRLLVLEDLLTIPHNI

8-2a13ii TCR	pMIG-II	EAIKLGNEFATMLLLLVPVLEVIFTLGGTRAQSVTQLDSHVSVSEGTPVLLRCNYSS SYSPSLFWYVQHPNKGLQLLLKYTSAATLVKGINGFEAEFKKSETSFHLTKPSAHM SDAAEYFCAVSVGSSYKLIFGSGTRLLVRPDIQNPDPAVYQLRDSKSSDKSVCLFTD FDSQTNVSQSKDSDVYITDKTVLDMRSMDFKSNSAVAWSNKSDFACANAFNNSIIP EDTFFPSPESSCDVKLVEKSFETDTNLNFQNLSVIGFRILLLKVAGFNLLMTLRLWSS GSGATNFSLLKQAGDVEENPGPMSNQVLCCVVLCFLGANTVAAGVIQSPRHLIKEK RETATLKCYPIPRHDTVYWYQQGPGQDPQFLISFYEKMQSDKGSIPDRFSAQQFSD YHSELNMSSLELGDSALYFCASSPTEWTSGDSSYEQYFGPGTRLTVTEDLLTIPHNI
17a11-2i TCR	pMIG-II	EAIKLGNEFATMLLLLVPVLEVIFTLGGTRSQQGEEDPQALSIQEGENATMNCSYKT SINNLQWYRQNSGRGLVHLILIRSNEREKHSGRLRVTLDTSKKSSSLLITASRAADT ASYFCATTNRDDKIIFGKGTRLHILPNIQNPDPAVYQLRDSKSSDKSVCLFTDFDSQT NVSQSKDSDVYITDKTVLDMRSMDFKSNSAVAWSNKSDFACANAFNNSIIPEDTFF PSPESSCDVKLVEKSFETDTNLNFQNLSVIGFRILLLKVAGFNLLMTLRLWSSGSGA TNFSLLKQAGDVEENPGPMSNQVLCCVVLCFLGANTVEAGVAQSPRYKIIEKRQSV AFWCNPISGHATLYWYQQILGQGPKLLIQFQNNGVVDDSQLPKDRFSAERLKGVD STLKIQPAKLEDSAVYLCASSLTAPELNNEQFFGPGTRLTVLEDLLTIPHNI
17a28 TCR	pMIG-II	EAIKLGNEFATMLLLLVPVLEVIFTLGGTRSQQGEEDPQALSIQEGENATMNCSYKT SINNLQWYRQNSGRGLVHLILIRSNEREKHSGRLRVTLDTSKKSSSLLITASRAADT ASYFCASSSGGTYKYIFGTGTRLKVLANIQNPDPAVYQLRDSKSSDKSVCLFTDFDS QTNVSQSKDSDVYITDKTVLDMRSMDFKSNSAVAWSNKSDFACANAFNNSIIPEDT FFPSPESSCDVKLVEKSFETDTNLNFQNLSVIGFRILLLKVAGFNLLMTLRLWSSGSG ATNFSLLKQAGDVEENPGPMSNQVLCCVVLCFLGANTVDVKVTQSSRYLVKRTGE KVFLECVQDMDHENMFWYRQDPGLGLRLIYFSYDVKMKEKGDIPEGYSVSREKK ERFSLILESASTNQTSMYLCASSLDLTDTQYFGPGTRLTVLEDLLTIPHNI
27a28 TCR	pMIG-II	EAIKLGNEFATMLLLLVPVLEVIFTLGGTRTQLLEQSPQFLSIQEGENLTVYCNSSSV FSSLQWYRQEPGEGPVLLVTVVTGGEVKKLKRLTFQFGDARKDSSLHITAAQPGDT GLYLCAGGSNYKLTFGKGTLLTVNPNIQNPDPAVYQLRDSKSSDKSVCLFTDFDSQ TNVSQSKDSDVYITDKTVLDMRSMDFKSNSAVAWSNKSDFACANAFNNSIIPEDTF FPSPESSCDVKLVEKSFETDTNLNFQNLSVIGFRILLLKVAGFNLLMTLRLWSSGSG ATNFSLLKQAGDVEENPGPMSNQVLCCVVLCFLGANTVDVKVTQSSRYLVKRTGE KVFLECVQDMDHENMFWYRQDPGLGLRLIYFSYDVKMKEKGDIPEGYSVSREKK ERFSLILESASTNQTSMYLCASSQFLAGGTEQYFGPGTRLTVTEDLLTIPHNI
29a28i TCR	pMIG-II	EAIKLGNEFATMLLLLVPVLEVIFTLGGTRDQQVKQNSPSLSVQEGRISILNCDYTN SMFDYFLWYKKYPAEGPTFLISISSIKDKNEDGRFTVFLNKSAKHLSLHIVPSQPGDS AVYFCAASAWSNQFYFGTGTSLTVIPNIQNPDPAVYQLRDSKSSDKSVCLFTDFDS QTNVSQSKDSDVYITDKTVLDMRSMDFKSNSAVAWSNKSDFACANAFNNSIIPEDT FFPSPESSCDVKLVEKSFETDTNLNFQNLSVIGFRILLLKVAGFNLLMTLRLWSSGSG ATNFSLLKQAGDVEENPGPMSNQVLCCVVLCFLGANTVDVKVTQSSRYLVKRTGE KVFLECVQDMDHENMFWYRQDPGLGLRLIYFSYDVKMKEKGDIPEGYSVSREKK ERFSLILESASTNQTSMYLCASSFGGPTRELFFGEGSRLTVLEDLLTIPHNI
29a28ii TCR	pMIG-II	EAIKLGNEFATMLLLLVPVLEVIFTLGGTRDQQVKQNSPSLSVQEGRISILNCDYTN SMFDYFLWYKKYPAEGPTFLISISSIKDKNEDGRFTVFLNKSAKHLSLHIVPSQPGDS AVYFCAASALSNQFYFGTGTSLTVIPNIQNPDPAVYQLRDSKSSDKSVCLFTDFDSQ TNVSQSKDSDVYITDKTVLDMRSMDFKSNSAVAWSNKSDFACANAFNNSIIPEDTF FPSPESSCDVKLVEKSFETDTNLNFQNLSVIGFRILLLKVAGFNLLMTLRLWSSGSG ATNFSLLKQAGDVEENPGPMSNQVLCCVVLCFLGANTVDVKVTQSSRYLVKRTGE KVFLECVQDMDHENMFWYRQDPGLGLRLIYFSYDVKMKEKGDIPEGYSVSREKK ERFSLILESASTNQTSMYLCASRFTGWAFFGQGTRLTVVEDLLTIPHNI

35a16 TCR	pMIG-II	EAIKLGNEFATMLLLLVPVLEVIFTLGGTRGQQLNQSPQSMFIQEGEDVSMNCTSSS IFNTWLWYKQDPGEGPVLLIALYKAGELTSNGRLTAQFGITRKDSFLNISASIPSDV GIYFCAGQSGSKMKTSYDKVIFGPGTSLSVIPNIQNPDPAVYQLRDSKSSDKSVCLF TDFDSQTNVSQSKDSDVYITDKTVLDMRSMDFKSNSAVAWSNKSDFACANAFNNS IIPEDTFFPSPESSCDVKLVEKSFETDTNLNFQNLSVIGFRILLLKVAGFNLLMTLRL WSSGSGATNFSLLKQAGDVEENPGPMSNQVLCCVVLCFLGANTVGEEVAQTPKHL VRGEGQKAKLYCAPIKGHSYVFWYQQVLKNEFKFLISFQNENVFDETGMPKERFS AKCLPNSPCSLEIQATKLEDSAVYFCASSLWDRYTEAFFGQGTRLTVVEDLLTIPHN I
13-1pa4-1 TCR	pMIG-II	EAIKLGNEFATMLLLLVPVLEVIFTLGGTRGENVEQHPSTLSVQEGDSAVIKCTYSD SASNYFPWYKQELGKGPQLIIDIRSNVGEKKDQRIAVTLNKTAKHFSLHITETQPED SAVYFCAASKYSTLTFGKGTMLLVSPDIQNPDPAVYQLRDSKSSDKSVCLFTDFDS QTNVSQSKDSDVYITDKTVLDMRSMDFKSNSAVAWSNKSDFACANAFNNSIIPEDT FFPSPESSCDVKLVEKSFETDTNLNFQNLSVIGFRILLLKVAGFNLLMTLRLWSSGSG ATNFSLLKQAGDVEENPGPMSNQVLCCVVLCFLGANTVDTEVTQTPKHLVMGMT NKKSLKCEQHMGHRAMYWYKQKAKKPPELMFVYSYEKLSINESVPSRFSPECPNS SLLNLHLHALQPEDSALYLCAASKYSTLTFGSGTRLTVVEDLLTIPHNI
16pb28 TCR	pMIG-II	EAIKLGNEFATMLLLLVPVLEVIFTLGGTRAQRVTQPEKLLSVFKGAPVELKCNYS YSGSPELFWYVQYSRQRLQLLLRHISRESIKGFTADLNKGETSFHLKKPFAQEEDSA MYYCALSHTGNQFYFGTGTSLTVIPNIQNPDPAVYQLRDSKSSDKSVCLFTDFDSQ TNVSQSKDSDVYITDKTVLDMRSMDFKSNSAVAWSNKSDFACANAFNNSIIPEDTF FPSPESSCDVKLVEKSFETDTNLNFQNLSVIGFRILLLKVAGFNLLMTLRLWSSGSG ATNFSLLKQAGDVEENPGPMSNQVLCCVVLCFLGANTVDVKVTQSSRYLVKRTGE KVFLECVQDMDHENMFWYRQDPGLGLRLIYFSYDVKMKEKGDIPEGYSVSREKK ERFSLILESASTNQTSMYLCASRLRGRREETQYFGPGTRLLVLEDLLTIPHNI
8-6pc4-1 TCR	pMIG-II	EAIKLGNEFATMLLLLVPVLEVIFTLGGTRAQSVTQLDSQVPVFEEAPVELRCNYSS SVSVYLFWYVQYPNQGLQLLLKYLSGSTLVESINGFEAEFNKSQTSFHLRKPSVHIS DTAEYFCAVSDRWGYQKVTFGTGTKLQVIPNIQNPDPAVYQLRDSKSSDKSVCLFT DFDSQTNVSQSKDSDVYITDKTVLDMRSMDFKSNSAVAWSNKSDFACANAFNNSI IPEDTFFPSPESSCDVKLVEKSFETDTNLNFQNLSVIGFRILLLKVAGFNLLMTLRLW SSGSGATNFSLLKQAGDVEENPGPMSNQVLCCVVLCFLGANTVDTEVTQTPKHLV MGMTNKKSLKCEQHMGHRAMYWYKQKAKKPPELMFVYSYEKLSINESVPSRFSP ECPNSSLLNLHLHALQPEDSALYLCASSQDRTGTPYEQYFGPGTRLTVTEDLLTIPH NI
6pc4-1 TCR	pMIG-II	EAIKLGNEFATMLLLLVPVLEVIFTLGGTRSQKIEQNSEALNIQEGKTATLTCNYTN YSPAYLQWYRQDPGRGPVFLLLIRENEKEKRKERLKVTFDTTLKQSLFHITASQPA DSATYLCALIGYQKVTFGTGTKLQVIPNIQNPDPAVYQLRDSKSSDKSVCLFTDFDS QTNVSQSKDSDVYITDKTVLDMRSMDFKSNSAVAWSNKSDFACANAFNNSIIPEDT FFPSPESSCDVKLVEKSFETDTNLNFQNLSVIGFRILLLKVAGFNLLMTLRLWSSGSG ATNFSLLKQAGDVEENPGPMSNQVLCCVVLCFLGANTVDTEVTQTPKHLVMGMT NKKSLKCEQHMGHRAMYWYKQKAKKPPELMFVYSYEKLSINESVPSRFSPECPNS SLLNLHLHALQPEDSALYLCASSQLGTDTNYGYTFGSGTRLTVVEDLLTIPHNI
26pd29 TCR	pMIG-II	EAIKLGNEFATMLLLLVPVLEVIFTLGGTRDAKTTQPPSMDCAEGRAANLPCNHSTI SGNEYVYWYRQIHSQGPQYIIHGLKNNETNEMASLIITEDRKSSTLILPHATLRDTA VYYCIVRVTQGSNYQLIWGAGTKLIIKPDIQNPDPAVYQLRDSKSSDKSVCLFTDFD SQTNVSQSKDSDVYITDKTVLDMRSMDFKSNSAVAWSNKSDFACANAFNNSIIPED TFFPSPESSCDVKLVEKSFETDTNLNFQNLSVIGFRILLLKVAGFNLLMTLRLWSSGS GATNFSLLKQAGDVEENPGPMSNQVLCCVVLCFLGANTVSAVISQKPSRDICQRGT SLTIQCQVDSQVTMMFWYRQQPGQSLTLIATANQGSEATYESGFVIDKFPISRPNLT FSTLTVSNMSPEDSSIYLCSATYRDRGLGTEAFFGQGTRLTVVEDLLTIPHNI

ptmCD1a	pMIG-II	MLFLLLPLLAVLPGGGNADGLKEPVSFHVIRISSFNNHSWKRNLVSGYLGHLQTHT SDRNCSTIIFLWPWSRGNFSNEEWKELEMLLHICCVRFLEGMRRYSRELQFEYPFEI QVTGGCELHSGKFSGSFLRLAYQGSDFISFQNNSWLPSPVAGNMAKRLCKVINQNQ HQNDIIHSLLSDTCPRLILGLLDAGKAHLQRQVKPEAWLSRGLSPGPGRLQLVCHV SGFYPKPVWVMWMRGEQEQQGTQRGDILPNADGTWYLRATQEVAAGEAADLSC RVKHSSLEGQDIILYWEHHSSMGLIILAGIVPLLLLIGLALWFRKRCFR*
ptmCD1b	pMIG-II	MLLLPFQLLAVLFPGGDSERAFQGPTSFHVIQTSSFTNSTWAQTQGSGWLDDLQIH GWDSDSGTAILLKPWSKGNFSDKEFAELEEIFRVYIFGFAQEVQDFAGDFQIQYPFEI QGIAGCELHSGGAIVSFLRGALRGLDFLSVKNASCVPSPEGGSKAQKVCALIMQYQ GIMETVRILLYETCPRYLLGVLHAGKADLQRQVKPEAWLSSGPSPGPGRLQLVCHV SGFYPKPVWVMWMRDEQEQRGTQLGDILPNANWTWYLQATLDVAAGEAAGLSC RVKHSSLEGQDIVLYWRNPTSTGSIVLAIMVPSLLLLLCLALWYMRRRSYQTIP*
ptmCD1c	pMIG-II	MLFLQFLLLAVLSGGDNADAQEHVSFYTIQILSFANQSWAQSQGSGWLDELQTHG WESESGRIIFLHTWSKSNFSNEELSDLELLFRVYFFGLTREIQDHASQDYSKYPFEVQ VKAGCELHSGKSPEGFFRVAFNGLDLLSFQNTTWVPSPDGGSLAPGVCHLLNHQY EGVTETVYNLIRSTCPRFLLGLLDAGKMYLHRQVRPEAWLSSRRSLGSGRLLLVCH ASGFYPKPVWVTWMRNEQEQLGTKHGDVLPNADGTWYLQVILEVASEETAGLSC RVRHSSLGGQDIILYWGHHFSMNWIALIVLVSLVILIVLVLRFKKHCSYQDIL*
ptmCD1d	pMIG-II	MGCLLFLLLWALLQAWGSAEVPQRLFPLRCLQISSFANSNWTRTDGLAWLGELQT HSWSNDSDTIRSLKPWSQGTFSDQQWEALQRVFRVYRSSFTRDVKEFAKMLRLAY PMELQVSAGCEVHPGNASHNFFHVAFQGSDILSFQGTSWEPAQEAPLWVNLAIQV LNQDKWTKETVQWLLNDTCPQFVSGLLESGKSELEKQVKPKAWLSRGPSPGPGRL QLVCHVSGFYPKPVWVKWMRGEQEQQGTQRGDILPNADETWYLRATLEVAAGE AAGLSCRVKHSSLEGQDIVLYWAGGSHTSVGLIALAVLACLLFLLALIVGFTFRFKR QTSYQGIL*

Appendix II: Soluble protein sequences

Table AII.1. Soluble human and macaque protein sequences and expression systems.

Protein	Expression system	Expression vector	Protein sequence
ptmCD1a	GnTI⁻ HEK 293S cells	pHLsec	TGLKEPVSFHVIRISSFNNHSWKRNLVSGYLGHLQTHTSDRNCSTIIFLWPWSRGNFSNEEWKELEMLLHICCVRFLEGMRRYSRELQFEYPFEIQVTGGCELHSGKFSGSFLRLAYQGSDFISFQNNSWLPSPVAGNMAKRLCKVINQNQHQNDIIHSLLSDTCPRLILGLLDAGKAHLQRQVKPEAWLSRGLSPGPGRLQLVCHVSGFYPKPVWVMWMRGEQEQQGTQRGDILPNADGTWYLRATQEVAAGEAADLSCRVKHSSLEGQDIILYWEGSLVPRGSGSRIARLEEKVKTLKAQNSELASTANMLREQVAQLKQKVMNHGSGLNDIFEAQKIEWHEHHHHHHH**GTL
ptmβ2m*	GnTI⁻ HEK 293S cells	pHLsec	TGIQRTPKIQVYSRHPPENGKPNFLNCYVSGFHPSDIEVDLLKNGEKMGKVEHSDLSFSKDWSFYLLYYTEFTPNEKDEYACRVNHVTLSGPRTVKWDRDMGSLVPRGSGSLTDTLQAETDQLEDKKSALQTEIANLLKEKEKLEFILAAH**GTL
ptmCD1b	GnTI⁻ HEK 293S cells	pHLsec	TGERAFQGPTSFHVIQTSSFTNSTWAQTQGSGWLDDLQIHGWDSDSGTAILLKPWSKGNFSDKEFAELEEIFRVYIFGFAQEVQDFAGDFQIQYPFEIQGIAGCELHSGGAIVSFLRGALRGLDFLSVKNASCVPSPEGGSKAQKVCALIMQYQGIMETVRILLYETCPRYLLGVLHAGKADLQRQVKPEAWLSSGPSPGPGRLQLVCHVSGFYPKPVWVMWMRDEQEQRGTQLGDILPNANWTWYLQATLDVAAGEAAGLSCRVKHSSLEGQDIVLYWRNPGSLTPRGVRLGSLNDIFEAQKIEWHEHHHHHH**GTL
ptmCD1c	GnTI⁻ HEK 293S cells	pHLsec	TGADAQEHVSFYTIQILSFANQSWAQSQGSGWLDELQTHGWESESGRIIFLHTWSKSNFSNEELSDLELLFRVYFFGLTREIQDHASQDYSKYPFEVQVKAGCELHSGKSPEGFFRVAFNGLDLLSFQNTTWVPSPDGGSLAPGVCHLLNHQYEGVTETVYNLIRSTCPRFLLGLLDAGKMYLHRQVRPEAWLSSRRSLGSGRLLLVCHASGFYPKPVWVTWMRNEQEQLGTKHGDVLPNADGTWYLQVILEVASEETAGLSCRVRHSSLGGQDIILYWGHHFGSLTPRGVRLGSLNDIFEAQKIEWHEHHHHHHH**GTL
ptmCD1d	GnTI⁻ HEK 293S cells	pHLsec	TGVPQRLFPLRCLQISSFANSNWTRTDGLAWLGELQTHSWSNDSDTIRSLKPWSQGTFSDQQWEALQRVFRVYRSSFTRDVKEFAKMLRLAYPMELQVSAGCEVHPGNASHNFFHVAFQGSDILSFQGTSWEPAQEAPLWVNLAIQVLNQDKWTKETVQWLLNDTCPQFVSGLLESGKSELEKQVKPKAWLSRGPSPGPGRLQLVCHVSGFYPKPVWVKWMRGEQEQQGTQRGDILPNADETWYLRATLEVAAGEAAGLSCRVKHSSLEGQDIVLYWGSGLNDIFEAQKIEWHEHHHHHH*GTKLLE
ptmβ2m	GnTI⁻ HEK 293S cells	pHLsec	TGIQRTPKIQVYSRHPPENGKPNFLNCYVSGFHPSDIEVDLLKNGEKMGKVEHSDLSFSKDWSFYLLYYTEFTPNEKDEYACRVNHVTLSGPRTVKWDRDM**GTL

*β2m contains an additional leucine zipper

huCD1a	GnTI⁻ HEK 293S cells	pHLsec	ETGLKEPLSFHVIWIASFYNHSWKQNLVSGWLSDLQTHTWDSNS STIVFLWPWSRGNFSNEEWKELETLFRIRTIRSFEGIRRYAHELQFE YPFEIQVTGGCELHSGKVSGSFLQLAYQGSDFVSFQNNSWLPYPV AGNMAKHFCKVLNQNQHENDITHNLLSDTCPRFILGLLDAGKAH LQRQVKPEAWLSHGPSPGPGHLQLVCHVSGFYPKPVWVMWMR GEQEQQGTQRGDILPSADGTWYLRATLEVAAGEAADLSCRVKHS SLEGQDIVLYWEGSLVPRGSGSRIARLEEKVKTLKAQNSELASTA NMLREQVAQLKQKVMNHGSGLNDIFEAQKIEWHEHHHHHH***L E
huβ2m	GnTI⁻ HEK 293S cells	pHLsec	EFKLATMGILPSPGMPALLSLVSLLSVLLMGCVAETGIQRTPKIQV YSRHPAENGKSNFLNCYVSGFHPSDIEVDLLKNGERIEKVEHSDL SFSKDWSFYLLYYTEFTPTEKDEYACRVNHVTLSQPKIVKWDRD MGSLVPRGSGSLTDTLQAETDQLEDKKSALQTEIANLLKEKEKLE FIXAAH***LE
17a28 TCR α	E. coli	pET30	EAIKLGNHMSQQGEEDPQALSIQEGENATMNCSYKTSINNLQWY RQNSGRGLVHLILIRSNEREKHSGRLRVTLDTSKKSSSLLITASRA ADTASYFCASSSGGTYKYIFGTGTRLKVLANIQNPDPPHNSTQHT
17a28 TCR β	E. coli	pET30	EAIKLGNHMDVKVTQSSRYLVKRTGEKVFLECVQDMDHENMFW YRQDPGLGLRLIYFSYDVKMKEKGDIPEGYSVSREKKERFSLILES ASTNQTSMYLCASSLDLTDTQYFGPGTRLTVLEDLLTIPHNI
27a28 TCR α	E. coli	pET30	EAIKLGNHMTQLLEQSPQFLSIQEGENLTVYCNSSSVFSSLQWYR QEPGEGPVLLVTVVTGGEVKKLKRLTFQFGDARKDSSLHITAAQP GDTGLYLCAGGSNYKLTFGKGTLLTVNPNIQNPDPAVYQLRDSK SSDKSVCLFTDFDSQTNVSQSKDSDVYITDKCVLDMRSMDFKSNS AVAWSNKSDFACANAFNNSIIPEDTFFPSPESS
27a28 TCR β	E. coli	pET30	EAIKLGNHMDVKVTQSSRYLVKRTGEKVFLECVQDMDHENMFW YRQDPGLGLRLIYFSYDVKMKEKGDIPEGYSVSREKKERFSLILES ASTNQTSMYLCASSQFLAGGTEQYFGPGTRLTVTEDLLTIPHNIKN VFPPEVAVFEPSEAEISHTQKATLVCLATGFYPDHVELSWWVNGK EVHSGVCTDPQPLKEQPALNDSRYALSSRLRVSATFWQNPRNHF RCQVQFYGLSENDEWTQDRAKPVTQIVSAEAWGRAD
29a28i TCR α	E. coli	pET30	MDQQVKQNSPSLSVQEGRISILNCDYTNSMFDYFLWYKKYPAEG PTFLISISSIKDKNEDGRFTVFLNKSAKHLSLHIVPSQPGDSAVYFC AASAWSNQFYFGTGTSLTVIPNIQNPDPAVYQLRDSKSSDKSVCL FTDFDSQTNVSQSKDSDVYITDKCVLDMRSMDFKSNSAVAWSNK SDFACANAFNNSIIPEDTFFPSPESS
29a28i TCR β	E. coli	pET30	MDVKVTQSSRYLVKRTGEKVFLECVQDMDHENMFWYRQDPGL GLRLIYFSYDVKMKEKGDIPEGYSVSREKKERFSLILESASTNQTS MYLCASSFGGPTRELFFGEGSRLTVLEDLLTIPHNIKNVFPPEVAV FEPSEAEISHTQKATLVCLATGFYPDHVELSWWVNGKEVHSGVC TDPQPLKEQPALNDSRYALSSRLRVSATFWQNPRNHFRCQVQFY GLSENDEWTQDRAKPVTQIVSAEAWGRAD
8-2a2 TCR α	E. coli	pET30	EAIKLGNHMAQSVTQLDSHVSVSEGTPVLLRCNYSSSYSPSLFWY VQHPNKGLQLLLKYTSAATLVKGINGFEAEFKKSETSFHLTKPSA HMSDAAEYFCVVVSGTYKYIFGTGTRLKVLANIQNPDPPHNSTQ HT
8-2a2 TCR β	E. coli	pET30	EAIKLGNHMEPEVTQTPSHQVTQMGQEVILRCVPISNHLYFYWYR QILGQKVEFLVSFYNNEISEKSEIFDDQFSVERPDGSNFTLKIRSTK LEDSAMYFCASSEALLLAGDQETQYFGPGTRLLVLEDLLTIPHNI

Appendix III: Single cell RNA-sequencing data

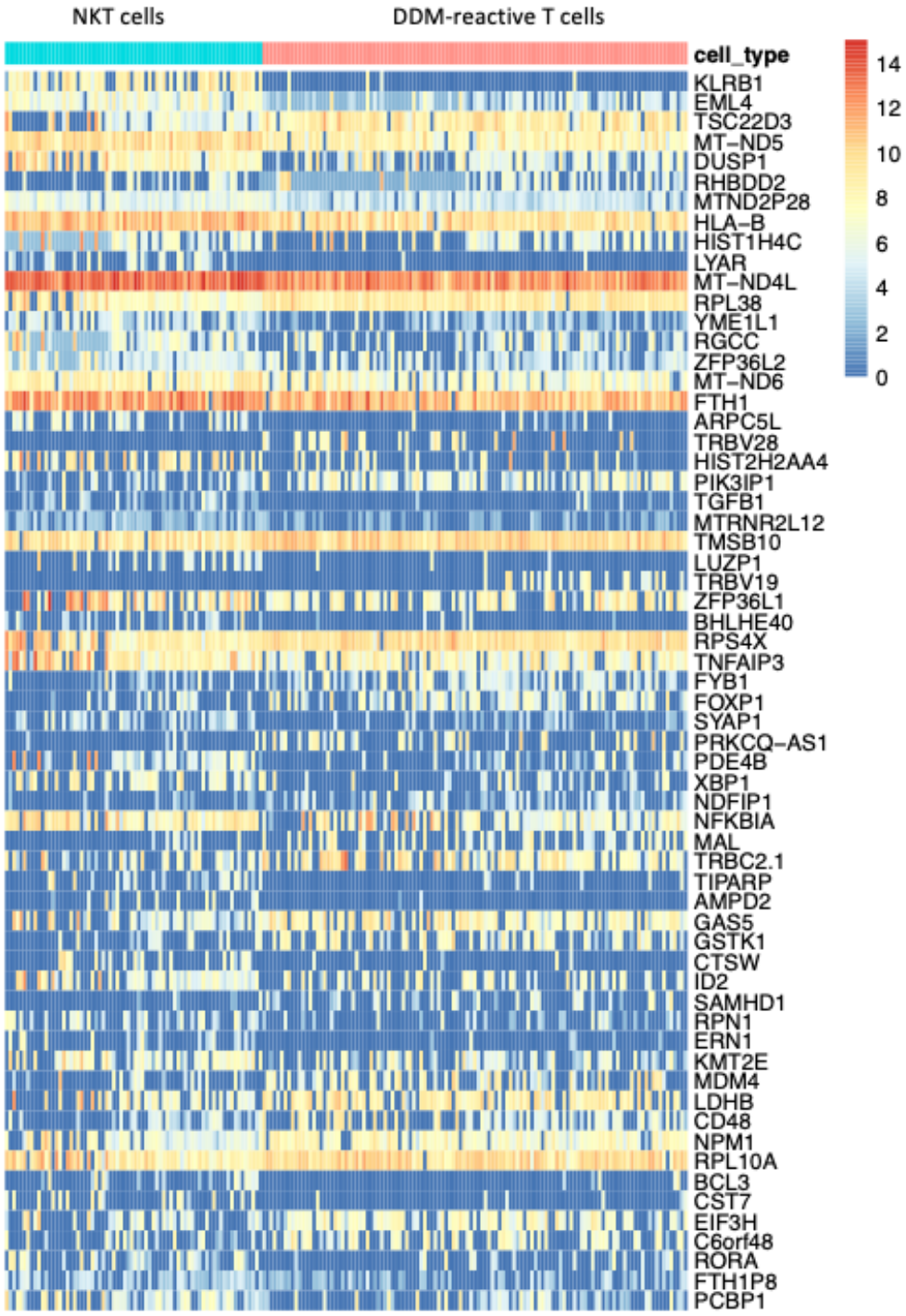

Figure AIII.I. Comparison of differentially expressed genes between DDM-reactive T cells and type I NKT cells. A gene expression heatmap displaying the top 62 differentially expressed genes between type I NKT cells (blue) and DDM-reactive T cells (red). Differential expression was calculated using the non-parametric Kruskal-Wallis Test with a p-value <0.01 and absolute log fold change >1.

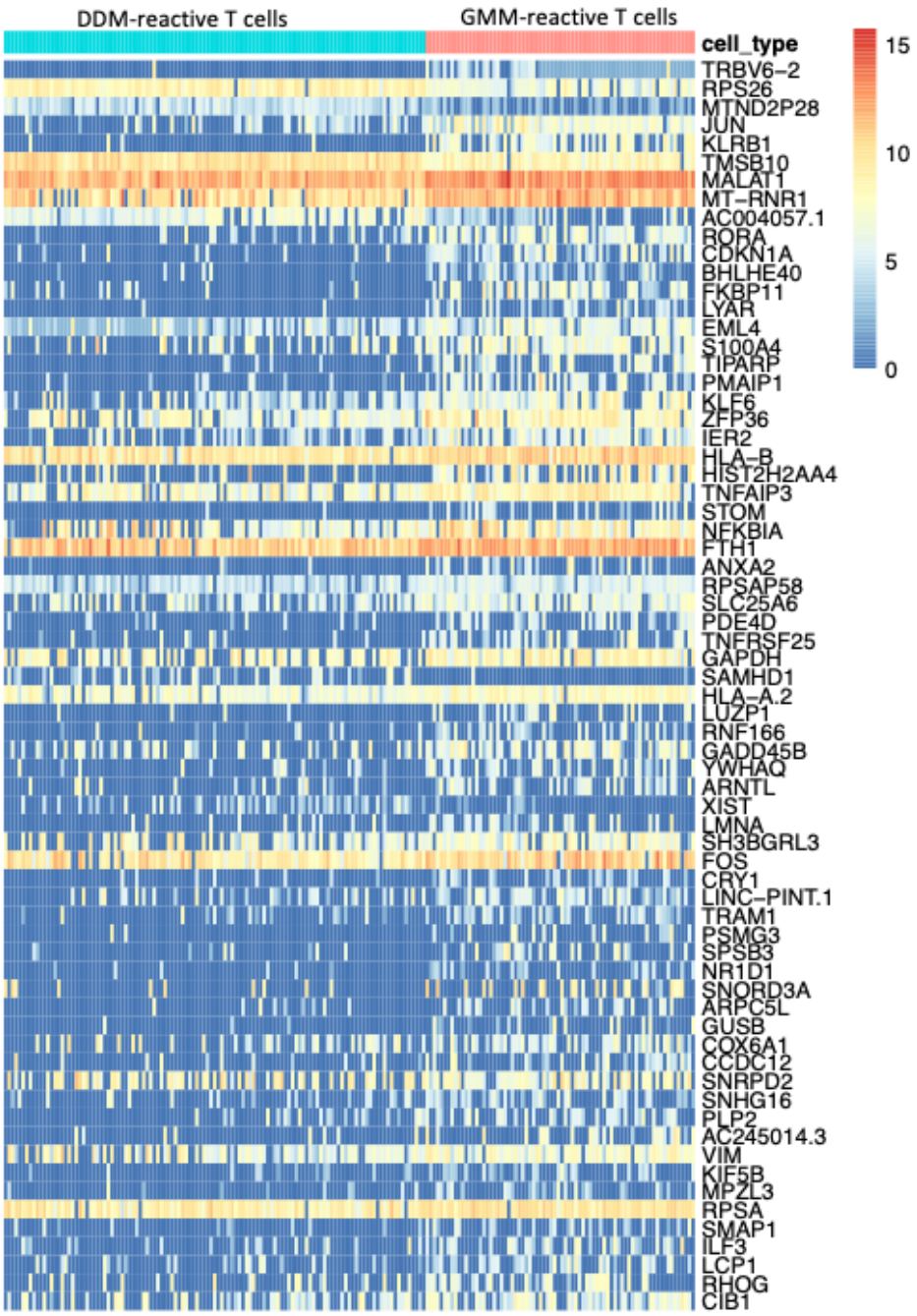

Figure AIII.II. Comparison of differentially expressed genes between DDM-reactive T cells and GMM-reactive T cells. A gene expression heatmap displaying the top 62 differentially expressed genes between type I NKT cells (blue) and DDM-reactive T cells (red). Differential expression was calculated using the non-parametric Kruskal-Wallis Test with a p-value <0.01 and absolute log fold change >1.

Appendix IV: Macaque CD1-restricted TCR sequences

TCR sequences from ptmCD1 tetramer$^+$ cells isolated from human PBMCs.

Table IV.1. Human ptmCD1a-restricted TCRs. Paired and unpaired TCR α- and β-chain sequences from sequencing of ptmCD1a tetramer$^+$ T cells. Tetramer$^+$ cells from human PBMCs were single cell-sorted and their TCRs were amplified and sequenced to determine their TCR gene usage.

TRAV	CDR3a	TRAJ	TRBV	CDR3b	TRBJ	Freq
26-1	CIVRVIGXGXGSYQLTF	28	28	CASSLSFLGTEAFF	1-1	1/5
38-1	CALRNFNKFYF	21	28	CASSPYGLAGGSLSSYNEQFF	2-1	1/5
25	-	43	28	CASSLSFLGTEAFF	1-1	2/5
17	-	29	-	-	-	1/5
8-2/8-4	CVVSDSGWISTGRYNKXIF	4	-	-	-	1/6
26-2	CILRDRSGGFGNVXHC	35	-	-	-	1/6
6	CALDEGQGGKLIF	23	20-1	CSAREVGTGTNQPQHF	1-5	1/6
29/DV5	-	49	14	-	2-5	1/6
26-2	CILRAAYXGAGSYQLTF	28	9	CASSVXTGYSEAFF	1-1	1/6
27	-	52	-	-	-	1/6

Table IV.2. Human ptmCD1c-restricted, TRAV9-2$^+$ TRBV4-1$^+$ TCRs. Human ptmCD1c-tetramer$^+$ T cells were single cell-sorted and their TCRs were amplified and sequenced to determine their TCR gene usage. Of 25 CD1c-restricted T cell clones identified from donor KG52, two were TRAV9-2$^+$ TRBV4-1$^+$ as shown here.

TRAV	CDR3a	TRAJ	TRBV	CDR3b	TRBJ	Freq
9-2	CALRYGGSNYKLTF	53*01	4-1	CASSQSYWAHEQYF	2-7	2/25
9-2	CALNRNQGGKLIF	23*01	4-1	CASSQGQGSPLHF	1-6	2/25

BIBLIOGRAPHY

ABOS GRACIA, B., LOPEZ RELANO, J., REVILLA, A., CASTRO, L., VILLALBA, M., MARTIN ADRADOS, B., REGUEIRO, J. R., FERNANDEZ-MALAVE, E., MARTINEZ NAVES, E. & GOMEZ DEL MORAL, M. 2017. Human Invariant Natural Killer T Cells Respond to Antigen-Presenting Cells Exposed to Lipids from Olea europaea Pollen. *Int Arch Allergy Immunol,* 173**,** 12-22.

ABUBAKAR, I., PIMPIN, L., ARITI, C., BEYNON, R., MANGTANI, P., STERNE, J. A., FINE, P. E., SMITH, P. G., LIPMAN, M., ELLIMAN, D., WATSON, J. M., DRUMRIGHT, L. N., WHITING, P. F., VYNNYCKY, E. & RODRIGUES, L. C. 2013. Systematic review and meta-analysis of the current evidence on the duration of protection by bacillus Calmette-Guerin vaccination against tuberculosis. *Health Technol Assess,* 17**,** 1-372, v-vi.

ACTON, S., RIGOTTI, A., LANDSCHULZ, K. T., XU, S., HOBBS, H. H. & KRIEGER, M. 1996. Identification of scavenger receptor SR-BI as a high density lipoprotein receptor. *Science,* 271**,** 518-20.

ACTON, S. L., SCHERER, P. E., LODISH, H. F. & KRIEGER, M. 1994. Expression cloning of SR-BI, a CD36-related class B scavenger receptor. *J Biol Chem,* 269**,** 21003-9.

ADAMS, E. J. & LUOMA, A. M. 2013. The adaptable major histocompatibility complex (MHC) fold: structure and function of nonclassical and MHC class I-like molecules. *Annu Rev Immunol,* 31**,** 529-61.

ADAMS, J. J., NARAYANAN, S., LIU, B., BIRNBAUM, M. E., KRUSE, A. C., BOWERMAN, N. A., CHEN, W., LEVIN, A. M., CONNOLLY, J. M., ZHU, C., KRANZ, D. M. & GARCIA, K. C. 2011. T cell receptor signaling is limited by docking geometry to peptide-major histocompatibility complex. *Immunity,* 35**,** 681-93.

ADLER, H. S., KUBSCH, S., GRAULICH, E., LUDWIG, S., KNOP, J. & STEINBRINK, K. 2007. Activation of MAP kinase p38 is critical for the cell-cycle-controlled suppressor function of regulatory T cells. *Blood,* 109**,** 4351-9.

ADLER, H. S. & STEINBRINK, K. 2008. MAP kinase p38 and its relation to T cell anergy and suppressor function of regulatory T cells. *Cell Cycle,* 7**,** 169-70.

AGEA, E., RUSSANO, A., BISTONI, O., MANNUCCI, R., NICOLETTI, I., CORAZZI, L., POSTLE, A. D., DE LIBERO, G., PORCELLI, S. A. & SPINOZZI, F. 2005. Human CD1-restricted T cell recognition of lipids from pollens. *J Exp Med,* 202**,** 295-308.

AHLERS, J. D. & BELYAKOV, I. M. 2010. Memories that last forever: strategies for optimizing vaccine T-cell memory. *Blood,* 115**,** 1678-89.

AI, J. W., RUAN, Q. L., LIU, Q. H. & ZHANG, W. H. 2016. Updates on the risk factors for latent tuberculosis reactivation and their managements. *Emerg Microbes Infect,* 5**,** e10.

ALBERTSON, D. G., FISHPOOL, R., SHERRINGTON, P., NACHEVA, E. & MILSTEIN, C. 1988. Sensitive and high resolution in situ hybridization to human chromosomes using biotin labelled probes: assignment of the human thymocyte CD1 antigen genes to chromosome 1. *EMBO J,* 7**,** 2801-5.

ALMEIDA, C. F., SUNDARARAJ, S., LE NOURS, J., PRAVEENA, T., CAO, B., BURUGUPALLI, S., SMITH, D. G. M., PATEL, O., BRIGL, M., PELLICCI, D. G., WILLIAMS, S. J., ULDRICH, A. P., GODFREY, D. I. & ROSSJOHN, J. 2019. Distinct CD1d docking strategies exhibited by diverse Type II NKT cell receptors. *Nat Commun,* 10**,** 5242.

ALONZO, E. S., GOTTSCHALK, R. A., DAS, J., EGAWA, T., HOBBS, R. M., PANDOLFI, P. P., PEREIRA, P., NICHOLS, K. E., KORETZKY, G. A., JORDAN, M. S. & SANT'ANGELO, D. B. 2010. Development of promyelocytic zinc finger and ThPOK-expressing innate gamma delta T cells is controlled by strength of TCR signaling and Id3. *J Immunol,* 184**,** 1268-79.

AMADORI, A., ZAMARCHI, R., DE SILVESTRO, G., FORZA, G., CAVATTON, G., DANIELI, G. A., CLEMENTI, M. & CHIECO-BIANCHI, L. 1995. Genetic control of the CD4/CD8 T-cell ratio in humans. *Nat Med,* 1**,** 1279-83.

AMARANTE-MENDES, G. P., ADJEMIAN, S., BRANCO, L. M., ZANETTI, L. C., WEINLICH, R. & BORTOLUCI, K. R. 2018. Pattern Recognition Receptors and the Host Cell Death Molecular Machinery. *Front Immunol,* 9**,** 2379.

AMIGORENA, S. & SAVINA, A. 2010. Intracellular mechanisms of antigen cross presentation in dendritic cells. *Curr Opin Immunol,* 22**,** 109-17.

ANDERSEN, P. & DOHERTY, T. M. 2005. The success and failure of BCG - implications for a novel tuberculosis vaccine. *Nat Rev Microbiol,* 3**,** 656-62.

ANDERSEN, P. & SCRIBA, T. J. 2019. Moving tuberculosis vaccines from theory to practice. *Nat Rev Immunol,* 19**,** 550-562.

ANGENIEUX, C., FRAISIER, V., MAITRE, B., RACINE, V., VAN DER WEL, N., FRICKER, D., PROAMER, F., SACHSE, M., CAZENAVE, J. P., PETERS, P., GOUD, B., HANAU, D., SIBARITA, J. B., SALAMERO, J. & DE LA SALLE, H. 2005. The cellular pathway of CD1e in immature and maturing dendritic cells. *Traffic,* 6**,** 286-302.

ANGENIEUX, C., SALAMERO, J., FRICKER, D., CAZENAVE, J. P., GOUD, B., HANAU, D. & DE LA SALLE, H. 2000. Characterization of CD1e, a third type of CD1 molecule expressed in dendritic cells. *J Biol Chem,* 275**,** 37757-64.

ANIPINDI, V. C., BAGRI, P., DIZZELL, S. E., JIMENEZ-SAIZ, R., JORDANA, M., SNIDER, D. P., STAMPFLI, M. R. & KAUSHIC, C. 2019. IL-17 Production by gammadelta(+) T Cells Is Critical for Inducing Th17 Responses in the Female Genital Tract and Regulated by Estradiol and Microbiota. *Immunohorizons,* 3**,** 317-330.

APOSTOLOU, I., CUMANO, A., GACHELIN, G. & KOURILSKY, P. 2000. Evidence for two subgroups of CD4-CD8- NKT cells with distinct TCR alpha beta repertoires and differential distribution in lymphoid tissues. *J Immunol,* 165**,** 2481-90.

ARICESCU, A. R., LU, W. & JONES, E. Y. 2006. A time- and cost-efficient system for high-level protein production in mammalian cells. *Acta Crystallogr D Biol Crystallogr,* 62**,** 1243-50.

ARSTILA, T. P., CASROUGE, A., BARON, V., EVEN, J., KANELLOPOULOS, J. & KOURILSKY, P. 1999. A direct estimate of the human alphabeta T cell receptor diversity. *Science,* 286**,** 958-61.

ASCH, A. S., BARNWELL, J., SILVERSTEIN, R. L. & NACHMAN, R. L. 1987. Isolation of the thrombospondin membrane receptor. *J Clin Invest,* 79**,** 1054-61.

AYROLDI, E., MIGLIORATI, G., BRUSCOLI, S., MARCHETTI, C., ZOLLO, O., CANNARILE, L., D'ADAMIO, F. & RICCARDI, C. 2001. Modulation of T-cell activation by the glucocorticoid-induced leucine zipper factor via inhibition of nuclear factor kappaB. *Blood,* 98**,** 743-53.

AYROLDI, E., ZOLLO, O., MACCHIARULO, A., DI MARCO, B., MARCHETTI, C. & RICCARDI, C. 2002. Glucocorticoid-induced leucine zipper inhibits the Raf-extracellular signal-regulated kinase pathway by binding to Raf-1. *Mol Cell Biol,* 22**,** 7929-41.

BABA, M., IMAI, T., NISHIMURA, M., KAKIZAKI, M., TAKAGI, S., HIESHIMA, K., NOMIYAMA, H. & YOSHIE, O. 1997. Identification of CCR6, the specific receptor for a novel lymphocyte-directed CC chemokine LARC. *J Biol Chem,* 272**,** 14893-8.

BAE, E. A., SEO, H., KIM, I. K., JEON, I. & KANG, C. Y. 2019. Roles of NKT cells in cancer immunotherapy. *Arch Pharm Res,* 42**,** 543-548.

BAGNARA, D., IBATICI, A., CORSELLI, M., SESSAREGO, N., TENCA, C., DE SANTANNA, A., MAZZARELLO, A., DAGA, A., CORVO, R., DE ROSSI, G., FRASSONI, F., CICCONE, E. & FAIS, F. 2009. Adoptive immunotherapy mediated by ex vivo expanded natural killer T cells against CD1d-expressing lymphoid neoplasms. *Haematologica,* 94**,** 967-74.

BAI, L., PICARD, D., ANDERSON, B., CHAUDHARY, V., LUOMA, A., JABRI, B., ADAMS, E. J., SAVAGE, P. B. & BENDELAC, A. 2012. The majority of CD1d-sulfatide-specific T cells in human blood use a semiinvariant Vdelta1 TCR. *Eur J Immunol,* 42**,** 2505-10.

BAKER, M. L. & MILLER, R. D. 2007. Evolution of mammalian CD1: marsupial CD1 is not orthologous to the eutherian isoforms and is a pseudogene in the opossum Monodelphis domestica. *Immunology,* 121**,** 113-21.

BALDAUF, H. M., PAN, X., ERIKSON, E., SCHMIDT, S., DADDACHA, W., BURGGRAF, M., SCHENKOVA, K., AMBIEL, I., WABNITZ, G., GRAMBERG, T., PANITZ, S., FLORY, E., LANDAU, N. R., SERTEL, S., RUTSCH, F., LASITSCHKA, F., KIM, B., KONIG, R., FACKLER, O. T. & KEPPLER, O. T. 2012. SAMHD1 restricts HIV-1 infection in resting CD4(+) T cells. *Nat Med,* 18**,** 1682-7.

BALK, S. P., BLEICHER, P. A. & TERHORST, C. 1989. Isolation and characterization of a cDNA and gene coding for a fourth CD1 molecule. *Proc Natl Acad Sci U S A,* 86**,** 252-6.

BALK, S. P., EBERT, E. C., BLUMENTHAL, R. L., MCDERMOTT, F. V., WUCHERPFENNIG, K. W., LANDAU, S. B. & BLUMBERG, R. S. 1991. Oligoclonal expansion and CD1 recognition by human intestinal intraepithelial lymphocytes. *Science,* 253**,** 1411-5.

BANGERT, C., FRIEDL, J., STARY, G., STINGL, G. & KOPP, T. 2003. Immunopathologic features of allergic contact dermatitis in humans: participation of plasmacytoid dendritic cells in the pathogenesis of the disease? *J Invest Dermatol,* 121**,** 1409-18.

BARCLAY, R. & RATLEDGE, C. 1988. Mycobactins and exochelins of Mycobacterium tuberculosis, M. bovis, M. africanum and other related species. *J Gen Microbiol,* 134**,** 771-6.

BAROUCH, D. H., KUNSTMAN, J., KURODA, M. J., SCHMITZ, J. E., SANTRA, S., PEYERL, F. W., KRIVULKA, G. R., BEAUDRY, K., LIFTON, M. A., GORGONE, D. A., MONTEFIORI, D. C., LEWIS, M. G., WOLINSKY, S. M. & LETVIN, N. L. 2002. Eventual AIDS vaccine failure in a rhesus monkey by viral escape from cytotoxic T lymphocytes. *Nature,* 415**,** 335-9.

BARRAL, D. C. & BRENNER, M. B. 2007. CD1 antigen presentation: how it works. *Nat Rev Immunol,* 7**,** 929-41.

BARRAL, D. C., CAVALLARI, M., MCCORMICK, P. J., GARG, S., MAGEE, A. I., BONIFACINO, J. S., DE LIBERO, G. & BRENNER, M. B. 2008. CD1a and MHC class I follow a similar endocytic recycling pathway. *Traffic,* 9**,** 1446-57.

BASSING, C. H., SWAT, W. & ALT, F. W. 2002. The mechanism and regulation of chromosomal V(D)J recombination. *Cell,* 109 Suppl**,** S45-55.

BATRAKOV, S. G. & BERGELSON, L. D. 1978. Lipids of the Streptomycettes. Structural investigation and biological interrelation a review. *Chem Phys Lipids,* 21**,** 1-29.
BATUWANGALA, T., SHEPHERD, D., GADOLA, S. D., GIBSON, K. J., ZACCAI, N. R., FERSHT, A. R., BESRA, G. S., CERUNDOLO, V. & JONES, E. Y. 2004. The crystal structure of human CD1b with a bound bacterial glycolipid. *J Immunol,* 172**,** 2382-8.
BECKER, L. C., BERGFELD, W. F., BELSITO, D. V., HILL, R. A., KLAASSEN, C. D., LIEBLER, D., MARKS, J. G., JR., SHANK, R. C., SLAGA, T. J., SNYDER, P. W. & ANDERSEN, F. A. 2012. Safety assessment of alkyl benzoates as used in cosmetics. *Int J Toxicol,* 31**,** 342S-72S.
BECKMAN, E. M., MELIAN, A., BEHAR, S. M., SIELING, P. A., CHATTERJEE, D., FURLONG, S. T., MATSUMOTO, R., ROSAT, J. P., MODLIN, R. L. & PORCELLI, S. A. 1996. CD1c restricts responses of mycobacteria-specific T cells. Evidence for antigen presentation by a second member of the human CD1 family. *J Immunol,* 157**,** 2795-803.
BECKMAN, E. M., PORCELLI, S. A., MORITA, C. T., BEHAR, S. M., FURLONG, S. T. & BRENNER, M. B. 1994. Recognition of a lipid antigen by CD1-restricted alpha beta+ T cells. *Nature,* 372**,** 691-4.
BEEKMAN, J. M. & COFFER, P. J. 2008. The ins and outs of syntenin, a multifunctional intracellular adaptor protein. *J Cell Sci,* 121**,** 1349-55.
BEHAR, S. M., DASCHER, C. C., GRUSBY, M. J., WANG, C. R. & BRENNER, M. B. 1999. Susceptibility of mice deficient in CD1D or TAP1 to infection with Mycobacterium tuberculosis. *J Exp Med,* 189**,** 1973-80.
BENDELAC, A., KILLEEN, N., LITTMAN, D. R. & SCHWARTZ, R. H. 1994. A subset of CD4+ thymocytes selected by MHC class I molecules. *Science,* 263**,** 1774-8.
BENDELAC, A., LANTZ, O., QUIMBY, M. E., YEWDELL, J. W., BENNINK, J. R. & BRUTKIEWICZ, R. R. 1995. CD1 recognition by mouse NK1+ T lymphocytes. *Science,* 268**,** 863-5.
BENLAGHA, K., WEI, D. G., VEIGA, J., TEYTON, L. & BENDELAC, A. 2005. Characterization of the early stages of thymic NKT cell development. *J Exp Med,* 202**,** 485-92.
BENLAGHA, K., WEISS, A., BEAVIS, A., TEYTON, L. & BENDELAC, A. 2000. In vivo identification of glycolipid antigen-specific T cells using fluorescent CD1d tetramers. *J Exp Med,* 191**,** 1895-903.
BENNETT, C. L., VAN RIJN, E., JUNG, S., INABA, K., STEINMAN, R. M., KAPSENBERG, M. L. & CLAUSEN, B. E. 2005. Inducible ablation of mouse Langerhans cells diminishes but fails to abrogate contact hypersensitivity. *J Cell Biol,* 169**,** 569-76.
BERESHCHENKO, O., MIGLIORATI, G., BRUSCOLI, S. & RICCARDI, C. 2019. Glucocorticoid-Induced Leucine Zipper: A Novel Anti-inflammatory Molecule. *Front Pharmacol,* 10**,** 308.
BERG, E. L., YOSHINO, T., ROTT, L. S., ROBINSON, M. K., WARNOCK, R. A., KISHIMOTO, T. K., PICKER, L. J. & BUTCHER, E. C. 1991. The cutaneous lymphocyte antigen is a skin lymphocyte homing receptor for the vascular lectin endothelial cell-leukocyte adhesion molecule 1. *J Exp Med,* 174**,** 1461-6.
BERGELSON, L. D., BATRAKOV, S. G. & PILIPENKO, T. 1970. A new glycolipid from Streptomyces. *Chem Phys Lipids,* 4**,** 181-90.

BESRA, G. S., MOREHOUSE, C. B., RITTNER, C. M., WAECHTER, C. J. & BRENNAN, P. J. 1997. Biosynthesis of mycobacterial lipoarabinomannan. *J Biol Chem,* 272**,** 18460-6.

BIENEMANN, K., IOUANNIDOU, K., SCHOENBERG, K., KRUX, F., REUTHER, S., FEYEN, O., BIENEMANN, K., SCHUSTER, F., UHRBERG, M., LAWS, H. J. & BORKHARDT, A. 2011. iNKT cell frequency in peripheral blood of Caucasian children and adolescent: the absolute iNKT cell count is stable from birth to adulthood. *Scand J Immunol,* 74**,** 406-11.

BILENKI, L., YANG, J., FAN, Y., WANG, S. & YANG, X. 2004. Natural killer T cells contribute to airway eosinophilic inflammation induced by ragweed through enhanced IL-4 and eotaxin production. *Eur J Immunol,* 34**,** 345-54.

BILLERBECK, E., KANG, Y. H., WALKER, L., LOCKSTONE, H., GRAFMUELLER, S., FLEMING, V., FLINT, J., WILLBERG, C. B., BENGSCH, B., SEIGEL, B., RAMAMURTHY, N., ZITZMANN, N., BARNES, E. J., THEVANAYAGAM, J., BHAGWANANI, A., LESLIE, A., OO, Y. H., KOLLNBERGER, S., BOWNESS, P., DROGNITZ, O., ADAMS, D. H., BLUM, H. E., THIMME, R. & KLENERMAN, P. 2010. Analysis of CD161 expression on human CD8+ T cells defines a distinct functional subset with tissue-homing properties. *Proc Natl Acad Sci U S A,* 107**,** 3006-11.

BIRKINSHAW, R. W., PELLICCI, D. G., CHENG, T. Y., KELLER, A. N., SANDOVAL-ROMERO, M., GRAS, S., DE JONG, A., ULDRICH, A. P., MOODY, D. B., GODFREY, D. I. & ROSSJOHN, J. 2015. alphabeta T cell antigen receptor recognition of CD1a presenting self lipid ligands. *Nat Immunol,* 16**,** 258-66.

BOBRYSHEV, Y. V., LORD, R. S., RAINER, S., JAMAL, O. S. & MUNRO, V. F. 1996. Vascular dendritic cells and atherosclerosis. *Pathol Res Pract,* 192**,** 462-7.

BOLTJES, A. & VAN WIJK, F. 2014. Human dendritic cell functional specialization in steady-state and inflammation. *Front Immunol,* 5**,** 131.

BONIFACE, K., BERNARD, F. X., GARCIA, M., GURNEY, A. L., LECRON, J. C. & MOREL, F. 2005. IL-22 inhibits epidermal differentiation and induces proinflammatory gene expression and migration of human keratinocytes. *J Immunol,* 174**,** 3695-702.

BONIFACE, K., GUIGNOUARD, E., PEDRETTI, N., GARCIA, M., DELWAIL, A., BERNARD, F. X., NAU, F., GUILLET, G., DAGREGORIO, G., YSSEL, H., LECRON, J. C. & MOREL, F. 2007. A role for T cell-derived interleukin 22 in psoriatic skin inflammation. *Clin Exp Immunol,* 150**,** 407-15.

BOOM, W. H., CANADAY, D. H., FULTON, S. A., GEHRING, A. J., ROJAS, R. E. & TORRES, M. 2003. Human immunity to M. tuberculosis: T cell subsets and antigen processing. *Tuberculosis (Edinb),* 83**,** 98-106.

BORG, N. A., WUN, K. S., KJER-NIELSEN, L., WILCE, M. C., PELLICCI, D. G., KOH, R., BESRA, G. S., BHARADWAJ, M., GODFREY, D. I., MCCLUSKEY, J. & ROSSJOHN, J. 2007. CD1d-lipid-antigen recognition by the semi-invariant NKT T-cell receptor. *Nature,* 448**,** 44-9.

BOURGEOIS, E. A., SUBRAMANIAM, S., CHENG, T. Y., DE JONG, A., LAYRE, E., LY, D., SALIMI, M., LEGASPI, A., MODLIN, R. L., SALIO, M., CERUNDOLO, V., MOODY, D. B. & OGG, G. 2015. Bee venom processes human skin lipids for presentation by CD1a. *J Exp Med,* 212**,** 149-63.

BOUSSO, P., CASROUGE, A., ALTMAN, J. D., HAURY, M., KANELLOPOULOS, J., ABASTADO, J. P. & KOURILSKY, P. 1998. Individual variations in the

murine T cell response to a specific peptide reflect variability in naive repertoires. *Immunity,* 9**,** 169-78.
BRADBURY, A., BELT, K. T., NERI, T. M., MILSTEIN, C. & CALABI, F. 1988. Mouse CD1 is distinct from and co-exists with TL in the same thymus. *EMBO J,* 7**,** 3081-6.
BRADLEY, L. M., DUNCAN, D. D., TONKONOGY, S. & SWAIN, S. L. 1991. Characterization of antigen-specific CD4+ effector T cells in vivo: immunization results in a transient population of MEL-14-, CD45RB- helper cells that secretes interleukin 2 (IL-2), IL-3, IL-4, and interferon gamma. *J Exp Med,* 174**,** 547-59.
BRENNAN, P. & BALLOU, C. E. 1967. Biosynthesis of mannophosphoinositides by Mycobacterium phlei. The family of dimannophosphoinositides. *J Biol Chem,* 242**,** 3046-56.
BRENNAN, P. & BALLOU, C. E. 1968. Biosynthesis of mannophosphoinositides by Mycobacterium phlei. Enzymatic acylation of the dimannophosphoinositides. *J Biol Chem,* 243**,** 2975-84.
BRENNAN, P. J., CHENG, T. Y., PELLICCI, D. G., WATTS, G. F. M., VEERAPEN, N., YOUNG, D. C., ROSSJOHN, J., BESRA, G. S., GODFREY, D. I., BRENNER, M. B. & MOODY, D. B. 2017. Structural determination of lipid antigens captured at the CD1d-T-cell receptor interface. *Proc Natl Acad Sci U S A,* 114**,** 8348-8353.
BRENNAN, P. J. & GOREN, M. B. 1979. Structural studies on the type-specific antigens and lipids of the mycobacterium avium. Mycobacterium intracellulare. Mycobacterium scrofulaceum serocomplex. Mycobacterium intracellulare serotype 9. *J Biol Chem,* 254**,** 4205-11.
BRENNAN, P. J. & NIKAIDO, H. 1995. The envelope of mycobacteria. *Annu Rev Biochem,* 64**,** 29-63.
BRENNAN, P. J., TATITURI, R. V., BRIGL, M., KIM, E. Y., TULI, A., SANDERSON, J. P., GADOLA, S. D., HSU, F. F., BESRA, G. S. & BRENNER, M. B. 2011. Invariant natural killer T cells recognize lipid self antigen induced by microbial danger signals. *Nat Immunol,* 12**,** 1202-11.
BRENNAN, P. J., TATITURI, R. V., HEISS, C., WATTS, G. F., HSU, F. F., VEERAPEN, N., COX, L. R., AZADI, P., BESRA, G. S. & BRENNER, M. B. 2014. Activation of iNKT cells by a distinct constituent of the endogenous glucosylceramide fraction. *Proc Natl Acad Sci U S A,* 111**,** 13433-8.
BRIGL, M., BRY, L., KENT, S. C., GUMPERZ, J. E. & BRENNER, M. B. 2003. Mechanism of CD1d-restricted natural killer T cell activation during microbial infection. *Nat Immunol,* 4**,** 1230-7.
BROSSAY, L., CHIODA, M., BURDIN, N., KOEZUKA, Y., CASORATI, G., DELLABONA, P. & KRONENBERG, M. 1998. CD1d-mediated recognition of an alpha-galactosylceramide by natural killer T cells is highly conserved through mammalian evolution. *J Exp Med,* 188**,** 1521-8.
BROWN, J. H., JARDETZKY, T. S., GORGA, J. C., STERN, L. J., URBAN, R. G., STROMINGER, J. L. & WILEY, D. C. 1993. Three-dimensional structure of the human class II histocompatibility antigen HLA-DR1. *Nature,* 364**,** 33-9.
BROWN-ELLIOTT, B. A. & WALLACE, R. J., JR. 2002. Clinical and taxonomic status of pathogenic nonpigmented or late-pigmenting rapidly growing mycobacteria. *Clin Microbiol Rev,* 15**,** 716-46.
BUETTNER, M., MEINKEN, C., BASTIAN, M., BHAT, R., STOSSEL, E., FALLER, G., CIANCIOLO, G., FICKER, J., WAGNER, M., ROLLINGHOFF, M. &

STENGER, S. 2005. Inverse correlation of maturity and antibacterial activity in human dendritic cells. *J Immunol,* 174**,** 4203-9.
BURUGUPALLI, S., ALMEIDA, C. F., SMITH, D. G. M., SHAH, S., PATEL, O., ROSSJOHN, J., ULDRICH, A. P., GODFREY, D. I. & WILLIAMS, S. J. 2020. α-Glucuronosyl and α-glucosyl diacylglycerides, natural killer T cell-activating lipids from bacteria and fungi. *Chemical Science,* 11**,** 2161-2168.
BUSCH, M., HERZMANN, C., KALLERT, S., ZIMMERMANN, A., HOFER, C., MAYER, D., ZENK, S. F., MUCHE, R., LANGE, C., BLOOM, B. R., MODLIN, R. L., STENGER, S. & NETWORK, T. B. 2016. Lipoarabinomannan-Responsive Polycytotoxic T Cells Are Associated with Protection in Human Tuberculosis. *Am J Respir Crit Care Med,* 194**,** 345-55.
CABANIOLS, J. P., FAZILLEAU, N., CASROUGE, A., KOURILSKY, P. & KANELLOPOULOS, J. M. 2001. Most alpha/beta T cell receptor diversity is due to terminal deoxynucleotidyl transferase. *J Exp Med,* 194**,** 1385-90.
CAI, Y., FLEMING, C. & YAN, J. 2012. New insights of T cells in the pathogenesis of psoriasis. *Cell Mol Immunol,* 9**,** 302-9.
CALABI, F., JARVIS, J. M., MARTIN, L. & MILSTEIN, C. 1989. Two classes of CD1 genes. *Eur J Immunol,* 19**,** 285-92.
CANNARILE, L., DELFINO, D. V., ADORISIO, S., RICCARDI, C. & AYROLDI, E. 2019. Implicating the Role of GILZ in Glucocorticoid Modulation of T-Cell Activation. *Front Immunol,* 10**,** 1823.
CAPONE, M., HOCKETT, R. D., JR. & ZLOTNIK, A. 1998. Kinetics of T cell receptor beta, gamma, and delta rearrangements during adult thymic development: T cell receptor rearrangements are present in CD44(+)CD25(+) Pro-T thymocytes. *Proc Natl Acad Sci U S A,* 95**,** 12522-7.
CARBONE, E., TERRAZZANO, G., MELIAN, A., ZANZI, D., MORETTA, L., PORCELLI, S., KARRE, K. & ZAPPACOSTA, S. 2000. Inhibition of human NK cell-mediated killing by CD1 molecules. *J Immunol,* 164**,** 6130-7.
CASTRO, G., LIU, X., NGO, K., DE LEON-TABALDO, A., ZHAO, S., LUNA-ROMAN, R., YU, J., CAO, T., KUHN, R., WILKINSON, P., HERMAN, K., NELEN, M. I., BLEVITT, J., XUE, X., FOURIE, A. & FUNG-LEUNG, W. P. 2017. RORgammat and RORalpha signature genes in human Th17 cells. *PLoS One,* 12**,** e0181868.
CAUX, C., DEZUTTER-DAMBUYANT, C., SCHMITT, D. & BANCHEREAU, J. 1992. GM-CSF and TNF-alpha cooperate in the generation of dendritic Langerhans cells. *Nature,* 360**,** 258-61.
CHANG, D. H., DENG, H., MATTHEWS, P., KRASOVSKY, J., RAGUPATHI, G., SPISEK, R., MAZUMDER, A., VESOLE, D. H., JAGANNATH, S. & DHODAPKAR, M. V. 2008. Inflammation-associated lysophospholipids as ligands for CD1d-restricted T cells in human cancer. *Blood,* 112**,** 1308-16.
CHANG, P. P., BARRAL, P., FITCH, J., PRATAMA, A., MA, C. S., KALLIES, A., HOGAN, J. J., CERUNDOLO, V., TANGYE, S. G., BITTMAN, R., NUTT, S. L., BRINK, R., GODFREY, D. I., BATISTA, F. D. & VINUESA, C. G. 2011. Identification of Bcl-6-dependent follicular helper NKT cells that provide cognate help for B cell responses. *Nat Immunol,* 13**,** 35-43.
CHEN, C. Y., HUANG, D., WANG, R. C., SHEN, L., ZENG, G., YAO, S., SHEN, Y., HALLIDAY, L., FORTMAN, J., MCALLISTER, M., ESTEP, J., HUNT, R., VASCONCELOS, D., DU, G., PORCELLI, S. A., LARSEN, M. H., JACOBS, W. R., JR., HAYNES, B. F., LETVIN, N. L. & CHEN, Z. W. 2009. A critical

role for CD8 T cells in a nonhuman primate model of tuberculosis. *PLoS Pathog,* 5**,** e1000392.
CHEN, L. & FLIES, D. B. 2013. Molecular mechanisms of T cell co-stimulation and co-inhibition. *Nat Rev Immunol,* 13**,** 227-42.
CHEN, L., GU, J., QIAN, Y., LI, M., QIAN, Y., XU, M., LI, J., WEN, Y., XIA, L., LI, J., XIA, Q., KONG, X. & WU, H. 2019a. Deletion of C-C Motif Chemokine Ligand 5 Worsens Invariant Natural Killer T-Cell-Mediated Hepatitis via Compensatory Up-regulation of CXCR2-Related Chemokine Activity. *Cell Mol Gastroenterol Hepatol,* 7**,** 623-639.
CHEN, P., DENG, W., LI, D., ZENG, T., HUANG, L., WANG, Q., WANG, J., ZHANG, W., YU, X., DUAN, D., WANG, J., XIA, H., CHEN, H., HUANG, W., LI, J., ZHANG, D., ZHONG, X. P. & GAO, J. 2019b. Circulating Mucosal-Associated Invariant T Cells in a Large Cohort of Healthy Chinese Individuals From Newborn to Elderly. *Front Immunol,* 10**,** 260.
CHEN, S., BONIFATI, S., QIN, Z., ST GELAIS, C., KODIGEPALLI, K. M., BARRETT, B. S., KIM, S. H., ANTONUCCI, J. M., LADNER, K. J., BUZOVETSKY, O., KNECHT, K. M., XIONG, Y., YOUNT, J. S., GUTTRIDGE, D. C., SANTIAGO, M. L. & WU, L. 2018. SAMHD1 suppresses innate immune responses to viral infections and inflammatory stimuli by inhibiting the NF-kappaB and interferon pathways. *Proc Natl Acad Sci U S A,* 115**,** E3798-E3807.
CHEN, X., WANG, X., BESRA, G. S. & GUMPERZ, J. E. 2007. Modulation of CD1d-restricted NKT cell responses by CD4. *J Leukoc Biol,* 82**,** 1455-65.
CHEN, Y., WANG, J., WANG, X., LI, X., SONG, J., FANG, J., LIU, X., LIU, T., WANG, D., LI, Q., WEN, S., MA, D., XIA, J., LUO, L., ZHENG, S. G., CUI, J., ZENG, G., CHEN, L., CHENG, B. & WANG, Z. 2019c. Pik3ip1 Is a Negative Immune Regulator that Inhibits Antitumor T-Cell Immunity. *Clin Cancer Res,* 25**,** 6180-6194.
CHENG, J. M., LIU, L., PELLICCI, D. G., REDDIEX, S. J., COTTON, R. N., CHENG, T. Y., YOUNG, D. C., VAN RHIJN, I., MOODY, D. B., ROSSJOHN, J., FAIRLIE, D. P., GODFREY, D. I. & WILLIAMS, S. J. 2017. Total Synthesis of Mycobacterium tuberculosis Dideoxymycobactin-838 and Stereoisomers: Diverse CD1a-Restricted T Cells Display a Common Hierarchy of Lipopeptide Recognition. *Chemistry,* 23**,** 1694-1701.
CHENG, T. Y., RELLOSO, M., VAN RHIJN, I., YOUNG, D. C., BESRA, G. S., BRIKEN, V., ZAJONC, D. M., WILSON, I. A., PORCELLI, S. & MOODY, D. B. 2006. Role of lipid trimming and CD1 groove size in cellular antigen presentation. *EMBO J,* 25**,** 2989-99.
CHENG, Y. & BELOV, K. 2014. Characterisation of non-classical MHC class I genes in the Tasmanian devil (Sarcophilus harrisii). *Immunogenetics,* 66**,** 727-35.
CHEUNG, K. L., JARRETT, R., SUBRAMANIAM, S., SALIMI, M., GUTOWSKA-OWSIAK, D., CHEN, Y. L., HARDMAN, C., XUE, L., CERUNDOLO, V. & OGG, G. 2016. Psoriatic T cells recognize neolipid antigens generated by mast cell phospholipase delivered by exosomes and presented by CD1a. *J Exp Med,* 213**,** 2399-2412.
CHIBA, H., MICHIBATA, H., WAKIMOTO, K., SEISHIMA, M., KAWASAKI, S., OKUBO, K., MITSUI, H., TORII, H. & IMAI, Y. 2004. Cloning of a gene for a novel epithelium-specific cytosolic phospholipase A2, cPLA2delta, induced in psoriatic skin. *J Biol Chem,* 279**,** 12890-7.

CHICZ, R. M., URBAN, R. G., LANE, W. S., GORGA, J. C., STERN, L. J., VIGNALI, D. A. & STROMINGER, J. L. 1992. Predominant naturally processed peptides bound to HLA-DR1 are derived from MHC-related molecules and are heterogeneous in size. *Nature,* 358**,** 764-8.

CHIKWAVA, K. & JAFFE, R. 2004. Langerin (CD207) staining in normal pediatric tissues, reactive lymph nodes, and childhood histiocytic disorders. *Pediatr Dev Pathol,* 7**,** 607-14.

CHOTHIA, C., BOSWELL, D. R. & LESK, A. M. 1988. The outline structure of the T-cell alpha beta receptor. *EMBO J,* 7**,** 3745-55.

CLARK, R. A., CHONG, B., MIRCHANDANI, N., BRINSTER, N. K., YAMANAKA, K., DOWGIERT, R. K. & KUPPER, T. S. 2006a. The vast majority of CLA+ T cells are resident in normal skin. *J Immunol,* 176**,** 4431-9.

CLARK, R. A., CHONG, B. F., MIRCHANDANI, N., YAMANAKA, K., MURPHY, G. F., DOWGIERT, R. K. & KUPPER, T. S. 2006b. A novel method for the isolation of skin resident T cells from normal and diseased human skin. *J Invest Dermatol,* 126**,** 1059-70.

CLEMETSON K.J., C. J. M. 2019. Platelet Receptors. *In:* A.D., M. (ed.) *Platelets.* Fourth Edition ed.

COHEN, N. R., GARG, S. & BRENNER, M. B. 2009. Chapter 1 Antigen Presentation by CD1. 102**,** 1-94.

COLONNA, M. 2010. Skin function for human CD1a-reactive T cells. *Nat Immunol,* 11**,** 1079-80.

COMSTOCK, G. W., LIVESAY, V. T. & WOOLPERT, S. F. 1974. The prognosis of a positive tuberculin reaction in childhood and adolescence. *Am J Epidemiol,* 99**,** 131-8.

CONSTANTINIDES, M. G., LINK, V. M., TAMOUTOUNOUR, S., WONG, A. C., PEREZ-CHAPARRO, P. J., HAN, S. J., CHEN, Y. E., LI, K., FARHAT, S., WECKEL, A., KRISHNAMURTHY, S. R., VUJKOVIC-CVIJIN, I., LINEHAN, J. L., BOULADOUX, N., MERRILL, E. D., ROY, S., CUA, D. J., ADAMS, E. J., BHANDOOLA, A., SCHARSCHMIDT, T. C., AUBE, J., FISCHBACH, M. A. & BELKAID, Y. 2019. MAIT cells are imprinted by the microbiota in early life and promote tissue repair. *Science,* 366.

COOK, D. N., PROSSER, D. M., FORSTER, R., ZHANG, J., KUKLIN, N. A., ABBONDANZO, S. J., NIU, X. D., CHEN, S. C., MANFRA, D. J., WIEKOWSKI, M. T., SULLIVAN, L. M., SMITH, S. R., GREENBERG, H. B., NARULA, S. K., LIPP, M. & LIRA, S. A. 2000. CCR6 mediates dendritic cell localization, lymphocyte homeostasis, and immune responses in mucosal tissue. *Immunity,* 12**,** 495-503.

COOPER, A. M. 2009. Cell-mediated immune responses in tuberculosis. *Annu Rev Immunol,* 27**,** 393-422.

COPPOLA, M., PIZZIGONI, A., BANFI, S., BASSI, M. T., CASARI, G. & INCERTI, B. 2000. Identification and characterization of YME1L1, a novel paraplegin-related gene. *Genomics,* 66**,** 48-54.

CORBETT, A. J., ECKLE, S. B., BIRKINSHAW, R. W., LIU, L., PATEL, O., MAHONY, J., CHEN, Z., REANTRAGOON, R., MEEHAN, B., CAO, H., WILLIAMSON, N. A., STRUGNELL, R. A., VAN SINDEREN, D., MAK, J. Y., FAIRLIE, D. P., KJER-NIELSEN, L., ROSSJOHN, J. & MCCLUSKEY, J. 2014. T-cell activation by transitory neo-antigens derived from distinct microbial pathways. *Nature,* 509**,** 361-5.

CORTELAZZO, S., PONZONI, M., FERRERI, A. J. & HOELZER, D. 2011. Lymphoblastic lymphoma. *Crit Rev Oncol Hematol,* 79**,** 330-43.
COSMI, L., DE PALMA, R., SANTARLASCI, V., MAGGI, L., CAPONE, M., FROSALI, F., RODOLICO, G., QUERCI, V., ABBATE, G., ANGELI, R., BERRINO, L., FAMBRINI, M., CAPRONI, M., TONELLI, F., LAZZERI, E., PARRONCHI, P., LIOTTA, F., MAGGI, E., ROMAGNANI, S. & ANNUNZIATO, F. 2008. Human interleukin 17-producing cells originate from a CD161+CD4+ T cell precursor. *J Exp Med,* 205**,** 1903-16.
COSULICH, M. E., RUBARTELLI, A., RISSO, A., COZZOLINO, F. & BARGELLESI, A. 1987. Functional characterization of an antigen involved in an early step of T-cell activation. *Proc Natl Acad Sci U S A,* 84**,** 4205-9.
COTTON, R. N., CHENG, T. Y., WEGRECKI, M., LE NOURS, J., ORGILL, D. P., POMAHAC, B., TALBOT, S. G., WILLIS, R. A., ALTMAN, J. D., DE JONG, A., OGG, G., VAN RHIJN, I., ROSSJOHN, J., CLARK, R. A. & MOODY, D. B. 2021. Human skin is colonized by T cells that recognize CD1a independently of lipid. *J Clin Invest,* 131.
COTTON, R. N., SHAHINE, A., ROSSJOHN, J. & MOODY, D. B. 2018. Lipids hide or step aside for CD1-autoreactive T cell receptors. *Curr Opin Immunol,* 52**,** 93-99.
COVENTRY, B. & HEINZEL, S. 2004. CD1a in human cancers: a new role for an old molecule. *Trends Immunol,* 25**,** 242-8.
CRAIG, F. E. & FOON, K. A. 2008. Flow cytometric immunophenotyping for hematologic neoplasms. *Blood,* 111**,** 3941-67.
CRAWFORD, J. M., KRISKO, J. M., MORRIS, G. A. & CHAMBERS, D. A. 1989. The distribution of Langerhans cells and CD1a antigen in healthy and diseased human gingiva. *Reg Immunol,* 2**,** 91-7.
CROOKS, G. E., HON, G., CHANDONIA, J. M. & BRENNER, S. E. 2004. WebLogo: a sequence logo generator. *Genome Res,* 14**,** 1188-90.
CROSBY, C. M. & KRONENBERG, M. 2018. Tissue-specific functions of invariant natural killer T cells. *Nat Rev Immunol,* 18**,** 559-574.
CROTZER, V. L. & BLUM, J. S. 2010. Autophagy and adaptive immunity. *Immunology,* 131**,** 9-17.
CROWE, N. Y., SMYTH, M. J. & GODFREY, D. I. 2002. A critical role for natural killer T cells in immunosurveillance of methylcholanthrene-induced sarcomas. *J Exp Med,* 196**,** 119-27.
CROWE, N. Y., ULDRICH, A. P., KYPARISSOUDIS, K., HAMMOND, K. J., HAYAKAWA, Y., SIDOBRE, S., KEATING, R., KRONENBERG, M., SMYTH, M. J. & GODFREY, D. I. 2003. Glycolipid antigen drives rapid expansion and sustained cytokine production by NK T cells. *J Immunol,* 171**,** 4020-7.
CUI, Y., KANG, L., CUI, L. & HE, W. 2009. Human gammadelta T cell recognition of lipid A is predominately presented by CD1b or CD1c on dendritic cells. *Biol Direct,* 4**,** 47.
CUI, Y. & WAN, Q. 2019. NKT Cells in Neurological Diseases. *Front Cell Neurosci,* 13**,** 245.
D'ANDREA, A., GOUX, D., DE LALLA, C., KOEZUKA, Y., MONTAGNA, D., MORETTA, A., DELLABONA, P., CASORATI, G. & ABRIGNANI, S. 2000. Neonatal invariant Valpha24+ NKT lymphocytes are activated memory cells. *Eur J Immunol,* 30**,** 1544-50.

DA SILVA, A. J., LI, Z., DE VERA, C., CANTO, E., FINDELL, P. & RUDD, C. E. 1997. Cloning of a novel T-cell protein FYB that binds FYN and SH2-domain-containing leukocyte protein 76 and modulates interleukin 2 production. *Proc Natl Acad Sci U S A,* 94**,** 7493-8.
DAFFE, M. & DRAPER, P. 1998. The envelope layers of mycobacteria with reference to their pathogenicity. *Adv Microb Physiol,* 39**,** 131-203.
DAS, R., SANT'ANGELO, D. B. & NICHOLS, K. E. 2010. Transcriptional control of invariant NKT cell development. *Immunol Rev,* 238**,** 195-215.
DASCHER, C. C. 2007. Evolutionary biology of CD1. *Curr Top Microbiol Immunol,* 314**,** 3-26.
DASCHER, C. C. & BRENNER, M. B. 2003. Evolutionary constraints on CD1 structure: insights from comparative genomic analysis. *Trends Immunol,* 24**,** 412-8.
DASCHER, C. C., HIROMATSU, K., XIONG, X., MOREHOUSE, C., WATTS, G., LIU, G., MCMURRAY, D. N., LECLAIR, K. P., PORCELLI, S. A. & BRENNER, M. B. 2003. Immunization with a mycobacterial lipid vaccine improves pulmonary pathology in the guinea pig model of tuberculosis. *Int Immunol,* 15**,** 915-25.
DAVENNE, T. & MCSHANE, H. 2016. Why don't we have an effective tuberculosis vaccine yet? *Expert Rev Vaccines,* 15**,** 1009-13.
DAVIS, M. M. 1990. T cell receptor gene diversity and selection. *Annu Rev Biochem,* 59**,** 475-96.
DAVIS, M. M. & BJORKMAN, P. J. 1988. T-cell antigen receptor genes and T-cell recognition. *Nature,* 334**,** 395-402.
DAY, E. B., GUILLONNEAU, C., GRAS, S., LA GRUTA, N. L., VIGNALI, D. A., DOHERTY, P. C., PURCELL, A. W., ROSSJOHN, J. & TURNER, S. J. 2011. Structural basis for enabling T-cell receptor diversity within biased virus-specific CD8+ T-cell responses. *Proc Natl Acad Sci U S A,* 108**,** 9536-41.
DE JONG, A., ARCE, E. C., CHENG, T. Y., VAN SUMMEREN, R. P., FERINGA, B. L., DUDKIN, V., CRICH, D., MATSUNAGA, I., MINNAARD, A. J. & MOODY, D. B. 2007. CD1c presentation of synthetic glycolipid antigens with foreign alkyl branching motifs. *Chem Biol,* 14**,** 1232-42.
DE JONG, A., CHENG, T. Y., HUANG, S., GRAS, S., BIRKINSHAW, R. W., KASMAR, A. G., VAN RHIJN, I., PENA-CRUZ, V., RUAN, D. T., ALTMAN, J. D., ROSSJOHN, J. & MOODY, D. B. 2014. CD1a-autoreactive T cells recognize natural skin oils that function as headless antigens. *Nat Immunol,* 15**,** 177-85.
DE JONG, A. & OGG, G. 2020. CD1a function in human skin disease. *Mol Immunol,* 130**,** 14-19.
DE JONG, A., PENA-CRUZ, V., CHENG, T. Y., CLARK, R. A., VAN RHIJN, I. & MOODY, D. B. 2010. CD1a-autoreactive T cells are a normal component of the human alphabeta T cell repertoire. *Nat Immunol,* 11**,** 1102-9.
DE JONG, R., BROUWER, M., HOOIBRINK, B., VAN DER POUW-KRAAN, T., MIEDEMA, F. & VAN LIER, R. A. 1992. The CD27- subset of peripheral blood memory CD4+ lymphocytes contains functionally differentiated T lymphocytes that develop by persistent antigenic stimulation in vivo. *Eur J Immunol,* 22**,** 993-9.
DE LA SALLE, H., MARIOTTI, S., ANGENIEUX, C., GILLERON, M., GARCIA-ALLES, L. F., MALM, D., BERG, T., PAOLETTI, S., MAITRE, B., MOUREY, L., SALAMERO, J., CAZENAVE, J. P., HANAU, D., MORI, L.,

PUZO, G. & DE LIBERO, G. 2005. Assistance of microbial glycolipid antigen processing by CD1e. *Science,* 310**,** 1321-4.
DE LALLA, C., LEPORE, M., PICCOLO, F. M., RINALDI, A., SCELFO, A., GARAVAGLIA, C., MORI, L., DE LIBERO, G., DELLABONA, P. & CASORATI, G. 2011. High-frequency and adaptive-like dynamics of human CD1 self-reactive T cells. *Eur J Immunol,* 41**,** 602-10.
DE LIBERO, G. & MORI, L. 2003. Self glycosphingolipids: new antigens recognized by autoreactive T lymphocytes. *News Physiol Sci,* 18**,** 71-6.
DE LIBERO, G. & MORI, L. 2007. Structure and biology of self lipid antigens. *Curr Top Microbiol Immunol,* 314**,** 51-72.
DE PAOLI, P., REITANO, M., BATTISTIN, S., CASTIGLIA, C. & SANTINI, G. 1984. Enumeration of human lymphocyte subsets by monoclonal antibodies and flow cytometry: a comparative study using whole blood or mononuclear cells separated by density gradient centrifugation. *J Immunol Methods,* 72**,** 349-53.
DE SANTO, C., ARSCOTT, R., BOOTH, S., KARYDIS, I., JONES, M., ASHER, R., SALIO, M., MIDDLETON, M. & CERUNDOLO, V. 2010. Invariant NKT cells modulate the suppressive activity of IL-10-secreting neutrophils differentiated with serum amyloid A. *Nat Immunol,* 11**,** 1039-46.
DE SANTO, C., SALIO, M., MASRI, S. H., LEE, L. Y., DONG, T., SPEAK, A. O., PORUBSKY, S., BOOTH, S., VEERAPEN, N., BESRA, G. S., GRONE, H. J., PLATT, F. M., ZAMBON, M. & CERUNDOLO, V. 2008. Invariant NKT cells reduce the immunosuppressive activity of influenza A virus-induced myeloid-derived suppressor cells in mice and humans. *J Clin Invest,* 118**,** 4036-48.
DEFRANCES, M. C., DEBELIUS, D. R., CHENG, J. & KANE, L. P. 2012. Inhibition of T-cell activation by PIK3IP1. *Eur J Immunol,* 42**,** 2754-9.
DEGUCHI, M., AIBA, S., OHTANI, H., NAGURA, H. & TAGAMI, H. 2002. Comparison of the distribution and numbers of antigen-presenting cells among T-lymphocyte-mediated dermatoses: CD1a+, factor XIIIa+, and CD68+ cells in eczematous dermatitis, psoriasis, lichen planus and graft-versus-host disease. *Arch Dermatol Res,* 294**,** 297-302.
DELLABONA, P., PADOVAN, E., CASORATI, G., BROCKHAUS, M. & LANZAVECCHIA, A. 1994. An invariant V alpha 24-J alpha Q/V beta 11 T cell receptor is expressed in all individuals by clonally expanded CD4-8- T cells. *J Exp Med,* 180**,** 1171-6.
DEMOULINS, T., GACHELIN, G., BEQUET, D. & DORMONT, D. 2003. A biased Valpha24+ T-cell repertoire leads to circulating NKT-cell defects in a multiple sclerosis patient at the onset of his disease. *Immunol Lett,* 90**,** 223-8.
DEPARTMENT OF HEALTH, G. O. A. 2013. The BCG vaccine: information and recommendations for use in Australia.
DESCOURS, B., CRIBIER, A., CHABLE-BESSIA, C., AYINDE, D., RICE, G., CROW, Y., YATIM, A., SCHWARTZ, O., LAGUETTE, N. & BENKIRANE, M. 2012. SAMHD1 restricts HIV-1 reverse transcription in quiescent CD4(+) T-cells. *Retrovirology,* 9**,** 87.
DESHAYES, C., ANGALA, S. K., MARION, E., BRANDLI, I., BABONNEAU, J., PREISSER, L., EYANGOH, S., DELNESTE, Y., LEGRAS, P., DE CHASTELLIER, C., STINEAR, T. P., JACKSON, M. & MARSOLLIER, L. 2013. Regulation of mycolactone, the Mycobacterium ulcerans toxin, depends on nutrient source. *PLoS Negl Trop Dis,* 7**,** e2502.
DEWITT, W. S., YU, K. K. Q., WILBURN, D. B., SHERWOOD, A., VIGNALI, M., DAY, C. L., SCRIBA, T. J., ROBINS, H. S., SWANSON, W. J., EMERSON,

R. O., BRADLEY, P. H. & SESHADRI, C. 2018. A Diverse Lipid Antigen-Specific TCR Repertoire Is Clonally Expanded during Active Tuberculosis. *J Immunol,* 201**,** 888-896.
DHODAPKAR, M. V. & KUMAR, V. 2017. Type II NKT Cells and Their Emerging Role in Health and Disease. *J Immunol,* 198**,** 1015-1021.
DI NARDO, A., WERTZ, P., GIANNETTI, A. & SEIDENARI, S. 1998. Ceramide and cholesterol composition of the skin of patients with atopic dermatitis. *Acta Derm Venereol,* 78**,** 27-30.
DIJKMAN, K., SOMBROEK, C. C., VERVENNE, R. A. W., HOFMAN, S. O., BOOT, C., REMARQUE, E. J., KOCKEN, C. H. M., OTTENHOFF, T. H. M., KONDOVA, I., KHAYUM, M. A., HAANSTRA, K. G., VIERBOOM, M. P. M. & VERRECK, F. A. W. 2019. Prevention of tuberculosis infection and disease by local BCG in repeatedly exposed rhesus macaques. *Nat Med,* 25**,** 255-262.
DODD, P. J., YUEN, C. M., SISMANIDIS, C., SEDDON, J. A. & JENKINS, H. E. 2017. The global burden of tuberculosis mortality in children: a mathematical modelling study. *Lancet Glob Health,* 5**,** e898-e906.
DOERNER, A. M., EDDLESTON, J., RAHNEMA, G., MILLER, M., BROIDE, D. & ZURAW, B. 2014. Deficiency Of The Glucocorticoid Induced Leucine Zipper Protein (GILZ) In Bronchial Epithelial Cells Enhances Allergic Airway Disease In A Murine Asthma Model. *D33. AIRWAY EPITHELIA ACTIVATION AND RESPONSES TO TREATMENT.* American Thoracic Society.
DOISNE, J. M., BARTHOLIN, L., YAN, K. P., GARCIA, C. N., DUARTE, N., LE LUDUEC, J. B., VINCENT, D., CYPRIAN, F., HORVAT, B., MARTEL, S., RIMOKH, R., LOSSON, R., BENLAGHA, K. & MARIE, J. C. 2009. iNKT cell development is orchestrated by different branches of TGF-beta signaling. *J Exp Med,* 206**,** 1365-78.
DOUGAN, S. K., KASER, A. & BLUMBERG, R. S. 2007. CD1 expression on antigen-presenting cells. *Curr Top Microbiol Immunol,* 314**,** 113-41.
DUECHTING, A., PRZYBYLA, A., KUERTEN, S. & LEHMANN, P. V. 2017. Delayed Activation Kinetics of Th2- and Th17 Cells Compared to Th1 Cells. *Cells,* 6.
DUHEN, T., GEIGER, R., JARROSSAY, D., LANZAVECCHIA, A. & SALLUSTO, F. 2009. Production of interleukin 22 but not interleukin 17 by a subset of human skin-homing memory T cells. *Nat Immunol,* 10**,** 857-63.
DUPUY, P., HESLAN, M., FRAITAG, S., HERCEND, T., DUBERTRET, L. & BAGOT, M. 1990. T-cell receptor-gamma/delta bearing lymphocytes in normal and inflammatory human skin. *J Invest Dermatol,* 94**,** 764-8.
DUSSEAUX, M., MARTIN, E., SERRIARI, N., PEGUILLET, I., PREMEL, V., LOUIS, D., MILDER, M., LE BOURHIS, L., SOUDAIS, C., TREINER, E. & LANTZ, O. 2011. Human MAIT cells are xenobiotic-resistant, tissue-targeted, CD161hi IL-17-secreting T cells. *Blood,* 117**,** 1250-9.
DYE, C., SCHEELE, S., DOLIN, P., PATHANIA, V. & RAVIGLIONE, M. C. 1999. Consensus statement. Global burden of tuberculosis: estimated incidence, prevalence, and mortality by country. WHO Global Surveillance and Monitoring Project. *JAMA,* 282**,** 677-86.
ELTAHLA, A. A., RIZZETTO, S., PIROZYAN, M. R., BETZ-STABLEIN, B. D., VENTURI, V., KEDZIERSKA, K., LLOYD, A. R., BULL, R. A. & LUCIANI, F. 2016. Linking the T cell receptor to the single cell transcriptome in antigen-specific human T cells. *Immunol Cell Biol,* 94**,** 604-11.

ENGEL, I., SEUMOIS, G., CHAVEZ, L., SAMANIEGO-CASTRUITA, D., WHITE, B., CHAWLA, A., MOCK, D., VIJAYANAND, P. & KRONENBERG, M. 2016. Innate-like functions of natural killer T cell subsets result from highly divergent gene programs. *Nat Immunol,* 17**,** 728-39.

ERNST, W. A., MAHER, J., CHO, S., NIAZI, K. R., CHATTERJEE, D., MOODY, D. B., BESRA, G. S., WATANABE, Y., JENSEN, P. E., PORCELLI, S. A., KRONENBERG, M. & MODLIN, R. L. 1998. Molecular interaction of CD1b with lipoglycan antigens. *Immunity,* 8**,** 331-40.

ESPOSITO, S., PUGNI, L., DALENO, C., RONCHI, A., VALZANO, A., SERRA, D., MOSCA, F. & PRINCIPI, N. 2011. Influenza A/H1N1 MF59-adjuvanted vaccine in preterm and term children aged 6 to 23 months. *Pediatrics,* 127**,** e1161-8.

ESSER, C., BARGEN, I., WEIGHARDT, H., HAARMANN-STEMMANN, T. & KRUTMANN, J. 2013. Functions of the aryl hydrocarbon receptor in the skin. *Semin Immunopathol,* 35**,** 677-91.

EXLEY, M., GARCIA, J., BALK, S. P. & PORCELLI, S. 1997. Requirements for CD1d recognition by human invariant Valpha24+ CD4-CD8- T cells. *J Exp Med,* 186**,** 109-20.

EXLEY, M., PORCELLI, S., FURMAN, M., GARCIA, J. & BALK, S. 1998. CD161 (NKR-P1A) costimulation of CD1d-dependent activation of human T cells expressing invariant V alpha 24 J alpha Q T cell receptor alpha chains. *J Exp Med,* 188**,** 867-76.

EXLEY, M. A., HOU, R., SHAULOV, A., TONTI, E., DELLABONA, P., CASORATI, G., AKBARI, O., AKMAN, H. O., GREENFIELD, E. A., GUMPERZ, J. E., BOYSON, J. E., BALK, S. P. & WILSON, S. B. 2008. Selective activation, expansion, and monitoring of human iNKT cells with a monoclonal antibody specific for the TCR alpha-chain CDR3 loop. *Eur J Immunol,* 38**,** 1756-66.

EYERICH, S., EYERICH, K., PENNINO, D., CARBONE, T., NASORRI, F., PALLOTTA, S., CIANFARANI, F., ODORISIO, T., TRAIDL-HOFFMANN, C., BEHRENDT, H., DURHAM, S. R., SCHMIDT-WEBER, C. B. & CAVANI, A. 2009. Th22 cells represent a distinct human T cell subset involved in epidermal immunity and remodeling. *J Clin Invest,* 119**,** 3573-85.

FARBER, D. L., YUDANIN, N. A. & RESTIFO, N. P. 2014. Human memory T cells: generation, compartmentalization and homeostasis. *Nat Rev Immunol,* 14**,** 24-35.

FAUNCE, D. E. & STEIN-STREILEIN, J. 2002. NKT cell-derived RANTES recruits APCs and CD8+ T cells to the spleen during the generation of regulatory T cells in tolerance. *J Immunol,* 169**,** 31-8.

FAURE, F., JITSUKAWA, S., MIOSSEC, C. & HERCEND, T. 1990. CD1c as a target recognition structure for human T lymphocytes: analysis with peripheral blood gamma/delta cells. *Eur J Immunol,* 20**,** 703-6.

FAUST, L., SCHREIBER, Y. & BOCKING, N. 2019. A systematic review of BCG vaccination policies among high-risk groups in low TB-burden countries: implications for vaccination strategy in Canadian indigenous communities. *BMC Public Health,* 19**,** 1504.

FAVREAU, M., VANDERKERKEN, K., ELEWAUT, D., VENKEN, K. & MENU, E. 2016. Does an NKT-cell-based immunotherapeutic approach have a future in multiple myeloma? *Oncotarget,* 7**,** 23128-40.

FEINGOLD, K. R. & GRUNFELD, C. 2000. The Effect of Inflammation and Infection on Lipids and Lipoproteins. *In:* FEINGOLD, K. R., ANAWALT, B., BOYCE,

A., CHROUSOS, G., DE HERDER, W. W., DUNGAN, K., GROSSMAN, A., HERSHMAN, J. M., HOFLAND, J., KALTSAS, G., KOCH, C., KOPP, P., KORBONITS, M., MCLACHLAN, R., MORLEY, J. E., NEW, M., PURNELL, J., SINGER, F., STRATAKIS, C. A., TRENCE, D. L. & WILSON, D. P. (eds.) *Endotext.* South Dartmouth (MA).

FELIO, K., NGUYEN, H., DASCHER, C. C., CHOI, H. J., LI, S., ZIMMER, M. I., COLMONE, A., MOODY, D. B., BRENNER, M. B. & WANG, C. R. 2009. CD1-restricted adaptive immune responses to Mycobacteria in human group 1 CD1 transgenic mice. *J Exp Med,* 206**,** 2497-509.

FERGUSSON, J. R., FLEMING, V. M. & KLENERMAN, P. 2011. CD161-expressing human T cells. *Front Immunol,* 2**,** 36.

FERGUSSON, J. R., SMITH, K. E., FLEMING, V. M., RAJORIYA, N., NEWELL, E. W., SIMMONS, R., MARCHI, E., BJORKANDER, S., KANG, Y. H., SWADLING, L., KURIOKA, A., SAHGAL, N., LOCKSTONE, H., BABAN, D., FREEMAN, G. J., SVERREMARK-EKSTROM, E., DAVIS, M. M., DAVENPORT, M. P., VENTURI, V., USSHER, J. E., WILLBERG, C. B. & KLENERMAN, P. 2014. CD161 defines a transcriptional and functional phenotype across distinct human T cell lineages. *Cell Rep,* 9**,** 1075-88.

FERNANDEZ, C. S., CAMERON, G., GODFREY, D. I. & KENT, S. J. 2012. Ex-vivo alpha-galactosylceramide activation of NKT cells in humans and macaques. *J Immunol Methods,* 382**,** 150-9.

FERNANDEZ, C. S., CHAN, A. C., KYPARISSOUDIS, K., DE ROSE, R., GODFREY, D. I. & KENT, S. J. 2009. Peripheral NKT cells in simian immunodeficiency virus-infected macaques. *J Virol,* 83**,** 1617-24.

FERNANDEZ, C. S., KELLEHER, A. D., FINLAYSON, R., GODFREY, D. I. & KENT, S. J. 2014. NKT cell depletion in humans during early HIV infection. *Immunol Cell Biol,* 92**,** 578-90.

FERNANDO, M. M., STEVENS, C. R., WALSH, E. C., DE JAGER, P. L., GOYETTE, P., PLENGE, R. M., VYSE, T. J. & RIOUX, J. D. 2008. Defining the role of the MHC in autoimmunity: a review and pooled analysis. *PLoS Genet,* 4**,** e1000024.

FEWOU, S. N., JACKMAN, N., MEER, G. V., BANSAL, R. & PFEIFFER, S. E. 2009. Functional Dynamics of Myelin Lipids*. *In:* LAJTHA, A., TETTAMANTI, G. & GORACCI, G. (eds.) *Handbook of Neurochemistry and Molecular Neurobiology: Neural Lipids.* Boston, MA: Springer US.

FINAK, G., MCDAVID, A., YAJIMA, M., DENG, J., GERSUK, V., SHALEK, A. K., SLICHTER, C. K., MILLER, H. W., MCELRATH, M. J., PRLIC, M., LINSLEY, P. S. & GOTTARDO, R. 2015. MAST: a flexible statistical framework for assessing transcriptional changes and characterizing heterogeneity in single-cell RNA sequencing data. *Genome Biol,* 16**,** 278.

FITHIAN, E., KUNG, P., GOLDSTEIN, G., RUBENFELD, M., FENOGLIO, C. & EDELSON, R. 1981. Reactivity of Langerhans cells with hybridoma antibody. *Proc Natl Acad Sci U S A,* 78**,** 2541-4.

FLEURIDOR, R., WILSON, B., HOU, R., LANDAY, A., KESSLER, H. & AL-HARTHI, L. 2003. CD1d-restricted natural killer T cells are potent targets for human immunodeficiency virus infection. *Immunology,* 108**,** 3-9.

FLOYD, K., GLAZIOU, P., ZUMLA, A. & RAVIGLIONE, M. 2018. The global tuberculosis epidemic and progress in care, prevention, and research: an overview in year 3 of the End TB era. *Lancet Respir Med,* 6**,** 299-314.

FORSTER, R., SCHUBEL, A., BREITFELD, D., KREMMER, E., RENNER-MULLER, I., WOLF, E. & LIPP, M. 1999. CCR7 coordinates the primary immune response by establishing functional microenvironments in secondary lymphoid organs. *Cell,* 99**,** 23-33.

FRANSWAY, A. F., ZUG, K. A., BELSITO, D. V., DELEO, V. A., FOWLER, J. F., JR., MAIBACH, H. I., MARKS, J. G., MATHIAS, C. G., PRATT, M. D., RIETSCHEL, R. L., SASSEVILLE, D., STORRS, F. J., TAYLOR, J. S., WARSHAW, E. M., DEKOVEN, J. & ZIRWAS, M. 2013. North American Contact Dermatitis Group patch test results for 2007-2008. *Dermatitis,* 24**,** 10-21.

FUHLBRIGGE, R. C., KIEFFER, J. D., ARMERDING, D. & KUPPER, T. S. 1997. Cutaneous lymphocyte antigen is a specialized form of PSGL-1 expressed on skin-homing T cells. *Nature,* 389**,** 978-81.

FUJII, S., SHIMIZU, K., OKAMOTO, Y., KUNII, N., NAKAYAMA, T., MOTOHASHI, S. & TANIGUCHI, M. 2013. NKT cells as an ideal anti-tumor immunotherapeutic. *Front Immunol,* 4**,** 409.

FUNG, T. C., OLSON, C. A. & HSIAO, E. Y. 2017. Interactions between the microbiota, immune and nervous systems in health and disease. *Nat Neurosci,* 20**,** 145-155.

GADOLA, S. D., ZACCAI, N. R., HARLOS, K., SHEPHERD, D., CASTRO-PALOMINO, J. C., RITTER, G., SCHMIDT, R. R., JONES, E. Y. & CERUNDOLO, V. 2002. Structure of human CD1b with bound ligands at 2.3 A, a maze for alkyl chains. *Nat Immunol,* 3**,** 721-6.

GALLEGOS, A. M., PAMER, E. G. & GLICKMAN, M. S. 2008. Delayed protection by ESAT-6–specific effector CD4+ T cells after airborne M. tuberculosis infection. *Journal of Experimental Medicine,* 205**,** 2359-2368.

GALLI, G., MEDINI, D., BORGOGNI, E., ZEDDA, L., BARDELLI, M., MALZONE, C., NUTI, S., TAVARINI, S., SAMMICHELI, C., HILBERT, A. K., BRAUER, V., BANZHOFF, A., RAPPUOLI, R., DEL GIUDICE, G. & CASTELLINO, F. 2009. Adjuvanted H5N1 vaccine induces early CD4+ T cell response that predicts long-term persistence of protective antibody levels. *Proc Natl Acad Sci U S A,* 106**,** 3877-82.

GANSUVD, B., GOODWIN, J., ASIEDU, C. K., JIANG, X. L., JARGAL, U., ANDRADES, P., EXLEY, M. A. & THOMAS, J. M. 2008. Invariant natural killer T cells from rhesus macaque spleen and peripheral blood are phenotypically and functionally distinct populations. *J Med Primatol,* 37**,** 1-11.

GANSUVD, B., HUBBARD, W. J., HUTCHINGS, A., THOMAS, F. T., GOODWIN, J., WILSON, S. B., EXLEY, M. A. & THOMAS, J. M. 2003. Phenotypic and functional characterization of long-term cultured rhesus macaque spleen-derived NKT cells. *J Immunol,* 171**,** 2904-11.

GARBOCZI, D. N., GHOSH, P., UTZ, U., FAN, Q. R., BIDDISON, W. E. & WILEY, D. C. 1996. Structure of the complex between human T-cell receptor, viral peptide and HLA-A2. *Nature,* 384**,** 134-41.

GARCIA, K. C. & ADAMS, E. J. 2005. How the T cell receptor sees antigen--a structural view. *Cell,* 122**,** 333-6.

GARCIA-ALLES, L. F., COLLMANN, A., VERSLUIS, C., LINDNER, B., GUIARD, J., MAVEYRAUD, L., HUC, E., IM, J. S., SANSANO, S., BRANDO, T., JULIEN, S., PRANDI, J., GILLERON, M., PORCELLI, S. A., DE LA SALLE, H., HECK, A. J., MORI, L., PUZO, G., MOUREY, L. & DE LIBERO, G. 2011. Structural reorganization of the antigen-binding groove of human CD1b for

presentation of mycobacterial sulfoglycolipids. *Proc Natl Acad Sci U S A,* 108**,** 17755-60.
GARCIA-ALLES, L. F., VERSLUIS, K., MAVEYRAUD, L., VALLINA, A. T., SANSANO, S., BELLO, N. F., GOBER, H. J., GUILLET, V., DE LA SALLE, H., PUZO, G., MORI, L., HECK, A. J., DE LIBERO, G. & MOUREY, L. 2006. Endogenous phosphatidylcholine and a long spacer ligand stabilize the lipid-binding groove of CD1b. *EMBO J,* 25**,** 3684-92.
GAUSLING, R., TROLLMO, C. & HAFLER, D. A. 2001. Decreases in interleukin-4 secretion by invariant CD4(-)CD8(-)V alpha 24J alpha Q T cells in peripheral blood of patientswith relapsing-remitting multiple sclerosis. *Clin Immunol,* 98**,** 11-7.
GAVIRAGHI, M., VIVORI, C., PAREJA SANCHEZ, Y., INVERNIZZI, F., CATTANEO, A., SANTOLIQUIDO, B. M., FRENQUELLI, M., SEGALLA, S., BACHI, A., DOGLIONI, C., PELECHANO, V., CITTARO, D. & TONON, G. 2018. Tumor suppressor PNRC1 blocks rRNA maturation by recruiting the decapping complex to the nucleolus. *EMBO J,* 37.
GEFEN, T., VAYA, J., KHATIB, S., RAPOPORT, I., LUPO, M., BARNEA, E., ADMON, A., HELLER, E. D., AIZENSHTEIN, E. & PITCOVSKI, J. 2015. The effect of haptens on protein-carrier immunogenicity. *Immunology,* 144**,** 116-26.
GEISLER, C., LARSEN, J. K. & PLESNER, T. 1988. Identification of alpha beta and gamma delta T cell receptor-positive cells. *Scand J Immunol,* 28**,** 741-5.
GEISSMANN, F., LEPELLETIER, Y., FRAITAG, S., VALLADEAU, J., BODEMER, C., DEBRE, M., LEBORGNE, M., SAELAND, S. & BROUSSE, N. 2001. Differentiation of Langerhans cells in Langerhans cell histiocytosis. *Blood,* 97**,** 1241-8.
GEORGAKILAS, A. G., MARTIN, O. A. & BONNER, W. M. 2017. p21: A Two-Faced Genome Guardian. *Trends Mol Med,* 23**,** 310-319.
GEORGIEV, H., RAVENS, I., BENARAFA, C., FORSTER, R. & BERNHARDT, G. 2016. Distinct gene expression patterns correlate with developmental and functional traits of iNKT subsets. *Nat Commun,* 7**,** 13116.
GERMAIN, R. N. 1994. MHC-dependent antigen processing and peptide presentation: providing ligands for T lymphocyte activation. *Cell,* 76**,** 287-99.
GHAZAEI, C. 2018. Mycobacterium tuberculosis and lipids: Insights into molecular mechanisms from persistence to virulence. *J Res Med Sci,* 23**,** 63.
GHERARDIN, N. A., REDMOND, S. J., MCWILLIAM, H. E. G., ALMEIDA, C. F., GOURLEY, K. H. A., SENEVIRATNA, R., LI, S., DE ROSE, R., ROSS, F. J., NGUYEN-ROBERTSON, C. V., SU, S., RITCHIE, M. E., VILLADANGOS, J. A., MOODY, D. B., PELLICCI, D. G., ULDRICH, A. P. & GODFREY, D. I. 2021. CD36 family members are TCR-independent ligands for CD1 antigen-presenting molecules. *Sci Immunol,* 6.
GHERARDIN, N. A., SOUTER, M. N., KOAY, H. F., MANGAS, K. M., SEEMANN, T., STINEAR, T. P., ECKLE, S. B., BERZINS, S. P., D'UDEKEM, Y., KONSTANTINOV, I. E., FAIRLIE, D. P., RITCHIE, D. S., NEESON, P. J., PELLICCI, D. G., ULDRICH, A. P., MCCLUSKEY, J. & GODFREY, D. I. 2018. Human blood MAIT cell subsets defined using MR1 tetramers. *Immunol Cell Biol,* 96**,** 507-525.
GIBBS, A., LEEANSYAH, E., INTROINI, A., PAQUIN-PROULX, D., HASSELROT, K., ANDERSSON, E., BROLIDEN, K., SANDBERG, J. K. & TJERNLUND, A. 2017. MAIT cells reside in the female genital mucosa and are biased towards

IL-17 and IL-22 production in response to bacterial stimulation. *Mucosal Immunol,* 10**,** 35-45.
GIGLI, G., CAIELLI, S., CUTULI, D. & FALCONE, M. 2007. Innate immunity modulates autoimmunity: type 1 interferon-beta treatment in multiple sclerosis promotes growth and function of regulatory invariant natural killer T cells through dendritic cell maturation. *Immunology,* 122**,** 409-17.
GILLERON, M., STENGER, S., MAZORRA, Z., WITTKE, F., MARIOTTI, S., BOHMER, G., PRANDI, J., MORI, L., PUZO, G. & DE LIBERO, G. 2004. Diacylated sulfoglycolipids are novel mycobacterial antigens stimulating CD1-restricted T cells during infection with Mycobacterium tuberculosis. *J Exp Med,* 199**,** 649-59.
GIRARDI, E. & ZAJONC, D. M. 2012. Molecular basis of lipid antigen presentation by CD1d and recognition by natural killer T cells. *Immunol Rev,* 250**,** 167-79.
GOBER, M. D., FISHELEVICH, R., ZHAO, Y., UNUTMAZ, D. & GASPARI, A. A. 2008. Human natural killer T cells infiltrate into the skin at elicitation sites of allergic contact dermatitis. *J Invest Dermatol,* 128**,** 1460-9.
GOBER, M. D. & GASPARI, A. A. 2008. Allergic contact dermatitis. *Curr Dir Autoimmun,* 10**,** 1-26.
GODFREY, D. I., KOAY, H. F., MCCLUSKEY, J. & GHERARDIN, N. A. 2019. The biology and functional importance of MAIT cells. *Nat Immunol,* 20**,** 1110-1128.
GODFREY, D. I., ROSSJOHN, J. & MCCLUSKEY, J. 2010. Fighting infection with your MAITs. *Nat Immunol,* 11**,** 693-5.
GODFREY, D. I., ULDRICH, A. P., MCCLUSKEY, J., ROSSJOHN, J. & MOODY, D. B. 2015. The burgeoning family of unconventional T cells. *Nat Immunol,* 16**,** 1114-23.
GOGOLAK, P., RETHI, B., SZATMARI, I., LANYI, A., DEZSO, B., NAGY, L. & RAJNAVOLGYI, E. 2007. Differentiation of CD1a- and CD1a+ monocyte-derived dendritic cells is biased by lipid environment and PPARgamma. *Blood,* 109**,** 643-52.
GOLD, M. C., EID, T., SMYK-PEARSON, S., EBERLING, Y., SWARBRICK, G. M., LANGLEY, S. M., STREETER, P. R., LEWINSOHN, D. A. & LEWINSOHN, D. M. 2013. Human thymic MR1-restricted MAIT cells are innate pathogen-reactive effectors that adapt following thymic egress. *Mucosal Immunol,* 6**,** 35-44.
GOLUBOVSKAYA, V. & WU, L. 2016. Different Subsets of T Cells, Memory, Effector Functions, and CAR-T Immunotherapy. *Cancers (Basel),* 8.
GOOSSENS, A. 2016. Cosmetic Contact Allergens. *Cosmetics,* 3**,** 5.
GOVERMAN, J. 2009. Autoimmune T cell responses in the central nervous system. *Nat Rev Immunol,* 9**,** 393-407.
GRANT, E. P., DEGANO, M., ROSAT, J. P., STENGER, S., MODLIN, R. L., WILSON, I. A., PORCELLI, S. A. & BRENNER, M. B. 1999. Molecular recognition of lipid antigens by T cell receptors. *J Exp Med,* 189**,** 195-205.
GRAS, S., KJER-NIELSEN, L., BURROWS, S. R., MCCLUSKEY, J. & ROSSJOHN, J. 2008. T-cell receptor bias and immunity. *Curr Opin Immunol,* 20**,** 119-25.
GRAS, S., VAN RHIJN, I., SHAHINE, A., CHENG, T. Y., BHATI, M., TAN, L. L., HALIM, H., TUTTLE, K. D., GAPIN, L., LE NOURS, J., MOODY, D. B. & ROSSJOHN, J. 2016. T cell receptor recognition of CD1b presenting a mycobacterial glycolipid. *Nat Commun,* 7**,** 13257.
GRAY, C. P., AROSIO, P. & HERSEY, P. 2002. Heavy chain ferritin activates regulatory T cells by induction of changes in dendritic cells. *Blood,* 99**,** 3326-34.

GRAY, C. P., FRANCO, A. V., AROSIO, P. & HERSEY, P. 2001. Immunosuppressive effects of melanoma-derived heavy-chain ferritin are dependent on stimulation of IL-10 production. *Int J Cancer,* 92**,** 843-50.
GREEN, A. M., DIFAZIO, R. & FLYNN, J. L. 2013. IFN-gamma from CD4 T cells is essential for host survival and enhances CD8 T cell function during Mycobacterium tuberculosis infection. *J Immunol,* 190**,** 270-7.
GRISERI, T., BEAUDOIN, L., NOVAK, J., MARS, L. T., LEPAULT, F., LIBLAU, R. & LEHUEN, A. 2005. Invariant NKT cells exacerbate type 1 diabetes induced by CD8 T cells. *J Immunol,* 175**,** 2091-101.
GUIARD, J., COLLMANN, A., GARCIA-ALLES, L. F., MOUREY, L., BRANDO, T., MORI, L., GILLERON, M., PRANDI, J., DE LIBERO, G. & PUZO, G. 2009. Fatty acyl structures of mycobacterium tuberculosis sulfoglycolipid govern T cell response. *J Immunol,* 182**,** 7030-7.
GUMPERZ, J. E., MIYAKE, S., YAMAMURA, T. & BRENNER, M. B. 2002. Functionally distinct subsets of CD1d-restricted natural killer T cells revealed by CD1d tetramer staining. *J Exp Med,* 195**,** 625-36.
HAIM-VILMOVSKY, L., WALKER, J. A., HENRIKSSON, J., MIAO, Z., NATAN, E., KAR, G., CLARE, S., BARLOW, J. L., CHARIDEMOU, E. & MAMANOVA, L. 2019. Rora regulates activated T helper cells during inflammation. *BioRxiv***,** 709998.
HAMANN, D., BAARS, P. A., REP, M. H., HOOIBRINK, B., KERKHOF-GARDE, S. R., KLEIN, M. R. & VAN LIER, R. A. 1997. Phenotypic and functional separation of memory and effector human CD8+ T cells. *J Exp Med,* 186**,** 1407-18.
HAN, M., HANNICK, L. I., DIBRINO, M. & ROBINSON, M. A. 1999. Polymorphism of human CD1 genes. *Tissue Antigens,* 54**,** 122-7.
HAN, X. & BUESO-RAMOS, C. E. 2007. Precursor T-cell acute lymphoblastic leukemia/lymphoblastic lymphoma and acute biphenotypic leukemias. *Am J Clin Pathol,* 127**,** 528-44.
HARA, T., JUNG, L. K., BJORNDAHL, J. M. & FU, S. M. 1986. Human T cell activation. III. Rapid induction of a phosphorylated 28 kD/32 kD disulfide-linked early activation antigen (EA 1) by 12-o-tetradecanoyl phorbol-13-acetate, mitogens, and antigens. *J Exp Med,* 164**,** 1988-2005.
HARANDI, A. M. 2018. Systems analysis of human vaccine adjuvants. *Semin Immunol,* 39**,** 30-34.
HARBECK, R. J. 1998. Immunophenotyping of bronchoalveolar lavage lymphocytes. *Clin Diagn Lab Immunol,* 5**,** 271-7.
HARDMAN, C. S., CHEN, Y. L., SALIMI, M., JARRETT, R., JOHNSON, D., JARVINEN, V. J., OWENS, R. J., REPAPI, E., COUSINS, D. J., BARLOW, J. L., MCKENZIE, A. N. J. & OGG, G. 2017. CD1a presentation of endogenous antigens by group 2 innate lymphoid cells. *Sci Immunol,* 2.
HASHIMOTO, K., HIRAI, M. & KUROSAWA, Y. 1995. A gene outside the human MHC related to classical HLA class I genes. *Science,* 269**,** 693-5.
HASHIMOTO, W., TANAKA, F., ROBBINS, P. D., TANIGUCHI, M., OKAMURA, H., LOTZE, M. T. & TAHARA, H. 2003. Natural killer, but not natural killer T, cells play a necessary role in the promotion of an innate antitumor response induced by IL-18. *Int J Cancer,* 103**,** 508-13.
HATZIIOANNOU, T., AMBROSE, Z., CHUNG, N. P., PIATAK, M., JR., YUAN, F., TRUBEY, C. M., COALTER, V., KISER, R., SCHNEIDER, D., SMEDLEY, J., PUNG, R., GATHUKA, M., ESTES, J. D., VEAZEY, R. S.,

KEWALRAMANI, V. N., LIFSON, J. D. & BIENIASZ, P. D. 2009. A macaque model of HIV-1 infection. *Proc Natl Acad Sci U S A,* 106**,** 4425-9.
HATZIIOANNOU, T. & EVANS, D. T. 2012. Animal models for HIV/AIDS research. *Nat Rev Microbiol,* 10**,** 852-67.
HAYDEN, M. S. & GHOSH, S. 2008. Shared principles in NF-kappaB signaling. *Cell,* 132**,** 344-62.
HAYES, S. M. & KNIGHT, K. L. 2001. Group 1 CD1 genes in rabbit. *J Immunol,* 166**,** 403-10.
HE, H., BISSONNETTE, R., WU, J., DIAZ, A., SAINT-CYR PROULX, E., MAARI, C., JACK, C., LOUIS, M., ESTRADA, Y., KRUEGER, J. G., ZHANG, N., PAVEL, A. B. & GUTTMAN-YASSKY, E. 2020. Tape strips detect distinct immune and barrier profiles in atopic dermatitis and psoriasis. *J Allergy Clin Immunol*.
HEWITT, E. W. 2003. The MHC class I antigen presentation pathway: strategies for viral immune evasion. *Immunology,* 110**,** 163-9.
HILL, D. L. & BALLOU, C. E. 1966. Biosynthesis of mannophospholipids by Mycobacterium phlei. *J Biol Chem,* 241**,** 895-902.
HINTZEN, R. Q., DE JONG, R., LENS, S. M., BROUWER, M., BAARS, P. & VAN LIER, R. A. 1993. Regulation of CD27 expression on subsets of mature T-lymphocytes. *J Immunol,* 151**,** 2426-35.
HIRABAYASHI, Y. 2012. A world of sphingolipids and glycolipids in the brain--novel functions of simple lipids modified with glucose. *Proc Jpn Acad Ser B Phys Biol Sci,* 88**,** 129-43.
HIRANO, T., KISHIMOTO, T., KURITANI, T., MURAGUCHI, A., YAMAMURA, Y., RALPH, P. & GOOD, R. A. 1979. In vitro immune response of human peripheral lymphocytes. IV. Specific induction of human suppressor T cells by an antiserum to the T leukemia cell line HSB. *J Immunol,* 123**,** 1133-40.
HIROMATSU, K., DASCHER, C. C., LECLAIR, K. P., SUGITA, M., FURLONG, S. T., BRENNER, M. B. & PORCELLI, S. A. 2002. Induction of CD1-restricted immune responses in guinea pigs by immunization with mycobacterial lipid antigens. *J Immunol,* 169**,** 330-9.
HIROSE, K., ITO, T. & NAKAJIMA, H. 2018. Roles of IL-22 in allergic airway inflammation in mice and humans. *Int Immunol,* 30**,** 413-418.
HIROSE, K., TAKAHASHI, K. & NAKAJIMA, H. 2013. Roles of IL-22 in Allergic Airway Inflammation. *J Allergy (Cairo),* 2013**,** 260518.
HOCHSTENBACH, F. & BRENNER, M. B. 1989. T-cell receptor delta-chain can substitute for alpha to form a beta delta heterodimer. *Nature,* 340**,** 562-5.
HOKANSON, J. E. & AUSTIN, M. A. 1996. Plasma triglyceride level is a risk factor for cardiovascular disease independent of high-density lipoprotein cholesterol level: a meta-analysis of population-based prospective studies. *J Cardiovasc Risk,* 3**,** 213-9.
HOLMES, R. S. 2012. Comparative Studies of Vertebrate Platelet Glycoprotein 4 (CD36). *Biomolecules,* 2**,** 389-414.
HOLST, J., SZYMCZAK-WORKMAN, A. L., VIGNALI, K. M., BURTON, A. R., WORKMAN, C. J. & VIGNALI, D. A. 2006. Generation of T-cell receptor retrogenic mice. *Nat Protoc,* 1**,** 406-17.
HOLZAPFEL, K. L., TYZNIK, A. J., KRONENBERG, M. & HOGQUIST, K. A. 2014. Antigen-dependent versus -independent activation of invariant NKT cells during infection. *J Immunol,* 192**,** 5490-8.

HOUTMAN, S. H., RUTTEMAN, M., DE ZEEUW, C. I. & FRENCH, P. J. 2007. Echinoderm microtubule-associated protein like protein 4, a member of the echinoderm microtubule-associated protein family, stabilizes microtubules. *Neuroscience,* 144**,** 1373-82.

HUANG, S., CHENG, T. Y., YOUNG, D. C., LAYRE, E., MADIGAN, C. A., SHIRES, J., CERUNDOLO, V., ALTMAN, J. D. & MOODY, D. B. 2011. Discovery of deoxyceramides and diacylglycerols as CD1b scaffold lipids among diverse groove-blocking lipids of the human CD1 system. *Proc Natl Acad Sci U S A,* 108**,** 19335-40.

HUANG, S., GILFILLAN, S., KIM, S., THOMPSON, B., WANG, X., SANT, A. J., FREMONT, D. H., LANTZ, O. & HANSEN, T. H. 2008. MR1 uses an endocytic pathway to activate mucosal-associated invariant T cells. *J Exp Med,* 205**,** 1201-11.

HUANG, S., MARTIN, E., KIM, S., YU, L., SOUDAIS, C., FREMONT, D. H., LANTZ, O. & HANSEN, T. H. 2009. MR1 antigen presentation to mucosal-associated invariant T cells was highly conserved in evolution. *Proc Natl Acad Sci U S A,* 106**,** 8290-5.

HUANG, W., HE, W., SHI, X., HE, X., DOU, L. & GAO, Y. 2018. The Role of CD1d and MR1 Restricted T Cells in the Liver. *Front Immunol,* 9**,** 2424.

HUGHES, M. M., YASSAI, M., SEDY, J. R., WEHRLY, T. D., HUANG, C. Y., KANAGAWA, O., GORSKI, J. & SLECKMAN, B. P. 2003. T cell receptor CDR3 loop length repertoire is determined primarily by features of the V(D)J recombination reaction. *Eur J Immunol,* 33**,** 1568-75.

HUH, J. Y., KIM, J. I., PARK, Y. J., HWANG, I. J., LEE, Y. S., SOHN, J. H., LEE, S. K., ALFADDA, A. A., KIM, S. S., CHOI, S. H., LEE, D. S., PARK, S. H., SEONG, R. H., CHOI, C. S. & KIM, J. B. 2013. A novel function of adipocytes in lipid antigen presentation to iNKT cells. *Mol Cell Biol,* 33**,** 328-39.

HUI, H., FULLER, K., ERBER, W. N. & LINDEN, M. D. 2015. Measurement of monocyte-platelet aggregates by imaging flow cytometry. *Cytometry A,* 87**,** 273-8.

HUNGER, R. E., SIELING, P. A., OCHOA, M. T., SUGAYA, M., BURDICK, A. E., REA, T. H., BRENNAN, P. J., BELISLE, J. T., BLAUVELT, A., PORCELLI, S. A. & MODLIN, R. L. 2004. Langerhans cells utilize CD1a and langerin to efficiently present nonpeptide antigens to T cells. *J Clin Invest,* 113**,** 701-8.

HUTLOFF, A., DITTRICH, A. M., BEIER, K. C., ELJASCHEWITSCH, B., KRAFT, R., ANAGNOSTOPOULOS, I. & KROCZEK, R. A. 1999. ICOS is an inducible T-cell co-stimulator structurally and functionally related to CD28. *Nature,* 397**,** 263-6.

HWANGBO, C., TAE, N., LEE, S., KIM, O., PARK, O. K., KIM, J., KWON, S. H. & LEE, J. H. 2016. Syntenin regulates TGF-beta1-induced Smad activation and the epithelial-to-mesenchymal transition by inhibiting caveolin-mediated TGF-beta type I receptor internalization. *Oncogene,* 35**,** 389-401.

IKEDA, K., KUNDU, R. K., IKEDA, S., KOBARA, M., MATSUBARA, H. & QUERTERMOUS, T. 2006. Glia maturation factor-gamma is preferentially expressed in microvascular endothelial and inflammatory cells and modulates actin cytoskeleton reorganization. *Circ Res,* 99**,** 424-33.

ILAN, Y. 2009. Alpha versus beta: are we on the way to resolve the mystery as to which is the endogenous ligand for natural killer T cells? *Clin Exp Immunol,* 158**,** 300-7.

ILLES, Z., KONDO, T., NEWCOMBE, J., OKA, N., TABIRA, T. & YAMAMURA, T. 2000. Differential expression of NK T cell V alpha 24J alpha Q invariant TCR chain in the lesions of multiple sclerosis and chronic inflammatory demyelinating polyneuropathy. *J Immunol,* 164**,** 4375-81.

IMOKAWA, G., ABE, A., JIN, K., HIGAKI, Y., KAWASHIMA, M. & HIDANO, A. 1991. Decreased level of ceramides in stratum corneum of atopic dermatitis: an etiologic factor in atopic dry skin? *J Invest Dermatol,* 96**,** 523-6.

INAGAKI, M., AOYAMA, M., SOBUE, K., YAMAMOTO, N., MORISHIMA, T., MORIYAMA, A., KATSUYA, H. & ASAI, K. 2004. Sensitive immunoassays for human and rat GMFB and GMFG, tissue distribution and age-related changes. *Biochim Biophys Acta,* 1670**,** 208-16.

INTERNATIONAL NOMENCLATURE COSMETIC INGREDIENT BEAUTY. *C12-15 Alkyl Benzoate* [Online]. Available: https://incibeauty.com/en/ingredients/10347-c12-15-alkyl-benzoate#:~:text=C12%2D15%20ALKYL%20BENZOATECAS%20number%3A%2068411%2D27%2D8&text=It%20is%20also%20often%20used,the%20touch%20silky%20and%20soft. [Accessed 11/11/20 2020].

ISHIHARA, S., NIEDA, M., KITAYAMA, J., OSADA, T., YABE, T., KIKUCHI, A., KOEZUKA, Y., PORCELLI, S. A., TADOKORO, K., NAGAWA, H. & JUJI, T. 2000. Alpha-glycosylceramides enhance the antitumor cytotoxicity of hepatic lymphocytes obtained from cancer patients by activating CD3-CD56+ NK cells in vitro. *J Immunol,* 165**,** 1659-64.

ITO, Y., VELA, J. L., MATSUMURA, F., HOSHINO, H., TYZNIK, A., LEE, H., GIRARDI, E., ZAJONC, D. M., LIDDINGTON, R., KOBAYASHI, M., BAO, X., BUGAYTSOVA, J., BOREN, T., JIN, R., ZONG, Y., SEEBERGER, P. H., NAKAYAMA, J., KRONENBERG, M. & FUKUDA, M. 2013. Helicobacter pylori cholesteryl alpha-glucosides contribute to its pathogenicity and immune response by natural killer T cells. *PLoS One,* 8**,** e78191.

JAHNG, A., MARICIC, I., AGUILERA, C., CARDELL, S., HALDER, R. C. & KUMAR, V. 2004. Prevention of autoimmunity by targeting a distinct, noninvariant CD1d-reactive T cell population reactive to sulfatide. *J Exp Med,* 199**,** 947-57.

JAHNG, A. W., MARICIC, I., PEDERSEN, B., BURDIN, N., NAIDENKO, O., KRONENBERG, M., KOEZUKA, Y. & KUMAR, V. 2001. Activation of natural killer T cells potentiates or prevents experimental autoimmune encephalomyelitis. *J Exp Med,* 194**,** 1789-99.

JAMES, C. A., XU, Y., AGUILAR, M. S., JING, L., LAYTON, E. D., GILLERON, M., MINNAARD, A. J., SCRIBA, T. J., DAY, C. L., WARREN, E. H., KOELLE, D. M. & SESHADRI, C. 2022. CD4 and CD8 co-receptors modulate functional avidity of CD1b-restricted T cells. *Nat Commun,* 13**,** 78.

JANEWAY, C. A., JR. 1992. The T cell receptor as a multicomponent signalling machine: CD4/CD8 coreceptors and CD45 in T cell activation. *Annu Rev Immunol,* 10**,** 645-74.

JARRETT, R., SALIO, M., LLOYD-LAVERY, A., SUBRAMANIAM, S., BOURGEOIS, E., ARCHER, C., CHEUNG, K. L., HARDMAN, C., CHANDLER, D., SALIMI, M., GUTOWSKA-OWSIAK, D., BERNARDINO DE LA SERNA, J., FALLON, P. G., JOLIN, H., MCKENZIE, A., DZIEMBOWSKI, A., PODOBAS, E. I., BAL, W., JOHNSON, D., MOODY, D. B., CERUNDOLO, V. & OGG, G. 2016a. Filaggrin inhibits generation of

CD1a neolipid antigens by house dust mite-derived phospholipase. *Sci Transl Med,* 8**,** 325ra18.
JARRETT, R., SALIO, M., LLOYD-LAVERY, A., SUBRAMANIAM, S., BOURGEOIS, E., ARCHER, C., CHEUNG, K. L., HARDMAN, C., CHANDLER, D., SALIMI, M., GUTOWSKA-OWSIAK, D., DE LA SERNA, J. B., FALLON, P. G., JOLIN, H., MCKENZIE, A., DZIEMBOWSKI, A., PODOBAS, E. I., BAL, W., JOHNSON, D., MOODY, D. B., CERUNDOLO, V. & OGG, G. 2016b. Filaggrin inhibits generation of CD1a neolipid antigens by house dust mite-derived phospholipase. *Sci Transl Med,* 8**,** 325ra18.
JENKINS, M. K., CHU, H. H., MCLACHLAN, J. B. & MOON, J. J. 2010. On the composition of the preimmune repertoire of T cells specific for Peptide-major histocompatibility complex ligands. *Annu Rev Immunol,* 28**,** 275-94.
JI, Z., HE, L., REGEV, A. & STRUHL, K. 2019. Inflammatory regulatory network mediated by the joint action of NF-kB, STAT3, and AP-1 factors is involved in many human cancers. *Proc Natl Acad Sci U S A,* 116**,** 9453-9462.
JO, J., TAN, A. T., USSHER, J. E., SANDALOVA, E., TANG, X. Z., TAN-GARCIA, A., TO, N., HONG, M., CHIA, A., GILL, U. S., KENNEDY, P. T., TAN, K. C., LEE, K. H., DE LIBERO, G., GEHRING, A. J., WILLBERG, C. B., KLENERMAN, P. & BERTOLETTI, A. 2014. Toll-like receptor 8 agonist and bacteria trigger potent activation of innate immune cells in human liver. *PLoS Pathog,* 10**,** e1004210.
JOHANSEN, J. D., ANDERSEN, T. F., THOMSEN, L. K., KJOLLER, M. & MENNE, T. 2000. Rash related to use of scented products. A questionnaire study in the Danish population. Is the problem increasing? *Contact Dermatitis,* 42**,** 222-6.
JOHNSON, W., BERGFELD, W. F., BELSITO, D. V., HILL, R. A., KLAASSEN, C. D., LIEBLER, D. C., MARKS, J. G., SHANK, R. C., SLAGA, T. J., SNYDER, P. W. & ANDERSEN, F. A. 2017. Safety Assessment of Benzyl Alcohol, Benzoic Acid and its Salts, and Benzyl Benzoate. *Int J Toxicol,* 36**,** 5S-30S.
JORDAN, M. S., BOESTEANU, A., REED, A. J., PETRONE, A. L., HOLENBECK, A. E., LERMAN, M. A., NAJI, A. & CATON, A. J. 2001. Thymic selection of CD4+CD25+ regulatory T cells induced by an agonist self-peptide. *Nat Immunol,* 2**,** 301-6.
KACZMAREK, R., PASCIAK, M., SZYMCZAK-KULUS, K. & CZERWINSKI, M. 2017. CD1: A Singed Cat of the Three Antigen Presentation Systems. *Arch Immunol Ther Exp (Warsz),* 65**,** 201-214.
KAEWPREEDEE, P., BOONRAT, P., TANSIRI, Y., ROWLAND-JONES, S. L. & HANSASUTA, P. 2019. Dimorphism in the T-cell receptor constant region affects T-cell function, phenotype and HIV outcome. *AIDS,* 33**,** 1421-1429.
KAGINA, B. M., ABEL, B., SCRIBA, T. J., HUGHES, E. J., KEYSER, A., SOARES, A., GAMIELDIEN, H., SIDIBANA, M., HATHERILL, M., GELDERBLOEM, S., MAHOMED, H., HAWKRIDGE, A., HUSSEY, G., KAPLAN, G., HANEKOM, W. A. & OTHER MEMBERS OF THE SOUTH AFRICAN TUBERCULOSIS VACCINE, I. 2010. Specific T cell frequency and cytokine expression profile do not correlate with protection against tuberculosis after bacillus Calmette-Guerin vaccination of newborns. *Am J Respir Crit Care Med,* 182**,** 1073-9.
KAIN, L., WEBB, B., ANDERSON, B. L., DENG, S., HOLT, M., COSTANZO, A., ZHAO, M., SELF, K., TEYTON, A., EVERETT, C., KRONENBERG, M., ZAJONC, D. M., BENDELAC, A., SAVAGE, P. B. & TEYTON, L. 2014. The

identification of the endogenous ligands of natural killer T cells reveals the presence of mammalian alpha-linked glycosylceramides. *Immunity,* 41**,** 543-54.
KALISH, R. S. 1990. The use of human T-lymphocyte clones to study T-cell function in allergic contact dermatitis to urushiol. *J Invest Dermatol,* 94**,** 108S-111S.
KALISH, R. S. & JOHNSON, K. L. 1990. Enrichment and function of urushiol (poison ivy)-specific T lymphocytes in lesions of allergic contact dermatitis to urushiol. *J Immunol,* 145**,** 3706-13.
KALISH, R. S., WOOD, J. A. & LAPORTE, A. 1994. Processing of urushiol (poison ivy) hapten by both endogenous and exogenous pathways for presentation to T cells in vitro. *J Clin Invest,* 93**,** 2039-47.
KAPLAN, D. H., IGYARTO, B. Z. & GASPARI, A. A. 2012. Early immune events in the induction of allergic contact dermatitis. *Nat Rev Immunol,* 12**,** 114-24.
KASHIWASE, K., KIKUCHI, A., ANDO, Y., NICOL, A., PORCELLI, S. A., TOKUNAGA, K., OMINE, M., SATAKE, M., JUJI, T., NIEDA, M. & KOEZUKA, Y. 2003. The CD1d natural killer T-cell antigen presentation pathway is highly conserved between humans and rhesus macaques. *Immunogenetics,* 54**,** 776-81.
KASMAR, A., VAN RHIJN, I. & MOODY, D. B. 2009. The evolved functions of CD1 during infection. *Curr Opin Immunol,* 21**,** 397-403.
KASMAR, A. G., VAN RHIJN, I., MAGALHAES, K. G., YOUNG, D. C., CHENG, T. Y., TURNER, M. T., SCHIEFNER, A., KALATHUR, R. C., WILSON, I. A., BHATI, M., GRAS, S., BIRKINSHAW, R. W., TAN, L. L., ROSSJOHN, J., SHIRES, J., JAKOBSEN, S., ALTMAN, J. D. & MOODY, D. B. 2013. Cutting Edge: CD1a tetramers and dextramers identify human lipopeptide-specific T cells ex vivo. *J Immunol,* 191**,** 4499-503.
KASPROWICZ, V. O., CHENG, T. Y., NDUNG'U, T., SUNPATH, H., MOODY, D. B. & KASMAR, A. G. 2016. HIV Disrupts Human T Cells That Target Mycobacterial Glycolipids. *J Infect Dis,* 213**,** 628-33.
KATELARIS, A. L., JACKSON, C., SOUTHERN, J., GUPTA, R. K., DROBNIEWSKI, F., LALVANI, A., LIPMAN, M., MANGTANI, P. & ABUBAKAR, I. 2020. Effectiveness of BCG Vaccination Against Mycobacterium tuberculosis Infection in Adults: A Cross-sectional Analysis of a UK-Based Cohort. *J Infect Dis,* 221**,** 146-155.
KAWAHARA, K., MOLL, H., KNIREL, Y. A., SEYDEL, U. & ZAHRINGER, U. 2000. Structural analysis of two glycosphingolipids from the lipopolysaccharide-lacking bacterium Sphingomonas capsulata. *Eur J Biochem,* 267**,** 1837-46.
KAWAI, Y., ASAI, K., MIURA, Y., INOUE, Y., YAMAMOTO, M., MORIYAMA, A., YAMAMOTO, N. & KATO, T. 2003. Structure and promoter activity of the human glia maturation factor-gamma gene: a TATA-less, GC-rich and bidirectional promoter. *Biochim Biophys Acta,* 1625**,** 246-52.
KAWANO, T., CUI, J., KOEZUKA, Y., TOURA, I., KANEKO, Y., MOTOKI, K., UENO, H., NAKAGAWA, R., SATO, H., KONDO, E., KOSEKI, H. & TANIGUCHI, M. 1997. CD1d-restricted and TCR-mediated activation of valpha14 NKT cells by glycosylceramides. *Science,* 278**,** 1626-9.
KAWASAKI, S., MORIGUCHI, R., SEKIYA, K., NAKAI, T., ONO, E., KUME, K. & KAWAHARA, K. 1994. The cell envelope structure of the lipopolysaccharide-lacking gram-negative bacterium Sphingomonas paucimobilis. *J Bacteriol,* 176**,** 284-90.

KAWASHIMA, T., NOROSE, Y., WATANABE, Y., ENOMOTO, Y., NARAZAKI, H., WATARI, E., TANAKA, S., TAKAHASHI, H., YANO, I., BRENNER, M. B. & SUGITA, M. 2003. Cutting edge: major CD8 T cell response to live bacillus Calmette-Guerin is mediated by CD1 molecules. *J Immunol,* 170**,** 5345-8.

KELLER, A. N., ECKLE, S. B., XU, W., LIU, L., HUGHES, V. A., MAK, J. Y., MEEHAN, B. S., PEDIONGCO, T., BIRKINSHAW, R. W., CHEN, Z., WANG, H., D'SOUZA, C., KJER-NIELSEN, L., GHERARDIN, N. A., GODFREY, D. I., KOSTENKO, L., CORBETT, A. J., PURCELL, A. W., FAIRLIE, D. P., MCCLUSKEY, J. & ROSSJOHN, J. 2017. Drugs and drug-like molecules can modulate the function of mucosal-associated invariant T cells. *Nat Immunol,* 18**,** 402-411.

KERZERHO, J., YU, E. D., BARRA, C. M., ALARI-PAHISSA, E., GIRARDI, E., HARRAK, Y., LAUZURICA, P., LLEBARIA, A., ZAJONC, D. M., AKBARI, O. & CASTANO, A. R. 2012. Structural and functional characterization of a novel nonglycosidic type I NKT agonist with immunomodulatory properties. *J Immunol,* 188**,** 2254-65.

KIM, C. H., JOHNSTON, B. & BUTCHER, E. C. 2002. Trafficking machinery of NKT cells: shared and differential chemokine receptor expression among V alpha 24(+)V beta 11(+) NKT cell subsets with distinct cytokine-producing capacity. *Blood,* 100**,** 11-6.

KIM, J. H., HU, Y., YONGQING, T., KIM, J., HUGHES, V. A., LE NOURS, J., MARQUEZ, E. A., PURCELL, A. W., WAN, Q., SUGITA, M., ROSSJOHN, J. & WINAU, F. 2016. CD1a on Langerhans cells controls inflammatory skin disease. *Nat Immunol,* 17**,** 1159-66.

KIM, S. K. & KARADENIZ, F. 2012. Biological importance and applications of squalene and squalane. *Adv Food Nutr Res,* 65**,** 223-33.

KIM, W. Y., KIM, H., JEON, Y. K. & KIM, C. W. 2010. Follicular dendritic cell sarcoma with immature T-cell proliferation. *Hum Pathol,* 41**,** 129-33.

KINJO, Y., WU, D., KIM, G., XING, G. W., POLES, M. A., HO, D. D., TSUJI, M., KAWAHARA, K., WONG, C. H. & KRONENBERG, M. 2005. Recognition of bacterial glycosphingolipids by natural killer T cells. *Nature,* 434**,** 520-5.

KIRCIK, L. H., DEL ROSSO, J. Q. & AVERSA, D. 2011. Evaluating Clinical Use of a Ceramide-dominant, Physiologic Lipid-based Topical Emulsion for Atopic Dermatitis. *J Clin Aesthet Dermatol,* 4**,** 34-40.

KITAMURA, H., IWAKABE, K., YAHATA, T., NISHIMURA, S., OHTA, A., OHMI, Y., SATO, M., TAKEDA, K., OKUMURA, K., VAN KAER, L., KAWANO, T., TANIGUCHI, M. & NISHIMURA, T. 1999. The natural killer T (NKT) cell ligand alpha-galactosylceramide demonstrates its immunopotentiating effect by inducing interleukin (IL)-12 production by dendritic cells and IL-12 receptor expression on NKT cells. *J Exp Med,* 189**,** 1121-8.

KJER-NIELSEN, L., PATEL, O., CORBETT, A. J., LE NOURS, J., MEEHAN, B., LIU, L., BHATI, M., CHEN, Z., KOSTENKO, L., REANTRAGOON, R., WILLIAMSON, N. A., PURCELL, A. W., DUDEK, N. L., MCCONVILLE, M. J., O'HAIR, R. A., KHAIRALLAH, G. N., GODFREY, D. I., FAIRLIE, D. P., ROSSJOHN, J. & MCCLUSKEY, J. 2012. MR1 presents microbial vitamin B metabolites to MAIT cells. *Nature,* 491**,** 717-23.

KLECHEVSKY, E., MORITA, R., LIU, M., CAO, Y., COQUERY, S., THOMPSON-SNIPES, L., BRIERE, F., CHAUSSABEL, D., ZURAWSKI, G., PALUCKA, A. K., REITER, Y., BANCHEREAU, J. & UENO, H. 2008. Functional

specializations of human epidermal Langerhans cells and CD14+ dermal dendritic cells. *Immunity,* 29**,** 497-510.
KOAY, H. F., GHERARDIN, N. A., ENDERS, A., LOH, L., MACKAY, L. K., ALMEIDA, C. F., RUSS, B. E., NOLD-PETRY, C. A., NOLD, M. F., BEDOUI, S., CHEN, Z., CORBETT, A. J., ECKLE, S. B., MEEHAN, B., D'UDEKEM, Y., KONSTANTINOV, I. E., LAPPAS, M., LIU, L., GOODNOW, C. C., FAIRLIE, D. P., ROSSJOHN, J., CHONG, M. M., KEDZIERSKA, K., BERZINS, S. P., BELZ, G. T., MCCLUSKEY, J., ULDRICH, A. P., GODFREY, D. I. & PELLICCI, D. G. 2016. A three-stage intrathymic development pathway for the mucosal-associated invariant T cell lineage. *Nat Immunol,* 17**,** 1300-1311.
KOAY, H. F., GHERARDIN, N. A., XU, C., SENEVIRATNA, R., ZHAO, Z., CHEN, Z., FAIRLIE, D. P., MCCLUSKEY, J., PELLICCI, D. G., ULDRICH, A. P. & GODFREY, D. I. 2019. Diverse MR1-restricted T cells in mice and humans. *Nat Commun,* 10**,** 2243.
KOAY, H. F., GODFREY, D. I. & PELLICCI, D. G. 2018. Development of mucosal-associated invariant T cells. *Immunol Cell Biol,* 96**,** 598-606.
KOBAYASHI, C., SHIINA, T., TOKIOKA, A., HATTORI, Y., KOMORI, T., KOBAYASHI-MIURA, M., TAKIZAWA, T., TAKAHARA, K., INABA, K., INOKO, H., TAKEYA, M., DRANOFF, G. & SUGITA, M. 2012. GM-CSF-independent CD1a expression in epidermal Langerhans cells: evidence from human CD1A genome-transgenic mice. *J Invest Dermatol,* 132**,** 241-4.
KONDO, T., TAKATA, H. & TAKIGUCHI, M. 2007. Functional expression of chemokine receptor CCR6 on human effector memory CD8+ T cells. *Eur J Immunol,* 37**,** 54-65.
KONO, F., HONDA, T., AINI, W., MANABE, T., HAGA, H. & TSURUYAMA, T. 2014. Interferon-gamma/CCR5 expression in invariant natural killer T cells and CCL5 expression in capillary veins of dermal papillae correlate with development of psoriasis vulgaris. *Br J Dermatol,* 170**,** 1048-55.
KOVALOVSKY, D., ALONZO, E. S., UCHE, O. U., EIDSON, M., NICHOLS, K. E. & SANT'ANGELO, D. B. 2010. PLZF induces the spontaneous acquisition of memory/effector functions in T cells independently of NKT cell-related signals. *J Immunol,* 184**,** 6746-55.
KOVALOVSKY, D., UCHE, O. U., ELADAD, S., HOBBS, R. M., YI, W., ALONZO, E., CHUA, K., EIDSON, M., KIM, H. J., IM, J. S., PANDOLFI, P. P. & SANT'ANGELO, D. B. 2008. The BTB-zinc finger transcriptional regulator PLZF controls the development of invariant natural killer T cell effector functions. *Nat Immunol,* 9**,** 1055-64.
KRAFT, M. L. 2016. Sphingolipid Organization in the Plasma Membrane and the Mechanisms That Influence It. *Front Cell Dev Biol,* 4**,** 154.
KRANGEL, M. S. 2009. Mechanics of T cell receptor gene rearrangement. *Curr Opin Immunol,* 21**,** 133-9.
KRENSKY, A. M. & CLAYBERGER, C. 2005. Granulysin: a novel host defense molecule. *Am J Transplant,* 5**,** 1789-92.
KROESEN, V. M., MADACKI, J., FRIGUI, W., SAYES, F. & BROSCH, R. 2019. Mycobacterial virulence: impact on immunogenicity and vaccine research. *F1000Res,* 8.
KRONENBERG, M. & KINJO, Y. 2009. Innate-like recognition of microbes by invariant natural killer T cells. *Curr Opin Immunol,* 21**,** 391-6.

KROVI, S. H. & GAPIN, L. 2016. Structure and function of the non-classical major histocompatibility complex molecule MR1. *Immunogenetics,* 68**,** 549-59.
KUMAR, P. 2017. IFNgamma-producing CD4(+) T lymphocytes: the double-edged swords in tuberculosis. *Clin Transl Med,* 6**,** 21.
KURIOKA, A., JAHUN, A. S., HANNAWAY, R. F., WALKER, L. J., FERGUSSON, J. R., SVERREMARK-EKSTROM, E., CORBETT, A. J., USSHER, J. E., WILLBERG, C. B. & KLENERMAN, P. 2017. Shared and Distinct Phenotypes and Functions of Human CD161++ Valpha7.2+ T Cell Subsets. *Front Immunol,* 8**,** 1031.
LAHOUASSA, H., DADDACHA, W., HOFMANN, H., AYINDE, D., LOGUE, E. C., DRAGIN, L., BLOCH, N., MAUDET, C., BERTRAND, M., GRAMBERG, T., PANCINO, G., PRIET, S., CANARD, B., LAGUETTE, N., BENKIRANE, M., TRANSY, C., LANDAU, N. R., KIM, B. & MARGOTTIN-GOGUET, F. 2012. SAMHD1 restricts the replication of human immunodeficiency virus type 1 by depleting the intracellular pool of deoxynucleoside triphosphates. *Nat Immunol,* 13**,** 223-228.
LANGEVELD-WILDSCHUT, E. G., BRUIJNZEEL, P. L., MUDDE, G. C., VERSLUIS, C., VAN IEPEREN-VAN DIJK, A. G., BIHARI, I. C., KNOL, E. F., THEPEN, T., BRUIJNZEEL-KOOMEN, C. A. & VAN REIJSEN, F. C. 2000. Clinical and immunologic variables in skin of patients with atopic eczema and either positive or negative atopy patch test reactions. *J Allergy Clin Immunol,* 105**,** 1008-16.
LANIO, N., SARMIENTO, E., GALLEGO, A., FERNANDEZ-YANEZ, J., PALOMO, J., PEREZ-ROJAS, J. & CARBONE, J. 2009. The potential role of T-cell memory distribution as predisposing factor for rejection in heart transplant recipients. *Transplant Proc,* 41**,** 2480-4.
LANTZ, O. & BENDELAC, A. 1994. An invariant T cell receptor alpha chain is used by a unique subset of major histocompatibility complex class I-specific CD4+ and CD4-8- T cells in mice and humans. *J Exp Med,* 180**,** 1097-106.
LAYRE, E., COLLMANN, A., BASTIAN, M., MARIOTTI, S., CZAPLICKI, J., PRANDI, J., MORI, L., STENGER, S., DE LIBERO, G., PUZO, G. & GILLERON, M. 2009. Mycolic acids constitute a scaffold for mycobacterial lipid antigens stimulating CD1-restricted T cells. *Chem Biol,* 16**,** 82-92.
LAYTON, E. D., YU, K. K. Q., SMITH, M. T., SCRIBA, T. J., DE ROSA, S. C. & SESHADRI, C. 2018. Validation of a CD1b tetramer assay for studies of human mycobacterial infection or vaccination. *J Immunol Methods,* 458**,** 44-52.
LE NOURS, J., PRAVEENA, T., PELLICCI, D. G., GHERARDIN, N. A., ROSS, F. J., LIM, R. T., BESRA, G. S., KESHIPEDDY, S., RICHARDSON, S. K., HOWELL, A. R., GRAS, S., GODFREY, D. I., ROSSJOHN, J. & ULDRICH, A. P. 2016. Atypical natural killer T-cell receptor recognition of CD1d-lipid antigens. *Nat Commun,* 7**,** 10570.
LEE, M. S., HANSPERS, K., BARKER, C. S., KORN, A. P. & MCCUNE, J. M. 2004. Gene expression profiles during human CD4+ T cell differentiation. *Int Immunol,* 16**,** 1109-24.
LEE, P. T., BENLAGHA, K., TEYTON, L. & BENDELAC, A. 2002. Distinct functional lineages of human V(alpha)24 natural killer T cells. *J Exp Med,* 195**,** 637-41.
LEE, Y. J., HOLZAPFEL, K. L., ZHU, J., JAMESON, S. C. & HOGQUIST, K. A. 2013. Steady-state production of IL-4 modulates immunity in mouse strains and is determined by lineage diversity of iNKT cells. *Nat Immunol,* 14**,** 1146-54.

LEE, Y. J., STARRETT, G. J., LEE, S. T., YANG, R., HENZLER, C. M., JAMESON, S. C. & HOGQUIST, K. A. 2016. Lineage-Specific Effector Signatures of Invariant NKT Cells Are Shared amongst gammadelta T, Innate Lymphoid, and Th Cells. *J Immunol,* 197**,** 1460-70.

LEEANSYAH, E., SVARD, J., DIAS, J., BUGGERT, M., NYSTROM, J., QUIGLEY, M. F., MOLL, M., SONNERBORG, A., NOWAK, P. & SANDBERG, J. K. 2015. Arming of MAIT Cell Cytolytic Antimicrobial Activity Is Induced by IL-7 and Defective in HIV-1 Infection. *PLoS Pathog,* 11**,** e1005072.

LEFRANC, M. P., GIUDICELLI, V., GINESTOUX, C., BODMER, J., MULLER, W., BONTROP, R., LEMAITRE, M., MALIK, A., BARBIE, V. & CHAUME, D. 1999. IMGT, the international ImMunoGeneTics database. *Nucleic Acids Res,* 27**,** 209-12.

LEFRANC, M. P., GIUDICELLI, V., GINESTOUX, C., JABADO-MICHALOUD, J., FOLCH, G., BELLAHCENE, F., WU, Y., GEMROT, E., BROCHET, X., LANE, J., REGNIER, L., EHRENMANN, F., LEFRANC, G. & DUROUX, P. 2009. IMGT, the international ImMunoGeneTics information system. *Nucleic Acids Res,* 37**,** D1006-12.

LEGOUX, F., SALOU, M. & LANTZ, O. 2017. Unconventional or Preset alphabeta T Cells: Evolutionarily Conserved Tissue-Resident T Cells Recognizing Nonpeptidic Ligands. *Annu Rev Cell Dev Biol,* 33**,** 511-535.

LEGOUX, F. P. & MOON, J. J. 2012. Peptide:MHC tetramer-based enrichment of epitope-specific T cells. *J Vis Exp*.

LEISHMAN, A. J., NAIDENKO, O. V., ATTINGER, A., KONING, F., LENA, C. J., XIONG, Y., CHANG, H. C., REINHERZ, E., KRONENBERG, M. & CHEROUTRE, H. 2001. T cell responses modulated through interaction between CD8alphaalpha and the nonclassical MHC class I molecule, TL. *Science,* 294**,** 1936-9.

LEPORE, M., DE LALLA, C., GUNDIMEDA, S. R., GSELLINGER, H., CONSONNI, M., GARAVAGLIA, C., SANSANO, S., PICCOLO, F., SCELFO, A., HAUSSINGER, D., MONTAGNA, D., LOCATELLI, F., BONINI, C., BONDANZA, A., FORCINA, A., LI, Z., NI, G., CICERI, F., JENO, P., XIA, C., MORI, L., DELLABONA, P., CASORATI, G. & DE LIBERO, G. 2014. A novel self-lipid antigen targets human T cells against CD1c(+) leukemias. *J Exp Med,* 211**,** 1363-77.

LEPORE, M., DE LALLA, C., MORI, L., DELLABONA, P., DE LIBERO, G. & CASORATI, G. 2015. Targeting leukemia by CD1c-restricted T cells specific for a novel lipid antigen. *Oncoimmunology,* 4**,** e970463.

LI, D., HONG, A., LU, Q., GAO, G. F., JIN, B., SCREATON, G. R. & XU, X. N. 2012a. A novel role of CD1c in regulating CD1d-mediated NKT cell recognition by competitive binding to Ig-like transcript 4. *Int Immunol,* 24**,** 729-37.

LI, D., WANG, L., YU, L., FREUNDT, E. C., JIN, B., SCREATON, G. R. & XU, X. N. 2009. Ig-like transcript 4 inhibits lipid antigen presentation through direct CD1d interaction. *J Immunol,* 182**,** 1033-40.

LI, J., REANTRAGOON, R., KOSTENKO, L., CORBETT, A. J., VARIGOS, G. & CARBONE, F. R. 2017. The frequency of mucosal-associated invariant T cells is selectively increased in dermatitis herpetiformis. *Australas J Dermatol,* 58**,** 200-204.

LI, S., CHOI, H. J., FELIO, K. & WANG, C. R. 2011a. Autoreactive CD1b-restricted T cells: a new innate-like T-cell population that contributes to immunity against infection. *Blood,* 118**,** 3870-8.

LI, S., SIMONI, Y., BECHT, E., LOH, C. Y., LI, N., LACHANCE, D., KOO, S.-L., LIM, T. P., TAN, E. K. W. & MATHEW, R. 2020. Human Tumor-Infiltrating MAIT Cells Display Hallmarks of Bacterial Antigen Recognition in Colorectal Cancer. *Cell Reports Medicine,* 1**,** 100039.

LI, X., POLACINO, P., GARCIA-NAVARRO, R., HU, S. L. & TSUJI, M. 2012b. Peripheral blood invariant natural killer T cells of pig-tailed macaques. *PLoS One,* 7**,** e48166.

LI, Y., INNOCENTIN, S., WITHERS, D. R., ROBERTS, N. A., GALLAGHER, A. R., GRIGORIEVA, E. F., WILHELM, C. & VELDHOEN, M. 2011b. Exogenous stimuli maintain intraepithelial lymphocytes via aryl hydrocarbon receptor activation. *Cell,* 147**,** 629-40.

LI, Y., YIN, Y. & MARIUZZA, R. A. 2013. Structural and biophysical insights into the role of CD4 and CD8 in T cell activation. *Front Immunol,* 4**,** 206.

LI, Z., LI, D., TSUN, A. & LI, B. 2015. FOXP3+ regulatory T cells and their functional regulation. *Cellular & Molecular Immunology,* 12**,** 558-565.

LIM, E. S., FREGOSO, O. I., MCCOY, C. O., MATSEN, F. A., MALIK, H. S. & EMERMAN, M. 2012. The ability of primate lentiviruses to degrade the monocyte restriction factor SAMHD1 preceded the birth of the viral accessory protein Vpx. *Cell Host Microbe,* 11**,** 194-204.

LIM, R. & ZAHEER, A. 1996. In vitro enhancement of p38 mitogen-activated protein kinase activity by phosphorylated glia maturation factor. *J Biol Chem,* 271**,** 22953-6.

LIN, C. C., BRADSTREET, T. R., SCHWARZKOPF, E. A., SIM, J., CARRERO, J. A., CHOU, C., COOK, L. E., EGAWA, T., TANEJA, R., MURPHY, T. L., RUSSELL, J. H. & EDELSON, B. T. 2014. Bhlhe40 controls cytokine production by T cells and is essential for pathogenicity in autoimmune neuroinflammation. *Nat Commun,* 5**,** 3551.

LIN, M. Y. & WELSH, R. M. 1998. Stability and diversity of T cell receptor repertoire usage during lymphocytic choriomeningitis virus infection of mice. *J Exp Med,* 188**,** 1993-2005.

LIPPERT, D. N. & WILKINS, J. A. 2012. Glia maturation factor gamma regulates the migration and adherence of human T lymphocytes. *BMC Immunol,* 13**,** 21.

LIPPI, G., TARGHER, G. & FRANCHINI, M. 2010. Vaccination, squalene and anti-squalene antibodies: facts or fiction? *Eur J Intern Med,* 21**,** 70-3.

LISSINA, A., LADELL, K., SKOWERA, A., CLEMENT, M., EDWARDS, E., SEGGEWISS, R., VAN DEN BERG, H. A., GOSTICK, E., GALLAGHER, K., JONES, E., MELENHORST, J. J., GODKIN, A. J., PEAKMAN, M., PRICE, D. A., SEWELL, A. K. & WOOLDRIDGE, L. 2009. Protein kinase inhibitors substantially improve the physical detection of T-cells with peptide-MHC tetramers. *J Immunol Methods,* 340**,** 11-24.

LITTMAN, D. R. 1998. Chemokine receptors: keys to AIDS pathogenesis? *Cell,* 93**,** 677-80.

LIU, Y., GOFF, R. D., ZHOU, D., MATTNER, J., SULLIVAN, B. A., KHURANA, A., CANTU, C., 3RD, RAVKOV, E. V., IBEGBU, C. C., ALTMAN, J. D., TEYTON, L., BENDELAC, A. & SAVAGE, P. B. 2006. A modified alpha-galactosyl ceramide for staining and stimulating natural killer T cells. *J Immunol Methods,* 312**,** 34-9.

LIU, Y., SHEPHERD, E. G. & NELIN, L. D. 2007. MAPK phosphatases--regulating the immune response. *Nat Rev Immunol,* 7**,** 202-12.

LIU, Y., XIONG, Y., NAIDENKO, O. V., LIU, J. H., ZHANG, R., JOACHIMIAK, A., KRONENBERG, M., CHEROUTRE, H., REINHERZ, E. L. & WANG, J. H. 2003. The crystal structure of a TL/CD8alphaalpha complex at 2.1 A resolution: implications for modulation of T cell activation and memory. *Immunity,* 18**,** 205-15.

LIVAK, F., TOURIGNY, M., SCHATZ, D. G. & PETRIE, H. T. 1999. Characterization of TCR gene rearrangements during adult murine T cell development. *J Immunol,* 162**,** 2575-80.

LOCKRIDGE, J. L., CHEN, X., ZHOU, Y., RAJESH, D., ROENNEBURG, D. A., HEGDE, S., GERDTS, S., CHENG, T. Y., ANDERSON, R. J., PAINTER, G. F., MOODY, D. B., BURLINGHAM, W. J. & GUMPERZ, J. E. 2011. Analysis of the CD1 antigen presenting system in humanized SCID mice. *PLoS One,* 6**,** e21701.

LOETSCHER, M., GERBER, B., LOETSCHER, P., JONES, S. A., PIALI, L., CLARK-LEWIS, I., BAGGIOLINI, M. & MOSER, B. 1996. Chemokine receptor specific for IP10 and mig: structure, function, and expression in activated T-lymphocytes. *J Exp Med,* 184**,** 963-9.

LOHNING, M., HUTLOFF, A., KALLINICH, T., MAGES, H. W., BONHAGEN, K., RADBRUCH, A., HAMELMANN, E. & KROCZEK, R. A. 2003. Expression of ICOS in vivo defines CD4+ effector T cells with high inflammatory potential and a strong bias for secretion of interleukin 10. *J Exp Med,* 197**,** 181-93.

LONNROTH, K., MIGLIORI, G. B., ABUBAKAR, I., D'AMBROSIO, L., DE VRIES, G., DIEL, R., DOUGLAS, P., FALZON, D., GAUDREAU, M. A., GOLETTI, D., GONZALEZ OCHOA, E. R., LOBUE, P., MATTEELLI, A., NJOO, H., SOLOVIC, I., STORY, A., TAYEB, T., VAN DER WERF, M. J., WEIL, D., ZELLWEGER, J. P., ABDEL AZIZ, M., AL LAWATI, M. R., ALIBERTI, S., ARRAZOLA DE ONATE, W., BARREIRA, D., BHATIA, V., BLASI, F., BLOOM, A., BRUCHFELD, J., CASTELLI, F., CENTIS, R., CHEMTOB, D., CIRILLO, D. M., COLORADO, A., DADU, A., DAHLE, U. R., DE PAOLI, L., DIAS, H. M., DUARTE, R., FATTORINI, L., GAGA, M., GETAHUN, H., GLAZIOU, P., GOGUADZE, L., DEL GRANADO, M., HAAS, W., JARVINEN, A., KWON, G. Y., MOSCA, D., NAHID, P., NISHIKIORI, N., NOGUER, I., O'DONNELL, J., PACE-ASCIAK, A., POMPA, M. G., POPESCU, G. G., ROBALO CORDEIRO, C., RONNING, K., RUHWALD, M., SCULIER, J. P., SIMUNOVIC, A., SMITH-PALMER, A., SOTGIU, G., SULIS, G., TORRES-DUQUE, C. A., UMEKI, K., UPLEKAR, M., VAN WEEZENBEEK, C., VASANKARI, T., VITILLO, R. J., VONIATIS, C., WANLIN, M. & RAVIGLIONE, M. C. 2015. Towards tuberculosis elimination: an action framework for low-incidence countries. *Eur Respir J,* 45**,** 928-52.

LOPEZ, K., IWANY, S. K., SULIMAN, S., REIJNEVELD, J. F., OCAMPO, T. A., JIMENEZ, J., CALDERON, R., LECCA, L., MURRAY, M. B., MOODY, D. B. & VAN RHIJN, I. 2020. CD1b Tetramers Broadly Detect T Cells That Correlate With Mycobacterial Exposure but Not Tuberculosis Disease State. *Front Immunol,* 11**,** 199.

LOTTEAU, V., TEYTON, L., PELERAUX, A., NILSSON, T., KARLSSON, L., SCHMID, S. L., QUARANTA, V. & PETERSON, P. A. 1990. Intracellular transport of class II MHC molecules directed by invariant chain. *Nature,* 348**,** 600-5.

LOWES, M. A., SUAREZ-FARINAS, M. & KRUEGER, J. G. 2014. Immunology of psoriasis. *Annu Rev Immunol,* 32**,** 227-55.

LOWIN, T. & STRAUB, R. H. 2011. Integrins and their ligands in rheumatoid arthritis. *Arthritis Res Ther,* 13**,** 244.
LUOMA, A. M., CASTRO, C. D. & ADAMS, E. J. 2014. gammadelta T cell surveillance via CD1 molecules. *Trends Immunol,* 35**,** 613-621.
LY, D., KASMAR, A. G., CHENG, T. Y., DE JONG, A., HUANG, S., ROY, S., BHATT, A., VAN SUMMEREN, R. P., ALTMAN, J. D., JACOBS, W. R., JR., ADAMS, E. J., MINNAARD, A. J., PORCELLI, S. A. & MOODY, D. B. 2013. CD1c tetramers detect ex vivo T cell responses to processed phosphomycoketide antigens. *J Exp Med,* 210**,** 729-41.
LY, D. & MOODY, D. B. 2014. The CD1 size problem: lipid antigens, ligands, and scaffolds. *Cell Mol Life Sci,* 71**,** 3069-79.
LYNN, R. C., WEBER, E. W., SOTILLO, E., GENNERT, D., XU, P., GOOD, Z., ANBUNATHAN, H., LATTIN, J., JONES, R., TIEU, V., NAGARAJA, S., GRANJA, J., DE BOURCY, C. F. A., MAJZNER, R., SATPATHY, A. T., QUAKE, S. R., MONJE, M., CHANG, H. Y. & MACKALL, C. L. 2019. c-Jun overexpression in CAR T cells induces exhaustion resistance. *Nature,* 576**,** 293-300.
MACHO-FERNANDEZ, E., CRUZ, L. J., GHINNAGOW, R., FONTAINE, J., BIALECKI, E., FRISCH, B., TROTTEIN, F. & FAVEEUW, C. 2014. Targeted delivery of alpha-galactosylceramide to CD8alpha+ dendritic cells optimizes type I NKT cell-based antitumor responses. *J Immunol,* 193**,** 961-9.
MACIOCIA, P. M., WAWRZYNIECKA, P. A., PHILIP, B., RICCIARDELLI, I., AKARCA, A. U., ONUOHA, S. C., LEGUT, M., COLE, D. K., SEWELL, A. K., GRITTI, G., SOMJA, J., PIRIS, M. A., PEGGS, K. S., LINCH, D. C., MARAFIOTI, T. & PULE, M. A. 2017. Targeting the T cell receptor beta-chain constant region for immunotherapy of T cell malignancies. *Nat Med,* 23**,** 1416-1423.
MADIGAN, C. A., CHENG, T. Y., LAYRE, E., YOUNG, D. C., MCCONNELL, M. J., DEBONO, C. A., MURRY, J. P., WEI, J. R., BARRY, C. E., 3RD, RODRIGUEZ, G. M., MATSUNAGA, I., RUBIN, E. J. & MOODY, D. B. 2012. Lipidomic discovery of deoxysiderophores reveals a revised mycobactin biosynthesis pathway in Mycobacterium tuberculosis. *Proc Natl Acad Sci U S A,* 109**,** 1257-62.
MAHIL, S. K., CATAPANO, M., DI MEGLIO, P., DAND, N., AHLFORS, H., CARR, I. M., SMITH, C. H., TREMBATH, R. C., PEAKMAN, M., WRIGHT, J., CICCARELLI, F. D., BARKER, J. N. & CAPON, F. 2017. An analysis of IL-36 signature genes and individuals with IL1RL2 knockout mutations validates IL-36 as a psoriasis therapeutic target. *Sci Transl Med,* 9.
MAK, T. W. & SAUNDERS, M. E. 2006. 28 - Allergy and Hypersensitivity. *In:* MAK, T. W. & SAUNDERS, M. E. (eds.) *The Immune Response.* Burlington: Academic Press.
MANGTANI, P., ABUBAKAR, I., ARITI, C., BEYNON, R., PIMPIN, L., FINE, P. E., RODRIGUES, L. C., SMITH, P. G., LIPMAN, M., WHITING, P. F. & STERNE, J. A. 2014. Protection by BCG vaccine against tuberculosis: a systematic review of randomized controlled trials. *Clin Infect Dis,* 58**,** 470-80.
MANOLOVA, V., KISTOWSKA, M., PAOLETTI, S., BALTARIU, G. M., BAUSINGER, H., HANAU, D., MORI, L. & DE LIBERO, G. 2006. Functional CD1a is stabilized by exogenous lipids. *Eur J Immunol,* 36**,** 1083-92.
MANSOUR, S., TOCHEVA, A. S., CAVE-AYLAND, C., MACHELETT, M. M., SANDER, B., LISSIN, N. M., MOLLOY, P. E., BAIRD, M. S., STUBS, G.,

SCHRODER, N. W., SCHUMANN, R. R., RADEMANN, J., POSTLE, A. D., JAKOBSEN, B. K., MARSHALL, B. G., GOSAIN, R., ELKINGTON, P. T., ELLIOTT, T., SKYLARIS, C. K., ESSEX, J. W., TEWS, I. & GADOLA, S. D. 2016. Cholesteryl esters stabilize human CD1c conformations for recognition by self-reactive T cells. *Proc Natl Acad Sci U S A,* 113**,** E1266-75.
MARKOWITZ, N., HANSEN, N. I., HOPEWELL, P. C., GLASSROTH, J., KVALE, P. A., MANGURA, B. T., WILCOSKY, T. C., WALLACE, J. M., ROSEN, M. J. & REICHMAN, L. B. 1997. Incidence of tuberculosis in the United States among HIV-infected persons. The Pulmonary Complications of HIV Infection Study Group. *Ann Intern Med,* 126**,** 123-32.
MARRACK, P., SCOTT-BROWNE, J. P., DAI, S., GAPIN, L. & KAPPLER, J. W. 2008. Evolutionarily conserved amino acids that control TCR-MHC interaction. *Annu Rev Immunol,* 26**,** 171-203.
MARRAKCHI, H., LANEELLE, M. A. & DAFFE, M. 2014. Mycolic acids: structures, biosynthesis, and beyond. *Chem Biol,* 21**,** 67-85.
MARTIN, B., HIROTA, K., CUA, D. J., STOCKINGER, B. & VELDHOEN, M. 2009a. Interleukin-17-producing gammadelta T cells selectively expand in response to pathogen products and environmental signals. *Immunity,* 31**,** 321-30.
MARTIN, E., TREINER, E., DUBAN, L., GUERRI, L., LAUDE, H., TOLY, C., PREMEL, V., DEVYS, A., MOURA, I. C., TILLOY, F., CHERIF, S., VERA, G., LATOUR, S., SOUDAIS, C. & LANTZ, O. 2009b. Stepwise development of MAIT cells in mouse and human. *PLoS Biol,* 7**,** e54.
MARTIN, L. H., CALABI, F. & MILSTEIN, C. 1986. Isolation of CD1 genes: a family of major histocompatibility complex-related differentiation antigens. *Proc Natl Acad Sci U S A,* 83**,** 9154-8.
MASON, D. 1998. A very high level of crossreactivity is an essential feature of the T-cell receptor. *Immunol Today,* 19**,** 395-404.
MASON, R. D., ROSE, R. D., SEDDIKI, N., KELLEHER, A. D. & KENT, S. J. 2008. Low pre-infection levels and loss of central memory CD4+ T cells may predict rapid progression in SIV-infected pigtail macaques. *Virology,* 381**,** 11-5.
MATSUDA, J. L., NAIDENKO, O. V., GAPIN, L., NAKAYAMA, T., TANIGUCHI, M., WANG, C. R., KOEZUKA, Y. & KRONENBERG, M. 2000. Tracking the response of natural killer T cells to a glycolipid antigen using CD1d tetramers. *J Exp Med,* 192**,** 741-54.
MATSUNAGA, I., BHATT, A., YOUNG, D. C., CHENG, T. Y., EYLES, S. J., BESRA, G. S., BRIKEN, V., PORCELLI, S. A., COSTELLO, C. E., JACOBS, W. R., JR. & MOODY, D. B. 2004. Mycobacterium tuberculosis pks12 produces a novel polyketide presented by CD1c to T cells. *J Exp Med,* 200**,** 1559-69.
MATSUNAGA, I., NAKA, T., TALEKAR, R. S., MCCONNELL, M. J., KATOH, K., NAKAO, H., OTSUKA, A., BEHAR, S. M., YANO, I., MOODY, D. B. & SUGITA, M. 2008. Mycolyltransferase-mediated glycolipid exchange in Mycobacteria. *J Biol Chem,* 283**,** 28835-41.
MATTEELLI, A., RENDON, A., TIBERI, S., AL-ABRI, S., VONIATIS, C., CARVALHO, A. C. C., CENTIS, R., D'AMBROSIO, L., VISCA, D., SPANEVELLO, A. & BATTISTA MIGLIORI, G. 2018. Tuberculosis elimination: where are we now? *Eur Respir Rev,* 27.
MATTNER, J., DEBORD, K. L., ISMAIL, N., GOFF, R. D., CANTU, C., 3RD, ZHOU, D., SAINT-MEZARD, P., WANG, V., GAO, Y., YIN, N., HOEBE, K., SCHNEEWIND, O., WALKER, D., BEUTLER, B., TEYTON, L., SAVAGE,

P. B. & BENDELAC, A. 2005. Exogenous and endogenous glycolipid antigens activate NKT cells during microbial infections. *Nature,* 434**,** 525-9.
MATULIS, G., SANDERSON, J. P., LISSIN, N. M., ASPARUHOVA, M. B., BOMMINENI, G. R., SCHUMPERLI, D., SCHMIDT, R. R., VILLIGER, P. M., JAKOBSEN, B. K. & GADOLA, S. D. 2010. Innate-like control of human iNKT cell autoreactivity via the hypervariable CDR3beta loop. *PLoS Biol,* 8**,** e1000402.
MCBRIDE, J. A. & STRIKER, R. 2017. Imbalance in the game of T cells: What can the CD4/CD8 T-cell ratio tell us about HIV and health? *PLoS Pathog,* 13**,** e1006624.
MCFARLAND, D. C., ZHANG, C., THOMAS, H. C. & T, L. R. 2006. Confounding effects of platelets on flow cytometric analysis and cell-sorting experiments using blood-derived cells. *Cytometry A,* 69**,** 86-94.
MCKENZIE, A. N. 2014. Type-2 innate lymphoid cells in asthma and allergy. *Ann Am Thorac Soc,* 11 Suppl 5**,** S263-70.
MEHTA, D., GUPTA, S., GAUR, S. N., GANGAL, S. V. & AGRAWAL, K. P. 1990. Increased leukocyte phospholipase A2 activity and plasma lysophosphatidylcholine levels in asthma and rhinitis and their relationship to airway sensitivity to histamine. *Am Rev Respir Dis,* 142**,** 157-61.
MELIAN, A., GENG, Y. J., SUKHOVA, G. K., LIBBY, P. & PORCELLI, S. A. 1999. CD1 expression in human atherosclerosis. A potential mechanism for T cell activation by foam cells. *Am J Pathol,* 155**,** 775-86.
MEMPEL, M., RONET, C., SUAREZ, F., GILLERON, M., PUZO, G., VAN KAER, L., LEHUEN, A., KOURILSKY, P. & GACHELIN, G. 2002. Natural killer T cells restricted by the monomorphic MHC class 1b CD1d1 molecules behave like inflammatory cells. *J Immunol,* 168**,** 365-71.
MESSAOUDI, I., ESTEP, R., ROBINSON, B. & WONG, S. W. 2011. Nonhuman primate models of human immunology. *Antioxid Redox Signal,* 14**,** 261-73.
MEUNIER, L., VIAN, L., LAGOUEYTE, C., LAVABRE-BERTRAND, T., DUPERRAY, C., MEYNADIER, J. & CANO, J. P. 1996. Quantification of CD1a, HLA-DR, and HLA class I expression on viable human Langerhans cells and keratinocytes. *Cytometry,* 26**,** 260-4.
MILES, J. J., DOUEK, D. C. & PRICE, D. A. 2011a. Bias in the alphabeta T-cell repertoire: implications for disease pathogenesis and vaccination. *Immunol Cell Biol,* 89**,** 375-87.
MILES, J. J., THAMMANICHANOND, D., MONEER, S., NIVARTHI, U. K., KJER-NIELSEN, L., TRACY, S. L., AITKEN, C. K., BRENNAN, R. M., ZENG, W., MARQUART, L., JACKSON, D., BURROWS, S. R., BOWDEN, D. S., TORRESI, J., HELLARD, M., ROSSJOHN, J., MCCLUSKEY, J. & BHARADWAJ, M. 2011b. Antigen-driven patterns of TCR bias are shared across diverse outcomes of human hepatitis C virus infection. *J Immunol,* 186**,** 901-12.
MILEY, M. J., TRUSCOTT, S. M., YU, Y. Y., GILFILLAN, S., FREMONT, D. H., HANSEN, T. H. & LYBARGER, L. 2003. Biochemical features of the MHC-related protein 1 consistent with an immunological function. *J Immunol,* 170**,** 6090-8.
MILLER, M. M., WANG, C., PARISINI, E., COLETTA, R. D., GOTO, R. M., LEE, S. Y., BARRAL, D. C., TOWNES, M., ROURA-MIR, C., FORD, H. L., BRENNER, M. B. & DASCHER, C. C. 2005. Characterization of two avian

MHC-like genes reveals an ancient origin of the CD1 family. *Proc Natl Acad Sci U S A,* 102**,** 8674-9.
MILLER, W. P., SRINIVASAN, S., PANOSKALTSIS-MORTARI, A., SINGH, K., SEN, S., HAMBY, K., DEANE, T., STEMPORA, L., BEUS, J., TURNER, A., WHEELER, C., ANDERSON, D. C., SHARMA, P., GARCIA, A., STROBERT, E., ELDER, E., CROCKER, I., CRENSHAW, T., PENEDO, M. C., WARD, T., SONG, M., HORAN, J., LARSEN, C. P., BLAZAR, B. R. & KEAN, L. S. 2010. GVHD after haploidentical transplantation: a novel, MHC-defined rhesus macaque model identifies CD28- CD8+ T cells as a reservoir of breakthrough T-cell proliferation during costimulation blockade and sirolimus-based immunosuppression. *Blood,* 116**,** 5403-18.
MILLS, G. B. & MOOLENAAR, W. H. 2003. The emerging role of lysophosphatidic acid in cancer. *Nat Rev Cancer,* 3**,** 582-91.
MINNIKIN, D. E., ABDOLRAHIMZADEH, H. & BADDILEY, J. 1971. The interrelation of polar lipids in bacterial membranes. *Biochim Biophys Acta,* 249**,** 651-5.
MIRZAEI, R., MOHAMMADZADEH, R., MAHDAVI, F., BADRZADEH, F., KAZEMI, S., EBRAHIMI, M., SOLTANI, F., KAZEMI, S., JEDA, A. S., DARVISHMOTEVALLI, M., YOUSEFIMASHOUF, R., KEYVANI, H. & KARAMPOOR, S. 2020. Overview of the current promising approaches for the development of an effective severe acute respiratory syndrome coronavirus 2 (SARS-CoV-2) vaccine. *Int Immunopharmacol,* 88**,** 106928.
MIYAMOTO, K., MIYAKE, S. & YAMAMURA, T. 2001. A synthetic glycolipid prevents autoimmune encephalomyelitis by inducing TH2 bias of natural killer T cells. *Nature,* 413**,** 531-4.
MIYAWAKI, T., KASAHARA, Y., TAGA, K., YACHIE, A. & TANIGUCHI, N. 1990. Differential expression of CD45RO (UCHL1) and its functional relevance in two subpopulations of circulating TCR-gamma/delta+ lymphocytes. *J Exp Med,* 171**,** 1833-8.
MIYAZAKI, K., MIYAZAKI, M., GUO, Y., YAMASAKI, N., KANNO, M., HONDA, Z., ODA, H., KAWAMOTO, H. & HONDA, H. 2010. The role of the basic helix-loop-helix transcription factor Dec1 in the regulatory T cells. *J Immunol,* 185**,** 7330-9.
MIZUMOTO, N. & TAKASHIMA, A. 2004. CD1a and langerin: acting as more than Langerhans cell markers. *J Clin Invest,* 113**,** 658-60.
MOLLAH, Z. U., AIBA, S., NAKAGAWA, S., MIZUASHI, M., OHTANI, T., YOSHINO, Y. & TAGAMI, H. 2003. Interleukin-3 in cooperation with transforming growth factor beta induces granulocyte macrophage colony stimulating factor independent differentiation of human CD34+ hematopoietic progenitor cells into dendritic cells with features of Langerhans cells. *J Invest Dermatol,* 121**,** 1397-401.
MONIN, L., WHETTLOCK, E. M. & MALE, V. 2020. Immune responses in the human female reproductive tract. *Immunology,* 160**,** 106-115.
MONTOYA, C. J., POLLARD, D., MARTINSON, J., KUMARI, K., WASSERFALL, C., MULDER, C. B., RUGELES, M. T., ATKINSON, M. A., LANDAY, A. L. & WILSON, S. B. 2007. Characterization of human invariant natural killer T subsets in health and disease using a novel invariant natural killer T cell-clonotypic monoclonal antibody, 6B11. *Immunology,* 122**,** 1-14.
MOODY, D. B. & COTTON, R. N. 2017. Four pathways of CD1 antigen presentation to T cells. *Curr Opin Immunol,* 46**,** 127-133.

MOODY, D. B. & PORCELLI, S. A. 2003. Intracellular pathways of CD1 antigen presentation. *Nat Rev Immunol,* 3**,** 11-22.
MOODY, D. B., REINHOLD, B. B., GUY, M. R., BECKMAN, E. M., FREDERIQUE, D. E., FURLONG, S. T., YE, S., REINHOLD, V. N., SIELING, P. A., MODLIN, R. L., BESRA, G. S. & PORCELLI, S. A. 1997. Structural requirements for glycolipid antigen recognition by CD1b-restricted T cells. *Science,* 278**,** 283-6.
MOODY, D. B. & SULIMAN, S. 2017. CD1: From Molecules to Diseases. *F1000Res,* 6**,** 1909.
MOODY, D. B., ULRICHS, T., MUHLECKER, W., YOUNG, D. C., GURCHA, S. S., GRANT, E., ROSAT, J. P., BRENNER, M. B., COSTELLO, C. E., BESRA, G. S. & PORCELLI, S. A. 2000. CD1c-mediated T-cell recognition of isoprenoid glycolipids in Mycobacterium tuberculosis infection. *Nature,* 404**,** 884-8.
MOODY, D. B., YOUNG, D. C., CHENG, T. Y., ROSAT, J. P., ROURA-MIR, C., O'CONNOR, P. B., ZAJONC, D. M., WALZ, A., MILLER, M. J., LEVERY, S. B., WILSON, I. A., COSTELLO, C. E. & BRENNER, M. B. 2004. T cell activation by lipopeptide antigens. *Science,* 303**,** 527-31.
MOODY, D. B., ZAJONC, D. M. & WILSON, I. A. 2005. Anatomy of CD1-lipid antigen complexes. *Nat Rev Immunol,* 5**,** 387-99.
MOORE, M. J., BLACHERE, N. E., FAK, J. J., PARK, C. Y., SAWICKA, K., PARVEEN, S., ZUCKER-SCHARFF, I., MOLTEDO, B., RUDENSKY, A. Y. & DARNELL, R. B. 2018. ZFP36 RNA-binding proteins restrain T cell activation and anti-viral immunity. *Elife,* 7.
MORITA, D., KATOH, K., HARADA, T., NAKAGAWA, Y., MATSUNAGA, I., MIURA, T., ADACHI, A., IGARASHI, T. & SUGITA, M. 2008. Trans-species activation of human T cells by rhesus macaque CD1b molecules. *Biochem Biophys Res Commun,* 377**,** 889-93.
MORITA, M., MOTOKI, K., AKIMOTO, K., NATORI, T., SAKAI, T., SAWA, E., YAMAJI, K., KOEZUKA, Y., KOBAYASHI, E. & FUKUSHIMA, H. 1995. Structure-activity relationship of alpha-galactosylceramides against B16-bearing mice. *J Med Chem,* 38**,** 2176-87.
MORITA, Y. S., PATTERSON, J. H., BILLMAN-JACOBE, H. & MCCONVILLE, M. J. 2004. Biosynthesis of mycobacterial phosphatidylinositol mannosides. *Biochem J,* 378**,** 589-97.
MOTSINGER, A., AZIMZADEH, A., STANIC, A. K., JOHNSON, R. P., VAN KAER, L., JOYCE, S. & UNUTMAZ, D. 2003. Identification and simian immunodeficiency virus infection of CD1d-restricted macaque natural killer T cells. *J Virol,* 77**,** 8153-8.
MOTSINGER, A., HAAS, D. W., STANIC, A. K., VAN KAER, L., JOYCE, S. & UNUTMAZ, D. 2002. CD1d-restricted human natural killer T cells are highly susceptible to human immunodeficiency virus 1 infection. *J Exp Med,* 195**,** 869-79.
MOTTA, S., MONTI, M., SESANA, S., CAPUTO, R., CARELLI, S. & GHIDONI, R. 1993. Ceramide composition of the psoriatic scale. *Biochim Biophys Acta,* 1182**,** 147-51.
MRAZ, V., GEISLER, C. & BONEFELD, C. M. 2020. Dendritic Epidermal T Cells in Allergic Contact Dermatitis. *Front Immunol,* 11**,** 874.
MUELLER, S. N., ZAID, A. & CARBONE, F. R. 2014. Tissue-resident T cells: dynamic players in skin immunity. *Front Immunol,* 5**,** 332.

MUNOZ-FONTELA, C., DOWLING, W. E., FUNNELL, S. G. P., GSELL, P. S., RIVEROS-BALTA, A. X., ALBRECHT, R. A., ANDERSEN, H., BARIC, R. S., CARROLL, M. W., CAVALERI, M., QIN, C., CROZIER, I., DALLMEIER, K., DE WAAL, L., DE WIT, E., DELANG, L., DOHM, E., DUPREX, W. P., FALZARANO, D., FINCH, C. L., FRIEMAN, M. B., GRAHAM, B. S., GRALINSKI, L. E., GUILFOYLE, K., HAAGMANS, B. L., HAMILTON, G. A., HARTMAN, A. L., HERFST, S., KAPTEIN, S. J. F., KLIMSTRA, W. B., KNEZEVIC, I., KRAUSE, P. R., KUHN, J. H., LE GRAND, R., LEWIS, M. G., LIU, W. C., MAISONNASSE, P., MCELROY, A. K., MUNSTER, V., ORESHKOVA, N., RASMUSSEN, A. L., ROCHA-PEREIRA, J., ROCKX, B., RODRIGUEZ, E., ROGERS, T. F., SALGUERO, F. J., SCHOTSAERT, M., STITTELAAR, K. J., THIBAUT, H. J., TSENG, C. T., VERGARA-ALERT, J., BEER, M., BRASEL, T., CHAN, J. F. W., GARCIA-SASTRE, A., NEYTS, J., PERLMAN, S., REED, D. S., RICHT, J. A., ROY, C. J., SEGALES, J., VASAN, S. S., HENAO-RESTREPO, A. M. & BAROUCH, D. H. 2020. Animal models for COVID-19. *Nature,* 586**,** 509-515.

MURAKAMI, M., YAMAMOTO, K., MIKI, Y., MURASE, R., SATO, H. & TAKETOMI, Y. 2016. The Roles of the Secreted Phospholipase A2 Gene Family in Immunology. *Adv Immunol,* 132**,** 91-134.

MUREITHI, M. W., COHEN, K., MOODLEY, R., POOLE, D., MNCUBE, Z., KASMAR, A., MOODY, D. B., GOULDER, P. J., WALKER, B. D., ALTFELD, M. & NDUNG'U, T. 2011. Impairment of CD1d-restricted natural killer T cells in chronic HIV type 1 clade C infection. *AIDS Res Hum Retroviruses,* 27**,** 501-9.

MURPHY, K. M. & WEAVER, C. 2020. *Janeway's Immunobiology*.

NAIR, B. 2001. Final report on the safety assessment of Benzyl Alcohol, Benzoic Acid, and Sodium Benzoate. *Int J Toxicol,* 20 Suppl 3**,** 23-50.

NAIR, S. & DHODAPKAR, M. V. 2017. Natural Killer T Cells in Cancer Immunotherapy. *Front Immunol,* 8**,** 1178.

NALDI, L., CAZZANIGA, S., GONCALO, M., DIEPGEN, T., BRUZE, M., ELSNER, P., COENRAADS, P. J., SVENSSON, A., BERTUCCIO, P., OFENLOCH, R. & GROUP, E. F. S. 2014. Prevalence of self-reported skin complaints and avoidance of common daily life consumer products in selected European Regions. *JAMA Dermatol,* 150**,** 154-63.

NEEFJES, J., JONGSMA, M. L., PAUL, P. & BAKKE, O. 2011. Towards a systems understanding of MHC class I and MHC class II antigen presentation. *Nat Rev Immunol,* 11**,** 823-36.

NEEFJES, J. J., SMIT, L., GEHRMANN, M. & PLOEGH, H. L. 1992. The fate of the three subunits of major histocompatibility complex class I molecules. *Eur J Immunol,* 22**,** 1609-14.

NESTLE, F. O., DI MEGLIO, P., QIN, J. Z. & NICKOLOFF, B. J. 2009. Skin immune sentinels in health and disease. *Nat Rev Immunol,* 9**,** 679-91.

NESTLE, F. O., ZHENG, X. G., THOMPSON, C. B., TURKA, L. A. & NICKOLOFF, B. J. 1993. Characterization of dermal dendritic cells obtained from normal human skin reveals phenotypic and functionally distinctive subsets. *J Immunol,* 151**,** 6535-45.

NGUYEN, T. K., KOETS, A. P., SANTEMA, W. J., VAN EDEN, W., RUTTEN, V. P. & VAN RHIJN, I. 2009. The mycobacterial glycolipid glucose monomycolate induces a memory T cell response comparable to a model protein antigen and no B cell response upon experimental vaccination of cattle. *Vaccine,* 27**,** 4818-25.

NGUYEN, T. K., KOETS, A. P., VORDERMEIER, M., JERVIS, P. J., COX, L. R., GRAHAM, S. P., SANTEMA, W. J., MOODY, D. B., VAN CALENBERGH, S., ZAJONC, D. M., BESRA, G. S. & VAN RHIJN, I. 2013. The bovine CD1D gene has an unusual gene structure and is expressed but cannot present alpha-galactosylceramide with a C26 fatty acid. *Int Immunol,* 25**,** 91-8.

NGUYEN, T. K., WIELAND, W., SANTEMA, W., HOEBOER, J., VAN EDEN, W., RUTTEN, V., KOETS, A. & VAN RHIJN, I. 2011. Immune response of cattle immunized with a conjugate of the glycolipid glucose monomycolate and protein. *Vet Immunol Immunopathol,* 142**,** 265-70.

NICOL, A., NIEDA, M., KOEZUKA, Y., PORCELLI, S., SUZUKI, K., TADOKORO, K., DURRANT, S. & JUJI, T. 2000. Human invariant valpha24+ natural killer T cells activated by alpha-galactosylceramide (KRN7000) have cytotoxic anti-tumour activity through mechanisms distinct from T cells and natural killer cells. *Immunology,* 99**,** 229-34.

NICOLAI, S., WEGRECKI, M., CHENG, T. Y., BOURGEOIS, E. A., COTTON, R. N., MAYFIELD, J. A., MONNOT, G. C., LE NOURS, J., VAN RHIJN, I., ROSSJOHN, J., MOODY, D. B. & DE JONG, A. 2020. Human T cell response to CD1a and contact dermatitis allergens in botanical extracts and commercial skin care products. *Sci Immunol,* 5.

NICOLAIDES, N. 1974. Skin lipids: their biochemical uniqueness. *Science,* 186**,** 19-26.

NIEDA, M., NICOL, A., KOEZUKA, Y., KIKUCHI, A., TAKAHASHI, T., NAKAMURA, H., FURUKAWA, H., YABE, T., ISHIKAWA, Y., TADOKORO, K. & JUJI, T. 1999. Activation of human Valpha24NKT cells by alpha-glycosylceramide in a CD1d-restricted and Valpha24TCR-mediated manner. *Hum Immunol,* 60**,** 10-9.

NIELSEN, M. M., WITHERDEN, D. A. & HAVRAN, W. L. 2017. gammadelta T cells in homeostasis and host defence of epithelial barrier tissues. *Nat Rev Immunol,* 17**,** 733-745.

NIEUWENHUIS, E. E., MATSUMOTO, T., EXLEY, M., SCHLEIPMAN, R. A., GLICKMAN, J., BAILEY, D. T., CORAZZA, N., COLGAN, S. P., ONDERDONK, A. B. & BLUMBERG, R. S. 2002. CD1d-dependent macrophage-mediated clearance of Pseudomonas aeruginosa from lung. *Nat Med,* 8**,** 588-93.

NOGRALES, K. E., ZABA, L. C., SHEMER, A., FUENTES-DUCULAN, J., CARDINALE, I., KIKUCHI, T., RAMON, M., BERGMAN, R., KRUEGER, J. G. & GUTTMAN-YASSKY, E. 2009. IL-22-producing "T22" T cells account for upregulated IL-22 in atopic dermatitis despite reduced IL-17-producing TH17 T cells. *J Allergy Clin Immunol,* 123**,** 1244-52 e2.

NOGUCHI, T., METZ, R., CHEN, L., MATTEI, M. G., CARRASCO, D. & BRAVO, R. 1993. Structure, mapping, and expression of erp, a growth factor-inducible gene encoding a nontransmembrane protein tyrosine phosphatase, and effect of ERP on cell growth. *Mol Cell Biol,* 13**,** 5195-205.

NORTH, R. J. & JUNG, Y. J. 2004. Immunity to tuberculosis. *Annu Rev Immunol,* 22**,** 599-623.

NURIEVA, R., THOMAS, S., NGUYEN, T., MARTIN-OROZCO, N., WANG, Y., KAJA, M. K., YU, X. Z. & DONG, C. 2006. T-cell tolerance or function is determined by combinatorial costimulatory signals. *EMBO J,* 25**,** 2623-33.

NURIEVA, R. I., LIU, X. & DONG, C. 2011. Molecular mechanisms of T-cell tolerance. *Immunol Rev,* 241**,** 133-44.

O'GARRA, A., REDFORD, P. S., MCNAB, F. W., BLOOM, C. I., WILKINSON, R. J. & BERRY, M. P. 2013. The immune response in tuberculosis. *Annu Rev Immunol,* 31**,** 475-527.
O'KEEFFE, J., GATELY, C. M., COUNIHAN, T., HENNESSY, M., LEAHY, T., MORAN, A. P. & HOGAN, E. L. 2008. T-cells expressing natural killer (NK) receptors are altered in multiple sclerosis and responses to alpha-galactosylceramide are impaired. *J Neurol Sci,* 275**,** 22-8.
OETTINGER, M. A., SCHATZ, D. G., GORKA, C. & BALTIMORE, D. 1990. RAG-1 and RAG-2, adjacent genes that synergistically activate V(D)J recombination. *Science,* 248**,** 1517-23.
OGG, G., CERUNDOLO, V. & MCMICHAEL, A. J. 2019. Capturing the antigen landscape: HLA-E, CD1 and MR1. *Curr Opin Immunol,* 59**,** 121-129.
OHTEKI, T. & MACDONALD, H. R. 1994. Major histocompatibility complex class I related molecules control the development of CD4+8- and CD4-8- subsets of natural killer 1.1+ T cell receptor-alpha/beta+ cells in the liver of mice. *J Exp Med,* 180**,** 699-704.
OKITA, M., GAUDETTE, D. C., MILLS, G. B. & HOLUB, B. J. 1997. Elevated levels and altered fatty acid composition of plasma lysophosphatidylcholine(lysoPC) in ovarian cancer patients. *Int J Cancer,* 71**,** 31-4.
OLAKANMI, O., SCHLESINGER, L. S., AHMED, A. & BRITIGAN, B. E. 2002. Intraphagosomal Mycobacterium tuberculosis acquires iron from both extracellular transferrin and intracellular iron pools. Impact of interferon-gamma and hemochromatosis. *J Biol Chem,* 277**,** 49727-34.
OLSON, C. M., JR., BATES, T. C., IZADI, H., RADOLF, J. D., HUBER, S. A., BOYSON, J. E. & ANGUITA, J. 2009. Local production of IFN-gamma by invariant NKT cells modulates acute Lyme carditis. *J Immunol,* 182**,** 3728-34.
OLSON, N. C., DOYLE, M. F., JENNY, N. S., HUBER, S. A., PSATY, B. M., KRONMAL, R. A. & TRACY, R. P. 2013. Decreased naive and increased memory CD4(+) T cells are associated with subclinical atherosclerosis: the multi-ethnic study of atherosclerosis. *PLoS One,* 8**,** e71498.
ONENGUT-GUMUSCU, S. & CONCANNON, P. 2002. Mapping genes for autoimmunity in humans: type 1 diabetes as a model. *Immunol Rev,* 190**,** 182-94.
ORME, I. M., ANDERSEN, P. & BOOM, W. H. 1993. T cell response to Mycobacterium tuberculosis. *J Infect Dis,* 167**,** 1481-97.
ORTALDO, J. R., YOUNG, H. A., WINKLER-PICKETT, R. T., BERE, E. W., JR., MURPHY, W. J. & WILTROUT, R. H. 2004. Dissociation of NKT stimulation, cytokine induction, and NK activation in vivo by the use of distinct TCR-binding ceramides. *J Immunol,* 172**,** 943-53.
OTEO, M., ARRIBAS, P., SETIEN, F., PARRA, J. F., MIRONES, I., GOMEZ DEL MORAL, M. & MARTINEZ-NAVES, E. 2001. Structural characterization of two CD1A allelic variants. *Hum Immunol,* 62**,** 1137-41.
PALETTA, D., FICHTNER, A. S., STARICK, L., PORCELLI, S. A., SAVAGE, P. B. & HERRMANN, T. 2015. Species Specific Differences of CD1d Oligomer Loading In Vitro. *PLoS One,* 10**,** e0143449.
PANNETIER, C., COCHET, M., DARCHE, S., CASROUGE, A., ZOLLER, M. & KOURILSKY, P. 1993. The sizes of the CDR3 hypervariable regions of the murine T-cell receptor beta chains vary as a function of the recombined germ-line segments. *Proc Natl Acad Sci U S A,* 90**,** 4319-23.
PAPPAS, A. 2009. Epidermal surface lipids. *Dermatoendocrinol,* 1**,** 72-6.

PARADIS, T. J., COLE, S. H., NELSON, R. T. & GLADUE, R. P. 2008. Essential role of CCR6 in directing activated T cells to the skin during contact hypersensitivity. *J Invest Dermatol,* 128**,** 628-33.
PAREKH, V. V., SINGH, A. K., WILSON, M. T., OLIVARES-VILLAGOMEZ, D., BEZBRADICA, J. S., INAZAWA, H., EHARA, H., SAKAI, T., SERIZAWA, I., WU, L., WANG, C. R., JOYCE, S. & VAN KAER, L. 2004. Quantitative and qualitative differences in the in vivo response of NKT cells to distinct alpha- and beta-anomeric glycolipids. *J Immunol,* 173**,** 3693-706.
PARK, J. Y., DIPALMA, D. T., KWON, J., FINK, J. & PARK, J. H. 2019. Quantitative Difference in PLZF Protein Expression Determines iNKT Lineage Fate and Controls Innate CD8 T Cell Generation. *Cell Rep,* 27**,** 2548-2557 e4.
PARK, Y. M. 2014. CD36, a scavenger receptor implicated in atherosclerosis. *Exp Mol Med,* 46**,** e99.
PEISER, M., TRALAU, T., HEIDLER, J., API, A. M., ARTS, J. H., BASKETTER, D. A., ENGLISH, J., DIEPGEN, T. L., FUHLBRIGGE, R. C., GASPARI, A. A., JOHANSEN, J. D., KARLBERG, A. T., KIMBER, I., LEPOITTEVIN, J. P., LIEBSCH, M., MAIBACH, H. I., MARTIN, S. F., MERK, H. F., PLATZEK, T., RUSTEMEYER, T., SCHNUCH, A., VANDEBRIEL, R. J., WHITE, I. R. & LUCH, A. 2012. Allergic contact dermatitis: epidemiology, molecular mechanisms, in vitro methods and regulatory aspects. Current knowledge assembled at an international workshop at BfR, Germany. *Cell Mol Life Sci,* 69**,** 763-81.
PELEG, E. & TIETZ, A. 1971. Glycolipids of a halotolerant moderately halophilic bacterium. *FEBS Lett,* 15**,** 309-312.
PELLICCI, D. G., KOAY, H. F. & BERZINS, S. P. 2020. Thymic development of unconventional T cells: how NKT cells, MAIT cells and gammadelta T cells emerge. *Nat Rev Immunol*.
PELLICCI, D. G., PATEL, O., KJER-NIELSEN, L., PANG, S. S., SULLIVAN, L. C., KYPARISSOUDIS, K., BROOKS, A. G., REID, H. H., GRAS, S., LUCET, I. S., KOH, R., SMYTH, M. J., MALLEVAEY, T., MATSUDA, J. L., GAPIN, L., MCCLUSKEY, J., GODFREY, D. I. & ROSSJOHN, J. 2009. Differential recognition of CD1d-alpha-galactosyl ceramide by the V beta 8.2 and V beta 7 semi-invariant NKT T cell receptors. *Immunity,* 31**,** 47-59.
PELLICCI, D. G. & ULDRICH, A. P. 2018. Unappreciated diversity within the pool of CD1d-restricted T cells. *Semin Cell Dev Biol,* 84**,** 42-47.
PELLICCI, D. G., ULDRICH, A. P., LE NOURS, J., ROSS, F., CHABROL, E., ECKLE, S. B., DE BOER, R., LIM, R. T., MCPHERSON, K., BESRA, G., HOWELL, A. R., MORETTA, L., MCCLUSKEY, J., HEEMSKERK, M. H., GRAS, S., ROSSJOHN, J. & GODFREY, D. I. 2014. The molecular bases of delta/alphabeta T cell-mediated antigen recognition. *J Exp Med,* 211**,** 2599-615.
PENA, J. C. & HO, W. Z. 2015. Monkey models of tuberculosis: lessons learned. *Infect Immun,* 83**,** 852-62.
PENA-CRUZ, V., ITO, S., DASCHER, C. C., BRENNER, M. B. & SUGITA, M. 2003. Epidermal Langerhans cells efficiently mediate CD1a-dependent presentation of microbial lipid antigens to T cells. *J Invest Dermatol,* 121**,** 517-21.
PENNINO, D., BHAVSAR, P. K., EFFNER, R., AVITABILE, S., VENN, P., QUARANTA, M., MARZAIOLI, V., CIFUENTES, L., DURHAM, S. R., CAVANI, A., EYERICH, K., CHUNG, K. F., SCHMIDT-WEBER, C. B. & EYERICH, S. 2013. IL-22 suppresses IFN-gamma-mediated lung inflammation in asthmatic patients. *J Allergy Clin Immunol,* 131**,** 562-70.

PENNOCK, N. D., WHITE, J. T., CROSS, E. W., CHENEY, E. E., TAMBURINI, B. A. & KEDL, R. M. 2013. T cell responses: naive to memory and everything in between. *Adv Physiol Educ,* 37**,** 273-83.
PEREIRA, C. S. & MACEDO, M. F. 2016. CD1-Restricted T Cells at the Crossroad of Innate and Adaptive Immunity. *J Immunol Res,* 2016**,** 2876275.
PICKER, L. J., MICHIE, S. A., ROTT, L. S. & BUTCHER, E. C. 1990. A unique phenotype of skin-associated lymphocytes in humans. Preferential expression of the HECA-452 epitope by benign and malignant T cells at cutaneous sites. *Am J Pathol,* 136**,** 1053-68.
PIGOZZI, B., BORDIGNON, M., BELLONI FORTINA, A., MICHELOTTO, G. & ALAIBAC, M. 2006. Expression of the CD1a molecule in B- and T-lymphoproliferative skin conditions. *Oncol Rep,* 15**,** 347-51.
PILONES, K. A., ARYANKALAYIL, J. & DEMARIA, S. 2012. Invariant NKT cells as novel targets for immunotherapy in solid tumors. *Clin Dev Immunol,* 2012**,** 720803.
PINTARELLI, G., NOCI, S., MASPERO, D., PETTINICCHIO, A., DUGO, M., DE CECCO, L., INCARBONE, M., TOSI, D., SANTAMBROGIO, L., DRAGANI, T. A. & COLOMBO, F. 2019. Cigarette smoke alters the transcriptome of non-involved lung tissue in lung adenocarcinoma patients. *Sci Rep,* 9**,** 13039.
PITCHER, C. J., HAGEN, S. I., WALKER, J. M., LUM, R., MITCHELL, B. L., MAINO, V. C., AXTHELM, M. K. & PICKER, L. J. 2002. Development and homeostasis of T cell memory in rhesus macaque. *J Immunol,* 168**,** 29-43.
POLLMANN, M., PARWARESCH, R., ADAM-KLAGES, S., KRUSE, M. L., BUCK, F. & HEIDEBRECHT, H. J. 2006. Human EML4, a novel member of the EMAP family, is essential for microtubule formation. *Exp Cell Res,* 312**,** 3241-51.
PORCELLI, S., BRENNER, M. B., GREENSTEIN, J. L., BALK, S. P., TERHORST, C. & BLEICHER, P. A. 1989. Recognition of cluster of differentiation 1 antigens by human CD4-CD8-cytolytic T lymphocytes. *Nature,* 341**,** 447-50.
PORCELLI, S., YOCKEY, C. E., BRENNER, M. B. & BALK, S. P. 1993. Analysis of T cell antigen receptor (TCR) expression by human peripheral blood CD4-8- alpha/beta T cells demonstrates preferential use of several V beta genes and an invariant TCR alpha chain. *J Exp Med,* 178**,** 1-16.
PORCELLI, S. A. & MODLIN, R. L. 1999. The CD1 system: antigen-presenting molecules for T cell recognition of lipids and glycolipids. *Annu Rev Immunol,* 17**,** 297-329.
PROVINE, N. M. & KLENERMAN, P. 2020. MAIT Cells in Health and Disease. *Annu Rev Immunol,* 38**,** 203-228.
QUINTANA, F. J., BASSO, A. S., IGLESIAS, A. H., KORN, T., FAREZ, M. F., BETTELLI, E., CACCAMO, M., OUKKA, M. & WEINER, H. L. 2008. Control of T(reg) and T(H)17 cell differentiation by the aryl hydrocarbon receptor. *Nature,* 453**,** 65-71.
RAHIMPOUR, A., KOAY, H. F., ENDERS, A., CLANCHY, R., ECKLE, S. B., MEEHAN, B., CHEN, Z., WHITTLE, B., LIU, L., FAIRLIE, D. P., GOODNOW, C. C., MCCLUSKEY, J., ROSSJOHN, J., ULDRICH, A. P., PELLICCI, D. G. & GODFREY, D. I. 2015. Identification of phenotypically and functionally heterogeneous mouse mucosal-associated invariant T cells using MR1 tetramers. *J Exp Med,* 212**,** 1095-108.
REANTRAGOON, R., CORBETT, A. J., SAKALA, I. G., GHERARDIN, N. A., FURNESS, J. B., CHEN, Z., ECKLE, S. B., ULDRICH, A. P., BIRKINSHAW,

R. W., PATEL, O., KOSTENKO, L., MEEHAN, B., KEDZIERSKA, K., LIU, L., FAIRLIE, D. P., HANSEN, T. H., GODFREY, D. I., ROSSJOHN, J., MCCLUSKEY, J. & KJER-NIELSEN, L. 2013. Antigen-loaded MR1 tetramers define T cell receptor heterogeneity in mucosal-associated invariant T cells. *J Exp Med,* 210**,** 2305-20.

REILEY, W. W., CALAYAG, M. D., WITTMER, S. T., HUNTINGTON, J. L., PEARL, J. E., FOUNTAIN, J. J., MARTINO, C. A., ROBERTS, A. D., COOPER, A. M. & WINSLOW, G. M. 2008. ESAT-6-specific CD4 T cell responses to aerosol Mycobacterium tuberculosis infection are initiated in the mediastinal lymph nodes. *Proceedings of the National Academy of Sciences,* 105**,** 10961-10966.

REININK, P. & VAN RHIJN, I. 2016. Mammalian CD1 and MR1 genes. *Immunogenetics,* 68**,** 515-23.

RELLOSO, M., CHENG, T. Y., IM, J. S., PARISINI, E., ROURA-MIR, C., DEBONO, C., ZAJONC, D. M., MURGA, L. F., ONDRECHEN, M. J., WILSON, I. A., PORCELLI, S. A. & MOODY, D. B. 2008. pH-dependent interdomain tethers of CD1b regulate its antigen capture. *Immunity,* 28**,** 774-86.

RES, P., BLOM, B., HORI, T., WEIJER, K. & SPITS, H. 1997. Downregulation of CD1 marks acquisition of functional maturation of human thymocytes and defines a control point in late stages of human T cell development. *J Exp Med,* 185**,** 141-51.

RHOADES, E. R., GEISEL, R. E., BUTCHER, B. A., MCDONOUGH, S. & RUSSELL, D. G. 2005. Cell wall lipids from Mycobacterium bovis BCG are inflammatory when inoculated within a gel matrix: characterization of a new model of the granulomatous response to mycobacterial components. *Tuberculosis (Edinb),* 85**,** 159-76.

RHODE, P. R., EGAN, J. O., XU, W., HONG, H., WEBB, G. M., CHEN, X., LIU, B., ZHU, X., WEN, J., YOU, L., KONG, L., EDWARDS, A. C., HAN, K., SHI, S., ALTER, S., SACHA, J. B., JENG, E. K., CAI, W. & WONG, H. C. 2016. Comparison of the Superagonist Complex, ALT-803, to IL15 as Cancer Immunotherapeutics in Animal Models. *Cancer Immunol Res,* 4**,** 49-60.

RIEGERT, P., WANNER, V. & BAHRAM, S. 1998. Genomics, isoforms, expression, and phylogeny of the MHC class I-related MR1 gene. *J Immunol,* 161**,** 4066-77.

RINCON, M., FLAVELL, R. A. & DAVIS, R. J. 2001. Signal transduction by MAP kinases in T lymphocytes. *Oncogene,* 20**,** 2490-7.

RIZZETTO, S., KOPPSTEIN, D. N. P., SAMIR, J., SINGH, M., REED, J. H., CAI, C. H., LLOYD, A. R., ELTAHLA, A. A., GOODNOW, C. C. & LUCIANI, F. 2018. B-cell receptor reconstruction from single-cell RNA-seq with VDJPuzzle. *Bioinformatics,* 34**,** 2846-2847.

ROCK, E. P., SIBBALD, P. R., DAVIS, M. M. & CHIEN, Y. H. 1994. CDR3 length in antigen-specific immune receptors. *J Exp Med,* 179**,** 323-8.

RODRIGUEZ-GARCIA, M., FORTIER, J. M., BARR, F. D. & WIRA, C. R. 2018. Isolation of Dendritic Cells from the Human Female Reproductive Tract for Phenotypical and Functional Studies. *J Vis Exp*.

RODRIGUEZ-GARCIA, M., SHEN, Z., BARR, F. D., BOESCH, A. W., ACKERMAN, M. E., KAPPES, J. C., OCHSENBAUER, C. & WIRA, C. R. 2017. Dendritic cells from the human female reproductive tract rapidly capture and respond to HIV. *Mucosal Immunol,* 10**,** 531-544.

ROSAT, J. P., GRANT, E. P., BECKMAN, E. M., DASCHER, C. C., SIELING, P. A., FREDERIQUE, D., MODLIN, R. L., PORCELLI, S. A., FURLONG, S. T. &

BRENNER, M. B. 1999. CD1-restricted microbial lipid antigen-specific recognition found in the CD8+ alpha beta T cell pool. *J Immunol,* 162**,** 366-71.
ROSSJOHN, J., PELLICCI, D. G., PATEL, O., GAPIN, L. & GODFREY, D. I. 2012. Recognition of CD1d-restricted antigens by natural killer T cells. *Nat Rev Immunol,* 12**,** 845-57.
ROTH, D. B. 2014. V(D)J Recombination: Mechanism, Errors, and Fidelity. *Microbiol Spectr,* 2.
ROURA-MIR, C., CATALFAMO, M., CHENG, T. Y., MARQUSEE, E., BESRA, G. S., JARAQUEMADA, D. & MOODY, D. B. 2005a. CD1a and CD1c activate intrathyroidal T cells during Graves' disease and Hashimoto's thyroiditis. *J Immunol,* 174**,** 3773-80.
ROURA-MIR, C., WANG, L., CHENG, T. Y., MATSUNAGA, I., DASCHER, C. C., PENG, S. L., FENTON, M. J., KIRSCHNING, C. & MOODY, D. B. 2005b. Mycobacterium tuberculosis regulates CD1 antigen presentation pathways through TLR-2. *J Immunol,* 175**,** 1758-66.
ROUT, N., ELSE, J. G., YUE, S., CONNOLE, M., EXLEY, M. A. & KAUR, A. 2010a. Heterogeneity in phenotype and function of CD8+ and CD4/CD8 double-negative Natural Killer T cell subsets in sooty mangabeys. *J Med Primatol,* 39**,** 224-34.
ROUT, N., ELSE, J. G., YUE, S., CONNOLE, M., EXLEY, M. A. & KAUR, A. 2010b. Paucity of CD4+ natural killer T (NKT) lymphocytes in sooty mangabeys is associated with lack of NKT cell depletion after SIV infection. *PLoS One,* 5**,** e9787.
ROUT, N., GREENE, J., YUE, S., O'CONNOR, D., JOHNSON, R. P., ELSE, J. G., EXLEY, M. A. & KAUR, A. 2012. Loss of effector and anti-inflammatory natural killer T lymphocyte function in pathogenic simian immunodeficiency virus infection. *PLoS Pathog,* 8**,** e1002928.
ROY, S., LY, D., CASTRO, C. D., LI, N. S., HAWK, A. J., ALTMAN, J. D., MEREDITH, S. C., PICCIRILLI, J. A., MOODY, D. B. & ADAMS, E. J. 2016. Molecular Analysis of Lipid-Reactive Vdelta1 gammadelta T Cells Identified by CD1c Tetramers. *J Immunol,* 196**,** 1933-42.
ROY, S., LY, D., LI, N. S., ALTMAN, J. D., PICCIRILLI, J. A., MOODY, D. B. & ADAMS, E. J. 2014. Molecular basis of mycobacterial lipid antigen presentation by CD1c and its recognition by alphabeta T cells. *Proc Natl Acad Sci U S A,* 111**,** E4648-57.
RUDOLPH, M. G., STANFIELD, R. L. & WILSON, I. A. 2006. How TCRs bind MHCs, peptides, and coreceptors. *Annu Rev Immunol,* 24**,** 419-66.
RULTEN, S. L., KINLOCH, R. A., TATEOSSIAN, H., ROBINSON, C., GETTINS, L. & KAY, J. E. 2006. The human FK506-binding proteins: characterization of human FKBP19. *Mamm Genome,* 17**,** 322-31.
RUSSANO, A. M., AGEA, E., CORAZZI, L., POSTLE, A. D., DE LIBERO, G., PORCELLI, S., DE BENEDICTIS, F. M. & SPINOZZI, F. 2006. Recognition of pollen-derived phosphatidyl-ethanolamine by human CD1d-restricted gamma delta T cells. *J Allergy Clin Immunol,* 117**,** 1178-84.
SABATINO, J. J., JR., HUANG, J., ZHU, C. & EVAVOLD, B. D. 2011. High prevalence of low affinity peptide-MHC II tetramer-negative effectors during polyclonal CD4+ T cell responses. *J Exp Med,* 208**,** 81-90.
SAG, D., KRAUSE, P., HEDRICK, C. C., KRONENBERG, M. & WINGENDER, G. 2014. IL-10-producing NKT10 cells are a distinct regulatory invariant NKT cell subset. *J Clin Invest,* 124**,** 3725-40.

SAITO, T., HOCHSTENBACH, F., MARUSIC-GALESIC, S., KRUISBEEK, A. M., BRENNER, M. & GERMAIN, R. N. 1988. Surface expression of only gamma delta and/or alpha beta T cell receptor heterodimers by cells with four (alpha, beta, gamma, delta) functional receptor chains. *J Exp Med,* 168**,** 1003-20.

SAKAGUCHI, S., SAKAGUCHI, N., ASANO, M., ITOH, M. & TODA, M. 1995. Immunologic self-tolerance maintained by activated T cells expressing IL-2 receptor alpha-chains (CD25). Breakdown of a single mechanism of self-tolerance causes various autoimmune diseases. *J Immunol,* 155**,** 1151-64.

SAKAI, S., KAUFFMAN, K. D., SCHENKEL, J. M., MCBERRY, C. C., MAYER-BARBER, K. D., MASOPUST, D. & BARBER, D. L. 2014a. Cutting edge: control of Mycobacterium tuberculosis infection by a subset of lung parenchyma-homing CD4 T cells. *J Immunol,* 192**,** 2965-9.

SAKAI, S., MAYER-BARBER, K. D. & BARBER, D. L. 2014b. Defining features of protective CD4 T cell responses to Mycobacterium tuberculosis. *Curr Opin Immunol,* 29**,** 137-42.

SAKAMOTO, H., LEE, S., ISHIZUKA, A., HINOSHITA, E., HORI, H., ISHIBASHI, N., KOMADA, K., NORIZUKI, M., KATSUMA, Y., AKASHI, H. & SHIBUYA, K. 2019. Challenges and opportunities for eliminating tuberculosis - leveraging political momentum of the UN high-level meeting on tuberculosis. *BMC Public Health,* 19**,** 76.

SALGUERO, F. J., WHITE, A. D., SLACK, G. S., FOTHERINGHAM, S. A., BEWLEY, K. R., GOOCH, K. E., LONGET, S., HUMPHRIES, H. E., WATSON, R. J., HUNTER, L., RYAN, K. A., HALL, Y., SIBLEY, L., SARFAS, C., ALLEN, L., ARAM, M., BRUNT, E., BROWN, P., BUTTIGIEG, K. R., CAVELL, B. E., COBB, R., COOMBES, N. S., DARBY, A., DAYKIN-PONT, O., ELMORE, M. J., GARCIA-DORIVAL, I., GKOLFINOS, K., GODWIN, K. J., GOURIET, J., HALKERSTON, R., HARRIS, D. J., HENDER, T., HO, C. M. K., KENNARD, C. L., KNOTT, D., LEUNG, S., LUCAS, V., MABBUTT, A., MORRISON, A. L., NELSON, C., NGABO, D., PATERSON, J., PENN, E. J., PULLAN, S., TAYLOR, I., TIPTON, T., THOMAS, S., TREE, J. A., TURNER, C., VAMOS, E., WAND, N., WIBLIN, N. R., CHARLTON, S., DONG, X., HALLIS, B., PEARSON, G., RAYNER, E. L., NICHOLSON, A. G., FUNNELL, S. G., HISCOX, J. A., DENNIS, M. J., GLEESON, F. V., SHARPE, S. & CARROLL, M. W. 2021. Comparison of rhesus and cynomolgus macaques as an infection model for COVID-19. *Nat Commun,* 12**,** 1260.

SALOMONSEN, J., SORENSEN, M. R., MARSTON, D. A., ROGERS, S. L., COLLEN, T., VAN HATEREN, A., SMITH, A. L., BEAL, R. K., SKJODT, K. & KAUFMAN, J. 2005. Two CD1 genes map to the chicken MHC, indicating that CD1 genes are ancient and likely to have been present in the primordial MHC. *Proc Natl Acad Sci U S A,* 102**,** 8668-73.

SANDBERG, J. K., FAST, N. M., PALACIOS, E. H., FENNELLY, G., DOBROSZYCKI, J., PALUMBO, P., WIZNIA, A., GRANT, R. M., BHARDWAJ, N., ROSENBERG, M. G. & NIXON, D. F. 2002. Selective loss of innate CD4(+) V alpha 24 natural killer T cells in human immunodeficiency virus infection. *J Virol,* 76**,** 7528-34.

SANDBERG, J. K., STODDART, C. A., BRILOT, F., JORDAN, K. A. & NIXON, D. F. 2004. Development of innate CD4+ alpha-chain variable gene segment 24 (Valpha24) natural killer T cells in the early human fetal thymus is regulated by IL-7. *Proc Natl Acad Sci U S A,* 101**,** 7058-63.

SANDERS, M. E., MAKGOBA, M. W., SHARROW, S. O., STEPHANY, D., SPRINGER, T. A., YOUNG, H. A. & SHAW, S. 1988. Human memory T lymphocytes express increased levels of three cell adhesion molecules (LFA-3, CD2, and LFA-1) and three other molecules (UCHL1, CDw29, and Pgp-1) and have enhanced IFN-gamma production. *J Immunol,* 140**,** 1401-7.

SANTEGOETS, S. J., GIBBS, S., KROEZE, K., VAN DE VEN, R., SCHEPER, R. J., BORREBAECK, C. A., DE GRUIJL, T. D. & LINDSTEDT, M. 2008. Transcriptional profiling of human skin-resident Langerhans cells and CD1a+ dermal dendritic cells: differential activation states suggest distinct functions. *J Leukoc Biol,* 84**,** 143-51.

SARWAR, N., DANESH, J., EIRIKSDOTTIR, G., SIGURDSSON, G., WAREHAM, N., BINGHAM, S., BOEKHOLDT, S. M., KHAW, K. T. & GUDNASON, V. 2007. Triglycerides and the risk of coronary heart disease: 10,158 incident cases among 262,525 participants in 29 Western prospective studies. *Circulation,* 115**,** 450-8.

SASAGAWA, T., OKITA, M., MURAKAMI, J., KATO, T. & WATANABE, A. 1999. Abnormal serum lysophospholipids in multiple myeloma patients. *Lipids,* 34**,** 17-21.

SASINDRAN, S. J. & TORRELLES, J. B. 2011. Mycobacterium tuberculosis infection and inflammation: what is beneficial for the host and for the bacterium? *Frontiers in microbiology,* 2**,** 2.

SAULE, P., TRAUET, J., DUTRIEZ, V., LEKEUX, V., DESSAINT, J. P. & LABALETTE, M. 2006. Accumulation of memory T cells from childhood to old age: central and effector memory cells in CD4(+) versus effector memory and terminally differentiated memory cells in CD8(+) compartment. *Mech Ageing Dev,* 127**,** 274-81.

SAVAGE, A. K., CONSTANTINIDES, M. G., HAN, J., PICARD, D., MARTIN, E., LI, B., LANTZ, O. & BENDELAC, A. 2008. The transcription factor PLZF directs the effector program of the NKT cell lineage. *Immunity,* 29**,** 391-403.

SCHADE, A. E., SCHIEVEN, G. L., TOWNSEND, R., JANKOWSKA, A. M., SUSULIC, V., ZHANG, R., SZPURKA, H. & MACIEJEWSKI, J. P. 2008. Dasatinib, a small-molecule protein tyrosine kinase inhibitor, inhibits T-cell activation and proliferation. *Blood,* 111**,** 1366-77.

SCHALL, T. J., JONGSTRA, J., DYER, B. J., JORGENSEN, J., CLAYBERGER, C., DAVIS, M. M. & KRENSKY, A. M. 1988. A human T cell-specific molecule is a member of a new gene family. *J Immunol,* 141**,** 1018-25.

SCHARF, L., LI, N. S., HAWK, A. J., GARZON, D., ZHANG, T., FOX, L. M., KAZEN, A. R., SHAH, S., HADDADIAN, E. J., GUMPERZ, J. E., SAGHATELIAN, A., FARALDO-GOMEZ, J. D., MEREDITH, S. C., PICCIRILLI, J. A. & ADAMS, E. J. 2010. The 2.5 A structure of CD1c in complex with a mycobacterial lipid reveals an open groove ideally suited for diverse antigen presentation. *Immunity,* 33**,** 853-62.

SCHATZ, D. G., OETTINGER, M. A. & BALTIMORE, D. 1989. The V(D)J recombination activating gene, RAG-1. *Cell,* 59**,** 1035-48.

SCHIOTT, A., LINDSTEDT, M., JOHANSSON-LINDBOM, B., ROGGEN, E. & BORREBAECK, C. A. 2004. CD27- CD4+ memory T cells define a differentiated memory population at both the functional and transcriptional levels. *Immunology,* 113**,** 363-70.

SCHNEIDER, U., SCHWENK, H. U. & BORNKAMM, G. 1977. Characterization of EBV-genome negative "null" and "T" cell lines derived from children with acute

lymphoblastic leukemia and leukemic transformed non-Hodgkin lymphoma. *Int J Cancer,* 19**,** 621-6.
SCHULTE, H., CULLEN, P. & ASSMANN, G. 1999. Obesity, mortality and cardiovascular disease in the Munster Heart Study (PROCAM). *Atherosclerosis,* 144**,** 199-209.
SCIBIOR, K., ROMANSKA-GOCKA, K., CZAJKOWSKI, R., PLACEK, W. & ZEGARSKA, B. 2019. Expression of CD1a, CD207, CD11b, CD11c, CD103, and HLA-DR receptors on the surface of dendritic cells in the skin of patients with atopic dermatitis. *Postepy Dermatol Alergol,* 36**,** 544-550.
SENESCHAL, J., CLARK, R. A., GEHAD, A., BAECHER-ALLAN, C. M. & KUPPER, T. S. 2012. Human epidermal Langerhans cells maintain immune homeostasis in skin by activating skin resident regulatory T cells. *Immunity,* 36**,** 873-84.
SESHADRI, C., SHENOY, M., WELLS, R. D., HENSLEY-MCBAIN, T., ANDERSEN-NISSEN, E., MCELRATH, M. J., CHENG, T. Y., MOODY, D. B. & HAWN, T. R. 2013. Human CD1a deficiency is common and genetically regulated. *J Immunol,* 191**,** 1586-93.
SESHADRI, C., THUONG, N. T., YEN, N. T., BANG, N. D., CHAU, T. T., THWAITES, G. E., DUNSTAN, S. J. & HAWN, T. R. 2014. A polymorphism in human CD1A is associated with susceptibility to tuberculosis. *Genes Immun,* 15**,** 195-8.
SHAHINE, A., REININK, P., REIJNEVELD, J. F., GRAS, S., HOLZHEIMER, M., CHENG, T. Y., MINNAARD, A. J., ALTMAN, J. D., LENZ, S., PRANDI, J., KUBLER-KIELB, J., MOODY, D. B., ROSSJOHN, J. & VAN RHIJN, I. 2019. A T-cell receptor escape channel allows broad T-cell response to CD1b and membrane phospholipids. *Nat Commun,* 10**,** 56.
SHAMSHIEV, A., DONDA, A., CARENA, I., MORI, L., KAPPOS, L. & DE LIBERO, G. 1999. Self glycolipids as T-cell autoantigens. *Eur J Immunol,* 29**,** 1667-75.
SHAMSHIEV, A., DONDA, A., PRIGOZY, T. I., MORI, L., CHIGORNO, V., BENEDICT, C. A., KAPPOS, L., SONNINO, S., KRONENBERG, M. & DE LIBERO, G. 2000. The alphabeta T cell response to self-glycolipids shows a novel mechanism of CD1b loading and a requirement for complex oligosaccharides. *Immunity,* 13**,** 255-64.
SHAMSHIEV, A., GOBER, H. J., DONDA, A., MAZORRA, Z., MORI, L. & DE LIBERO, G. 2002. Presentation of the same glycolipid by different CD1 molecules. *J Exp Med,* 195**,** 1013-21.
SHARPE, S. A., WHITE, A. D., SIBLEY, L., GLEESON, F., HALL, G. A., BASARABA, R. J., MCINTYRE, A., CLARK, S. O., GOOCH, K., MARSH, P. D., WILLIAMS, A. & DENNIS, M. J. 2017. An aerosol challenge model of tuberculosis in Mauritian cynomolgus macaques. *PLoS One,* 12**,** e0171906.
SHAULIAN, E. & KARIN, M. 2002. AP-1 as a regulator of cell life and death. *Nat Cell Biol,* 4**,** E131-6.
SHI, Y., CHEN, L., LIOTTA, L. A., WAN, H. H. & RODGERS, G. P. 2006. Glia maturation factor gamma (GMFG): a cytokine-responsive protein during hematopoietic lineage development and its functional genomics analysis. *Genomics Proteomics Bioinformatics,* 4**,** 145-55.
SIELING, P. A., JULLIEN, D., DAHLEM, M., TEDDER, T. F., REA, T. H., MODLIN, R. L. & PORCELLI, S. A. 1999. CD1 Expression by Dendritic Cells

in Human Leprosy Lesions: Correlation with Effective Host Immunity. *The Journal of Immunology,* 162**,** 1851-1858.
SIELING, P. A., PORCELLI, S. A., DUONG, B. T., SPADA, F., BLOOM, B. R., DIAMOND, B. & HAHN, B. H. 2000. Human double-negative T cells in systemic lupus erythematosus provide help for IgG and are restricted by CD1c. *J Immunol,* 165**,** 5338-44.
SIMONI, Y., DIANA, J., GHAZARIAN, L., BEAUDOIN, L. & LEHUEN, A. 2013. Therapeutic manipulation of natural killer (NK) T cells in autoimmunity: are we close to reality? *Clin Exp Immunol,* 171**,** 8-19.
SIMS, J. E., TUNNACLIFFE, A., SMITH, W. J. & RABBITTS, T. H. 1984. Complexity of human T-cell antigen receptor beta-chain constant- and variable-region genes. *Nature,* 312**,** 541-5.
SKAPER, S. D., FACCI, L., ZUSSO, M. & GIUSTI, P. 2018. An Inflammation-Centric View of Neurological Disease: Beyond the Neuron. *Front Cell Neurosci,* 12**,** 72.
SMALLEY, I. & SMALLEY, K. S. M. 2018. ERK Inhibition: A New Front in the War against MAPK Pathway-Driven Cancers? *Cancer Discov,* 8**,** 140-142.
SMYTH, M. J., CROWE, N. Y., PELLICCI, D. G., KYPARISSOUDIS, K., KELLY, J. M., TAKEDA, K., YAGITA, H. & GODFREY, D. I. 2002. Sequential production of interferon-gamma by NK1.1(+) T cells and natural killer cells is essential for the antimetastatic effect of alpha-galactosylceramide. *Blood,* 99**,** 1259-66.
SNOW, G. A. & WHITE, A. J. 1969. Chemical and biological properties of mycobactins isolated from various mycobacteria. *Biochem J,* 115**,** 1031-50.
SOLER, P., MOREAU, A., BASSET, F. & HANCE, A. J. 1989. Cigarette smoking-induced changes in the number and differentiated state of pulmonary dendritic cells/Langerhans cells. *Am Rev Respir Dis,* 139**,** 1112-7.
SOMNAY-WADGAONKAR, K., NUSRAT, A., KIM, H. S., CANCHIS, W. P., BALK, S. P., COLGAN, S. P. & BLUMBERG, R. S. 1999. Immunolocalization of CD1d in human intestinal epithelial cells and identification of a beta2-microglobulin-associated form. *Int Immunol,* 11**,** 383-92.
SOTZIK, F., BOYD, A. & SHORTMAN, K. 1993. Surface antigens of human thymocyte populations defined by CD3, CD4 and CD8 expression: CD1a is expressed by mature thymocytes but not peripheral T cells. *Immunol Lett,* 36**,** 101-6.
SOURDIVE, D. J., MURALI-KRISHNA, K., ALTMAN, J. D., ZAJAC, A. J., WHITMIRE, J. K., PANNETIER, C., KOURILSKY, P., EVAVOLD, B., SETTE, A. & AHMED, R. 1998. Conserved T cell receptor repertoire in primary and memory CD8 T cell responses to an acute viral infection. *J Exp Med,* 188**,** 71-82.
SPADA, F. M., GRANT, E. P., PETERS, P. J., SUGITA, M., MELIAN, A., LESLIE, D. S., LEE, H. K., VAN DONSELAAR, E., HANSON, D. A., KRENSKY, A. M., MAJDIC, O., PORCELLI, S. A., MORITA, C. T. & BRENNER, M. B. 2000. Self-recognition of CD1 by gamma/delta T cells: implications for innate immunity. *J Exp Med,* 191**,** 937-48.
SRIBENJA, S., LI, M., WONGKHAM, S., WONGKHAM, C., YAO, Q. & CHEN, C. 2009. Advances in thymosin beta10 research: differential expression, molecular mechanisms, and clinical implications in cancer and other conditions. *Cancer Invest,* 27**,** 1016-22.
STAX, A. M., TUENGEL, J., GIRARDI, E., KITANO, N., ALLAN, L. L., LIU, V., ZHENG, D., PANENKA, W. J., GUILLAUME, J., WONG, C. H., VAN

CALENBERGH, S., ZAJONC, D. M. & VAN DEN ELZEN, P. 2017. Autoreactivity to Sulfatide by Human Invariant NKT Cells. *J Immunol,* 199**,** 97-106.

STENGER, S., HANSON, D. A., TEITELBAUM, R., DEWAN, P., NIAZI, K. R., FROELICH, C. J., GANZ, T., THOMA-USZYNSKI, S., MELIAN, A., BOGDAN, C., PORCELLI, S. A., BLOOM, B. R., KRENSKY, A. M. & MODLIN, R. L. 1998. An antimicrobial activity of cytolytic T cells mediated by granulysin. *Science,* 282**,** 121-5.

STENGER, S., MAZZACCARO, R. J., UYEMURA, K., CHO, S., BARNES, P. F., ROSAT, J. P., SETTE, A., BRENNER, M. B., PORCELLI, S. A., BLOOM, B. R. & MODLIN, R. L. 1997. Differential effects of cytolytic T cell subsets on intracellular infection. *Science,* 276**,** 1684-7.

STERN, N. & TIETZ, A. 1973. Glycolipids of a halotolerant, moderately halophilic bacterium. II. Biosynthesis of glucuronosyldiglyceride by cell-free particles. *Biochim Biophys Acta,* 296**,** 136-44.

STEWART, C. R., STUART, L. M., WILKINSON, K., VAN GILS, J. M., DENG, J., HALLE, A., RAYNER, K. J., BOYER, L., ZHONG, R., FRAZIER, W. A., LACY-HULBERT, A., EL KHOURY, J., GOLENBOCK, D. T. & MOORE, K. J. 2010. CD36 ligands promote sterile inflammation through assembly of a Toll-like receptor 4 and 6 heterodimer. *Nat Immunol,* 11**,** 155-61.

STORKUS, W. J., ALEXANDER, J., PAYNE, J. A., DAWSON, J. R. & CRESSWELL, P. 1989. Reversal of natural killing susceptibility in target cells expressing transfected class I HLA genes. *Proc Natl Acad Sci U S A,* 86**,** 2361-4.

STRID, J., TIGELAAR, R. E. & HAYDAY, A. C. 2009. Skin immune surveillance by T cells--a new order? *Semin Immunol,* 21**,** 110-20.

STROMINGER, J. L. 2010. An alternative path for antigen presentation: group 1 CD1 proteins. *J Immunol,* 184**,** 3303-5.

SUBLESKI, J. J., JIANG, Q., WEISS, J. M. & WILTROUT, R. H. 2011. The split personality of NKT cells in malignancy, autoimmune and allergic disorders. *Immunotherapy,* 3**,** 1167-84.

SUBRAMANIAM, S., ASLAM, A., MISBAH, S. A., SALIO, M., CERUNDOLO, V., MOODY, D. B. & OGG, G. 2016. Elevated and cross-responsive CD1a-reactive T cells in bee and wasp venom allergic individuals. *Eur J Immunol,* 46**,** 242-52.

SUGITA, M., GRANT, E. P., VAN DONSELAAR, E., HSU, V. W., ROGERS, R. A., PETERS, P. J. & BRENNER, M. B. 1999. Separate pathways for antigen presentation by CD1 molecules. *Immunity,* 11**,** 743-52.

SUN, H., CHARLES, C. H., LAU, L. F. & TONKS, N. K. 1993. MKP-1 (3CH134), an immediate early gene product, is a dual specificity phosphatase that dephosphorylates MAP kinase in vivo. *Cell,* 75**,** 487-93.

SURH, C. D. & SPRENT, J. 1994. T-cell apoptosis detected in situ during positive and negative selection in the thymus. *Nature,* 372**,** 100-3.

SWAIN, S. L., CROFT, M., DUBEY, C., HAYNES, L., ROGERS, P., ZHANG, X. & BRADLEY, L. M. 1996. From naive to memory T cells. *Immunol Rev,* 150**,** 143-67.

SZYMCZAK, A. L., WORKMAN, C. J., WANG, Y., VIGNALI, K. M., DILIOGLOU, S., VANIN, E. F. & VIGNALI, D. A. 2004. Correction of multi-gene deficiency in vivo using a single 'self-cleaving' 2A peptide-based retroviral vector. *Nat Biotechnol,* 22**,** 589-94.

TAHERI, M., DANESH, H., BIZHANI, F., BAHARI, G., NADERI, M. & HASHEMI, M. 2019. Association between genetic variants in CD1A and CD1D genes and pulmonary tuberculosis in an Iranian population. *Biomed Rep,* 10**,** 259-265.

TAI, A. Y. C., ATHAN, E., FRIEDMAN, N. D., HUGHES, A., WALTON, A. & O'BRIEN, D. P. 2018. Increased Severity and Spread of Mycobacterium ulcerans, Southeastern Australia. *Emerg Infect Dis,* 24.

TAKAHASHI, T., CHIBA, S., NIEDA, M., AZUMA, T., ISHIHARA, S., SHIBATA, Y., JUJI, T. & HIRAI, H. 2002. Cutting edge: analysis of human V alpha 24+CD8+ NK T cells activated by alpha-galactosylceramide-pulsed monocyte-derived dendritic cells. *J Immunol,* 168**,** 3140-4.

TARD, C., ROUXEL, O. & LEHUEN, A. 2015. Regulatory Role of Natural Killer T Cells in Diabetes. *Biomed J*.

TATITURI, R. V., WATTS, G. F., BHOWRUTH, V., BARTON, N., ROTHCHILD, A., HSU, F. F., ALMEIDA, C. F., COX, L. R., EGGELING, L., CARDELL, S., ROSSJOHN, J., GODFREY, D. I., BEHAR, S. M., BESRA, G. S., BRENNER, M. B. & BRIGL, M. 2013. Recognition of microbial and mammalian phospholipid antigens by NKT cells with diverse TCRs. *Proc Natl Acad Sci U S A,* 110**,** 1827-32.

TATITURI, R. V. V., ILLARIONOV, P. A., DOVER, L. G., NIGOU, J., GILLERON, M., HITCHEN, P., KRUMBACH, K., MORRIS, H. R., SPENCER, N., DELL, A., EGGELING, L. & BESRA, G. S. 2007. Inactivation of Corynebacterium glutamicum NCgl0452 and the role of MgtA in the biosynthesis of a novel mannosylated glycolipid involved in lipomannan biosynthesis. *J Biol Chem,* 282**,** 4561-4572.

TAZI, A., BONAY, M., GRANDSAIGNE, M., BATTESTI, J. P., HANCE, A. J. & SOLER, P. 1993a. Surface phenotype of Langerhans cells and lymphocytes in granulomatous lesions from patients with pulmonary histiocytosis X. *Am Rev Respir Dis,* 147**,** 1531-6.

TAZI, A., BOUCHONNET, F., GRANDSAIGNE, M., BOUMSELL, L., HANCE, A. J. & SOLER, P. 1993b. Evidence that granulocyte macrophage-colony-stimulating factor regulates the distribution and differentiated state of dendritic cells/Langerhans cells in human lung and lung cancers. *J Clin Invest,* 91**,** 566-76.

TEGLA, C. A., CUDRICI, C. D., NGUYEN, V., DANOFF, J., KRUSZEWSKI, A. M., BOODHOO, D., MEKALA, A. P., VLAICU, S. I., CHEN, C., RUS, V., BADEA, T. C. & RUS, H. 2015. RGC-32 is a novel regulator of the T-lymphocyte cell cycle. *Exp Mol Pathol,* 98**,** 328-37.

TERABE, M. & BERZOFSKY, J. A. 2008. The role of NKT cells in tumor immunity. *Adv Cancer Res,* 101**,** 277-348.

TESTI, R., PHILLIPS, J. H. & LANIER, L. L. 1989. T cell activation via Leu-23 (CD69). *J Immunol,* 143**,** 1123-8.

TEUNISSEN, M. B. M., YEREMENKO, N. G., BAETEN, D. L. P., CHIELIE, S., SPULS, P. I., DE RIE, M. A., LANTZ, O. & RES, P. C. M. 2014. The IL-17A-producing CD8+ T-cell population in psoriatic lesional skin comprises mucosa-associated invariant T cells and conventional T cells. *J Invest Dermatol,* 134**,** 2898-2907.

THEDREZ, A., DE LALLA, C., ALLAIN, S., ZACCAGNINO, L., SIDOBRE, S., GARAVAGLIA, C., BORSELLINO, G., DELLABONA, P., BONNEVILLE, M., SCOTET, E. & CASORATI, G. 2007. CD4 engagement by CD1d potentiates activation of CD4+ invariant NKT cells. *Blood,* 110**,** 251-8.

THIPPESHAPPA, R., KIMATA, J. T. & KAUSHAL, D. 2020. Toward a Macaque Model of HIV-1 Infection: Roadblocks, Progress, and Future Strategies. *Front Microbiol,* 11**,** 882.

THOMAS, S. Y., HOU, R., BOYSON, J. E., MEANS, T. K., HESS, C., OLSON, D. P., STROMINGER, J. L., BRENNER, M. B., GUMPERZ, J. E., WILSON, S. B. & LUSTER, A. D. 2003. CD1d-restricted NKT cells express a chemokine receptor profile indicative of Th1-type inflammatory homing cells. *J Immunol,* 171**,** 2571-80.

THOME, J. J., YUDANIN, N., OHMURA, Y., KUBOTA, M., GRINSHPUN, B., SATHALIYAWALA, T., KATO, T., LERNER, H., SHEN, Y. & FARBER, D. L. 2014. Spatial map of human T cell compartmentalization and maintenance over decades of life. *Cell,* 159**,** 814-28.

THORSBY, E. & RONNINGEN, K. S. 1993. Particular HLA-DQ molecules play a dominant role in determining susceptibility or resistance to type 1 (insulin-dependent) diabetes mellitus. *Diabetologia,* 36**,** 371-7.

TILLOY, F., TREINER, E., PARK, S. H., GARCIA, C., LEMONNIER, F., DE LA SALLE, H., BENDELAC, A., BONNEVILLE, M. & LANTZ, O. 1999. An invariant T cell receptor alpha chain defines a novel TAP-independent major histocompatibility complex class Ib-restricted alpha/beta T cell subpopulation in mammals. *J Exp Med,* 189**,** 1907-21.

TOHN, R., BLUMENFELD, H., HAERYFAR, S. M., VEERAPEN, N., BESRA, G. S., PORCELLI, S. A. & DELOVITCH, T. L. 2011. Stimulation of a shorter duration in the state of anergy by an invariant natural killer T cell agonist enhances its efficiency of protection from type 1 diabetes. *Clin Exp Immunol,* 164**,** 26-41.

TORINA, A., GUGGINO, G., LA MANNA, M. P. & SIRECI, G. 2018. The Janus Face of NKT Cell Function in Autoimmunity and Infectious Diseases. *Int J Mol Sci,* 19.

TRATTNER, A., SLODOWNIK, D., JBARAH, A. & INGBER, A. 2009. Questionnaire study of the prevalence of allergic contact dermatitis from cosmetics in Israel. *Dermatitis,* 20**,** 284-6.

TREINER, E., DUBAN, L., BAHRAM, S., RADOSAVLJEVIC, M., WANNER, V., TILLOY, F., AFFATICATI, P., GILFILLAN, S. & LANTZ, O. 2003. Selection of evolutionarily conserved mucosal-associated invariant T cells by MR1. *Nature,* 422**,** 164-9.

TREINER, E., DUBAN, L., MOURA, I. C., HANSEN, T., GILFILLAN, S. & LANTZ, O. 2005. Mucosal-associated invariant T (MAIT) cells: an evolutionarily conserved T cell subset. *Microbes Infect,* 7**,** 552-9.

TRIFARI, S., KAPLAN, C. D., TRAN, E. H., CRELLIN, N. K. & SPITS, H. 2009. Identification of a human helper T cell population that has abundant production of interleukin 22 and is distinct from T(H)-17, T(H)1 and T(H)2 cells. *Nat Immunol,* 10**,** 864-71.

TROWSDALE, J. 2011. The MHC, disease and selection. *Immunol Lett,* 137**,** 1-8.

TUBO, N. J., MCLACHLAN, J. B. & CAMPBELL, J. J. 2011. Chemokine receptor requirements for epidermal T-cell trafficking. *Am J Pathol,* 178**,** 2496-503.

TUNNACLIFFE, A., KEFFORD, R., MILSTEIN, C., FORSTER, A. & RABBITTS, T. H. 1985. Sequence and evolution of the human T-cell antigen receptor beta-chain genes. *Proc Natl Acad Sci U S A,* 82**,** 5068-72.

TURNER, S. J., DIAZ, G., CROSS, R. & DOHERTY, P. C. 2003. Analysis of clonotype distribution and persistence for an influenza virus-specific CD8+ T cell response. *Immunity,* 18**,** 549-59.
TURNER, S. J., DOHERTY, P. C., MCCLUSKEY, J. & ROSSJOHN, J. 2006. Structural determinants of T-cell receptor bias in immunity. *Nat Rev Immunol,* 6**,** 883-94.
UCHE, U. U., PICCIRILLO, A. R., KATAOKA, S., GREBINOSKI, S. J., D'CRUZ, L. M. & KANE, L. P. 2018. PIK3IP1/TrIP restricts activation of T cells through inhibition of PI3K/Akt. *J Exp Med,* 215**,** 3165-3179.
UHLEN, M., FAGERBERG, L., HALLSTROM, B. M., LINDSKOG, C., OKSVOLD, P., MARDINOGLU, A., SIVERTSSON, A., KAMPF, C., SJOSTEDT, E., ASPLUND, A., OLSSON, I., EDLUND, K., LUNDBERG, E., NAVANI, S., SZIGYARTO, C. A., ODEBERG, J., DJUREINOVIC, D., TAKANEN, J. O., HOBER, S., ALM, T., EDQVIST, P. H., BERLING, H., TEGEL, H., MULDER, J., ROCKBERG, J., NILSSON, P., SCHWENK, J. M., HAMSTEN, M., VON FEILITZEN, K., FORSBERG, M., PERSSON, L., JOHANSSON, F., ZWAHLEN, M., VON HEIJNE, G., NIELSEN, J. & PONTEN, F. 2015. Proteomics. Tissue-based map of the human proteome. *Science,* 347**,** 1260419.
ULDRICH, A. P., LE NOURS, J., PELLICCI, D. G., GHERARDIN, N. A., MCPHERSON, K. G., LIM, R. T., PATEL, O., BEDDOE, T., GRAS, S., ROSSJOHN, J. & GODFREY, D. I. 2013. CD1d-lipid antigen recognition by the gammadelta TCR. *Nat Immunol,* 14**,** 1137-45.
ULRICHS, T., MOODY, D. B., GRANT, E., KAUFMANN, S. H. & PORCELLI, S. A. 2003. T-cell responses to CD1-presented lipid antigens in humans with Mycobacterium tuberculosis infection. *Infect Immun,* 71**,** 3076-87.
UNUTMAZ, D., KEWALRAMANI, V. N. & LITTMAN, D. R. 1998. G protein-coupled receptors in HIV and SIV entry: new perspectives on lentivirus-host interactions and on the utility of animal models. *Semin Immunol,* 10**,** 225-36.
USSHER, J. E., BILTON, M., ATTWOD, E., SHADWELL, J., RICHARDSON, R., DE LARA, C., METTKE, E., KURIOKA, A., HANSEN, T. H., KLENERMAN, P. & WILLBERG, C. B. 2014. CD161++ CD8+ T cells, including the MAIT cell subset, are specifically activated by IL-12+IL-18 in a TCR-independent manner. *Eur J Immunol,* 44**,** 195-203.
VAN BLOKLAND, S. C., WIERENGA-WOLF, A. F., VAN HELDEN-MEEUWSEN, C. G., DREXHAGE, H. A., HOOIJKAAS, H., VAN DE MERWE, J. P. & VERSNEL, M. A. 2000. Professional antigen presenting cells in minor salivary glands in Sjogren's syndrome: potential contribution to the histopathological diagnosis? *Lab Invest,* 80**,** 1935-41.
VAN DE BERG, P. J., HOEVENAARS, E. C., YONG, S. L., VAN DONSELAAR-VAN DER PANT, K. A., VAN TELLINGEN, A., FLORQUIN, S., VAN LIER, R. A., BEMELMAN, F. J. & TEN BERGE, I. J. 2012. Circulating lymphocyte subsets in different clinical situations after renal transplantation. *Immunology,* 136**,** 198-207.
VAN DER VLIET, H. J., NISHI, N., DE GRUIJL, T. D., VON BLOMBERG, B. M., VAN DEN EERTWEGH, A. J., PINEDO, H. M., GIACCONE, G. & SCHEPER, R. J. 2000. Human natural killer T cells acquire a memory-activated phenotype before birth. *Blood,* 95**,** 2440-2.
VAN DER VLIET, H. J., VON BLOMBERG, B. M., HAZENBERG, M. D., NISHI, N., OTTO, S. A., VAN BENTHEM, B. H., PRINS, M., CLAESSEN, F. A., VAN DEN EERTWEGH, A. J., GIACCONE, G., MIEDEMA, F., SCHEPER,

R. J. & PINEDO, H. M. 2002. Selective decrease in circulating V alpha 24+V beta 11+ NKT cells during HIV type 1 infection. *J Immunol,* 168**,** 1490-5.
VAN DER VLIET, H. J., VON BLOMBERG, B. M., NISHI, N., REIJM, M., VOSKUYL, A. E., VAN BODEGRAVEN, A. A., POLMAN, C. H., RUSTEMEYER, T., LIPS, P., VAN DEN EERTWEGH, A. J., GIACCONE, G., SCHEPER, R. J. & PINEDO, H. M. 2001. Circulating V(alpha24+) Vbeta11+ NKT cell numbers are decreased in a wide variety of diseases that are characterized by autoreactive tissue damage. *Clin Immunol,* 100**,** 144-8.
VAN GENT, R., VAN TILBURG, C. M., NIBBELKE, E. E., OTTO, S. A., GAISER, J. F., JANSSENS-KORPELA, P. L., SANDERS, E. A., BORGHANS, J. A., WULFFRAAT, N. M., BIERINGS, M. B., BLOEM, A. C. & TESSELAAR, K. 2009. Refined characterization and reference values of the pediatric T- and B-cell compartments. *Clin Immunol,* 133**,** 95-107.
VAN KAER, L. & JOYCE, S. 2010. The hunt for iNKT cell antigens: alpha-galactosidase-deficient mice to the rescue? *Immunity,* 33**,** 143-5.
VAN KAER, L., PAREKH, V. V. & WU, L. 2015a. The Response of CD1d-Restricted Invariant NKT Cells to Microbial Pathogens and Their Products. *Front Immunol,* 6**,** 226.
VAN KAER, L. & WU, L. 2018. Therapeutic Potential of Invariant Natural Killer T Cells in Autoimmunity. *Front Immunol,* 9**,** 519.
VAN KAER, L., WU, L. & PAREKH, V. V. 2015b. Natural killer T cells in multiple sclerosis and its animal model, experimental autoimmune encephalomyelitis. *Immunology,* 146**,** 1-10.
VAN PUIJVELDE, G. H. M. & KUIPER, J. 2017. NKT cells in cardiovascular diseases. *Eur J Pharmacol,* 816**,** 47-57.
VAN RHIJN, I., GHERARDIN, N. A., KASMAR, A., DE JAGER, W., PELLICCI, D. G., KOSTENKO, L., TAN, L. L., BHATI, M., GRAS, S., GODFREY, D. I., ROSSJOHN, J. & MOODY, D. B. 2014. TCR bias and affinity define two compartments of the CD1b-glycolipid-specific T Cell repertoire. *J Immunol,* 192**,** 4054-60.
VAN RHIJN, I., KASMAR, A., DE JONG, A., GRAS, S., BHATI, M., DOORENSPLEET, M. E., DE VRIES, N., GODFREY, D. I., ALTMAN, J. D., DE JAGER, W., ROSSJOHN, J. & MOODY, D. B. 2013a. A conserved human T cell population targets mycobacterial antigens presented by CD1b. *Nat Immunol,* 14**,** 706-13.
VAN RHIJN, I., KOETS, A. P., IM, J. S., PIEBES, D., REDDINGTON, F., BESRA, G. S., PORCELLI, S. A., VAN EDEN, W. & RUTTEN, V. P. 2006. The bovine CD1 family contains group 1 CD1 proteins, but no functional CD1d. *J Immunol,* 176**,** 4888-93.
VAN RHIJN, I., LY, D. & MOODY, D. B. 2013b. CD1a, CD1b, and CD1c in immunity against mycobacteria. *Adv Exp Med Biol,* 783**,** 181-97.
VAN RHIJN, I. & MOODY, D. B. 2015. CD1 and mycobacterial lipids activate human T cells. *Immunol Rev,* 264**,** 138-53.
VAN RHIJN, I., NGUYEN, T. K., MICHEL, A., COOPER, D., GOVAERTS, M., CHENG, T. Y., VAN EDEN, W., MOODY, D. B., COETZER, J. A., RUTTEN, V. & KOETS, A. P. 2009. Low cross-reactivity of T-cell responses against lipids from Mycobacterium bovis and M. avium paratuberculosis during natural infection. *Eur J Immunol,* 39**,** 3031-41.
VAN SMEDEN, J., JANSSENS, M., KAYE, E. C., CASPERS, P. J., LAVRIJSEN, A. P., VREEKEN, R. J. & BOUWSTRA, J. A. 2014. The importance of free fatty

acid chain length for the skin barrier function in atopic eczema patients. *Exp Dermatol,* 23**,** 45-52.
VELDHOEN, M., HIROTA, K., CHRISTENSEN, J., O'GARRA, A. & STOCKINGER, B. 2009. Natural agonists for aryl hydrocarbon receptor in culture medium are essential for optimal differentiation of Th17 T cells. *J Exp Med,* 206**,** 43-9.
VENKEN, K., DECRUY, T., ASPESLAGH, S., VAN CALENBERGH, S., LAMBRECHT, B. N. & ELEWAUT, D. 2013. Bacterial CD1d-restricted glycolipids induce IL-10 production by human regulatory T cells upon cross-talk with invariant NKT cells. *J Immunol,* 191**,** 2174-83.
VENKEN, K., SEEUWS, S., ZABEAU, L., JACQUES, P., DECRUY, T., COUDENYS, J., VERHEUGEN, E., WINDELS, F., CATTEEUW, D., DRENNAN, M., VAN CALENBERGH, S., LAMBRECHT, B. N., YOSHIMURA, A., TAVERNIER, J. & ELEWAUT, D. 2014. A bidirectional crosstalk between iNKT cells and adipocytes mediated by leptin modulates susceptibility for T cell mediated hepatitis. *J Hepatol,* 60**,** 175-82.
VESIKARI, T., GROTH, N., KARVONEN, A., BORKOWSKI, A. & PELLEGRINI, M. 2009. MF59-adjuvanted influenza vaccine (FLUAD) in children: safety and immunogenicity following a second year seasonal vaccination. *Vaccine,* 27**,** 6291-5.
VESIKARI, T., KNUF, M., WUTZLER, P., KARVONEN, A., KIENINGER-BAUM, D., SCHMITT, H. J., BAEHNER, F., BORKOWSKI, A., TSAI, T. F. & CLEMENS, R. 2011. Oil-in-water emulsion adjuvant with influenza vaccine in young children. *N Engl J Med,* 365**,** 1406-16.
VINCENT, M. S., LESLIE, D. S., GUMPERZ, J. E., XIONG, X., GRANT, E. P. & BRENNER, M. B. 2002. CD1-dependent dendritic cell instruction. *Nat Immunol,* 3**,** 1163-8.
VINCENT, M. S., XIONG, X., GRANT, E. P., PENG, W. & BRENNER, M. B. 2005. CD1a-, b-, and c-Restricted TCRs Recognize Both Self and Foreign Antigens. *The Journal of Immunology,* 175**,** 6344-6351.
VIVIER, E., UGOLINI, S., BLAISE, D., CHABANNON, C. & BROSSAY, L. 2012. Targeting natural killer cells and natural killer T cells in cancer. *Nat Rev Immunol,* 12**,** 239-52.
VOCANSON, M., HENNINO, A., ROZIERES, A., POYET, G. & NICOLAS, J. F. 2009. Effector and regulatory mechanisms in allergic contact dermatitis. *Allergy,* 64**,** 1699-714.
VOILLET, V., BUGGERT, M., SLICHTER, C. K., BERKSON, J. D., MAIR, F., ADDISON, M. M., DORI, Y., NADOLSKI, G., ITKIN, M. G., GOTTARDO, R., BETTS, M. R. & PRLIC, M. 2018. Human MAIT cells exit peripheral tissues and recirculate via lymph in steady state conditions. *JCI Insight,* 3.
VON STEBUT, E., BOEHNCKE, W. H., GHORESCHI, K., GORI, T., KAYA, Z., THACI, D. & SCHAFFLER, A. 2019. IL-17A in Psoriasis and Beyond: Cardiovascular and Metabolic Implications. *Front Immunol,* 10**,** 3096.
VYNNYCKY, E. & FINE, P. E. 2000. Lifetime risks, incubation period, and serial interval of tuberculosis. *Am J Epidemiol,* 152**,** 247-63.
WAKABAYASHI, T., HU, D. L., TAGAWA, Y., SEKIKAWA, K., IWAKURA, Y., HANADA, K. & NAKANE, A. 2005. IFN-gamma and TNF-alpha are involved in urushiol-induced contact hypersensitivity in mice. *Immunol Cell Biol,* 83**,** 18-24.

WALKER, L. S. & ABBAS, A. K. 2002. The enemy within: keeping self-reactive T cells at bay in the periphery. *Nat Rev Immunol,* 2**,** 11-9.
WALTON, L. J., MACEY, M. G., THORNHILL, M. H. & FARTHING, P. M. 1998. Intra-epithelial subpopulations of T lymphocytes and Langerhans cells in oral lichen planus. *J Oral Pathol Med,* 27**,** 116-23.
WANG, C. Y., YU, P. F., HE, X. B., FANG, Y. X., CHENG, W. Y. & JING, Z. Z. 2016. alphabeta T-cell receptor bias in disease and therapy (Review). *Int J Oncol,* 48**,** 2247-56.
WANG, F., ONO, T., KALERGIS, A. M., ZHANG, W., DILORENZO, T. P., LIM, K. & NATHENSON, S. G. 1998. On defining the rules for interactions between the T cell receptor and its ligand: a critical role for a specific amino acid residue of the T cell receptor beta chain. *Proc Natl Acad Sci U S A,* 95**,** 5217-22.
WANG, G. C., DASH, P., MCCULLERS, J. A., DOHERTY, P. C. & THOMAS, P. G. 2012. T cell receptor alphabeta diversity inversely correlates with pathogen-specific antibody levels in human cytomegalovirus infection. *Sci Transl Med,* 4**,** 128ra42.
WANG, Y., CHEN, B., LI, Y., ZHOU, D. & CHEN, S. 2011. PNRC accumulates in the nucleolus by interaction with B23/nucleophosmin via its nucleolar localization sequence. *Biochim Biophys Acta,* 1813**,** 109-19.
WATANABE, Y., WATARI, E., MATSUNAGA, I., HIROMATSU, K., DASCHER, C. C., KAWASHIMA, T., NOROSE, Y., SHIMIZU, K., TAKAHASHI, H., YANO, I. & SUGITA, M. 2006. BCG vaccine elicits both T-cell mediated and humoral immune responses directed against mycobacterial lipid components. *Vaccine,* 24**,** 5700-7.
WEAVER, T. A., CHARAFEDDINE, A. H., AGARWAL, A., TURNER, A. P., RUSSELL, M., LEOPARDI, F. V., KAMPEN, R. L., STEMPORA, L., SONG, M., LARSEN, C. P. & KIRK, A. D. 2009. Alefacept promotes co-stimulation blockade based allograft survival in nonhuman primates. *Nat Med,* 15**,** 746-9.
WEGRECKI, M., OCAMPO, T. A., GUNASINGHE, S. D., VON BORSTEL, A., TIN, S. Y., REIJNEVELD, J. F., CAO, T. P., GULLY, B. S., LE NOURS, J., MOODY, D. B., VAN RHIJN, I. & ROSSJOHN, J. 2022. Atypical sideways recognition of CD1a by autoreactive gammadelta T cell receptors. *Nat Commun,* 13**,** 3872.
WERBROUCK, J., LAMBRECHT, C. & GOOSSENS, A. 2015. C12-15 alkyl benzoate: a new cosmetic allergen? *Contact Dermatitis,* 73**,** 249-50.
WESLEY, J. D., TESSMER, M. S., CHAUKOS, D. & BROSSAY, L. 2008. NK cell-like behavior of Valpha14i NK T cells during MCMV infection. *PLoS Pathog,* 4**,** e1000106.
WEST, J. A., OLSEN, S. L., MITCHELL, J. M., PRIDDLE, R. E., LUKE, J. M., AKEFELDT, S. O., HENTER, J. I., TURVILLE, C. & KANNOURAKIS, G. 2014. Polyclonal T-cells express CD1a in Langerhans cell histiocytosis (LCH) lesions. *PLoS One,* 9**,** e109586.
WIELAND BROWN, L. C., PENARANDA, C., KASHYAP, P. C., WILLIAMS, B. B., CLARDY, J., KRONENBERG, M., SONNENBURG, J. L., COMSTOCK, L. E., BLUESTONE, J. A. & FISCHBACH, M. A. 2013. Production of alpha-galactosylceramide by a prominent member of the human gut microbiota. *PLoS Biol,* 11**,** e1001610.
WIKBY, A., MANSSON, I. A., JOHANSSON, B., STRINDHALL, J. & NILSSON, S. E. 2008. The immune risk profile is associated with age and gender: findings

from three Swedish population studies of individuals 20-100 years of age. *Biogerontology,* 9**,** 299-308.
WILKINS, A. L., KAZMIN, D., NAPOLITANI, G., CLUTTERBUCK, E. A., PULENDRAN, B., SIEGRIST, C. A. & POLLARD, A. J. 2017. AS03- and MF59-Adjuvanted Influenza Vaccines in Children. *Front Immunol,* 8**,** 1760.
WILKINSON, S. G. 1968. Glycolipids containing glucose and uronic acids in Pseudomonas species. *Biochim Biophys Acta,* 152**,** 227-9.
WILKINSON, S. G. 1969. Lipids of Pseudomonas diminuta. *Biochim Biophys Acta,* 187**,** 492-500.
WILLIAMS, A., PEH, C. A. & ELLIOTT, T. 2002. The cell biology of MHC class I antigen presentation. *Tissue Antigens,* 59**,** 3-17.
WOLF, A. J., DESVIGNES, L., LINAS, B., BANAIEE, N., TAMURA, T., TAKATSU, K. & ERNST, J. D. 2008. Initiation of the adaptive immune response to Mycobacterium tuberculosis depends on antigen production in the local lymph node, not the lungs. *The Journal of experimental medicine,* 205**,** 105-115.
WOLF, B. J., TATITURI, R. V., ALMEIDA, C. F., LE NOURS, J., BHOWRUTH, V., JOHNSON, D., ULDRICH, A. P., HSU, F. F., BRIGL, M., BESRA, G. S., ROSSJOHN, J., GODFREY, D. I. & BRENNER, M. B. 2015. Identification of a Potent Microbial Lipid Antigen for Diverse NKT Cells. *J Immunol,* 195**,** 2540-51.
WOLF, R., ORION, E., RUOCCO, E., BARONI, A. & RUOCCO, V. 2013. Contact dermatitis: facts and controversies. *Clin Dermatol,* 31**,** 467-478.
WOLK, K., KUNZ, S., WITTE, E., FRIEDRICH, M., ASADULLAH, K. & SABAT, R. 2004. IL-22 increases the innate immunity of tissues. *Immunity,* 21**,** 241-54.
WOLK, K. & SABAT, R. 2006. Interleukin-22: a novel T- and NK-cell derived cytokine that regulates the biology of tissue cells. *Cytokine Growth Factor Rev,* 17**,** 367-80.
WOLLENBERG, A., KRAFT, S., HANAU, D. & BIEBER, T. 1996. Immunomorphological and ultrastructural characterization of Langerhans cells and a novel, inflammatory dendritic epidermal cell (IDEC) population in lesional skin of atopic eczema. *J Invest Dermatol,* 106**,** 446-53.
WOLOSIK, K., KNAS, M., ZALEWSKA, A., NICZYPORUK, M. & PRZYSTUPA, A. W. 2013. The importance and perspective of plant-based squalene in cosmetology. *J Cosmet Sci,* 64**,** 59-66.
WOLUCKA, B. A., MCNEIL, M. R., KALBE, L., COCITO, C. & BRENNAN, P. J. 1993. Isolation and characterization of a novel glucuronosyl diacylglycerol from Mycobacterium smegmatis. *Biochim Biophys Acta,* 1170**,** 131-6.
WORLD HEALTH ORGANIZATION. 2019. *Global Tuberculosis Report* [Online]. World Health Organisation. Available: https://www.who.int/tb/publications/global_report/en/ [Accessed 2020].
WU, D., XING, G. W., POLES, M. A., HOROWITZ, A., KINJO, Y., SULLIVAN, B., BODMER-NARKEVITCH, V., PLETTENBURG, O., KRONENBERG, M., TSUJI, M., HO, D. D. & WONG, C. H. 2005. Bacterial glycolipids and analogs as antigens for CD1d-restricted NKT cells. *Proc Natl Acad Sci U S A,* 102**,** 1351-6.
WU, J. J., ROTH, R. J., ANDERSON, E. J., HONG, E. G., LEE, M. K., CHOI, C. S., NEUFER, P. D., SHULMAN, G. I., KIM, J. K. & BENNETT, A. M. 2006. Mice lacking MAP kinase phosphatase-1 have enhanced MAP kinase activity and resistance to diet-induced obesity. *Cell Metab,* 4**,** 61-73.

WU, L. & VAN KAER, L. 2009. Natural killer T cells and autoimmune disease. *Curr Mol Med,* 9**,** 4-14.
XIONG, Y., HANNON, G. J., ZHANG, H., CASSO, D., KOBAYASHI, R. & BEACH, D. 1993. p21 is a universal inhibitor of cyclin kinases. *Nature,* 366**,** 701-4.
YAMAGUCHI, H., HIRAI, M., KUROSAWA, Y. & HASHIMOTO, K. 1997. A highly conserved major histocompatibility complex class I-related gene in mammals. *Biochem Biophys Res Commun,* 238**,** 697-702.
YANG, B. H., HAGEMANN, S., MAMARELI, P., LAUER, U., HOFFMANN, U., BECKSTETTE, M., FOHSE, L., PRINZ, I., PEZOLDT, J., SUERBAUM, S., SPARWASSER, T., HAMANN, A., FLOESS, S., HUEHN, J. & LOCHNER, M. 2016. Foxp3(+) T cells expressing RORgammat represent a stable regulatory T-cell effector lineage with enhanced suppressive capacity during intestinal inflammation. *Mucosal Immunol,* 9**,** 444-57.
YANG, C., LIU, X., CHENG, T., XIAO, R., GAO, Q., MING, F., JIN, M., CHEN, H. & ZHOU, H. 2019. LYAR Suppresses Beta Interferon Induction by Targeting Phosphorylated Interferon Regulatory Factor 3. *J Virol,* 93.
YANG, J. Q., KIM, P. J. & SINGH, R. R. 2012. Brief treatment with iNKT cell ligand alpha-galactosylceramide confers a long-term protection against lupus. *J Clin Immunol,* 32**,** 106-13.
YANG, Z., WANG, C., WANG, T., BAI, J., ZHAO, Y., LIU, X., MA, Q., WU, X., GUO, Y., ZHAO, Y. & REN, L. 2015. Analysis of the reptile CD1 genes: evolutionary implications. *Immunogenetics,* 67**,** 337-46.
YAO, X. S., DIAO, Y., SUN, W. B., LUO, J. M., QIN, M. & TANG, X. Y. 2007. Analysis of the CDR3 length repertoire and the diversity of TCR alpha chain in human peripheral blood T lymphocytes. *Cell Mol Immunol,* 4**,** 215-20.
YORK, I. A. & ROCK, K. L. 1996. Antigen processing and presentation by the class I major histocompatibility complex. *Annu Rev Immunol,* 14**,** 369-96.
YOSHIDA, A., IMAYAMA, S., SUGAI, S., KAWANO, Y. & ISHIBASHI, T. 1997. Increased number of IgE positive Langerhans cells in the conjunctiva of patients with atopic dermatitis. *Br J Ophthalmol,* 81**,** 402-6.
YOSHIDA, K., KUBO, A., FUJITA, H., YOKOUCHI, M., ISHII, K., KAWASAKI, H., NOMURA, T., SHIMIZU, H., KOUYAMA, K., EBIHARA, T., NAGAO, K. & AMAGAI, M. 2014. Distinct behavior of human Langerhans cells and inflammatory dendritic epidermal cells at tight junctions in patients with atopic dermatitis. *J Allergy Clin Immunol,* 134**,** 856-64.
YOUNG, D. C., KASMAR, A., MORASKI, G., CHENG, T. Y., WALZ, A. J., HU, J., XU, Y., ENDRES, G. W., UZIEBLO, A., ZAJONC, D., COSTELLO, C. E., MILLER, M. J. & MOODY, D. B. 2009. Synthesis of dideoxymycobactin antigens presented by CD1a reveals T cell fine specificity for natural lipopeptide structures. *J Biol Chem,* 284**,** 25087-96.
YU, C. Y. & MILSTEIN, C. 1989. A physical map linking the five CD1 human thymocyte differentiation antigen genes. *EMBO J,* 8**,** 3727-32.
YU, K. K. Q., WILBURN, D. B., HACKNEY, J. A., DARRAH, P. A., FOULDS, K. E., JAMES, C. A., SMITH, M. T., JING, L., SEDER, R. A., ROEDERER, M., KOELLE, D. M., SWANSON, W. J. & SESHADRI, C. 2019. Conservation of molecular and cellular phenotypes of invariant NKT cells between humans and non-human primates. *Immunogenetics,* 71**,** 465-478.
YUE, F. Y., MERCHANT, A., KOVACS, C. M., LOUTFY, M., PERSAD, D. & OSTROWSKI, M. A. 2008. Virus-specific interleukin-17-producing CD4+ T

cells are detectable in early human immunodeficiency virus type 1 infection. *J Virol,* 82**,** 6767-71.
YUROVSKY, V. V., BLEECKER, E. R. & WHITE, B. 1996. Restricted T-cell antigen receptor repertoire in bronchoalveolar T cells from normal humans. *Hum Immunol,* 50**,** 22-37.
ZAHEER, A. & LIM, R. 1996. In vitro inhibition of MAP kinase (ERK1/ERK2) activity by phosphorylated glia maturation factor (GMF). *Biochemistry,* 35**,** 6283-8.
ZAJONC, D. M., CANTU, C., 3RD, MATTNER, J., ZHOU, D., SAVAGE, P. B., BENDELAC, A., WILSON, I. A. & TEYTON, L. 2005a. Structure and function of a potent agonist for the semi-invariant natural killer T cell receptor. *Nat Immunol,* 6**,** 810-8.
ZAJONC, D. M., CRISPIN, M. D., BOWDEN, T. A., YOUNG, D. C., CHENG, T. Y., HU, J., COSTELLO, C. E., RUDD, P. M., DWEK, R. A., MILLER, M. J., BRENNER, M. B., MOODY, D. B. & WILSON, I. A. 2005b. Molecular mechanism of lipopeptide presentation by CD1a. *Immunity,* 22**,** 209-19.
ZAJONC, D. M., ELSLIGER, M. A., TEYTON, L. & WILSON, I. A. 2003. Crystal structure of CD1a in complex with a sulfatide self antigen at a resolution of 2.15 A. *Nat Immunol,* 4**,** 808-15.
ZAJONC, D. M. & GIRARDI, E. 2014. A gammadelta T-cell glimpse of glycolipids. *Immunol Cell Biol,* 92**,** 99-100.
ZAJONC, D. M. & WILSON, I. A. 2007. Architecture of CD1 proteins. *Curr Top Microbiol Immunol,* 314**,** 27-50.
ZEDDA, L., FORLEO-NETO, E., VERTRUYEN, A., RAES, M., MARCHANT, A., JANSEN, W., CLOUTING, H., ARORA, A., BEATTY, M. E., GALLI, G., DEL GIUDICE, G. & CASTELLINO, F. 2015. Dissecting the immune response to MF59-adjuvanted and nonadjuvanted seasonal influenza vaccines in children less than three years of age. *Pediatr Infect Dis J,* 34**,** 73-8.
ZEISSIG, S., MURATA, K., SWEET, L., PUBLICOVER, J., HU, Z., KASER, A., BOSSE, E., IQBAL, J., HUSSAIN, M. M., BALSCHUN, K., ROCKEN, C., ARLT, A., GUNTHER, R., HAMPE, J., SCHREIBER, S., BARON, J. L., MOODY, D. B., LIANG, T. J. & BLUMBERG, R. S. 2012. Hepatitis B virus-induced lipid alterations contribute to natural killer T cell-dependent protective immunity. *Nat Med,* 18**,** 1060-8.
ZEMMOUR, J., LITTLE, A. M., SCHENDEL, D. J. & PARHAM, P. 1992. The HLA-A,B "negative" mutant cell line C1R expresses a novel HLA-B35 allele, which also has a point mutation in the translation initiation codon. *J Immunol,* 148**,** 1941-8.
ZENG, Z., CASTANO, A. R., SEGELKE, B. W., STURA, E. A., PETERSON, P. A. & WILSON, I. A. 1997. Crystal structure of mouse CD1: An MHC-like fold with a large hydrophobic binding groove. *Science,* 277**,** 339-45.
ZHANG, N., PAN, H. F. & YE, D. Q. 2011. Th22 in inflammatory and autoimmune disease: prospects for therapeutic intervention. *Mol Cell Biochem,* 353**,** 41-6.
ZHANG, X., REN, D., GUO, L., WANG, L., WU, S., LIN, C., YE, L., ZHU, J., LI, J., SONG, L., LIN, H. & HE, Z. 2017. Thymosin beta 10 is a key regulator of tumorigenesis and metastasis and a novel serum marker in breast cancer. *Breast Cancer Res,* 19**,** 15.
ZHANG, Y., REYNOLDS, J. M., CHANG, S. H., MARTIN-OROZCO, N., CHUNG, Y., NURIEVA, R. I. & DONG, C. 2009. MKP-1 is necessary for T cell activation and function. *J Biol Chem,* 284**,** 30815-24.

ZHANG, Y., SPRINGFIELD, R., CHEN, S., LI, X., FENG, X., MOSHIRIAN, R., YANG, R. & YUAN, W. 2019. alpha-GalCer and iNKT Cell-Based Cancer Immunotherapy: Realizing the Therapeutic Potentials. *Front Immunol,* 10**,** 1126.

ZHAO, Y., FISHELEVICH, R., PETRALI, J. P., ZHENG, L., ANATOLIEVNA, M. A., DENG, A., ECKERT, R. L. & GASPARI, A. A. 2008. Activation of keratinocyte protein kinase C zeta in psoriasis plaques. *J Invest Dermatol,* 128**,** 2190-7.

ZHOU, D., CANTU, C., 3RD, SAGIV, Y., SCHRANTZ, N., KULKARNI, A. B., QI, X., MAHURAN, D. J., MORALES, C. R., GRABOWSKI, G. A., BENLAGHA, K., SAVAGE, P., BENDELAC, A. & TEYTON, L. 2004a. Editing of CD1d-bound lipid antigens by endosomal lipid transfer proteins. *Science,* 303**,** 523-7.

ZHOU, D., CHEN, B., YE, J. J. & CHEN, S. 2004b. A novel crosstalk mechanism between nuclear receptor-mediated and growth factor/Ras-mediated pathways through PNRC-Grb2 interaction. *Oncogene,* 23**,** 5394-404.

ZHOU, D., MATTNER, J., CANTU, C., 3RD, SCHRANTZ, N., YIN, N., GAO, Y., SAGIV, Y., HUDSPETH, K., WU, Y. P., YAMASHITA, T., TENEBERG, S., WANG, D., PROIA, R. L., LEVERY, S. B., SAVAGE, P. B., TEYTON, L. & BENDELAC, A. 2004c. Lysosomal glycosphingolipid recognition by NKT cells. *Science,* 306**,** 1786-9.

ZHOU, D., ZHONG, S., YE, J. J., QUACH, K. M., JOHNSON, D. L. & CHEN, S. 2007. PNRC is a unique nuclear receptor coactivator that stimulates RNA polymerase III-dependent transcription. *J Mol Signal,* 2**,** 5.

ZHU, Z., HE, X., JOHNSON, C., STOOPS, J., EAKER, A. E., STOFFER, D. S., BELL, A., ZARNEGAR, R. & DEFRANCES, M. C. 2007. PI3K is negatively regulated by PIK3IP1, a novel p110 interacting protein. *Biochem Biophys Res Commun,* 358**,** 66-72.